POROUS GRAPHITIC CARBON, A NEW

MATERIAL FOR HIGH PERFORMANCE

LIQUID CHROMATOGRAPHY

By

Bulvinder Kaur, B.Sc., M.Sc.

Thesis submitted for the
Degree of Doctor of Philosophy
University of Edinburgh
1986

Postgraduate Lecture Courses Attended

(1) Fortran Computer Course   - 1 week course

        Dr. C.N.M. Pounder

(2) The Use of Microcomputers with   - 5 lectures
        Instrumentation

        Dr. A.G. Rowley and Mr. A. King

(3) "Of Mussels, Moses and Micrograms" - 1 lecture

        Dr. G.A. Best

        (Clyde River Purification Board)

(4) Chemical Technology & Industrial   - 6 lectures
        Chemistry

        Dr. A.J.S. Nicoll, Dr. L.H. Mustoe
        and Dr. R.S. Sinclair

        (Paisley College of Technology)

(5) Least Square Methods   - 5 lectures

        Professor Joel Tellinghuisen

(6) "An Explosive Lecture"   - 1 lecture

        Dr. D.R. Marshall

(7) "Molecular Electronics"   - 5 lectures

        Professor R.W. Munn and
        Professor J.O. Williams

        (U.M.I.S.T.)

(8) Joint Meeting of the Chromatography - 3 meetings
        and Electrophoresis Group

(9) East of Scotland HPLC Users' Group - 8 meetings

(10) 9th International Symposium on   - 1 week conference
        Column Liquid Chromatography
        held in Edinburgh

To my darling daughter, Heather

and my loving family.

Abstract

This thesis is divided into four parts. In the first part, the history of chromatography is described. Different modes of chromatography are briefly discussed and a survey of stationary phases being used in High Performance Liquid Chromatography (HPLC) is made. The need for a non-polar reversed-phase stationary phase is highlighted. A brief survey of the use of carbon by other workers in liquid chromatography is also made.

The second part of the thesis deals with the production and structural study of porous graphitic carbon (PGC). The different stages of production of PGC are discussed. Pore volume and surface area studies on PGC have also been made. A detailed structural study of PGC has been presented.

The third part of the thesis deals with the literature survey of the formation of surface complexes on carbon and the gas reactions of carbon, an understanding of which was necessary for the production and control of the final quality of PGC.

The fourth part of the thesis deals with the use of PGC in HPLC. A packing method for PGC has been investigated. Different batches of PGC's produced have been tested with standard test solutes. A separation of a wide variety of solutes, including polymethylphenols, polymethylbenzenes, alkylbenzenes, bases, acids, polyaromatic hydrocarbons, phenyl ketones and phthalates on PGC have been achieved. Analgesics can also be separated. Solvent strengths on PGC has been investigated using different solvents and different solutes.

CONTENTS

Part I

HISTORY AND PRINCIPLES OF LC AND SURVEY
OF STATIONARY PHASES IN LC. THE USE OF CARBON IN LC

Part II

PRODUCTION AND STRUCTURE OF POROUS CARBON

P A R T   1

(HISTORY AND PRINCIPLES OF LC AND SURVEY

OF STATIONARY PHASES IN LC

THE USE OF CARBON IN LC)

CHAPTER 1

HISTORICAL BACKGROUND AND BASIC CONCEPTS OF LC

1.0 <u>General Remarks</u>

Liquid chromatography represents an important branch of analytical chemistry and is now accepted as a powerful and versati le analytical technique.   Molnar and Horvath noted its popularity to be due to its relative simplicity and its high degree of reproducibility.[1a] It is a separation technique which involves applying a sample to one end of a rigidly held bed of some partitioning material. Subsequently a fluid or mobile phase is passed through the bed and washes the sample down the column, thereby, brings about the separation of the components of the sample.   This may be explained in terms of thermodynamic and kinetic effects as is discussed in detail in chapter 2.

A liquid chromatographic system is composed of the following components; a pump which pumps a liquid, generally termed mobile phase, through a column packed with a suitable packing material which bears the stationary partitioning phase.   The sample to be analysed is introduced into the top of the column by means of an injection system.   A detector placed at the end of the column detects different components of the sample as they emerge, hopefully separated, from the column.

The heart of a liquid chromatographic system is the column and the success of a particular analysis depends to a great measure on the ability of the column to bring about the desired separation.   A large number of packing materials having a variety of stationary phases are currently being used in liquid chromatography and these are discussed in greater detail in section 1.4.   The particular subject of this thesis

is the development, characterisation and the use of a
novel form of carbon as a stationary phase in liquid
chromatography.   The use of carbon is not new in liquid
chromatography.   Indeed, active carbons had been used for
many years[1b] but due to certain undesired properties possessed
by such carbons their use in liquid chromatography has de-
clined in recent years.   Only very recently has the potential
of carbon again been recognized but now in the form of
graphitized carbon rather than active carbon.   The work to
be described in this thesis follows earlier work by Knox and
Gilbert[2] on a form of carbon which they called porous
glassy carbon.   Broadly, what has now been achieved as a
result of the work described below, is a reliable method of
production of a high grade chromatographic carbon, a com-
prehensive elucidation of the structure of this material
and a fairly extensive examination or study of its application
in modern HPLC.   We believe that the work of this thesis
has opened a new field in liquid chromatography.

1.1   Historical background of Chromatography

The discovery of chromatography is generally accorded
to Michael Tswett, a Russian botanist and who has become
known as the father of chromatography because of the crucial
contributions which he made to both the practice and the
understanding of this technique.   In 1903, Tswett[3] was the
first scientist to show how components could be separated
by elution through a column of adsorbent;   Tswett separated
a solution of coloured leaf pigments by passing it through

a column packed with adsorbent chalk particles.   He was the
first to recognize that separation arose because of different
affinities of substances for the adsorbent with which the
column was packed.   Unfortunately at that time, chemists at
large did not recognize the potential of chromatography and
the method was ignored until Kuhn and Lederer[4] in the 1930's
revived the technique to separate carotene isomers.   In 1938,
Reichstein and Van Euw[5] used adsorption chromatography for
the separation of natural products.   In 1940, Wilson[6] put
forward the first mathematical theory of chromatography.
He offered a qualitative description of nonequilibrium and
its importance in chromatography, and related it to longitu-
dinal band dispersion.   He also proposed that peak tailing
was due to too low rates of adsorption and desorption, and
that such effects could be reduced by decreasing the rate at
which liquid flows through the column.   The principles
enunciated by J.N. Wilson are applicable to all forms of
chromatography.

In 1941, Martin and Synge[7] developed the plate theory
of chromatography, which was the first theory to describe the
development of a zone profile under the influence of non-
equilibrium in the presence of a linear partition isotherm.
They deduced the rule that the plate height, H, is proportional
to flow velocity and the square of the particle diameter.
Non-specific conclusions were reached regarding the variations
of H with experimental conditions.   The well known Gaussian
profile was first noted by them.   They also recognized that
liquid chromatography could be carried out at high speed.
They stated that "high performance in liquid chromatography

could be achieved by using very small particles and a high pressure difference across the length of the column". Unfortunately, the Martin-Synge treatment was largely irrelevant to adsorption chromatography as practised in the period 1940-1960 since the adsorption isotherms in practical separation systems were seriously non-linear and peak dispersion arose much more from this than from non-optimization Therefore, during this period theoretical treatments of adsorption chromatography were based on the assumed non-linearity of the adsorption isotherm. In 1943, Devault[8] and Weiss[9] improved on the equilibrium theory originated by Wilson.

The next great step was the break from restrictions and limitations of the nonequilibrium theory. Walter,[10] Sillen[11] and Thomas[12] made the contribution to this advancement. Thomas's first treatment of nonequilibrium theory appeared in 1944. Thomas introduced a Langmuir mechanism term starting with the equation of mass conservation. He obtained equations of effluent concentrations as a function of time. He considered close-to-equilibrium conditions whereby the flow rate is slow enough to prevent large departures from equilibrium. He also obtained formulae from which the adsorption and desorption rates could be obtained from experimental solute concentration curves of chromatography.

In 1947, Boyd, Myers and Adamson[13] described ion-exchange kinetics in terms of diffusion through a liquid film. They were the first to predict zone structure in terms of independent rate and equilibrium constants.

In 1952, Lapidus and Amundson[14] developed a theory which

contained as parameters a mass transfer coefficient and a longitudinal coefficient. At the same time, James and Martin[15] described the first use of gas liquid partition chromatography. Their analysis of fatty acids by partition between nitrogen and silicone oil distributed on a diatomaceous earth support led to the explosive growth in the application of this technique.

The second decade of chromatographic theory (1950-1960) involved the development of asymptotic theories which evolved around the concept that an effective and practical chromatographic operation requires sufficient running time to obtain narrow and well-separated zones. When the time is sufficiently long for this, however, the sorption-desorption kinetics are proceeding with only slight departure from equilibrium. In 1955, Giddings and Eyring[16] introduced probability (statistical) concepts into the description of molecular migration in chromatography. The theory was extended to the complex two-site adsorption problem, and a simplified expression was shown to be valid for one-site adsorption after a sufficient time. This approach was the forerunner of the random walk theory of chromatography, the simplest known chromatographic theory.

In 1956, van Deemter, Zuiderweg and Klinkenberg[17] put forward a theory using the long-time approximation. Zone spreading was expressed in terms of the height equivalent to a theoretical plate. The most important feature of their treatment was to express the HETP as a sum of three terms each with a different velocity dependence. The subsequent application of the so-called 'van Deemter equation' was largely responsible for the rapid development of efficient gas

chromatographic techniques.

Giddings,[18] in 1957, gave an expression in terms of Gaussian concentration profiles originating from effective diffusion process for a simple reversible adsorption-desorption reaction.

In 1958, Golay[19] first applied the successful combination of long but practical time periods and simplicity in the form of Gaussian, plate height or effective diffusion concepts to a diffusion controlled mechanism - the sorption and desorption of a solute with an open capillary column, the wall of which was assumed to possess a uniform coating of liquid stationary phase.

The development of a generalized non-equilibrium theory of chromatography was started by Giddings in 1959[20] for the purpose of calculating the influence of any complex combination of sorption and desorption steps, whether controlled by diffusion or single step reactions. This theory was subsequently elaborated and is fully described in Giddings' "Dynamics of Chromatography".[21]

1.2 Basic Concepts and Definitions

1.2.1 Basic Concepts

To illustrate the chromatographic process Snyder and Kirkland[22] considered a hypothetical separation of a three-component mixture in an LC column.

Figure 1.2.1 shows such a hypothetical situation. The three compounds A, B and C were considered, and are represented by

BASIC CONCEPTS
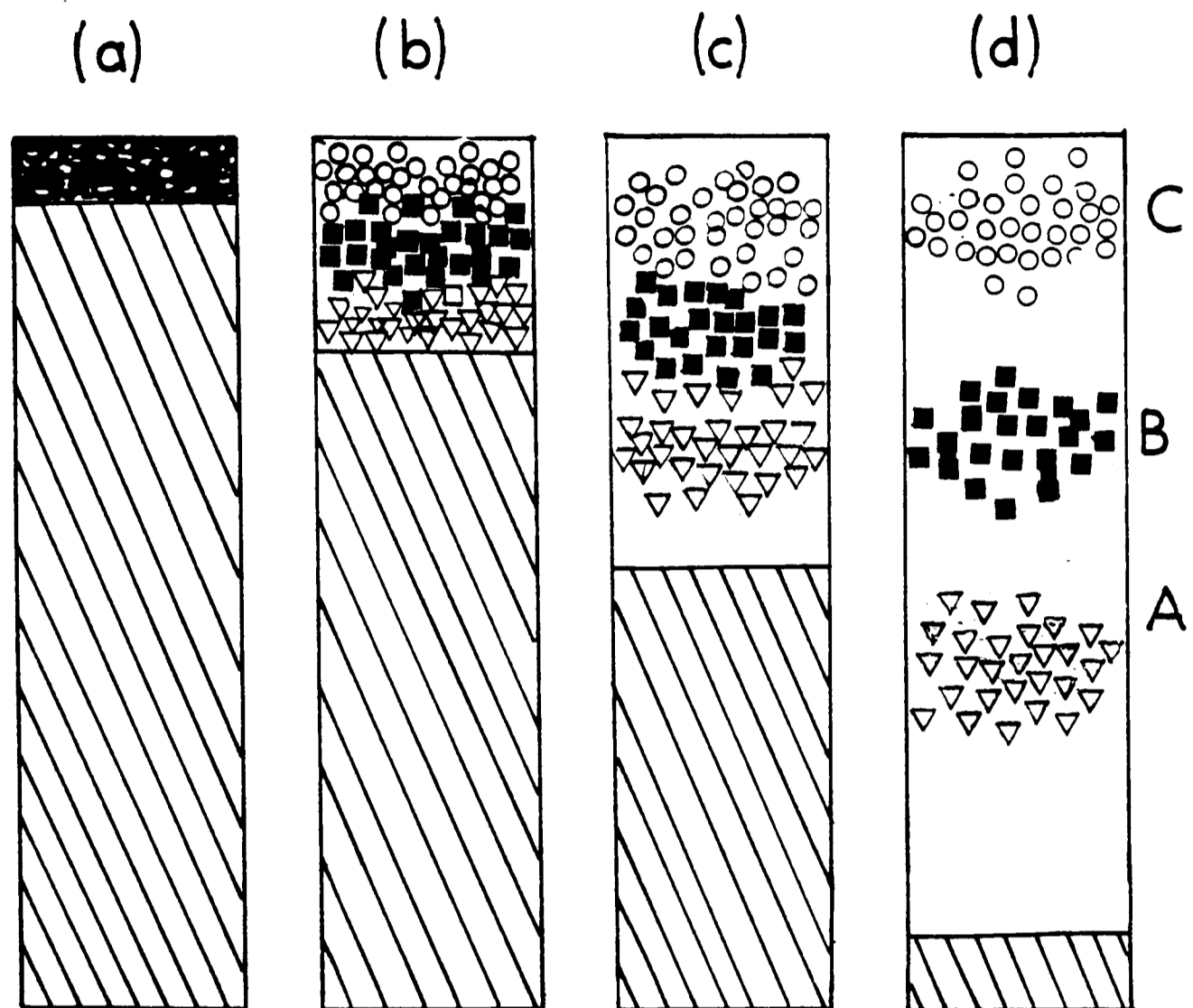
FIG.1.2-1: HYPOTHETICAL SEPARATION
OF A 3-COMPONENT
SAMPLE; ▽ COMPOUND A
▪ COMPOUND B
∘ COMPOUND C

(from ref. 21)

triangles (A), squares (B), and circles (C).   The following

four successive stages of the separation are illustrated.

(i) Application of a sample containing compounds A, B and C

to the top of the column under static conditions (no flow of

eluent).

(ii) The solvent or mobile phase begins to flow down the

column and, in doing so, begins to affect a partial separation

of compounds A, B and C.

(iii) Greater separation of compounds A, B and C is seen as

the mobile phase moves farther down the column.

(iv) The chromatographic separation is essentially complete

with A, B and C being depicted by three well separated bands

moving down the column.   At this stage, two distinct features

of a chromatographic process becomes apparent.   Firstly,

different compounds have moved down the column at different

rates.   This is termed differential migration which is the

basis of separation in LC.   Secondly, there is a spread of

molecules of one given compound due to the fact that the

migration rates of individual molecules are not identical.

This is termed molecular spreading or peak dispersion in LC.

How does differential migration arise in a chromatographic

separation?   In a chromatographic system there are two phases

namely the moving or mobile phase and the stationary phase.

Figure 1.2-2 gives a good representation of these two zones.[23]

Different compounds have different equilibrium distributions,

between these two phases due to their different affinities.

The phenomenon of differential migration is illustrated in

figure 1.2-3 in the case of a single stationary phase particle

Wall   Streamline   Stationary   Mobile
                      Zone   Zone
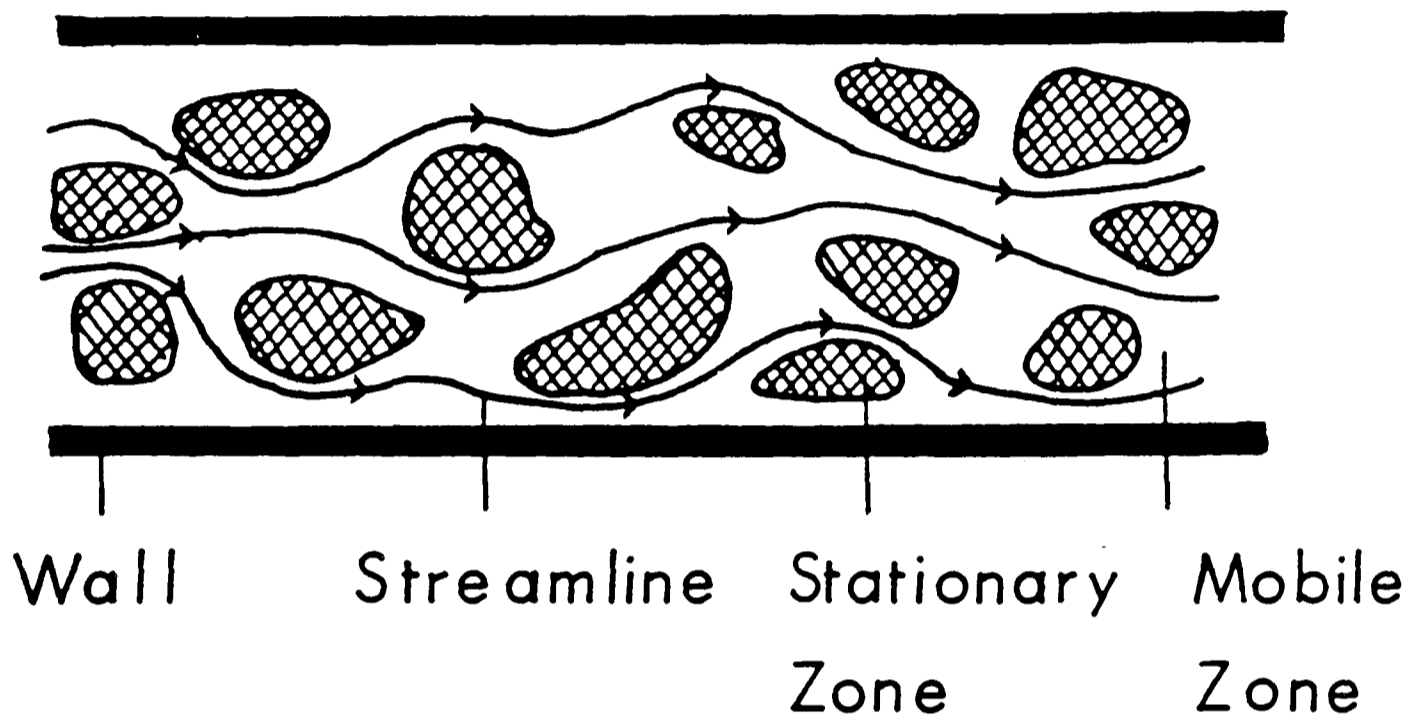
FIG. 1.2 - 2 : FORMAL REPRESENTATION
OF COLUMN STRUCTURE
SHOWING STATIONARY
AND MOBILE ZONE
(from Ref. 22)
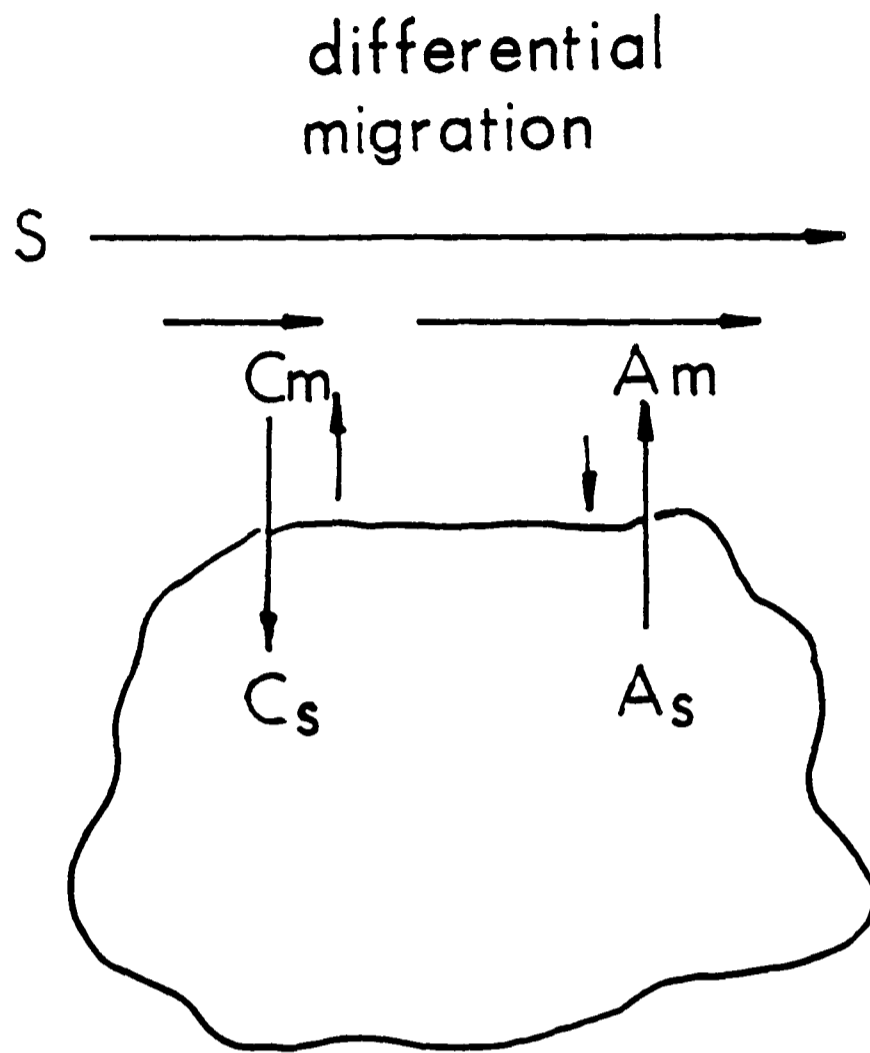
FIG.1.2-3: THE BASIS OF RETENTION
IN LC (from ref.21)

and for two compounds A and C. Compound C, due to its greater affinity to the stationary phase, is present mainly in the stationary phase at equilibrium with only a small fraction of its molecules in the moving phase. On the other hand, compounds such as A which have greater affinity for the mobile phase spend a greater proportion of their time in this phase and lesser time in the stationary phase. Since molecules move along the column only when they are in the mobile phase, the speed which each compound moves through the column is determined by the fraction of molecules of that compound in the moving phase at any moment, compounds such as C thus move slowly through the column and compounds such as A move more rapidly. The relative migration rate is, therefore, determined by variables which affect the equilibrium distribution of each compound namely the mobile phase composition, the type of stationary phase and the separation temperature. The relative migration rate is determined by thermodynamic considerations.

The second feature of a chromatographic separation is band dispersion. This is governed by kinetic considerations. Molecular or band spreading is brought about by the following rate processes:

(1) Axial molecular diffusion.

(2) Flow pattern effects.

(3) The finite rate of mass transfer processes within and between the mobile and stationary phases.

which, according to van Deemter et al[17] gave independent contributions to band dispersion. Axial molecular diffusion is no different from any kind of molecular diffusion and it

depends on the time of residence of molecules in the column, for a column of given length the time of residence is inversely proportional to velocity. Flow pattern effects arise from the random nature of the packing and from the fact that streamlines of different lengths and random variations of velocity along each flow line exists. This results in the spread of residence time in the column since this is essentially independent of velocity. The mass transfer contribution arises from the fact that when a solute molecule finds itself within a particle it lags behind the band as a whole and when in the moving phase it tends to rush ahead; it thus performs a random walk about the centre of the band, and so when different molecules are considered with each performing its own independent walk one gets a sort of a band since the distance by which the solute molecule lags behind or goes ahead of that band as a whole is proportional to the flow velocity. The contribution to H is proportional to the velocity.

In general, as shown later in Chapter 2, Section 2.2, the dispersion is affected by flow velocity, diffusion rates, particle size, goodness of column packing, and the degree of retention. Of these, the particle size is the most important since equilibration time is proportional to the square of the particle diameter. Thus the smallest possible particles consistent with the pressure drop available should be used in any form of chromatography driven by pressurised eluent.

1.2.2 Definitions

The time, t_R, that elapses between injection and elution of a solute is called the retention time or elution time and the volume of eluent, V_R, passed into the column during this time is called the retention or elution volume of the solvent (see figure 1.2-4). V_R and t_R are related through the equation:

$$V_R = t_R f_V \qquad (1.2-1)$$

where f_V is the volumetric flow rate.

The degree of retention of a solute is given by the phase capacity ratio, k', and is defined by:

$$k' = \frac{t_R - t_m}{t_m} \qquad (1.2-2)$$

$$= \frac{V_R - V_m}{V_m} \qquad (1.2-3)$$

where t_m is the retention time for a solute that is unretained by the stationary phase and V_m is the retention volume of such a solute. V_m is also equal to the volume of eluent in the column.

The linear flow velocity, u, denotes the rate of movement of eluent along the column and is related to retention time, t_m, and column length, L, by:

$$u = \frac{L}{t_m} \qquad (1.2-4)$$

In well behaved chromatography where the partition
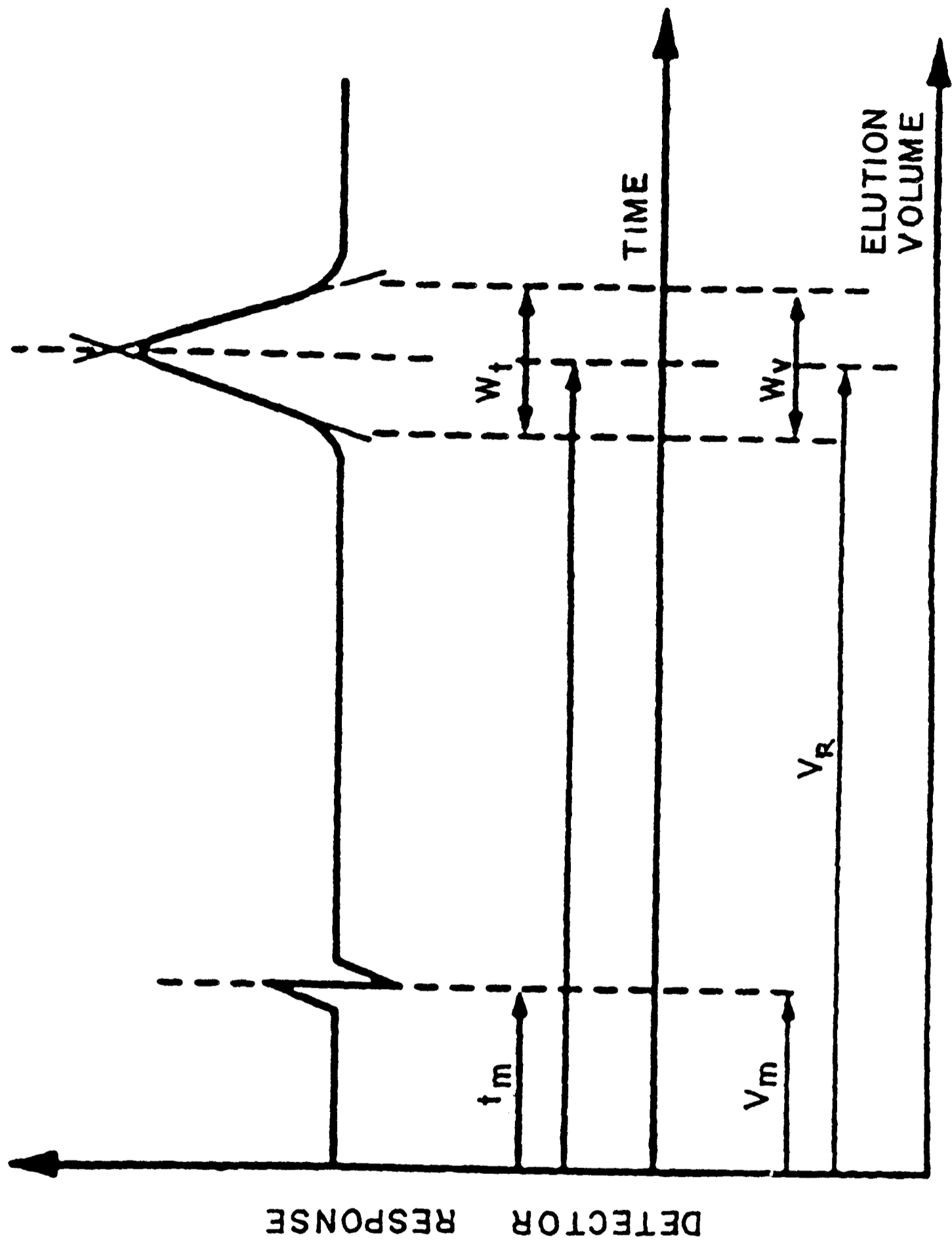
FIG. 12-4: PARAMETERS FOR DEFINING RETENTION AND PEAK WIDTH

isotherm is linear and where there is no dead volume effects the elution peaks should be Gaussian. Both theory and practice agree that the width of a solute band increases as the square root of the distance migrated. This result may be stated as:

$$\sigma = \sqrt{H\,L} \qquad\qquad (1.2\text{-}5)$$

where σ is the standard deviation of the Gaussian curve, L is the column length and H is termed the height equivalent to a theoretical plate (HETP) originally introduced by Martin and Synge.[7] H is the term used by most chromatographers to gauge column performance. The smaller the plate height, the better the performance.

In terms of the peak width at the base in the elution record (figure 1.2-4) which is denoted by either W_t measured in time units or by W_v when measured in volume units, the band dispersion parameters, H can be expressed as:

$$H = \frac{1}{16}\left(\frac{W_z}{L}\right)^2 = \frac{L}{16}\left(\frac{W_t}{t_R}\right)^2 \qquad (1.2\text{-}6)$$

This allows the plate height to be calculated from the chart record. The number of theoretical plates to which a column is equivalent is given by:

$$N = \frac{L}{H} \qquad\qquad (1.2\text{-}7)$$

$$= 16\left(\frac{L}{W_z}\right)^2 \qquad\qquad (1.2\text{-}7a)$$

$$= 16\left(\frac{t_R}{W_t}\right)^2 \qquad\qquad (1.2\text{-}7b)$$

$$= 16\left(\frac{V_R}{W_v}\right)^2 \qquad\qquad (1.2\text{-}7c)$$

The greater the number of plates a column can produce, the better the column performance.

It is often more convenient to describe the plate height not in absolute terms but in terms of the number of particles corresponding to H.   This quantity, h, is called the reduced plate height and was first introduced by Giddings[21] and is equal to:

$$h = \frac{H}{d_p} \qquad\qquad (1.2\text{-}8)$$

where h is a measure of the degree of band dispersion produced by the packing considered in relation to the particle size.

Each dispersion process discussed in section 1.2.1 contributes independently to the total plate height and, on a particle scale, depends upon the balance between the flow of eluent over a particle and the diffusion of solute across a particle.   Van Deemter et al.[17] first appreciated that the total plate height could be expressed as a sum of three terms contributed by the different dispersion processes, and the van Deemter equation can be simply represented by:

$$H = A + \frac{B}{v} + Cv \qquad\qquad (1.2\text{-}9)$$

where v is the flow velocity, and the constants, A, B and C are associated with the plate height terms due to eddy diffusion, longitudinal diffusion and mass transfer respectively.   Each of these independent contributions are dealt with in greater detail in Chapter 2, Section 2.2.

The van Deemter equation was then modified by Giddings and later by Knox and co-workers[24-26] and represented in terms of the reduced plate height as:

$$h = A\nu^{1/3} + \frac{B}{\nu} + C\nu \qquad (1.2-10)$$

where ν is called the reduced linear velocity of the eluent and is defined as:

$$\nu = \frac{ud_p}{D_m} \qquad (1.2-11)$$

where D_m is the diffusion coefficient of the solute in the eluent.   The reduced velocity first introduced by Giddings[21] is a measure of the rate of flow over a particle relative to the rate of diffusion within a particle.

The log-log of h versus ν in figure 1.2-5 shows how the different terms contribute to H and emphasizes that H has a minimum value.

1.3   Different Modes of Chromatography

Chromatography can be carried out in a wide variety of ways, and can be classified according to several quite different criteria namely column configuration, scale of operation, the nature of the mobile phase, the nature, composition and the structure of the stationary phase and the
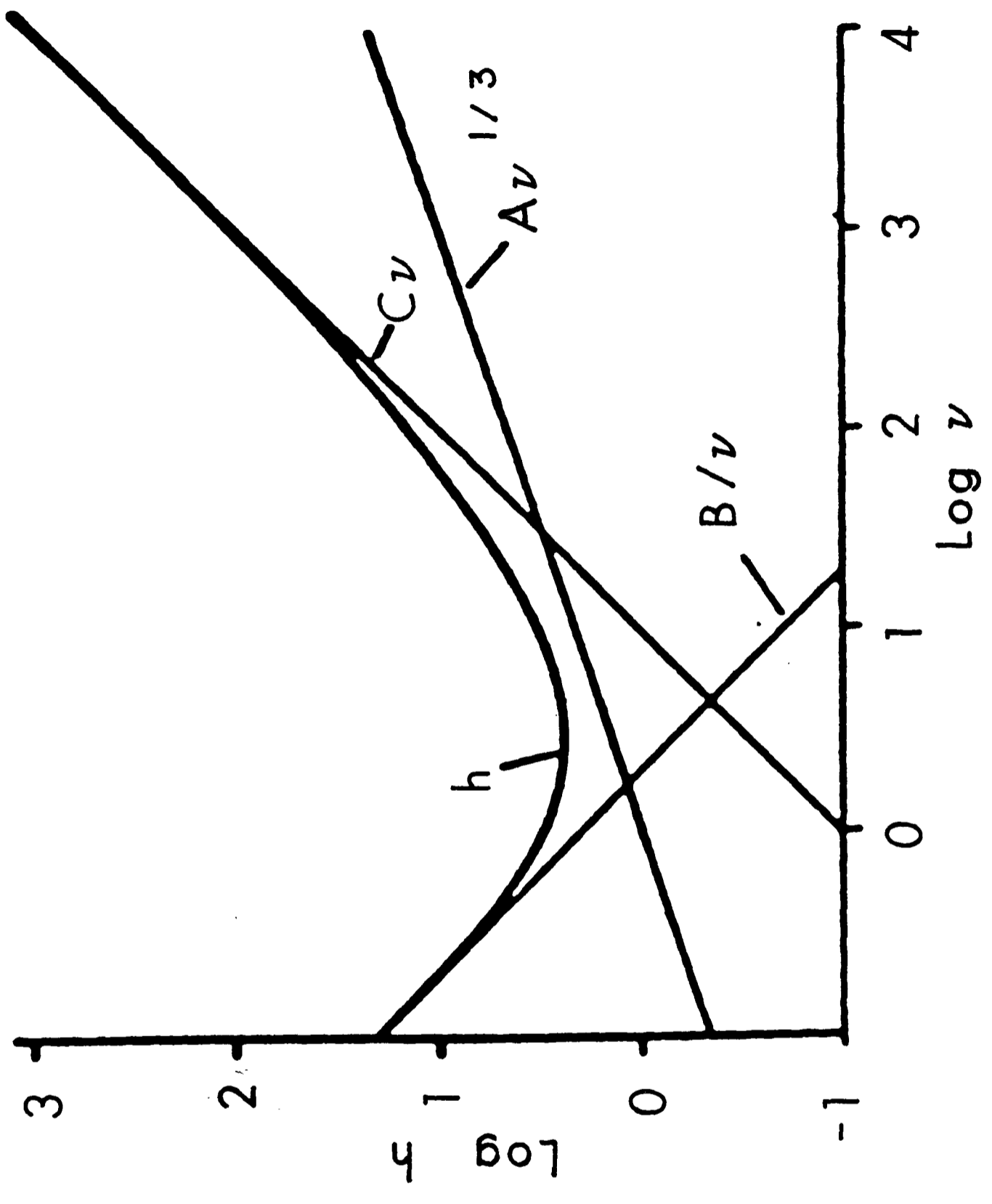
FIG.1.2-5: DEPENDENCE OF h UPON ν

nature of the molecular forces which hold the solute
molecules within the mobile and stationary zones.   This is
illustrated in table 1.3-1.   In open-bed chromatography
the paper or the glass plates are covered with adsorbents
like alumina or silica.   On the other hand, classical column
chromatography was performed in columns that were gravity fed.
Modern HPLC is carried out in a pressurized system compared to
classical gravity fed system.   In terms of scale of operation,
this ranges from microgram level in analytical LC up to kilogram
level in preparative scale chromatography.   The work of this
thesis is concerned only with analytical scale HPLC.

The different branches of chromatography as determined
by the nature of the phases or of the type of molecular
interactions involved are:

(i) Molecular Exclusion Chromatography (MEC) or gel permeation
chromatography (GPC).   In this mode, molecules are separated
according to their size by passage down a column packed with
a micro-porous material which is usually a porous wide pore
silica gel or cross-linked polystyrene for high pressure
applications.   Large molecules are excluded from the pores of the
packing while smaller molecules may permeate the pores partially
or totally depending upon their size.   In exclusion chromato-
graphy the largest molecules emerge from the column first and
the smallest last.

(ii) Ion Exchange Chromatography (IEC).   The column is packed
either with ion exchange resin beads, with surface layer ion
exchange particles (pellicular materials) or bonded porous

Table 1.3-1   Forms of chromatography

A.   Division According to Form of Column

OPEN COLUMN   Paper Chromatography, Thin-layer
                   Chromatography

CLOSED COLUMN   Column Chromatography

OPEN COLUMN   Capillary Chromatography

Mode of Elution   Single Elution - using an initially dry
                   column, e.g. in thin-layer chromatography.

                   Repetitive Elution - using a column
                   already contaminated with eluent.

B.   Division According to Mobile Phase

GASEOUS ELUENT   Gas Chromatography

LIQUID ELUENT   Liquid Chromatography

SUPERCRITICAL   Supercritical fluid chromatography
   FLUID

C.   Division According to Scale

up to 1 mg   Analytical Chromatography

10 - 100 mg   Small Scale Preparative Chromatography

100 mg - 10 g   Preparative Chromatography

>10 g   Large or Industrial Scale Preparative
                   Chromatography

Table 1.3-1 (contd.)

D.   Division According to Nature of Stationary Phase

    High Surface Area   Liquid-Solid or Gas-Solid
    Absorbent   Chromatography

    Liquid   Liquid-Liquid Chromatography

                               Gas-Liquid Partition Chromatography

    Ion-Exchange Resin   Ion-Exchange Chromatography

    Bonded Stationary Phase   Bonded Phase or Reversed Phase
                               Liquid Chromatography

                               or Gas Chromatography

    Wide Pore Packing   Exclusion Chromatography

ion-exchangers. This technique is used in the separation of ionic or ionizable compounds. The support material, therefore, consists of a matrix onto which a charge-bearing group is chemically bonded. Cation exchangers contain negatively charged groups and are used for exchanging cationic species while anionic exchangers contain positively charged groups and are used for exchanging anionic species.

(iii) <u>Liquid -solid Adsorption Chromatography</u> (LSAC). An adsorbent such as silica gel or alumina or other material of large surface area is used as the partitioning material. LSAC is suitable for the separation of a wide range of organic materials which are soluble in non-polar or moderately polar organic solvents. Chromatography on carbon falls within this category.

(iv) <u>Liquid-liquid Partition Chromatography</u> (LLC). The stationary phase is a liquid supported on a solid. The supporting solid may be either a completely porous material such as a wide pore silica gel or porous glass or it may be a superficially porous (pellicular) material. LLC is applicable to a wide range of organic and inorganic solutes and one can use either a polar stationary phase and a non-polar mobile phase or the reverse.

(v) <u>Liquid-solid Partition Chromatography</u>. Here the stationary phase is chemically bonded to the surface of the support which is normally silica. The great advantage of the bonded phase compared to liquid stationary phases is that they are insoluble in solvents and are thermally stable.

1.3.1 Major Operational Modes

The two main operational modes are normal phase chromatography represented by adsorption chromatography and reversed-phase chromatography. The technique of reversed-phase chromatography was introduced by Howard and Martin[27] in 1950 for the separation of polar molecules. At this time, the technique was not widely used in LC because of the instability of column packings. But with the introduction of chemically bonded reversed-phase materials like ODS-silica in 1970 and carbon, this reversed phase method has become widely used. The mobile phase is generally a mixture of water and a non-uv absorbing organic modifier. In RPLC the lower the polarity of the mobile phase the greater is the eluting power (methanol is a stronger solvent than water) and substances are eluted in a general order of decreasing polarity. The advantages and disadvantages of RPLC are tabulated in table 1.3-2.

Recent ideas on the mechanism of reversed-phase chromatography are contained in references[28-31]. Stated simply, the hydrophobic surface extracts the more lipophilic component of the eluent to form an organic rich layer at the particle surface in which the chromatographically useful partitioning takes place. The retentions of various members within a class of compounds in reversed-phase chromatography have been correlated to their solubilities in the eluent. Although reversed-phase chromatography is suited to the separation of polar molecules, non-polar molecules can also be successfully separated by using an eluent which is sufficiently rich in the organic component (eg methanol) to cause the solutes to elute in a reasonable time.

Table 1.3-2   Advantages and Disadvantages of RPLC

ADVANTAGES

1) Samples with a wide range of polarities and molecular weights can be easily separated, hence its broad scope.

2) Ionic or ionizable compounds can be separated by manipulating secondary chemical equilibria such as ionization control and ion-pairing in the aqueous mobile phase.

3) Special selectivities such as structural, steric and enantiomeric can be achieved by specific mobile phase additives.

4) The general rapidity of mobile-phase column equilibration because of weak surface attraction energies of the non-polar stationary phase. (Hydrophobic counter ions in ion-pair chromatography may necessitate longer equilibration times).

5) General ease of use.

6) Can be used as a trace enrichment method in which samples injected in solvents weaker than the mobile phase are preconcentrated at the head of the column.

DISADVANTAGES

1) For silica-based chemically bonded phases the usable pH range in order to maintain stable columns is limited between 2 and 7.5. Atwood et al.[56] have partly surmounted this problem by presaturating the mobile phase with silicates which, therefore, permits high pH values to be used at least for short periods of time.

2) The presence of unreacted, accessible silanols in the silica surface causes chemical instability and gives rise to poor peak shapes and irreproducible retention times between columns due to solute adsorption.

1.4 Column Packing Materials

In the evolution of modern LC, the principal focus
has been on the column, which forms the central element of
every LC system. Pellicular packings approximately 30-50μm
in diameter or so called porous layered beads (superficially
porous packings, controlled surface porosity supports) were
widely used in the early to mid '70s but have now been
relegated to use in quickly replaced guard columns. For
analytical HPLC, the microparticulates in the range of 5μm and
10μm are the most widely used packings today, but larger
porous packings find use in high performance preparative
chromatography.

The different modes of LC require the use of different
stationary phases which can be broadly divided into three
main categories as:

(a) Adsorbents.

(b) Polymer-coated supports.

(c) Chemically bonded stationary phases.

A comprehensive list of the various types of packing
materials available for HPLC has been compiled by Major.[32]

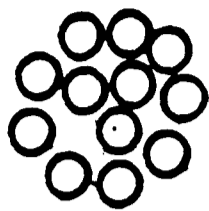## 1.4.1 Adsorbents

The earliest types of HPLC packing materials were large
porous adsorbents (>30μm) such as Lichrosorb (Merck) and
Porasils (Waters). These large particles had poor mass
transfer characteristics due to the large diffusion distances.
In 1968 Kirkland[33] began to use 'superficially porous' packing
materials (also called 'controlled surface porosity', pellicular)

which were non-porous spherical glass beads covered with a thin layer (1-2μm) of porous silica or alumina as seen in figure 1.4-1. Examples of pellicular supports include Zipax (DuPont), Corasil I and II (Waters), Pellosil (Whatman) and Perisorb A (Merck). These supports have low surface areas and are normally used for liquid-liquid partition chromatography, although some can also be used for adsorption chromatography. These pellicular materials, however, have low sample capacity. The most efficient HPLC packings are fully porous particles with diameters of around 5μm. These microparticulate particles combine higher capacity with shorter diffusion distances. Adsorbents for LSC have been classified by Snyder and Poppe[34] as in Table 1.4-1. The two most commonly used adsorbents are silica and alumina. Fairly wide pores (>5nm) are desirable in adsorbents so that solutes are not trapped in the small pores and give rise to tailed peaks. A comprehensive list of commercially available adsorbents are given in Appendix 1.

1.4.2 Polymer Coated Supports

Synthetic cross-linked polymers such as Dowex 1-8x resin were initially used as ion-exchange materials by Cohn and co-workers,[35,36] Volkin et al.[37] and Anderson et al.[38] who developed ion-exchangers as column packings for the separation of bases, nucleotides and nucleosides. Many older organic gels are of microporous types. These materials had the disadvantage that they changed their volumes in organic solvents and under different pH and ionic strength conditions. They were soft and deformed at high pressure and had poor mass

6 um
Porous

30 um
Porous
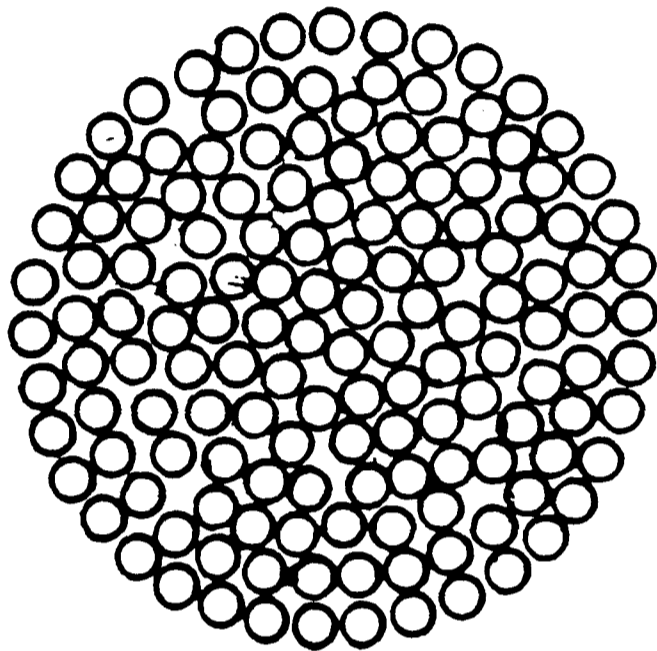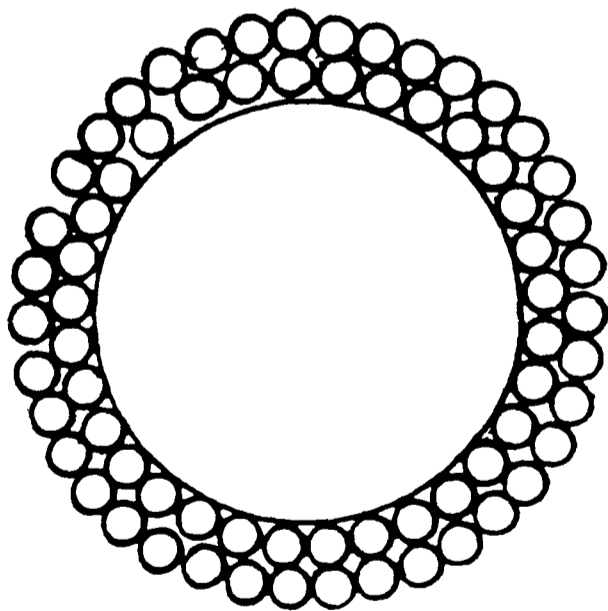
30 um
Pellicular

FIG.1.4 - 1: DIFFERENT TYPES OF PARTICLES USED IN HPLC

Table 1.4-1

Classification of LSC Adsorbents (34)

Adsorbents	General Class	Examples
I	Polar Inorganic	Silica
		Alumina
II	Non Polar Inorganic	Graphite
		Charcoal
III	Polar Bonded Phase	Amino-propyl (C_3NH_2)
		Cyano-propyl (C_3CN)
		Diol Phase $(-O-CH_2-CHOH-CH_2OH)$
IV	Non Polar Bonded Phase	C_8, C_{18} Bonded Phase

transfer characteristics.   Recently macroporous gels have become available.   These gels, like silica, are rigid because there are tightly polymerized regions where solvent and solute cannot penetrate.

In 1967, Horvath et al.[39] developed a pellicular ion-exchange resin.   They coated the surface of glass beads with a polystyrene/divinylbenzene polymer.   Sulphonation of the resulting polymer produced a layer of cation-exchange resin over the glass bead surface, and,similarly,chloromethylation followed by reaction with a tertiary amine produced an anion-exchange resin.   Some of the new organic materials like Styragel, Spherogel, TSK gel and Chromex had good mechanical stability, shorter diffusion distances, low swelling charac-teristics and have stable physical properties like silica gel. A range of porous layer beads coated with ion-exchange resins is now commercially available and include SAX and Zipax SCX (DuPont), AS Pellionex SAX (Whatman) and Pellicular Anion (Varian).   Glass beads (or superficially porous glass beads) could also be coated with hydrocarbon or polyamide polymers. In 1963, Endres and Hörmann[40] published an excellent review on polyamide column chromatography.   Pellicular polyamide was further developed by DuPont and Northgate Laboratories in 1970 and marketed under the name Pellidon.   Examples of each type are collected in Appendix 2.

1.4.3   Chemically Bonded Stationary Phases

According to Majors[32] 65% of HPLC users resort to the reversed phase mode and since 1977 the number of listed reversed phase (RP) materials packings has tripled, some of

which are given in Appendix 3. There are several methods available for the preparation of bonded phases for HPLC. These are as follows.

(i) <u>Reactions with alcohols and amines</u> (Halasz brushes)

The first chemically bonded phases for HPLC were prepared by Halasz and Sebestian[41] by esterifying the silanol (Si-OH) groups on the surface of silica with an alcohol as shown in figure 1.4-2. A further range of bonded materials was prepared by conversion of silica to silica chloride by treatment with thionyl chloride, followed by reaction of the surface chloride groups with amine as shown in figure 1.4-3.[42] These new phases had strands of organic chains (bristles) pointing away from the silica surface, and became known as "Halasz brushes". They are commercially available from Waters as Durapak supports. Their main disadvantage is their limited hydrolytic stability (within the range 4-7) due to hydrolysis of the Si-OR and Si-NR bonds.

(ii) <u>Reaction with organosilanes</u>

Modern commercially available bonded materials are based on reactions between organochloro- or alkyoxysilanes and the surface silanol groups. Such reactions can be carried out under a range of conditions as discussed in detail by Majors.[43] There are two general approaches to the bonding of organosilanes to silica and these are discussed in turn.

(a) Anhydrous conditions

In this instance, dry silica is heated at reflux with octadecyltrichlorosilane in toluene under conditions which exclude water from the reaction mixture.[43,44] In the absence
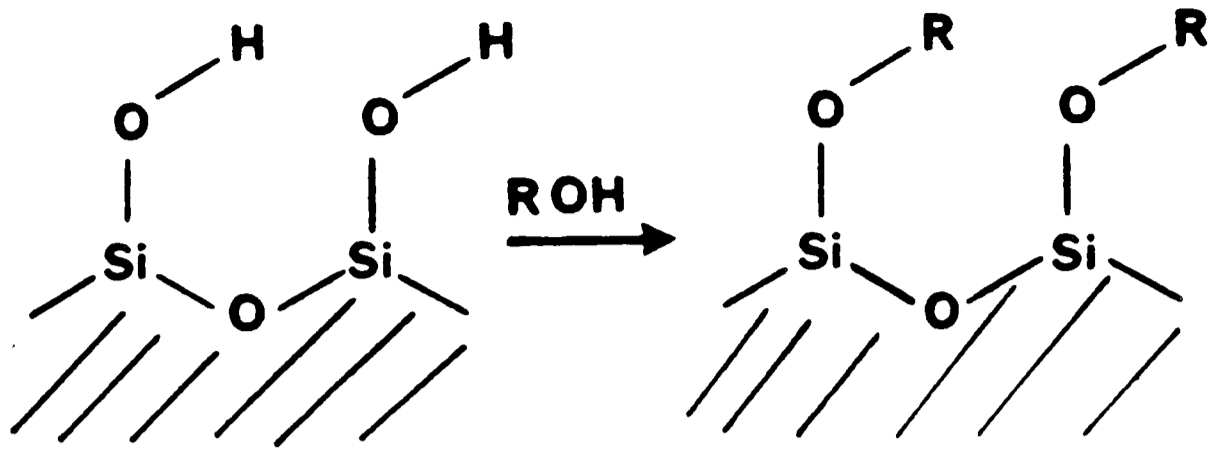
FIG.1.4-2 : ESTERIFICATION OF
SILANOL GROUPS
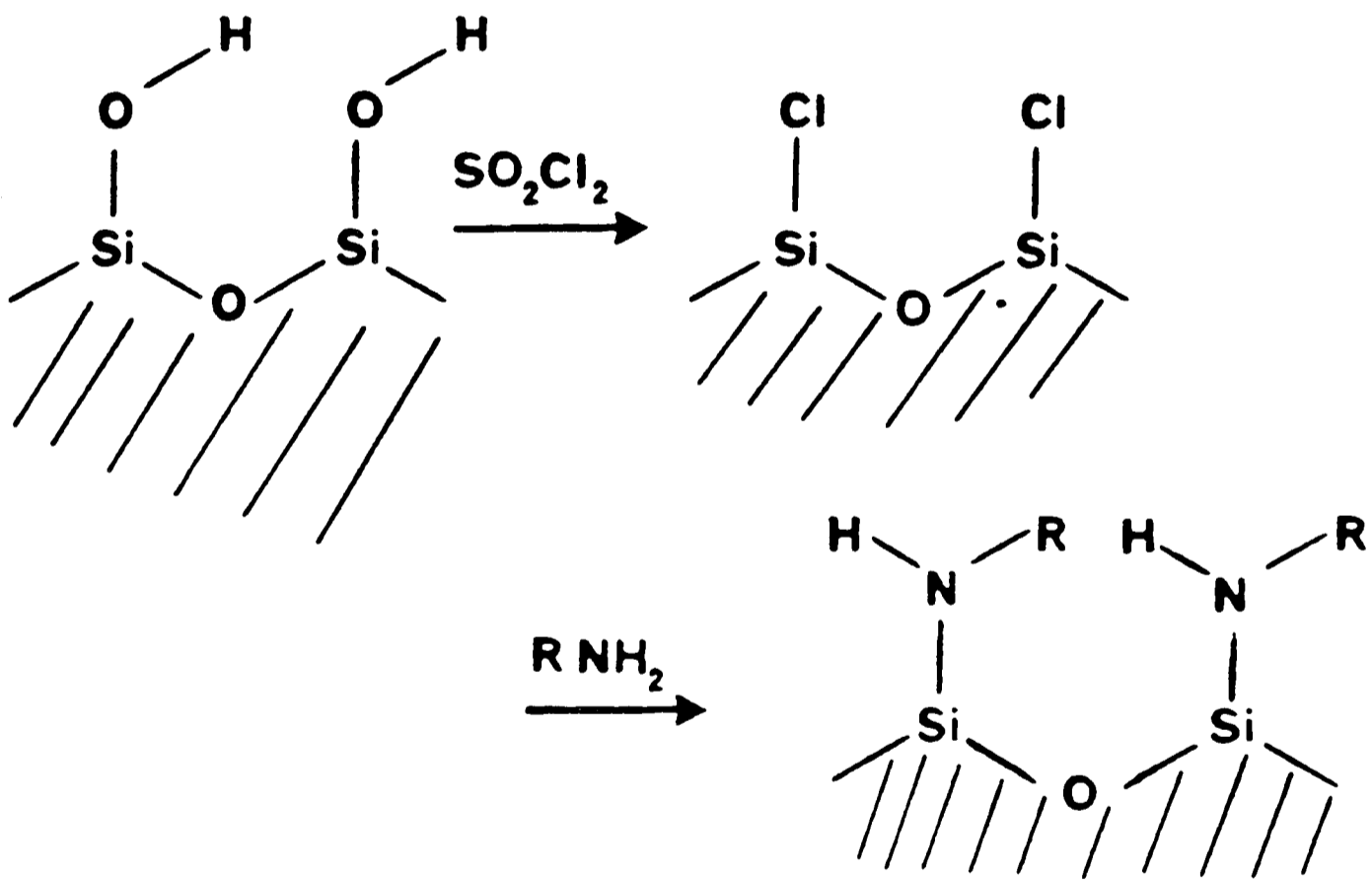
FIG.1.4-3: CHLORINATION OF
SILANOLS GROUPS

of water no hydrolysis of the Si-Cl bonds in the chlorosilane takes place and bonding occurs by elimination of HCl between the organosilane and one or more of the surface silanol groups. After removal of excess reagents, subsequent hydrolysis converts unreacted Si-Cl groups to silanol groups as depicted in figure 1.4-4. In practice, however, the presence of residual silanol groups arising either from hydrolysis of Si-Cl bonds as shown, or by non-reaction of a surface silanol site may confer chromatographically undesirable adsorptive properties on the material. These residual silanol groups should then be "capped", for example, with trimethylsilyl groups,[45] although this is not always done in practice so that some commercial materials have substantial adsorptive properties due to SiOH groups. Some of the widely used commercially available phases based on this reaction include Bondapak supports (Waters), Hypersil supports (Shandon Southern), Partisil-10 ODS (Whatman) and Spherisorb-ODS (Phase Separations). A wide range of bonded phases are prepared by this scheme. No capping is required in the recent materials made from monochloroalkyl-dimethylsilane.

The advantage of supports prepared in this way is that the Siloxane (Si-O-Si) bonds formed during the reaction are relatively stable to hydrolysis. There is a paucity of detailed information on the stability of bonded phases, but such supports are generally held to be stable in the pH range 2-8. Around pH 2, the organic groups are cleaved from the support and at about pH 8, silica itself starts to dissolve. The stability of the bonded phase is also governed by the ionic strength of the mobile phase and the column operating temperature.
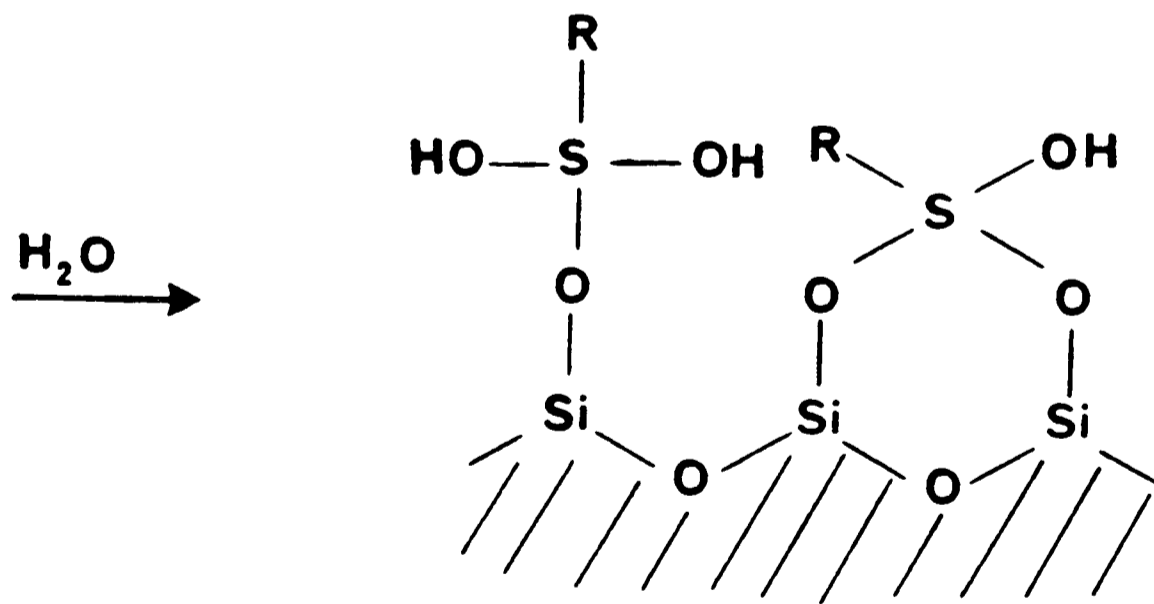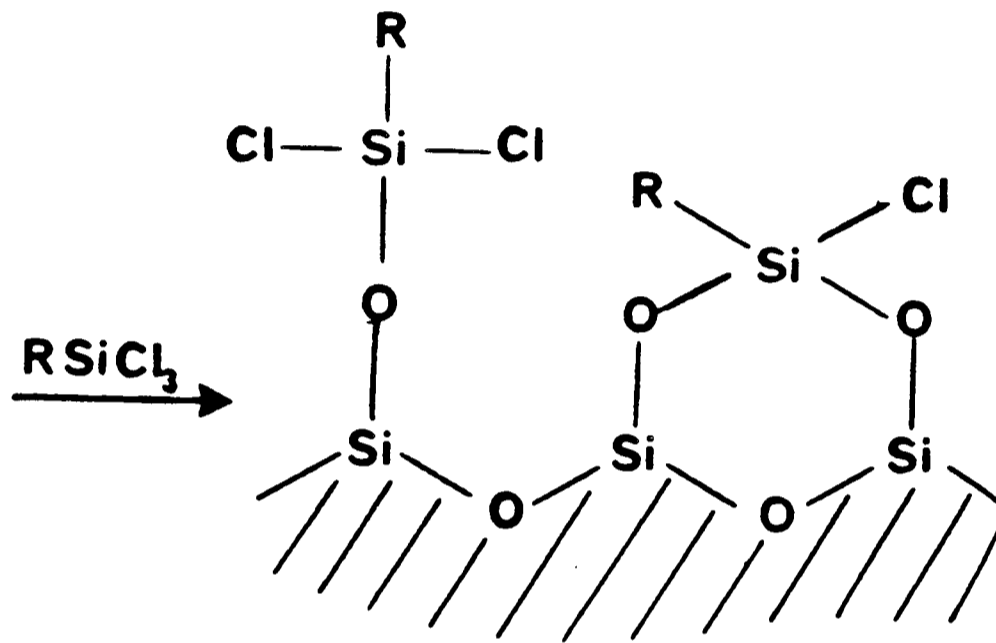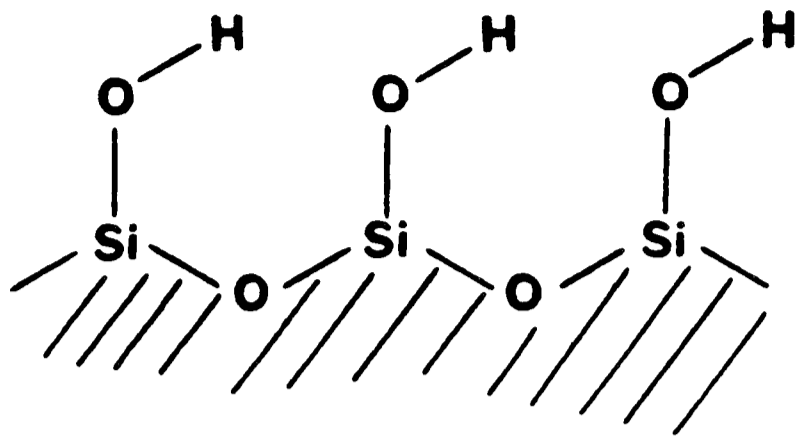
FIG. 14-4 : REACTION WITH ALKYL-TRICHLOROSILANES

(b)   Reaction with hydrolysis

As shown in figure 1.4-5 an alternative scheme for the
reaction of organosilanes with siliceous surfaces is first
to hydrolyse the organochloro- or alkoxysilane to the silane-
triol and to partially polymerise the latter.   The resulting
polymer is then bonded to the support surface by multiple
attachments via stable siloxane linkages.[46,47] This is the
method of preparation of the DuPont Permaphases in which
the organic group may be octadecyl, ν-glycidoxypropyl ("ether")
or a quaternary ammonium group.   The siloxane linkages again
offer good hydrolytic stability on these supports .

According to the review by Majors[32] the use of di- and
trichloro- or ethoxyoctadecylsilanes for the preparation of
bonded phases is being replaced by the monochloro- and mono-
ethoxydimethyloctadecylsilane reactions because the former
can react with one or two hydroxyl groups and are subject to
polymerization reactions giving rise to polymerized bonded
phases.   The advantage of monochloro- or monoalkyoxysilane
reagents like trimethylchlorosilane (TMS) or phenyldimethyl-
chlorosilane (PDS) is that their reaction ensures a reproduc-
ible monolayer coverage.   Furthermore, the monomeric (bristle)
phases may have faster solute mass transfer kinetics and
hence have superior column performance.   The surface coverage
of silanol groups is a maximum for trimethylchlorosilane of
around $48\mu mol/m^2$ whereas the concentration of Si-OH groups is
around $9\mu mol/m^2$.   Although even under the most exhaustive
silanization only about 55% of silanol groups can be
derivatized.[51,52]   The work of Unger et al.[51] has also shown
that there is no difference in behaviour between the bonded
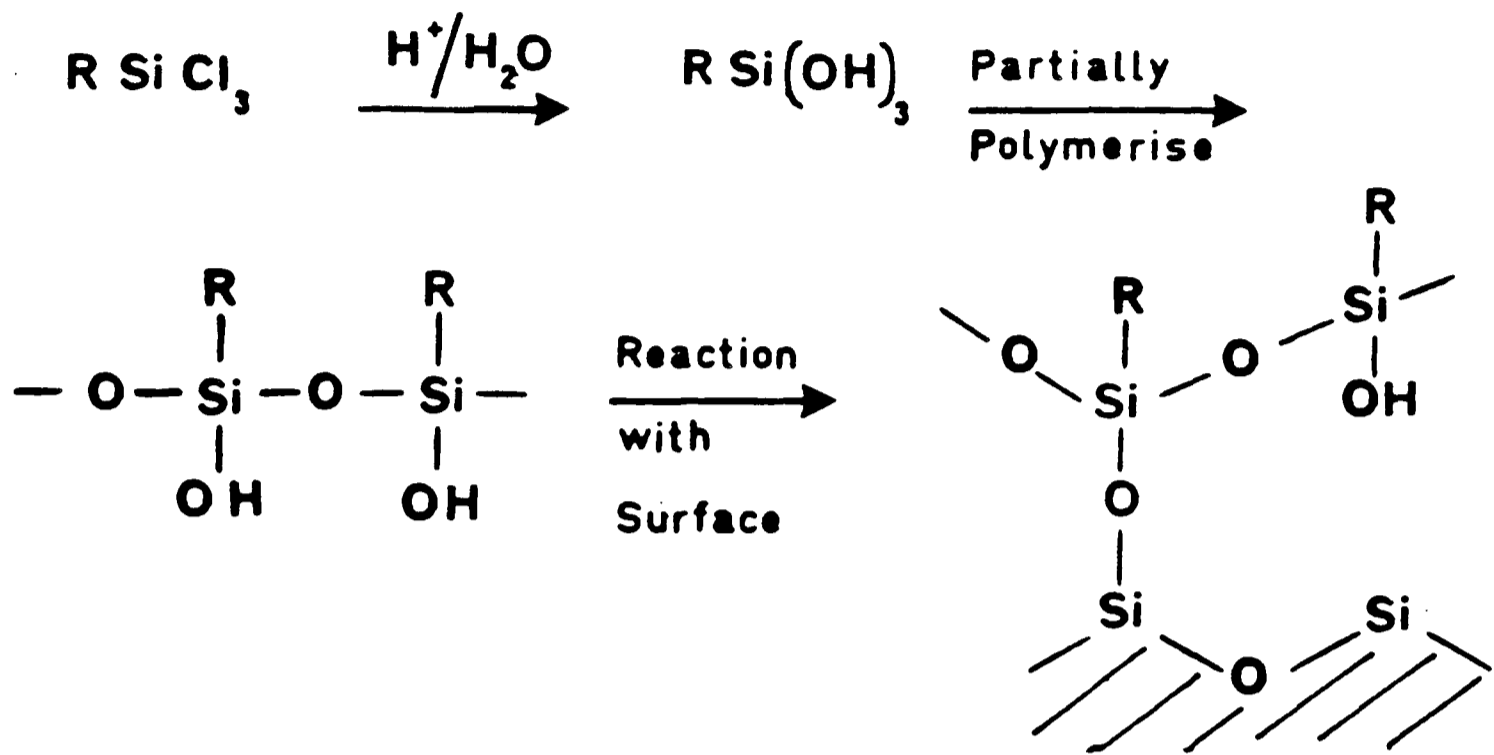
FIG.1.4-5: FORMATION OF BONDED POLYMERIC STATIONARY PHASE

short chain n-alkane packings and ODS types.   The prepara-
tion and characterization of chemically bonded stationary
phases has been the subject of a number of studies[45,53,54]
and recent reviews.[54-56]

(iii) <u>Reactions involving Grignard and Organo-lithium</u>
      <u>Reagents</u>

Organic groups can be bonded to the surface of silica via
direct Si-C bonds, by reaction of thionyl chloride with
Grignard or organolithium reagents.[48-50]   (Figure 1.4-6).
These supports also possess good hydrolytic stability.

The present success of reversed-phase liquid chromato-
graphy (RPLC) entirely relies on the performance achievable
with columns packed with chemically bonded phases.   These
reversed-phase materials still do not behave in a totally
hydrophobic manner because their hydrophobic character
depends on the type of n-alkyl chain bonded and on the surface
coverage.   This can be observed in the chemical instability
of reversed-phase packings in aqueous eluents which can be
attributed to the reactivity of siloxane groups anchoring the
alkyl group and to the presence of residual silanol groups.
Some improvements have been made in improving the stability
of silica-based packings, mainly by "protecting" the surface
with polymeric phase or high surface coverage or by the use
of precolumns which saturate the mobile phase with dissolved
silica or bonded phase.   Atwood <u>et al.</u>[57] presaturated the
mobile phase with silicates which, therefore, permitted high
pH values to be used at least for short periods of time.
One cannot neglect the known solubility of silica in water and
the liability of the siloxane bonds to basic hydrolysis.
Whenever silica-based packings are used at high pHs, high
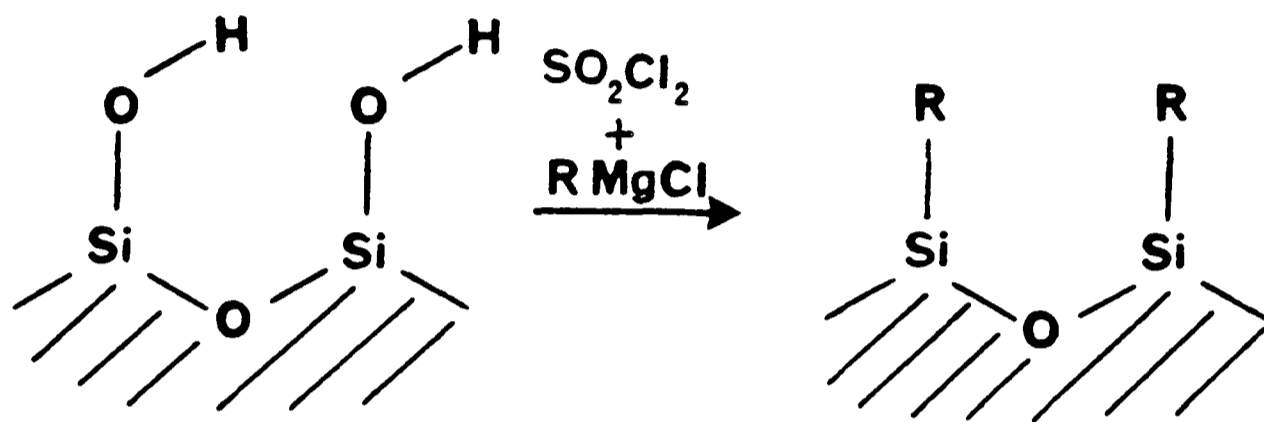
FIG.1.4 - 6 : ALKYLATION OF GRIGNARD REAGENT

buffer strengths, in the presence of tetraalkylammonium salts and at elevated temperatures, shortened column lifetimes will have to be accepted. Increasing attention has, therefore, been devoted to the development of non-polar adsorbents exhibiting an improved pH stability over the alkyl-bonded silica material.

The survey of modern HPLC materials just given highlights some of the disadvantages of existing materials, in particular, the hydrolytic unstability of bonded silicas. There is, therefore, a need for chemically stable and physically robust materials specially reversed-phase materials which is only particularly met by the new polymeric packings.

A carbon which could be used in LC especially in a graphitized form offers a possible alternative, but formidable difficulties exist in producing such a material to a state where it can be used effectively in LC. This thesis is concerned with meeting this challenge.

CHAPTER 1

REFERENCES

1a. Molnar, I. and Horvath, C, Clin.Chem., 22 (1976) 1497.

1b. Tiselius, A., Kolloid.-Z., 105 (1943) 101.

2. Knox, J.H. and Gilbert, M.T., UK Patent No.7939449,
    U.S. Patent No. 4,263,268, Fed.Rep.Germany P2946688-4.

3. Tswett, M., Proc. Warsaw Soc.Nat.Sci (Bio) 14 (1903) No.6.

4. Kuhn, R. and Lederer, E., Naturwiss, 19 (1931) 306.

5. Reichstein, T. and Van Euw, .Helv.Chim.Acta, 21 (1938)
    1197.

6. Wilson, J.N., J.Am.Chem.Soc., 62 (1940) 1583.

7. Martin, A.J.P. and Synge, R.L.M., Biochem.J., 35 (1941)
    1358.

8. De Vault, D., J.Am.Chem.Soc., 65 (1943) 532.

9. Weiss, J., J.Chem.Soc., (1943) 297.

10. Walter, J.E., J.Chem.Phys., 13 (1945) 332.

11. Sillen, L.G., Arkiv.Kemi.Mineral Geol., A22, No.15
    (1946); Nature, 166 (1950) 722.

12. Thomas, H.C., J.Am.Chem.Soc., 66 (1944) 1664;
    Ann.N.Y. Acad.Sci., 49 (1948) 161.

13. Boyd, G.E., Myers, L.S. and Adamson, A.W., J.Am.Chem.
    Soc., 69 (1947) 2849.

14. Lapidus, L. and Amundson, N.R., J.Phys.Chem., 56 (1952)
    984.

15. James, A.T. and Martin, A.J.P., Biochem.J., 50 (1952) 679.

16. Giddings, J.C. and Eyring, H., J.Phys.Chem., 59 (1955)
    416.

17. van Deemter, J.J., Zuiderweg, F.J. and Klinkenberg, A., Chem.Eng.Sci., 5 (1956) 271.

18. Giddings, J.C., J.Chem.Phys., 26 (1957) 1755.

19. Golay, M.J.E. in Gas Chromatography, 1958; D.H. Desty, ed., Academic Press, New York, 1958, p.36.

20. Giddings, J.C., J.Chem.Phys., 31 (1959) 1462.

21. Giddings, J.C. in Dynamics of Chromatography, Part I, Marcel Dekker, Inc., New York, N.Y., 1965.

22. Snyder, L.R. and Kirkland, J.J. in Introduction to Modern Liquid Chromatography, John Wiley, New York, 1974.

23. Knox, J.H. in High Performance Liquid Chromatography, Edinburgh University Press, Edinburgh, 1980.

24. Kennedy, G.J. and Knox, J.H., J.Chr.Sci., 10 (1972) 549.

25. Knox, J.H. and Vasvari, G., J.Chr., 83 (1973) 181.

26. Knox, J.H. and Pryde, A., J.Chr., 112 (1975) 171.

27. Howard, G.A. and Martin, A.J.P., Biochem.J., 56 (1950) 532.

28. Henry, R.A. and Schmidt, J.A., Chromatographia, 3 (1970) 116.

29. Cooper, M.J. and Anders, R.W., Anal.Chem., 46 (1974) 1849.

30. Morozowich, W. and Douglas, S.L., Prostaglandins, 10 (1975) 19.

31. Fitzpatrick, F.A., Anal.Chem., 48 (1976) 499.

32. Majors, R.E., J. Chr.Science, 18 (1980) 488.

33. Kirkland, J.J., Anal.Chem., 40 (1968) 391.

34. Snyder, L.R. and Poppe, H., J. Chromatogr., 184 (1980) 363.

35. Cohn, W.E., J.Amer.Chem.Soc., 72 (1950) 1471.

36. Cohn, W.E. and Bollum, F.J., Biochem.Biophys.Acta, 48 (1961) 588.

37. Volkin, E., Kitym, J.X. and Cohn, W.B., Jacs, 73 (1951) 1533.

38. Anderson, N.G., Green, J.G., Barber, M.L., and Ladd, F.C., Sr., Anal.Biochem., 6 (1963) 153.

39. Horvath, C.G., Preiss, B.A. and Lipsky, S.R., Anal.Chem., 39 (1967) 1422.

40. Endres, H., and Hörmann, H., Angew.Chem.Internat.Ed., 2 (1963) 254.

41. Halasz, I. and Sebestian, I., Angew.Chem.Internat.Ed., 8 (1969) 453.

42. Su, S.C., Hartkopf, A.V. and Karger, B.L., J.Chr. 119 (1976) 523.

43. Majors, R.E. and Hopper, M.J., J.Chr.Science, 12 (1974) 767.

44. Kirkland, J.J., Chromatographia, 8 (1975) 661.

45. Kirkland, J.J., Chromatographia, 12 (1975) 661.

46. Kirkland, J.J. and Yates, P.C., US Patent 3,722,181 March 1973.

47. Kirkland, J.J., J.Chr.Sci., 9 (1971) 206.

48. Locke, D.C., Schmermund, J.T. and Banner, B., Anal. Chem., 44 (1972) 90.

49. Sebestian, I. and Halasz, I., Chromatographia, 7 (1974) 371.

50. Saunders, D.H., Barford, R.A., Magidman, P., Olzewski, L.Y., Rothbart, H.L., Anal.Chem., 46 (1974) 834.

51. Unger, K.K., Becker, N. and Roumeliotis, P., J.Chr., 125 (1976) 115.

52. Colin, H. and Guiochon, G., J.Chr., 141 (1977) 289.

53. Scott, R.P.W. and Kucera, P., Chromatographia, 142 (1977) 213.

54. Grushka, E. and Kikta, E.J., Jr., Anal.Chem., 49 (1977) 1004A.

55. Cox, G.B., J.Chr.Sci., 15 (1977) 385.

56. Atwood, A.G., Schmidt, G.J. and Slavin, W., J.Chr., 171 (1979) 109.

CHAPTER 2

PRINCIPLES OF LIQUID CHROMATOGRAPHY

2.1 Thermodynamics of Liquid Chromatography

When the molecules of a substance X to be separated
are introduced into the column they distribute themselves
between the mobile and stationary phases as noted in section
1.2.1. Giddings[1] has shown that it is an essential feature
of efficient chromatography that the ratio of the amount of
solute in the stationary phase and the amount of solute in
the mobile phase averaged over the band must be equal to the
equilibrium ratio.   When the molecules are in the mobile
phase they move at the speed of the mobile phase, u, but when
in the stationary phase they are static.   Thus the relative
band migration rate is given by:

$$R = \frac{\text{Speed of band}}{\text{Speed of mobile phase}}$$

$$= \frac{(\text{amount of X in mobile phase})}{(\text{amount of mobile and stationary phase})} = \frac{q_m}{q_s + q_m}$$

$$= \frac{1}{(1 + k')} \tag{2.1-1}$$

where $k' = \dfrac{(\text{amount of X in stationary phase})}{(\text{amount of X in mobile phase})}$

at equilibrium

$$= \frac{q_s}{q_m} \tag{2.1-2}$$

Because of the near-equilibrium assumption discussed
in section 2.2.5 q_s and q_m can be regarded as equilibrium

values and can be given as:

$$q_s = C_s V_s \qquad\qquad (2.1\text{-}3)$$

and $\qquad q_m = C_m V_m \qquad\qquad (2.1\text{-}4)$

where C_s, C_m are the equilibrium concentrations of the solute in the stationary and mobile phases and V_s, V_m are the volumes of the stationary and eluent phases. Thus:

$$k' = \frac{C_s V_s}{C_m V_m}$$

$$= \frac{K V_s}{V_m} \qquad\qquad (2.1\text{-}5)$$

where K is the distribution coefficient of the solute between the two phases.

When the separation of a pair of solutes X and Y is considered, the ratios of the distances between the points of injection and the zone centres depend on the thermodynamics of the system, that is, the nature of the mobile phase, the stationary phase or both. Quantitatively, separation is discussed in terms of resolution, which is defined as:

$$R_s = \frac{\Delta z}{4\sigma} \qquad\qquad (2.1\text{-}6)$$

where Δz is the distance between adjacent peak maxima and σ is the standard deviation of the Gaussian concentration profile generated by the dynamic column processes.

2.1.1 Thermodynamics of adsorption chromatography

According to Snyder[2] the adsorption of a polyatomic molecule X from solution in an eluent E can be represented by the following chemical reaction analogue.

$$X_m + nE_a \rightleftharpoons X_a + nE_m \qquad (2.1-7)$$

where subscripts m and a refer to the mobile and adsorbed phases respectively, n is the number of eluent molecules displaced by the adsorption of one solute molecule. For adsorption chromatography equation (2.1-5) can be written in terms of the weight of the adsorbent in the column, w, or by the surface area of the adsorbent, A, in the column.

That is,
$$k' = \frac{C_s' w}{C_m V_m}$$

$$= K_{ads} \cdot \frac{w}{V_m} \qquad (2.1-8)$$

and
$$k' = \frac{C_s'' A}{C_m V_m}$$

$$= K_a \frac{A}{V_m} \qquad (2.1-9)$$

where K_{ads} is generally called the adsorption coefficient (measured in $cm^3 g^{-1}$) and C_s' is the concentration of adsorbate in moles per unit weight or alternatively, where K_a is the superficial adsorption coefficient (measured in $cm^3 m^{-2}$) and

C_s'' is the adsorbate concentration in moles per unit area of adsorbent surface.

In LSC, there is a competition between solvent and sample molecules for the fixed 'active' sites on the surface.[3,4] The adsorption of sample molecules requires the desorption of solvent molecules to permit the accommodation of sample molecules on the surface. The capacity factor k' is, therefore, determined by the net energy of adsorption of sample molecules and the net energy of adsorption is given as the sum of interaction energies. The adsorption coefficient of a component between the mobile and stationary phases depends on the type of interaction forces, mainly on dispersion (non-polar) and on hydrogen bonding between the sample components, solvent and adsorbent, which will be dealt with in greater detail in Chapter 9.

2.1.1.1 Adsorption isotherm

The equilibrium relationship between adsorbed and non-adsorbed samples at a given temperature can be given by the adsorption isotherm. This is a plot of the concentration of solute in the adsorbed phase versus the concentration of solute in the nonadsorbed phase at a given temperature. Linearity of the plot is equivalent to a constant distribution coefficient, K, in the separation. Separations in which K is independent of sample concentration are referred to as linear isotherm separations; which for most chromatographic separations occur at low sample concentration. A non-linear sample isotherm affects both the shape of the sample band and the rate at which

they migrate through the bed. Three isotherm types may
be distinguished at low sample concentrations; linear, convex
and concave (see Figure 2.1-1) where the effect of isotherm
type on band shape is also shown. Adsorption chromato-
graphic separations have typical convex isotherms, indicating
that K decreases with increasing sample concentration. In
this situation, the symmetrical sample bands are described by
faster migration of high concentration portions of the band
resulting in a skewed elution band. Band asymmetry or
'tailing' in adsorption chromatography can be evidence of
isotherm non-linearity (slow desorption kinetics can also
lead to band tailing).

In the region of isotherm linearity, where the solute
concentration is small, the lateral interactions of each solute
molecule in the adsorbed phase will be with eluent molecules
only. For adsorption from a liquid phase the Langmuir
isotherm takes the form:

$$\theta = \frac{K_{th}N_x}{1+K_{th}N_x} \qquad \text{(liquid)} \qquad \text{(2.1-10)}$$

where θ is the fractional coverage of the adsorbent surface
by adsorbed X, K_{th} the thermodynamic equilibrium constant
(or relative adsorption affinity of X) for the adsorption
process and N_x the mole fraction of X in the unadsorbed phase.
The derivation of the Langmuir isotherm assumes a maximum of
single monolayer adsorption, equivalent sites and no inter-
actions between adjacent adsorbate molecules.

For low sample concentrations, $K_{th}N_x$ becomes small and
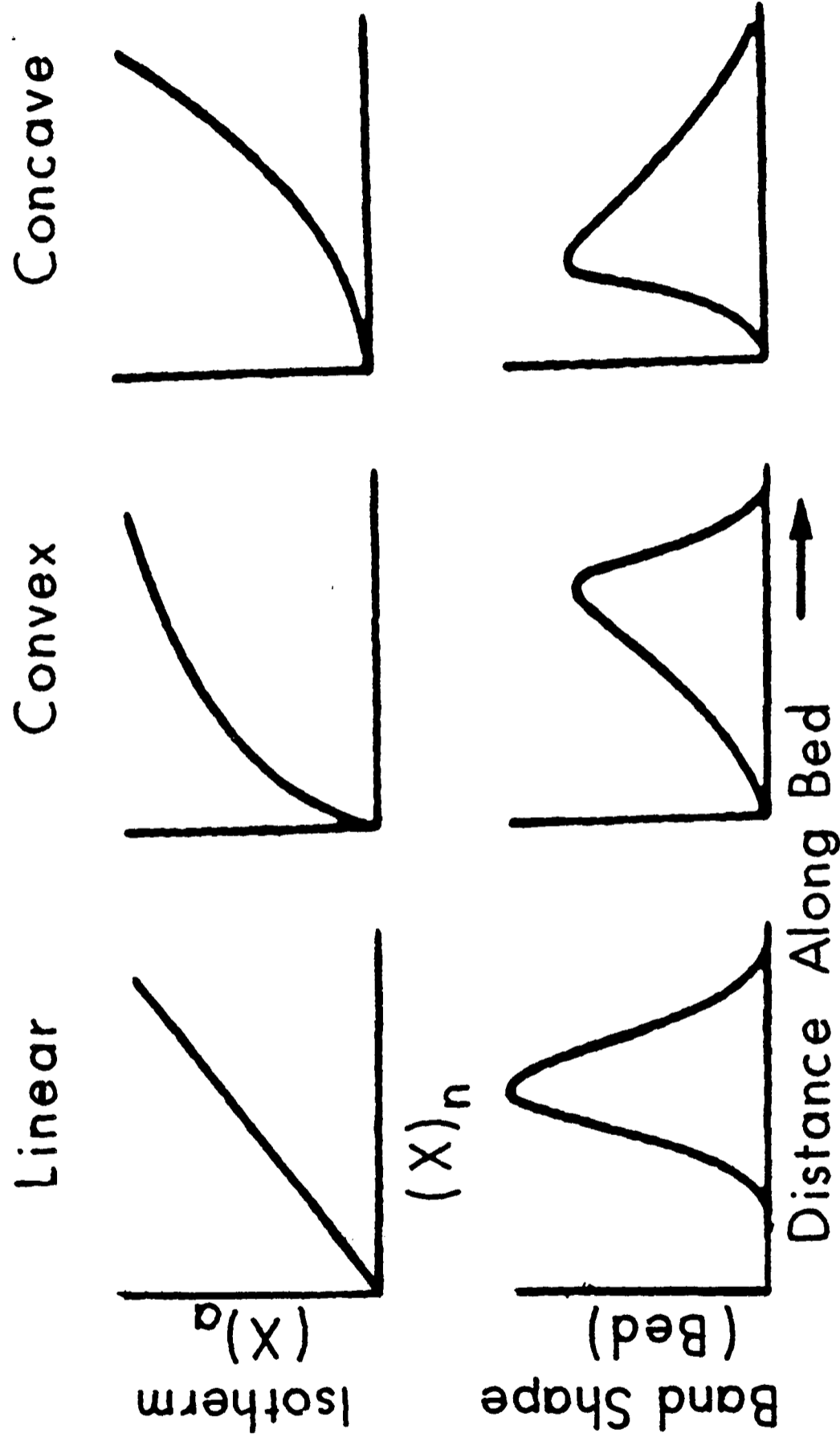
FIG. 2.1-1: ISOTHERM TYPES AND ITS EFFECT ON BAND SHAPE

equation (2.1-10) reduces to:

$$\frac{a}{N_x} = K_{th} \qquad (2.1-11)$$

that is, the sample distribution coefficient becomes constant at low sample concentrations. If the monolayer capacity (moles/gram) is defined as $N°$, equation (2.1-10) then can be rewritten as:

$$\frac{(X)_a}{N°} = \frac{K°(X)_u}{1+K°(X)_u} \qquad (2.1-12)$$

where $K°$ is the constant value of K at low sample concentrations.

Rearranging equation (2.1-12)

$$\frac{1}{(X)_a} = \frac{1}{N°} + \frac{1}{K_{th}N°(X)_u} \qquad (2.1-13)$$

For a Langmuir isotherm, a plot of $1/(X)_a$ versus $1/(X)_u$ will be linear, and the intercept of this plot on the $1/(X)_a$ axis is equal to $1/N°$.

Unfortunately, the major assumption of uniform sites does not often hold and the dependence of K on coverage can be severe even at near-zero coverage. It is, therefore, necessary to deactivate the active sites. In the case of carbon, an ideal material would have uniform sites.

2.1.2 Thermodynamics of partition chromatography

Liquid-liquid partition chromatography depends upon the

different distribution coefficient of the components of a
mixture between a stationary and a mobile phase which are
immiscible. The stationary phase is an inert packing
material coated with a polar (triethylene glycol) or non-
polar (squalane) stationary phase. The distribution
coefficient is related to the capacity factor, k', by:

$$k' = D\left(\frac{V_s}{V_m}\right) \qquad (2.1\text{-}14)$$

which is similar to equation (2.1-5).

Karger et al.[5] have derived the following equation,
which describes the distribution coefficient, D, of a solute,
i, between stationary and mobile phase.

$$\log D = \frac{V_i}{RT}\left[(\delta_i-\delta_m)^2-(\delta_i-\delta_s)^2\right] \qquad (2.1\text{-}15)$$

where V_i is the molar volume of the solute, i, and $\delta_i, \delta_s, \delta_m$
are the solubility parameters of the solute, stationary phase
and mobile phase.

The solubility parameters as defined by Hildebrand and
co-workers[6,7] are given by:

$$\delta_i = (\Delta H_{vap}/V_i)^{\frac{1}{2}} \qquad (2.1\text{-}16)$$

Combining equation (2.1-14) and (2.1-15) gives:

$$\ln k' = \ln\left(\frac{V_s}{V_m}\right) + \frac{V_i}{RT}\left[(\delta_i-\delta_m)^2-(\delta_i-\delta_s)^2\right] \qquad (2.1\text{-}17)$$

2.2   Kinetics of Liquid Chromatography

2.2.1   Introduction

As recognized in Chapter 1, Section 1.2.1, band or molecular dispersion is governed by kinetic considerations and is brought about by three rate processes, namely axial molecular diffusion, flow pattern effects and the finite rate of mass transfer processes within and between the mobile and stationary phases.   Figure 2.2-1[8a] gives an illustration of band dispersion during a chromatographic process, where the molecules of one compound C, represented by crosses, is considered.   At the injection point, the molecules are represented by a narrow line as in figure 2.2-1(A) but as these molecules move along the column they become spread over a wider portion of the column as shown in figure 2.2-1(B). Each of the three different rate processes will now be discussed separately.

2.2.1.1   Mass transfer processes

The rate of mass transfer within and between phases in chromatography may be controlled by either of two mechanisms. (i) Adsorption-desorption kinetic processes which may be single or multistep as can occur in adsorption chromatography and (ii) diffusion-controlled phase transfer kinetics which are important in partition chromatography and include mass transfer within the flowing part of the mobile phase, within the stagnant mobile phase and within the stationary phase.

A — Initial Band Width

B — Final Band Width — Eddy Diffusion
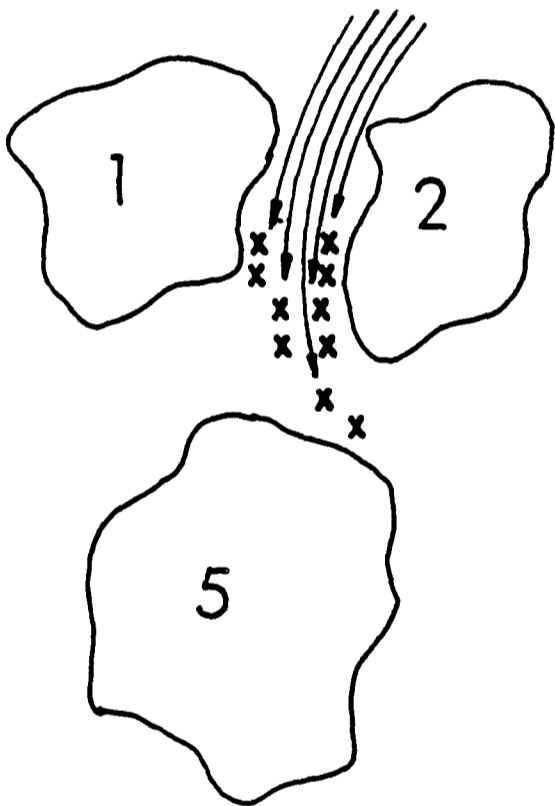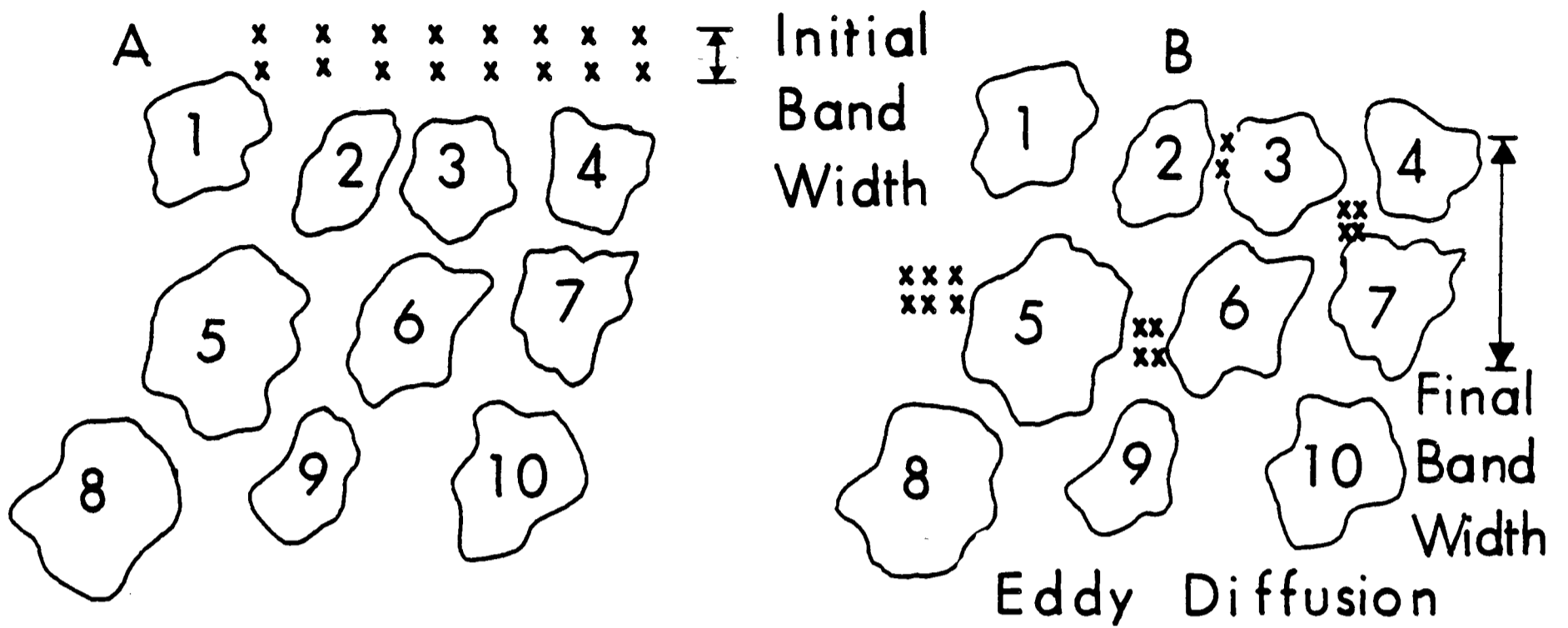
Mobile Phase Mass Transfer

C
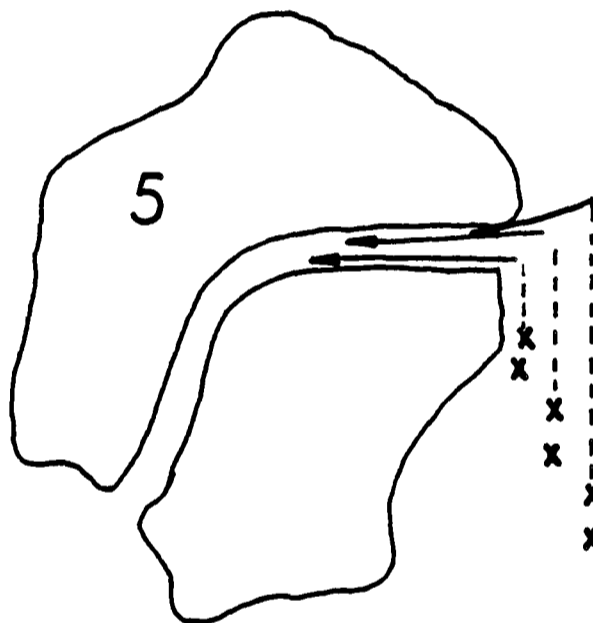
Stagnant Mobile Phase Transfer

D
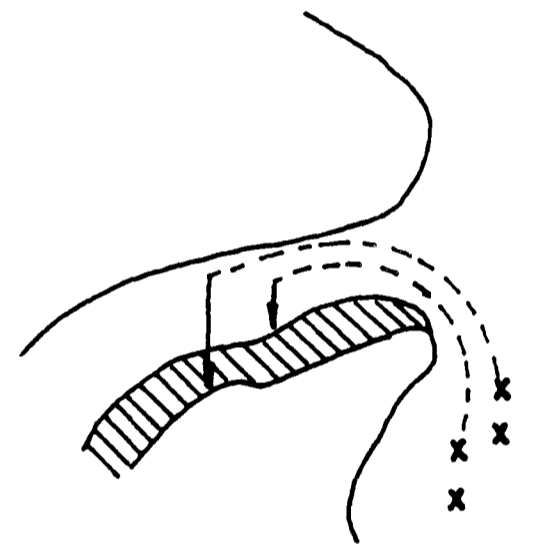
Stationary Phase Mass Transfer

E

FIG. 2.2-1 : KINETIC CONSIDERATIONS

Mobile phase mass transfer. In a single flow stream, different flow rates exist for different parts of that flow stream. Sample molecules in the centre of a flow stream move fastest and hence travel greater distances in a given time compared to molecules moving in a flow stream adjacent to a particle. This dispersive effect is reduced by diffusion of solute across the flow stream and by decrease of flow velocity. Figure 2.2-1(C) shows such a situation between particle 1 and 2.

Stagnant phase mass transfer. This type of contribution arises in the case of porous column packing particles. The mobile phase in the pores of these particles is stagnant. Molecules diffuse in and out of these pores to different depths of the pores. Molecules diffusing only a short distance into the pore diffuse back into the mobile phase quickly and, therefore, travel a greater distance down the column. Those molecules that diffuse further into the pore spend more time in the pore and less time in the mobile phase and, therefore, travel slowly down the column. This dispersive effect is reduced by increasing the diffusion rate or reducing flow velocity. Figure 2.2-1(D) illustrates stagnant phase mass transfer where the pore of a single particle 5 is shown.

Stationary phase mass transfer. Molecules penetrate to different depths of the stationary phase. Those molecules which penetrate deep into the stationary phase travel slowly through the column as compared to those molecules which spend only a little time in the stationary phase. This is shown in

figure 2.2-1(E).   Fast diffusion or low flow rate reduces
this form of dispersion.

2.2.1.2   Axial molecular diffusion

Molecular diffusion in the flow or longitudinal direction
contributes most at low or very low velocities.   Its contri-
bution to spreading can be calculated in terms of diffusion
coefficients and a structural parameter, γ, with a value near
unity.   The theory of γ has been discussed by Knox and
McLaren.[8b]

2.2.1.3   Flow pattern effects

Flow pattern effects include channelling (and other
effects of packing inhomogeneity) and was termed the 'Eddy
Diffusion' term by van Deemter et al.[8c]   This is represented
in figure 2.2-1(B).   Different solvent flow streams exist
within the column of a LC system.   Sample molecules, there-
fore, take different paths through the packed bed.   Molecules
following narrow paths as paths between particles 2 and 3
travel much more slowly as compared with molecules taking
wider paths as between particles 5 and 6.   This is essentially
a geometrical effect but is reduced by transverse diffusion
in the mobile phase as discussed above.

2.2.2   Theoretical plate model

As discussed earlier in Section 2.2 solutes injected at
the top of the column are subjected to zone or band spreading
as they progress through the column.   In 1941, Martin and
Synge[9] were the first to introduce the band dispersion

parameter, which is called the height equivalent to a theoretical plate or H, to characterize chromatographic zone spreading and thus resolution. Following Martin and Synge the plate height may be defined as "the thickness of the layer such that the solution issuing from it is in equilibrium with the mean concentration of solute in the nonmobile phase throughout the layer". The theoretical plate model was introduced into chromatography because of its effectiveness in describing the distillation procedures. It was the first model to describe the development of a solute concentration profile under the conditions of non-equilibrium processes and when the isotherm was linear.

The model, therefore, pictures a discontinuous concentration profile of the solute distributed in plates. According to Keulemans[10] a chromatographic column in the plate model is likened to a Craig distribution apparatus consisting of a series of interconnected but distinct bed sections or theoretical plates. Passage of solvent through the bed is visualized to take place in steps as in the operation of the Craig apparatus. In each step the solvent (plus any un-adsorbed sample) in plates N_0, N_1, N_2, etc shifts over to the next higher number plate and fresh solvent enters plate N_0, equilibrium taking place at each step according to the distribution coefficient (see Table 2.2-1[8a] and figure 2.2-2[8a]). Mathematically, the distribution of X on the adsorbent bed is given by the successive terms of the binomial expansion $(x+y)^n$ where n is the number of solvent transfers that have taken place. As shown in figure 2.2-2, as X moves down

Table 2.2-1   (from reference 8a)

Migration of Sample X in Craig Distribution Model

Transfer number	Total amount of X in each plate after solvent transfer						Amount of X tranferred from each plate during following transfer					
	N_0	N_1	N_2	N_3	N_4	N_5	N_0	N_1	N_2	N_3	N_4	N_5
0	1	0	0	0	0	0	1/2	0	0	0	0	0
1	1/2	1/2	0	0	0	0	1/4	1/4	0	0	0	0
2	1/4	2/4	1/4	0	0	0	1/8	1/4	1/8	0	0	0
3	1/8	3/8	3/8	1/8	0	0	1/16	3/16	3/16	1/16	0	0
4	1/16	4/16	6/16	4/16	1/16	0	1/32	1/8	3/16	1/8	1/32	0
5	1/32	5/32	10/32	10/32	5/32	1/32	1/64	5/64	5/32	5/32	5/64	1/64
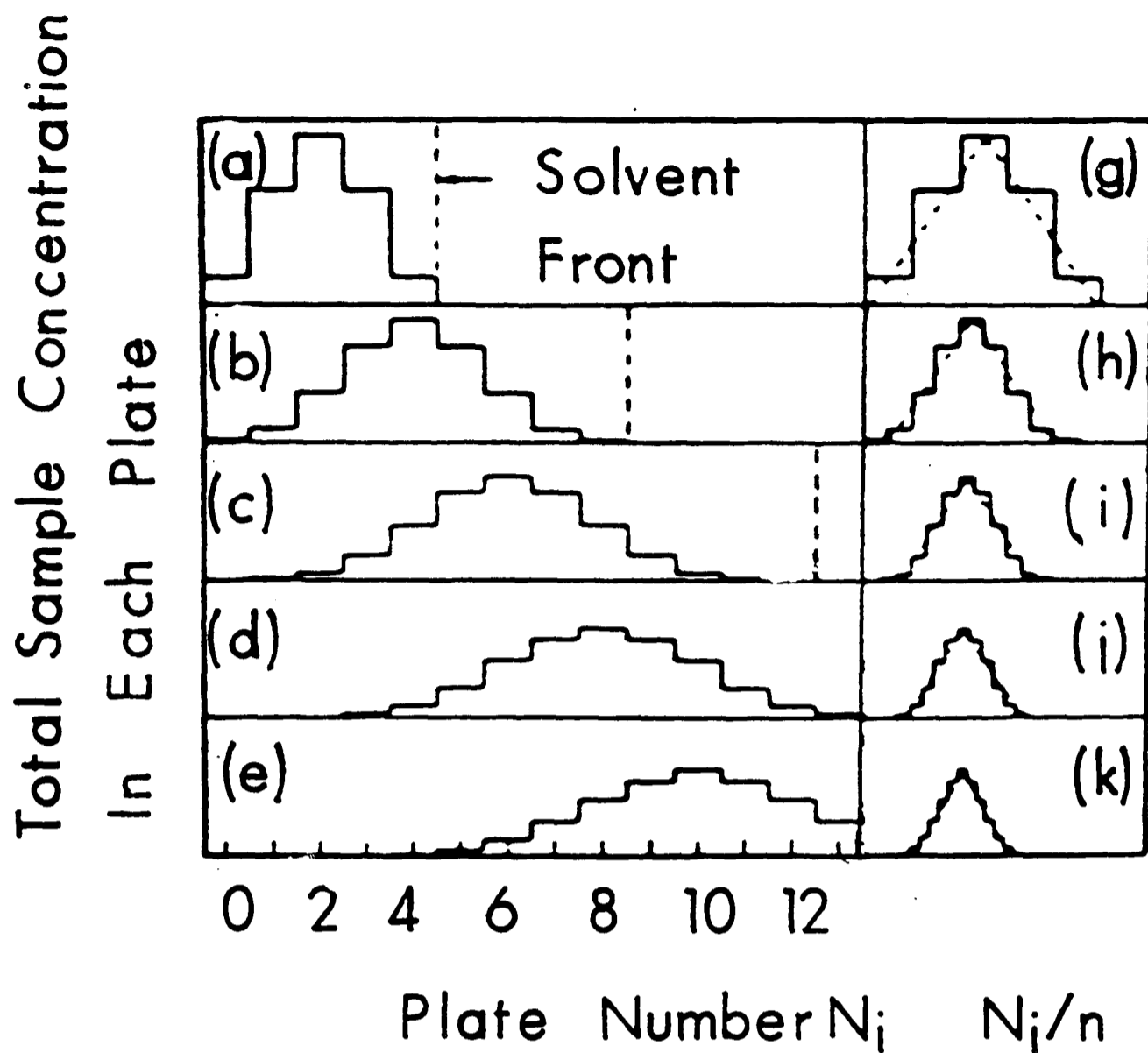
FIG. 2.2 - 2: DISTRIBUTION OF SAMPLE ON THE ADSORBENT BED AFTER VARYING DEGREES OF SOLVENT TRANSFER, ACCORDING TO THE CRAIG DISTRIBUTION MODEL: (a,g) 4 TRANSFERS; (b,h) 8 TRANSFERS; (c,i) 12 TRANFERS; (e,k) 20 TRANSFERS (from Ref. 8a)

the adsorbent bed, for large values of n, a symmetrical concentration distribution converging to a Gaussian distribution is formed (figure 2.2-3).

The band width can be defined by the standard deviation σ of the Gaussian curve and this is found to be equal to $\sqrt{HL}$ where H is the plate height and L is the distance migrated by the centre of the zone. One useful prediction of the model is that the zone width, proportional to σ, increases with the square root of the zone migration distance L. Therefore, the plate height for a uniform column may be defined as:

$$H = \frac{\sigma^2}{L} \qquad (2.2-1)$$

In a nonuniform column where concentration and velocity gradients exist the plate height is then the increment in the variance σ^2 per unit length of migration.

$$H = \frac{d\sigma^2}{dL} \qquad (2.2-2)$$

Giddings[1] has criticized the theory for the irrelevance to the details of kinetic phenomena of the chromatographic process, the assumption of plate wide equilibrium and the discrete nature of the plates. Its failure to allow for longitudinal diffusion effects has also been criticized.

2.2.3 <u>Random walk model</u>

Chromatographic migration can be described in terms of the simple random walk model to account for molecular
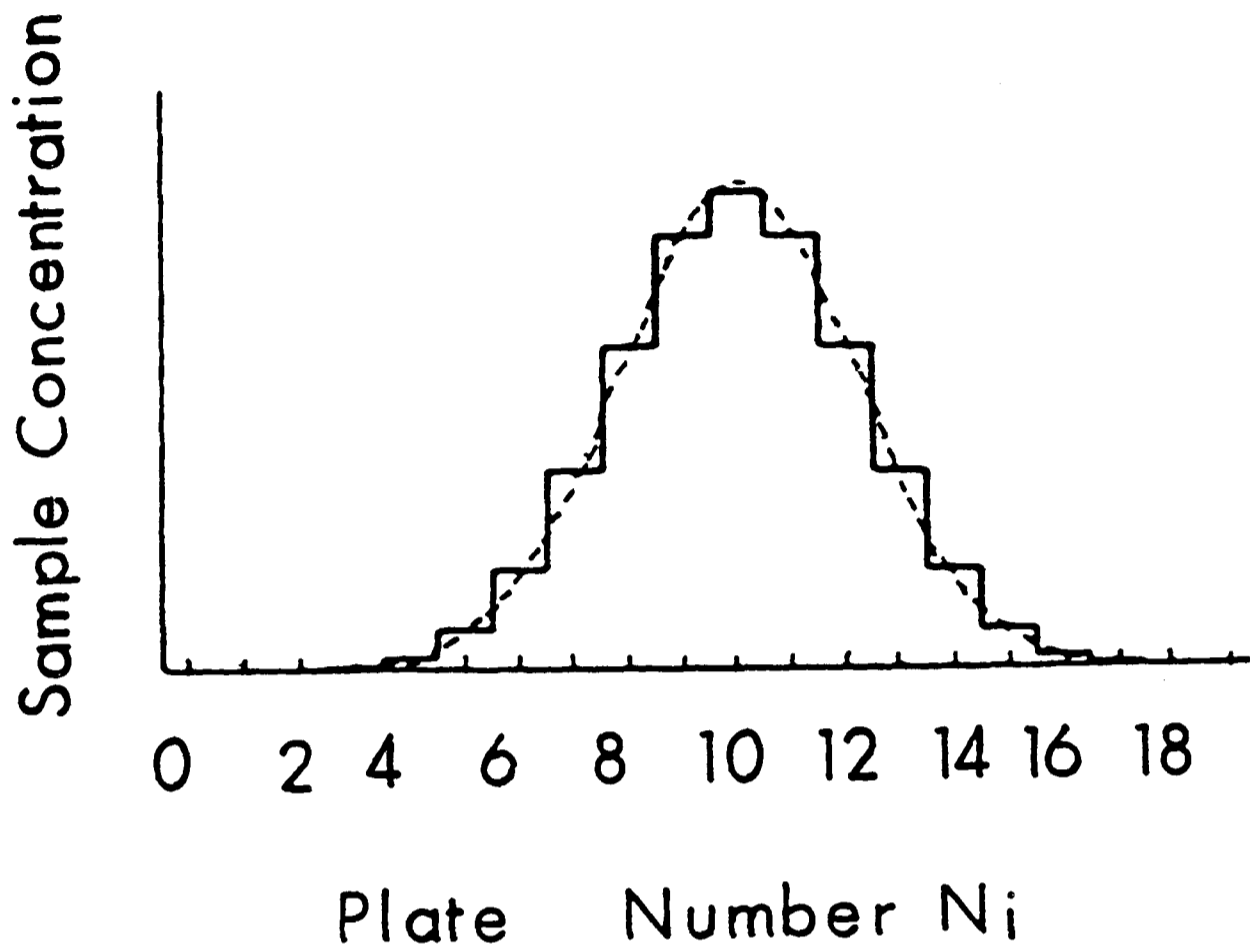
FIG. 2.2 - 3: APPROACH OF BAND SHAPE
TO A GAUSSIAN DISTRIBUTION.
SOLID LINE, CRAIG DISTRIBUTION
MODEL AFTER 20 TRANSFERS
(R = 0.5); DASHED LINE,
GAUSSIAN CURVE (from Ref. 8a)

displacement. The model provides the simplest and most direct calculation of the effects of dynamic molecular processes on zone structure. If a large number of molecules were started at a given origin, the operation of a many step-random walk would lead to their dispersion. The standard deviation (or quarter width) σ of the resulting Gaussian concentration is simply:

$$\sigma = \ell\sqrt{n} \qquad\qquad (2.2\text{-}3)$$

where ℓ is the fixed step length and n, the number of steps taken.

In terms of variance:

$$\sigma^2 = \ell^2 n \qquad\qquad (2.2\text{-}4)$$

for any number of simultaneous random processes such as those occurring in a chromatographic system:

$$\sigma^2 = \sigma_1^2 + \sigma_2^2 + \sigma_3^2 + \ldots \qquad\qquad (2.2\text{-}5)$$

A combination of equation (2.2-4), which gives σ^2 for each individual random process, and equation (2.2-5), which shows how the σ^2 of component processes adds together to form the final chromatographic zone, is sufficient for a quantitative treatment. Einstein's[11] equation relating σ^2 to the diffusion coefficient D is:

$$\sigma^2 = 2Dt_D \qquad\qquad (2.2\text{-}6)$$

where t_D is the time period over which diffusion occurs. The equation can replace equation (2.2-3) for the calculation of σ^2 values arising from molecular diffusion. To estimate the 'average' time which a molecule needs to diffuse a distance d from its starting point, d_t, may be equal to σ. The time required would then be obtained from equation (2.2-6) as:

$$t_D = \frac{d^2}{2D} \qquad\qquad (2.2-7)$$

where t_D is the time spent by solute molecules through the distance, L.

2.2.3.1 Longitudinal molecular diffusion

Equation (2.2-6) can now be used in terms of random processes to calculate the contribution to the plate height made by molecular diffusion. Consider solute molecules travelling in the mobile phase with the average mobile phase velocity v,

$$\text{then} \qquad t_m = \frac{L}{v} \qquad\qquad (2.2-8)$$

where t_m is the column dead time, that is, the average time for the passage of inert, nonsorbing molecules to position L. Using equation (2.2-6):

$$\sigma^2 = 2D_m t_m$$

$$= 2D_m \frac{L}{v} \qquad\qquad (2.2-9)$$

where D_m is the diffusion coefficient in the mobile fluid. The actual distance diffused is reduced due to tortuous and constricted nature of the path, thus the obstructive factor γ,[12,13] slightly less than unity (about 0.6) is applicable in packed columns.

Thus
$$\sigma^2 = 2\gamma D_m \frac{L}{v} \qquad (2.2-10)$$

Using equation (2.2-1)

$$H = \frac{\sigma^2}{L}$$

$$= \frac{2\gamma D_m}{v} \qquad (2.2-11)$$

Equation (2.2-11) represents the contribution to plate height due to molecular diffusion by random processes.

Under some circumstances, longitudinal diffusion in the stationary phase can also contribute to the plate height.

Then
$$\sigma^2 = 2D_s t_s \qquad (2.2-12)$$

where D_s is the diffusion coefficient of solute in the stationary phase and t_s is the time spent in the stationary phase. Using Le Rosen's equation[14]

$$\frac{t_s}{t_m} = \frac{1-R}{R} = k' \qquad (2.2-13)$$

where R is the equilibrium fraction of solute in the mobile phase and is equal to 1/1+k'.

Then substituting equation (2.2-13) into equation (2.2-12)

$$\sigma^2 = \frac{2D_s t_m (1-R)}{R} \qquad (2.2-14)$$

And using equations (2.2-8) and (2.2-1)

$$t_m = \frac{L}{v}$$

and $\quad H = \dfrac{\sigma^2}{L}$

then $\quad H = \dfrac{2\gamma_s D_s}{v} \dfrac{(1-R)}{R} \qquad (2.2-15)$

Longitudinal molecular diffusion, therefore, gives a contribution inversely proportional to the flow velocity which can be abbreviated as B/v where B is a constant related to the diffusivity of the solute.

2.2.3.2 Adsorption-desorption kinetics

This process is an abrupt molecular process and involves sites with different adsorption energies. Molecular desorption occurs if and only if they possess sufficient activation energy to cause the necessary rearrangement of rupture of chemical or physical bonding. Solute molecules adsorb and desorb in accordance with the law of first order kinetics; the rate of the process is proportional to the total number of molecules able to react. For each process there is a rate constant or transition rate, k, which is the constant of proportionality in the rate law and represents the fraction

of the available molecules reacting in one second.
That is,

$$- \frac{dc}{dt} = k_c \qquad (2.2-16)$$

If k_d is the mean desorption rate and k_a is the mean
adsorption rate
Then

$$t_d = \frac{1}{k_a} \qquad (2.2-17)$$

$$\text{and} \quad t_a = \frac{1}{k_d} \qquad (2.2-18)$$

where t_d and t_a are the mean desorption and adsorption time
respectively.

During the migration of a chromatographic zone, adsorp-
tion and desorption occur frequently at random.
There is a transfer of activating energy in and out of the
molecular bonds.   A desorption process is seen as a random
step forward, allowing mobility of the molecules in the
mobile phase and an adsorption process is seen as a random
step backwards retarding the movement of molecules.   The
total number of random steps, therefore, involved during
zone migration through the distance L would be the number of
forward steps plus the number of backward steps which is
equal to twice the number of adsorptions as each adsorption
is followed by desorption.

If t_a is the time a molecule remains in the mobile phase
moving with mean flow velocity, v , before being adsorbed.
Then, distance (segment) covered before adsorption

$$= vt_a$$

Number of segments to reach distance L

$$= \frac{L}{v t_a}$$

= number of adsorptions

Number of random walk steps is

$$n = 2 \times \text{number of adsorptions}$$

$$= \frac{2L}{v t_a} \qquad (2.2\text{-}19)$$

On the other hand, in the same period, t_a, the zone centre is also moving.   The zone migrates only a fraction R as fast as the free molecule.

∴. Advance in time by the zone

$$= R v t_a$$

Relative Displacement or step length of molecule

$$= v t_a - R v t_a$$

$$\text{or} \quad \ell = (1-R) v t_a$$

Using equations (2.2-4) and (2.2-19)

Then

$$\sigma^2 = (1-R)^2 v^2 t_a^2 \times \frac{2L}{v t_a}$$

$$= (1-R)^2 v t_a L$$

Using equation (2.2-1)

$$H = 2(1-R)^2 vt_a \qquad (2.2\text{-}20)$$

In terms of mean desorption time

$$\frac{t_a}{t_d} = \frac{R}{1-R}$$

$$H = 2R(1-R)vt_d \qquad (2.2\text{-}21)$$

Equation (2.2-21) is an important equation. It applies to both heterogenous and uniform surfaces. The plate height contribution due to kinetic or non-equilibrium effects is proportional to the flow velocity, v, t_a or t_d, the time necessary to make a transition between the mobile and stationary phases (therefore, it is necessary to increase the rate of transition) and it is also proportional to $R(1-R)$, a quantity which acquires a maximum at $R=\frac{1}{2}$ and is relatively small near the extremes where $R=0$ and $R=1$.

2.2.3.3 Diffusion-controlled sorption-desorption kinetics

This type of phenomenon is important in the partition systems (gas liquid or liquid-liquid) where a bulk stationary phase exists and a change occurs gradually as molecules diffuse in and out of localized regions. The simple random walk process is similar to that of adsorption-desorption kinetics and equation (2.2-21) is applicable which gives the plate height, H, in terms of R, v and the mean desorption time, t_a; the only difference being that the rate of release

by diffusion is controlled by the diffusion coefficient while the desorption from surfaces is controlled by the rate constant k_d.

Using equation

$$t_D = \frac{d^2}{2D_s} \qquad (2.2-22)$$

where D_s is the diffusion coefficient for solute in the stationary phase and d, the distance diffused. When substituted into equation (2.2-21) the plate height contribution is found to be:

$$H = 2R (1-R)d^2 v/D_s \qquad (2.2-23)$$

In equation (2.2-21) H is reduced by increasing sorption and desorption rates (decreasing t_d). In this case, however, the increased rate is affected by reducing d to its absolute minimum; that is, the stationary liquid should be dispersed in very small units. It is also desirable to choose liquids with large D_s.

2.2.3.4 Diffusion in the mobile phase

The nature of this diffusion is more complicated than that in the stationary phase. Only recently has it been possible to account quantitatively for some of the major components of zone spreading caused by these diffusion processes.[15,16] According to Giddings[17] velocity inequalities which lead to zone spreading originate within the mobile phase in the following ways:

a. Transchannel Contribution, where a high velocity exists in the centre of a flow system, and a low velocity near the walls and diffusion leads to the exchange of molecules between these regions.

b. Transparticle Effect. The existence of stagnant mobile phase in porous supports which is surrounded by mobile fluid in a state of motion. The interchange through the stagnant mobile phase gives rise to transparticle effect, seen in partition chromatography.

c. Short-range interchannel Effect. In a packed bed, small tightly packed regions are joined together by a rather loosely filled space composed of large channels. A significant velocity differential occurs between the large open channels and the smaller surrounding ones.

d. Long-range interchannel Effect. Throughout a given cross-section of the column no single undulation of the pattern could be exactly repeated, thereby giving rise to variations in the average velocity within each undulation or repeating flow unit. The diffusion back and forth among these units leads to a long-range interchannel effect.

e. Transcolumn Diffusion. Velocity differences are found to exist between the outer regions (influence of wall on packing density) and the centre of the column (due to bending of a column) or between one outer region and another. Transfer of solute molecules between velocity extremes must occur through diffusion on a column-wide scale.

Employing the random walk model, the contribution to plate height by these processes is given by:

$$H = \frac{w_i d_p{}^2 v}{D_m} \qquad (2.2\text{-}24)$$

where $w_i = \frac{w_\alpha^2 w_\beta^2}{2}$ and w_α and w_β depends on the particle effect categorized above.

$$w_\alpha = \frac{S}{\bar{d}p} \qquad (2.2\text{-}25)$$

where S is the distance a molecule must diffuse to reach one extreme from another

$$\text{and} \quad w_\beta = \frac{\Delta v}{v} \qquad (2.2\text{-}26)$$

where Δv is the difference between the extreme and the mean velocity, v.

The values of w_α, w_β and w_i have been tabulated for all the five effects in table 2.2-2. It is very difficult to generalize transcolumn effects. For straight columns, transcolumn inhomogeneity is due to size separation effect where larger support particles settle near the outside, allowing greater permeability and increased flow rate. Smaller particles settle near the centre.[18,19] In addition, there is the wall effect[20] due to the narrow gap between the wall and adjacent particles. Generally, the velocity near the outside is 10% greater than the average, and that near the centre is 10% or so less. The bending or coiling of a chromatographic column can also lead to transcolumn effect[21] common in GC. A molecule near the inside bend is progressing more rapidly than its outside counterpart because its path is shorter, its velocity is greater (this results from larger pressure

Table 2.2-2

Approximate magnitude of the parameters w_i, Λ_i and $v_{\frac{1}{2}}$.

Type of Velocity Inequality	w_i	λ_i	$v_{\frac{1}{2}}=2\lambda_i/w_i$
1. Transchannel	0.01	0.5	10^2
2. Transparticle	0.1	10^4	2×10^5
3. Short-range interchannel	0.5	0.5	2
4. Long-range interchannel	2	0.1	0.1
5a. Transcolumn	0.02-10	0.4-200	40
5b. Transcolumn (coiled)	$0-10^2$	$0-10^3$	40

gradient which is a consequence of the total column pressure drop being distributed over a shorter path). Therefore, in transcolumn effects, H should be expressed in terms of column diameter (or radius) and not particle diameter.

Hence

$$H = 0.004 r_c^2 v / D_m \qquad (2.2-27)$$

where r_c is the tube radius.

For transcolumn variation in permeability

$$H = 8 r_c^4 \, v / R_o^2 \, D_m \qquad (2.2-28)$$

where R_o is the coil radius or radius of curvature of the bend.

2.2.3.5 Eddy diffusion

Eddy diffusion is the consequence of the same velocity inequalities.   A separate eddy diffusion term may be identified with each of the five categories of velocity inequalities and the plate height contribution would be:

$$H = w_\beta^2 w_\lambda dp \qquad (2.2-29)$$

where w_λ is a structural parameter, near unity.

For a given velocity inequality i,

$$H = 2 \lambda_i dp \qquad (2.2-30)$$

where $$\lambda_i = w_\beta^2 w_\lambda / 2 \qquad (2.2-31)$$

The various values of λ_i have also been tabulated in table 2.2-2.

The classical theory of eddy diffusion assumes that solute molecules follow fixed streampaths down the column and the eddy diffusion term will be a structural property. In fact, solute molecules frequently undergo lateral diffusion and can be carried into new flow channels and its path becomes highly segmented containing many random walk steps. Therefore, the assumption that H was the sum of the contributions from the flow mechanism, H_f, and from the diffusion mechanism, H_D, as in the classical theory of eddy diffusion, seems unjustified. The coupling theory of eddy diffusion developed by Giddings[17] gives H to be equal to:

$$H = \frac{1}{1/H_f + 1/H_D} \qquad (2.2-32)$$

in contrast with

$$H = H_f + H_D \quad \text{(classical theory} \qquad (2.2-33)$$
$$\text{eddy diffusion)}$$

An equation of this type applies to all categories of velocity inequality, thus yielding a summed expression[17,22] ΣH for the final plate height term.

$$H = \sum_i \frac{1}{\frac{1}{2}\lambda_i d_p + D_m/w_i v d_p^2} \qquad (2.2-34)$$

Dividing each side by d_p, and substituting for $d_p v/D_m = v$ we obtain

$$h = \sum_i \frac{1}{1/2\lambda_i + 1/w_i v} \qquad (2.2-35)$$

where h is the reduced plate height and ν the reduced

velocity. Also, the reduced transition velocity, which is

a dimensionless number dependent only on the structural

factors λ_i and w_i, and independent of diffusivity and mean

particle diameter, is given by:

$$\nu_{\frac{1}{2}} = 2\lambda_i / w_i \qquad (2.2-36)$$

If $\nu_{\frac{1}{2}}$ is determined for one mobile phase, its value will

be fixed in that column for any other possible mobile phases.

2.2.4 Rigorous Stochastic Theory

In predicting the random model, an arbitrary decision

must be made on what to take as the length and number of steps.

In addition, the model is based on a fixed number of steps for

all participating molecules which in sorption-desorption

kinetics, a variable number of steps are taken. The length

of step taken is also notoriously variable.

Giddings and Eyring[23] studied the random sorption-

desorption processes of chromatography and derived a rigorous

expression for the concentration profile of solute molecules

emerging from the end of the column in terms of probability,

density function or distribution function P. This stochastic

approach was derived for a single kind of adsorption site or

for any first order exchange process.

The approach assumes that there is a definite non-varying

constant, k_a, representing the probability per unit time that

the molecule will adsorb on the surface. This first order

rate constant is accompanied by a first-order desorption

constant k_d. The assumption that k_a and k_d are non-varying

constants, independent of time or of the molecules history

causes a departure from diffusion-controlled kinetics.

According to this rigorous approach, for a large number of

adsorptions and desorptions, if the molecule started its

migration in the mobile phase, its distribution function P

is then equal to:

$$P = \frac{k_d k_a t_m}{2\sqrt{\pi}} \frac{\exp[-(\sqrt{k_d t_s} - \sqrt{k_a t_m})^2]}{t_s^{3/4}} \qquad (2.2\text{-}37)$$

A slightly different probability distribution is obtained

if the molecule starts its migration in an adsorbed state

(in paper chromatography).

Then

$$P = \frac{k_d}{2\sqrt{\pi}(k_a k_d t_m)^{1/4}} \frac{\exp[-(\sqrt{k_d t_s} - \sqrt{k_a t_m})^2]}{t_s^{1/4}} \qquad (2.2\text{-}38)$$

where t_s and t_m are the time spent in the stationary and

mobile phases, respectively. The above two expressions have

been derived for a large number of adsorptions and desorptions

when the elapsed time is large compared to the time required

for adsorption or desorption. These two asymtotic expressions

can be expressed in the form of a Gaussian profile[24], which is

$$P = \text{constant} \times \exp(-k_d \Delta t_s^2 / 4\overline{t}_s) \qquad (2.2\text{-}39)$$

which is identical to the Gaussian profile

$$P = \text{constant} \times \exp(-\Delta t_s^2 / 2\tau^2) \qquad (2.2\text{-}40)$$

in its dependence on the time Δt_s which is the departure of t_s from the mean, $\bar{t}_s$.

The plate height contribution due to this approach is

$$H = 2R(1-R)v/k_d \qquad (2.2-41)$$

This equation is identical to that derived by the random walk model provided that $1/k_d$ is replaced by the mean desorption time t_d.

This one-site stochastic theory of Giddings and Eyring[23] has since been extended. Giddings[25] has formulated two-site theory in terms of complex double summations. Giddings developed a somewhat simplified integral expression from which a sample profile was computed. McQuarrie[26] has formulated both the two site and the general n-site problem but the results are too complex to be readily usable.

2.2.5 Non-Equilibrium and Generalized Non-Equilibrium Theories

The non-equilibrium approach is based on entirely different considerations than the random walk approach and stochastic theory. The single molecular events of the random walk approach and the stochastic theory have been replaced by the overall concentration changes at a given point down the column which result from the flow and kinetic processes of chromato-graphy.

As a concentration profile, representing a chromatographic zone, moves down the column, both the leading edge and tail

end of the zone have concentrations of solute that are more than and less than the equilibrium respectively. This is explained in terms of non-equilibrium and the degree of non-equilibrium is dependent on the rate of sorption and desorption of solutes and velocity of migration.[22,23] The non-equilibrium approach is, therefore, used only for the calculation of the C (or rate) term in the plate height expression which is related to the transfer of solutes between regions having different velocities. C is often called the mass transfer term or the non-equilibrium term.

The plate height contribution by this consideration is identical to the equation derived from stochastic theory and with the equation derived from the random walk theory which is

$$H = 2R(1-R) \, v/k_d \qquad\qquad (2.2-42)$$

On the derivation of this equation two assumptions have been made, namely a near-equilibrium assumption where a rapid exchange of solute between the mobile and stationary phase maintain a near-equilibrium condition and the assumption of the existence of a uniform or one-site surface containing equivalent or homogenous sites. Mass transfer by diffusional transport has been neglected in this consideration.

The non-equilibrium theory has been extended and generalized in view of the known complexity of chromatographic materials. The generalized non-equilibrium theory is, therefore, applicable to a number of real chromatographic problems, like the existence of heterogenous surfaces, the existence of

mixed mass-transfer mechanism where both mass transfer by step-wise kinetics and diffusional transport are considered.

The contributions to H by different chromatographic processes have been tabulated in table 2.2-3 according to the various approaches and theories discussed above.

Table 2.2-3

Contributions to H by different chromatographic processes.

Processes	H Plate height	Model
Longitudinal molecular	$H=2\gamma D_m/v$	Random Walk Model
Adsorption-desorption	$H=2R(1-R)v/t_d$	Random Walk Model
(1-site)	$H=2R(1-R)v/k_d$	Rigorous Stochastic and Non-equilibrium theory (NET)
	$H=2R(1-R)v/k_d$	Generalized N.E.T.
Multi-site Adsorption	$H=2R(1-R)v/t_d$	Generalized N.E.T.
$A_1 \quad A_2$		
$A_1 \quad A_3$		
$A_1 \quad A_n$		
Adsorption of Complex Molecules	$H=\dfrac{2(1-R)\ v}{k_{12}f_2+k_{14}f_4}$	Generalized N.E.T.[a]
Adsorption in Partition Chr.	$H=2(1-R\ v/k_{12}+$ $2X_3^* Rv.k_{32}$ $X_1^*=R,\ X_2^*+X_3^*=1-R$	Generalized N.E.T.[a]
Diffusion in Esationary Phase	$H=2R(1-R)d^3/D_s$	Generalized N.E.T.[a] Applicable to st.ph[b] as uniform film or pores of uniform bore and depth d.
	$H=\dfrac{1}{16}R(1-R)\dfrac{d_p^2 v}{D_s}$ dp=rod diameter dp/2-pore	Applicable to stationary phase existing in rod-shaped units when length is > diameter (paper chromatogr.)

Table 2.2-3 (cont.)

Processes	H Plate height	Model
	$H=qR(1-R)d^2/D_s$ q-configuration	Applicable to a column for all units of stationary phase
Diffusion-controlled Sorption-desorption Processes	$H=2R(1-R)d^2v/D_s$	Random Walk Model
Velocity Inequalities	$H=w_i d_p^2 v/D_M$ Transcolumn $H=0.004r_c^2v/D_m$	Random Walk Model
Eddy Diffusion	$H=2\lambda_i d_p$	Classical Theory
	$H=\sum_i \dfrac{1}{1/2\lambda_i d_p + D_m/w_i v d_p^2}$	

D_m, D_s = Diffusion coefficient of solute in mobile and stationary phase respectively.

v = mobile phase velocity

γ = obstructive factor

R = equilibrium faction of solute in the mobile phase

= $1/1+k'$

C_d = mean desorption time

k_d = mean desorption rate

k_{12}, k_{14}, k_{32} = rate constants for adsorption step

f_2, f_4 = fraction proceeding from initial to complete adsorption

d = depth of stationary phase

d_p = rod diameter

q = configuration factor

$$w_i = \frac{S^2 \, Dv^2}{2d_p^2 v^2}$$ where S is the distance a molecule must diffuse to reach one extreme from another.

CHAPTER 2

REFERENCES

1. Giddings, J.C. in Dynamics of Chromatography, Part I, Marcel Dekker, Inc., New York, N.Y., 1965.

2. Snyder, L.R. in Principles of Adsorption Chromatography, Marcel Dekker, New York, 1968.

3. Huber, J.F.K., in Comprehensive Analytical Chemistry (Wilson, C.L. and Wilson, D.W., eds.), Vol.IIB, Elsevier, Amsterdam, 1968.

4. Snyder, L.R., in Modern Practice of Liquid Chromatography, (Kirkland, J.J., ed.), Wiley (Interscience), New York, 1971, p.143.

5. Karger, B.L. Snyder, L.R. and Horvath, C., in 'An Introduction to Separation Science', Wiley (Interscience), New York, 1973.

6. Hildebrand, J.H. and Scott, R.L. in Regular Solutions, Prentice Hall, Englewood Cliffs, New Jersey, 1962.

7. Hildebrand, J.H. and Scott, R.L., in Solubility of Non-electrolytes, 3rd ed. Reinhold Publishing Corp., New York, 1949.

8a. Snyder, L.R. and Kirkland, J.J. in Introduction to Modern Liquid Chromatography, John Wiley, New York, N.Y., 1974.

8b. Knox, J.H. and McLaren, L., Anal.Chem., 36 (1964) 1477.

8c. van Deemter, J.J., Zuiderweg, F.J. and Klinkenberg, A., Chem.Eng.Sci., 5 (1956) 271.

9. Martin, A.J.P. and Synge, R.L.M., Biochem.J., 35C (1941) 1358.

10. Keulemans, A.I.M. in Gas Chromatography, 2nd ed., Reinhold, New York, 1957.

11. Einstein, A., Ann.der Physik, 17 (1905) 549.

12. Horne, D.S., Knox, J.H. and McLaren, L., Separation Science, 1 (1966) 531.

13. Knox, J.H. and McLaren, L., Anal.Chem., 36 (1964) 1477.

14. LeRosen, A.L., J.Am.Chem.Soc., 62 (1940) 1583.

15. Giddings, J.C., Anal.Chem., 34 (1962) 1186.

16. Perrett, R.H. and Purnell, J.H., Anal.Chem., 35 (1963) 430.

17. Giddings, J.C., Anal.Chem., 35 (1963) 439; 33 (1961) 962; J.Phys.Chem., 68 (1964) 184.

18. Klein, P.D., Anal.Chem., 33 (1961) 1737.

19. Kiselev, A.V., Yu. S. Nikitin, Petrova, R.S., Shcherbakova, K.D. and Ya, J. Yashin, Anal.Chem., 36 (1964) 1527.

20. Young, D.M. and Crowell, A.D. in Physical Adsorption of Gases, Butterworth, London, 1962.

21. McClellan, A.L. and Harnesberger, H.F., J.Colloid Interface Sci., 23 (1967) 577.

22. Giddings, J.C., Anal.Chem., 35 (1963) 1338.

23. Giddings, J.C. and Eyring, H., J.Phys.Chem., 59 (1955) 416.

24. Giddings, J.C., J.Chem.Phys., 26 (1957) 1755.

25. Giddings, J.C., J.Chem.Phys., 26 (1957) 169.

26. McQuarrie, D.A., J.Chem.Phys., 38 (1963) 437.

CHAPTER 3

HISTORY OF CARBON AND REQUIREMENTS

OF A GOOD LC STATIONARY PHASE

3.1 Historical background of carbon in LC

In classical liquid chromatography, prior to 1955, charcoal was among the most popular of chromatographic adsorbents.[1,2] The early fundamental studies carried out by Tiselius and co-workers in column liquid chromatography all used activated carbons.[3,4] At this time, activated carbons were widely used for the study of adsorption of hydrocarbons without substituted groups[5,6] and of hydrocarbons containing them.[2,7-9] Some papers discuss the adsorption isotherms,[2,6] others are concerned with the heats of wetting.[10,11] However, its use gradually decreased due to the poor peak shapes so often obtained and the competition from silica gel in TLC. However, with the realisation of the disadvantages of silica based particles an intense search for new adsorbents is now occurring owing to the rapid proliferation of HPLC. Due to the fact that chemically bonded phases are not stable under all conditions and cannot solve all separation problems, there is a growing need to find non-polar adsorbents in LC. Carbon adsorbents are, therefore, of special interest and they offer a pronounced lipophilic or reversed-phase surface.

A carbon adsorbent in the form of diamond was used by Telepchak[12] for the separation of benzene and anthracene. The chromatograms are shown in figure 3.1-1 (a and b). In spite of its unique mechanical properties and nearly non-polar surface, this material has not found application due to its low specific surface area and high cost. However, in the last few years, following the extensive work of Kiselev,[13,14] Liberti and others[15] in GC graphitized carbon blacks have

Solutes:

1. Benzene
2. Anthracene

(a)

1 + 2

Inject

8 mins

(b)

1

2

Inject

24 mins
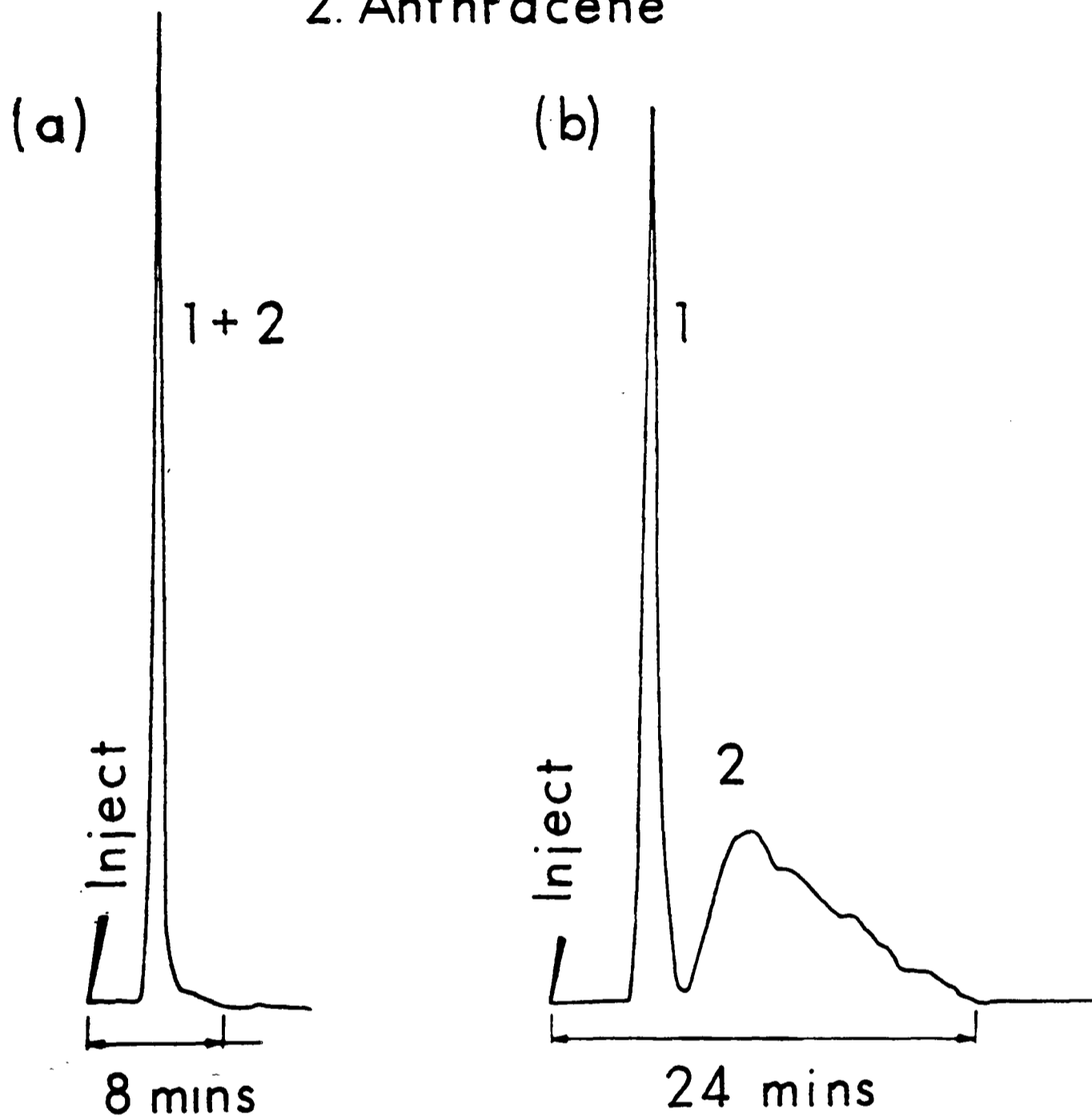
Flow Rate: 0.2 ml / min

Eluent: (a): 50% Methanol / H_2O

(b) 30% Methanol / H_2O

FIG. 3.1-1: REVERSED - PHASE ADSORPTION ON DIAMOND (ref. 12)

been used in LC.   These are composed of colloidal particles

of graphitized carbons with an average diameter between 0.01

and 0.5μm.   The microparticles cannot, of course, be used

directly in chromatography but they must be pellitized to

form aggregates but, unfortunately, such aggregates are very

fragile and are easily destroyed by shear forces due to the

liquid flow during column operation or column packing.   In

addition, graphitized carbon blacks (GCTB) generally have a

low surface area ($5-10m^2g^{-1}$) are, therefore, easily overloaded.

A form of graphitized carbon black is now marketed by Supelco

under the trade name Carbopack for GC.   This material was

developed by Liberti and co-workers[15] and is in the form of

weakly bound spherical pellets, but made from Saran Charcoal

rather than carbon black.   It has been used recently in LC[15]

but can withstand only relative low pressures and is too

fragile to be regarded as a realistic candidate for a LC

packing material.

Benzene and other hydrocarbons can be pyrolyzed into

various forms of pyrolytic carbon.[16-18]   If this pyrolytic

carbon is deposited on carbon black particles their hardness is

much increased.[19]   Barmakova et al.[16] applied this idea to

GC.   Guiochon and co-workers[20] used this technique in LC.

They started from carbon black aggregates of 5-50μm in size.

Carbon black was obtained from Cabot, Neuilly, France (Sterling

FTFF) as the basis for a material of small specific surface

area and Black Pearls from Cabot, Boston, U.S.A. for larger

specific surface area.   The mechanical strength of the trial

material was much greater than the original aggregates but

was still insufficient for LC.   They subsequently performed

the pyrolysis of benzene on silica gels such as Spherosil
XOA 600, and XOB 75 and 75μm Partisil instead of carbon black.
The percentage of pyrocarbon deposited was somewhat critical
for the amount deposited should eliminate the sorption pro-
perties of the silica while not giving so thick a layer that
pores were completely blocked and efficiently reduced; 15-20%
proved the optimum but up to 50% deposition still gave useful
materials.   Unger et al.[21] adopted another approach using
purified and calcined active charcoal and cokes which were
mechanically hard but had very low surface areas of only a
few $m^2 g^{-1}$.   More recently still, Plzak et al.[22] prepared a
new carbon adsorbent by reduction of polytetrafluoroethylene
(PTFE) with alkali-metal amalgams in vacuo at 100°C.   This
procedure produced a highly active carbon of extremely large
surface area in the region of 2000 $m^2 g^{-1}$.   The so-called
"Jado-Carbon" could be modified by various treatments including
high-temperature heating treatment to give materials of areas
as low as 20 $m^2 g^{-1}$.   The carbon powder obtained exhibits very
good mechanical properties for packing HPLC columns but shows
poor chromatographic characteristics.

Inspite of the efforts made to produce suitable carbons
for LC, it is readily seen from the published chromatograms
that poor chromatographic performance has been obtained so
far.   Peaks are badly tailed especially when solutes are
significantly retained and plate efficiencies are low.   This
is attributed to the fact that the surface of carbon adsorbent
is heterogenous and strong adsorption of molecules occurs at
rare but particularly active sites on the adsorbent surface.
In summary, the only carbon to give good peak shapes is

graphitized carbon black (Carbopack) but this is too weak for HPLC.

A novel carbon was recently described by Knox and Gilbert[23] and which was originally called porous glassy carbon. They conceived the idea of making porous carbon by impregnating the pores of a silica template by a polymer such as the phenol-hexamine resin. The material was subsequently carbonised at 900°C in an inert atmosphere. The template was dissolved out by alcoholic KOH at 120°C and the carbon obtained was heated in argon at temperatures greater than 2340°C to improve its surface, remove micropores and provide adequate mechanical strength. The method of production of PGC has now been improved so that its kinetic performance in LC has been enhanced. The details of the production and its modifications will be dealt with in greater detail in Chapter 6.

3.2 <u>Desirable characteristics of a column packing material with reference to carbon</u>

To be applicable as a packing in HPLC, a particulate carbon should possess the following characteristics: (i) sufficient hardness to withstand high pressures, (ii) a well-defined, reproducible and stable surface which shows no change during chromatographic work or storage, (iii) a specific surface area in the range of 50 to 500 m^2/g to give adequate retention of solutes and to maintain a reasonable linear sample capacity, (iv) a mean pore size not less than 10nm and an absence of micropores in order to ensure rapid mass transfer of solutes

into and out of the particles, (v) ease of preparation by
a simply controlled, low-cost process (vi) uniform surface
energy to give linear adsorption isotherm.

An essential requirement of any final material for HPLC
is that it must possess sufficient hardness to withstand high
pressures and high eluent flow rates during column packing
and operation. The hardness of carbon is directly related
to its molecular and pore structures. Layer-type materials
such as graphite are soft whereas amorphous glassy carbons
possess high mechanical strength due to their microcrystalline
mosaic structure. Between these two limiting cases a large
number of structural intermediates exists. One of them is
the so-called turbostratic structure proposed by·Biscoe and
Warren.[24] The layers in such carbon materials are 'arranged
roughly parallel and equidistant but are not otherwise
mutually oriented'. It may be concluded that because of their
low mechanical strength highly ordered graphite-like carbons
are less likely to be suited as packings in HPLC than amorphous
carbons.

Particle porosity also has an important effect on
mechanical strength. In general, particles are too fragile
for HPLC when the particle porosity exceeds about 70% (a
typical silica gel, for example, has a particle porosity of
about 55%). Each population of pores contributes to the total
specific surface area. In general, active carbons have high
surface areas whereas graphitized materials have low surface
areas. Carbons having high surface areas due to micropores
are not suitable for use in liquid chromatography on account

of slow mass transfer and too high retention. Undoubtedly, one of the major problems in the manufacture of porous carbons suitable for HPLC arises from the extreme difficulty of eliminating micropores.

CHAPTER 3

REFERENCES

1. Cassidy, H.G. in Adsorption and Chromatography, Wiley (Interscience), New York, 1951.

2. Williams, R.J.P., Hagdahl, C. and Tiselius, A., Arkiv Kemi, 7 (1954) 1.

3. Tiselius, A., Kolloid-Z., 105 (1943) 101.

4. Tiselius, A., and Hahn, L., Kolloid-Z., 105 (1943) 177.

5. van der Waarden, M., J.Colloid Sci., 6 (1951) 443.

6. Hansen, R.S. and Hansen, R.D., J.Phys.Chem., 59 (1955) 496.

7. Wachell, J.L. and Cassidy, H.G., J.Am.Chem.Soc., 65 (1943) 665.

8. Bodforss, I. and Ethrlen, I., Kgl.Fysiolgraf Sällskap. Lund.Forh, 15 (1945) 3.

9. Hesse, G. and Sauter, O., Naturwissenchaften, 34 (1947) 277.

10. Kiselev, V.F., Dokl.Akad.Nauk SSSR, 89 (1953) 113.

11. Kraus, G., J.Phys.Chem., 59 (1955) 343.

12. Telepchak, M.J., Chromatographia, 6 (1973) 234.

13. Kiselev, A.V. and Yashin, Ya.I., Zh.Fiz.Khim., 40 (1966) 603.

14. Kiselev, A.V., Kuznetsov, A.V., Filatova, I.Yu. and Shcherbakova, K., Zh.Fiz.Khim., 44 (1970) 1272.

15. Ciccioli, P., Tappa, R., DiCorcia, A., Liberti, A., J.Chr., 206 (1981) 35.

16. Barmakova, T.V., Kiselev, A.V. and Kovaleva, N.V., Kolloid Zh., 36 (1974) 133.

17. Makarov, K.I. and Pechik, V.K., Carbon, 12 (1974) 391.

18. Fitzer, E., Mueller, K., Schaeffer, W., Chemistry and Physics of Carbon, Vol.7, Marcel Dekker Inc., New York, 1971.

19. Brown, A.R.G., Hall, A.R. and Watt, W., Nature, 172 (1953) 1145.

20. Colin, H., Eeon, C. and Guiochon, G., J.Chr., 119 (1976) 41.

21. Unger, K., Roumeliotis, P., Mueller, H. and Goetz, H., J.Chr., 202 (1980) 3.

22. Plzak, Z., Dousek, F.P., Jansta, J., J.Chr., 147 (1978) 137.

23. Knox, J.H. and Gilbert, M.T., U.K.Patent No.7939449; U.S.Patent No.4,263,268; Fed.Rep.Germany P294 6688-4.

24. Biscoe, J. and Warren, B.E., J.Appl.Phys., 13 (1942) 364.

PART II

PRODUCTION AND STRUCTURE

OF POROUS CARBON

Chapter 4

Production and Structure of Carbons - General

4.1 Production of Polymeric Carbons

4.1.1 Introduction

Carbon exists in many forms, but of these only two, diamond and graphite, can be completely characterized. These are the true allotropes of carbon and both occur naturally. However, a wide range of artificial bulk carbons have been prepared for industrial use. These include dense electrode carbons, nuclear reactor carbons, active carbons (for decolorizing materials), carbon flims and glassy carbons. Artificially produced carbons can be categorized into cokes and chars but this historic distinction between the types of carbon is not clear cut because a continuous gradation exists between the two types.

Organic compounds are the main and almost exclusive raw materials for the production of synthetic carbons and graphites. When many high polymers are heated in an inert atmosphere to temperatures above 300°C they lose much of their non-carbon content as organic vapours and leave a residue consisting of carbon. The process is termed carbonization or pyrolysis. Until recently, two types of carbon were distinguished. If the material passed through a liquid or tarry state immediately prior to carbonization the resultant carbon is termed a coke: if it does not pass through such an intermediate phase, the resultant product is called a char. The most common and, indeed, the earliest known char is charcoal which is the carbon produced by carbonizing wood. Correspondingly the most common coke is produced by the pyrolysis or partial

combustion of coal or heavy oil. However, more recently other methods of making carbons have been developed. Carbon fibres are produced by the carbonization of different polymers.[1,2] A relatively new form of carbon, glassy carbon, can now be produced by the carbonization of phenolic resins[3] which are also the basis of production of the novel form of carbon, porous glassy carbon (or PGC for short) which is the subject of this thesis. The pyrolysis of the resin is now discussed in more detail.

4.1.2 Phenolic Resins

Phenolic resins constitute an important group of polymers in which the chain consists of phenolic groups linked by methylenes ($-CH_2$). They are formed by a condensation reaction between phenol and hexamine (or formaldehyde) with elimination of ammonia and water. They can be produced by either a one-stage or a two-stage process.

In the one-stage process, phenol is reacted with excess formaldehyde so that the phenol-to-formaldehyde (P:F) molar ratio is less than one. The mixture is heated in the presence of alkaline catalysts such as sodium hydroxide or ammonia. The actual degree of polycondensation can be controlled to form either a 'resol' which is a short low molecular weight, linear polymer and completely soluble in the alkaline solution or a 'resitol' which is a long linear polymer with slight amount of cross-linking between chains. Resitol is insoluble in alkaline solution but readily soluble in organic solvents. When heated to a higher temperature, resitol undergoes extensive

cross-linking to form a hard and insoluble resin.

When the amount of formaldehyde is reduced so that the P:F ratio is greater than one, it requires a two-stage process to form a phenolic resin. The reaction is allowed to proceed in the presence of an acid catalyst until no further chemical changes take place. The resin formed called 'Novalac' is fusible and soluble in organic solvents. It is then ground and treated with hexamine to form a hard, infusible resin with methylene cross-links.

If, on the other hand, hexamine $[N_4(CH_2)_6]$ is used instead of formaldehyde, no catalyst is required, and, no matter what the P:F ratio is, the resin is made in a one-step process because the ammonia released acts as a catalyst in the process. The use of hexamine, therefore, simplifies the whole procedure and for this reason was adopted for the production of PGC.

According to Zinke[4] nitrogen in the resin exists in the form of dimethylene-amino bridges. In a resin with excess phenol, nitrogen is eliminated as ammonia resulting in the formation of methylene bridges giving a phenol-methylene structure as shown in figure 4.1-1. It has been established that a nitrogen-free resin is formed by heating 6 phenol: 1 hexamine (molar ratio) and that all the nitrogen in hexamine escapes as ammonia during polymerization. Fitzer et al.[5] consider that between 100 and 300°C polymerization continues to form long chain polymers.

4.1.3 Carbonization of Phenolic Resins

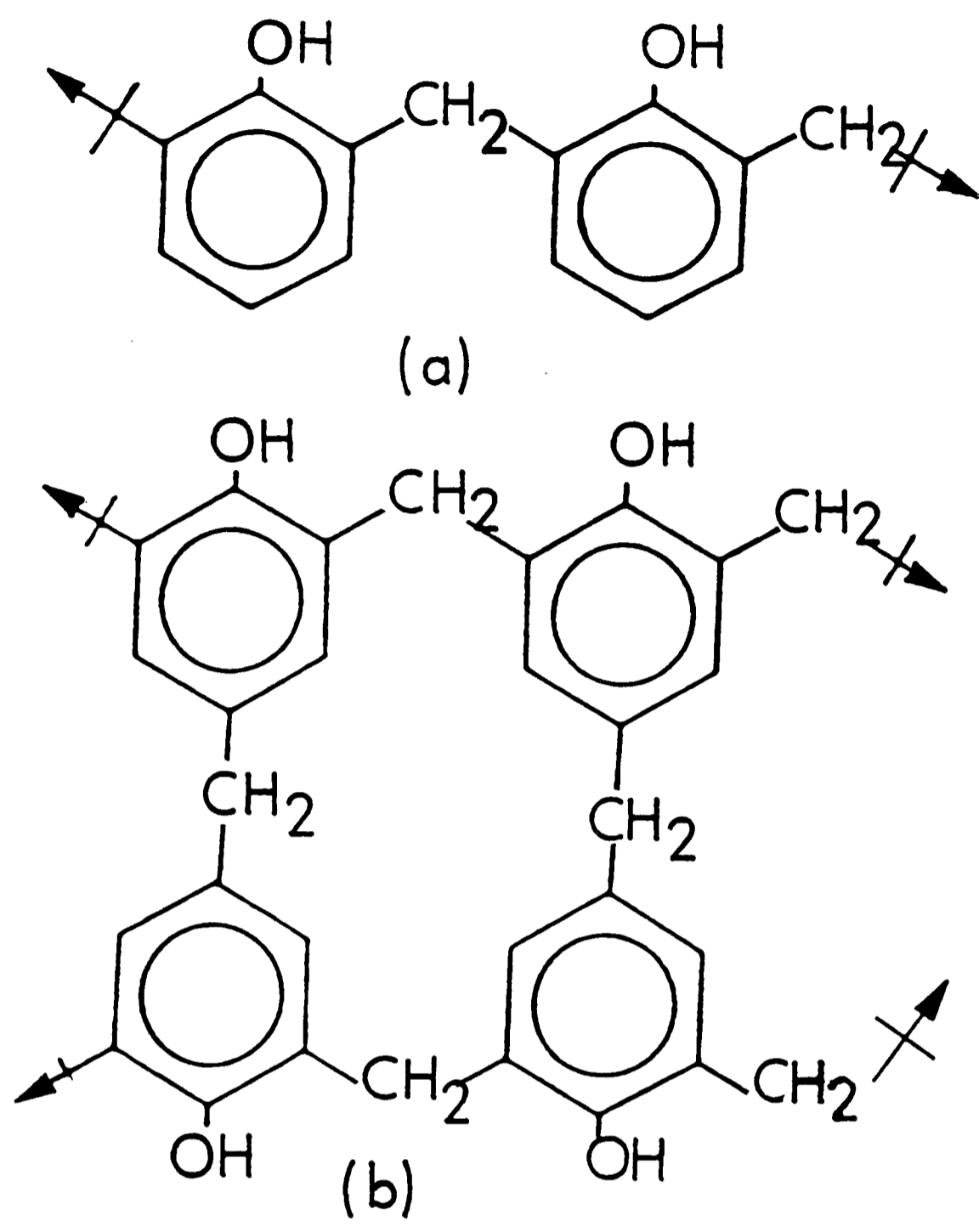Carbonization (pyrolysis) of polymers is normally carried

FIG. 4.1-1 : (a) STRUCTURE OF LINEAR
POLYMER OF PHENOL-HEXAMINE;
(b) STRUCTURE OF RESIN OF
PHENOL-HEXAMINE

out in an inert atmosphere and its various stages are illustrated in figure 4.1-2.[6,7] When strongly cross-linked polymers containing oxygen are pyrolysed, it is evident that condensation, oxidation, dehydration and decomposition may occur as both parallel and sequential reactions. In almost all cases, pyrolysis takes place in the solid state. The first step in the pyrolysis of phenolic resins, as the polymer is heated from 300°C, is assumed to be the formation of ether bonds (III) by the reaction of two phenolic groups, accompanied by the release of water. In parallel to this reaction, a condensation of a phenolic group with a methylene group occurs to yield a triphenyl-methane structure (IV). The cyclic ether diphenylpyran (V), identified as being produced above 400°C, can be explained by a chemical condensation of two phenolic groups accompanied by cyclization.

Due to instability at temperatures around 400°C, the pyran ring releases methane and yields the more stable furan ring (VI). Above 450°C, the remaining methylene bridge (VII) is oxidized by the water of pyrolysis to form keto groups (VIII). Above 400°C, the keto groups release carbon monoxide, thus yielding the biphenyl structures (IX). There are no definite data available regarding the further course of the pyrolysis. Dibenzofuran (VI) is assumed to be formed at temperatures above 600°C.

Solid-state pyrolysis results in the formation of aromatic sheets or groups that are randomly oriented with respect to each other. There is not sufficient mobility of these groups for rearrangement to occur to give ordered groups. While limited rotation becomes possible in the biphenyl
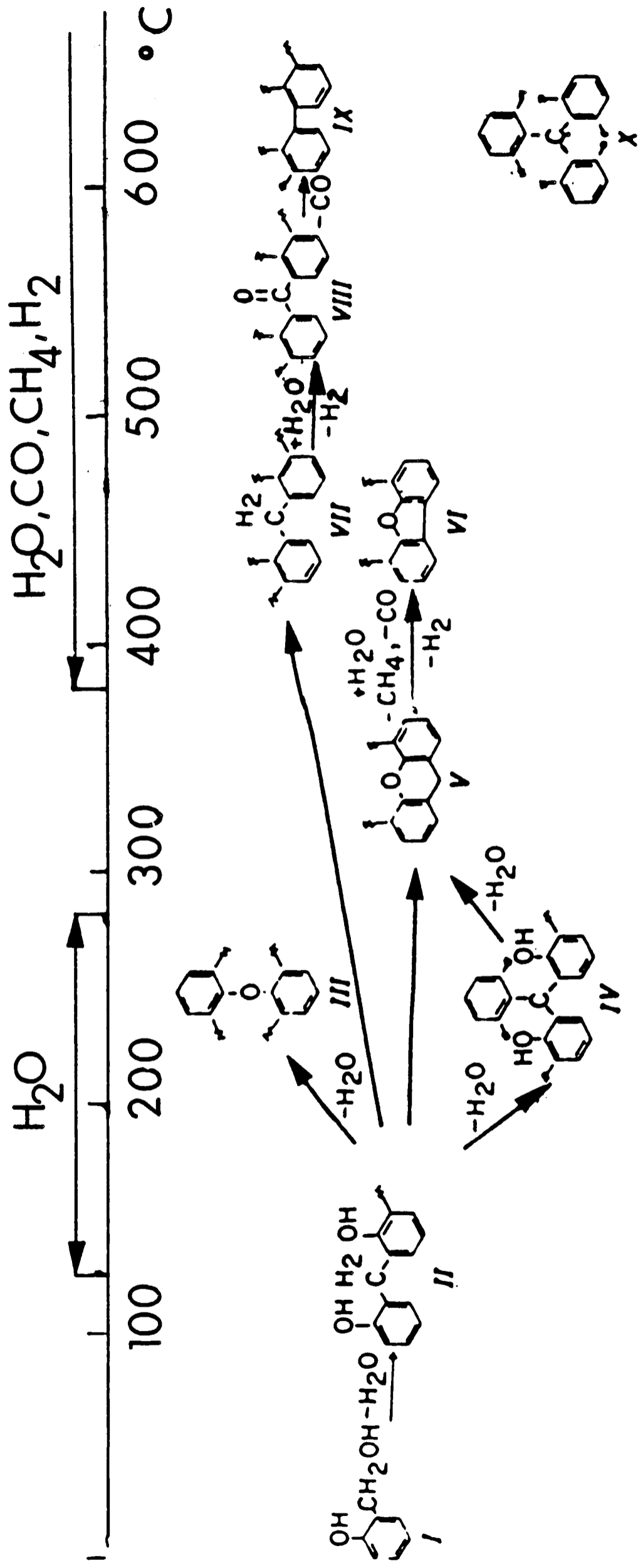
FIG. 4.1 - 2: SCHEMATIC OF THE PYROLSIS OF PHENOL - FORMALDEHYDE POLYMER (from Refs. 6,7)

structures (IX), it is not sufficient to result in good graphitizability. At the same time, the strong cross-link-ages renders the release of low molecular weight fragments difficult and this leads to a high carbon yield. In the case of phenolic polymers the carbon yields amounts to 84%[8-10] of the original carbon or about 50% of the original polymer weight. The pyrolysis gases consist primarily of water, carbon monoxide, carbon dioxide, methane and hydrogen.

Figure 4.1-3[11] shows the weight loss of a 12:1 and 6:1 resin as a function of heat treatment temperature. A marked weight loss is observed between 300 and 400°C which corresponds to the change in chemical structure detected by infra-red spectroscopy.[11] The rate of weight loss decreases gradually up to 1250°C and, thereafter, the weight remains constant. The weight loss of a resin is highly dependent on the molar ratio of phenol to hexamine. The weight loss of the 6:1 mixture follows the same shape as that of the 12:1 mixture but the final weight loss is reduced to 49.6% compared to 60% because the 12:1 mixture contains excess phenol molecules which cannot be linked together with methylene bridges. The weight loss of the resin is accompanied by a sharp decrease in bulk density of the resin as illustrated in figure 4.1-4[12] but above 500°C, the density increases rapidly with the removal of a relatively small mass of material - mainly hydrogen as shown in figure 4.1-5[12] while the body of the material shrinks.

The rate of heating during pyrolysis has a profound influence on both the carbon yield and the carbon properties and the temperature programme may be adjusted to control the
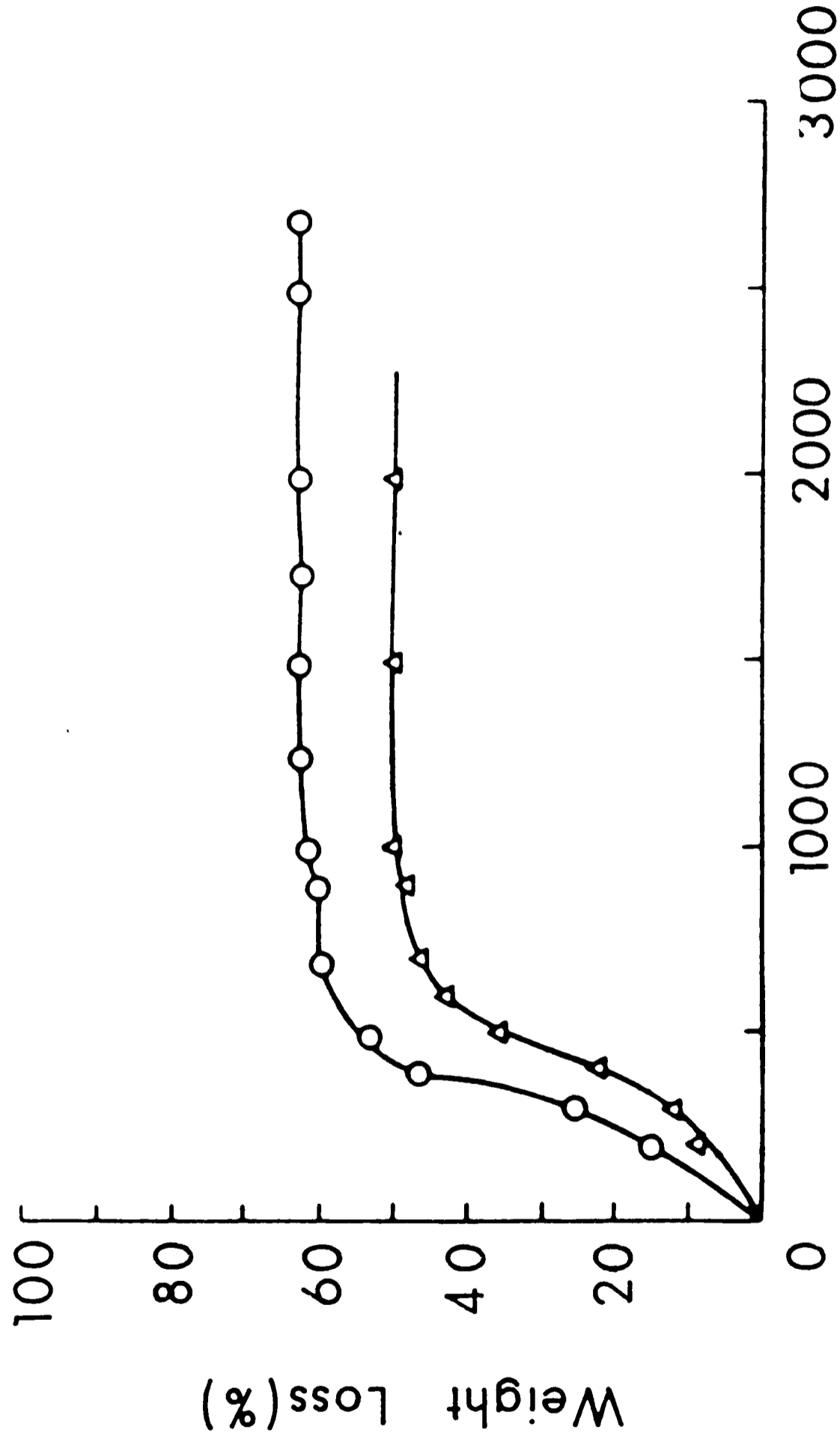
FIG. 4.1 - 3 : WEIGHT LOSS OF PHENOLIC RESINS DURING

PYROLYSIS. o 12 PHENOL : 1 HEXAMINE ;

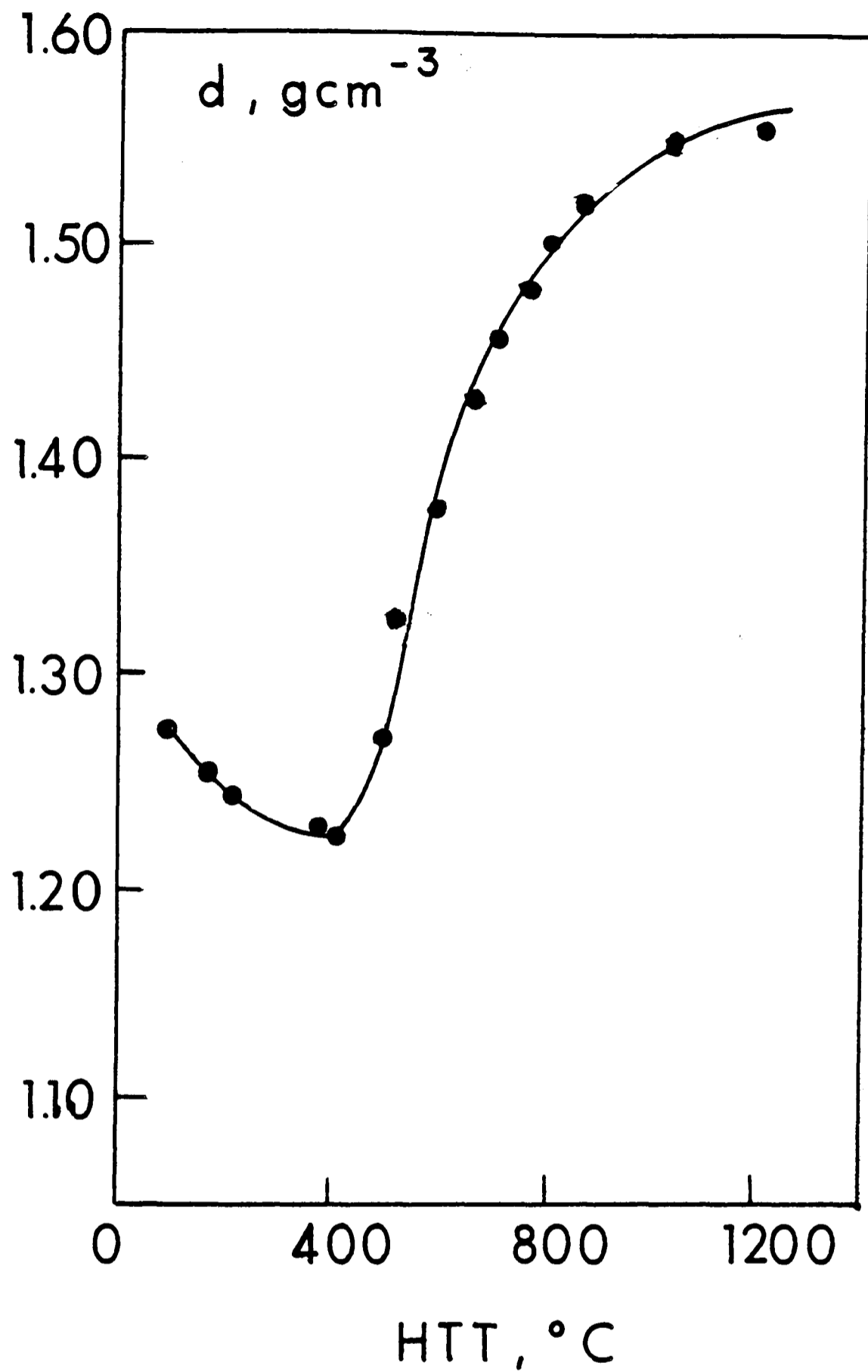△ 6 PHENOL : 1 HEXAMINE (from Ref. 11)

FIG. 4.1 - 4 : BULK DENSITY OF PYROLYZED
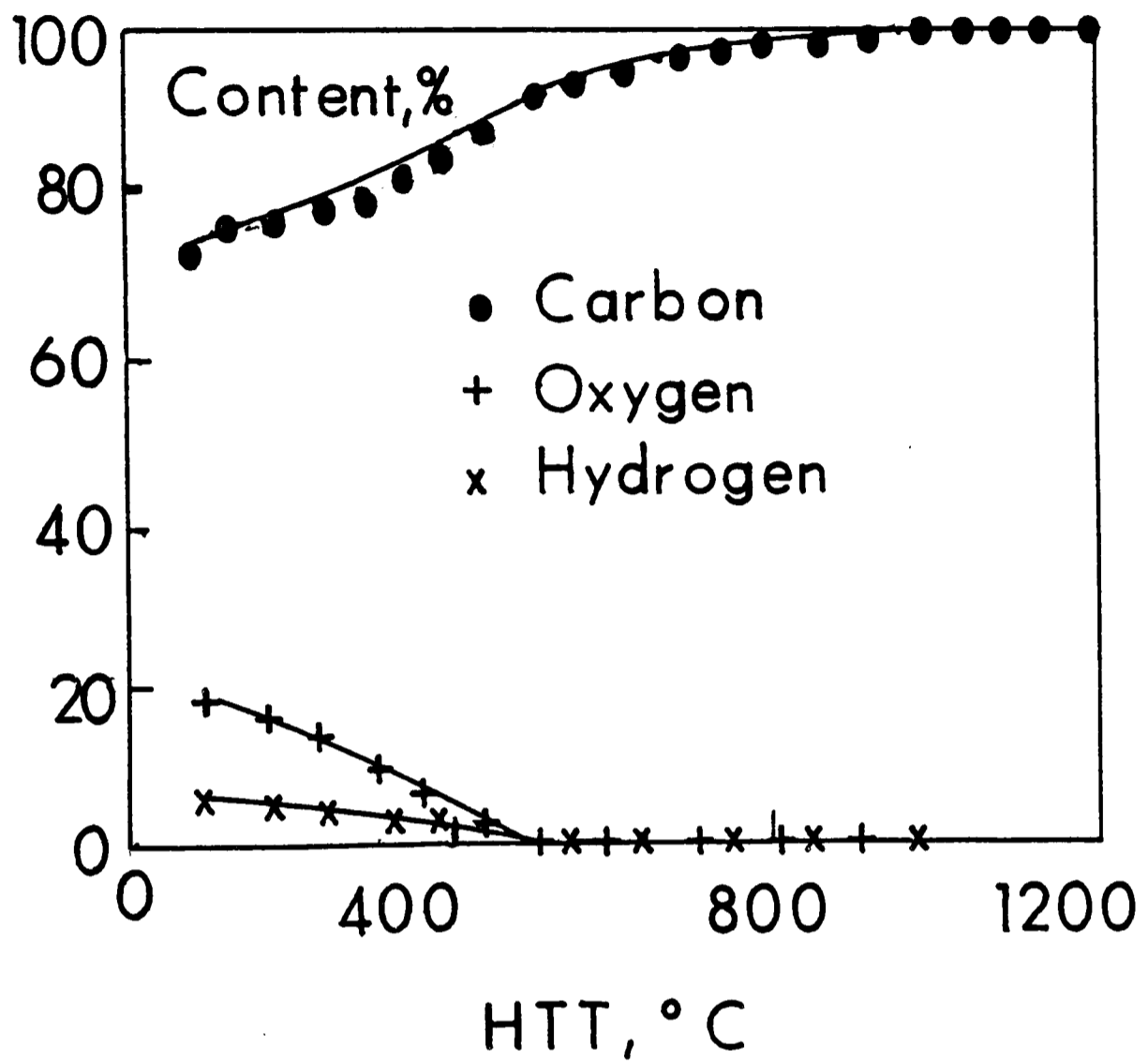PHENOLIC RESIN (from Ref.12)

FIG.4.1 - 5: CHEMICAL COMPOSITION OF PYROLYSED PHENOLIC RESIN (from Ref. 12)

morphology of the final carbon for the purpose of obtaining certain quality characteristics. The morphology is influenced not only by the chemistry of the reactions but also by the mass and heat transport phenomena during the pyrolysis. It depends on whether the compounds to be pyrolyzed are solid, liquid or gaseous, as well as on the rate of energy input and rate of diffusion to the carbon nuclei of molecules undergoing pyrolysis. The morphology also depends on the ease of escape of the volatile by-products. Dense carbon without micro-scopically detectable pores is obtained either by slow gas phase pyrolysis of hydrocarbons (pyrolytic carbon deposition) or by slow carbonization of non-melting cross-linked polymers (formation of glass-like carbon with uniform pores having a diameter of 25Å or less).

4.1.4 High Temperature Treatments (HTT)

Carbons obtained at temperatures up to 1000°C are generally highly microporous with very high surface areas. Such carbons have been found unsuitable for use in liquid chromatography due to their high retention of solutes and the poor peak shapes arising from non-linear adsorption isotherms for solutes. There is, therefore, the need to subject the carbon to higher heating temperatures to bring about the structural rearrangement necessary for the closing up of micropores. The distinction between high temperature treat-ments of carbons and true graphitization and the effect of temperature on the structure of carbons will be discussed in section 4.2.

4.2 Structure of Carbons

4.2.1 Introduction

The structure of carbon has intrigued crystallographers for decades. Part of the fascination stems from the fact that, in addition to its two well-defined allotropic forms, diamond and graphite, carbon can take a great number of quasi-crystalline forms varying continuously from the near amorphous to the highly crystalline state. The history of X-ray studies on carbon and graphite is closely linked to the development of theory and experiment of X-ray diffraction itself. Graphite was one of the first substances investigated by X-ray diffraction and the study of carbons will be made in comparison with that of graphite.

4.2.2 Structure of Graphite

The valence electrons of carbon permit trigonal and π bonding between each atom and its three neighbours. Such bonding results in the formation of a two-dimensional hexagonal lattice as shown in figure 4.2-1. The hexagonal form of graphite is the equilibrium state of the element carbon over a large range of temperatures and pressures including the normal conditions. It consists of two-dimensional flat sheets which are stacked in a ABABAB sequence above each other as shown in figure 4.2-2(a). Debye and Scherrer[13] had first proposed that planes were registered one above the other in a AAAA sequence. Hull[14], on the other hand, disagreed with the Debye-Scherrer postulate[13] and proposed that adjacent layers
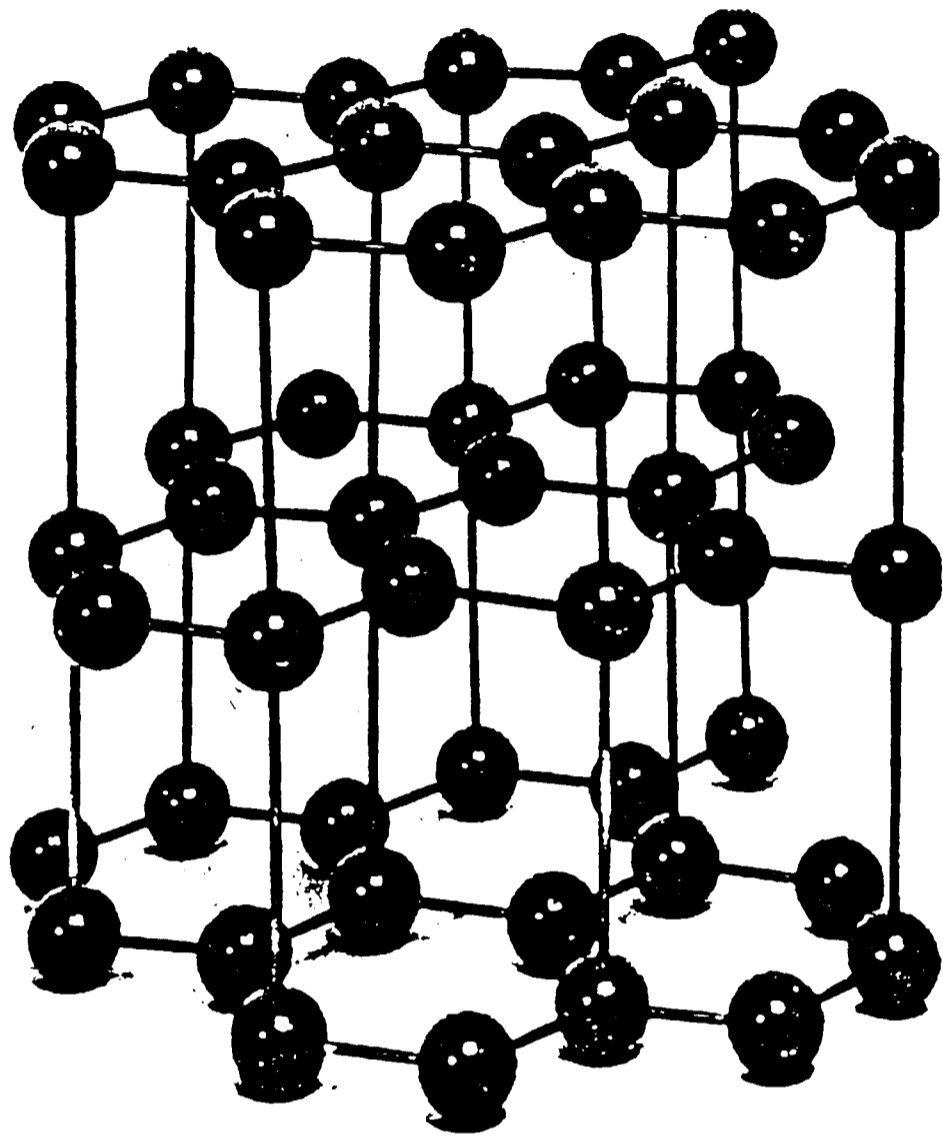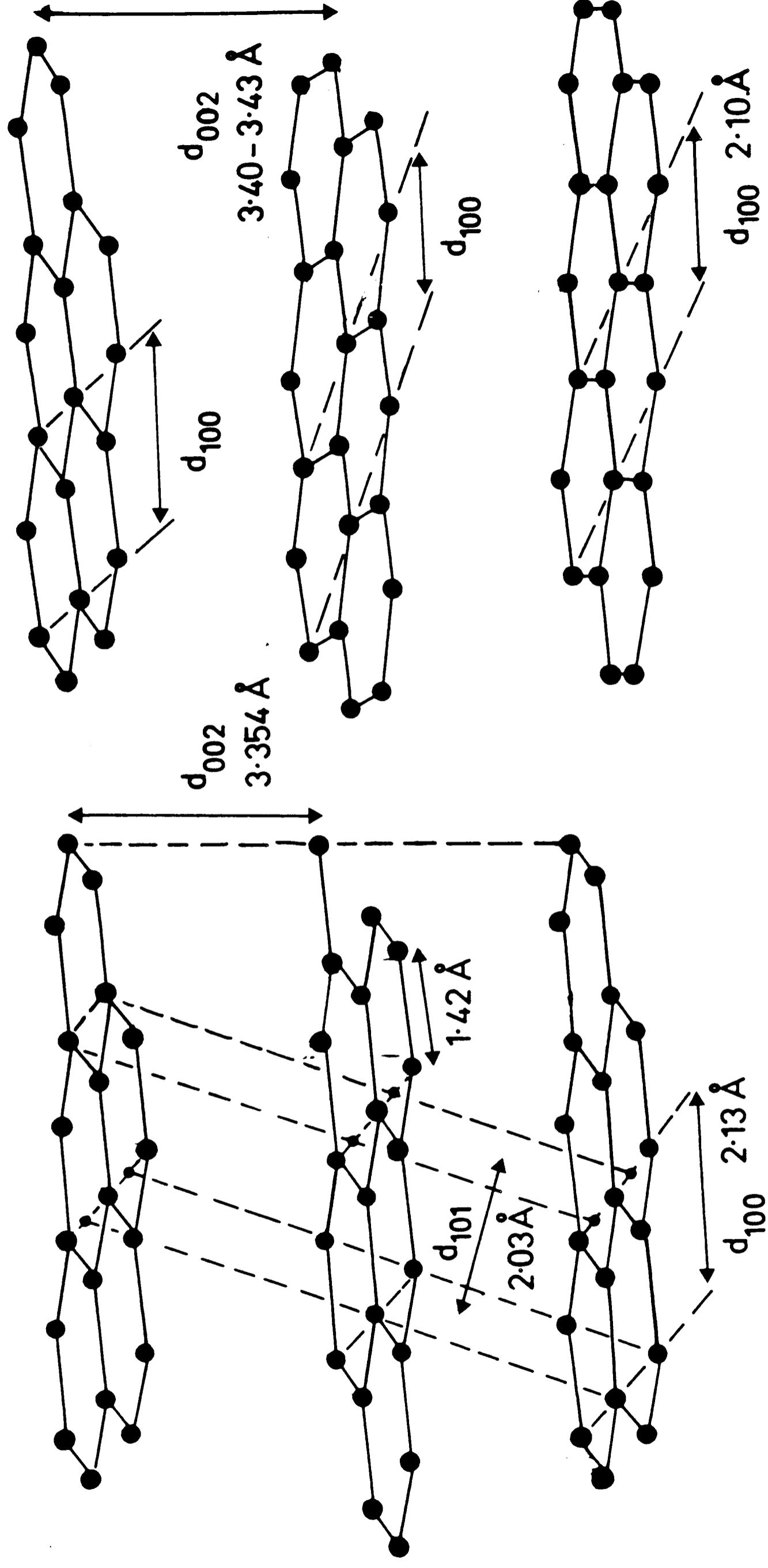
FIG. 4.2 - 1: HEXAGONAL LATTICE OF GRAPHITE

FIG. 4.2 – 2 : 3D – GRAPHITE (a) AND 2D – GRAPHITE (b)

(a)

(b)

d_{002} 3.354 Å

d_{100} 2.13 Å

d_{101} 2.03 Å

1.42 Å

d_{002} 3.40 – 3.43 Å

d_{100}

d_{100} 2.10 Å

were translated by a bond length and that only alternate
layers had identical projections.   This sequence is desig-
nated A-B-A-B-A ... , its cell is represented by a simple
hexagonal lattice.   It is now accepted that the equilibrium
structure of graphite is that proposed by Hull[14] and con-
firmed by Bernal.[15]   The hexagonal lattice became the
accepted lattice for a graphite.

The hexagonal lattice consists of plane layers of carbon
atoms covalently bonded in a regular open-centred hexagonal
array.   The distance between carbon atoms is $1.42\overset{o}{A}$ while
between perfect sheets the interlayer spacing is $3.354\overset{o}{A}$.   The
bonds in the basal plane are extremely stiff and strong and so
the modulus in the a-direction is very high;   the material
can withstand temperatures of 3300°C before breaking up by
thermal degradation alone.   The bonds between the planes
are of the weak van der Waals type and so the crystal can be
sheared and cleaved easily in the plane perpendicular to
the c-axis even at very low temperatures.

Later studies of graphite have revealed lines in X-ray
patterns in addition to those expected for the Bernal struc-
ture.   Lipson and Stokes[16] succeeded in interpreting some
supplementary lines in powder photographs of well crystallized
graphite.   These lines indicate the existence of another
lattice besides the hexagonal;   the difference between the
two resides in the stacking sequence of the layers which is
ABCABC rather than ABABAB of the Bernal structure.   This
form, termed the rhombohedral form, occurs to the extent of
a few percent in most samples of graphite.

4.2.3 X-Ray Diffraction Study of Carbons

4.2.3.1 Measurement of crystallite sizes

The layer diameter, L_a, and the stack height, L_c, of the crystal considered as a right cylinder are measured in the crystallographic a and c direction and may be obtained from measurements of diffraction peaks. The interlayer spacing is obtained from the angle at which the corresponding peak is diffracted.

In 1918, Scherrer[17] gave an expression relating the edge dimension, L, of a cubic crystal to the pure X-ray diffraction line width, B, given by a powder comprised of such crystals:

$$L = K \lambda / B \cos \theta$$

where λ is the wavelength of the X-ray radiation, θ is the Bragg angle and K is a constant of the order of unity (Scherrer constant). The validity and applicability of this formula has been reviewed by Drenck[18] and by Klug and Alexander[19]. Line breadths, B, may be measured in radians at different fraction of the peak height, usually half peak height. In this case, K is close to unity. Accordingly:

$$L = 1.00 \ \lambda / B_{(\frac{1}{2})} \cos \theta$$

Warren[20] was the first to show that carbon black either "graphitized" or "as formed" at around 1000°C are not truly amorphous but rather contain atomic spacings close to those within a single graphite sheet. He suggested that carbon is a heterogenous mixture of atomic groupings ranging from single graphite sheets up to crystallites several layers thick.

In 1941, Warren[21] made a further advance of presenting the relation between crystal size and line broadening of two-dimensional reflections from random-layer lattices as exemplified by the dimension L_a and the 110, 100 and 002 reflections due to the graphitic layers of turbostratic carbons. He obtained an equation similar to that of Scherrer but with a value of the constant K = 1.84, that is

$$L_a = 1.84\lambda/B_{\frac{1}{2}} \cos \theta \text{ (for turbostratic carbons)}$$

Franklin[22] found that the layer diameter in pyrolytic carbons as calculated using Warren's method was one order lower than that determined with an electron microscope. Diamond[23] explained this by showing that a Gaussian strain distribution in an aromatic layer which would be caused by bending or twisting of graphite sheets would considerably reduce the average layer diameter determined by X-ray diffraction. No significant discrepancy has however been reported between the calculated crystallite size, L_c, and the average thickness observed in graphite crystallites.

Soon after the development of the theory of diffraction for random layer lattices, Biscoe and Warren[24] showed experimentally that the layers present in carbon are arranged roughly parallel and equidistant but are not otherwise mutually oriented. The layer spacing was found to be somewhat greater than that found in graphite. In figure 4.2-2 the layer arrangement in graphite is compared with that found in turbostratic carbons.

In using Warren's formula, both the 100 and 110 reflections

will give a 'mean diameter' of the graphite layers although
it is found that the two reflections do not always give the
same result!

Also, the proper application of the Scherrer and Warren
formula to very small crystals is doubtful.   This is because
such small crystals are associated with very diffuse reci-
procal lattice points for which the interference function
may be non-zero over an appreciable volume about this point.[25]
It is because of these objections that Diamond[23,25,26] evolved
his method for measuring the crystal size of very small
crystals of turbostratic carbons.   Diamond[27] used a slightly
modified Scherrer-type equation relating L_a to the width of the
110 band, that is:

$$L_{1\,10} = 0.71\lambda/\Delta \sin \theta$$

Diamond's empirical formula holds for $8\overset{\circ}{A} < L_a < 20\overset{\circ}{A}$.

Thus there appears to be some disagreement about the
value of the Scherrer constant.   Diamond proposes 0.71 while
Warren uses 1.84.

Using the usual Scherrer equation[28] for the height of
the crystallites, L_c,

$$L_c = 0.94\lambda/B_{(oo\ell)} \cos \theta$$

Biscoe and Warren found that the L_a and L_c of carbons
were proportional to one another.   This result and those of
Franklin[29] and others[30,31] have shown that L_a is usually in the
range $L_c < L_a < 2L_c$.

The mean diameter, L_a, measured in the a-direction, is

usually determined from the (110) line, whereas the average
thickness measured in the c-direction, L_c, is most commonly
measured from the (002) line.

4.2.3.2 X-Ray diffraction patterns of graphite and glassy carbon

X-Ray crystallography is a very powerful tool for
deciphering the structure of the wide variety of carbons
available.   A crystalline material such as natural graphite,
gives sharp, well-defined X-ray diffraction lines, materials
with lower degrees of crystallinity give more diffuse peaks
or indeed complete absence of certain peaks.   Natural
graphite has been extensively studied by X-ray crystallo-
graphers.   As discussed earlier, there is perfect orientation
(ABABAB or ABCABC) between layers as represented in figure
4.2-2 (a).   The X-ray diffractions of graphite,
therefore, show a definite three-dimensional structure which
represents the stable Bernal structure.   The peak of highest
intensity is derived from the spacing between extensive
graphite sheets and is designated (002) with a Bragg or inter-
layer spacing of 3.355Å.   A second type of peak, (100),
related to the spacing between carbon atoms within a sheet is
also observed.   At the same time, because of perfect orien-
tation between the layers, strong (hkl) lines are seen.

Figure 4.2-3 illustrates the X-ray diffraction pattern
of natural graphite and the gradual transition to the pattern
for two-dimensional graphites.[32]   Gay and Gasparoux[33] have
calculated the relative intensities of diffraction peaks for
graphite as shown in figure 4.2-4.
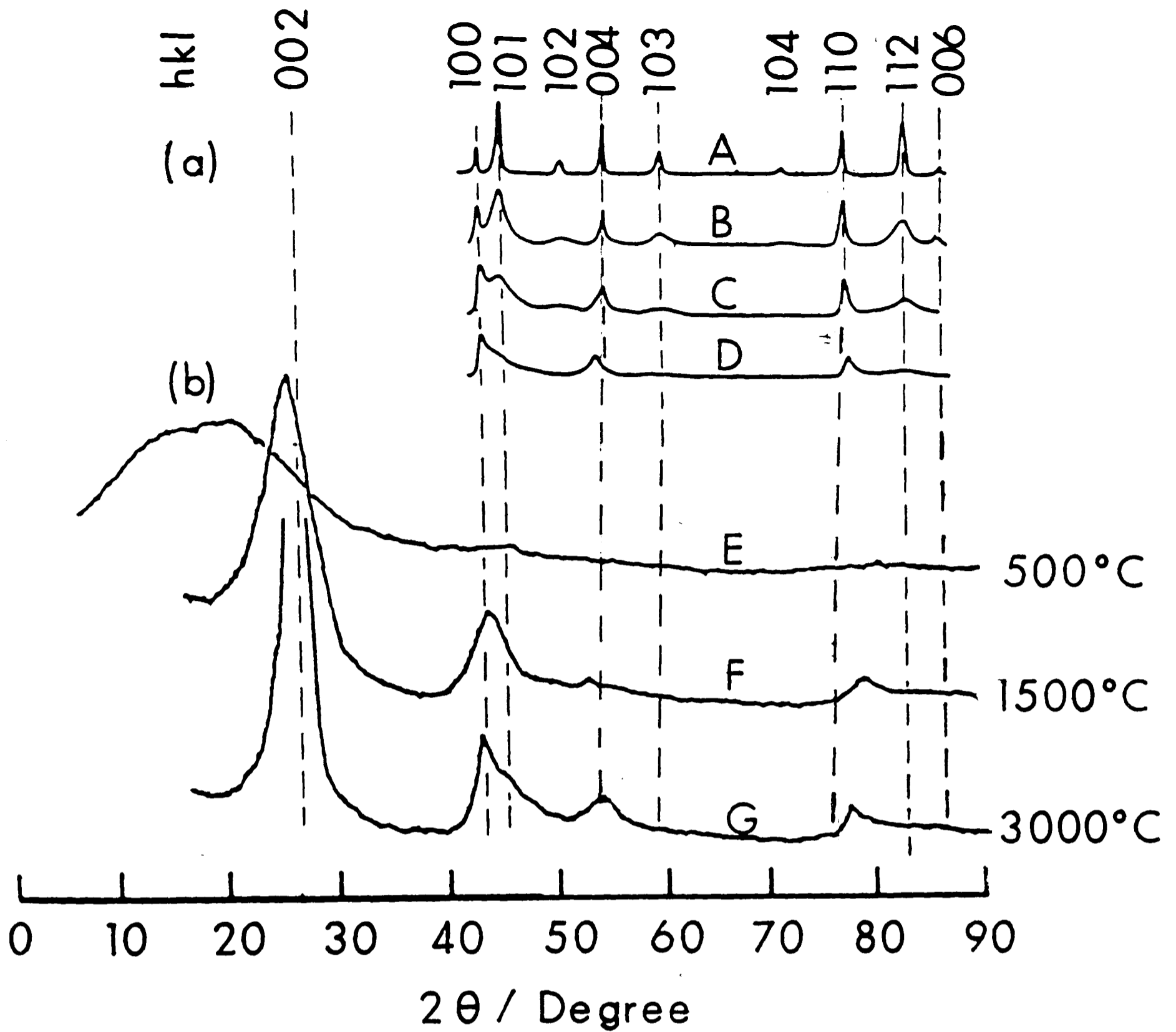
FIG. 4.2-3 : X-RAY DIFFRACTION PATTERNS SHOWING (a) TRANSITION FROM 3d-2d -Graphites, A   D   (b) GLASSY CARBON AT DIFFERENT TEMPS.
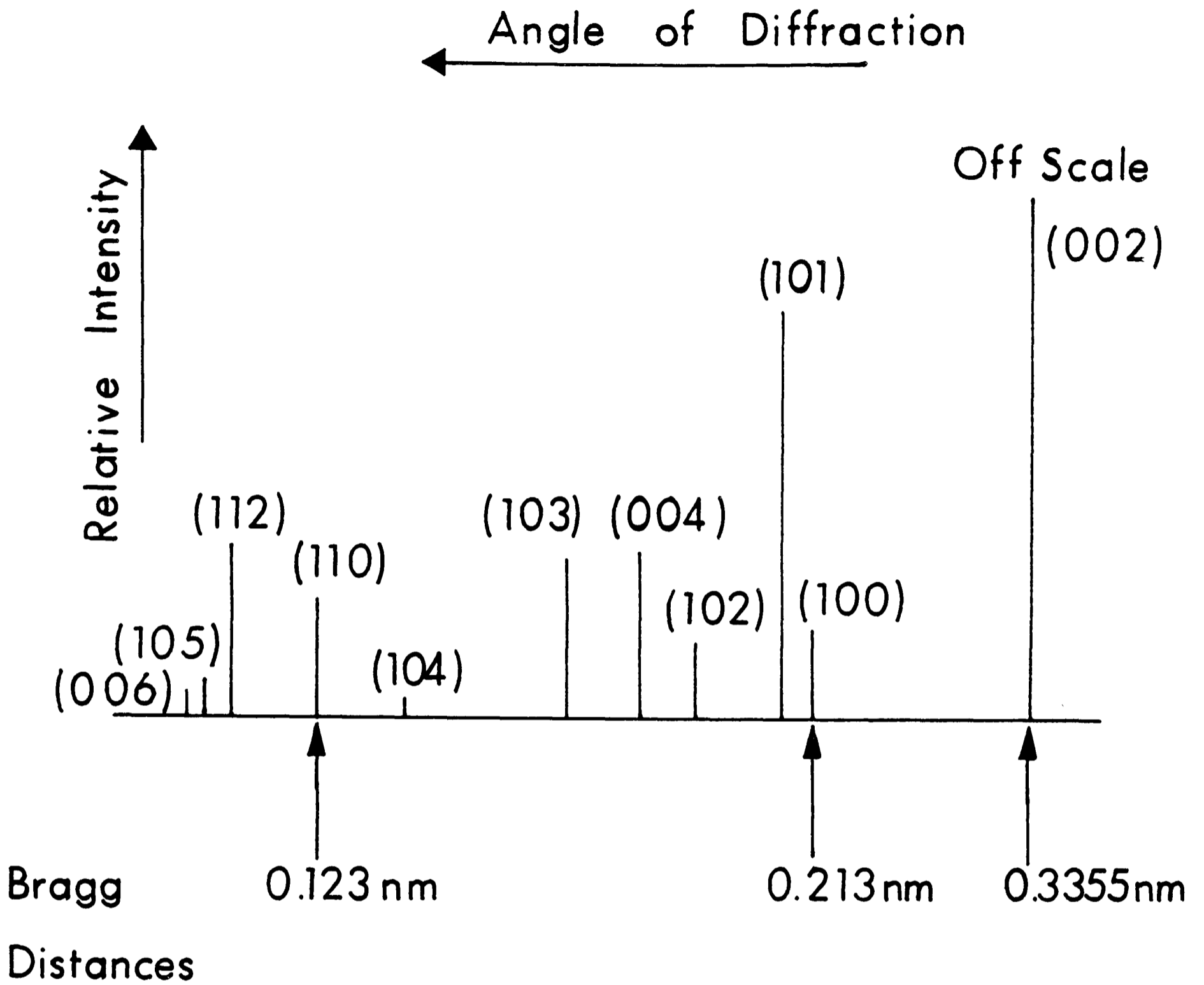
FIG. 4.2 - 4 : RELATIVE   DIFFRACTION
INTENSITIES   OF   GRAPHITE
(from   Ref. 33)

The (00ℓ) lines are very intense and (hkℓ) lines are clearly present. The strong peak at (101) is related to the extent to which extensive graphite sheets are in ABABAB registration. According to Jenkins and Kawamura[34] only carbons which show a definite (101) line can really be defined as graphites. As we pass from a three-dimensional crystal to a two-dimensional crystal there is the gradual disappearance of the (hkℓ) lines and the displacement of the (00ℓ) lines towards lower angles.

Most carbons heated to very high temperatures (temperatures greater than 2000°C) do show extensive graphite-like layers, but only random orientation of the layers as shown in figure 4.2-2(b).

X-ray diffractograms of these carbons show only three peaks corresponding to two-dimensional ordering with the (00ℓ) peaks displaced towards slightly lower angles due to a greater spacing between layers. The (100) peak, which is due to diffraction within each layer, is also observed. The absence of (101) peak or the (hkℓ) lines in these carbons indicate the 'turbostratic' character of these carbons. The peaks are also broad and asymmetrical which is typical of non-graphitic carbons. The X-ray diffractogram of glassy carbon (produced from phenolic resin) also illustrated in figure 4.2-3[35] shows still broader peaks. The (002) diffraction line is very broad, and displaced still further towards low angles and the (101) peak is completely absent. The (100) peak is broad and diffuse and merges into the (004) band. On the other hand, the X-ray diffractogram of amorphous carbon is extremely broad as seen in figure 4.2-3 for glassy carbon heated to 500°C.

4.2.4 Graphitization

4.2.4.1 The meaning of graphitization

As discussed earlier in the section, the stable Bernal structure represents the equilibrium structure of graphite. At pressures below about 130 kbar, carbon in any other form tends to evolve into the Bernal structure if given an opportunity to do so.   This is the process of graphitization. The development of the stable Bernal structure can occur by way of two very different processes.   The first involves the transformation from one well ordered relatively perfect crystallographic phase to another; the second involves the development of an ordered crystalline structure from an initially disordered or defective solid.   Examples of the first would be the thermal graphitization of diamond[35-37] and the transformation of rhombohedral graphite (ABCABC stacking) to the equilibrium hexagonal ABABAB stacking[35-44].   The process which occurs in most synthetic carbons represents transformation of the second type.   Thus, the term graphitization should strictly be used only to refer to the development of three-dimensional order or crystallinity in an initially disordered carbon or a carbon with a different ordered structure.

Based on this ability or inability of carbons to develop the stable Bernal structure two forms of carbon can be distinguished namely the "hard" nongraphitizing carbons and the "soft" graphitizing carbons.   The "hard" carbons which include glassy or vitreous carbon, cellulose carbon and several types

of carbon fibres and chars, retain a very imperfect structure even after prolonged treatment at very high temperatures under ordinary ambient pressures. Substantially complete graphitization of such carbons can be achieved only under the influence of combined high pressure and high temperature, or through the action of catalytic agents such as metal carbides at elevated temperatures. On the other hand, with diamond and the "soft" carbons such as conventional petroleum and pitch cokes, pyrolytic carbons full graphitization can occur at ambient pressure as a result of thermal treatment alone. In these cases, graphitization is a thermally activated process[46].

Hard and soft carbons can be distinguished by a study of the X-ray diffraction pattern of carbons. According to Franklin[45] graphitizing and non-graphitizing carbons can be easily distinguished by a difference of the apparent stack height and the apparent layer size observed well below the range of temperatures in which graphitization occurs. For equal apparent layer area, the apparent stack height (average number of layers per stack) is greater for a graphitizing than for a non-graphitizing carbon; thus, the layer stacking is more perfect in graphitizing than in non-graphitizing carbons. A minimum value of layer diameter (L_a) 100-150Å for layer ordering is required at lower temperatures if the carbon is to be graphitizable[45].

Following the explanation of graphitization it has been postulated that the degree of graphitization,(g) can be calculated from $\bar{d}$, the mean interlayer spacing of the material derived from X-ray diffraction measurements by the equation:

$$g = \frac{3.440 - \bar{d}}{3.440 - 3.354}$$

$$= \frac{3.440 - \bar{d}}{0.086}$$

$\bar{d}$ is known to decrease monotonically with the development of the structure from $\bar{d} \geqslant 0.344$ nm in disordered carbon to 0.3354 nm for near perfect graphite at room temperature.
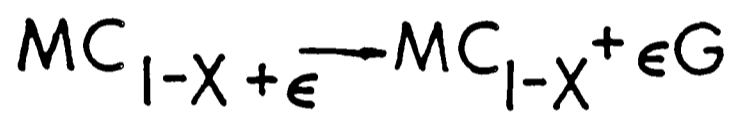
4.2.4.2 Nature of the graphitization process

The carbonization of phenolic resins up to 1000°C leads to the formation of disordered or amorphous carbons. Heating to temperatures up to 3000°C[46] then produces partially ordered or turbostratic carbons which include small clusters of carbon atoms some of which have a proto-graphitic structure. The model is often called the turbostratic model and was first proposed by Warren[46]. Carbon blacks can also be described by the turbostratic model. In these forms of carbon, graphitic planes of aromatic rings, though present, are not regularly registered as seen in graphite but are randomly orientated. The turbostratic model has been extensively explored and developed by Warren and co-workers[46-51], Franklin[45,52,53] and Bacon[54-58]. According to these workers, the growth of both apparent crystallite size and layer ordering in graphitization occurs due to the growth of both whole layer plane segments rather than the motion of individual atoms. The inadequacies of the turbostratic model was first pointed out by Mering and Maire[59]. They proposed a model based on the existence

of 'interstitial' carbon atoms firmly attached to each side
of each plane of disordered graphitized carbons. These
interstitials are assumed to be the cause of the lattice
distortion and increased interlayer spacing. Different
concentrations of interstitial defects account for the
differences in the properties and graphitization behaviour
of carbons[60,61]. Schiller and Mering[62] explained the
graphitization process in terms of an initial transition from
a random to an ordered arrangement of the interstitials
relative to the hexagonal structure of the layers to which
they are attached followed by the removal of these defects
from first one side and then the other of each layer resulting
in the formation of an ordered ABABAB stacking sequence and
the properties of graphite. Mering acknowledged two
deficiencies of the model. Firstly, the studies were done
on a single class of graphitizing carbons (polyvinylchloride
and conventional pitch cokes) and its applicability to other
carbon types such as carbon blacks was not established.
Secondly, there is little direct evidence for the physical
reality of the postulated interstitial imperfections. As in
Mering's model, Ruland[63,64] also attributed graphitization
to the annealing out of defects and Pacault[65] also indicated
that the elimination of defects during high heat treatment
is important in the graphitization process. Graphitization
can, therefore, be more aptly described in terms of the
progressive removal of defects within and between the layers
which stabilize the disordered structure.

4.2.4.3 Catalytic Graphitization

It is well established that the rate and degree of graphitization can be greatly accelerated bu the presence of some catalysts. This enhancement, is, of course, most dramatic in the case of carbons which do not graphitize significantly under the influence of thermal treatment alone. For these carbons the effectiveness of a graphitization aid depends on its ability to promote a substantial reorganization of the structure.

A number of carbides and carbide-forming metals are well-known graphitization catalysts[66,67]. According to Fitzer et al.[66] and Gillot et al.,[67] fine carbide particles can burrow randomly through a glassy carbon matrix, ingesting carbon on the leading surface of the particle and depositing it as graphite at the tailing surface as illustrated in figure 4.2-5. It is postulated that free metal diffuses along the surface of the carbide particle to react with disordered carbon. In this way, 2-5 weight percent of vanadium carbide can completely graphitize furfuryl alcohol coke in 20 hrs at 2200°C.[67] Schwartz and Bokros[68] worked on the graphitization of pyrolytic carbon codeposited with titanium. A titanium content of 5-7% resulted in complete graphitization after 4 hrs at 2200°C. Nickel is another well known catalyst for graphitization and, at high pressures, it is important for the formation of diamond[69-71]. Robertson[71] also reported catalytic effects of iron and cobalt. The nickel apparently catalyzes the pyrolysis process[72] as well as the graphitization. In addition, the influence of iron on the graphitization of

DISORDERED CARBON

CARBIDE

M

C

M

GRAPHITE

$MC_{1-X} + \epsilon C \longrightarrow MC_{1-X} + \epsilon$

OR

$M + (1-X)C \longrightarrow MC_{1-X}$

$MC_{1-X} + \epsilon \longrightarrow MC_{1-X} + \epsilon G$

OR

$MC_{1-X} \longrightarrow M + (1-X)G$
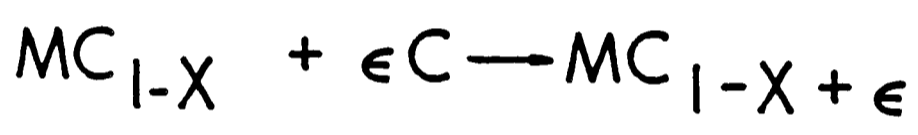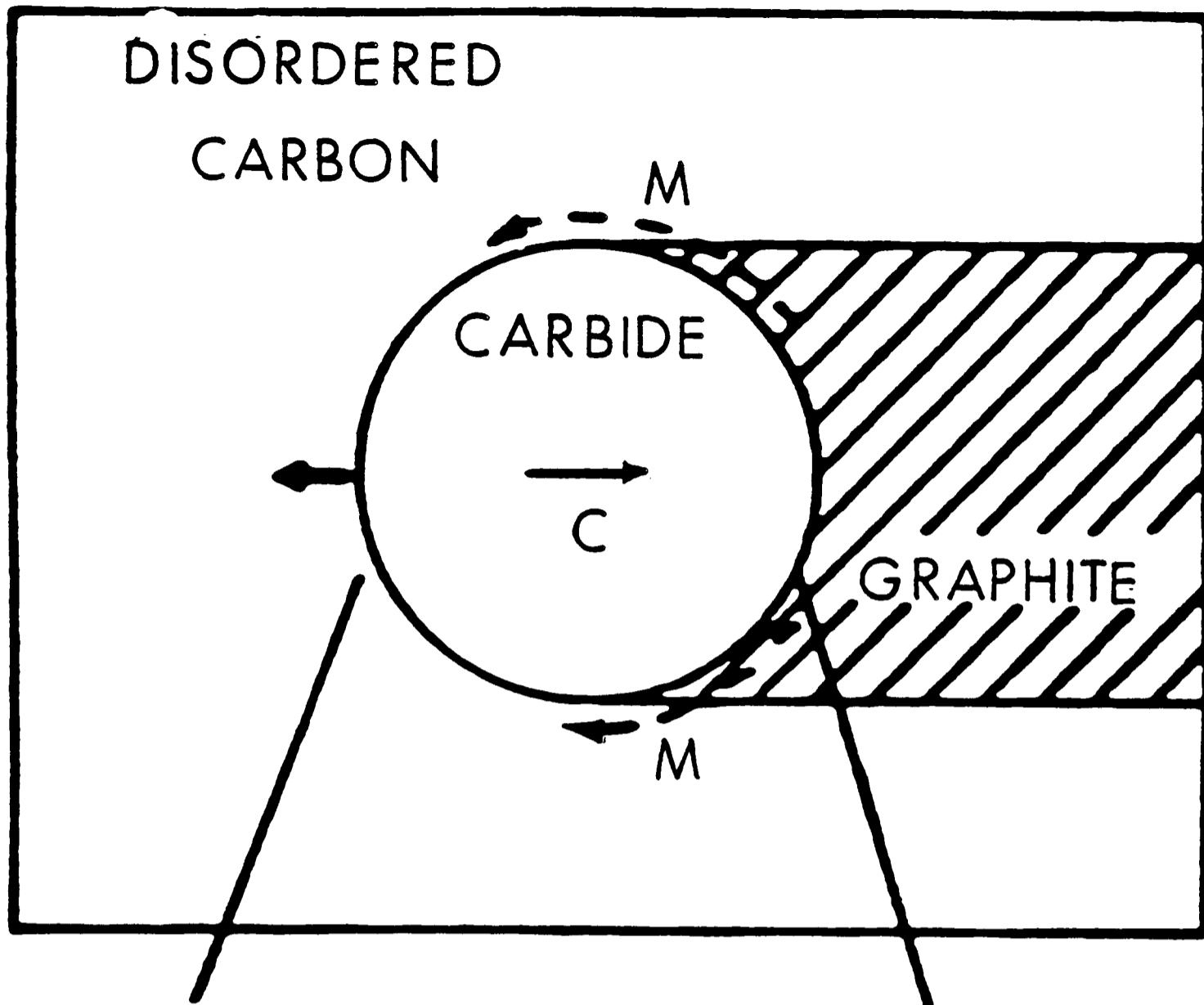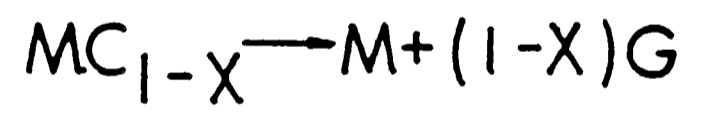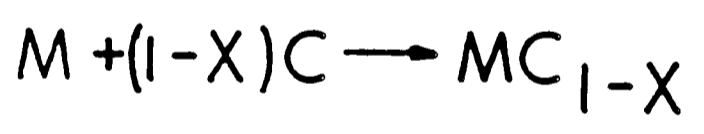
FIG. 4.2 - 5 : MIGRATION OF CARBIDE PARTICLE THROUGH VITREOUS CARBON MATRIX CONSUMING DISORDERED CARBON AND DISPOSITING GRAPHITE (Refs. 68,69)

hard carbons has been attributed to the formation and decomposition of iron carbide (Fe_3C) under certain conditions[73,74].

Observations made by Noda and Inagaki[75,76] showed that graphitization of petroleum coke and carbon black was enhanced by oxidizing atmospheres. The effect decreased with decreasing pressure in air (1 atm to 10^{-2} Torr). It seems likely that oxygen attacks chemically active defect sites, such as distorted or cross-link bonds, which must be removed for graphitization to proceed. A mechanism of this type has also been suggested by Pearce and Heintz[77].

CONCLUSIONS: CHAPTER 4

Today, there are a large number of synthetic carbons available commercially. The X-ray diffraction technique can be valuable in studying the structure of the available carbons, bearing in mind that only carbons exhibiting X-ray diffraction pattern characteristic of the true Bernal Structure can be termed true 3d-graphites.

Some amorphous carbons are called "soft" carbons, as heating to temperatures in the range 2500-3000°C, form true three-dimensional graphite crystallites having the Bernal Structure in which graphitic layers of hexagonally arranged carbon atoms are present correctly registered in the sequence ABABAB... Other amorphous carbons are called "hard" carbons and these carbons will not form 3-dimensional Bernal graphite when heated to 2500-3000°C. Instead they form graphites with random orientation of graphitic sheets. These graphites are also called turbostratic graphites. They do not convert to 3-dimensional graphite except under high pressure and temperature combined, or through metal catalyzed graphitization. The turbostratic graphites may also be called 2-dimensional graphites. Layer spacing in 3-D graphite is 3.354Å while in 2-D graphite it is around 3.40Å. The two forms are easily distinguished by X-ray crystallography since the 3-D graphites show (hkℓ) reflections and, in particular, a strong (101) reflection whereas the 2-D graphites show only (ooℓ) and (hko) reflections which are rather diffuse and may be asymmetric reflecting crystallite size in the region of 100Å. Some forms of carbon will, therefore, be examined in Chapter 6

to determine their structure.

The phenol-formaldehyde resins used in the work yield 2-dimensional graphites as do carbon blacks on heating to high temperatures.

References Chapter 4

1. Shindo, A., J.Ceram.Ass.Japan 69 (1961) C195.

2. Tang, M.M. and Bacon, R., Carbon 2 (1964) 211.

3. Davidson, J.W., Brit.Patent 860,342 (1961).

4. Zinke, A., J.Appl.Chem., 1 (1951) 257.

5. Fitzer, E., Schäfer, W. and Yamada, S. Carbon, 7 (1969) 643.

6. Ouchi, K. and Honda, H., Fuel, 38 (1959) 429.

7. Christu, N., Fitzer, E., Kalka, J. and Schäffer, W., J.Chem.Phys. (Special Issue), p.50 (1969).

8. Schäfer, W., J.Chim.Phys. (Special Issue), p.50 (1969).

9. Schäfer, W., Ph.D.Thesis, Karlsruhe University, W.Germany, 1969.

10. Fitzer, E. and Schäfer, W., Carbon, 8 (1970) 353.

11. Jenkins, G.M. and Kawamura, K. in Polymeric Carbons, Cambridge University Press, 1976.

12. Fitzer, E. and Schäfer, W., Carbon, 7 (1970) 643.

13. Debye, P. and Scherrer, P. Physik.Z., 18 (1917) 291.

14. Hull, A.W., Phys.Rev., 20 (1922) 113.

15. Bernal, J.D. Proc.Roy.Soc.(London), A100 (1924) 749.

16. Lipson, H. and Stokes, A.R., Proc.Roy.Soc.(London) A181 (1942) 93.

17. Scherrer, P., Nachr.Ges.Wissensch.Gottingen, 2 (1918) 98.

18. Drenck, K., Ph.D.Thesis, Copenhagen (1959).

19. Klug, H.P. and Alexander, L.E., X-Ray Diffraction Procedures, John Wiley, New York (1954).

20. Warren, B.E., J.Chem.Phys., 2 (1934) 551.

21. Warren, B.E., Phys.Rev., 59 (1941) 693.

22. Franklin, R.E., Proc.Roy.Soc.(London), A209 (1951) 196.

23. Diamond, R., Proceedings of the Third Carbon Conference, p.367, Pergamon Press, London and New York (1959).

24. Biscoe, J. and Warren, B.E., J.Appl.Phys., 13 (1942) 364.

25. Diamond, R. Ph.D.Thesis, Cambridge (1956).

26. Diamond, R., Acta Cryst., 10 (1957) 359.

27. Diamond, R., Acta Cryst., 11 (1958) 129.

28. Scherrer, P., Nachr.Akad.Ges.Wiss.Gottingen, 2 (1918) 98.

29. Franklin, R.E., Proc.Roy.Soc.(London), A209 (1951) 196.

30. Mering, J. and Maire, J., J.Chim.Phys., 57 (1960) 803.

31. Austin, A.E., Proceedings of the Third Conference on Carbon, Buffalo, 1957, Permanon Press, New York, 1959, p.389.

32. Kurydyumov, A.V. and Pilyankevich, A.N., Crystallography, Vol.13, 1968, 245.

33. Gay, R. and Gasparoux, H., Les Carbones, Vol.1, p.63.

34. Noda, T., Inagaki, M., Yamada, S., J.of Non-crystalline Solids 1 (1969) 285.

35. Ishikawa, T. and Yoshizawa, S., Kogyo Kagaku Zasshi, 66 (1963) 933.

36. Mizushima, S., Proc.Conf.Carbon, 5th, Penn.State, 1961, Vol.2, Pergamon, New York, 1963, p.439.

37. Pandic, B., Proc.2nd.Conf.On Industrial Carbon and Graphite, Soc.Chem.Industry, 1966, p.131.

38. Noda, T., Inagaki, M. and Sekiya, T., Paper-III 24-1, Symposium on Carbon, Tokyo, 1964; Carbon, 3 (1965) 175.

39. Fishbach, D.B., Appl.Phys.Letters, 3 (1963) 1968; Fishbach, D.B., Nature, 200 (1963) 1281.

40. Bragg, R.H., Crooks, D.D., Fenn, R.E.,Jr., and Hammond, M.L., Carbon, 1 (1964) 171.

41. Kotlensky, W.V. and Martens, H.E. Proc.Conf.Carbon, 5th Penn.State, 1961, Vol.2, Pergamon Press, 1963, p.625.

42. Moore, A.W., Ubbelohde, A.R. and Young, D.A., Proc. Roy.Soc.(London), A280 (1964) 153.

43. Noda, T., Carbon, 6 (1968) 125.

44. Bale, E.S., Paper III-3, Conference on Structural Studies of Partially Ordered Materials, University of Sussex, April, 1969.

45. Franklin, R.E., Proc.Roy.Soc.(London), A209 (1951) 196.

46. Warren, B.E., Phys.Rev., 59 (1941) 693.

47. Biscoe, J. and Warren, B.E., J.Appl.Phys., 13 (1942) 364.

48. Houska, C.R. and Warren, B.E., J.Appl.Phys., 25 (1954) 1503.

49. Warren, B.E., Proc.Conf.Carbon, 1st and 2nd, Buffalo, 1953, 1955, Waverly Press, University of Buffalo, Buffalo, N.Y., 1956, p.49.

50. Warren, B.E. and Bodenstein, P., Acta Cryst., 18 (1965) 262.

51. Warren, B.E. and Bodenstein, P., Acta Cryst., 20 (1966) 602.

52. Franklin, R.E., Acta Cryst., 3 (1950) 107.

53. Franklin, R.E., Acta Cryst., 4 (1951) 253.

54. Bacon, G.E., Acta Cryst., 3 (1950) 137.

55. Bacon, G.E., Acta Cryst., 4 (1951) 558.

56. Bacon, G.E., Acta Cryst., 5 (1952) 492.

57. Bacon, G.E., Acta Cryst., 7 (1954) 359.

58. Bacon, G.E., Proc.Conf.Carbon, 3rd, Buffalo, 1957, Pergamon Press, New York, 1959, p.475.

59. Mering, J. and Maire, J., J.Chim.Phys., 57 (1960) 803.

60. Schiller, C., Mering, J., Cornualt, P. and F. du Chaffaut, Carbon, 5 (1967) 385.

61. Schiller, C., Mering, J., Cornault, P. and F. du Chaffaut, Carbon, 5 (1967) 507.

62. Schiller, C. and Mering, J., Paper S161, 8th Conference on Carbon, Buffalo, New York, June 1967.

63. Ruland, W., Acta Cryst., 18 (1965) 992.

64. Ruland, W., in Chemistry and Physics of Carbon (P.L. Walker,Jr.ed.), Vol.4, Dekker, New York, 1968, p.1.

65. Pacault, A., in Chemistry and Physics of Carbon (P.L. Walker,Jr.ed.), Vol.7, Dekker, New York, p.107.1967

66. Fitzer, E. and Kegel, B., Carbon, 6 (1968) 433.

67. Gillot, J., Lux, B., Cornault, P. and F.du Chaffaut, Ber.Deut.Keram.Ges., 45 (1968) 224.

68. Schwartz, A.S. and Bokros, J.C., Carbon, 5 (1967) 325.

69. Banerjee, B.C., Hirt, T.J. and Walker, P.L.,Jr., Nature, 192 (1961) 593.

70. Karu, A.E. and Beer, M., J.Appl.Phys., 37 (1966) 2179.

71. Robertson, S.D., Nature, 221 (1969) 1044.

72. Yamai, Y., Nishiyama, Y. and Takahashi, M., Carbon, 6 (1968) 593.

73. Albert, P., Paper 36, Paris Conf. Aspects Fundamentaux de la Carbonisation et de la Graphitisation, Paris, June, 1968.

74. Oberlin, A., Rousseau, F. and Rouchy, J.P., Paper 33, Paris Conf., June 1968, Aspects Fundamentaux de la Carbonisation et de la Graphitisation, J.Chim.Phys., (Special Issue, April), p.160 (1969).

75. Noda, T. and Inagaki, M., Nature, 196 (1962) 772.

76. Noda, T., and Inagaki, M., Carbon, 2 (1964) 127.

77. Pearce, M.L. and Heintz, E.A., J.Phys.Chem., 70 (1966) 1935.

CHAPTER 5

EXPERIMENTAL METHODS AND EQUIPMENTS USED IN PRODUCTION AND CHARACTERIZATION OF POROUS 2D-GRAPHITIC CARBON (PGC)

EXPERIMENTAL METHODS AND EQUIPMENT

5.1 Production of Porous 2 D-Graphitic Carbon (PGC)

5.1.1 Introduction

Knox and Gilbert[1] described a general scheme for the production of a porous carbon which they called porous glassy carbon. As will be discussed in Chapter 6, structural study of this carbon indicated that, in fact it is a 2 D-graphitic carbon. In their process, a phenol-hexamine polymer was produced within a porous template such as silica gel. The silica-polymer material was then heated in an inert atmosphere (nitrogen) up to a temperature of 900°C to carbonise the polymer. Silica was then dissolved out by boiling alcoholic potassium hydroxide. Thermal gravimetric analysis was used to measure the amount of silica that remained in the carbon. The amorphous carbon formed at this stage was then subjected to high temperature treatments to improve its performance in LC. This general scheme is illustrated in figure 5.1.-1. By this method, two reasonably good batches of PGC were produced; (PGC 26 and PGC 19); both used porous silica which was commercially available. Of the two batches, PGC 19, a large particle material, performed very well in GC. PGC 26, a small particulate material designed for HPLC, was found to be very fragile and gave high back pressures which allowed a maximum flow rate of only 0.5 ml/min. but, nevertheless, gave encouraging separation of test solutes. The polymerization pathway of these two batches of PGC is illustrated in figure 5.1-2. In the production of PCG 26, phenol-hexamine (1:3
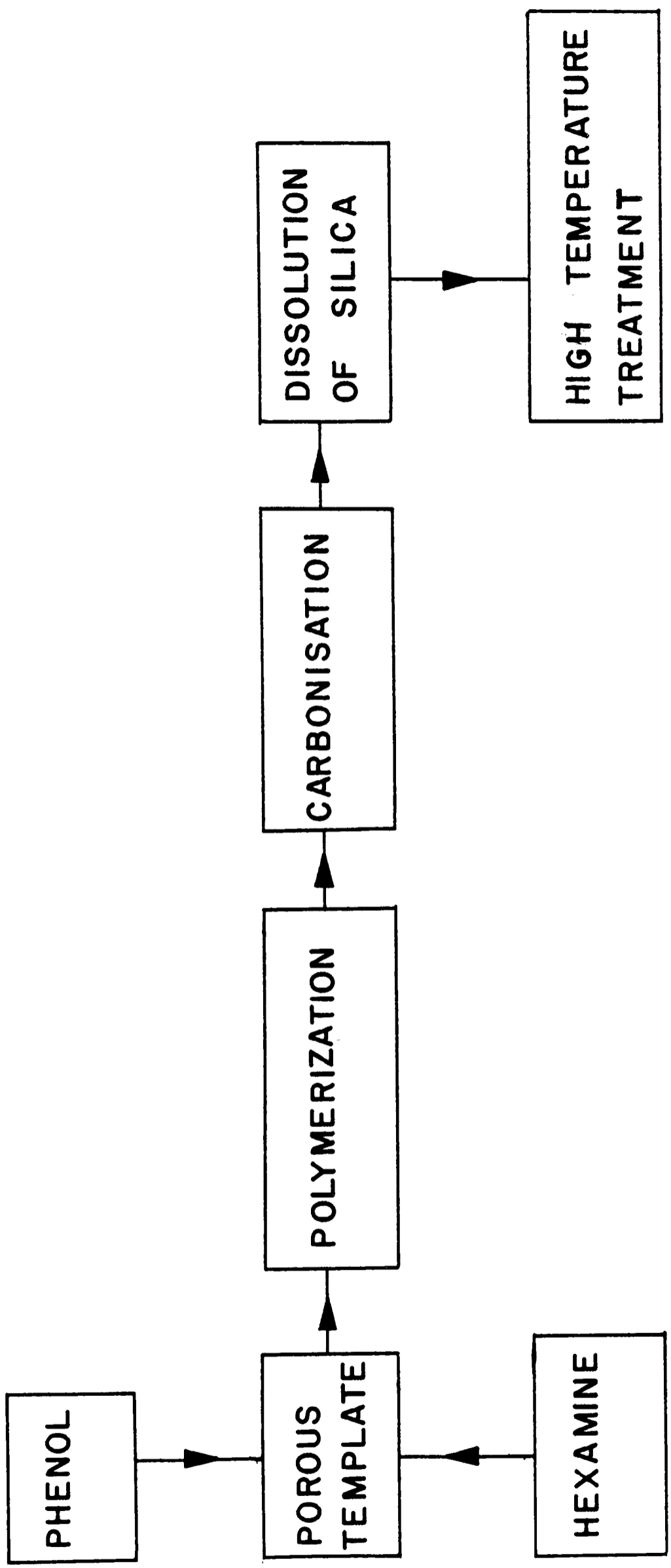
FIG. 5.1-1: GENERAL SCHEME FOR PRODUCTION OF PGC

PGC 26

PHENOL → | HYPERSIL | ── Loaded by evaporation of solution ──→ 150°C 5 hrs → POLYMER

HEXAMINE →

PGC 19

PHENOL → | CPG 60°C,5hrs | → 150°C 5 hrs → POLYMER
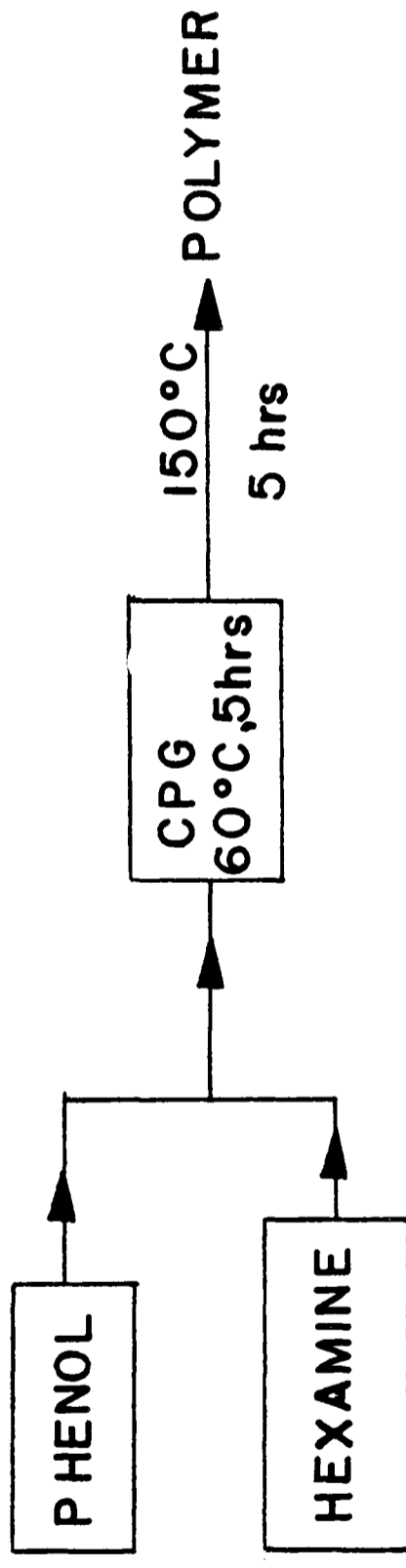
HEXAMINE →
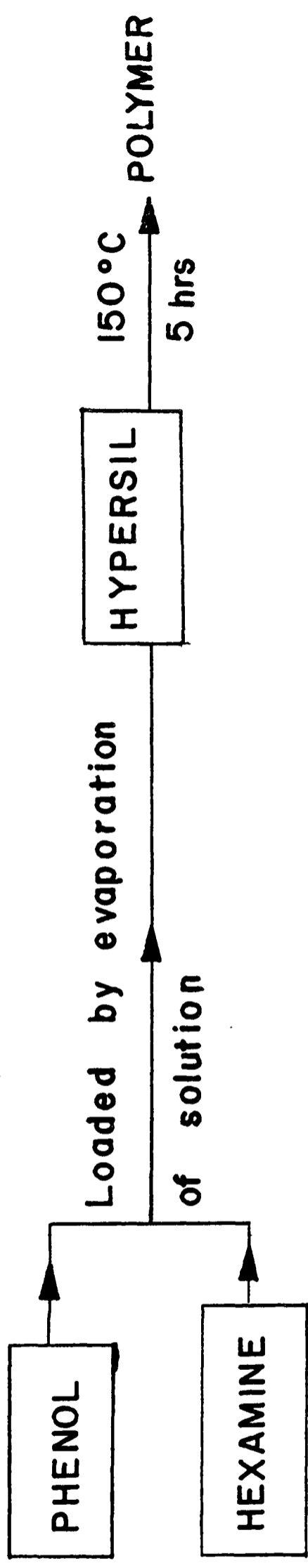
FIG.5.1 - 2 : POLYMERIZATION PATHWAY OF EARLIER
BATCHES OF PGC

molar ratio) melt was loaded on to Hypersil (a 5 μm spherical silica gel) by evaporation of acetone; the material was then subsequently polymerized at 150°C for five hours. Excess phenol-hexamine was used compared with the amount required to fill the pore volume of the silica template. Carbonisation was carried out at 1°C/min up to 400°C and then rapidly to 900°C for five hours. Silica was then dissolved out but 40% of silica still remained in the carbon. In the production of PGC 19, a phenol-hexamine molar ratio of 4:1 was used to fill the pores of the very porous but expensive Corning Porous Glass (CPG) used as template. Phenol-hexamine were melted at 60°C and CPG later added for the impregnation of the polymer at 60°C for 5 hours. The temperature was then raised to 150°C. By this method a relatively high degree of polymer impregnation was achieved.

The results obtained from the early experiments on production of PGC provided a number of conclusions and pointers to desirable improvements both in regard to the template silica gel and to the subsequent stages.

(1) Because of the cost of high grade silica gels it was desirable to develop a cheap in-house method of producing spherical silica gels which could be used as template for GC and LC materials.

(2) Early samples of PGC were too fragile to be routinely used for HPLC. To increase strength it would be necessary to employ more porous templates than those obtainable commercially so that on pyrolysis of the polymer the maximum carbon content could be achieved in the final particles. This necessitated preparation of very porous silica gels and

reinforced the desirability of (1) above.

(3) The difficulty of dissolving out the silica for PGC 26 indicated that the structural units of Hypersil were not sufficiently fused together to give good access to the dissolving reagent (KOH). Thus some type of hydrothermal or sintering treatment would be required to produce an ideal silica gel template. Since sintering is well known to reduce both surface area and pore volume, whereas hydrothermal treatment at moderate temperatures recuces only surface area, while retaining pore volume the second would be preferred.

In regard to the subsequent stages in the procedure a number of other improvements seemed desirable.

(1) Complete pore filling was found to be desirable. Furthermore, hexamine dissolved in phenol melt should be used for polymerization.

(2) Temperature programming of the pyrolysis stage.

(3) Control of dissolution of silica and

(4) High temperature treatment - the importance of avoiding oxidation at high temperatures.

The developments in the process described follow the above suggestions and are further discussed in Chapter 6. The use of new techniques and specially designed equipment were required to achieve this objective. The materials and equipment used in the production of PGC are now discussed.

5.1.2   Experimental

5.1.2.1   Materials

Silica sols were used as starting materials for production of silica gel templates which included Ludox HS40 (Du Pont, Hitchin, Herts, England) and Syton X-30 (Monsanto Ltd., Victoria Street, London) containing 40% w/w and 30% w/w of silica respectively.   Properties of these sols given by manufacturers are listed in table 5.1-1.   Phenol and hexamine, used to form the polymer later to be carbonized, were BDH analar reagents (Birmingham, England).   Petroleum Ether (BP 100-120°C), used in the production of silica gel, was BDH reagent and was the dispersion medium for forming the silica gel emulsion.   Acetone used for washing silica gel was also BDH analar reagent.   Span 80 used as an emulsifier stabilizer was obtained from Fluorochem (Derbyshire, England).

5.1.2.2   Equipment used for the production of PGC

Silverson mixer with variable speed adjustment was used for emulsification (model no.L2R from Silverson Machines Ltd., Waterside, Chesham, England).   By varying the speed of the Silverson mixer the particle sizes can be controlled.   Water baths used for thermosetting were obtained from Grant Instruments (Cambridge).   Drying of samples was carried out in a Belling oven (Townson & Mercer Ltd., Croydon, England).   A 2-litre Autoclave manufactured by C.W. Cook & Sons Ltd. (Albion Works, Birmingham, England) was employed in the preparation of silica (see figure 5.1-3).   The maximum temperature attainable was 400°C, and had a pressure limitation of 300 bars.

Table 5.1-1. Properties of Syton X-30 and Ludox

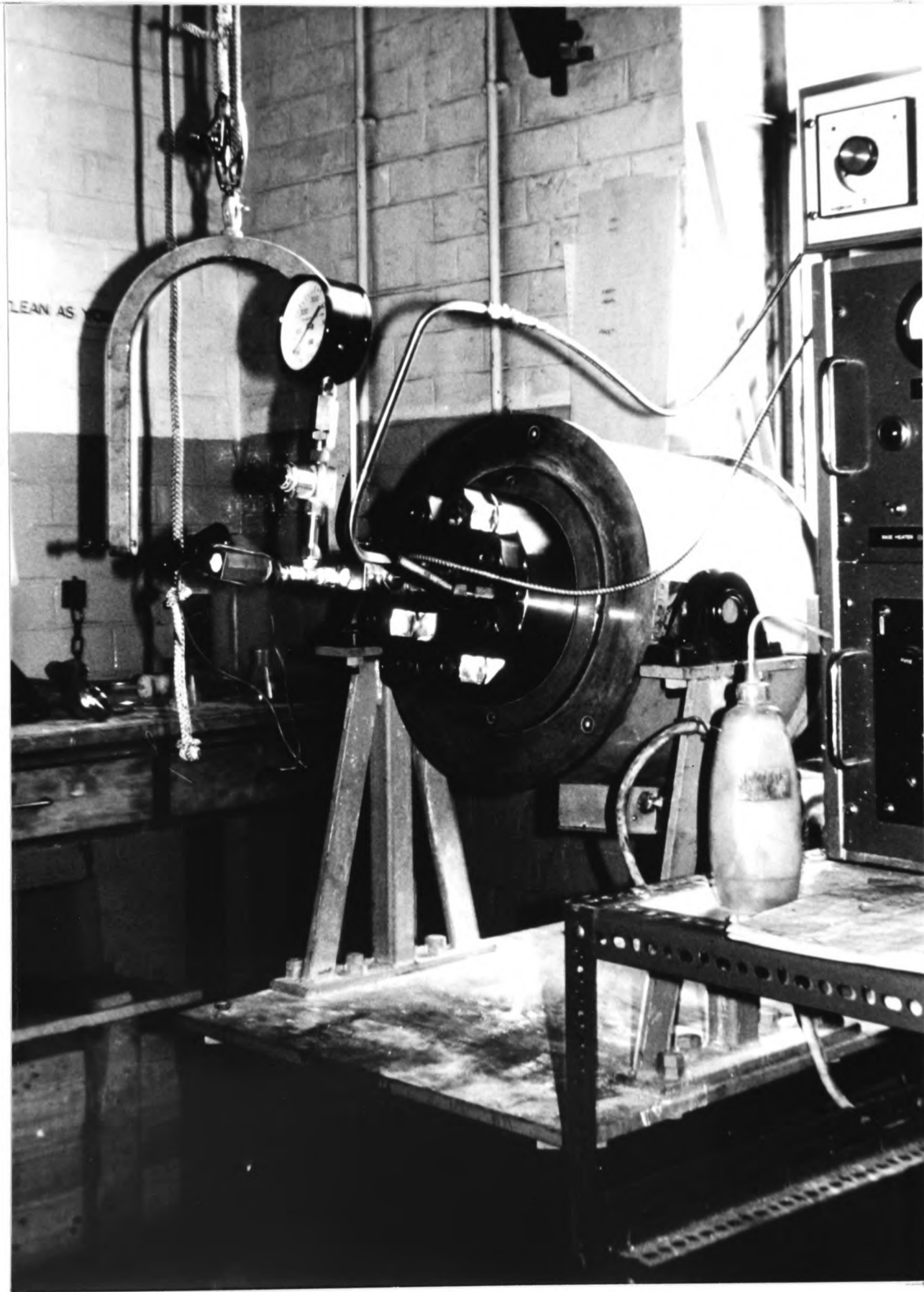|	Syton X-30	Ludox HS40
Particle size (nm)	25	13-14
Specific surface area (m^2/g)	250	210-230
SiO_2 content (% w/w)	30	40
pH (25°C, 77°F)	9.9	9.7
Na_2O content (% w/w) Titratable alkali	0.34	0.43
SiO_2/Na_2O (ratio)	88	90
Chlorides (as NaCl), wt %	0.007	0.01
Viscosity (centipoise)	5.5 at 20°C	17.5 at 25°C
Specific Gravity	1.2 at 15.5°C	1.3 at 25°C

FIG. 5.1 - 3 : ROCKING   AUTOCLAVE

The autoclave rocked at the rate of 20-30 rocks per minute. A Buchner funnel was used to filter both silica and carbon before final drying in the oven. A large Gallenkamp muffle furnace from East Kilbride, Scotland (internal dimensions, 416 x 182 x 130 mm) was used for sintering off silica gels. In early experiments, impregnation and polymerization were carried out in round-bottomed flasks in a K4 electronic oil bath. Subsequently, a rotary apparatus was constructed as shown in figure 5.1-4. It comprised a Towers oven (Towers and Company Ltd., Widnes, Cheshire, England) controlled by a Bikini temperature regulator. The oven was mounted on its side. 3 or 5 litre round flasks rotated on bearing supports by a rotary Büchi motor (supplied by Orme Scientific Ltd., Manchester, England) through a spherical joint. Three furnaces were used for carbonisation. In the early stages of production a Carbolite tube furnace type CFM1-1400 + PiD as shown in figure 5.1-5, was used (Carbolite, Sheffield, England). A temperature programmer series 104, which was obtained from W.G. Pye and Company Ltd., Cambridge, England, was fitted to the carbolite furnace. Samples were contained in stainless steel boats of 20 ml capacity. One end of the ceramic tube was stoppered and the other end was fitted with brass fittings having an inlet for purging of nitrogen and an outlet for the removal of by-products of pyrolysis. Later, the large Gallenkamp furnace, which was used for sintering, was also used for carbonization so as to increase the batch size of carbon produced. Stainless steel beakers of 350 ml capacity were constructed. These were fitted with lids having an inlet tubing for purging of
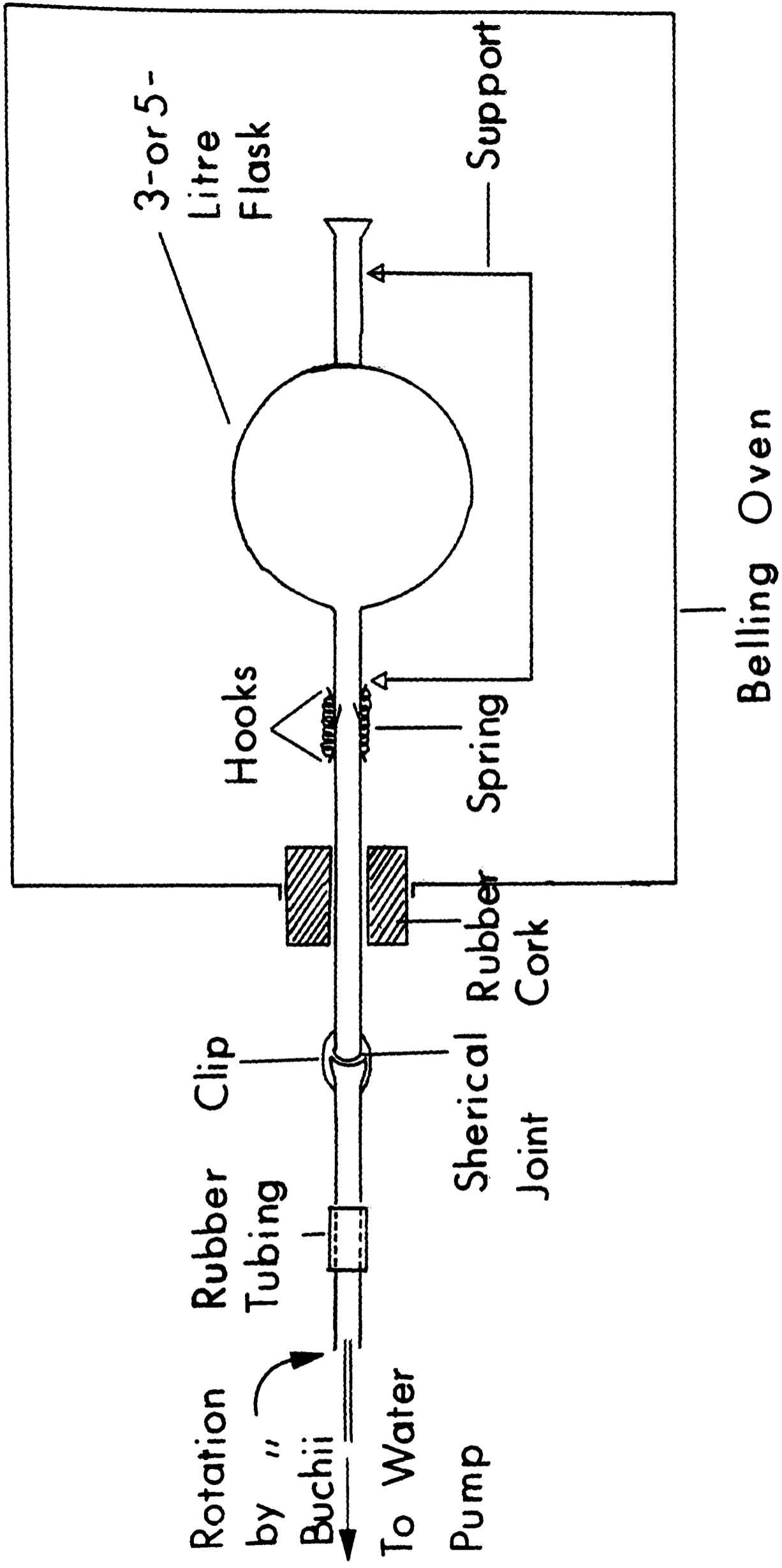
FIG. 5.1-4: ROTARY APPARATUS FOR POLYMERIZATION

FIG. 5.1-5: CARBOLITE TUBE FURNACE

nitrogen (shown in figure 5.1-6). A hole was present in the lid to allow for the release of by-products into the fume-cupboard. The temperature was regulated by means of a Bikini temperature regulator. As there was the need to further increase the batch size and to regulate the temperature precisely, a special rotary furnace (see figure 5.1-7) was used for carbonisation. This furnace was designed in collaboration with Carbolite Furnaces Ltd., Bamford Mill, Bamford, Sheffield, England. The detailed specifications are given in Table 5.1-2. The furnace was designed to rotate a nickel chromium alloy (Inconel 600) retort which extended through the furnace to rest on rollers at each end. The retort was sealed with an O-ringed stainless steel flange which was fitted to a sprocket drive mechanism. The retort could be purged with nitrogen through the rotary seal. The furnace case was hinged at the rear end and opened to allow easy access for retort removal. The retort could contain up to 2 litres of sample. The noxious pyrolysis products were condensed into Wolfe bottles containing 1M sodium hydroxide and the nitrogen remaining was scrubbed in a tower packed with glass beads down which sodium hydroxide (1M) was pumped by a peristaltic pump (Watson Marlow model) at 4 ml per minute. The gas was then vented into a fume cupboard. Nitrogen was controlled by a pressure regulator fed by a length of teflon tubing at the rate of 10 mls per minute. The furnace was fitted with a combined ramp programmer and temperature controller system model 702 automatic controller from Cambridge Process Controls. The microprocessor system in the unit allows fully automatic operation
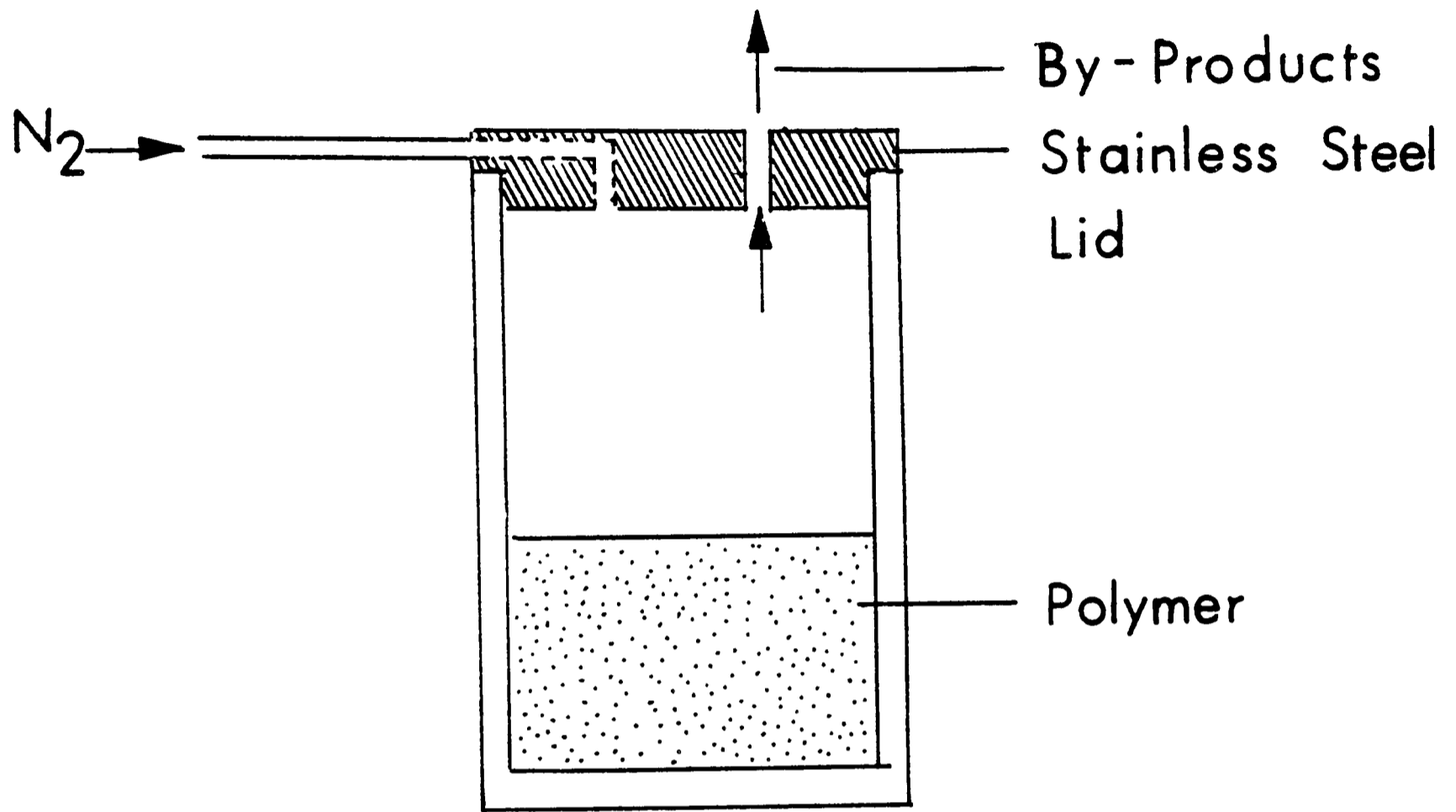
FIG. 5.1 - 6 : STAINLESS STEEL BEAKER

FOR CARBONISATION
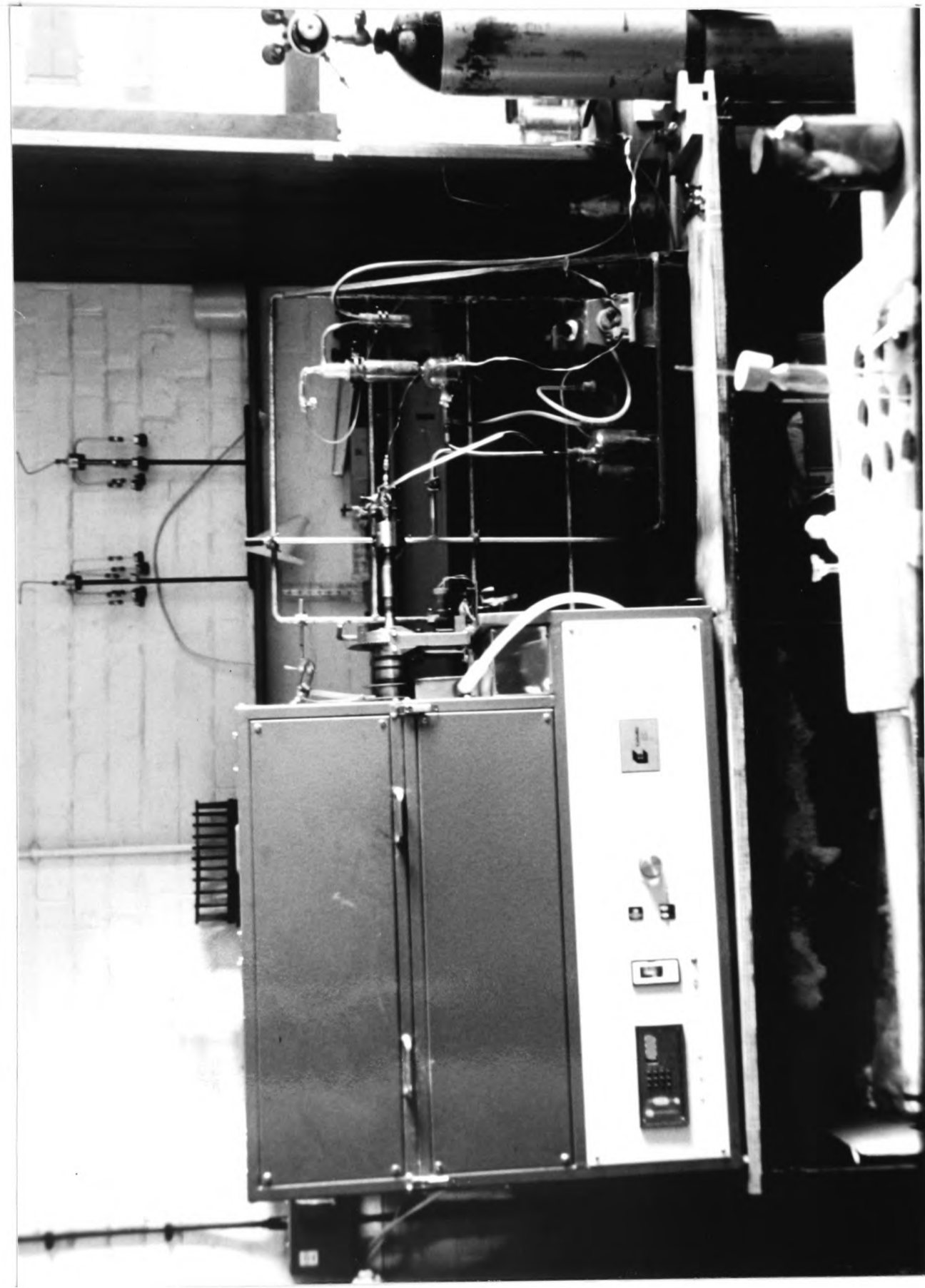
FIG. 5.1-7: ROTARY FURNACE FOR CARBONIZATION

Table 5.1-2. Detailed Specifications of Rotary Furnace

Type of Furnace   - Rotating Retort Furnace

Maximum Operating Temperature   - 1400°C

Retort Dimensions   - 500 mm long x 150 mm I/D
                                     (usable)

Heating Elements   - Silicon Carbide elements
                                     mounted axially about the
                                     retort

Temperature Sensors   - Pt/Pt 13%Rh thermocouples

Temperature Control   - Cambridge Process Controls
                                     702 - 6 segment ramp and
                                     hold programmer/controller

Over-temperature Protection   - Eurotherm 106 controller

Power Control   - Solid State Relays

Maximum Power Consumption   - 12 kW.

Power Supply Required   - 415/240 Volt, 3 phase, 50 Hz,
                                     4 wire and earth, isolated and
                                     fused at 40 amps per pH

Retort   - Inconel 600 with stainless
                                     steel and flanges

Rotating Drive   - DC motor with reduction gearbox

Rotation Speed Control   - Potentiometric speed controller
                                     settable between 0 and 5 RPM

Approximate Overall Dimensions   - 1000 mm H x 700 mm W x 1100 mm L

of the furnace through the complete operating cycle, to a time and temperature sequence programme stored in the unit's memory. This programme is loaded into the memory using a simple calculator style keyboard and display on the front panel of the instrument which is shown in figure 5.1-8. The specifications of the automatic controller are shown in Table 5.1-3. Figure 5.1-9 shows the programming cycle for the carbonization of PGC. Later experiments showed that the plastic tubing used for purging nitrogen allowed small amounts of oxygen into the carbonization system. In the more recent production of carbon these tubings have been replaced by stainless steel tubings.

Dissolution of silica was carried out using stainless steel beakers. The material was well stirred and heated by magnetic stirrers (Voss Instruments Ltd., Essex, England). Thermogravimetric analysis, to determine the percentage of silica still remaining, was carried out with a Stanton Redcroft TG770 thermogravimetric analyser (Stanton Redcroft, London, England). A high temperature furnace for temperatures greater than 2000°C is not available at present in the Department of Chemistry and therefore batches of carbon were sent to one of the following places for further heat treatment.

(i)   Anglo-Great Lakes (AGL), Newburn Haugh, Newcastle-upon-Tyne.

(ii)   Atomic Weapons Research Establishment (A.W.R.E.), Ministry of Defence, Aldermaston, U.K.

(iii) Dr. C. Jenkins, Department of Metallurgy, University College of Swansea, Wales, U.K.

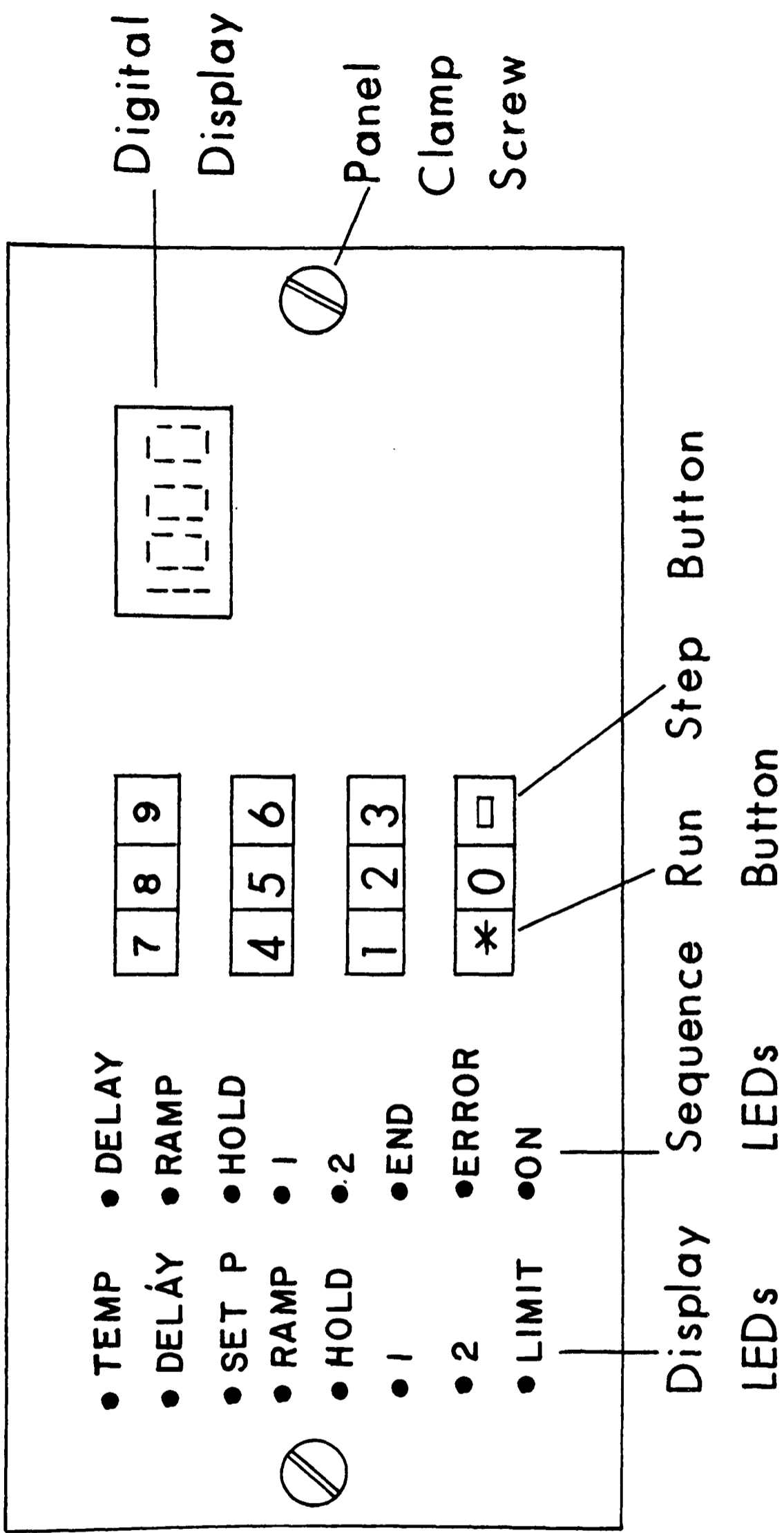(iv)   British Petroleum, Sunbury-on-Thames, Middlesex, U.K.

FIG 5.1-8: FRONT DISPLAY LAYOUT OF THE CARBONISATION FURNACE

Table 5.1-3. Specification of the Automatic Controller

Switch-on time delay   - 0-99hr.59mins. in 1 minute
                                 steps. Delay counts down
                                 to zero then furnace
                                 switches on.

Three Set Points   - 0-1599°C

Three Temperature Ramps   - 5-500°C/hr. First ramp
                                 always increasing, second
                                 and third ramps up or down
                                 depending on subsequent set
                                 points

Three Hold times at Set Point - 0-99hr.59mins. in 1 minute
                                 steps

Temperature Control   - Three term PID

Power Adjust facility   - 0-100% via keyboard entry

Input   - Type R thermocouple (Pt/Pt
                                 13%Rh).

Output   - Logic Drive 15 V.DC.
                                 Fast cycle

Optional Relays   - Volt-free contacts available
                                 at various parts of cycle.
                                 Relay board to be available
                                 as retrofit kit

Safety   - Thermocouple break or reverse
                                 polarity switch off output.
                                 Cold junction compensation
                                 provided.

Electrical supply   - 220/240 or 110/120 Volt 50/60
                                 Hz

Dimensions   - 192mm Wide x 96mm High x 220mm
                                 Deep Double DIN cutout.

FIG. 5.1 - 9 : PROGRAMMING CYCLE FOR THE CARBONISATION OF PGC
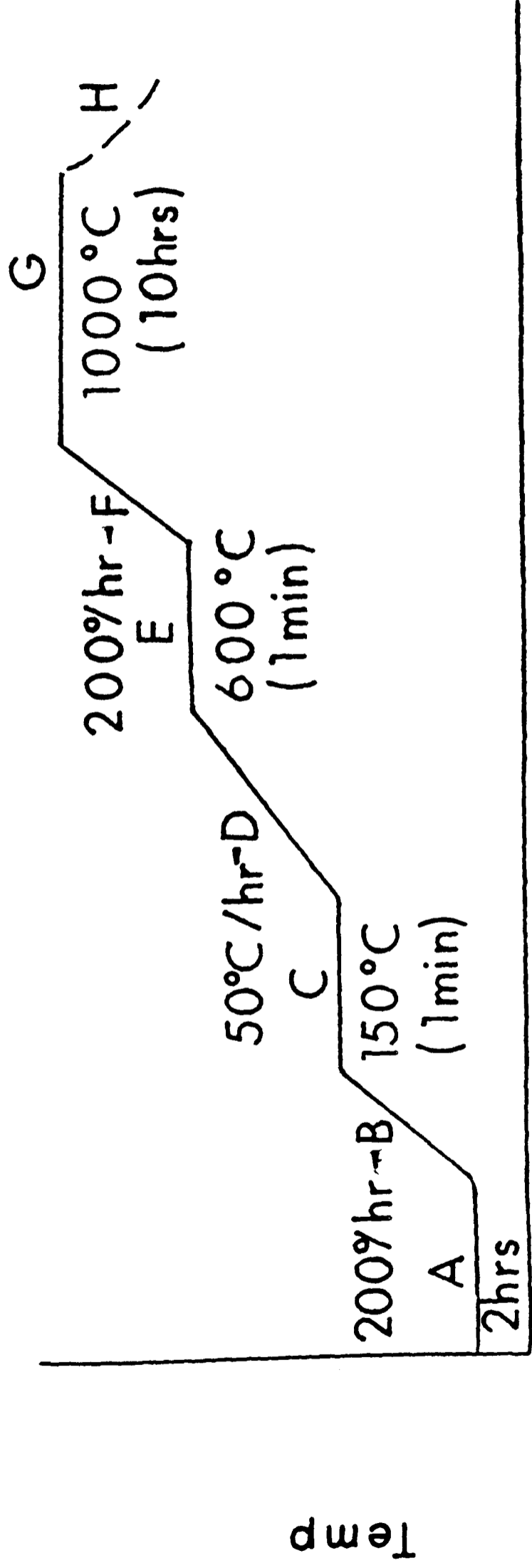
A   Switch-on delay (2 hrs)
B   Ramp 1
C   Hold 1 at Set Point 1
D   Ramp 2
E   Hold 2 at Set Point 2
F   Ramp 3
G   Hold 3 at Set Point 3
H   Switch off and natural cool to ambient

(v) Le Carbone-Lorraine, Gennevilliers, France.

(vi) Centorr Associates, Inc., Suncook, New Hampshire,

U.S.A.

Anglo-Great Lakes Firing Procedure

The graphitizing furnace shown in figure 5.1-10 consists of a 9 ft long carbon tube of approximate 4" bore. The heated portion is 2 ft long. The material to be fired was contained in a well sealed 110 ml graphite capsule which fitted into a larger container of about 1350 ml. The ends of the furnace are capped and pure nitrogen or Argon was passed through the end caps under slight positive pressure. The graphite tube is contained within a bed of carbon black.

The firing regimes for PGCs 57, 59 and 62 are shown in figure 5.1-11.

AWRE Firing Procedure

The apparatus (SPEMBLY FURNACE SB40) used at AWRE is shown in figure 5.1-12. The samples are heated in a stream of argon at 10 cu.ft/hr or 0.5 litres per minute giving a linear velocity of 2.6 cm/min and the total time in the furnace as a whole of 35 minutes.

Firing of samples was conducted by Dr. C. Thomas of AWRE and the firing regime is also illustrated in figure 5.1-11.

Firing Procedure at University College of Swansea by Dr. C. Jenkins

The graphitizing furnace is essentially the same as that

FIG. 5.1-10: AGL GRAPHITIZING FURNACE
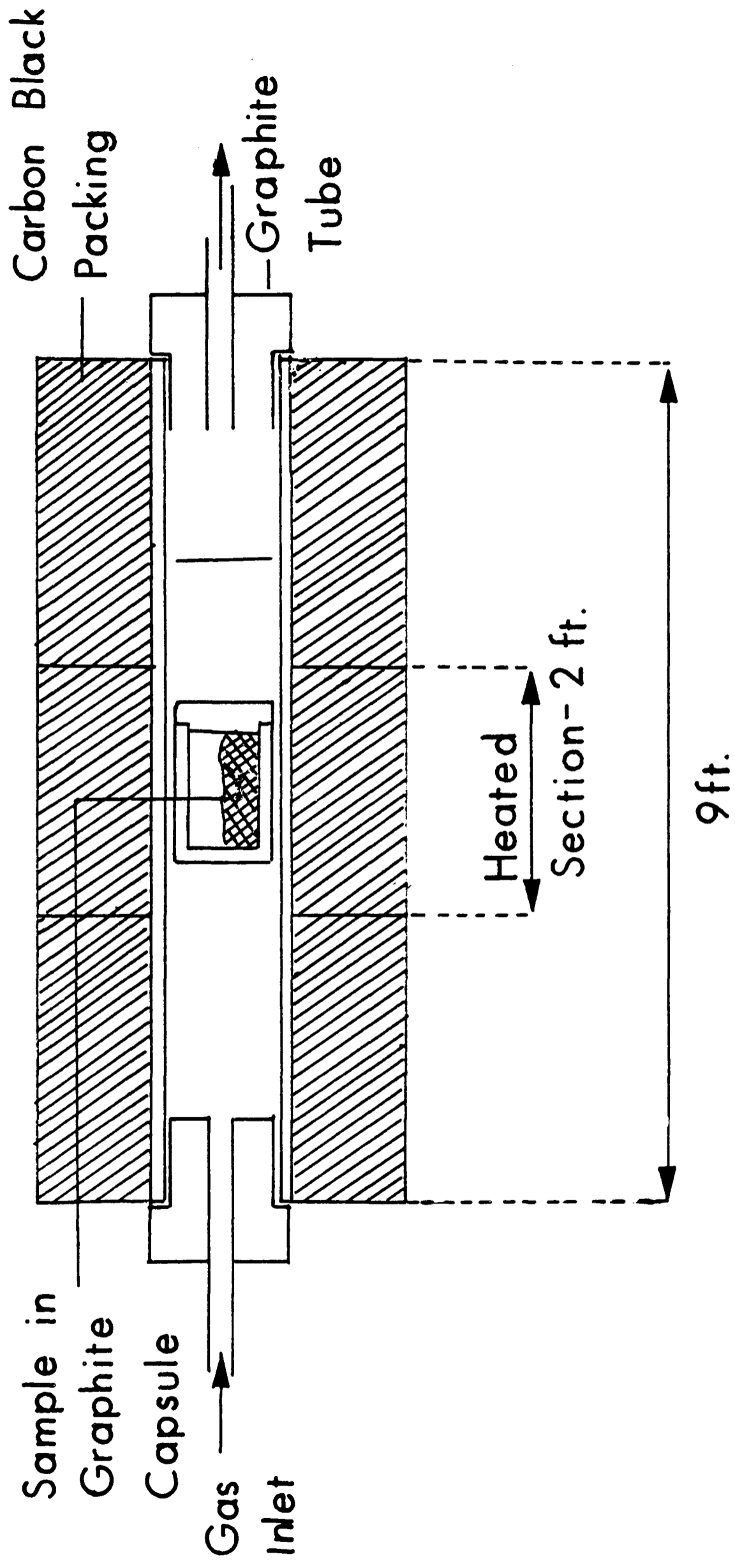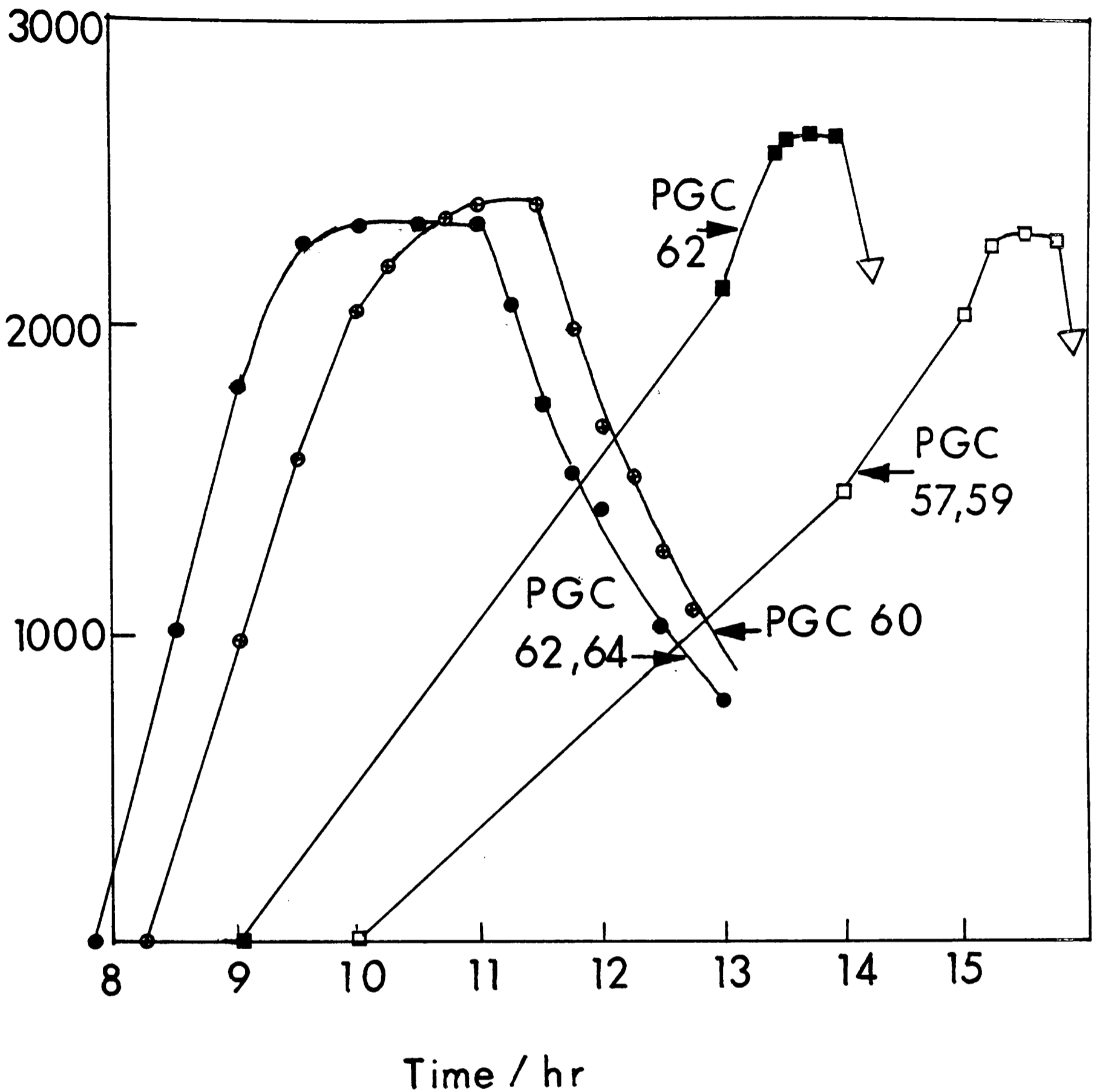
FIG. 5.1-11: FIRING REGIMES FOR PGCs HEATED AT AWRE (●,⊙) AND AT AGL (■,□)

Hot Zone
∽ 30 cms

Total
Length
∽ 100 cms

Graphite
Resistance
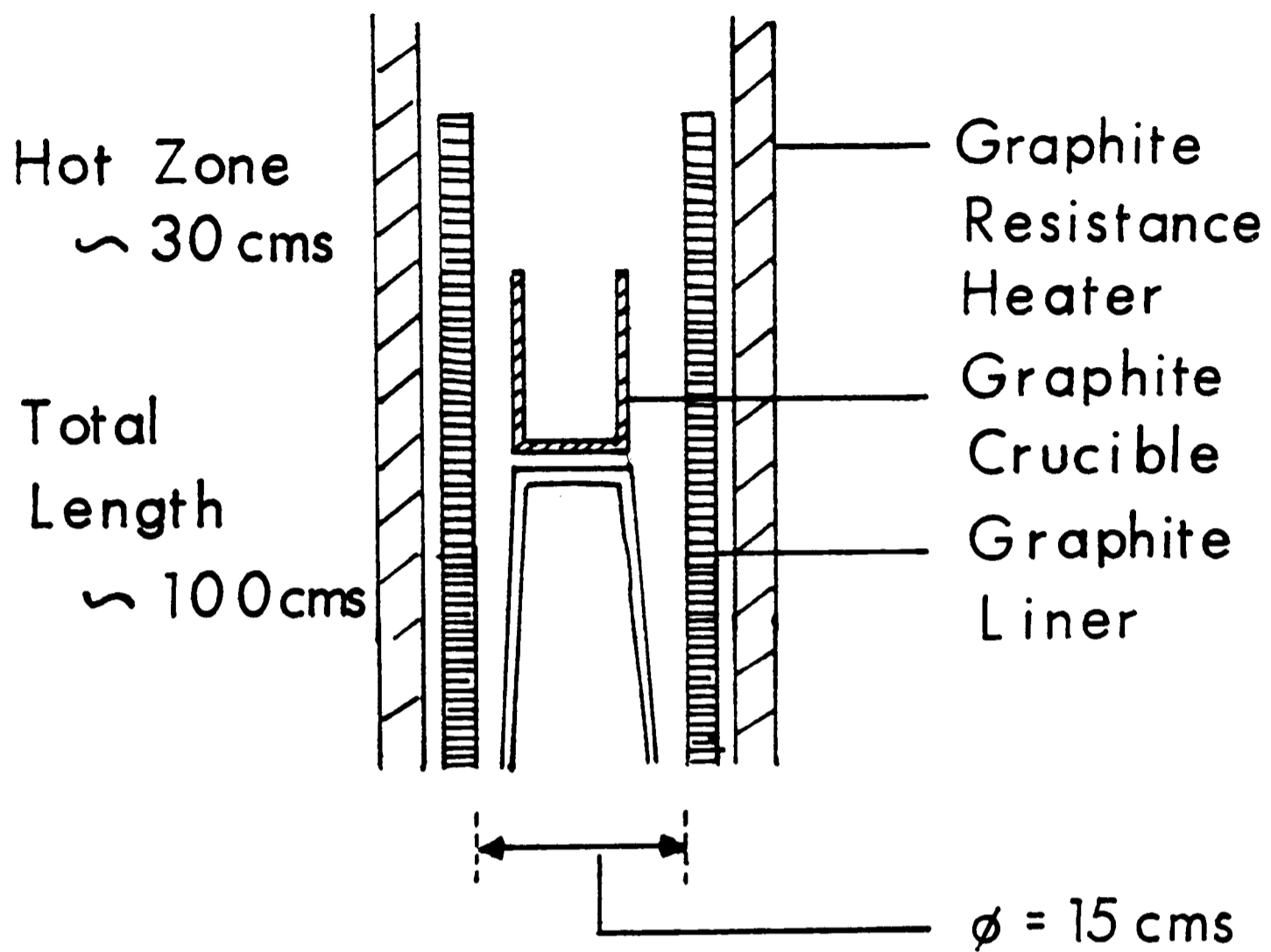Heater

Graphite
Crucible

Graphite
Liner

∅ = 15 cms

FIG. 5.1-12: FIRING APPARATUS
USED AT AWRE

of AWRE except that the furnace is smaller with a heated zone of 10 cm long, and 8 cm diameter. The firing regimes are illustrated in figure 5.1-13.

British Petroleum Firing Procedure

The apparatus used at BP is shown in figure 5.1-14. Helium gas is purged in through holes in the lid of the crucible then up the chimney. Hence some ventilation of the samples is achieved. The samples were first rapidly heated to 1500°C and then at rate of 30°C/min to 2500°C.

Carbone-Lorraine Firing Procedure

The graphitizing furnace used by Carbone-Lorraine is a tube furnace resembling that of Anglo-Great Lakes as shown in figure 5.1-10. The samples were heated in Argon at a rate of 3°C/min from ambient to 1100°C, then at a rate of 4°C/min from 1100°C to 1800°C. Further heating to 2500°C was carried out at a rate of 6°C/min, and the temperature was held for 15 minutes at this temperature.

Centorr Firing Procedure

The samples were fired in a vacuum by Centorr using a High-temperature Vacuum Furnace model 14 which is illustrated in figure 5.1-15. The furnace is mounted on a single pole floor stand with the Vacuum System (or the Evacuation System) immediately behind (or to one side) for maximum efficiency. A vacuum of 10^{-5} Torr is attainable. The furnace consists of a double wall all stainless steel (304L) water-jacketed chamber, inside of which is the heat zone (3" diameter x 3"

Temperature (°C)

Time (Minutes)
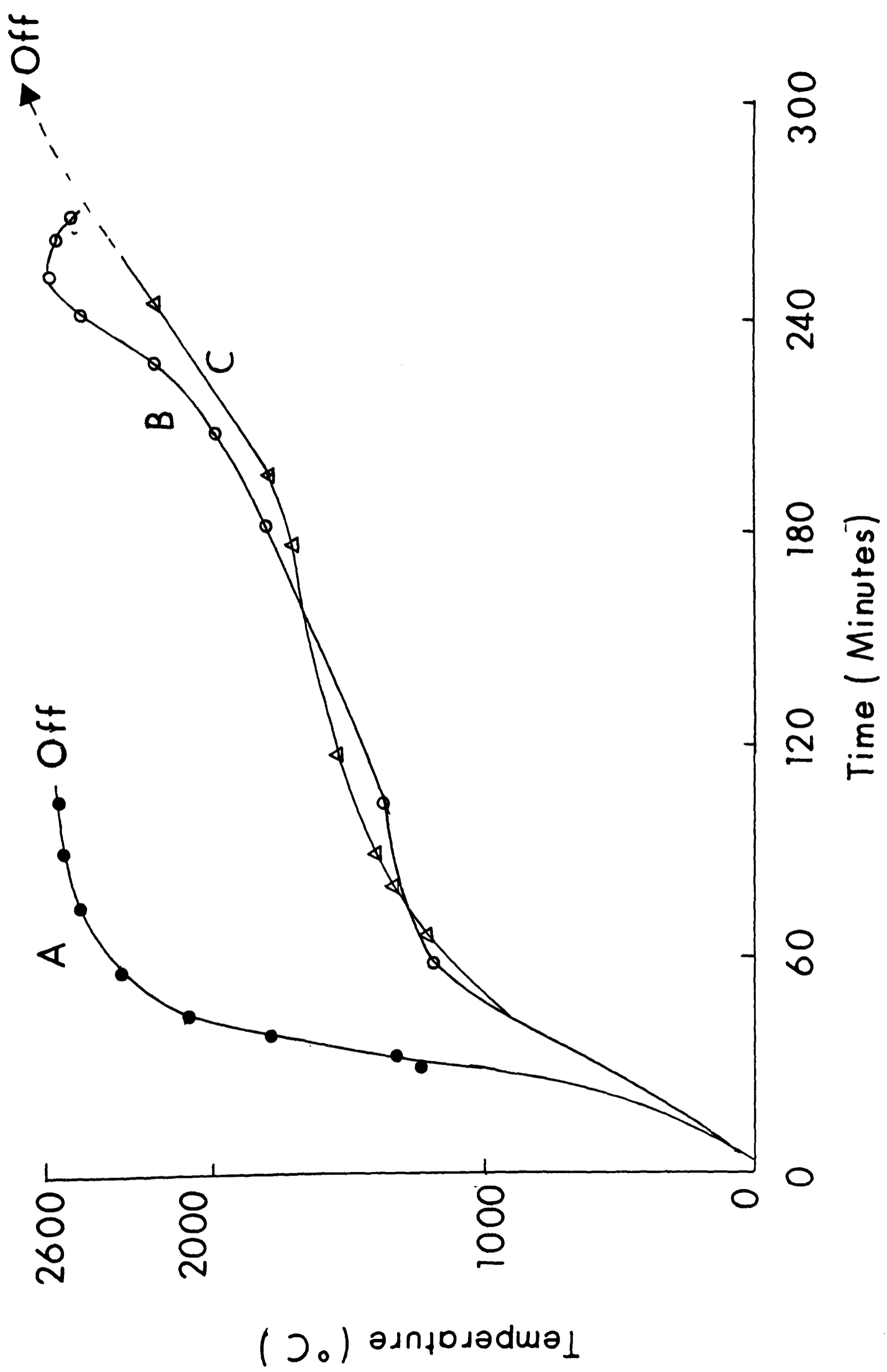
FIG. 5.1-13 : FIRING REGIME AT SWANSEA FOR PGC 70

Graphite Crucible

He →

Water Cooled Jacket

Chimney

Carbon Rod Support

Window

Graphite Heating Element
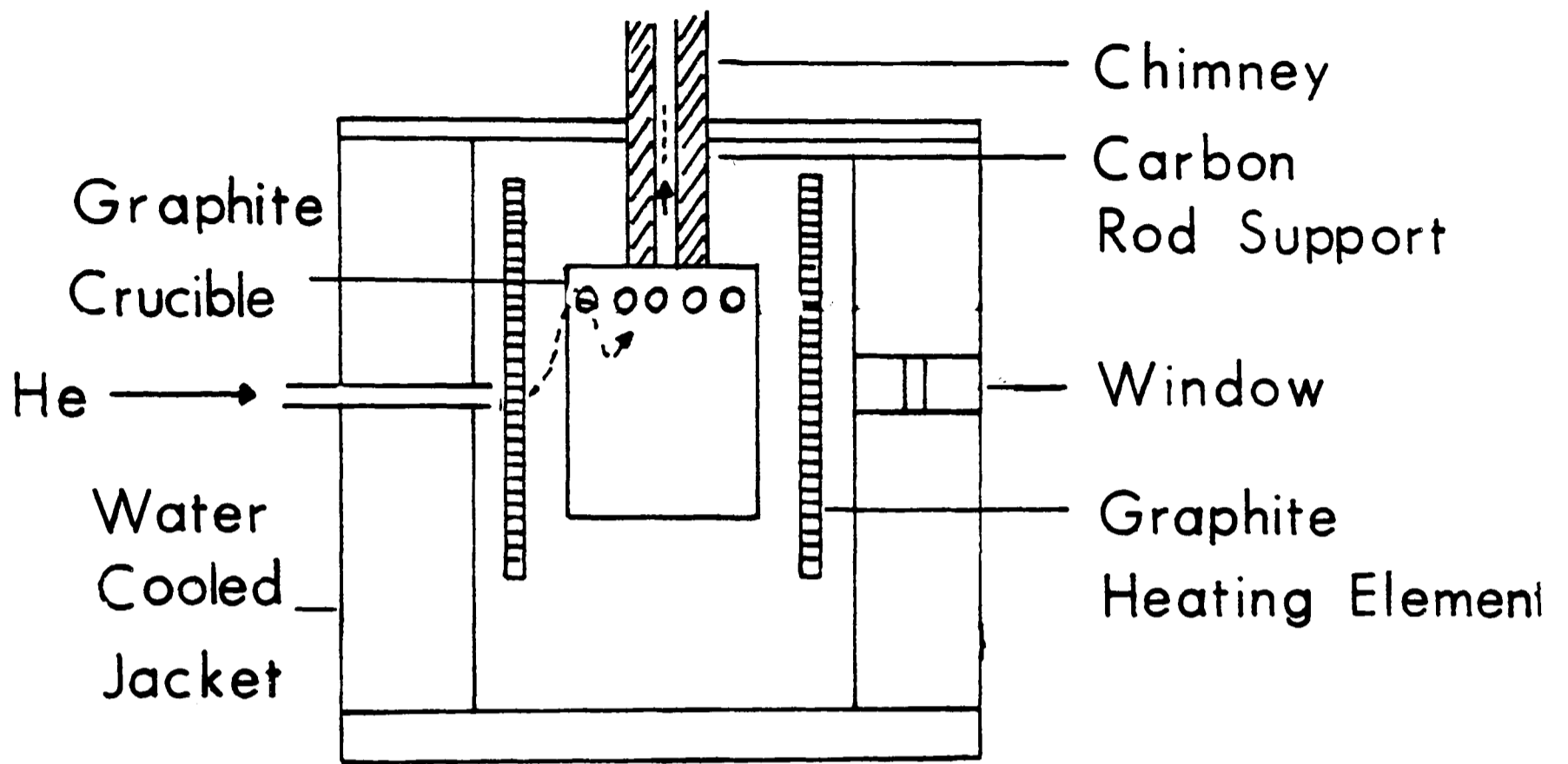
FIG. 5.1 -14 : FIRING APPARATUS AT BRITISH PETROLEUM

Lid

Flange

Power Feed

Top Shield

Water
Cooled Body

Side Shield

Heater Element

Work Support

Bottom Shield

Flange

Lid
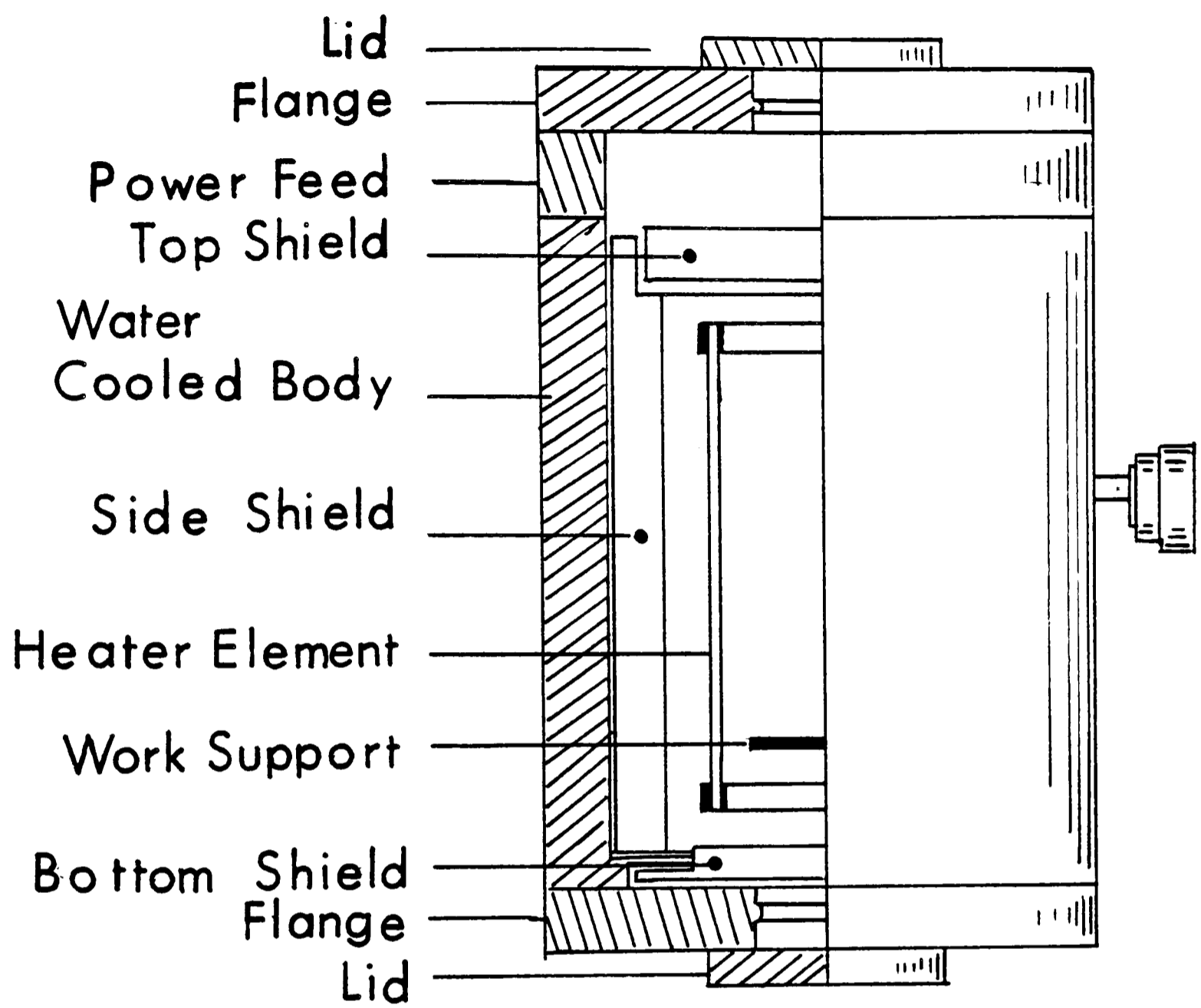
FIG. 5.1 - 15: CENTORR HIGH TEMPERATURE VACUUM FURNACE

high).   The heat zone is resistance heated.   The heating
element is made of solid graphite.   Heat shielding is by
Graphite Felt pressed into solid form.   Loading is done
through the Top Cover.   The firing procedure was as follows:

Slow evacuation (with rough vacuum pump).

Backfilled with Argon slowly.

Evacuated and backfilled again.

Evacuated and kept under vacuum

Heated from ambient to 1800°C at 5°C/min.

Backfilled with Argon.

Heated from 1800°C to 2500°C at 7°C/min.

Held for 15 minutes at 2500°C.

Power off - allowed to cool naturally.

5.2 Characterization of PGC

A large number of techniques were utilised in the characterization of PGC, namely:

(i)   Surface area measurements.

(ii)   Pore volume measurements.

(iii) X-Ray diffraction.

(iv)   Scanning electron microscopy.

(v)   Transmission electron microscopy.

(vi)   X-Ray fluorescence.

5.2.1 Materials

The following carbons were used in the structural studies:

(1)   PGC which was produced by the method described in Section 6.1.

(2)   Carbopack B, a graphitized carbon black, which was supplied by Supelco, Bellefonte, Pennsylvania, U.S.A.

(3)   'Graphite' felt supplied by Carbolite Furnaces (Carbolite, Sheffield, England).

(4)   Vulcan pelletized carbon black supplied by Cabot Corporations (U.S.A.).

(5)   Black Pears and Carbon-coated Silica which were kindly gifted by Dr. H. Colin, Department of Analytical Chemistry, Ecole Polytechnique, Palaiseau, France.

(6)   Carbon electrode which was taken from an EverReady Battery.

5.2.2 Equipment used for the characterization of PGC

5.2.2.1 Surface Area Measurements

Surface area was measured by a home built apparatus by the B.E.T. method illustrated in figure 5.2-1.

Gas adsorption provides an easy method for surface area determination. The quantity of gas, adsorbed on the surface, can be determined as a function of the gas phase pressure, at constant temperature, to give an adsorption isotherm. From this isotherm, it is possible to deduce the amount of gas needed to cover the complete surface area with a one molecule thick layer, which in turn allows determination of the surface area of the sample.

The equation that describes the B.E.T. adsorption is given as:

$$\frac{P}{V_{ads}(P_0-P)} = \frac{1}{V_m C(T)} + \frac{[C(T)-1]P}{V_m C(T) P_0}$$

where

P = equilibrium adsorbate gas at temperature T.

V_{ads} = volume of gas adsorbed at P and T.

P_0 = the saturation vapour pressure of the adsorbate.

V_m = volume of gas corresponding to monolayer coverage.

$$C(T) \; \alpha \; \exp \; (\Delta H_{ads} - \Delta Hliq)/R.T$$

Now a plot of $P/V_{ads}(P_0-P)$ against the relative pressure P/P_0 will be a straight line with a slope and an intercept
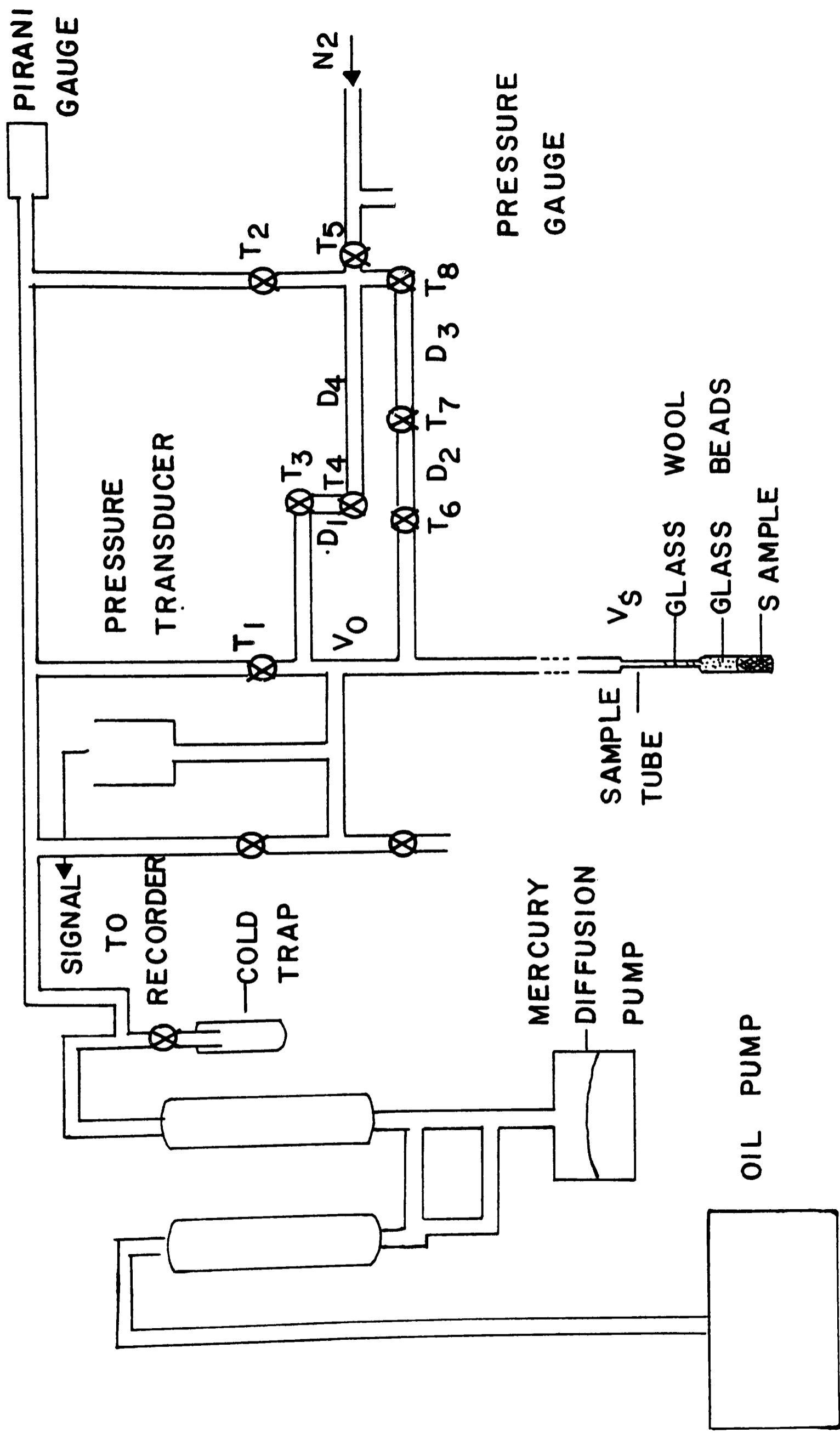
FIG. 5.2 -1 : APPARATUS FOR SURFACE AREA MEASUREMENT BY B.E.T METHOD

such that $-V_m = 1/G + I$ where G is the gradient and I is the intercept. Since the size of the adsorbate molecules is known the surface area is given by:

$$Area = Constant \times V_m$$

which in this case gives:

$$Surface\ Area = 4.35\ V_m m^2 g^{-1}$$

This was the basic theory for the surface area determination which for the purposes of calculation required the determination of the equilibrium pressure (P) and the amount of gas adsorbed (V_{ads}) by experimental methods.

Samples were degassed at about 300°C, and then surrounded by liquid nitrogen. A dose of gas was put into the dozing volume (D_1, D_2, D_3 or D_4) at a known pressure. The tap into the sample volume was opened and the system was allowed to reach equilibrium. This equilibrium pressure was recorded and then the procedure was repeated several times. The total volume of gas adsorbed (V_{ads}) at equilibrium Pressure P can be calculated as shown in Table 5.2-1, which is

$$\sum_{n=1}^{n} (V_{D_n} P_{D_n} - V_{D_n} P_n) - V_0 P_n$$

$$or \sum_{n=1}^{n} \{V_{D_n} (P_{D_n} - P_n) - V_0 P_n\}$$

And for a constant dozer pressure then:

Amount adsorbed is equal to

$$n V_D P_{D_n} \sum_{n=1}^{n} (V_{D_n} P_n - V_0 P_n)$$

Table 5.2-1: Calculation of the amount of gas adsorbed by the sample

V_o = Volume of sample tube V_s and volume V_o shown in figure 5.2-1

Doze No.	Doze Volume (ml)	Doze Pressure (mV)	Equilibrium Pressure (mV)	Amount dozed (ml.mV)	Cumulative amount dozed (ml.mV)	Cumulative amount dozed (ml.mV)
D_1	V_{D_1}	P_{D_1}	P_1	$V_{D_1} P_{D_1} - V_{D_1} P_1$	$V_{D_1} P_{D_1} - V_{D_1} P_1$	$(V_{D_1} P_{D_1} - V_{D_1} P_1) - V_0 P_1$
D_2	V_{D_2}	P_{D_2}	P_2	$V_{D_2} P_{D_2} - V_{D_2} P_2$	$V_{D_1} P_{D_1} - V_{D_1} P_1 +$ $V_{D_2} P_{D_2} - V_{D_2} P_2$	$\{(V_{D_1} P_{D_1} - V_{D_1} P_1) - V_0 P_1\}$ $+\{(V_{D_2} PD_2 - V_{D_2} P_2) - V_0 P_2\}$
—	—	—	—	—	—	—
—	—	—	—	—	—	—
—	—	—	—	—	—	—
D_n	V_{D_n}	P_{D_n}	P_n	$V_{D_n} P_{D_n} - V_{D_n} P_n$	$\sum_{n=1}^{n} (V_{D_n} P_{D_n} - V_{D_n} P_n)$	$\sum_{n=1}^{n} (V_{D_n} P_{D_n} - V_{D_n} P_n) - (V_0 P_n)$

5.2.2.2 <u>Pore Volume Determination</u>

Pore volumes of PGCs were measured either by mercury porosimetry or by titration with the solvent 2,2,4-trimethyl-pentane (iso-octane). Pore volumes of silica templates were measured by titration with water.

5.2.2.2.1 Mercury Porosimetry

A calibrated glass tube as shown in figure 5.2-2 was used known weights of silica, glass wool and mercury were taken in the tube and a pressure (500 psi) was then exerted onto the top of the mercury using a solvent pump so that the mercury entered the spaces between the silica particles but not into the pores. The level of the mercury was noted by means of a travelling vernier telescope. The pore volume of the sample, in this case, silica, was then calculated as follows:

Let mass of silica taken = x gms

Taking density of silica = 2.2 gms/cm^3

Then volume due to silica = (x/2.2) cm^3

Similarly,

Let mass of glass wool taken = y gms

Then volume due to glass wool taking

the density of glass woold to be 2.40 gm/cm^3 = (y/2.4) cm^3

And let mass of mercury taken = z gms

Volume due to mercury = (z/13.6) cm^3

Therefore,

Total volume account for = (x/2.2 + y/2.4 + z/13.5) cm^3

Pressure

0
0.1
0.2
0.3
0.4
0.5
0.6
0.7
0.8
0.9
1.0

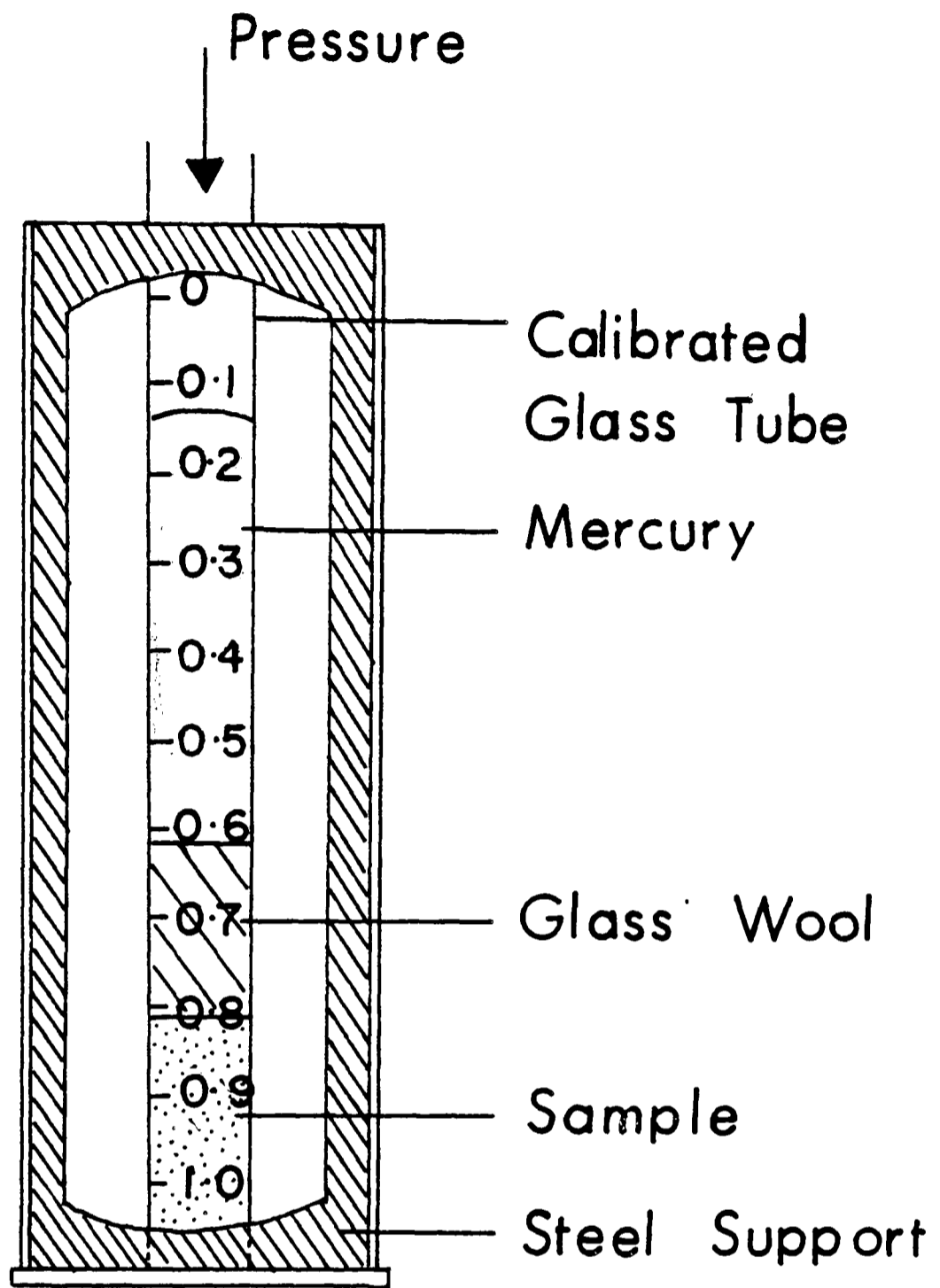Calibrated Glass Tube

Mercury

Glass Wool

Sample

Steel Support

FIG.5.2 -2 : APPARATUS FOR MEASURING PORE VOLUME

If the level of mercury noted $\equiv$ Z cm^3 as the tube is calibrated.

Then any volume not accounted for by silica, glass and mercury is due to pores in the silica.

$\therefore$ Total Pore Volume = Z - (x/2.2 + y/2.4 + z/13.6) cm^3

And Pore Volume of silica = $\frac{1}{x}$ {Z-(x/2.2 + y/2.4 + z/13.6)} $cm^3 g^{-1}$

5.2.2.2.2 Solvent Titration

Weight amounts of samples were titrated with water (in the case of silica) or 2,2,4-trimethylpentane (in the case of carbon) and the amount of solvent needed to just wet the sample was noted. The pore volume of the sample was then calculated as the amount of solvent in cm^3 needed to just wet one gram of sample.

5.2.2.3 <u>Structural study of PGC and other carbons</u>

5.2.2.3.1 X-Ray powder diffraction

Results were obtained using a Philips powder diffracto-meter (Pye-Unicam, Cambridge, England). Samples were loaded by an automatic sample changer (type PW 1170/02). The goniometer (PW 1050/80) was mounted on a highly stabilised X-ray generator (PW 1730/10) that provided $CuK_{\alpha1,2}$ radiation (mean λ = 1.5418$\overset{\circ}{A}$). Scanning was controlled by a motor control unit (PW 1394). Detection was controlled by a channel control unit (PW 1390) and fed to a pen recorder (PM 8203). An AMR focussing monochromater (model AMR 3-202E) was fitted immediately before the detector (PW 1965/60).

Samples were finally ground and carefully packed into slide holders and analysed.

5.2.2.3.2 Scanning electron microscopy

A Cambridge Instruments type 604 stereoscan scanning electron microscope fitted with a Praktica L2 camera was used. Samples were coated with gold (SEM coating unit E5100, Polaron Equipment Ltd) prior to analysis. Fine powders were dispersed on aluminium pegs and coated with a film of gold.

5.2.2.3.3 High resolution electron microscopy and electron diffraction

This was carried out by Dr. G.R. Millward of the Department of Physical Chemistry, University of Cambridge using a Jeol 200-CX instrument (Jeol at Cambridge University). The instrument, operated at 200 keV, was fitted with a top-entry goniometer stage modified to enable the specimens to be moved parallel to the incident beam (Z-lift) as described by Thomas et al.[2]. Under the operating conditions used, it has a resolution of 2.4Å . Specimens for examination were deposited from a suspension in acetone into carbon "holey" films. Only particles positioned over the holes were imaged under high resolution.

5.2.2.4 Identification of trace elements in samples of PGC and other carbons

The identification of trace elements was carried out by X-ray fluorescence. The instrument used was Philips X-ray

Spectrometer PV 1450 (Pye-Unicam, Cambridge, England) with chromium target X-ray tube (60 KV, 20mA), LiF analysing crystal (d = 4.027Å), flow counter and scintillation counter and fine collimator and air path. Samples were held on Mylar in plastic cups. Scans ran from 38-60 degrees 2θ and from 84-102 degrees 2θ.

Chapter 5: References

1. Knox, J.H. and Gilbert, M.T., U.K. Patent No.7939449,
    U.S. Patent No. 4,263,268.   Fed.Rep.Germany
    P2946688-4.

2. Thomas, J.M., Jefferson, D.A., Millward, G.R.   Joel
    News, 23 (1965) 7.

CHAPTER 6

PRODUCTION AND CHARACTERIZATION OF POROUS 2D-GRAPHITIC
CARBON (PGC) DEVELOPMENT, RESULTS AND DISCUSSION.

6.1 Production of PGC

6.1.1 Method development of PGC

The development of the method of production of PGC suitable for use in LC can be divided into four main phases relating to the general scheme for the production of PGC given in figure 5.1-1 viz. Phase 1, Phase 2, Phase 3 and Phase 4.

6.1.1.1 Phase 1: Study of impregnation of hydrogel

Phase 1 represented the first attempt in producing PGC from a home made silica template. Ludox, which is a colloidal dispersion of silica, was the starting material for the template. Batches 49-59 were produced in Phase 1 according to the outline procedure given in Figure 6.1-1.

In the preparation of PGC 49, Ludox was first gelled by adding 14 ml of 50% concentrated nitric acid to 1000 ml Ludox, and then allowing the acidified Ludox to stand in a water bath at 50°C. The hydrogel thus formed was broken up and the fragments were allowed to equilibrate five times with 15 ml acetone. In this way the acetone replaced the water in the hydrogel. After equilibration with acetone, the silica gel was then allowed to stand in contact with phenol melt at 80°C in an oil bath to allow the phenol to replace the acetone. PGC 50-59 were not equilibrated with acetone, but the hydrogel was allowed to equilibrate directly with phenol melt at 80°C in an oil bath. In the case of PGC 49, there was ultimately 24% of carbon in the silica gel/carbon particle after firing at 900°C; in the case of PGC 50, 28%. Since
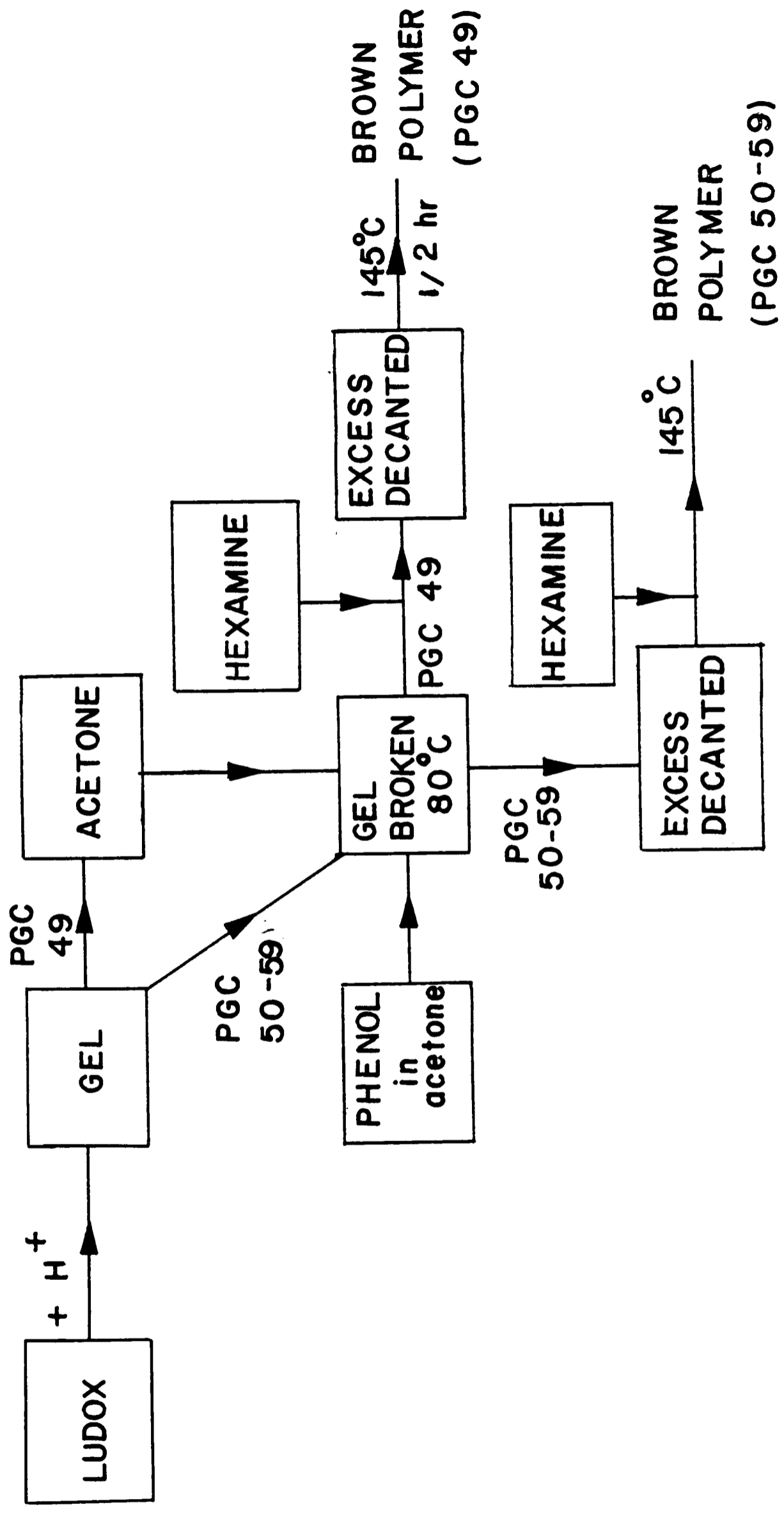
FIG. 6.1-1: DEVELOPMENT OF PGC (PHASE 1)

little difference in carbon content was observed and since the time and work involved in the equilibration with acetone was significant it was decided that in the production of later batches of PGCs this equilibration step would be omitted.

Impregnation and polymerization was carried out in two different ways. In the first, for the production of PGC 49, both phenol and hexamine (3:1 molar ratio) were added to the acetone loaded gel at 80°C and left overnight to equilibrate, the excess red liquid was then decanted; polymerization was then carried out at 145°C for half an hour. In the production of PGC 50-59, only phenol was added to the hydrogel at 80°C and the excess was decanted, a measured amount of hexamine was then added. Polymerization was allowed to proceed at 145°C for 4-5 hours.

Calculation of the amount of hexamine required

Let volume of Ludox (HS40) used = x ml.

Weight of phenol taken = x gms.

After equilibration, it is assumed that all the water in the gelled Ludox is replaced by phenol.

Density of Ludox at 25°C = 1.3 g/cm^3

Ludox type HS40 contains 40% (w/w) of silica and 60% (w/w) of water.

x ml of hydrogel (gelled Ludox) will contain (60% of 13x) gm

of water   = 0.078x ml of water

Let volume of liquid decanted off be = y ml.

Volume of phenol decanted off will be (y - 0.078x) ml.

Weight of phenol decanted off = (y - 0.078x) 1.047 gms.

Weight of phenol in the gel = x - [(y - 0.078x) 1.047]

Taking the weight ratio of phenol:hexamine to be equal to 2.

Then weight of hexamine to be used

$$= \frac{1}{2} \{x-[(y - 0.078x) \ 1.047]\}$$

These batches of silica gel/polymer were then carbonised.
The silica/polymer obtained by this procedure was formed in
fairly large lumps and, therefore, there was the necessity
to grind and fractionate.   This had the further advantage that
the ground fragments would not be totally encased in excess
polymer.   It was found that grinding and fractionation had to
be carried out after carbonization but before dissolution of
silica to prevent fragmentation.   Carbonization was carried
out in nitrogen using the Carbolite furnace (PGC 49) and
Gallenkamp furnace (PGS50-59) at 1°C/min from 150°C to 400°C
then at 4°C/min from 400°C to 1000°C.   The temperature was
held at 1000°C for 10 hours.

The dissolution of silica was brought about by one of the
following methods:

(i)   Heating the silica/carbon with 50° solution of 5M KOH
and ethanol at 100°C.

(ii) Heating with fused KOH at 450°C or a mixture of NaOH and
KOH at 235°C in a stainless steel vessel followed by heating
in 50% ethanol and water to wet the carbon and to dissolve out
the potassium silicate.

(iii) Treatment with hydrofluoric acid.   This is based on the
volatility of silicon tetrafluoride formed when hydrofluoric
acid is added to silica and heat is applied.

$$4HF + SiO_2 \rightarrow SiF_{4(g)} + 2H_2O$$
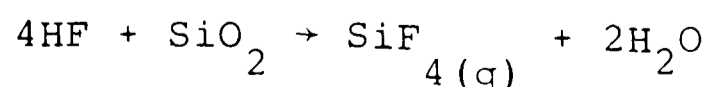
A platinum crucible was used because of the reactivity of hydrofluoric acid. The difference in weight between the original sample and the sample treated with hydrofluoric acid gives the percentage of silica in the sample.

Table 6.1-1 lists data on dissolution of silica in PGC 57 by different methods. Alcoholic potassium hydroxide does not seem to be suitable for the dissolution of silica. Treatment with fused KOH at 450°C, or a mixture of NaOH/KOH, or hydrofluoric acid were effective in dissolving out silica. In this phase, therefore, method (ii) was the treatment chosen for the dissolution of silica.

The samples were sent to Anglo-Great Lakes for further firing at temperatures greater than 2000°C according to the firing regime illustrated in figure 5.1-11.

Conclusions and Considerations that led on to Phase 2

(i) PGCs produced at this first phase of development were not satisfactory in LC due to the development of high back pressures and badly shaped peaks. There was, therefore, still the necessity of producing a stronger material.

(ii) The PGCs produced at this stage were in the form of chips with a size range of 5-20 μm.

(iii) The dissolution of silica by fused KOH at 450°C was undesirable as the treatment resulted in the corrosion of the stainless steel beakers bringing about contamination with metallic impurities and very probably oxidation of the carbon product. The difficulty of dissolving silica suggested that

Table 6.1-1   Data on Dissolution of Silica in PGC 57

Method   % Weight loss using

                                          Thermogravimetric analysis

5% Ethanol/KOH   60

5% Ethanol/KOH, then   64

50% Ethanol/KOH

Fused KOH at 450°C   98

Fused KOH/NaOH at 235°C   90

TGA was done in air from ambient to 1000°C
at 30°c/min

the colloidal units were insufficiently well connected so that access to the dissolving solution was poor. We were also uncertain at this stage as to whether geometrical integrity of the template was preserved at the dissolution stage.

(iv) Severe weight loss of 30-60% was found with samples sent to AGL for firing. At this stage the reason for the weight loss was still unclear.

6.1.1.2 Phase 2: Establishment of Geometric Stability of PGC

In the second phase of development, the template was produced in the form of cylindrical pellets. A cylindrical stainless steel vessel (figure 6.1-2) was filled with acidified Ludox which was allowed to gel slightly. The vessel was then connected to a pumping system, and gelled Ludox was extruded into acetone through a 1/4" stainless steel tubing.

The "sphagetti" strands, 1 cm long, were then washed with 0.1M nitric acid, and allowed to stand overnight at 80°C. Final washing of the "sphagetti" strands was done in 2.5% ammonium hydroxide and then the strands were subjected to hydrothermal treatment in an autoclave at 220°C in order to consolidate the structure. Prior to impregnating with the polymer, the strands were dried and sintered at 600°C for 16 hours to further strengthen the template. The whole process is outlined in figure 6.1-3(a). The pore volume of the silica gel strands produced were 0.86 cm^3/g.

Impregnation and polymerization for PGC 60 was carried out as in PGC 50-59 using 3:1 molar ratio of phenol:hexamine

Eluent from Pump

Stainless Steel

Eluent

Gelled Ludox

Stainless Steel
Cylindrical Vessel

7"

1/4"

Sphagetti Strands
Acetone
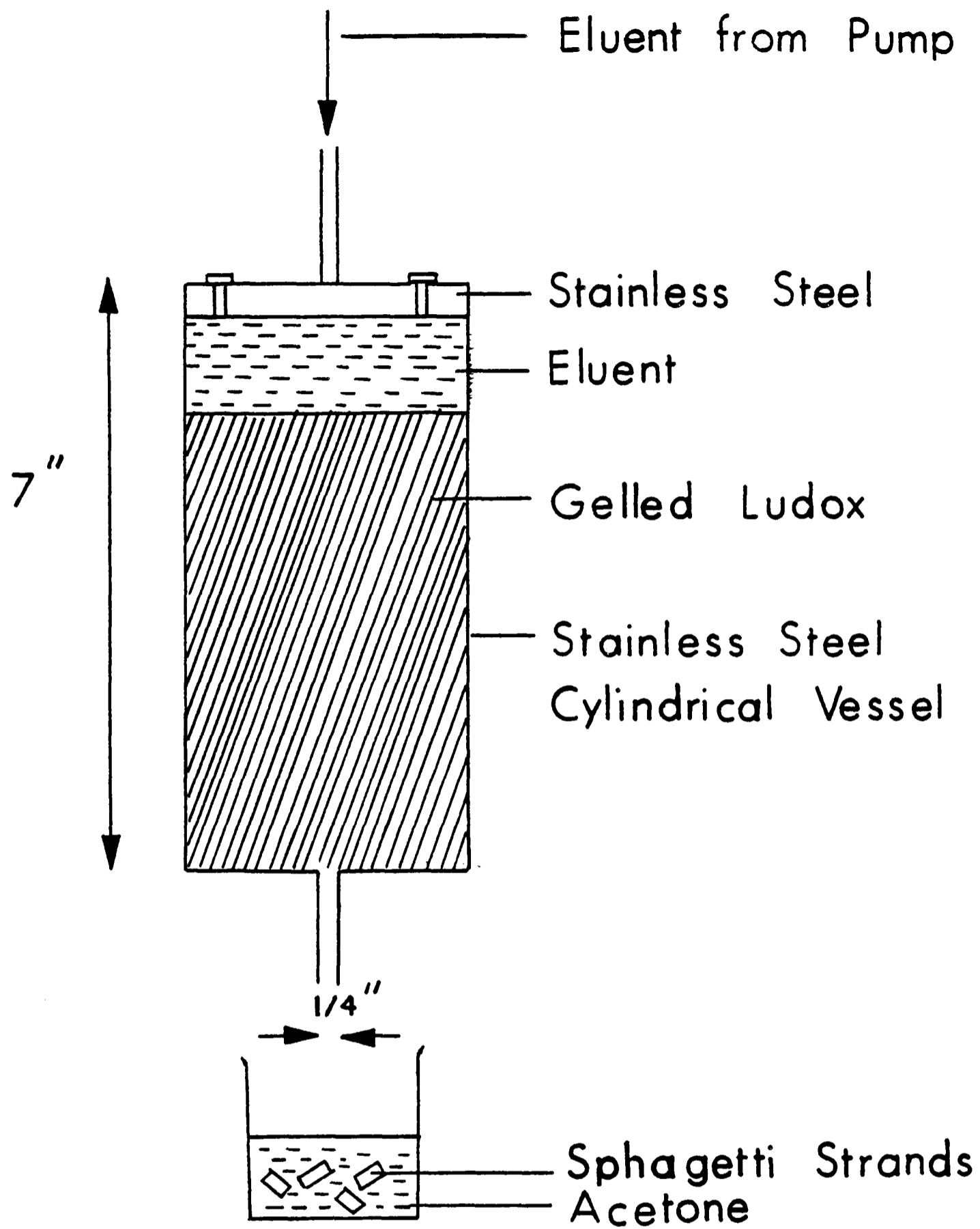
FIG. 6.1 - 2 : APPARATUS   FOR   MAKING

SPHAGETTI   STRANDS

(a) Production of template (for PGC 60-62)

```
                    +
              + H
LUDOX ─────────────────► GEL ─────► SPHAGETTI ─────► ACETONE
                                     STRANDS              │
                                                          │
                                                          ▼
SINTERED ◄──── HYDROTHERMAL ◄──── DISTILLED ◄──── 0.1M HNO₃
 600°C        TREATMENT            WATER            80°C
              220°C                                overnight
```

FIG. 6.1-3 : DEVELOPMENT OF PGC (PHASE 2)

[Figure 6.1-3(b)] but using dried, sintered silica gel rather than hydrogel. Carbonization was carried out as in Phase 1 using the Gallenkamp muffle furnace. Grinding of the carbon strands and fractionation to obtain narrow range of particle sizes was done after carbonization. Dissolution of silica was now car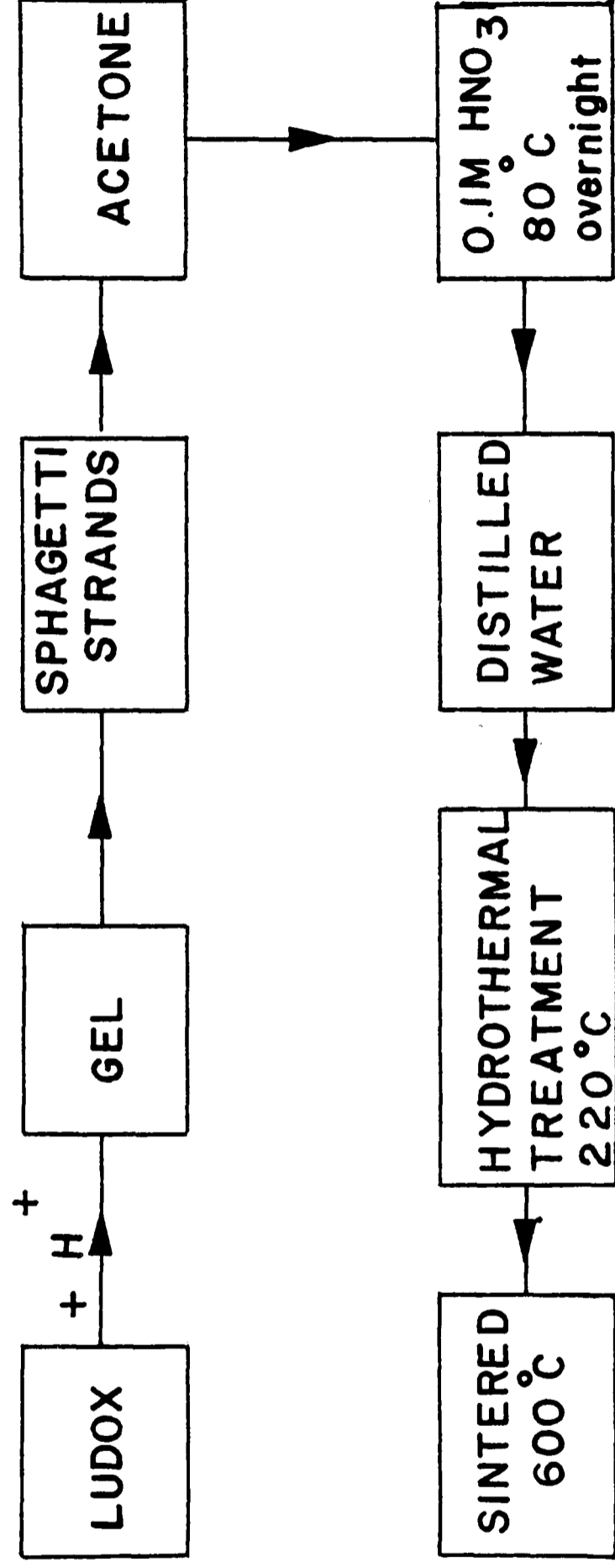ried out in aqueous KOH as it was found that ethanol, though allowing the wetting of carbon, produced an environment in which the potassium silicate was insoluble. Later, with a greater knowledge of PGC, it was noted that PGC heated at 1000°C (amorphous), was highly hydrophilic and that a wetting agent was not necessary after all!

PGC 60 was sent to AWRE for higher heat treatment to be fired according to the firing regime in Figure 5.1-11. The batch sent to AWRE was successfully used in GC.

It was also noticed that both the dimensions of the "sphagetti" template and the PGC ultimately formed remained the same. No significant dimensional shrinkage was seen.

Calculation of the amount of phenol and hexamine required
for total pore volume filling

Let total weight of silica gel taken

$$= x \text{ gms}$$

If the pore volume of the silica gel is y cm^3/g

∴ Total pore volume available for filling of polymer

$$= xy \text{ cm}^3$$

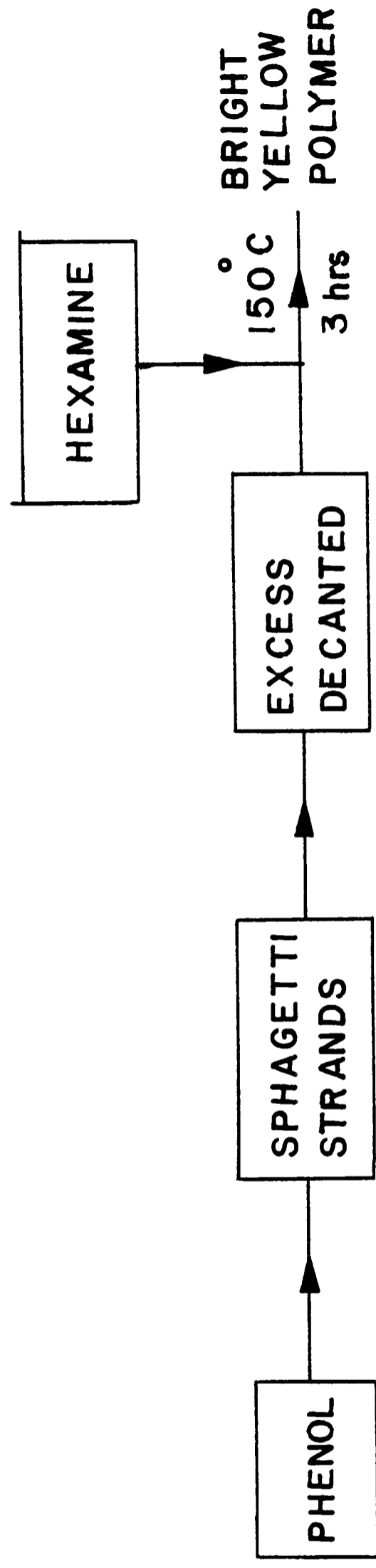Taking phenol:hexamine   = 6:1 (weight ratio)

Then phenol-hexamine   = 7.614:1 (volume ratio)

Volume fraction of phenol required

$$= 7.614xy/8.615$$

$$= 0.88xy \text{ cm}^3$$

(b) Production of PGC 60

PHENOL →→ SPHAGETTI STRANDS →→ EXCESS DECANTED

HEXAMINE →

150°C

3 hrs

↑

BRIGHT YELLOW POLYMER

Static Polymerization

FIG. 6.1-3 : DEVELOPMENT OF PGC (PHASE 2)

Weight of phenol required

$$= (0.88xy \times 1.0472) \text{ gms}$$

$$= 0.92xy \text{ gms}$$

Volume fraction of hexamine required

$$= xy/8.614$$

$$= 0.12xy \text{ cm}^3$$

Weight of hexamine required

$$= (0.12xy \times 1.33) \text{ gms}$$

$$= 0.16xy \text{ gms}$$

Therefore in a typical case:

If pore volume of the silica gel is

$$= 1.4 \text{ cm}^3/g$$

and the total weight of silica gel taken

$$= 200 \text{ gms}$$

Then, total pore volume available for filling of polymer

$$= 280 \text{ cm}^3$$

Taking phenol:hexamine (volume ratio) to be 7.614:1

Then volume fraction of phenol required

$$= 246.4$$

And weight of phenol required

$$= 264.4 \times 1.0472$$

$$= 258.03 \text{ mgs}$$

Volume fraction of hexamine required

$$= 33.60$$

weight of hexamine required

$$= (33.60 \times 1.33) \text{ gms}$$

$$= 44.69 \text{ gms}$$

Conclusion

This was the first phase that saw the complete dissolution of silica prior to higher heat treatment. The dissolution of silica had always proved to be one of the major problems during the earlier stages of development of PGCs like PGCs 26 and 49-59. Fused KOH at 450°C was the only way of dissolving out almost completely the silica present. On the other hand, the silica gel structure has been consolidated by hydrothermal treatment in the sphagetti strands. Because of this reason there was an easy access to the silica gel by the dissolving KOH. Furthermore, no dimensional shrinkage was observed.

6.1.1.3 <u>Phase 3</u>: <u>Establishment of a Final "Dry Impregnation" Method</u>.

Initially, sphagetti strands were still used as templates for the production of PGCs 61 and 62. Three main changes were incorporated at this stage, namely:

(i) The phenol-hexamine ratio was optimized. The phenol-hexamine molar ratio was changed to be in the range that would produce a form of glassy carbon according to Kawamura and Jenkins[1]. 8.9:1 molar ratio was chosen based on a 6:1 weight ratio of phenol:hexamine. According to Jenkins and Kawamura[2] the percentage yield of phenol hexamine molar ratio is increased.

(ii) The process of impregnation of the polymer was improved by using phenol-hexamine mix as melt rather than simply molten phenol. Phenol was first initially melted at 60°C. Hexamine was then dissolved in the phenol melt at 80°-90°C. The amount of phenol and hexamine melt to be used was calculated to allow just under 100% pore filling of the template so as to result in a free flowing material.

(iii) Impregnation and polymerization temperatures were rigorously controlled. Impregnation was allowed to proceed overnight and then again at 120°C before hardening at 150°C for 5 hours. The temperature was raised from 120°C to 150°C slowly at the rate of 5°C/hour. Both impregnation and polymerization were carried out dynamically in an oil bath, that is, continuous rotation was maintained throughout so as to allow good agitation of the contents (figure 6.1-4a).

The process of production of PGC 64 is illustrated in figure 6.1-4(b) which is similar to the above process. The silica template, however, was a commercially available Hypersil (Shandon Southern). Carbonization was carried out at 1°C/min up to 400°C, and then at 1000°C for 5 hours. The silica was dissolved out using aqueous KOH at 100°C.

PGCs 61-64 were sent to AWRE for higher heat treatment to be fired to 2340°C according to the firing regime in figure 5.1-11. A batch of PGC 62 was also sent to Anglo Great Lakes to be fired at 2600°C. The batch sent to Anglo Great Lakes did not prove useful in chromatography, whereas the same
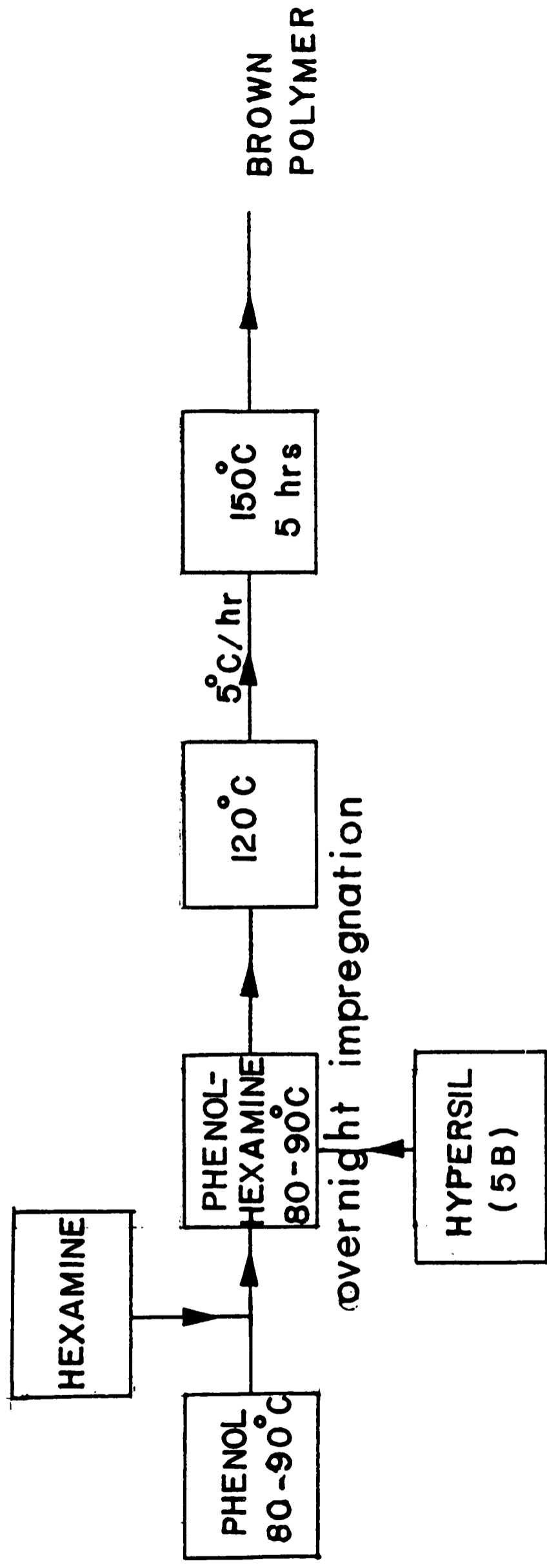
(a) Production of PGC 61-62
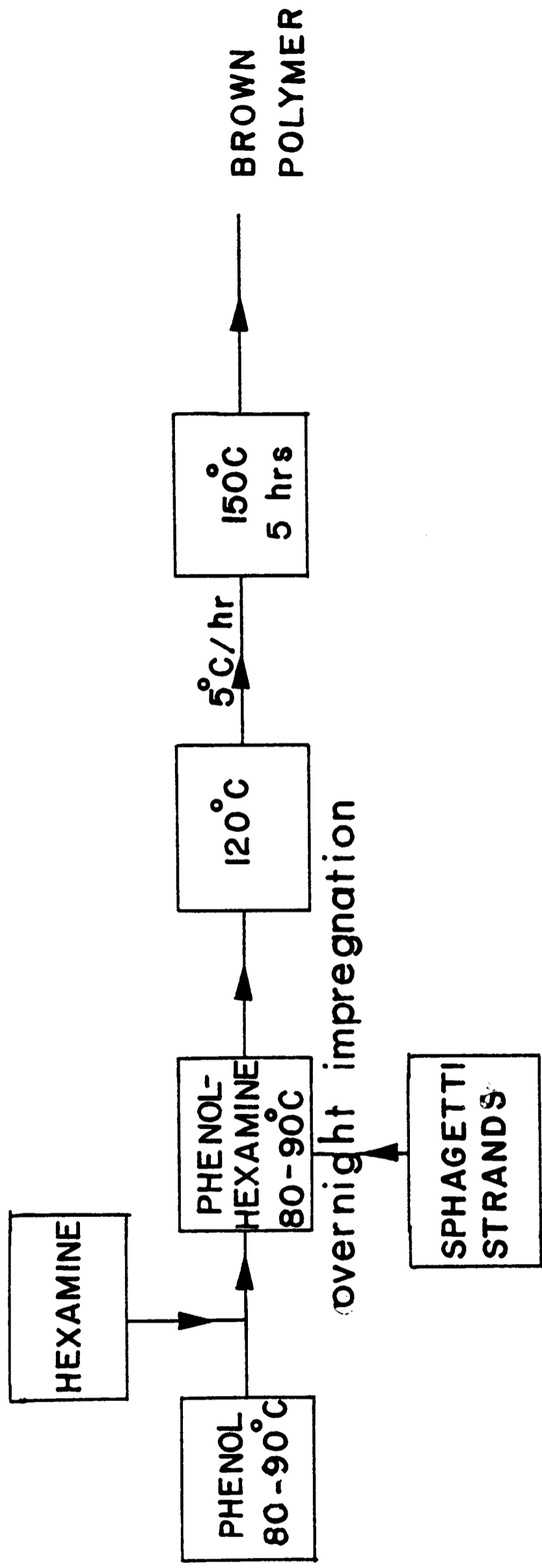
Dynamic Impregnation And Polmerization

FIG. 6.1-4: DEVELOPMENT OF PGC (PHASE 3)

(b) Production of PGC 64

FIG. 6.1-4: DEVELOPMENT OF PGC (PHASE 3)

Dynamic Impregnation And Polmerization

material fired at AWRE was successfully used in GC.

Conclusions

(i)   The third phase of the development saw a great number of modifications culminating in the production of successful batches of PGCs.   PGCs 61 and 62 performed well in GC and PGC 64 in LC.

(ii) Table 6.1-2 lists the weight and molar ratios of phenol-hexamine in the production of the different batches of PGCs. The successful batches of PGCs had a molar ratio in between that quoted or necessary for the production of glassy carbon. This represents an important consideration as noted later in Section 6.2 in the structural study of PGC, it is the inter-twined graphitic ribbons like those found in glassy carbon that contributes to the strength and rigidity of PGC.   PGC 26, an earlier batch proved to be very fragile in LC, giving high back pressure.

(iii) Dynamic rotation at all stages of production greatly improved impregnation, polymerization and carbonization procedure.   100% filling of the pores by the polymer also ensured that the maximum amount of polymer was incorporated giving a higher percentage of carbon content.   A free flowing material was also produced.

(iv) The efficiency of the Anglo Great Lakes firing regime was now questionable as the part batch PGC 62 sent to AGL proved unsuccessful whereas the part batch 62 fired at AWRE proved to be a better material.   Severe weight loss was again observed when the sample was fired at AGL.   The weight loss is

Table 6.1-2   Weight and Molar Ratios of Phenol-Hexamine
in the Production of the Different Batches
of PGCs

| PGCs | PHENOL : HEXAMINE | |
	WEIGHT RATIO	MOLAR RATIO
19	1 : 4.5	1 : 3
26	2.7 : 1	4 : 1
49-60	2 : 1	3 : 1
61-78	6 : 1	8.9 : 1
Glassy Carbon[1]		6 : 1-24 : 1

NOTE: Percentage yield of carbon is increased as the
phenol:hexamine molar ratio is increased[2]

not readily explained. The most probable explanation seems to be oxidation by water vapour possibly present in the Argon used to flush the sample. The weight loss was greater for samples heated to only 1000°C. Such samples would have a more active surface so would oxidize faster assuming oxidation rate to be controlled by kinetics not diffusion. Later batches of PGCs were then sent to AWRE for high temperature firing. As there was the need to increase the batch size of PGCs heated to temperatures greater than 2000°C, other places of firing were sought. Carbone Lorraine and Centorr Associates have now proved to be able to meet the requirements of high temperature treatment so as to produce good batches of PGCs.

6.1.1.4   Phase 4: Preparation of Special Large Pore Volume Silica Gel

Subsequent to the success of PGC 64 in LC, there was then a necessity to produce 5μm spherical porous silica template. The process of production of the template is indicated in figure 6.1-5. The following steps can be followed for 500 ml of Ludox used.

(i)   Emulsification step

1500 ml of Pet-ether (100-120) containing 45 ml (3%) of span 80 is warmed in a water bath at 45-50°C. In a separate container, 500 ml of Ludox was also warmed up gently. Just before emulsification, 14 ml (1.4%) of 50% nitric acid was added to the Ludox and well stirred. The acidified Ludox was then added to the warm Pet-ether/span. The mixture was
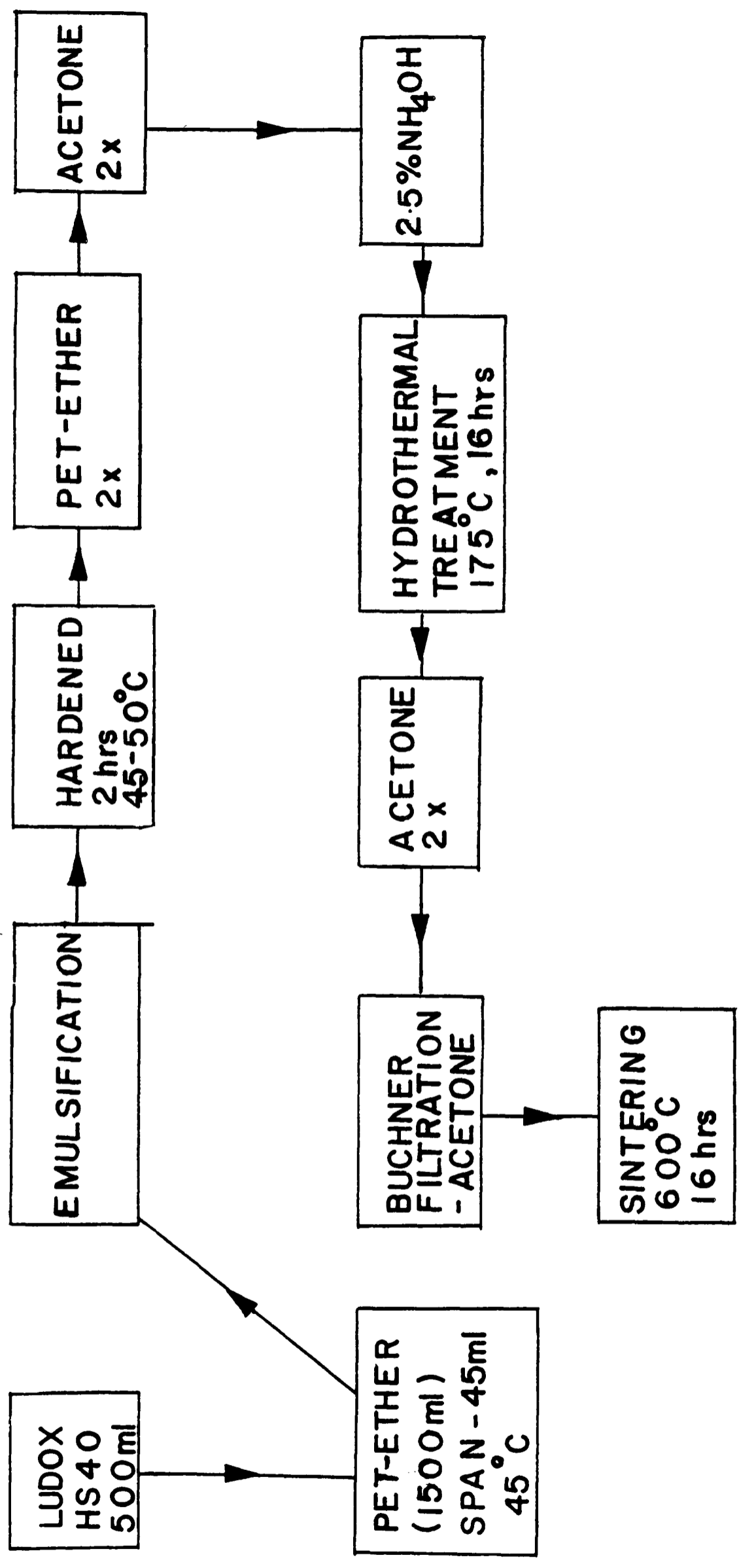
(a) Production of template for PGCs 66-78

FIG. 6.1-5: DEVELOPMENT OF PGC (PHASE 4)

then emulsified using a Silverson mixer at about 4000 revolutions a minute for 10 minutes.

(ii) Hardening step

After emulsification, the mixture is replaced in the water bath and left to stand at 45-50°C for 2 hours. It is important, for the production of small particle sizes, that the temperature of the bath does not rise beyond this temperature as higher temperatures cause clumping of the particles.

(iii) Initial washing step

Pet-ether/span was then decanted off gently and fresh Pet-ether was then added and well stirred. After allowing the particles to settle, the Pet-ether was again decanted off and another washing with Pet-ether was often necessary. After the third washing with Pet-ether, the silica gel was then washed twice with acetone. The final washing was done with 2.5% aqueous ammonium hydroxide.

(iv) Hydrothermal treatment

Hydrothermal treatment in an autoclave was carried out at 175°C for 16 hours in 2.5% aqueous ammonium hydroxide. After the treatment, the silica gel was completely washed and dried using a Buchner funnel and acetone as the solvent.

(v) Sintering

The dried silica gel was then sintered in the Gallenkamp muffle furnace at 600°C for 16 hours.

The pore volumes and surface areas of the silica gel templates and some batches of PGCs before and after high heat

treatment are given in section 6.2.

6.1.2 Important Considerations in the Production of 5μm Silica Gel Template

Several considerations should be noted so as to be able to reproduce 5μm silica gel particles.   These include:

(i)   Since there can be batch to batch variation of the silica sol, it is important that the pH of the silica sol should be adjusted with the pH meter so as to give a definite pH of 5.5.

(ii) The washing procedure of silica gel prior to hydrothermal treatment has further been modified so as to produce 5μm particles that do not stick together.   In the process described in phase 4, acetone was added to Pet-ether after the hardening step.   It was found that the addition of acetone to Pet-ether brought about clumping together of the silica particles.   Therefore, after hardening, the Pet-ether should be decanted off and replaced with BMM solution.   In 1 litre of distilled water, the BMM solution should contain:

0.8M   sodium nitrate

0.09M conc HNO$_3$

0.15M NH$_4$OH

1.75M acetone

The BMM solution is a modification of MM1 solution of Ritchie[3] which contains:

1M   NaNO$_3$

0.1M   conc HNO$_3$

0.74M acetone

Ammonium hydroxide is a necessary reagent in BMM solution
as it prevents settling and sticking of silica gel particles
before hydrothermal treatment.   In the BMM solution there
is also a greater concentration of acetone.   This has the
effect of reducing drastically the time required to allow
the silica gel particles to settle during the washing process
after hardening with Pet-ether, reducing the time from 48
hours to 24 hours, that is, from 2 days to 1 day.   This is
important as the time required to produce batches of 5μm
silica particles can be reduced as 2 BMM solution washes are
recommended thereby saving 2 days.

(iii) After hydrothermal treatment and then allowing the
silica gel particles to settle the ammonium hydroxide solution
should be decanted off and acetone added.   The silica gel
particles should not be allowed to stand overnight in the
ammonium hydroxide solution as by doing this the silica gel
particles again have the tendency to stick together.   Further-
more, before filtration, using the Buchner funnel, care should
be taken so that all the water in the silica gel particles
should be replaced by acetone.   This can be done by decanting
and replacing with acetone two more times, and then allowing
the silica gel particles to stand in acetone for a minimum
of 1 day.   Should water be present in the silica gel
particles then filtration through the Buchner funnel becomes
extremely slow.   If this is observed then the silica gel
particles should be given further washings of acetone and
allowed to stand in acetone for another day.   Furthermore,
the water that may still be present in the silica gel particles

may bring about sticking of particles so that the ultimate product of dry silica may contain groups of silica particles sticking together. Therefore, it is absolutely necessary to get rid of all the water in the silica gel particles before filtration.

(iv) It has also been found that sticking together of particles occurs at the time of gelation during the hardening process. Therefore, the process could be greatly improved if the emulsion in the Pet-ether is rotated during the hardening process. Rotation of the emulsion during the hardening process would have the effect of producing better quality individual particles of silica.

6.1.3 Important Considerations in the Reproducible Production of PGC

The reproduction of successful batches of PGCs was not without problems. These included:

(i) Oxidation of PGC at different stages.

(ii) Irreproducible heating rates of PGCs at different stages.

(iii) The presence of fine "needles" as contaminants in PGC.

(iv) Impurity of the inert gases used.

(v) Metallic impurities prior to high heat treatment.

Oxidation of PGCs

Carbon is very susceptible to oxidation reactions as shall be discussed in Chapter 7. The oxidation of PGC during its

formation would, therefore, lead to the presence of adventitious groups on the surface. It was, therefore, necessary to take all precautions to prevent oxidation at different stages of production of PGC. These precautions include:

(i) The inlet purging system for the inert gas was made up of stainless steel tubings rather than PTFE tubings which would allow diffusion of gases from the atmosphere.

(ii) The ceramic tube used at later stages of the production of PGC during heat treatment was discarded. This tube was found to be porous to some extent at higher temperatures.

(iii) The presence of moisture at different stages of heating should be avoided. Therefore, it was absolutely necessary that during carbonization an initial slow heating program was necessary so that the moisture was removed before it had the chance to oxidize the surface. Furthermore, it had been found that PGC heated to 1000°C (amorphous PGC) was highly hydrophilic. Therefore, exposure of PGC to the atmosphere before high temperature treatment brought about adsorption of water vapour. Rapid heating of PGC when it was sent away for high heat treatment had, therefore, a destructive effect on the surface of PGC as oxidation was more critical at higher temperatures. Precautions were also taken against the presence of moisture in the inert gas which was used to purge the carbonization and high temperature systems.

As noted earlier, the samples of PGCs sent to Anglo Great Lakes suffered severe weight losses. This was probably due to the oxidation of the samples due to either the

impurity of the inert gases, or inadequate flushing of the system prior to high temperature treatment.

Heating Rates of Carbonization and High-temperature Treatment

Achieving definite heating rates at both the carbonization and high temperature treatment stage has also been the problem in reproducing PGC. With the purchase of the specially modified carbonization furnace from Carbolite Furnaces, which had the ability of temperature programming, the problem of irreproducible heating rates at the carbonization stage was eliminated. PGC was heated at 50°C/hr from 200°C to 600°C and then at 200°C/hr to 1000°C where the temperature was held for 10 hours. In addition, since further heating is dependent on furnaces belonging to others, achieving true heating rates at temperatures greater than 1000°C had presented a great problem. Some batches of PGCs sent to different places of firing produced PGCs that differed in quality. PGC 62, as discussed earlier, was an example. British Petroleum and Anglo Great Lakes produced bad batches of PGCs, and good batches of PGCs were fired either at AWRE, Carbone Lorraine or Centorr. PGC 70 that was heated at three different rates by Dr. Jenkins in the University College of Swansea as shown by the heating regime in figure 5.1-13 has definitely proved that slow heating rates of 10°C/minute or less are important during high temperature treatments. The various test chromatograms of these three batches are shown in Figure 8.2-4 in Chapter 8. The batches of PGCs that were heated at slow heating rates (Batches A and B)

produced PGCs that gave sharp, symmetrical peaks for test solutes discussed in Chapter 8.

Presence of Needles as Contaminants in PGCs

It had been found that bad batches of PGCs were badly contaminated with fine needles (the structure of these needles is discussed in section 6.2). These needles are now thought to be dense graphitic needles formed by the pyrolytic deposition from vapours released by heating above 1000°C. A proper purging system is, therefore, desirable at higher temperatures. It had been found that reheating PGCs to 1000°C after the dissolution of silica (second heat treatment) had helped to get rid of these needles.

Once formed, these needles are difficult to get rid of in LC samples of PGCs. Fractionation by sieving can remove needles from GC samples of PGCs although scanning electron microscopic studies (discussed in section 6.2) show that although needles can be removed from GC samples, some needles do still stick on the surface of GC particles. Therefore, it is necessary that formation of needles should be avoided in order to produce good batches of PGCs.

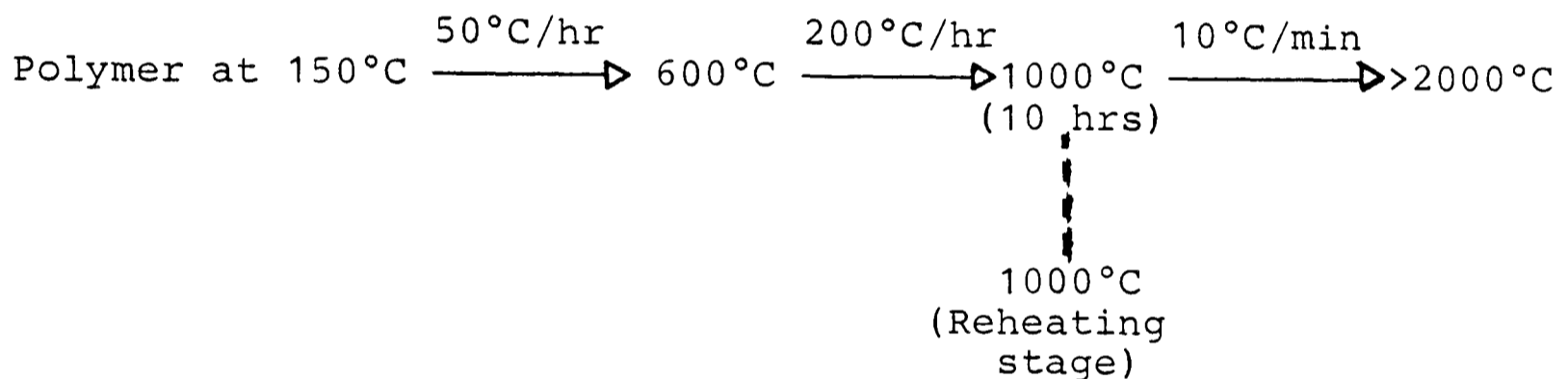## Metallic Impurities in PGCs

As noted in section 4.2.4.3 catalytic graphitization can be important during high heat treatment of carbons and this could be relevant in the high temperature treatment of PGCs. Metallic impurities present in some batches of PGCs could produce irreproducible batches of PGCs. Trace metal

analysis in PGCs by X-ray fluorescence is discussed in section 6.2.

6.1.4 Conclusions on Production of PGC

1. The method of production of a PGC suitable for LC is now clearly defined, and the precautions necessary at different stages are now noted. Precautions against oxidation are particularly important considerations.

2. Slow heating rates at different stages seems to be desirable. Briefly, this can be represented by the general scheme below.

```
                    50°C/hr              200°C/hr           10°C/min
Polymer at 150°C ──────────▷ 600°C ──────────▷1000°C ──────────▷>2000°C
                                            (10 hrs)
                                               ╏
                                               ╏
                                               ╏
                                            1000°C
                                           (Reheating
                                            stage)
```

3. The reheating stage in (2) at 1000°C is important in eliminating contamination with needles which may pose packing problems as will be noted later in Section 8.1.

6.2   Characterization of PGC

6.2.1   Surface Area and Pore Volume Measurements

The surface area and pore volume measurements of the silica templates and some batches of PGCs before and after firing to high temperatures has been tabulated in table 6.2-1.   PGCs given high temperature treatments have surface areas and pore volumes greater than the surface areas and pore volumes of the templates used to make the PGCs.   The silica templates used for the production of PGCs can now be reproduced, each batch having a surface area of approximately $50m^2 g^{-1}$ and pore volume of 1.4-1.5 $cm^3 g^{-1}$.   60% of the surface area is lost as PGCs are heated from 1000°C to temperatures greater than 2000°C;   the final PGC having a surface area of approximately 150 $m^2 g^{-1}$.   PGC 19, made from commercially available Corning Porous Glass, have an extremely low surface area of 21 $m^2 g^{-1}$.   Later batches of PGCs show greater percentages of carbon, at least 99%, indicating that most of the silica template has been removed.

6.2.2   Structure of PGC and other Commercial Carbons

Figure 6.2-1a is the X-ray diffractogram of PGC after heating to 1000°C and after the silica has been removed completely.   The carbon obtained at this stage has a large surface area (300-400 $m^2 g^{-1}$) due to the presence of micropores and is unsuitable for liquid chromatography.   Two broad diffuse maximas are seen in the X-ray diffractogram, one at an angle around 22° and the other at around 42°.

Table 6.2-1

DATA ON CARBONS

| BATCH NO	TEMPLATE			CARBON BEFORE FIRING		FIRING TEMP + PLACE °C	CARBON AFTER FIRING		
		Area m²/g	Vp cm³/g	Area m²/g	% C TGA		Area m²/g	Vp cm³/g Hg Method	Vp cm³/g Solvent Method*
19		12.5	1.0	81		2350AWRE	21	1.54	–
57	Hydrogel-Chips	~180	1.4 Estimated	370	>97	2600	68	. 1.25	1.6
60	Sphagetti which broke up on dissolution of silica by fused KOH	95	0.86	591	>97	2400 AWRE	79	0.77	0.81
61	Sphagetti for GC ground to required sizes after graphitisn.	70	1.44	183	>97	2400 AWRE	134	2.10	2.30
64	Shandon spher- ical silica 5μm LC	53	1.75	210	>97	2340 AWRE	154	1.72	1.76
200	WLCU silica 60-180μm	41	1.40		99	2340 AWRE			
68	WLCU silica 5μm	52	1.44	195	99.5	2340 AWRE	152	1.69	1.74

* Solvent used was 2,2,4 Trimethylpentane
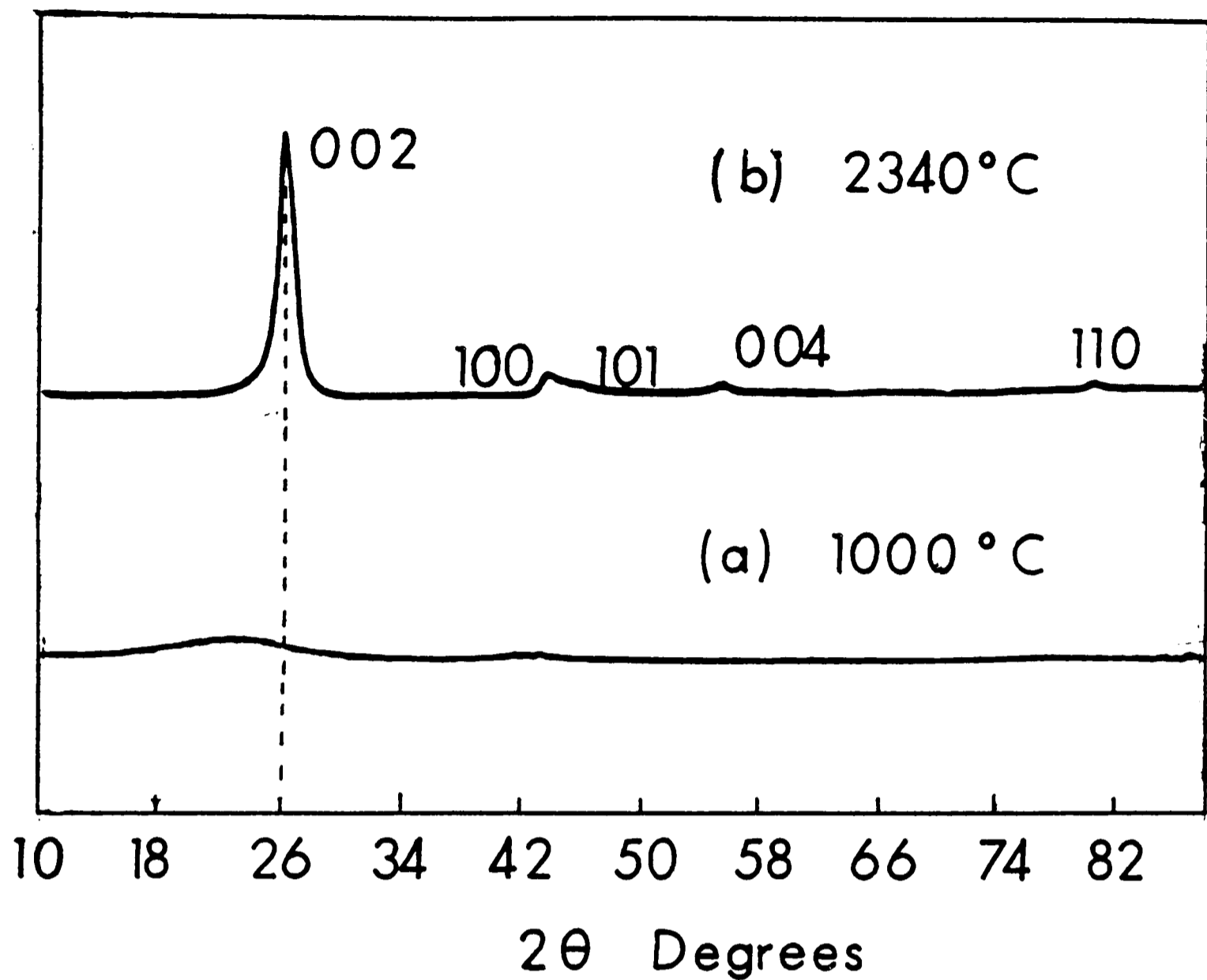
FIG. 6.2-1 : X-RAY DIFFRACTOGRAMS OF AMORPHOUS (a) AND HIGH TEMPERATURE TREATED (b) PGC 64

These broad reflections correspond to an amorphous structure. A study of the high resolution electron micrograph (figure 6.2-2) confirms the amorphous nature of PGC where no structure is seen at the 10Å level. As PGC is heated to high temperatures, the diffraction peaks become sharper and move towards higher angles as shown in figure 6.2-1(b). This diffractogram should be compared with diffractograms of PGCs that are unsuitable for LC which are shown in figure 6.2-3. For a good batch of PGC there is a sharp (002) diffraction peak corresponding to an interlayer spacing of 3.43Å. The (004) band is also discernible. Two dimensional (hk) lines are clearly seen, which include the (100) and the (110) lines. It is clearly seen that the (101) line is completely absent indicating that PGC is two dimensional. This would indicate that PGC differs from true graphite in that the layers that are present do not have regular orientation. High resolution electron micrographs of two good batches of high heat-treated PGCs show the development of extensive graphite-like sheets which are strongly interconnected [figures 6.2-4(a) and 6.2-4(b)]. These interconnecting sheets are responsible for giving strength to PGC and its successful use in LC. The presence of flat angular surfaces in PGC can also be clearly seen. Bad batches of PGCs do not show such extensive development of graphitic sheets [Figure 6.2-4(c)]. In Carbopack, however, the crystallites are larger and can be seen to be independent of each other. This probably accounts for the fragile nature of this material (Figure 6.2-5). The surface of Carbopack is also highly angular with flat graphitic areas. Although PGC is made from the same precursor as
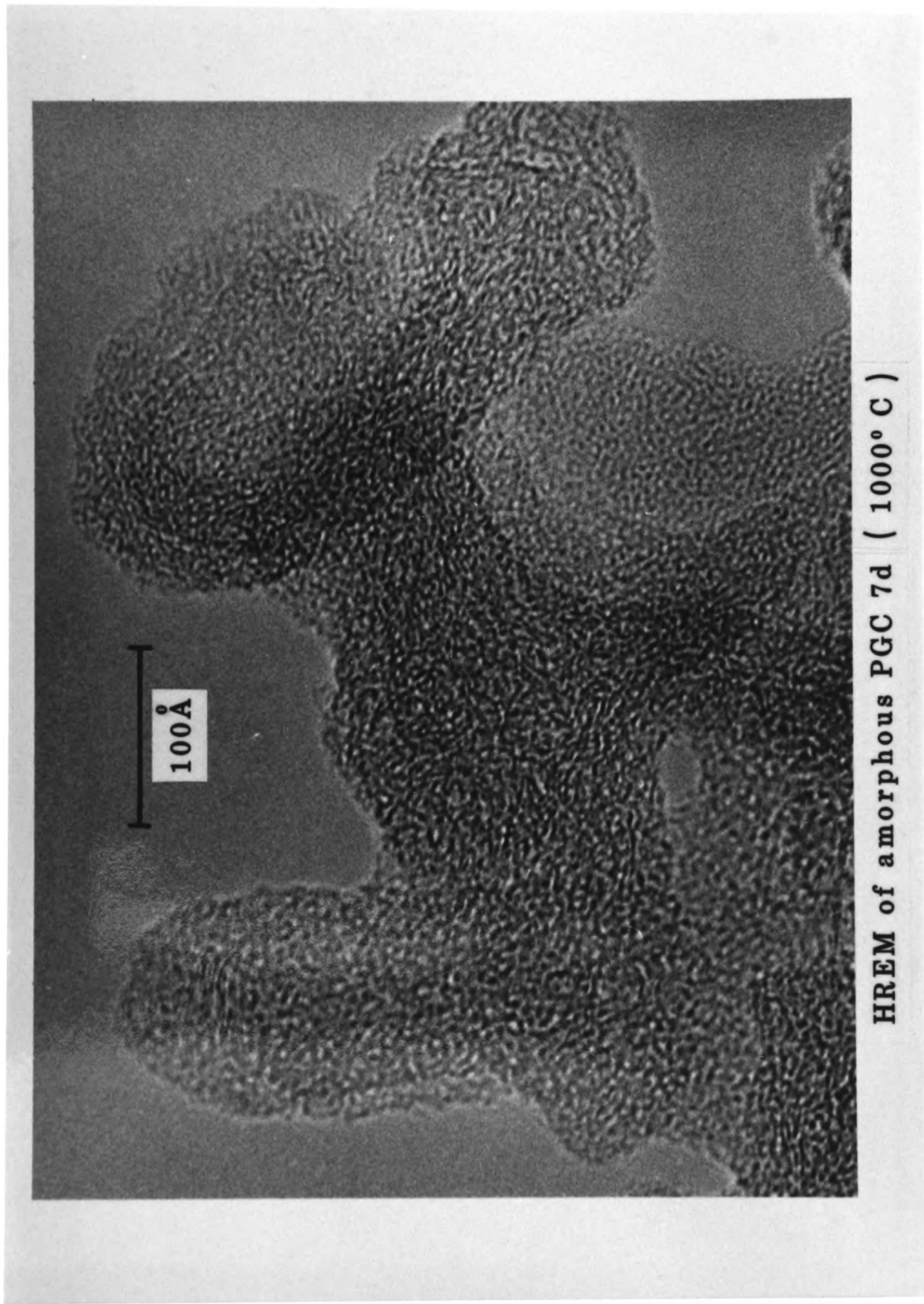
100Å

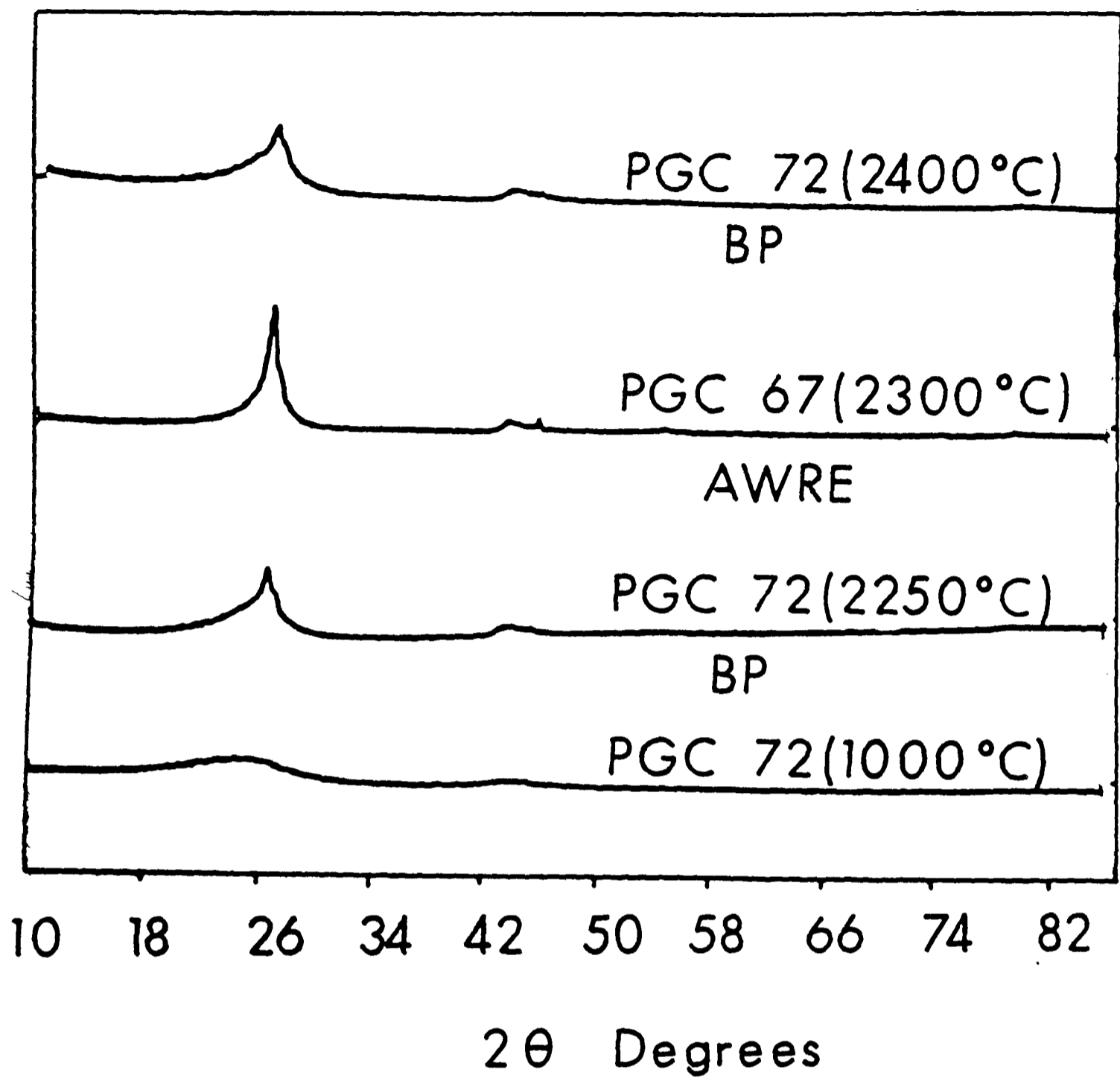HREM of amorphous PGC 7d (1000° C)

FIG. 6.2 -2 :

PGC 72(2400°C)

BP

PGC 67(2300°C)

AWRE

PGC 72(2250°C)

BP

PGC 72(1000°C)

2θ Degrees

FIG. 6.2-3: X-RAY DIFFRACTOGRAMS OF BAD BATCHES OF PGCs.

100Å

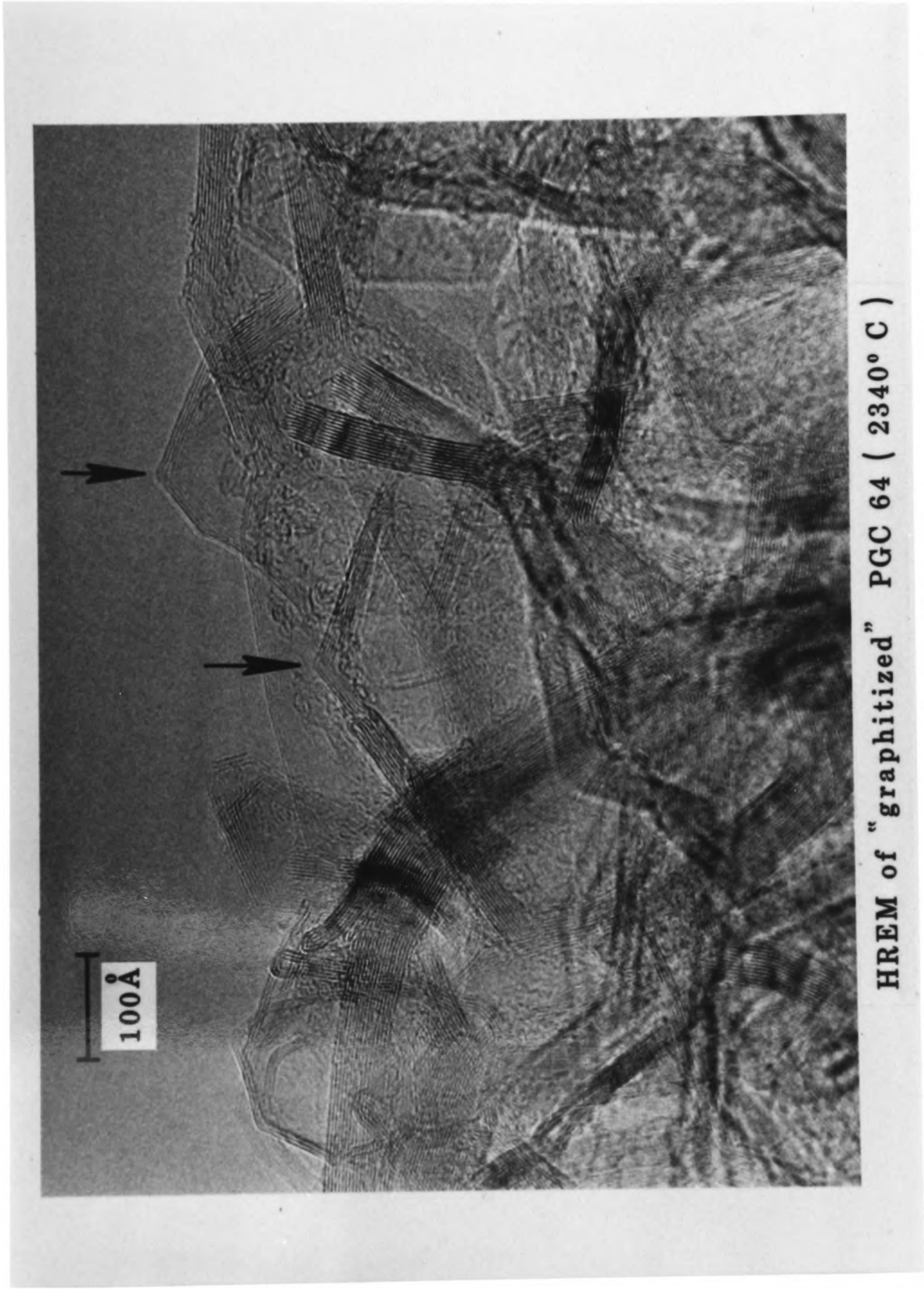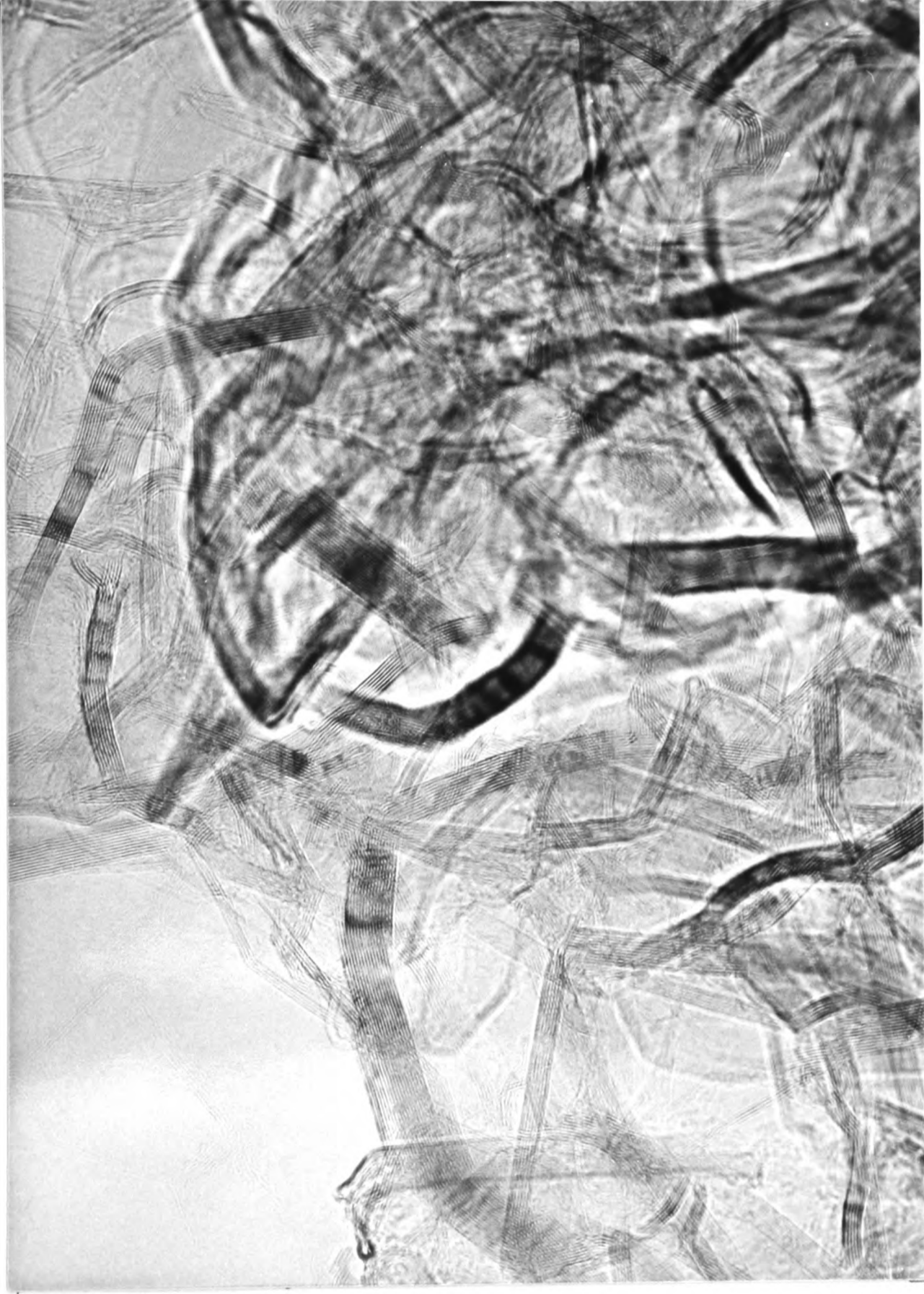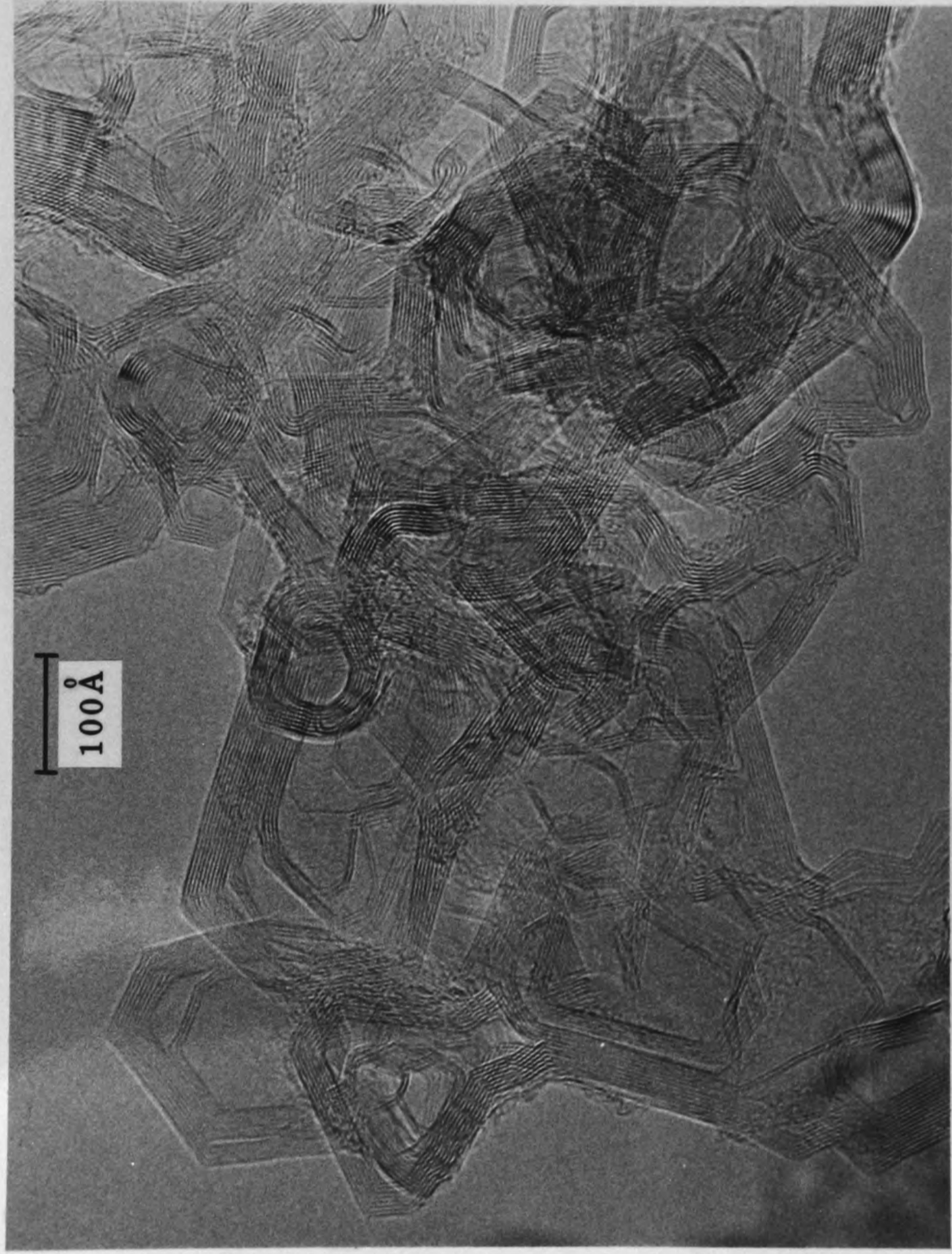HREM of "graphitized" PGC 64 (2340° C)

FIG. 6.2 - 4(a)

FIG. 6. 2 - 4(b): HREM OF PGC 70 - B

FIG. 6.2 - 4(c): HREM OF OXIDIZED PGC 69

100Å

HREM of graphitized carbon black: "CARBOPACK"

FIG. 6.2-5

glassy carbon, its structure appears to be quite different. From the study of HREM and X-ray diffraction PGC would most appropriately mean "Porous 2d-graphitic carbon" and not "Porous glassy carbon" as it was originally called.

The layer ordering of PGC can also be followed by electron diffraction, where there is a distinct formation of the (002) ring [Figure 6.2-6(b)] when compared to amorphous PGC [Figure 6.2-6(a)].

The highly porous nature of PGC can be clearly seen in the scanning electron micrographs (Figures 6.2-7 and 6.2-8) and high resolution electron micrographs (Figure 6.2-9) PGC has a pore volume of 1.7 cm^3g^{-1}.

Figure 6.2-10 shows X-ray diffractograms of PGCs and carbons used in LC. All carbons performing well in LC have similar 2d-diffraction patterns. On the other hand, Black Pearls and carbon coated silica particles are amorphous and, therefore, have been found to give poor results in LC.

Tables 6.2-2 and 6.2-3 give the calculated crystallite sizes, L_a and L_c, respectively, of PGC, Carbopack and graphite. PGCs have layer diameters of around 100Å and layer thickness of around 70Å. The crystallite sizes of both PGC and Carbopack are very much smaller than those of natural graphite.

The interlayer spacings, d (002), obtained for both Carbopack and PGC are similar to, but greater than, that of graphite and is equal to 3.43Å (Table 6.2-4). On the other hand, the Bragg spacing for carbon atoms within each layer, d (100), is slightly less than that of graphite with a value of 2.13Å. "Black Pearls", a non-graphitized carbon, has the greatest d (002) and d (100) spacings indicating its remoteness

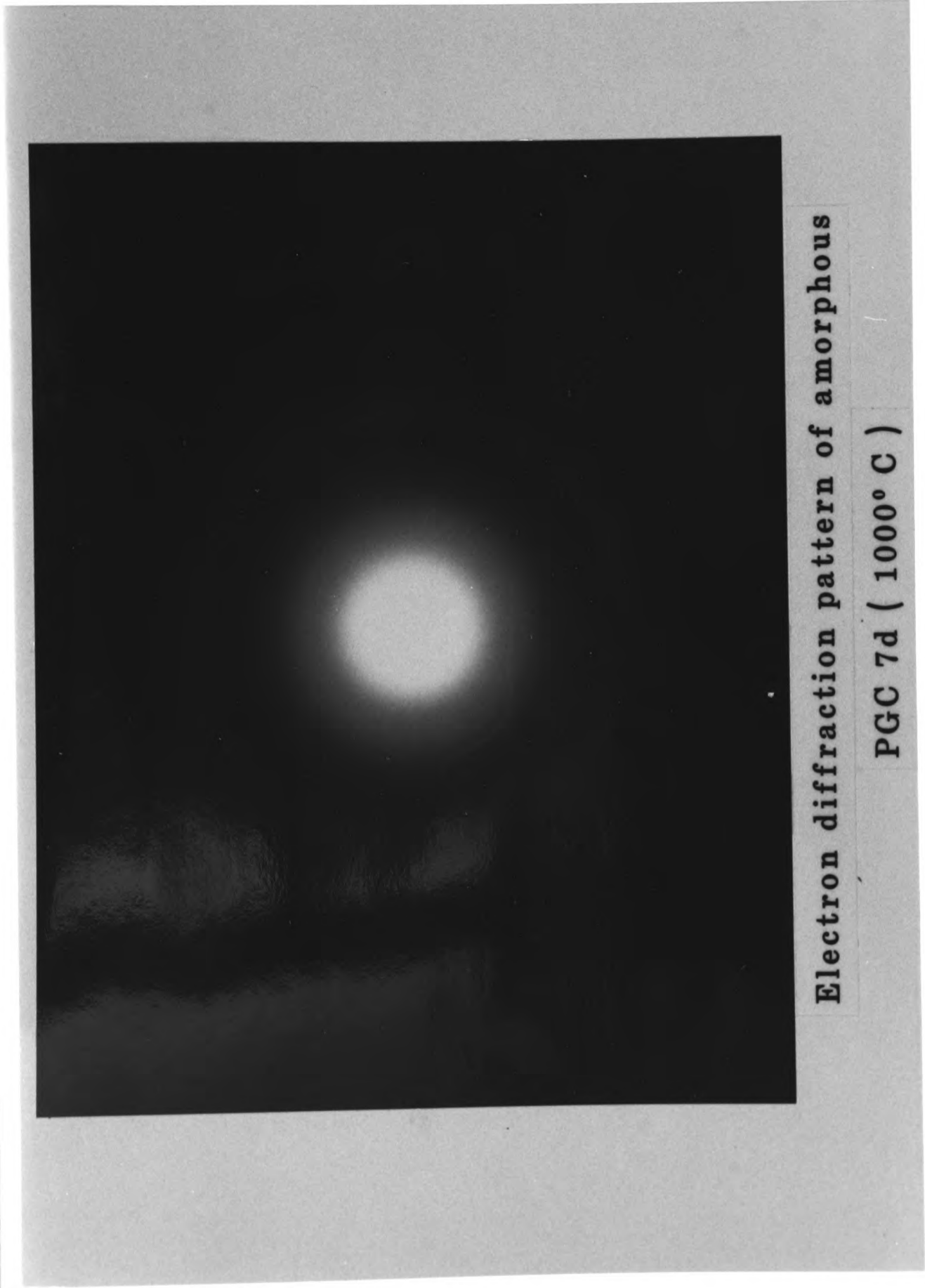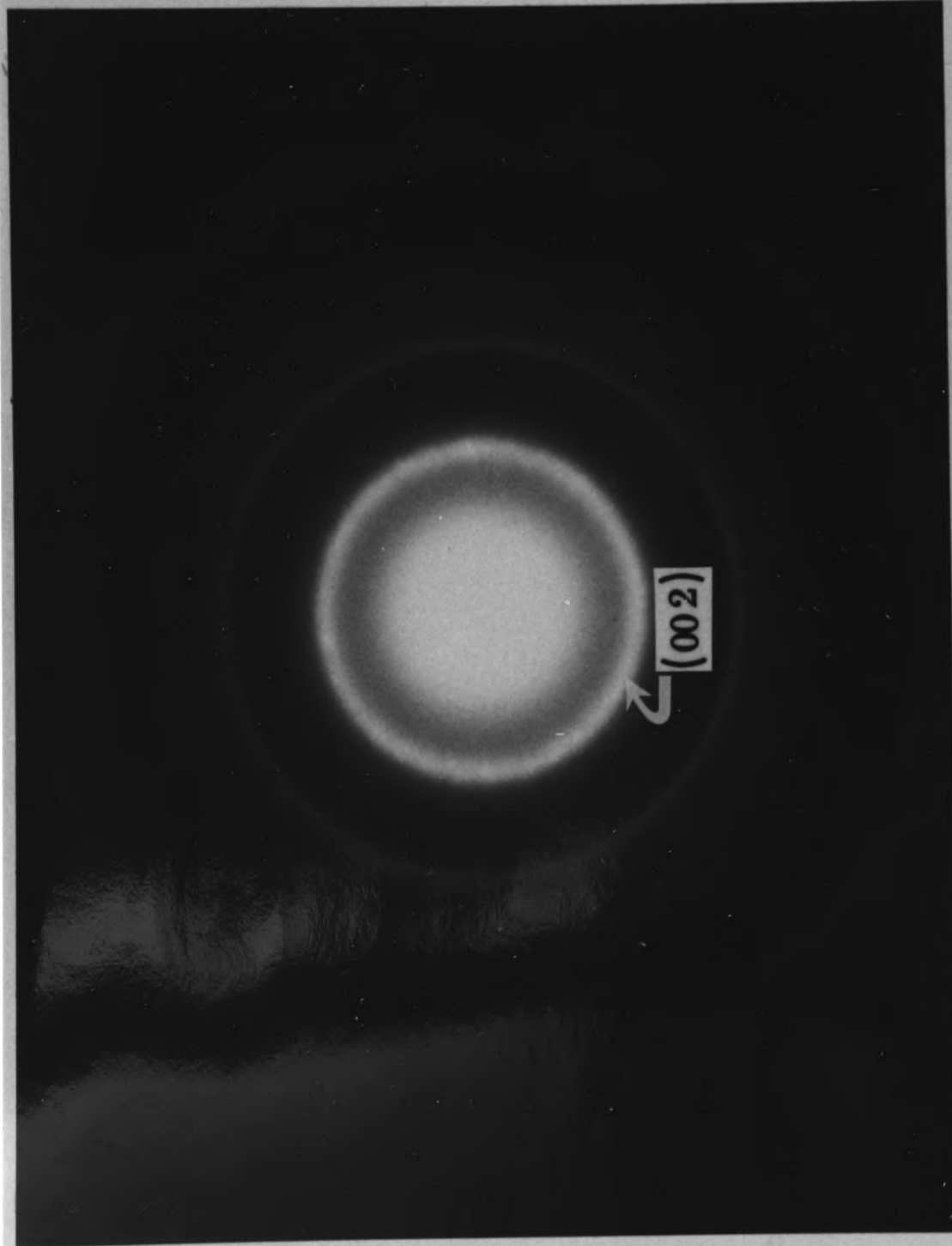Electron diffraction pattern of amorphous
PGC 7d (1000° C)

FIG. 6.2 -6(a)

[002]

Electron diffraction pattern of "graphitized"

PGC 205 (2500° C) showing (002) band

FIG.6.2 - 6(b)

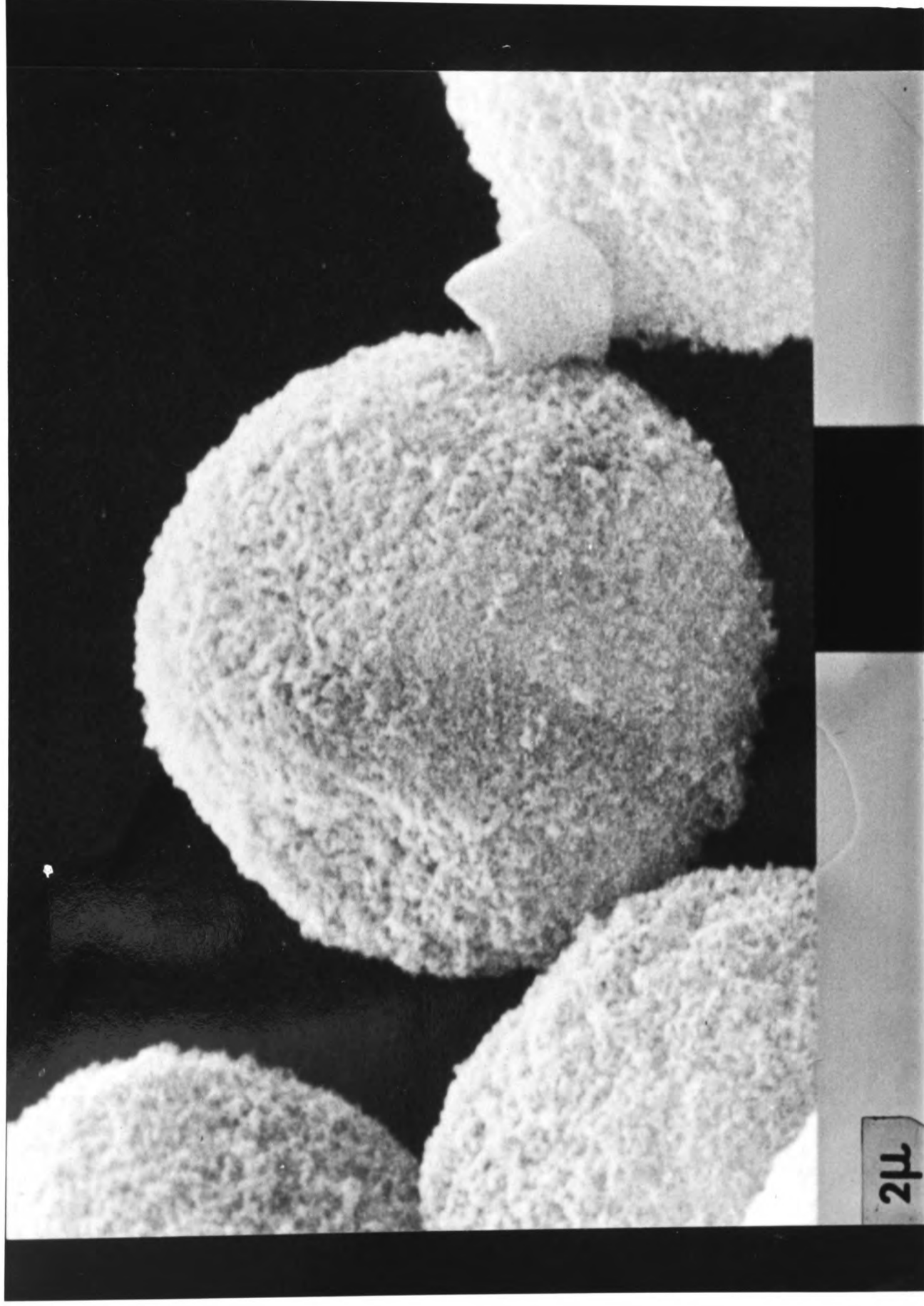FIG. 6.2-7 : SEM OF PGC PARTICLES
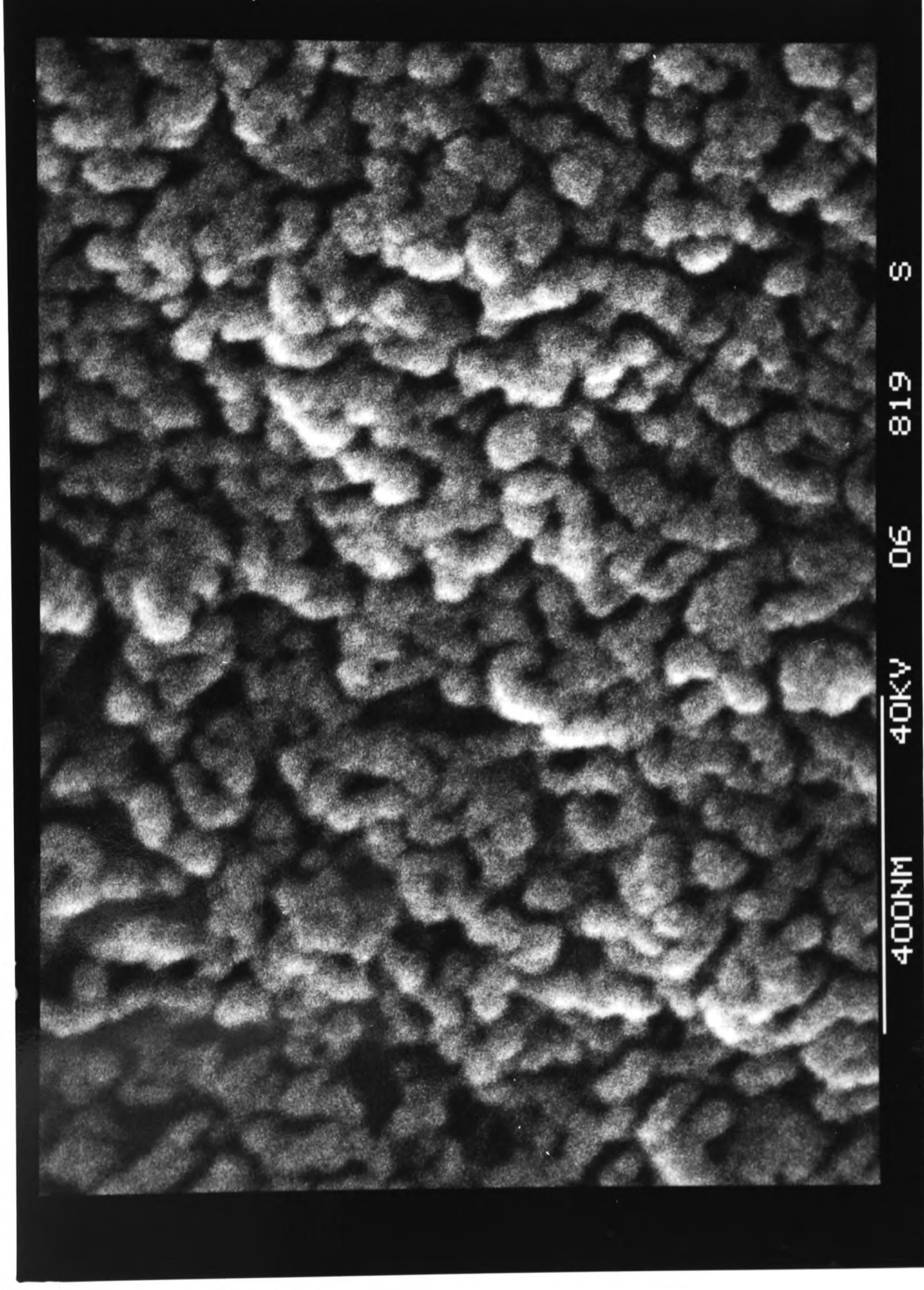
FIG.6.2-8: SEM SHOWING SURFACE OF PGC

Image caption text (visible in micrograph): 400NM 40KV 06 819 S

EM of PGC 64 (2340° C)

1 µm

FIG. 6.2 - 9

002

100
101
004
110
112

PGC 57 with "needles"

Carbopack with "needles"

PGC 64 (LC)

PGC 212 (GC)

Carbopack - no "needles"

Carbon for catalysis

Pyrocarbon on BP

Pyrocarbon on silica gel

20   30   40   50   60   70   80

2θ / degree
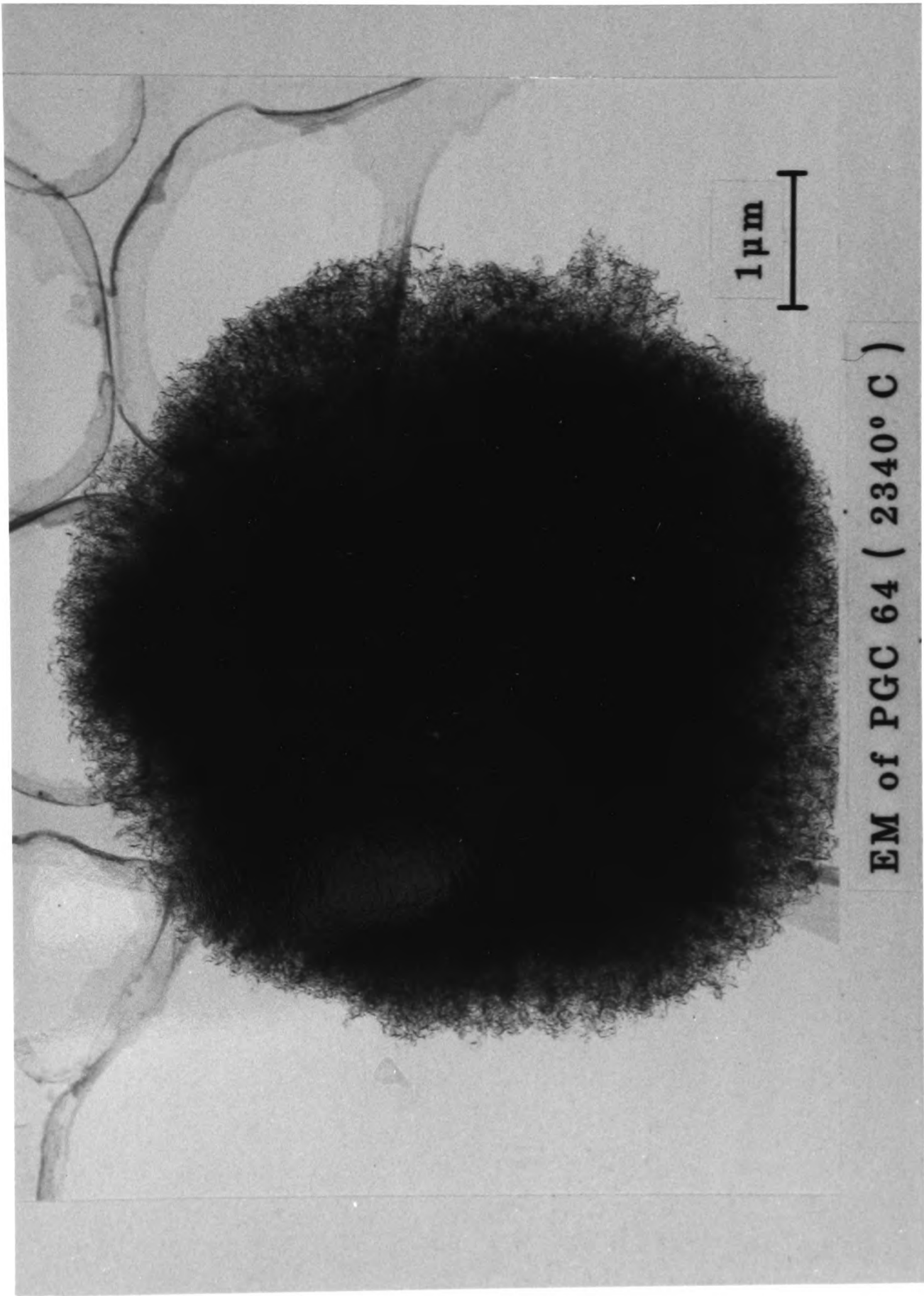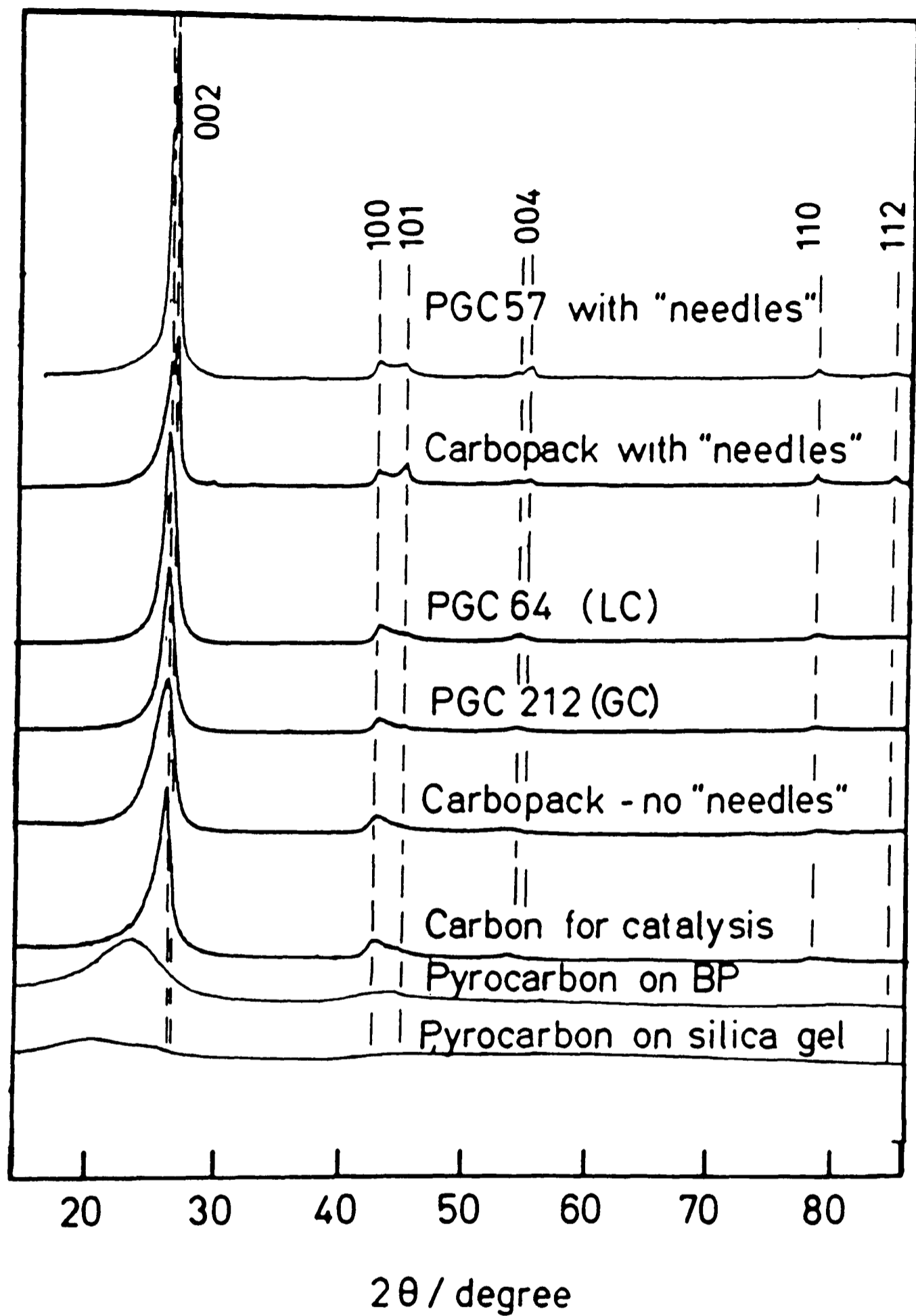
FIG. 6.2-10: X-RAY DIFFRACTOGRAMS
OF POSSIBLE CHROMATOGRAPHIC
CARBONS

Table 6.2-2 L_a - Layer Diameter in Carbons

	B/Radians	θ/deg	L_a (100) $\overset{\circ}{A}$
Graphite	0.01	21.2	304.oo
Carbopack	0.02933	21.2	103.49
PGC 64 (2340°)	0.02933	21.2	103.49
PGC 205-208 (2500°C)	0.02095	21.2	144.89
PGC 57 (2600°C)	0.01730	21.2	175.68

$$L_a = 1.84 \ \lambda/B\cos\theta$$

B = intrinsic peak breadth at half height in radians

Table 6.2-3 L_c - Layer Thickness in Carbons

	B/Radians	θ/deg	L_c (002)
Graphite	0.01	13.3	250.0
Carbopack	0.02933	13.0	49.77
PGC 64 (2340°C)	0.02025	13.0	70.24
PGC 70B (2500°C)	0.02025	13.0	70.24
PGC 205-208 (2500°C) GC	0.02025	13.0	70.24

$$L_c = k\lambda/B\cos\theta$$

K = 0.86 for L_c measurements and B is the intrinsic peak breadth at half peak height.

Table 6.2-4   Bragg Spacings for Carbons

	θ/deg	d(002) $\overset{\circ}{A}$	θ/deg	d(100) $\overset{\circ}{A}$	θ/deg	d(101) $\overset{\circ}{A}$
Graphite	13.3	3.35	21.2	2.13	22.3	2.03
Needles	13.3	3.35	21.2	2.13	22.3	2.03
Carbopack	13.0	3.43	21.2	2.13	-	-
PGC 64	13.0	3.43	21.2	2.13	-	-
Colins Black Pearls	12.2	3.65	21.0	2.15	-	-

$$d = 0.7709/Sin\theta$$

from the true graphitic structure.

The variation of crystallite sizes and Bragg spacing of PGC at different temperatures are shown in tables 6.2-5 and 6.2-6 respectively. These can be represented by figure 6.2-11 which clearly shows the increase and decrease of crystallite sizes and Bragg spacing respectively with increasing heat treatment temperatures. The intensity of the (002) diffraction peak also increases as shown in figure 6.2-12.

As noted earlier, most samples of carbon including carbopack are contaminated with needles. This can be clearly seen in the scanning electron micrograph in Figure 6.2-13. These needles which are about 10μm long and 1μm wide are highly graphitic and dense as seen in the high resolution electron micrographs (Figure 6.2-14). The presence of needles can also be detected using X-ray crystallography. Figures 6.2-15(b) and 6.2-16(b) show the X-ray diffractograms of Carbopack and PGC 201 respectively, both contaminated with needles. The (002) and the (004) diffraction peaks are doubled. The prominent (101) and (112) peaks typical of graphite can also be clearly seen when these samples are fractionated by sieving so as to remove the needles, the extra diffraction peaks disappear [Figures 6.2-15(a) and 6.2-16(a)].

The diffraction angles of PGC and Carbopack with and without needles have been tabulated (Table 6.2-7) and compared with the diffraction angles of graphite. It is clearly evident that these needles are highly graphitic. The regular layer ordering present in the needles are shown in

Table 6.2-5   Variation of Crystallite Size (L_a and L_c) due to Different Temperature Treatments on PGC 212

Temperatures °C	B/Radians	L_c (Å)	B/Radians	L_a (Å)
1000°C	0.10473	13.58	0.06982	43.48
1965	0.02793	50.93	0.03491	86.95
2140	0.02444	58.20	0.03351	90.58
2280	0.02095	67.90	0.03142	96.61
2500	0.02025	70.24	0.02793	108.68

θ for L_c = 13.0 deg.

L_a = 21.2 deg.

Table 6.2-6   Variation of Interlayer Spacing $d_{(002)}$ Due
to Different Temperature Treatments on
PGC 212

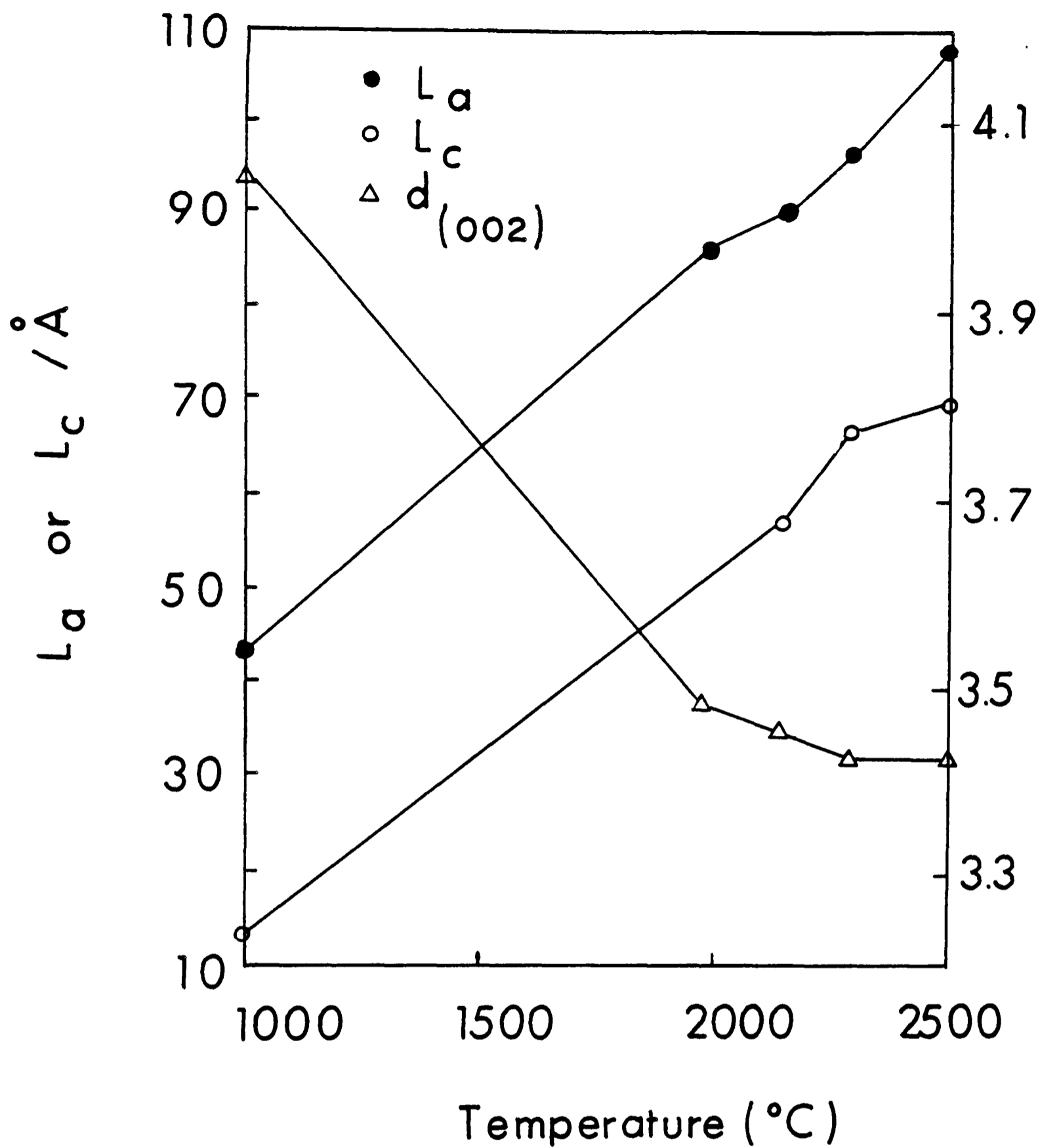| Temperatures °/C	θ/deg	$d_{(002)}$ $\overset{\circ}{A}$
1000°C	11.0	4.04
1965	12.8	3.48
2140	12.9	3.45
2280	13.0	3.43
2500	13.0	3.43

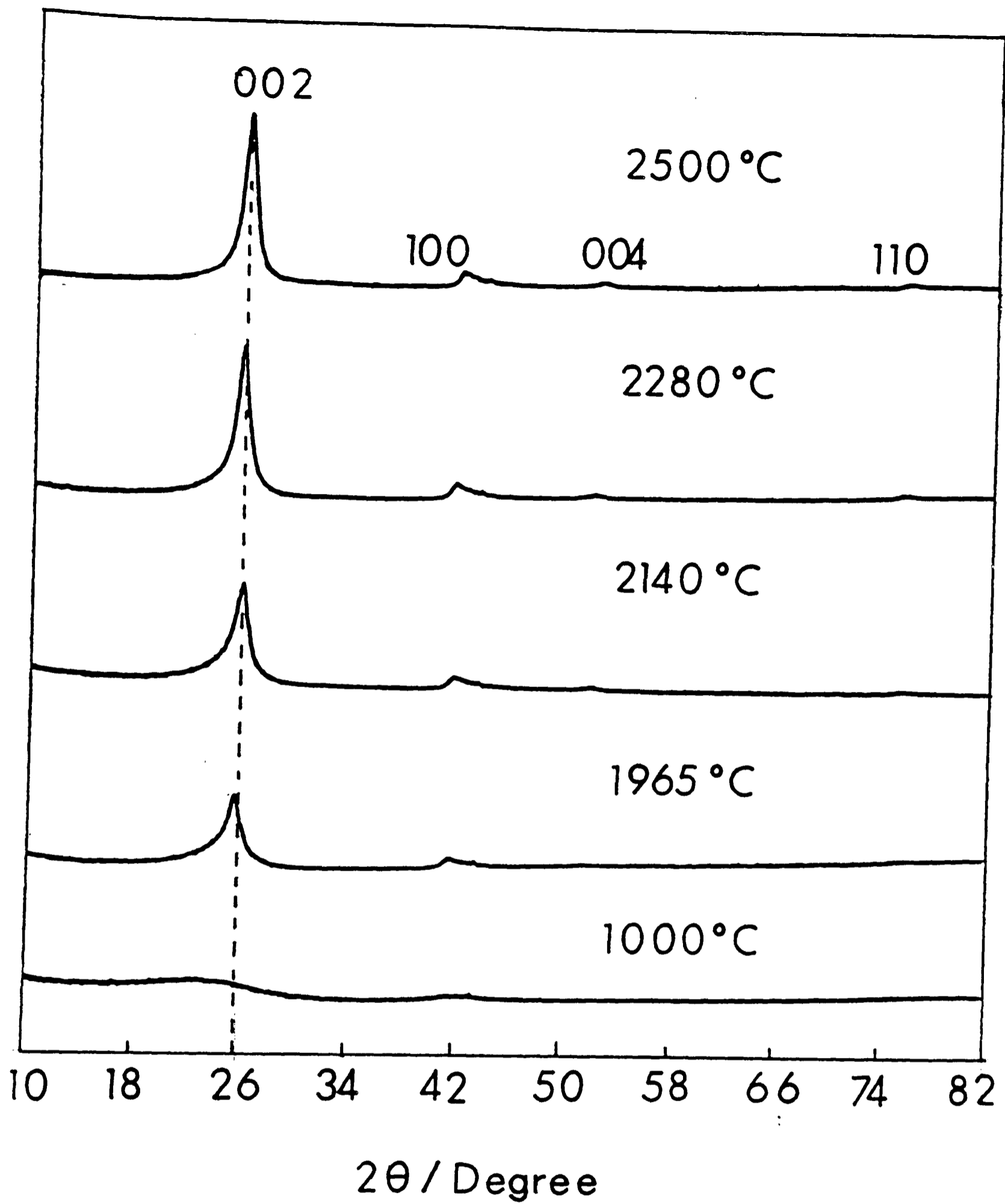FIG. 6.2 -11: VARIATION OF CRYSTALLITE SIZE(L_a AND L_c) WITH DIFFERENT TEMPERATURE TREATMENTS FOR PGC 212

FIG. 6.2-12 : EFFECT OF TEMPERATURE ON
X-RAY DIFFRACTION PATTERNS
OF PGC 212.

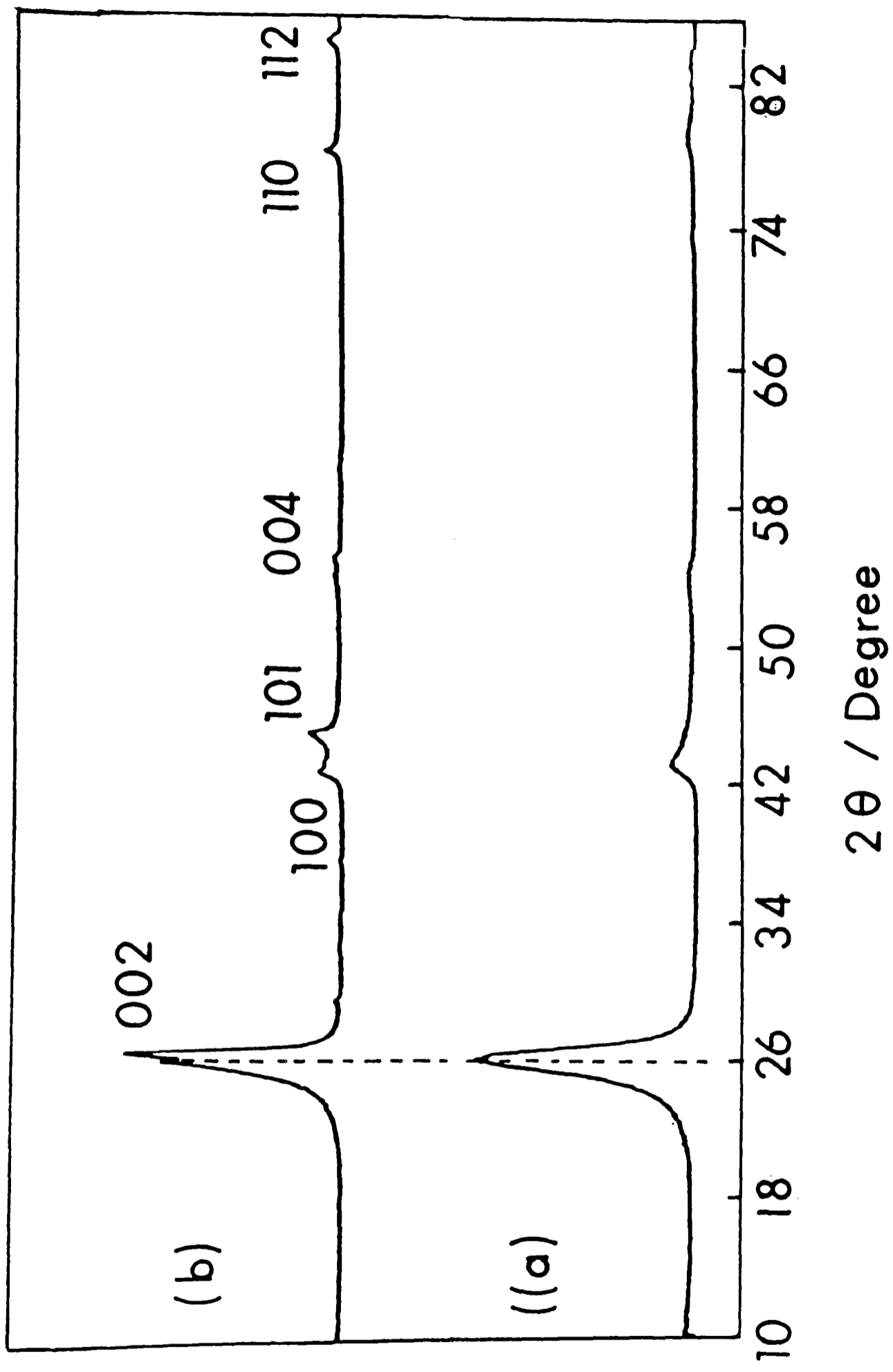FIG. 6.2-13: SEM OF PGC CONTAMINATED WITH NEEDLES

FIG.6.2-14 : SEM OF NEEDLES

FIG. 6.2-15 : X-RAY DIFFRACTOGRAMS OF CARBOPACK
WITH (b) AND WITHOUT (a) NEEDLES.

PGC Spheres

002

26.0°

(a)

002

26.4°

26.0°

(b)

PGC Needles & Spheres

d_{002} = 3.405 , 3.354 Å

004
53.5°
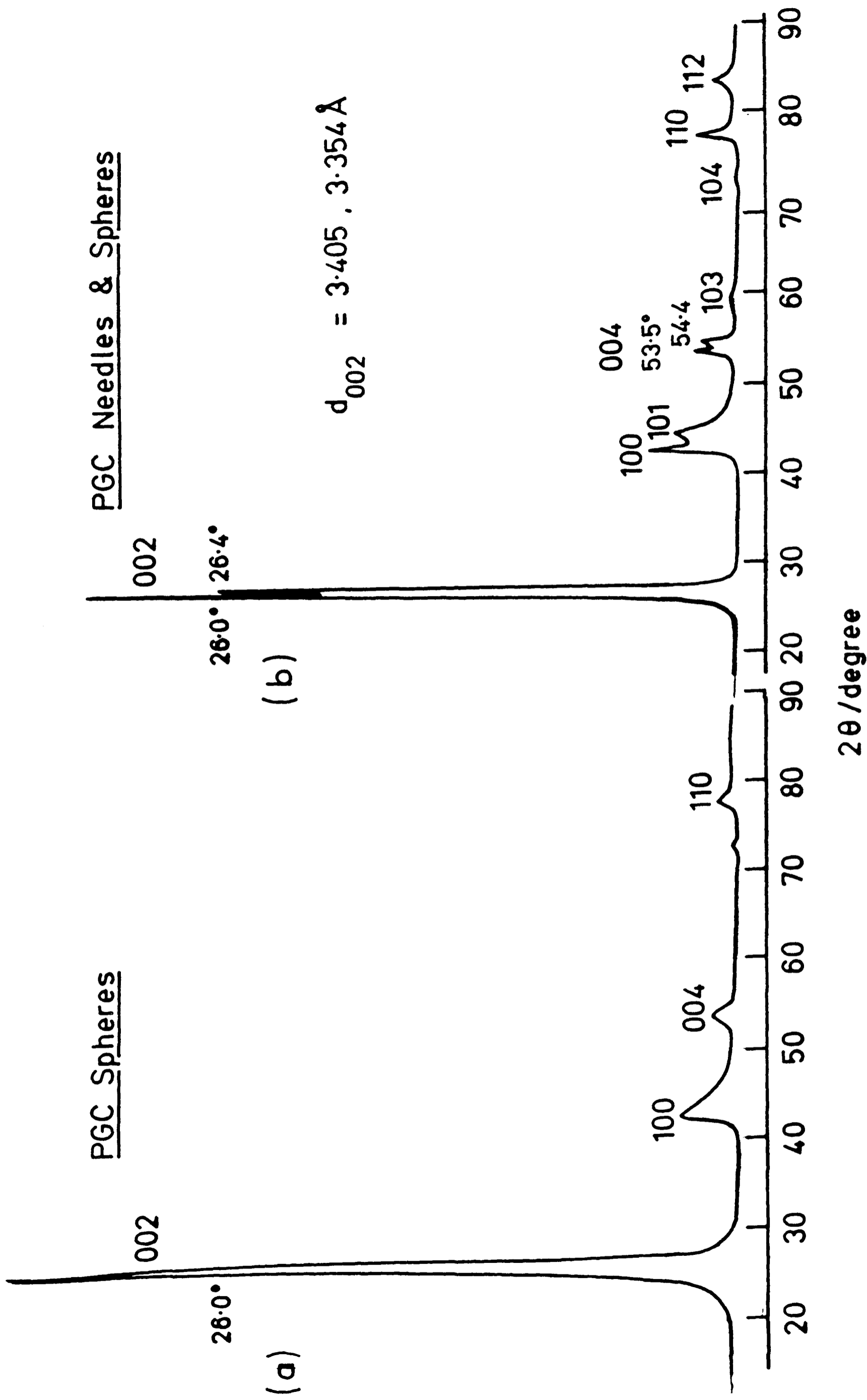54.4

100
101
103
104
110
112

100

004

110

2θ/degree

FIG. 6.2-16 : X-RAY DIFFRACTOGRAMS OF PGC WITH (b) AND
WITHOUT (a) NEEDLES

Table 6.2-7　Diffraction Angles of PGC and Carbopack with and without Needles, Compared with those of Graphite

X-Ray Diffraction Peaks	2θ Degrees				
	Graphite	PGC without needles	PGC with needles	Carbopack without needles	Carbopack with needles
002	26.6	26.0	26.0, 26.6	26.0	26.0, 26.6
100	42.4	42.4	42.4	42.4	42.4
101	44.5	–	44.6	–	42.4
102	50.5	–	–	–	–
004	54.5	53.4	53.4, 54.4	53.4	54.8
103	59.9	–	–	–	
104	71.6	–	–	–	
110	79.5	77.6	77.4	77.6	77.6
112	83.7	–	83.6	–	83.8

Figures 6.2-18 and 6.2-19.

Two reasons may be put forward to account for the presence of these needles. Firstly, there is still the presence of high molecular weight aromatic hydrocarbons which, at high temperatures, volatilise and then deposit pyrolytic carbon. At the same time, at temperatures greater than 1000°C, impurities present in the carbons may act as catalytic nuclei around which aromatics can easily recondense and graphitize. This is evident by HREM in Figure 6.2-20 where a concavity is seen at the tip of a formed graphitic needle, the concavity may represent the position of a metal particle which has evaporated away at higher temperatures.

The study of the X-ray diffractograms of PGC 77 cont-aminated with iron deliberately [PGC 77(Fe)] and PGC carefully prepared to exclude such contamination (PGC Quartz) shows the presence of a distinct shoulder in the diffractogram of PGC-Fe (Figure 6.2-21). This can be due to the presence of needles. Therefore, it would appear that the presence of metal impurities would enhance the formation of needles. In addition, a study of the HREM of PGC 77(Fe) and PGC 77 (Quartz) further confirms the idea that metals induce graphitization as a greater degree of graphitization is seen in PGC 77(Fe) (Figures 6.2-22 and 6.2-23).

Analysis of the X-ray diffractograms of several commer-cially available carbons (Figure 6.2-24) highlights the misuse of the term 'graphite'. The graphite felt supplied by Carbolite furnaces does not show any structure close to graphite. In fact, it is a totally amorphous material! The carbon electrodes from batteries appear to compose of two
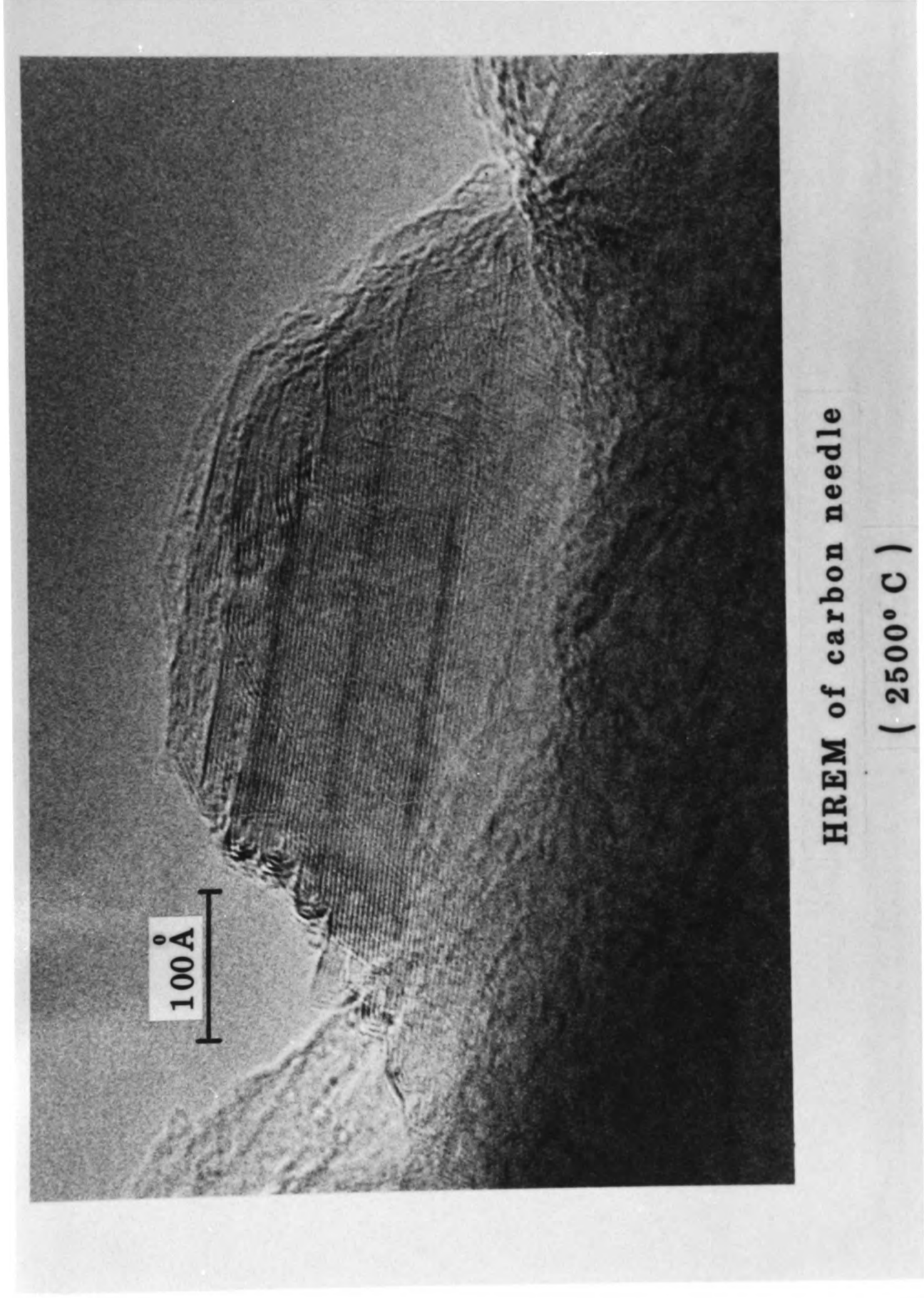
100Å

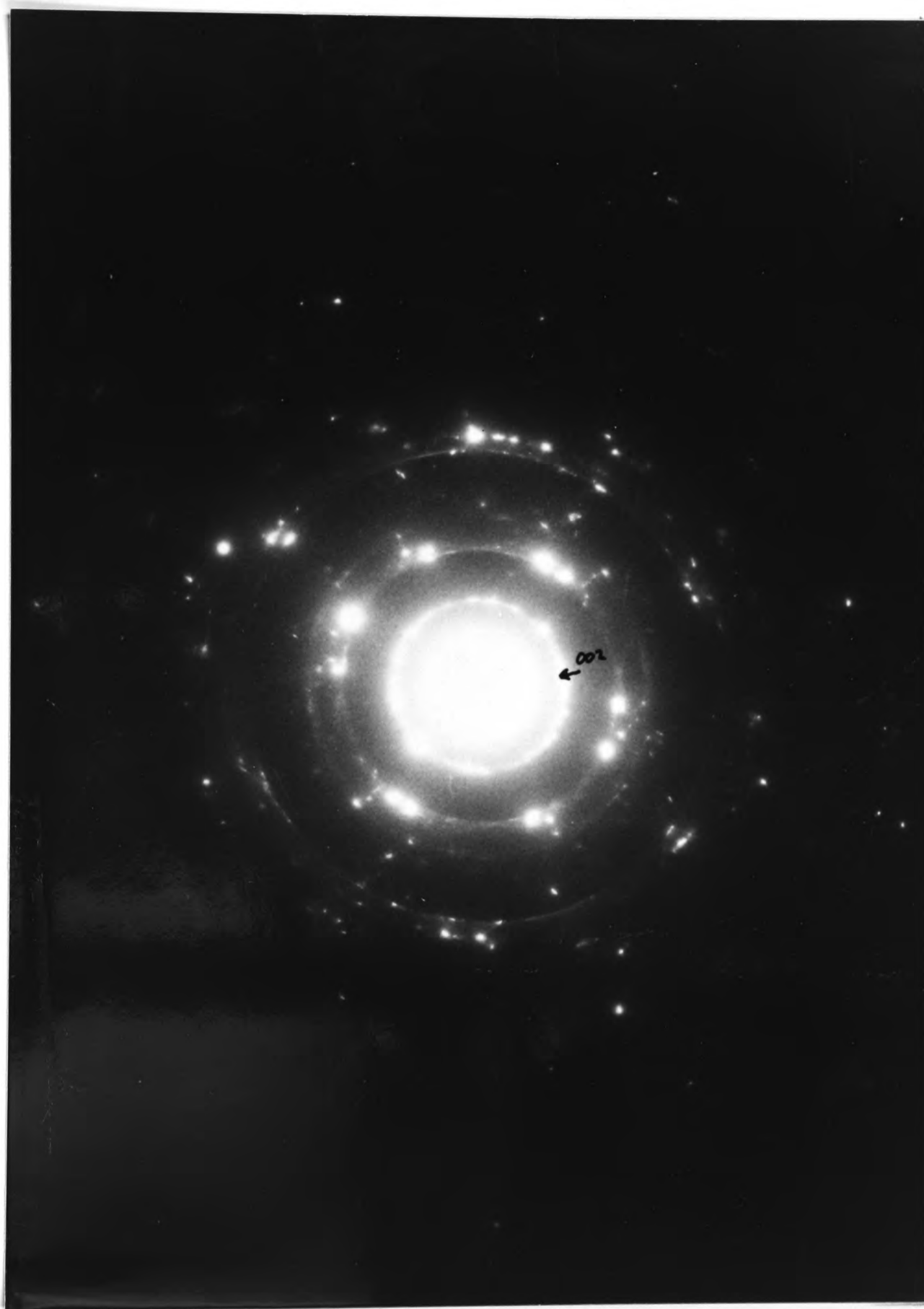HREM of carbon needle

(2500° C)

FIG. 6.2 - 18

FIG. 6.2 - 19 : ELECTRON   DIFFRACTION

PATTERN   OF   NEEDLE
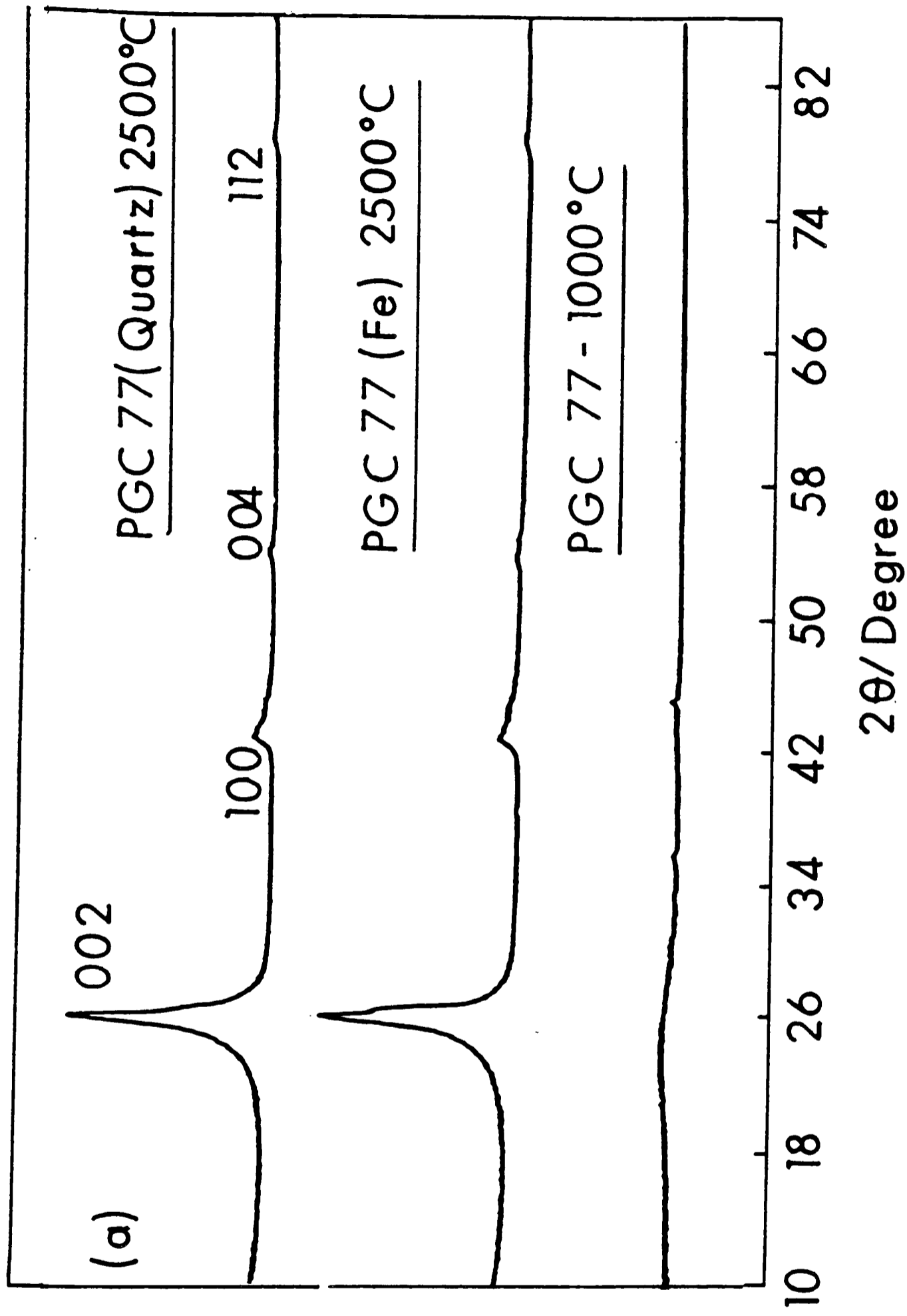
FIG. 6.2 - 20 : HREM OF NEEDLE SHOWING CONCAVITY

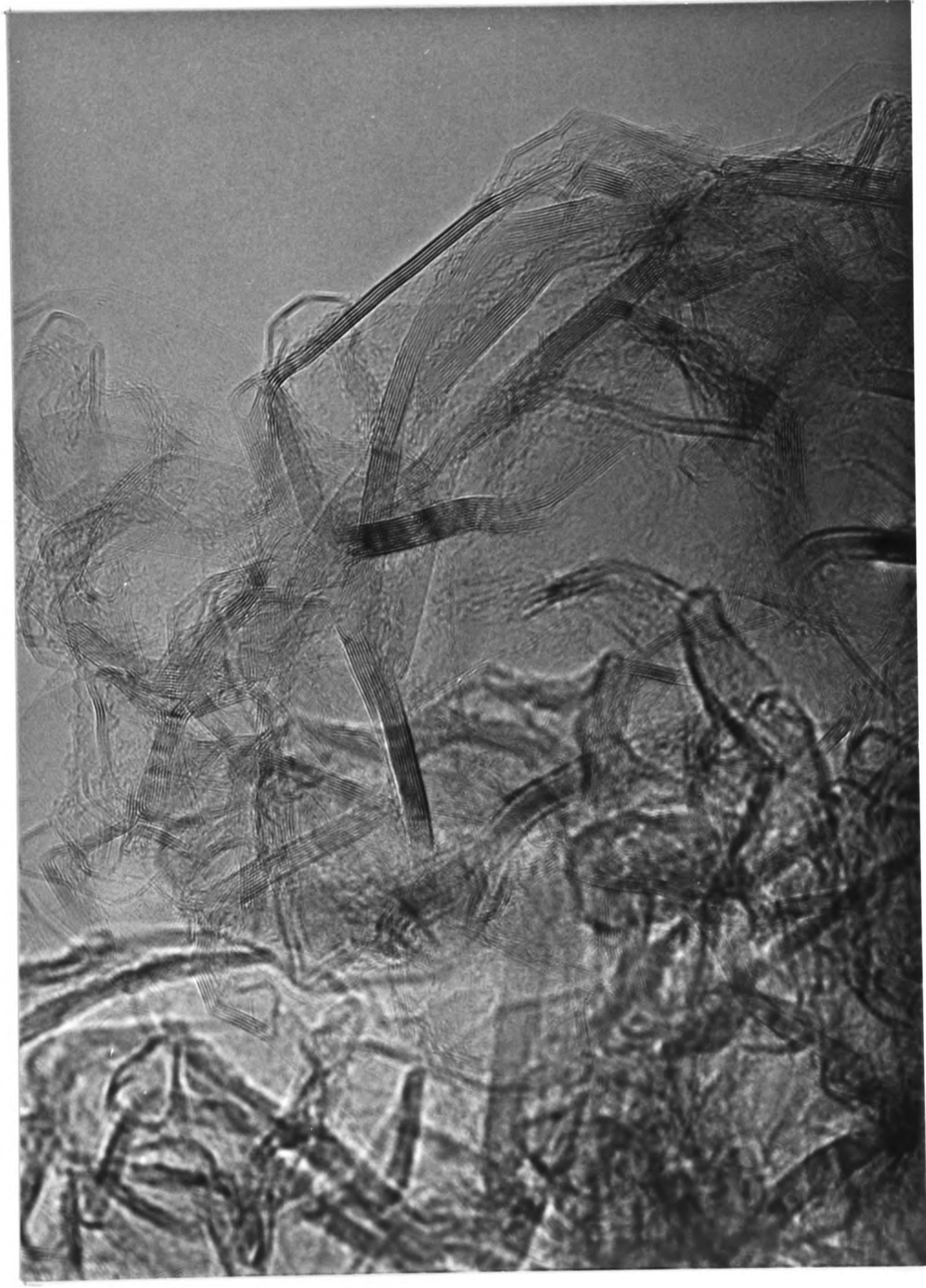FIG. 6.2 - 21 : X - RAY DIFFRACTOGRAMS OF PGC 77 WITH (b) AND WITHOUT (a) IRON AND OF AMORPHOUS PGC 77 (c)

FIG. 6.2-22: HREM OF PGC 77(IRON)

FIG. 6.2 - 23 : HREM OF PGC 77 (QUARTZ)

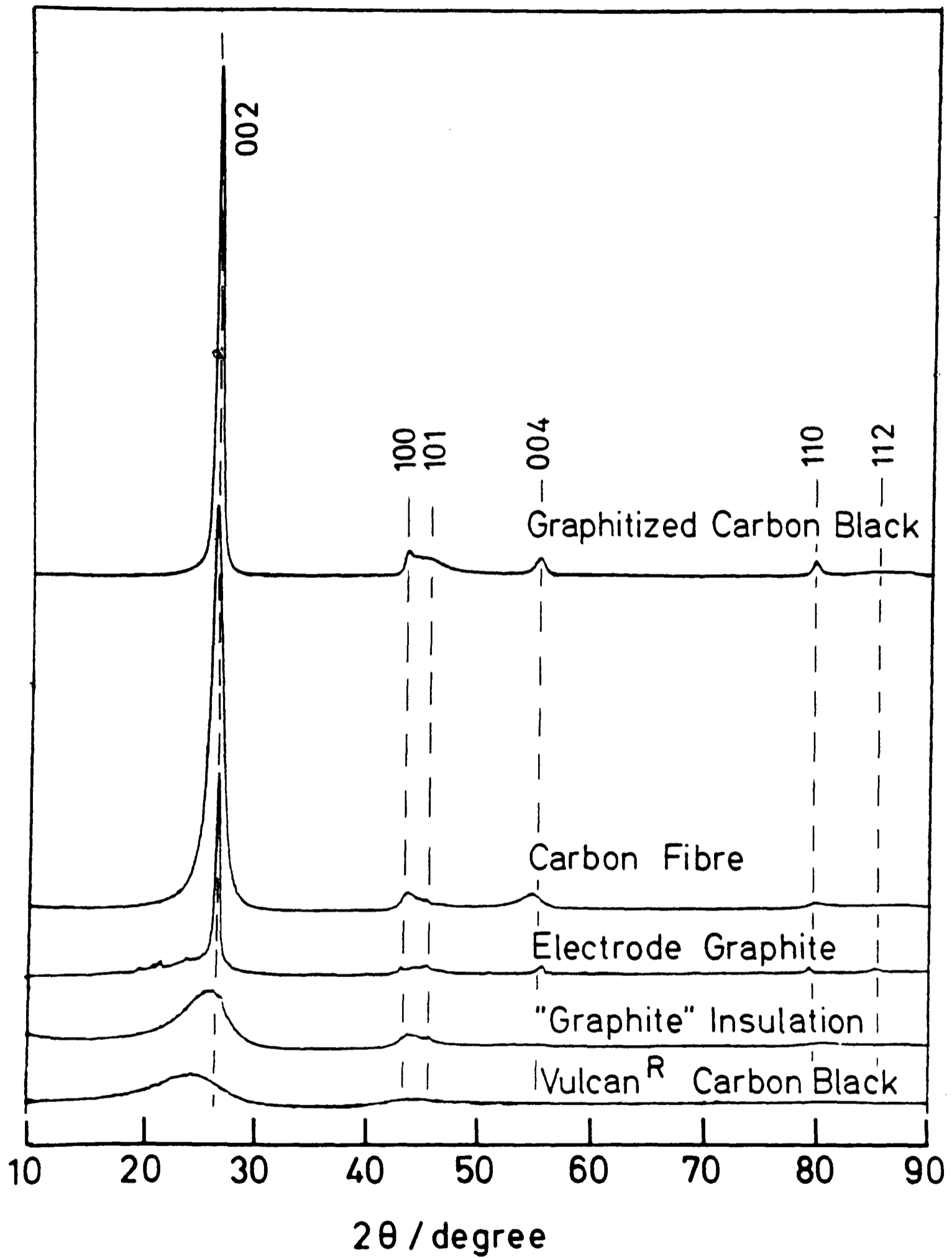# X-RAY DIFFRACTOGRAMS OF COMMERCIAL CARBONS

FIG. 6.2 - 24 : X - RAY DIFFRACTOGRAMS OF COMMERCIAL CARBONS.

phases, small crystallites of graphite being present in an otherwise amorphous matrix. The graphitized carbon black studied also do not have the structure of true graphite but, in fact, have the two-dimensional structure seen in PGC.

6.2.3   Identification of Trace Elements in PGC and other Carbons

PGCs, carbopack, Colin's Black Pearls and carbon-coated silicas all contained the same trace elements viz. Zinc, Copper, Nickel, Iron, Titanium and Calcium.   Table 6.2-8 shows the types of metals detected in the different samples and figures 6.2-25 and 6.2-26 show X-ray fluorescence traces of PGC 57 and 61 respectively at 1000°C and at temperatures greater than 2000°C.   In general, the concentration of con-taminants noted above were reduced by high temperature treat-ment.

Some earlier batches of PGCs (PGC 57 and 59) contained huge amounts of metallic impurities compared with the recent batches of PGCs (PGC 61) as can be seen from Figures 6.2-25 and 6.2-26.   This could be due to the fact that with the earlier batches of PGCs dissolution of silica was carried out using fused KOH at 450°C.   This had, in fact, caused corrosion of the stainless steel vessel, and the process was discontinued.

However, some of the samples of PGCs came back with higher metal content of some contaminants.   The vessel or crucible used and general precautions taken at higher temperatures seemed to be important.   When the samples were

Table 6.2-8

Data on metal content in different carbons

Height / CM

ELEMENTS	PGC 57 1000°C	PGC 57 2600°C	PGC 60 1000°C	PGC 60 2400°C	PGC 60 2600°C	PGC 61 1000°C	PGC 61 2600°C	PGC 59 ASH	CARBOPACK ASH	CARBOPACK	BP ASH	BP	BLACK PEARLS	CARBON COATED SILICA
W	13	OS↑	–	–	–	–	–	20	–	–	–	–	–	–
Ba	–	–	–	31↑	–	–	27↑	–	63	60	112	112	–	–
Zn	OS	65↓	28	25↓	–	15	–	32	14	28	19	78	16	38
Cu Kβ	35	50↑	57	13↓	13↓	10	32↑	–	–	15	10	50	13	48
Cu Kα	OS	OS	OS	42	66↑	36	110	26	21	53	35	OS	40	OS
Ni Kβ	29	–	57	–	–	–	–	–	–	–	–	–	–	–
Ni Kα	137	29↑	OS	25	17	21	8↓	23	11	16	11	15	9	43
Fe Kβ	63	23↓	70	14↓	–	10	–↑	5	39	63	43	74	12	20
Fe Kα	OS	145↓	OS	55	22↓	53	16	40	223	OS	240	OS	43	108
Ti	50	OS↑	20	78↑	55↑	109	68↓	223	70	19	211	OS	–	41
Ca	13	22↑	4	42↑	–	2	–	3	73	37	40	40	18	12
Co	33	10↓												

Total height for full scale intensity = 250cm.

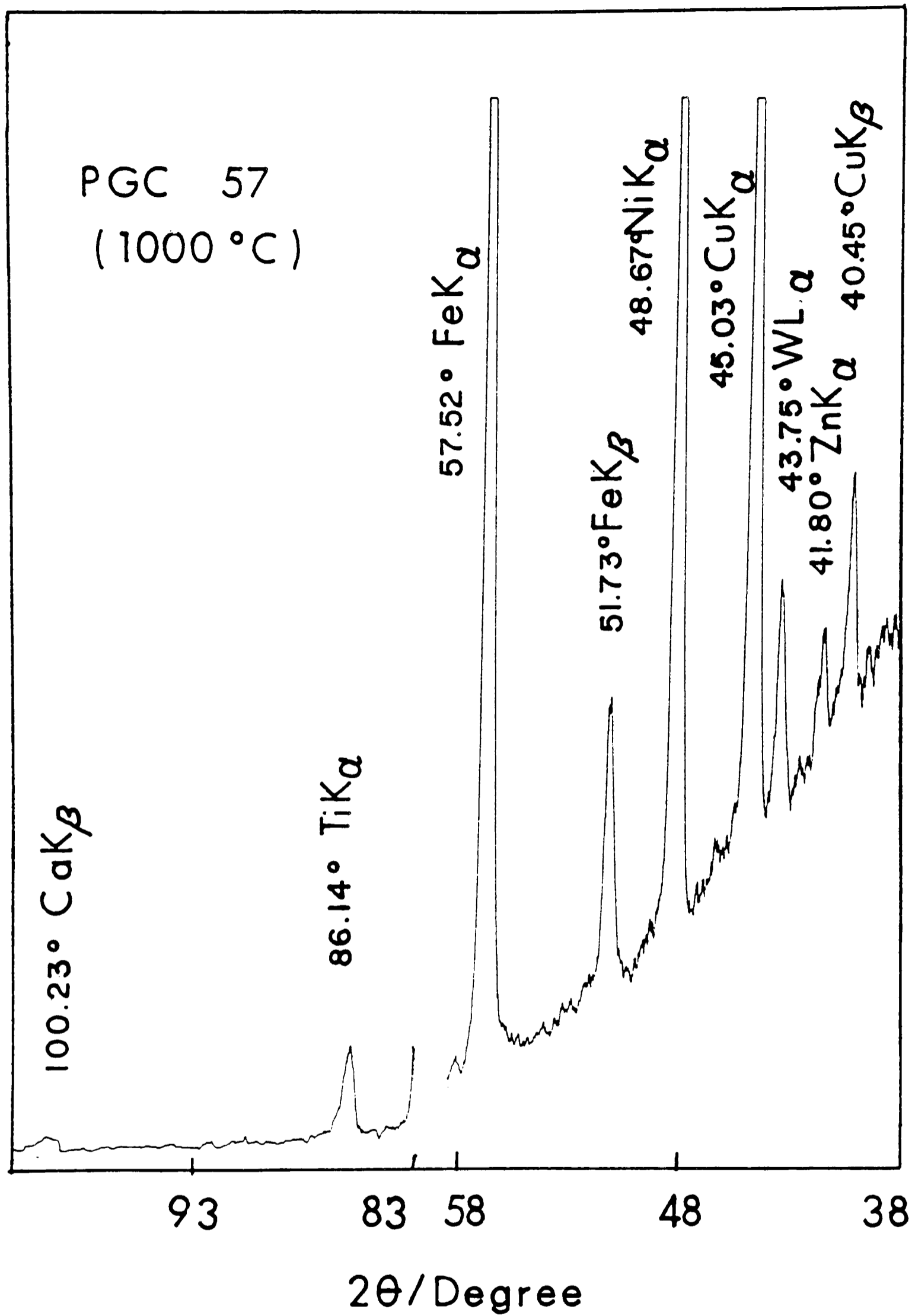Trace-Height (0↔83)cm   Large (16↔250)cm   Medium (84↔167)cm   OS – offscale

FIG. 6.2 - 25 (a) : X - RAY FLUORESCENCE OF
AN EARLY BATCH OF PGC
BEFORE HIGH HEAT TREATMENT
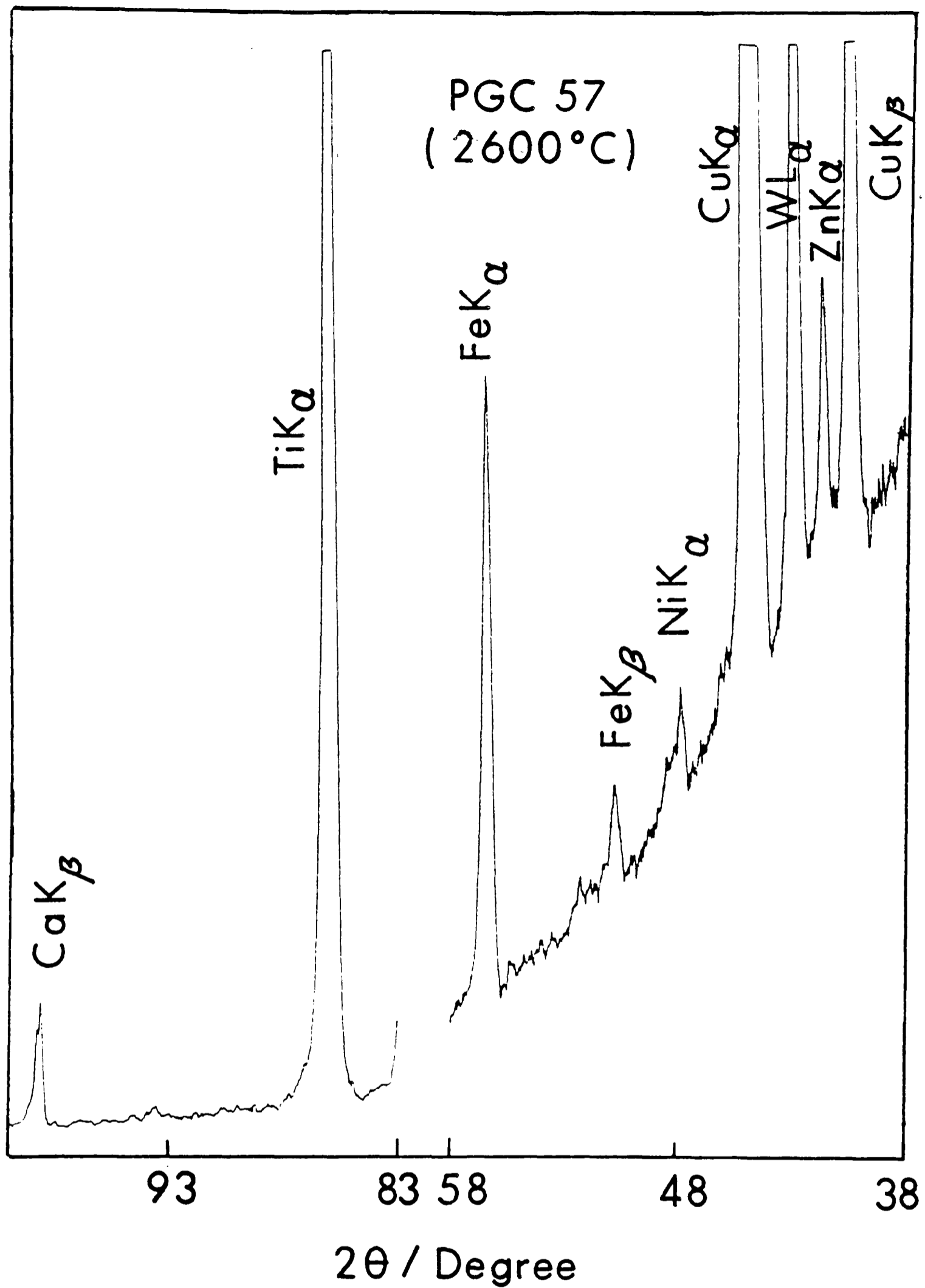
FIG. 6.2 - 25 (b): X-RAY FLUORESCENCE OF AN EARLY BATCH OF PGC AFTER HIGH HEAT TREATMENT
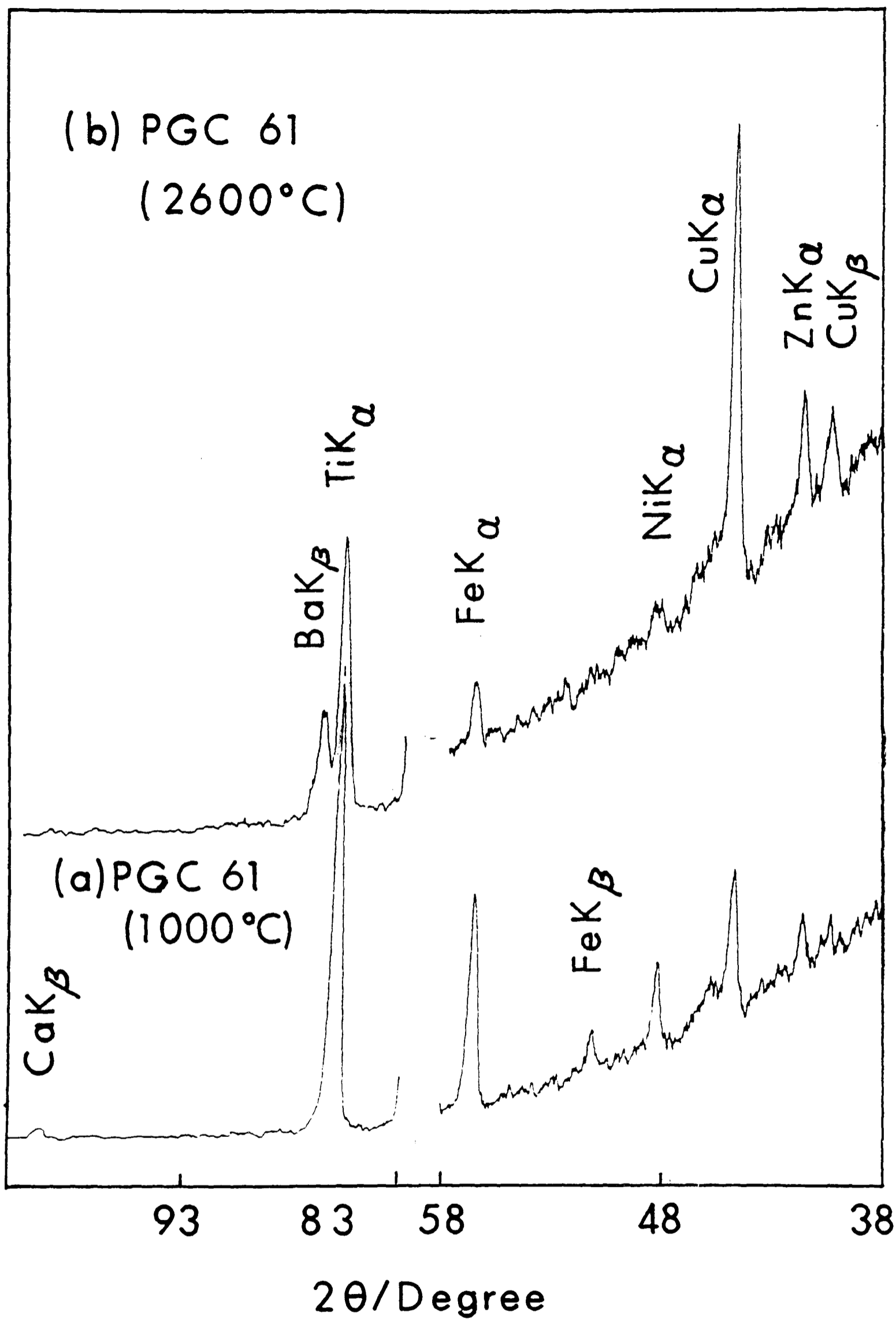
(b) PGC 61
(2600°C)

(a) PGC 61
(1000°C)

FIG. 6.2-26 : X-RAY FLUORESCENCE OF A LATER
BATCH OF PGC BEFORE (a) AND
AFTER (b) HIGH HEAT TREATMENT.

heated at Anglo Great Lakes, PGCs 57 and 59 showed con-
tamination of tungsten, copper, titanium and copper. When
samples were heated at Swansea, there was the contamination
of barium apart from titanium and copper (PGCs 60 and 61).
Atomic Weapons Research Establishment (AWRE) incorporated
contaminants like calcium, barium and uranium!! X-ray
fluorescence traces of different carbons are shown in Figure
6.2-27.

6.2.4 Conclusions

1. PGC has been incorrectly named as porous glassy carbon.
Its proper name should be porous 2d-graphitic carbon due to
its two dimensional nature.

2. It is fairly common to find the term 'graphitized' used
in a much less rigorous fashion. Carbon products which have
been treated to some arbitrarily high temperature (see 2500°C
or above) are very often called graphite or said to have been
graphitized by virtue of such treatment alone, without regard
to their final structure. As noted in section 4.2, graphites
have 3-dimensional Bernal structure. The wrong usage is
based on the misconception that the structure of a carbon is
determined primarily by the maximum temperature of treatment
without regard to the nature of the precursor or the treat-
ment time, and that all carbons treated to a particular
temperature have the same structure regardless of their
origins. 'Graphite' Felt as seen in section 6.2-2 has an
amorphous structure despite the fact that it has been heat
treated at temperatures near 3000°C. "Pyrolytic graphite"
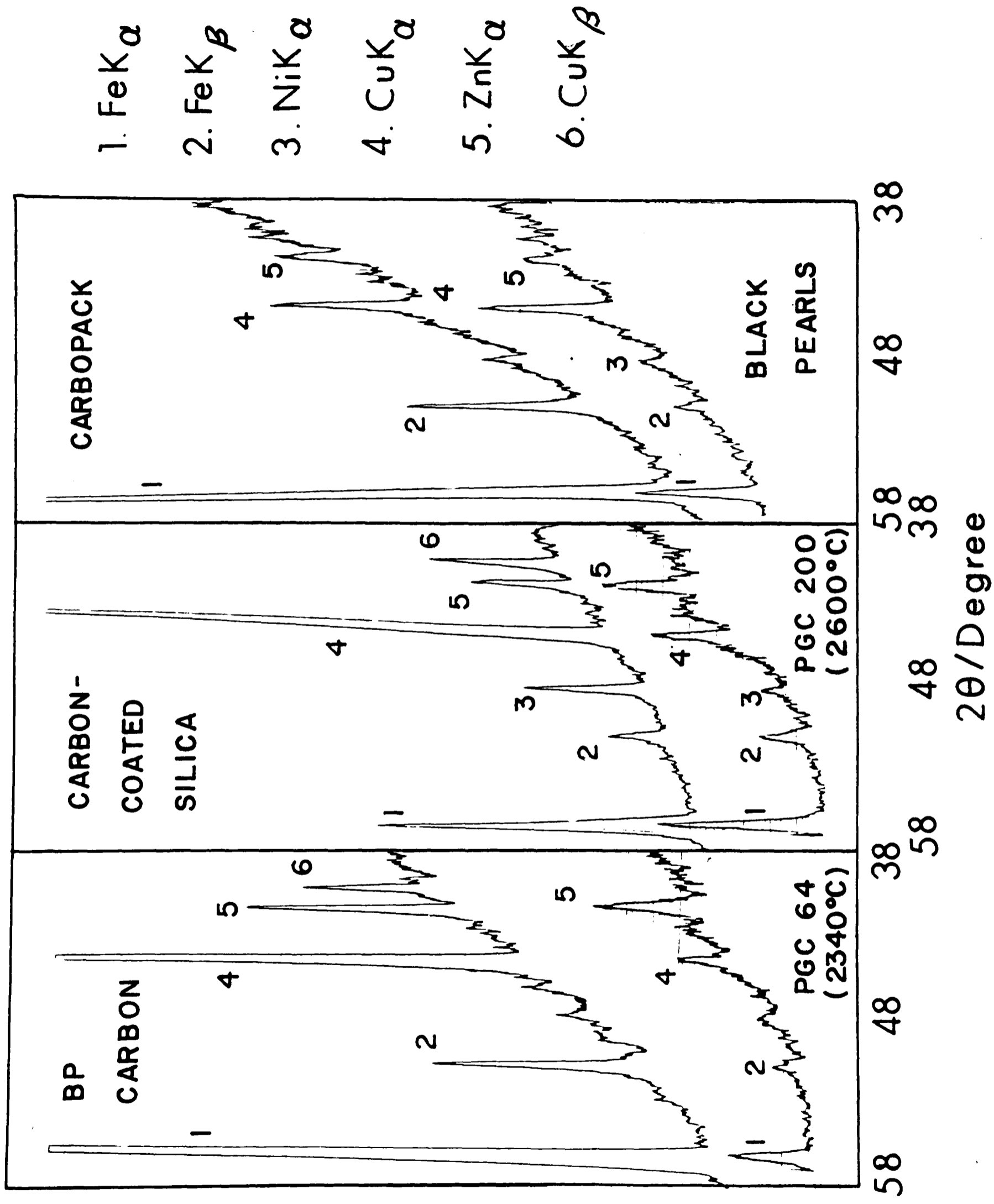a term commonly applied to as deposited pyrolytic carbon has

1. FeKα
2. FeKβ
3. NiKα
4. CuKα
5. ZnKα
6. CuKβ

FIG. 6.2 - 27 : X-RAY FLUORESCENCE OF DIFFERENT CARBONS

2θ/Degree

CARBOPACK

BLACK PEARLS

CARBON-COATED SILICA

PGC 200 (2600°C)

BP CARBON

PGC 64 (2340°C)

the two-dimensional amorphous structure typical of un-graphitized carbons. 'Graphite' fibers and fabrics and 'graphitized' carbon blacks are other examples. 'Graphitized' carbon blacks, which have been heat treated to 3000°C, do not have the Bernal 3-dimensional structure of graphite but possess only two-dimensional or turbostratic order. This misuse of terminology is certainly confusing. While one might hope that the terms graphite and graphitization could be reserved to those carbon materials which develop substantially the three-dimensionally ordered graphite structure, it is probably now too late to expect a general adoption of such a recommendation. At best we could expect that the origin of the material, the maximum treatment temperature and the time at the temperature will be used to specify the thermal treatment history of less perfect carbons and that the term 'graphite' be used for 2- or 3-dimensional ordered carbons.

3.   Contamination of high temperature 2-dimensional graphites with needles seems to be a common feature of all carbons heated to higher temperatures. A proper purging system is, therefore, desirable in order to eliminate these needles.

4.   Structural study by HREM confirms why PGC is a much stronger material than graphitized carbon blacks by clearly showing that it is made up of interconnecting graphitic sheets.

Chapter 6

References

1. Kawamura, K. and Jenkins, G.M., J. Materials Science 5 (1970) 262.

2. Jenkins, G.M., Kawamura, K. in Polymeric Carbons, Cambridge University Press, 1976.

3. Richie, H., private communication.

Part III

(THE STUDY OF CARBONS)

CHAPTER 7

THE STUDY OF CARBONS

7.1   Surface Complexes on Carbon

7.1.1   Introduction

A very large number of studies of chemisorption of gases and vapours have been made on carbons of diverse forms ranging from chars, activated carbons, carbon blacks and cokes.   In all these carbons, the portion of carbon which exists in the form of disordered, single, unstacked, graphite-like layers is the more susceptible to chemisorption of gases and vapours, while the portion which shows some degree of well-ordered parallel stacking is the less susceptible.   In addition to graphite layers there are many exposed defects, dislocations and discontinuities in the layer planes of the microcrystalline carbons, apart from the edges of the carbon layers.   Such sites, called the 'active' sites, are associated with high concentrations of unpaired electron spin and, there-fore, are expected to play a significant role in chemisorption. Moreover, charcoals and activated carbons, being porous, and carbon blacks, being composed essentially of spherical particles of colloidal dimensions, have large internal and external surface areas for unit weight respectively.   The surface carbon atoms located at the active sites, due to residual valencies, show a strong tendency to chemisorb other elements such as oxygen, hydrogen, nitrogen, chlorine, bromine, iodine and sulphur and give rise to nonstoichiometric stable surface compounds called surface complexes.   Many of the surface reactions of charcoals and carbon blacks arise either because of their tendency to chemisorb other elements or because of the existence of a superficial layer of the chemically bonded

elements. It is now known that almost all types of carbons are covered with oxygen complexes unless special care is taken to eliminate them. These complexes are often the source of the property by which a carbon becomes useful or effective in particular applications.

7.1.2 Carbon-oxygen Complexes

7.1.2.1 Formation of carbon-oxygen complexes

Several methods of forming carbon-oxygen surface complexes have been reported in recent years; the commonest of these involve the reactions with oxidizing gases.

7.1.2.1.1 Reactions with oxygen

Oxygen is chemisorbed more readily than most other elements and carbon-oxygen complexes are the most important in influencing surface reactions of carbons. Smith,[1] in 1863, was probably the first worker to suggest that when oxygen is adsorbed on a carbon surface it undergoes a chemical change. He found that adsorption of oxygen on charcoal did not cease after a month, and that while nitrogen and other gases adsorbed on charcoal could be easily removed, oxygen could be removed only on strong heating and then as carbon dioxide. Rhead and Wheeler[2,3], Lowry and Huelett[4] all confirmed that the gases evolved when charcoal is heated to 900°C consisted entirely of carbon dioxide and carbon monoxide, the former predominating at lower temperatures and the latter at higher temperatures. Further evidence for chemisorption of oxygen on carbons was furnished by the work of Langmuir[5],

Lambert[6] and Lepin[7]. Ward and Rideal[8] found that the heat
of adsorption of oxygen on charcoal even at 0°C, was of the
order 165 KJ/mole; suggesting the chemical nature of the
interaction involved. Other workers[9-11] reported even
higher values, ranging from 160 to 250 KJ/mole.

According to Puri et al[12] the chars of sugar and coconut
shells continue to pick up oxygen slowly from air but rapidly
from oxygen atmosphere at room temperature. In
oxygen, the process was completed in twelve hours but in air
it took almost three months for completion. The presence of
moisture had very little effect on the rate of pick-up. The
same value for oxygen content, characteristic of the charcoal
and the temperature of carbonisation, was obtained in every
case. The values were appreciably less if they had been
carbonized at higher temperatures.

7.1.2.1.2 Reactions with nitrous oxide

A number of reactions between carbons and the oxides of
nitrogen resulting in the chemisorption of oxygen have been
reported[13-18]. Smith and co-workers[17] using Graphon and sugar
charcoal found that the interaction with nitrous oxide in the
temperature range of 400-650°C, first involved a rapid oxida-
tion of the active centres, giving rise to carbon-oxygen
surface complexes and free nitrogen. This oxidation was
followed by a slow reaction in which the complexes were oxidized
to gaseous carbon dioxide and more free nitrogen was produced.
The following reaction mechanism was suggested:

$$N_2O + (C) \xrightarrow{\text{fast}} N_2 + (CO)$$

surface-complex

$$N_2O + (CO) \xrightarrow{\text{slow}} N_2 + CO + (CO)$$

$$(CO) \longrightarrow CO$$
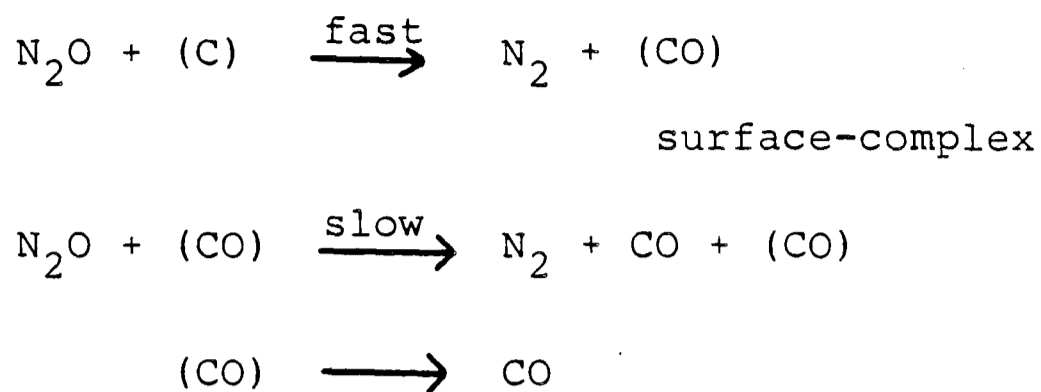
(where entities in parenthesis are meant to represent surface atoms or groups).

Later, Smith et al[18] extended this work by using nitric oxide in place of nitrous oxide. At temperatures up to 200°C, they observed a rapid fixation of oxygen with production of free nitrogen. At higher temperatures, particularly between 450 and 600°C, nitrogen, carbon monoxide and carbon dioxide were produced besides surface oxygen complexes. The authors postulated that a molecule of nitric oxide reacts with another molecule at the site of the oxygen complex on the surface to give nitrogen and carbon dioxide, and an oxygen complex on the adjacent carbon atom. The new oxygen complex served as a site for further adsorption of nitric oxide, and thus the reaction was continued. The preceding mechanism was represented by the following scheme:

$$2NO + 2(C') \longrightarrow N_2 + 2(C'O)$$

$$NO + (C'O) \rightleftharpoons (OC'\text{\_ \_ \_ \_}ON)$$

$$NO + (OC'\text{\_ \_ \_ \_}ON) + (C'') \longrightarrow C'O_2 + N_2 + (C''O)$$

$$NO + (OC'\text{\_ \_ \_ \_}ON) + (C''') \longrightarrow C'O_2 + N_2 + C'''O$$
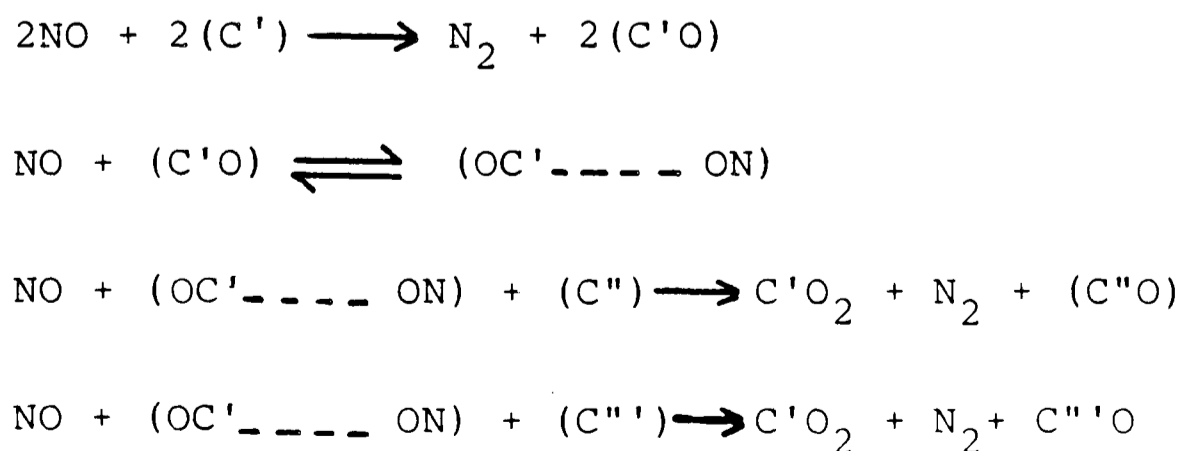
The entities enclosed in the parenthesis represent species chemisorbed on the carbon surface.

7.1.2.1.3 Reactions with water vapour

A number of investigations have been reported on reactions of activated carbons and carbon blacks with water vapour at different temperatures, under static as well as dynamic conditions[19-25]. The work of Smith, Pierce and Joel[19] indicated that the treatment resulted in the formation of a hydrogen complex as well as two oxygen complexes, one that decomposed easily as carbon dioxide and the other, which was more stable, decomposing as carbon monoxide when heated to temperatures above 500°C. This was confirmed by Singh, Parkash and Puri[22] who further proved that nearly 60% of the oxygen fixed as a complex was disposed of as carbon dioxide and the rest as carbon monoxide. According to them, the (CO) complex was formed only between 200° and 400°C and not at higher temperatures. This was explained as due to oxidation of this complex to gaseous carbon dioxide by water vapour at higher temperatures.

$$H_2O + (C) \longrightarrow H_2 + (CO)$$

$$(CO) + H_2O \longrightarrow CO_2 + H_2$$

These observations are significant in showing that the more stable (CO) complex, which ordinarily can be desorbed completely only on heating in vacuum to about 1000°C, can be eliminated by heating in a current of steam for six to eight hours even at 400°C.

7.1.2.1.4 Reactions with carbon dioxide

Reactions of carbon with carbon dioxide have been reviewed by Walker, Rusinko and Austin[26]. It has been suggested[27,28] that carbon dioxide oxidizes carbons to carbon monoxide, forming oxygen complexes as intermediates. The various steps of the reactions are:

$$CO_2 + (C) \xrightarrow{\text{fast}} CO + (CO)$$

$$(CO) \longrightarrow CO$$

$$CO + (CO) \longrightarrow CO_2 + (C)$$
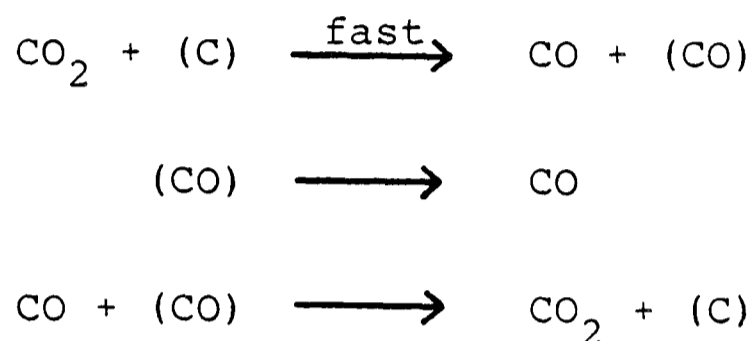
Deiz, Carpenter and Arnold[29] observed three increasing levels of interaction between carbon and carbon dioxide: (1) pure physical adsorption, (2) formation of an adsorption complex having a bicarbonate structure and (3) formation of an adsorption complex with a carbonate complex.

7.1.2.2 Temperature of formation of carbon-oxygen complexes

Walker and co-workers[30-33] studied chemisorption of oxygen on Graphon, a highly graphitized carbon black in the temperature range 300-625°C at low pressures up to 0.5mmHg. A sharp increase in the saturation amount of oxygen adsorbed at temperatures of about 400°C was observed. Later, in 1968, Walker[34] suggested that only the carbon atoms located at the edges of the basal planes were active in chemisorbing oxygen. Lussow[35], however, on account of his work suggested that

chemisorption of oxygen at 625°C occurs not only at the edge atoms but also at lattice intersections and defects.

Hennig[36] from microscopic examination of single graphite crystals concluded that at temperatures below 800°C the oxidation rate of the edge carbon atoms was about twenty times as high as that of the carbon atoms at the cleavage surface.

7.1.2.3 Decomposition of carbon-oxygen complexes

The surface oxygen complexes formed on treatment of carbons with oxygen or oxidizing gases are generally stable even under high vacuum, at all temperatures below the temperature of formation[37]. They are generally stable to about 250°C when outgassed around this temperature, the gas evolved consists mostly of carbon dioxide and water vapour. Around 500°C, the evolution of carbon monoxide commences and with increasing temperatures the ratio CO_2/CO continuously decreases. Above 600°C, the gas evolved is largely carbon monoxide. Hydrogen comes off as steam to about 500°C - occasionally to 700°C - and above that, as the elementary gas which comes off in large quantities in the region of 700-1000°C[12,38-40].

Johnson[41,42] showed that the combined oxygen in carbon blacks comes off on evacuating slowly at 400°C and rapidly at 955°C in the form of carbon dioxide and carbon monoxide. Anderson and Emmett[43,44] heated a few samples of carbon blacks in vacuum at different temperatures. Puri and co-workers[12,38-40] subjected carbon blacks to a treatment of vacuum pyrolysis but emphasized that such treatment should be carried out with

gradually increasing temperature so that the carbon dioxide

evolved at 200-300°C temperature range could be absorbed

in sodium hydroxide as soon as it was formed and so escaped

reduction to carbon monoxide at the higher temperatures.

Similarly, the chemisorbed water was removed at much lower

temperatures (<500°C) to minimize the chances of its inter-

acting with carbon at higher temperatures. Caltharp and

Hackerman[45] conducted a thermal decomposition of the com-

plexes on Spheron-6 by passing a stream of purified helium

over a sample of the carbon black which had been pre-dried

at 150°C. Smith et al[46] heated their samples in a current

of hydrogen at 1000°C to remove carbon-oxygen complexes and

to obtain clean surfaces. Puri, Kumar and Singh[47] showed

that the treatment of charcoals in a current of hydrogen at

600°C for sixteen hours causes a complete elimination of

oxygen as well as partial elimination of hydrogen. According

to these workers, there were no indications of reformation

of these complexes on mere exposure to air at room tempera-

ture.

On the other hand, however, Lohenstein and Deitz[48] showed

that the treatment of bone char with hydrogen at 400°C results

in enhanced chemisorption of oxygen at 200°C and concluded

that the hydrogen treatment causes the formation of some C-H

bonds. Emmett[49] observed an increase in surface area of

carbons when heated with hydrogen as carbon atoms are lost

from the surface producing methane resulting in surface

etching. This is analogous to treatment with steam or

carbon dioxide where oxides of carbon are produced when

steam is passed.

7.1.2.4 Acid-base Character of Carbons in Relation to Chemisorbed Oxygen

The acidic or basic character of a carbon depends upon its history of formation and, in particular, upon the temperature at which it has been heated. King[50] reported that charcoal activated in air or oxygen at a particular temperature has a specific pH value characteristic of that temperature. Singh, Sharma and Puri[51] showed that the pH value of sugar charcoal in aqueous suspension, which was close to 3, increased as the charcoal was outgassed at increasing temperatures. It increased to 7 at 750°C and rose further to about 8.6 at 1000°C.

Puri et al[52] and Smith[53] have shown that carbons outgassed at high temperatures and exposed to oxygen between 200° and 700°C adsorb appreciable amounts of strong bases but very little of strong acids. The optimum temperature for the development of maximum capacity to adsorb bases has been shown to lie close to 400°C, which corresponds to the temperature of maximum fixation of oxygen. On the other hand, if outgassed carbons are exposed to oxygen either below 200°C or above 700°C they adsorb strong acids but very little strong bases.

7.1.2.5 Acidic Surface Oxides

The presence of acidic surface oxides has been implied since the time it became known that oxygen-containing carbons can neutralize appreciable amounts of alkalies irreversibly[52,54-57]. According to Puri et al.[52,54], Weller and Young[55] and Boehm et al.[56] if a suspension of charcoal or carbon black

is agitated with a moderate excess of a strong alkali, preferably in an atmosphere of nitrogen, for a sufficiently long time, extending to two or three days, it is possible to obtain maximum and reproducible values.

Studebaker[58] carried out potentiometric titrations of a number of carbon blacks in a non-aqueous medium (ethylene diamine) using 0.1N sodium amino ethoxide as the titrant. The acidity values obtained were much higher than that obtained at titrating with sodium hydroxide in an aqueous medium. On the other hand, Rivin[59] did not find any difference in acidity values whether by titrating in aqueous or in non-aqueous medium using strongly basic lithium aluminium hydroxide in diethyl sorbitol.

According to Puri and co-workers the amount of sodium hydroxide or barium hydroxide needed to neutralize charcoals[12, 38,39] and commercial carbon blacks[54] were found to be equivalent to the amounts of the (CO_2) complexes. As the amount of the complexes decreased on outgassing the samples at increasing temperatures, the capacity for base-adsorption decreased correspondingly. When the entire amount of the complex was eliminated on outgassing at around 700°C the carbon completely lost the property to neutralize alkali even though it retained an appreciable amount of oxygen. This is illustrated by titration curves of sugar and coconut charcoals in figure 7.1-1[60] and some commercial carbon blacks in figure 7.1-2[54] using barium hydroxide as the titrant. The points of inflection of the titration curves of the sugar and coconut charcoal (Fig. 7.1-1) are quite sharp and resemble very closely the titration curve of carbonic acid in the case of carbons
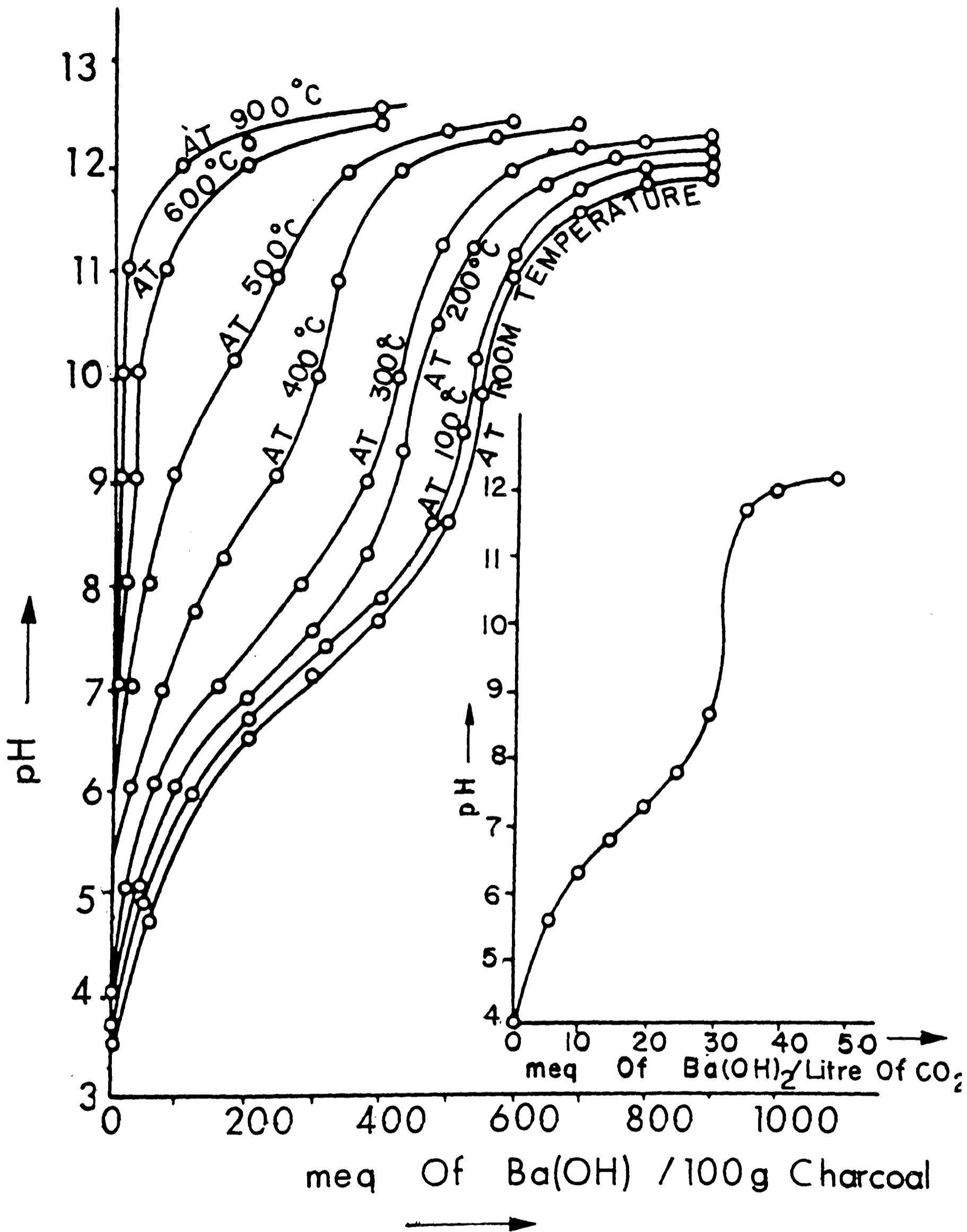
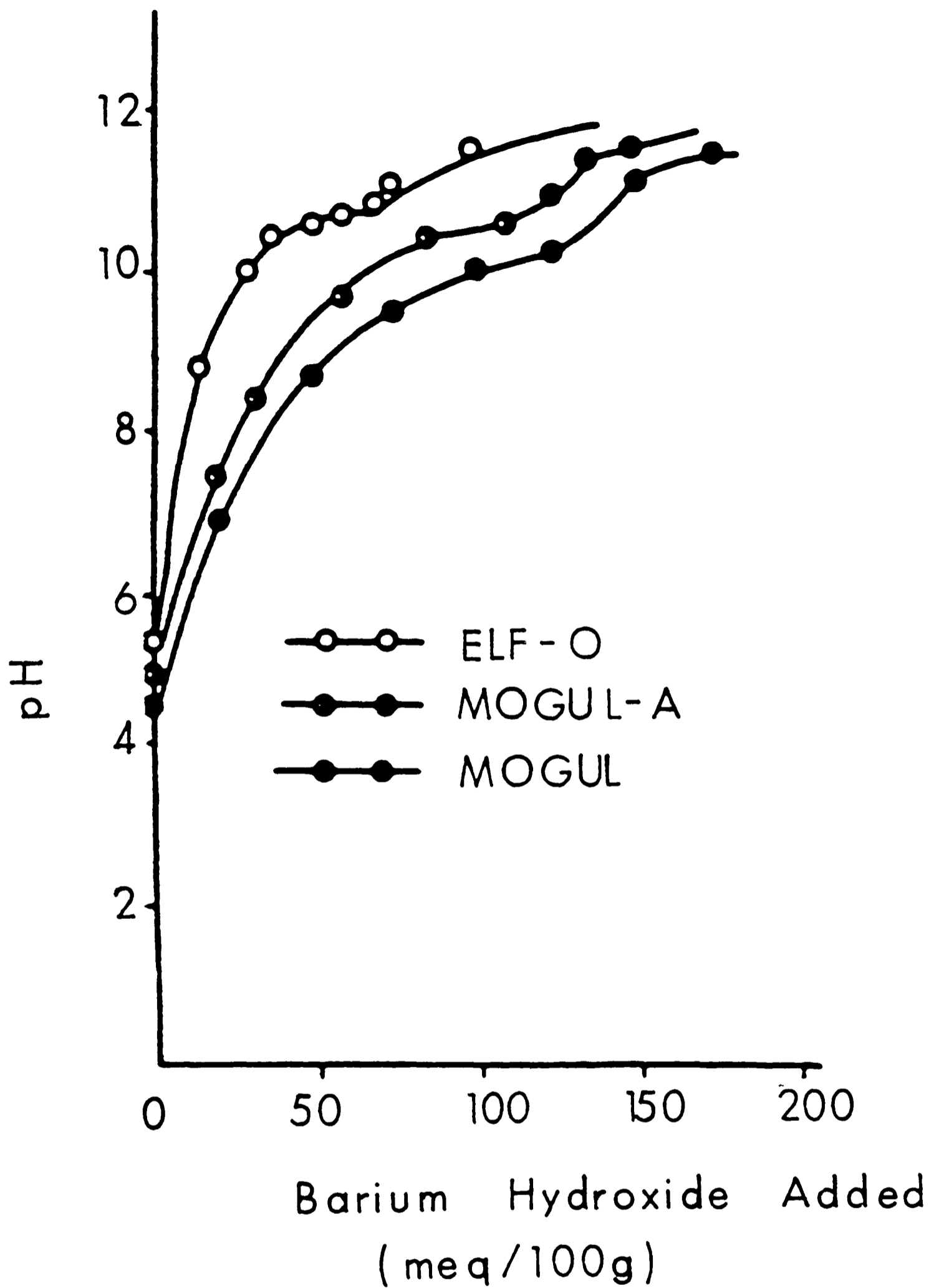FIG. 7.1-1 : TITRATION CURVES OF SUGAR CHARCOAL OUTGASSED AT DIFFERENT TEMPERATURES, AND OF CO₂ WITH Ba(OH)₂ (Ref.60)

FIG. 7.1-2 : TITRATION CURVES OF
VARIOUS CARBON BLACKS
WITH BARIUM HYDROXIDE
(from Ref. 54)

of high acidity.   As the acidity decreases with the increase in the temperature of evacuation the curves become flat and the points of break are not easily detected[57,61]. Puri et al.[54,60] on the other hand, questioned the existence of strongly acidic groups on the surface of activated carbons and carbon blacks because the titration curves obtained for carbon blacks (Fig.7.1-2) were flat and without a break and unlike those on sugar charcoal did not resemble those of strong acids, but instead indicate the presence of much weaker acid groups, of strength comparable to that of a phenol group. The pK values taken as pH values at half neuralizations lie between 9 and 10.

When Mogul was subjected to oxidation with nitric acid whereby its surface acidity was as high as 530 mE/100 g the titration curve shows a sharp inflexion with a pK value of about 5.5[54] (Figure 7.1-3).   Puri and Bansal[54] subjected the oxidized Mogul to partial evacuations to eliminate increasing amounts of the (CO_2) complex at different tempera- tures whose titrations are also given together with that of the original Mogul.

Kruyt and Kadt[62,63] and Schweitzer and Goodrich[64] attributed acidity of carbon blacks to carboxyl groups. Hofmann and Ohlerich[65] and Studebaker et al.[66] also suggested the presence of phenolic groups to account for the non- hydrolyzed fraction of the products.   According to Garten and Weiss[67], acidity of carbons is primarily due to three functional groups namely phenols, f-lactones and n-lactones. They also questioned the existence of carboxylic groups.
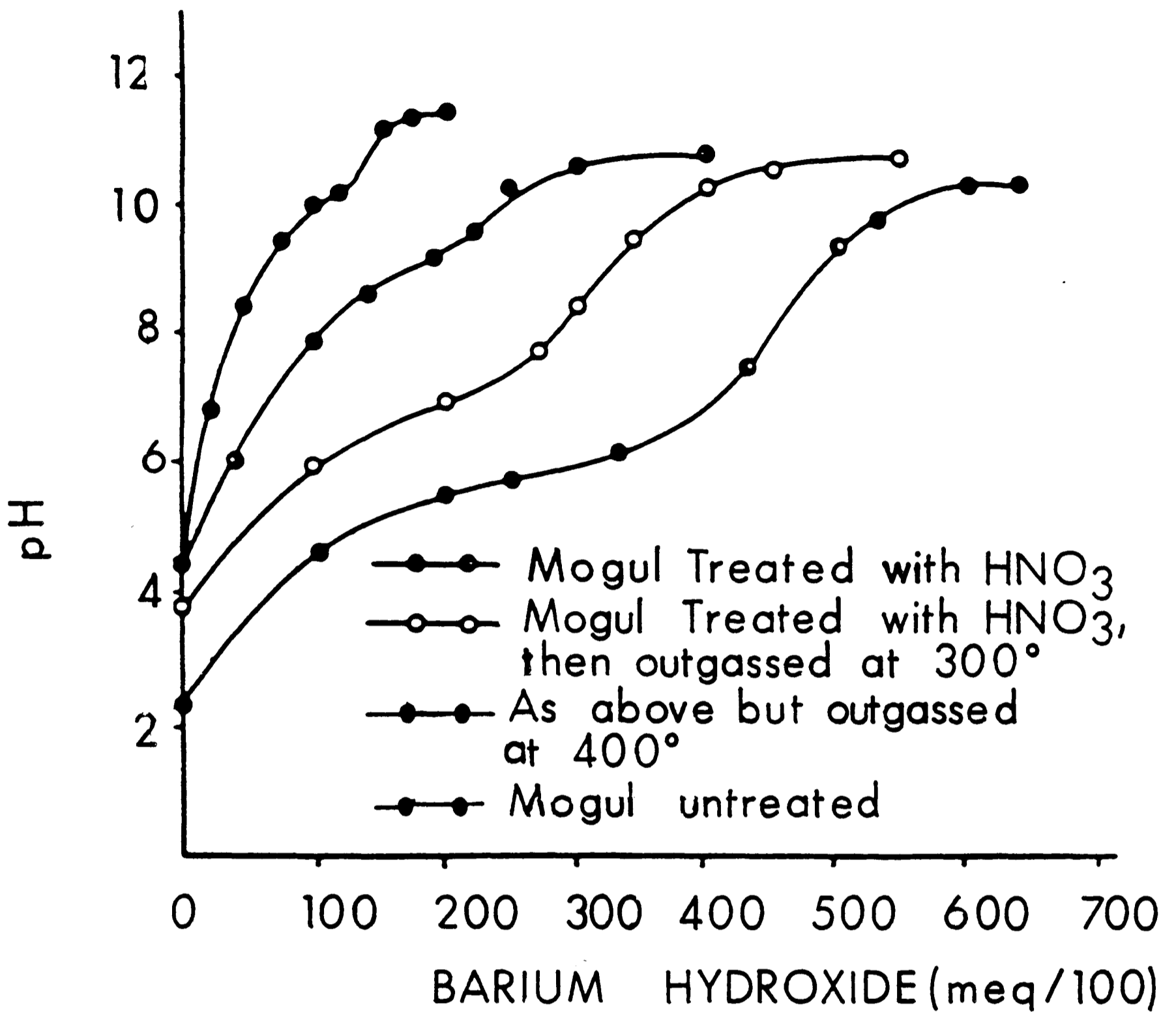
FIG. 7.1 - 3 : TITRATION CURVES OF MOGUL WITH BARIUM HYDROXIDE (from Ref. 54)

7.1.2.6 Influence of Carbon-oxygen Complexes on Surface Behaviour of Carbon

The presence or absence of 'surface oxides' determines the surface properties of carbonaceious or graphitic materials. The findings of Hennig[36] indicated that functional groups are located mostly on the edge atoms of the graphitic planes and as these edges constitute the main adsorbing surface, the oxygen complexes have a considerable influence on surface behaviour and surface reactions of carbon.

7.1.2.6.1 Adsorption of electrolytes

The influence on adsorption of electrolytes, particularly acids and bases, has already been discussed. Smith[53] has reported adsorption of sulphur dioxide at sites of oxygen complexes.

7.1.2.6.2 Hydrophobicity

Pure carbon is hydrophobic. The hydrophobicity decreases if oxygen is present. Functional groups formed by oxidation makes the carbon hydrophilic by providing sites for the chemisorption of water molecules. Pierce and Smith[68], Dubinin, Zaverine, and Serpenski[69], McDermot and Arnell[70] all support the cluster theory of hysteresis. They are of the opinion that oxygen provides active centres at which sorption of water proceeds in the form of isolated clusters through hydrogen bonds. These clusters then grow in size, as more adsorption takes place on adsorbed water molecules which are secondary adsorption centres by means of hydrogen bonds and ultimately they merge at a higher relative vapour pressure to form a

continuous layer on nonporous carbons and to bridge the walls of the pores on porous carbons. The hysteresis arises from the fact that while adsorption proceeds the formation of clusters, desorption takes place from continuous layers in non-porous carbons and from menisci in the case of porous carbons. The steep rise in the adsorption isotherm curves, in fig.7.1-4, in the region of mean equilibrium relative pressures of 0.3 to 0.5 is connected with the appearance and growth of these complexes from the associated water molecules. Adsorption and desorption isotherm of water possess an S-like shape typical of active carbons and are characterized by a clearly defined hysteresis region. However, very little benzene is adsorbed since carbon micropores are inaccessible for this larger molecule.

7.1.2.6.3 Selective adsorption

Kipling and co-workers[71-73] and Puri et al.[74,75] showed that the presence of combined oxygen imparts polar character to carbons, as a result of which they exercise preferential adsorption for a more polar component of a binary mixture. Spheron-6 which contains oxygen, preferred methanol from its solution in benzene, while Graphon, which was essentially free of oxygen, preferred benzene. According to Puri and co-workers[74,75] these preferences are much greater than those shown by silica gel whose surface largely consists of polar silanol (Si-OH) functional groups. They also point out that these preferential adsorptions are due to the presence of large amounts of CO_2 complex on the carbon surface. On the other hand, if the amount of the complex is decreased by
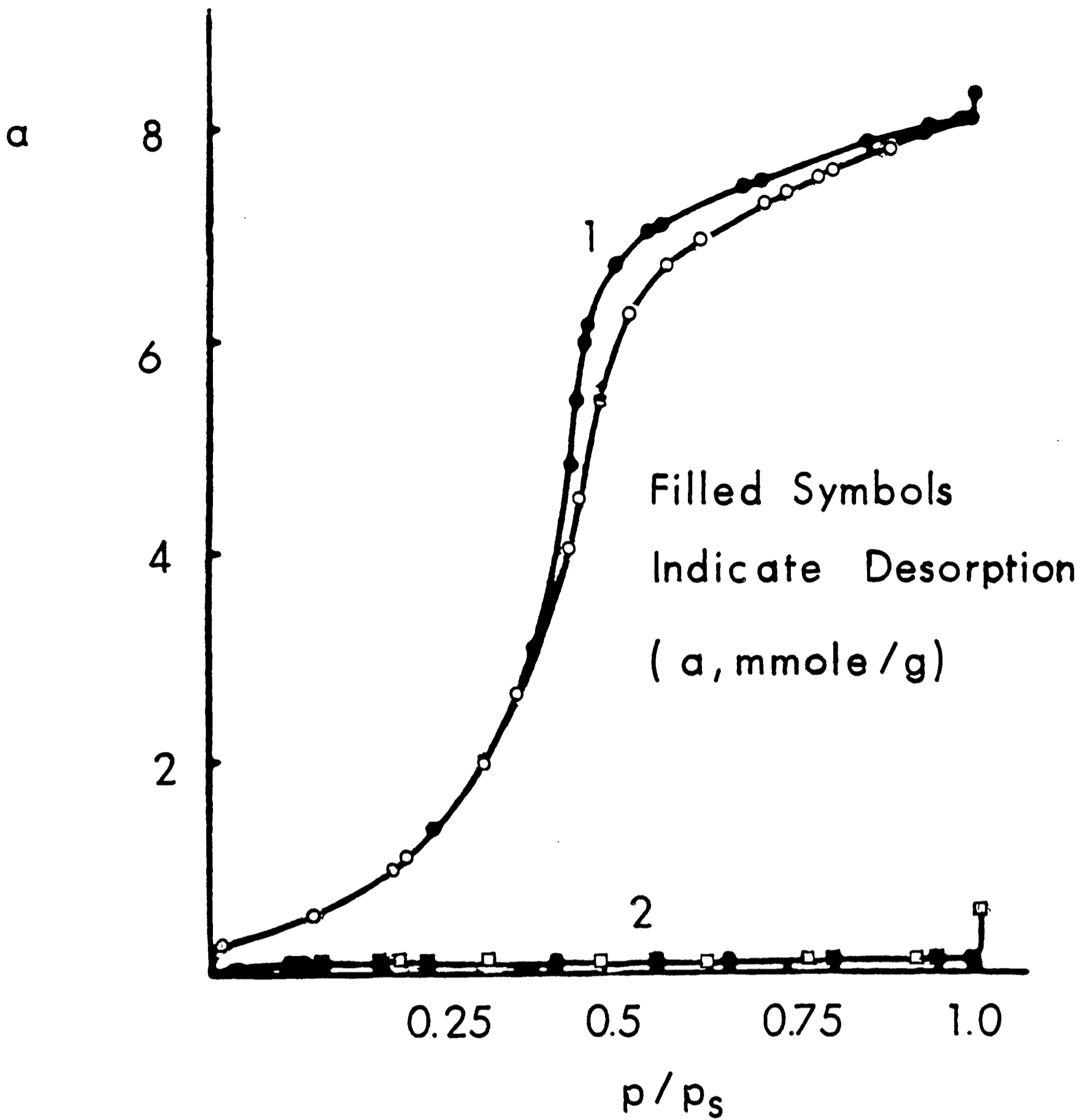
FIG. 7.1 - 4 : SORPTION AND DESORPTION
ISOTHERMS OF VAPOURS ON
CARBON AT 20°C. 1, WATER
2, BENZENE.(from Ref. 106)

outgassing the carbons at 750°C so that appreciable amounts of oxygen are still retained by carbons, they show less preference for both ethanol and methanol and more for benzene. It appears that quinone groups, which form part of the CO complex promote preference for benzene.

Thus, while one part of the combined oxygen (present as CO_2 complex) promotes preferential adsorption of alcohols, another part (present as CO complex) promotes preferential adsorption of benzene. These results indicate the need to determine not only the total oxygen but also the form in which it is evolved in order to assess correctly the performance and surface behaviour of carbons[74].

Note: The adsorption of benzene, on the other hand, can be said mainly to be due to flat graphitic surfaces not oxygen complexes.

7.1.2.7 Functional Groups of Carbon-oxygen Complexes

Several types of polar, groups have been identified on oxidized carbon surfaces[76]. The most common species are carboxyl,R-COOH, phenolic hydroxyl,R-OH, and carbonyl,R>C=O,R being the graphitic substance in each case. Other possible groups, the identification of which is less firmly established, include a) lactones, possibly a condensation product of adjacent carbonyl and carboxyl groups, b) quinoid structures[57] from the oxidation of adjacent phenolic hydroxyles and c) hydroperoxides   R ->C-O-O-H[77].

(a)
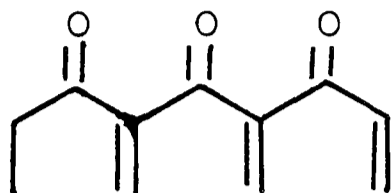
(b)

The presence of quinone groups on the surface of carbons have been confirmed by a number of workers[40,54,57,66,78-80]. During the reaction with diazo-methane the nitrogen content of the samples was found to increase[78] due to the formation of pyrazoline rings:
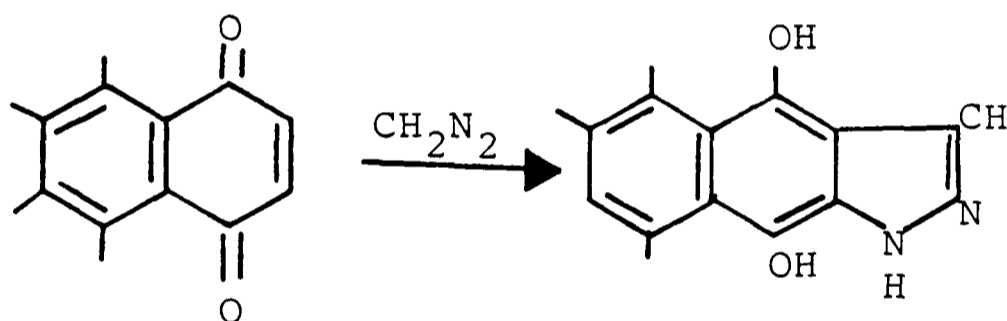
Studebaker et al.[66] analysed twelve carbon blacks and concluded that nearly 18% of the total oxygen was present in 1,4 quinone form. The evidence for the presence of simple quinones or quinones in association with phenols through hydrogen bonding seems to be fairly convincing.

The surface oxide layer has been studied by specific chemical reactions and by employing spectroscopic, potentiometric and polarographic techniques. As a result of these investigations, the existence of such functional groups as carboxyls, phenols, lactones of fluorescein type (f-lactones), normal

lactones, aldehydes, quinones, hydroquinones and ethereal structures have been postulated. The validity of applying organic reactions for identification and estimation of surface groups can be questioned.

According to Boehm et al.[81] the functional groups present on graphite crystallites react only slowly and incompletely. The chances for completing the reaction in the case of micro-crystalline carbons would be far less, because of the large surface area and, in many cases, the microporous nature of these materials and the inaccessibility of sites to reagent molecules. Moreover, the groups on the surface are not likely to behave in the same way as those present in simple organic compounds because of possible association between adjacent groups and steric hindrances. The infrared spectra can only be of limited help. As has been rightly pointed out[82], it is often difficult to obtain clear evidence from the spectra because of continuous background absorption[83] and also because of the likelihood that the various functional groups may not be present as simple, independent, nonassociated structures.

The various methods for analysing the functional groups on carbons have been tabulated in table 7.1-1. The results of Studebaker et al.[66] indicated that for every 3.2 atoms of oxygen found in carboxylic groups one atom of oxygen was present in phenolic groups. Furnace blacks contained 5%; channel blacks, 9% and carbon blacks 8-19% of their total oxygen as carboxyl groups.

Table 7.1-1

Functional Group	Methods of Analysis	References
A. <u>Determination of carboxyl groups</u>	1. <u>Titration with sodium bicarbonate</u> Carbon fibers, refluxed with an excess of calcium acetate in a water slurry for 24 hr. $2R\text{-}COOH + (CH_3COO)_2Ca$ $\rightarrow (RCOO)_2Ca + 2CH_3COOH$ Acetic acid formed by the reaction is then titrated with N/50 KOH.	The technique was developed by Donnet et al.[84] Herrick et al. employed the technique to carbon fibres[85]
	2. <u>Methylation with diazo-methane</u> $RCOOH + CH_2N_2 \rightarrow$ $R\text{-}COOCH_3 + N_2$ The methyl esters formed can then be hydrolyzed with dilute hydrochloric acid.	Studebaker et al.[66] used the method in a number of carbon blacks
	3. <u>Reaction with thionyl chloride</u> to give an acid chloride which can $R\text{-}COOH + SOCl_2 \rightarrow RCOCl +$ $SO_2 + HCl$	Donnet[86]

be characterized by further
reaction with dimethyl ani-
line to give an anilide.

4. Decomposition of carboxyl   Puri and Bansal[40,54]

groups at 900°C.

5. Reaction with Grignard   Villars[61] used

reagent (methyl magnesium   the method for

iodide). Amount of CH_4 carbon blacks

evolved was measured

$R-COOH + CH_3HgI \rightarrow$

$\quad R-COOMgI + CH_4$
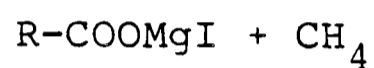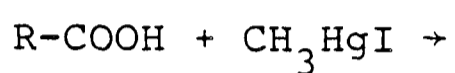
6. Carbons heated with   Studebaker et al.[66]

calcium acetate and the   and Boehm et al.[56]

amount of acetic acid set

free is measured.

Table 7.1-1 (cont.)

B. **Determina-**   **1. Titration with sodium**   Boehm[87]
tion of   **hydroxide and with sodium**
hydroxyl   **carbonate**
group

Surface phenolic hydro-
xyls appear to be neutra-
lized by sodium hydroxide
but not by sodium carbonate
so the difference between
the NaOH and Na_2CO_3 titra-
tion values gives a
measure of phenolic
hydroxyl concentration.

2. Methylation with diazo-   Goan and Prosen[88]
methane   used the method for

$$R-OH + CH_2N_2 \rightarrow$$
$$R-OCH_3 + N_2$$

carbon fibres and
Studebaker[66] on
carbon black

3. Reaction with Grignard   Villars[61] on carbon
reagent   blacks

$$R-OH + CH_3MgI \rightarrow ROMgI$$
$$+ CH_4 \text{ (measured)}$$

Table 7.1-1 (cont.)

C. Determination of carbonyl groups

1. Reaction with diazomethane to give a cyclic pyrazoline

$$\text{(p-benzoquinone)} + CH_2N_2 \longrightarrow \text{(dihydroxy indazole)}$$
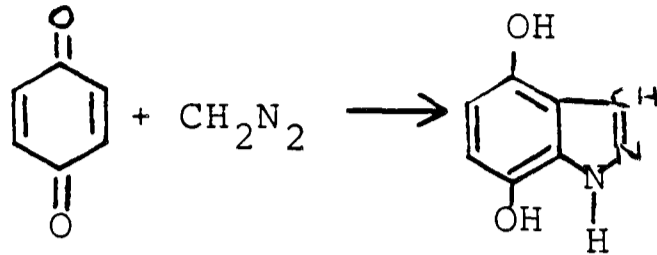
Method was developed by Studebaker[89]. None of the methods 1,2 or 3 have been used with carbon fibers.

2. Hydrogen titration using a platinium hydrogenation catalyst

$$\text{(p-benzoquinone)} + H_2 \xrightarrow{\ Pt\ } \text{(hydroquinone, OH / OH)}$$
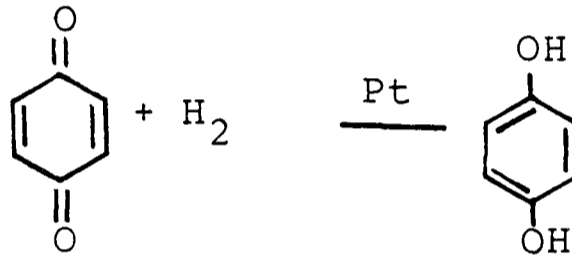
3. Reaction with sodium borohydride

$$4\ \text{(p-benzoquinone)} + NaBH_4 + 2H \longrightarrow 4\ \text{(hydroquinone)} + NaBO_2$$

Method was developed by Studebaker[66]

7.1.2.8 Hypothetical Structures of Carbon-oxygen Complexes

Several hypothetical structures and formulae have been assigned to carbon-oxygen surface complexes, Langmuir[90] assuming each oxygen atom to be chemically bonded to a surface carbon atom, assigned the following structure.

```
Oxygen layer at
the surface          O      O      O      O
                     ||     ||     ||     ||
Body of the         C      C      C      C
filament          /   \  /   \  /   \  /   \
                 C     C     C     C     C
```

This hypothesis explained the difficulty in removing oxygen from carbons.

Pyrolysis studies conducted on charcoals and carbon blacks indicates that the oxygen complexes are of more than one type and that the composition of the evolve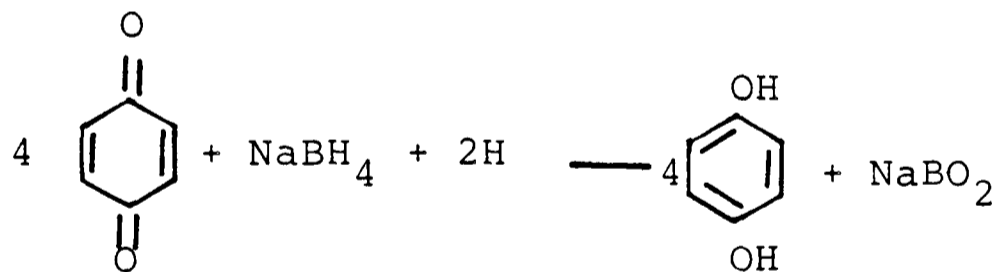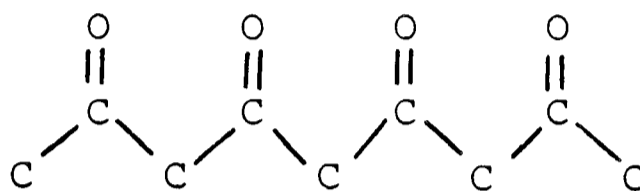d gas, at a particular temperature, depends on the type and the amount of the complex decomposing at that temperature. There are also indications that there are definite surface groups which evolve carbon dioxide and similarly there are distinct groups responsible for the evolution of carbon monoxide and water vapour. It has been suggested[56,59,91] that carbon dioxide is derived from carboxylic groups and their derivatives such as lactones while carbon monoxide is mainly a decomposition product of quinones, hydroquinones, and phenols. Water appears to come from hydroquinone.

Blench and Garner[92] and Garner[93] also suggested the existence of three different surface oxides on charcoal because the adsorbed oxygen was liberated in three forms

namely as oxygen, as carbon monoxide and as carbon dioxide. Garner and Mckie[94] suggested the following structural forms of the complexes.

$$
\underset{\text{I}}{C - \overset{\overset{\displaystyle O}{\|}\overset{\displaystyle O}{\|}}{C} - C}
\qquad
\underset{\text{II}}{C - \overset{\overset{\displaystyle O-O}{\diagdown\diagup}}{C} - C}
\qquad
\underset{\text{III}}{- \overset{\overset{\displaystyle O}{\|}}{C} - \overset{\overset{\displaystyle O}{\|}}{C} - \overset{\overset{\displaystyle O}{\|}}{C} - C -}
$$
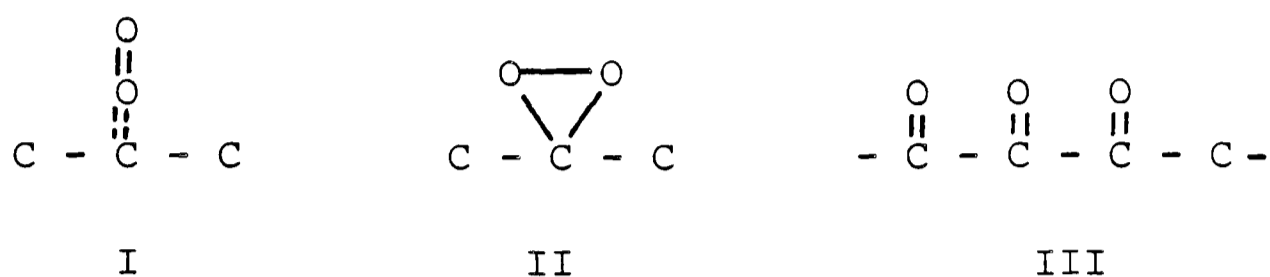
Formula I represents the process of physical adsorption and oxygen can be recovered unchanged.   Formulae II and III represent the process of chemical combination.   Structure II evolves carbon dioxide and structure III evolves carbon monoxide on heating.

Shilov et al.[95] in order to explain adsorption of acids and bases by carbons, suggested the existence of three different surface oxides.

(A)   (B)   or   (C)
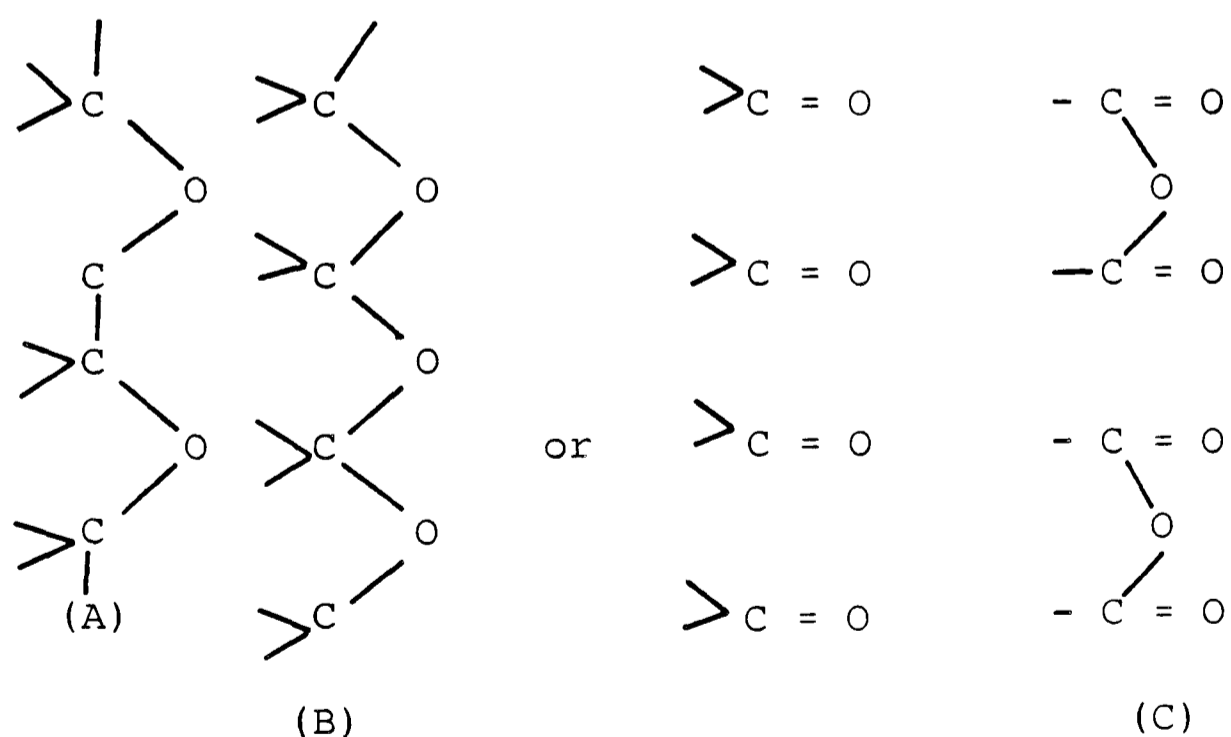
A and B were supposed to be alkaline and C acidic.   The presence of acidic oxide was supported by Lepin[96] but the existence of alkaline oxides was questioned.

7.1.3 Carbon-Hydrogen Surface Complexes

Carbons are pyrolyzed residues of organic compounds and the presence of hydrogen is expected. It is present as chemisorbed water and as phenolic, hydroquinonic, possibly carboxylic groups and in direct combination with carbon atoms. It is eliminated as elementary gas only when carbons are outgassed at temperatures above 500-600°C. It is not completely eliminated even if the temperature is raised _in vacuo_ to 1200°C. The total hydrogen content in carbon blacks that have been analyzed varies between 0.01% and 0.8%[97]. This quantity, although very small, is significant because of the low atomic weight of hydrogen compared to carbon. Thus according to Studebaker[97] one hydrogen atom was present for every 3.2 carbon atoms present at the edges of the layer planes.

Treatment of carbons in a current of hydrogen at 1000°C has been used for the removal of oxygen complexes[19,47,48]. No carbon-hydrogen complexes are formed during the treatment. Indeed, according to Puri _et al._[47], an appreciable portion of the combined hydrogen is eliminated during the process.

Although both Studebaker[98] and Smith _et al._[19] did not notice any change in surface area during treatment in hydrogen at any of the temperatures, Emmett[23], on the other hand, reported an appreciable increase in surface area together with a loss of carbon as methane during the treatment. Hydrogen treatment may, therefore, cause some degree of surface etching which could be undesirable.

7.2 Gas Reactions with Carbon

7.2.1 Introduction

Gas reactions of carbon and carbonaceous materials contribute substantially to the world's energy requirements. Principally, these are the reactions of carbon with oxygen, or air, steam, and carbon dioxide. The exothermic reaction with oxygen is still the major source of energy in the world. The endothermic reaction of carbon with steam produces carbon monoxide and hydrogen, which are used either directly as gaseous fuels or as synthesis gas to be converted catalytically to a series of hydrocarbon fuels. The reaction of hydrogen with carbon to produce methane may be important industrially in future. The gas-carbon reactions have been an integral part of our industrial economy for many years. More recently, the use of graphite as a moderator material in nuclear reactors has created a new need for minimizing the reaction of carbon with its ambient atmosphere.

The kinetics of the gasification reactions of carbon have been the subject of much study and several excellent reviews[99-103] which survey most of the significant fundamental work of the last fifty years. In order to study primary chemical reactions and to determine their kinetics free from the interfering effects of mass and heat transfer phenomena many experimental studies have been conducted under special conditions with respect to (a) the pressure, (b) gas velocity, (c) type of carbon sample and (d) method of heating. Letort and co-workers[104,105], Langmuir[106], Strickland-Constable[107], Vastola and Walker[108,109] have indicated that the reactions

of steam, carbon dioxide and oxygen at pressures in the

range 10^{-3}mm of mercury were first order between 1000°C and

1800°C.

### 7.2.2 General Mechanisms for the Gas-carbon Reactions

One of the main steps involved in a gas-carbon reaction

is the chemisorption of the gas (in whole or in part) on the

carbon surface. Most workers agree that chemisorption occurs

only on a relatively small fraction of the total surface[110-112].

Oxygen is chemisorbed on 6% of the total surface of amorphous

carbons at 200°C[110], hydrogen and water vapour is chemisorbed

on 4% of a graphite[111] and 0.5% of a charcoal surface chemi-

sorbs carbon monoxide[112]. Nitrogen is chemisorbed on 0.4% of

the surface[111] while argon and helium are not adsorbed.

In chemisorption, the surface atoms must have free valence

electrons in order to form strong chemical bonds with gas

molecules or atoms. Work by Ingram and Austen,[113] and Winslow

et al.[114], and by Hennig and Smaller[115] using electron

paramagnetic resonance absorption techniques, have confirmed

the presence of unpaired electrons in various types of carbons,

the number of unpaired electrons being a complex function of

carbon heat-treatment temperature.[113,114] Ingram and Austen[113]

further concluded that these unpaired electrons are located

primarily at, or close to, the carbon surface.

Chemisorption experiments have shown the carbon surface

to be heterogeneous. In addition to the normal sources of

heterogeneity (holes and dislocation in the lattice), carbon

is a multicrystalline material, which means that its surface,

in most instances, will be composed of different crystallographic planes.   The degree of heterogeneity in carbon surfaces will depend upon the percentage of different crystallographic planes composing the surface and size, and will affect gas-carbon reactions.   Walker et al.[99] have considered two main orientations of crystallites in the carbon surface namely (i) crystallites with their basal planes parallel to the surface, and (ii) crystallites with their basal planes perpendicular to the surface.   According to Grisdale[116] the rate of oxidation of carbon crystallites is 17 times faster in the direction parallel to the basal planes (along their edges) than perpendicular to them.   This indicates that the specific reactivity of a carbon would be at a minimum when its surface contains a maximum of crystallites with their basal planes parallel to the surface.   Smith and Polley[117] compared the oxidation rates of original and 'graphitized'* (2700°C) samples of Sterling FT carbon black, which have almost the same surface areas (15.4 and 16.6 m²/g).   The orientation of the two samples is shown in figure 7.2-1.   In the original carbon black, there are a number of exposed edges in the surfaces for reaction to occur at a relatively high rate.   On the other hand, they picture the graphitized carbon black as being in the shape of a polyhedron with its entire surface composed of crystallites with their basal planes parallel to the surface.   They found that the oxidation rate of original Sterling FT carbon black was twelve times greater than that of 'graphitized' carbon black.

* NOTE: Walker et al.[99] and Smith and Polley[117] used the term 'graphitized' to mean heated to an elevated temperature above 2200°C and does not mean the carbon has 100% graphitic structure.
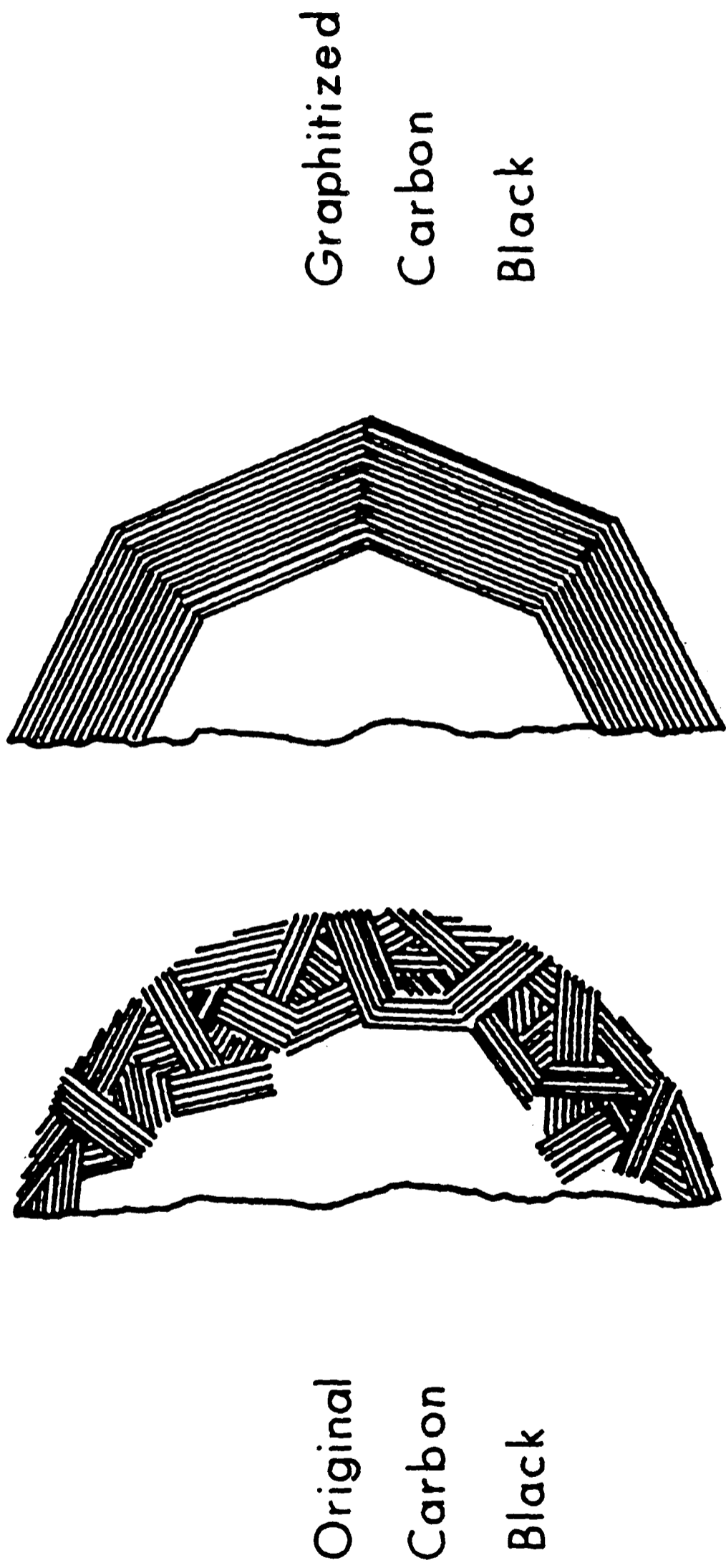
Graphitized
Carbon
Black

Original
Carbon
Black

FIG. 7.2 - 1: ARRANGEMENT OF CRYSTALLITES IN AN ORIGINAL
AND GRAPHITIZED (2700°C) PARTICLE OF STERLING
FT CARBON (from Ref. 117)

7.2.2.1 Carbon-carbon Dioxide Reaction

There is a general agreement that the rate of gasification of carbon by carbon dioxide can be expressed by a Langmuir-type equation[118-121] (31) which takes the form:

$$\text{Rate} = \frac{k_1 P_{CO_2}}{1 + k_2 P_{CO} + k_3 P_{CO_2}} \qquad (7.2-1)$$

where P_{CO_2} and P_{CO} are the partial pressures of carbon dioxide and carbon monoxide and the constants k_1, k_2 and k_3 are functions of one or more rate constants.

There are several hypothetical mechanisms which give the required form of rate equation (7.2-1), the steps of which are analogous to the general scheme used to represent a catalytic reaction:

(1) $S + R \rightleftharpoons SR$

(2) $SR \rightleftharpoons SP$

(3) $SP \rightleftharpoons S + P$
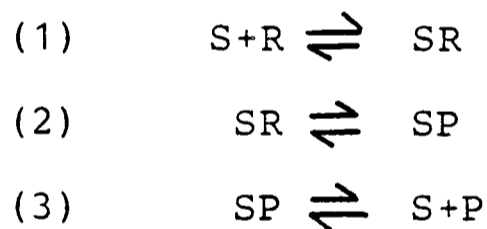
where S represents the catalytic surface, R represents the reactant(s) and P represents the product(s).

For the gasification of carbon by carbon dioxide the scheme can be represented as:

(1) $C_f + CO_{2(g)} \underset{k_{-1}}{\overset{k_1}{\rightleftharpoons}} CO(g) + C(O)$

(2) $C(O) \underset{k_{-3}}{\overset{k_3}{\rightleftharpoons}} CO(g)$

(3) $CO(g) + C_f \underset{k_{-2}}{\overset{k_2}{\rightleftharpoons}} C(CO)$
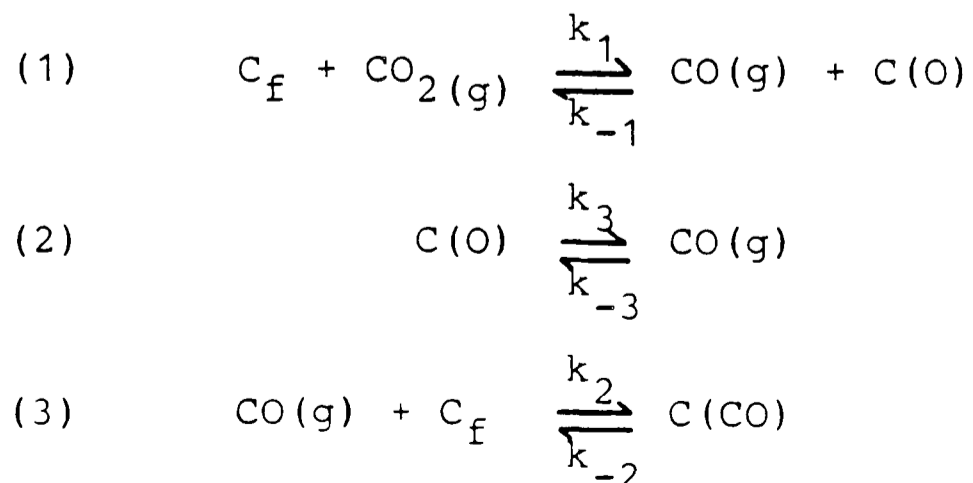
where C_f = free carbon sites and $C(O)$ = surface bound oxygen

$C(CO)$ = surface bound CO.

Mechanism A applies when the rates of the back reactions of reaction (1) and (2) are negligible.

Mechanism A:

(1) $\qquad C_f + CO_{2(g)} \xrightarrow{k_1} CO_{(g)} + C(O)$

(2) $\qquad C(O) \xrightarrow{k_3} CO_{(g)}$

(3) $\qquad CO_{(g)} + C_{(f)} \underset{k_{-2}}{\overset{k_2}{\rightleftharpoons}} C(CO)$
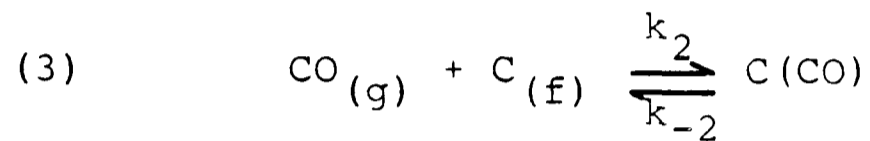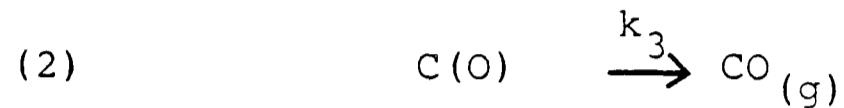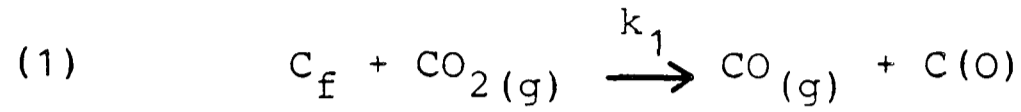
in which k_1, k_3, k_2 and k_{-2} are the rate constants for these reactions. At steady state, the rates of formation and removal of the surface complexes are equal. The rate of gasification in this type of mechanism can be obtained as follows.

Assuming $[C_f] + [C(O)] + [C(CO)] = C_{Total}$ = constant

$$= C_t$$

Then

$$\frac{dCO}{dt} = 2k_1 C_f \cdot CO_2$$

$$k_1 C_f \cdot CO_2 = k_3 C(O)$$

$$k_2 \cdot CO\ C_f = k_{-2} C(CO)$$

$$C(O) = \frac{k_1}{k_3} CO_2 \cdot C_f$$

and $\qquad C(CO) = \dfrac{k_2}{k_{-2}} CO \cdot C_f$

$$\therefore \quad C_f \left(1 + \frac{k_1}{k_3} CO_2 + \frac{k_2}{k_{-2}} CO\right) = C_t$$

$$\therefore \quad \text{Rate} = \frac{2k_1 C_t CO_2}{1 + \dfrac{k_1}{k_3} CO_2 + \dfrac{k_2}{k_{-2}} CO} \qquad (7.2\text{-}2)$$

which is equivalent to equation (7.2-1)

Mechanism B applies where the rate of the back reaction of reaction (2) is negligible and where reaction (3) is not important.

Mechanism B:

(1) $\qquad C_f + CO_{2(g)} \underset{k_{-1}}{\overset{k_1}{\rightleftharpoons}} C(O) + CO_{(g)}$
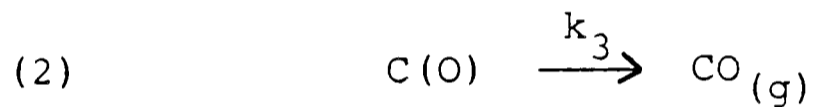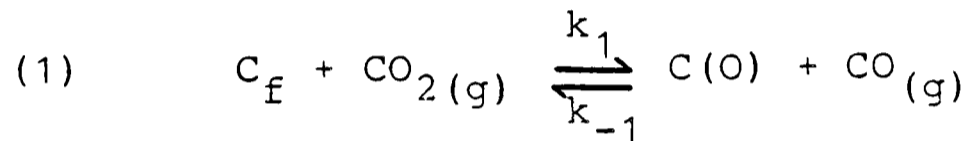
(2) $\qquad\qquad C(O) \xrightarrow{k_3} CO_{(g)}$

and the rate of gasification can be calculated as follows:

$$\text{Rate} = 2k_1 C_f \cdot CO_2$$

$$k_1 C_f \cdot CO_2 = k_{-1} C(O) \cdot CO + k_3 C(O)$$

if $\qquad C_f + C(O) = C_{Total}$

Then $\qquad C_f \left(\dfrac{k_3 + k_1 CO_2 + k_{-1} CO}{k_{-1} CO + k_3} \right) = C_{Tot.}$

$$\text{Rate} = \frac{2k_1 CO_2 \cdot C_t (k_{-1} CO + k_3)}{k_3 + k_1 CO_2 + k_{-1} CO} \qquad (7.2\text{-}3)$$

Mechanism A and B both state that carbon monoxide retards the gasification of carbon by carbon dioxide.

Mechanism A has been strongly supported by Gadsby and co-workers[112] who found that a large part of the oxygen on the surface of charcoal was due to the adsorption of carbon monoxide. On the other hand, Reif[120], Ergun[122], Key[123] and Strickland-Constable[124] all support mechanism B.

There are two schools of thought as regards the study of oxygen and exchange reactions occurring during the over-all gasification of carbon with carbon dioxide. Bonner and Turkevich[125] and Brown[128] by using radioactive carbon, C^{14}, as a tracer confirm that some carbon from the original carbon dioxide is transferred on to the carbon surface. Brown[128] states that this carbon transfer occurs to a greater extent in sugar carbons than in graphite. He suggests that when carbon dioxide reacts with a small fraction of the active surface of carbons, the carbon dioxide deposits its carbon atom on the surface and its oxygen atoms depart with two new carbon atoms giving rise to surface rearrangement. Other workers[127-145] indicate that equation (1) of either mechanisms expresses an oxygen exchange phenomenon, not the carbon transfer from solid to gas phase by isotropic tracer techniques. Studies of surface reactions[106,134-138] with carbon-oxygen systems have demonstrated the ability of carbons to retain oxygen at certain sites on their surfaces by chemical bonding. On an initially cleaned carbon surface, carbon dioxide is reduced to carbon monoxide at temperatures as low as $450°$[139]. The oxygen lost by carbon dioxide remains on the carbon

surface.[102,106,138,140,141] These studies demonstrate
the ability of certain carbon atoms to detach an oxygen
atom from a carbon dioxide molecule.   In a reverse manner,
oxygen retained on the surface can be removed by carbon mon-
oxide.[102,103,110,111,141]

The equilibrium constant of the oxygen exchange reaction,
K_1, is given by:

$$\frac{k_1(C_t)}{k_2(C_t)} = K_1 = \frac{(CO)(C_O)}{(CO_2)(C_f)} \qquad (7.2-4)$$

Ergun and Mentser[146] have made quantitative measurements
of oxygen exchange on Spheron 6, a carbon black at 800° and
850° in flowing CO_2-CO mixtures.   The derived numerical
values of the parameters $k_1(C_t)$, $k_2(C_t)$ and K_1 are given in
table 7.2-1.   The experimentally determined values of
equilibrium constant K_1 of the oxygen exchange reaction are
plotted as a function of temperature in fig.7.2-2.   The dashed
line corresponds to data obtained with carbons   (activated
carbon, activated graphite, Ceylon graphite).   At low
temperatures, values of K_1 for coke are lower; at 1200°C
they become identical with those of relatively pure carbons.
The apparent heat of reaction is about 27 kcal/mole for coke
as compared with 23 kcal.mole for carbons.   Ergun and
Mentser accounted the differences to be due to large amounts
of mineral matter present in coke which can react with carbon
dioxide and carbon monoxide.

Table 7.2-1   Kinetic parameters for dynamic oxygen

exchange between CO_2 and CO over carbon

(from Ref. 146)

| Temperature °C | $k_1(C_t)$ | $k_1'(C_t)$ | K_1 |
	sites/g sec x 10^{-18}		
800	0.094	0.77	0.12
850	0.22	1.33	0.17

$$E_1 = 41 \text{ kcal/mole}$$

$$E_1' = 26 \text{ kcal/mole}$$
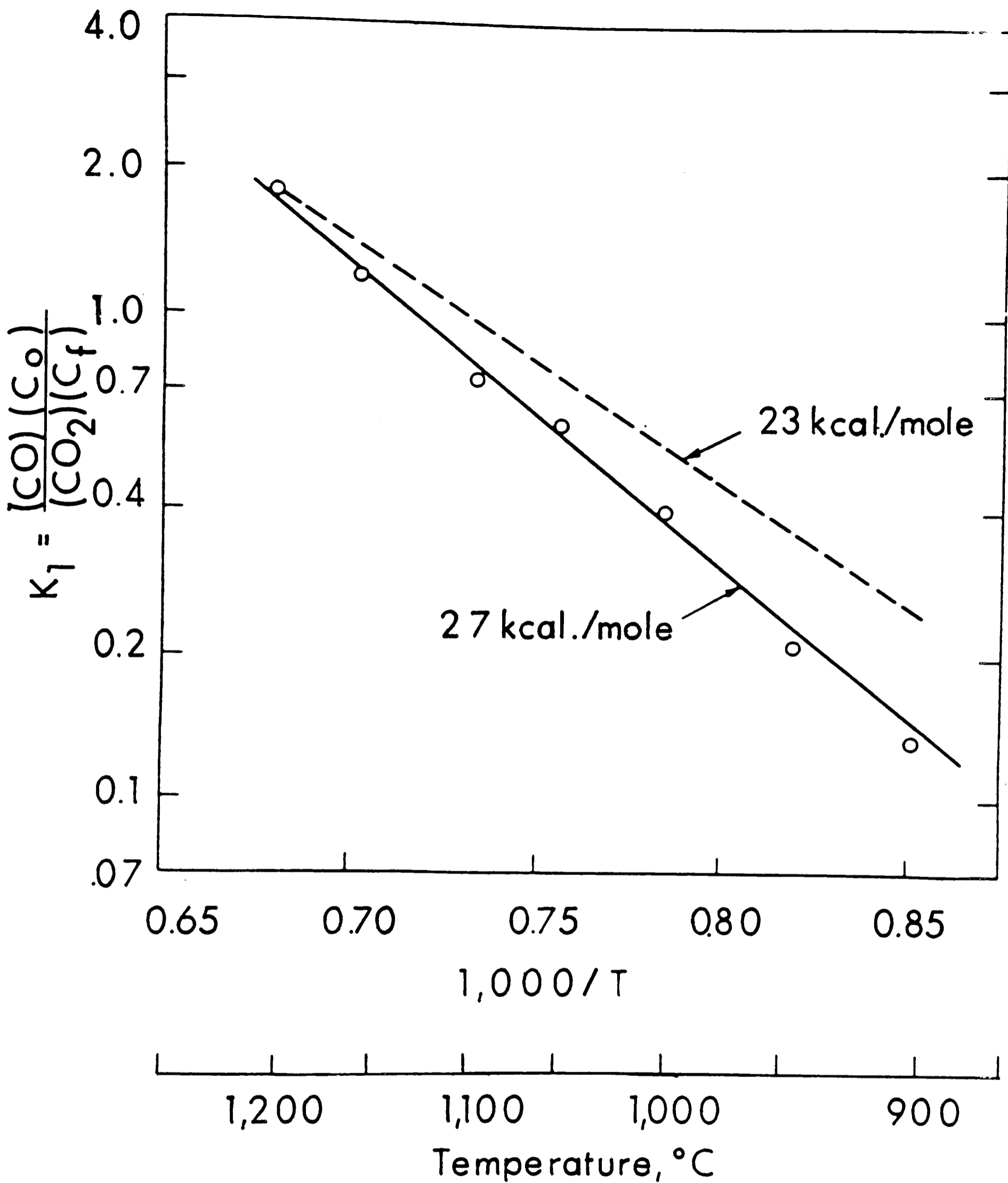
$$\Delta E = 15 \text{ kcal/mole}$$

FIG. 7.2-2: EQUILIBRIUM CONSTANT OF THE OXYGEN EXCHANGE REACTION OVER COKE BETWEEN CO_2 AND CO AS A FUNCTION OF TEMPERATURE. (from Ref 146)

7.2.2.2 Carbon-Steam Reaction

There is a general agreement[147-151] that experimental data on the rate of gasification of carbon by steam also fit a langmuir type equation which takes the form:

$$Rate = \frac{k_1 H_2 O}{1 + k_2 P_{H_2} + k_3 P_{H_2 O}} \qquad (7.2-5)$$

where $P_{H_2 O}$ and P_{H_2} are the partial pressures of steam and hydrogen and the constants k_1, k_2 and k_3 are functions of one or more rate constants. This equation is identical to that of the carbon-carbon dioxide reaction.

Gadsby et al.[149] and Johnstone et al.[150] have suggested the following mechanism:

Mechanism A:

$$(1) \qquad C_f + H_2 O_{(g)} \underset{k_{-1}}{\overset{k_1}{\rightleftharpoons}} C(H_2 O)^{\cdot}$$

$$(2) \qquad C(H_2 O) \overset{k_3}{\longrightarrow} CO_{(g)} + H_{2(g)}$$

$$(3) \qquad C_f + H_{2(g)} \underset{k_{-2}}{\overset{k_2}{\rightleftharpoons}} C(H_2)$$
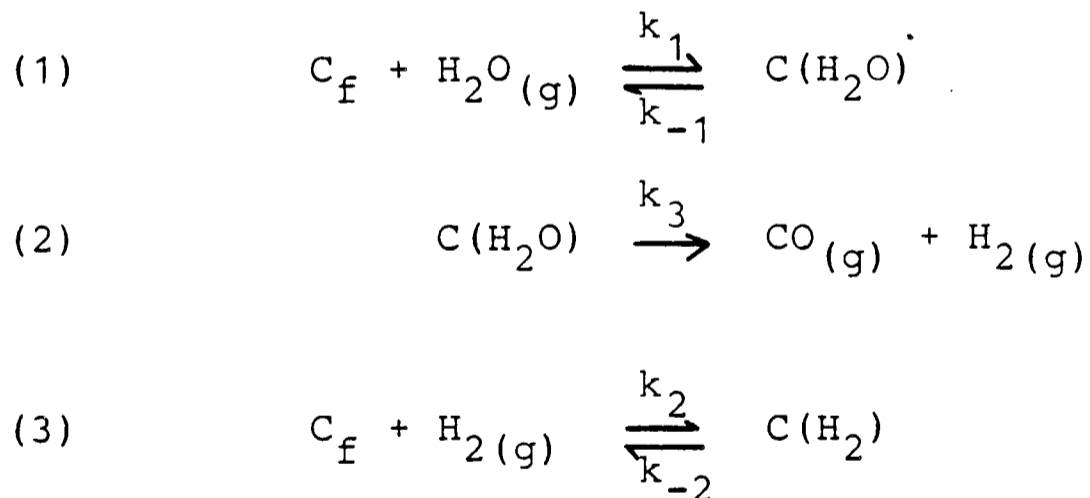
At steady states, the rates of formation and removal of the surface complexes are equal. The rate of gasification of carbon by steam can then be represented as:

$$\text{Rate} = \frac{\dfrac{k_1 k_3}{k_{-1} + k_3} \, P_{H_2O}}{1 + \dfrac{k_2}{k_{-2}} P_{H_2} + \dfrac{k_1}{k_{-1} + k_3} P_{H_2O}} \qquad (7.2\text{-}6)$$
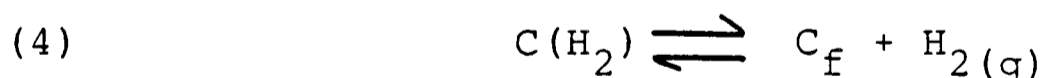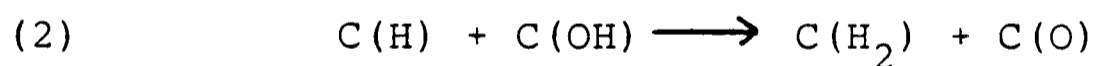
The mechanism of the carbon-steam reaction is discussed in more detail by Long and Sykes[148]. They propose that the steam molecule decomposes at the carbon surface into a hydrogen atom and hydroxyl radical both of which chemisorb rapidly on adjacent carbon sites. This is followed by the hydrogen atom on the chemisorbed hydroxyl radical joining the hydrogen atom on the adjacent carbon site and leaving as a hydrogen molecule. Therefore, on further breakdown of the steps in mechanism A may be written as:

(1) $\qquad 2C_f + H_2O_{(g)} \longrightarrow C(H) + C(OH)$

(2) $\qquad C(H) + C(OH) \longrightarrow C(H_2) + C(O)$

(3) $\qquad C(O) \longrightarrow CO_{(g)}$

(4) $\qquad C(H_2) \rightleftharpoons C_f + H_{2(g)}$
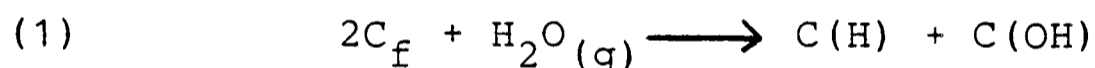
On the other hand, Ergun and Mentser[152] and Reif[120] suggest a second mechanism to be operative.

Mechanism B:

(1) $\qquad C_f + H_2O_{(g)} \underset{k_{-1}}{\overset{k_1}{\rightleftharpoons}} C(O) + H_{2(g)}$

(2) $\qquad C(O) \xrightarrow{k_3} CO_{(g)}$

(3) $\qquad CO_{(g)} + C(O) \underset{k_{-2}}{\overset{k_2}{\rightleftharpoons}} CO_{2(g)} + C_f$
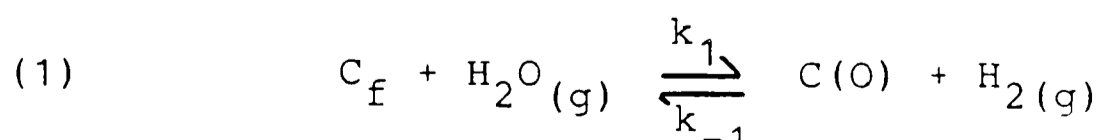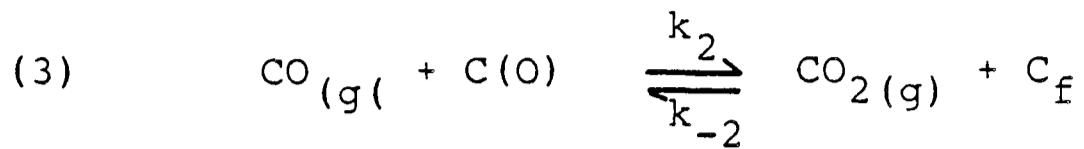
The actual gasification is represented by step (2) which involves the occupied sites, that is, an occupied site leaves the solid phase to form carbon monoxide. The carbon monoxide formed can, as does hydrogen, remove oxygen from occupied sites to form carbon dioxide (step 3) which, in turn, can be reduced by a reaction site to form carbon monoxide.

References   Chapter 7

1.   Smith, R.A., Proc.Roy.Soc. (London), 12 (1863) 425.

2.   Rhead, T.F.E. and Wheeler, R.V., J.Chem.Soc., 101 (1912) 846.

3.   Rhead, T.F.E. and Wheeler, R.V., J.Chem.Soc., 103 (1913) 461.

4.   Lowry, H.H. and Huelett, C.A., J.Am.Chem.Soc., 42 (1920) 1409.

5.   Langmuir, J., J.Am.Chem.Soc., 37 (1915) 1139.

6.   Lambert, J.D., Trans.Faraday Soc., 32 (1931) 249.

7.   Lepin, L., Physik Z. Sowjetunion, 4 (1957) 849.

8.   Ward, A.F.C.H. and Rideal, E.K., J.Chem.Soc., (1927) 3117.

9.   Keyes, F.G. and Marshall, M.J., J.Chem.Soc. (1924) 1154.

10. Marshall, M.J. and Bramston-Cook, J.Am.Chem.Soc., 51 (1929) 2019.

11. D. McKie, J.Chem.Soc., (1928) 2870.

12. Puri, B.R., Myer, Y.P. and Sharma, L.R., J.Indian Chem.Soc., 33 (1956) 781.

13. Shah, M.S., J.Chem.Soc., 1929, 2661.

14. Shah, M.S., J.Chem.Soc., 1929, 2676.

15. Strickland-Constable, R.F., Trans.Faraday Soc., 34 (1938) 1374.

16. Madley, G.G. and Strickland-Constable, R.F., Trans. Faraday Soc., 49 (1953) 1312.

17. Smith, R.N., Lessini, D. and Mooi, J., J.Phys.Chem., 61 (1957) 81.

18. Smith, R.N., Swinehart, J. and Lessini, D.,
    J.Phys.Chem., 63 (1959) 544.

19. Smith, R.N., Pierce, G. and Joel, C.D., J.Phys.
    Chem., 58 (1954) 298.

20. Beeck, O., Rev.Mod.Phys., 20 (1948) 127.

21. Studebaker, M.L., Rubber Chem.Technol., 30 (1957)
    1400.

22. Singh, D.D., Prakash, S. and Puri, B.R., Chem.& Ind.
    (London), 18 (1959).

23. Emmett, P.H., Chem.Rev., 43 (1948) 69.

24. Muller, S. and Cobb, J.W., J.Chem.Soc., 177 (1940).

25. Strickland-Constable, R.F., Proc.Roy.Soc. (London),
    A189 (1947) 1.

26. Walker, P.L., Jr., Rusinko, F., Jr., and Austin, L.G.,
    in Chemistry and Physics of Carbon, Vol.2 (1966) p.275.

27. Harker, H., Marsh, H. and Wyne-Jones, W.F.K.,
    First Conference on Industrial Carbon and Graphite,
    London (1957), Society of Chemical Industry, London
    (1958) p.291.

28. Reif, A.E., J.Phys.Chem., 56 (1952) 785.

29. Deitz, V.R., Carpenter, F.G. and Arnold, R.G., Carbon,
    2 (1965) 245.

30. Laine, N.R., Vastola, F.J. and Walker, P.L., Jr.,
    J.Phys.Chem., 67 (1963) 2030.

31. Laine, N.R., Vastola, F.J. and Walker, P.L., Jr.,
    Proceedings of the Fifth Conference on Carbon,
    Penn.State, 1961, Vol.II, Pergamon Press, New York, 1963,
    p.211.

32. Hart, P.J., Vastola, F.J. and Walker, P.L., Jr.,
    Carbon, 5 (1967) 363.

33. Lussow, R.O., Vastola, F.J. and Walker, P.L., Jr.,
    Carbon, 5 (1967) 591.

34. Walker, P.L., Jr., Carbon, 6 (1968) 194.

35. Lussow, R.O., Private Communication quoted by
    W.J. Thomas, Carbon, 3 (1966) 435.

36. Hennig, G.R., Proceedings of the Fifth Conference on
    Carbon, Penn.State, 1961, Vol.I, Pergamon Press,
    New York, 1961, p.143.

37. Puri, B.R., Chemistry and Physics of Carbon, Vol.6,
    p.191.

38. Puri, B.R., Myer, Y.P. and Sharma, L.R., Res.Bull.
    Punjab University, No.88, 53 (1956).

39. Puri, B.R., Myer, Y.P. and Sharma, L.R., Chem.& Ind.
    (London), B.I.F., Review, R30 (1956).

40. Puri, B.R. and Bansal, R.C., Carbon, 1 (1964) 457.

41. Johnson, C.R., Ind.Eng.Chem., 20 (1928) 904.

42. Johnson, C.R., Ind.Eng.Chem., 21 (1929) 1288.

43. Anderson, R.B. and Emmett, P.H., J.Phys.Chem., 51
    (1947) 1308.

44. Anderson, R.B. and Emmett, P.H., J.Phys.Chem., 56
    (1952) 753.

45. Caltharp, M.T. and Hackerman, N., J.Phys.Chem., 72
    (1968) 1171.

46. Smith, R.N., Pierce, G. and Joel, C.D., J.Phys.Chem.,
    58 (1954) 298.

47. Puri, B.R., Kumar, B., and Singh, D.D., J.Sci.Ind.
    Res. (India), 200 (1961) 366.

48. Lohenstein, W.R. and Deitz, V.R., J.Phys.Chem., 59 (1953) 481.

49. Emmett, P.H., Chem.Rev., 43 (1948) 69.

50. King, A., J.Chem.Soc., 1935, 889.

51. Singh, D.D., Sharma, L.R. and Puri, B.R., J.Sci.Ind. Res. (India), 18B, 172 (1959).

52. Puri, B.R., Singh, D.D., Nath, J. and Sharma, L.R., Ind.Eng.Chem., 50 (1958) 1071.

53. Smith, R.N., Quarterly Rev., 13 (1959) 287.

54. Puri, B.R. and Bansal, R.C., Carbon, 1 (1964) 451.

55. Weller, S.W. and Young, T.F., J.Am.Chem.Soc., 71 (1948) 4155.

56. Boehm, H.P., Diehl, E., Heck, W. and Sappok, R., Angew Chem., 3 (1964) 669.

57. Garten, V.A. and Weiss, D.E., Austral.J.Chem., 8 (1955) 68.

58. Studebaker, M.L., Proceedings of the Fifth Conference on Carbon, Penn.State, 1961, Vol.II, Pergamon Press, New York, 1963, p.189.

59. Rivin, D., The Fourth Rubber Tech.Conf. (London) p.1 (1962).

60. Puri, B.R., Singh, G. and Sharma, L.R., J.Indian Chem. Soc., 34 (1957) 357.

61. Villars, D.S., J.Am.Chem.Soc., 70 (1948) 3655.

62. Kruyt, H.R. and de Kadt, G.S., Kolloid Z., 47 (1929) 44.

63. Kruyt, H.R. and de Kadt, G.S., Kolloid Chem. Beiheffe, 32 (1931) 249.

64. Schweitzer, C.W. and Goodrich, W.C., Rubber Age (N.Y.) 55 (1944) 469.

65. Hofmann, U. and Ohlerich, G., Angew.Chem., 62 (1950) 16.

66. Studebaker, M.L., Huffman, E.W.D., Wolfe, A.C. and Nabors, L.G., Ind.Eng.Chem., 48 (1956) 162.

67. Garten, V.A. and Weiss, D.E., Rev.Pure Appl.Chem., 7 (1957) 69.

68. Pierce, C. and Smith, R.N., J.Phys.Chem., 54 (1950) 784.

69. Dubinin, M.M., Zaverina, E.D. and Serpinski, V.V., J.Chem.Soc., 1955, 1760.

70. McDermot, H.L., and Arnell, A.C., J.Phys.Chem., 58 (1954) 492.

71. Kipling, J.J. and Gasser, C.G., J.Phys.Chem., 64 (1960) 710.

72. Kipling, J.J. and Tester, D.A., J.Chem.Soc., 1949, 4123.

73. Gasser, C.G. and Kipling, J.J., Proceedings of the Fourth Conference on Carbon, New York, 1960, p.55.

74. Puri, B.R., Kumar, S. and Sandle, N.K., Indian J.Chem., 1 (1963) 418.

75. Puri, B.R., Carbon, 4 (1966) 391.

76. McKee, D.W. and Mimeault, V.J., Chemistry and Physics of Carbon, Vol.8, p.221.

77. Zarif'yants, Y.A., Kiselev, V.F., Lezhnev, N., Novikova, I. and Fedorov, G.G., Dokl.Akad.Nauk SSSR, 143 (1962) 1358.

78. Lindeburg, B. and Paju, J., Svensk.Kem.Tidsk., 65 (1953) 9.

79. Puri, B.R. and Bedi, K.M., Indian J.Chem., 2 (1964) 215.

80. Hallum, J.V. and Drushell, H.V., J.Phys.Chem., 62 (1958) 110.

81. Boehm, H.P., Hofmann, U. and Clauss, A., Proceedings of the Third Conference on Carbon, Buffalo, 1957, Pergamon Press, New York, 1959, p.241.

82. Garten, V.A., Weiss, D.E. and Willis, J.B., Austral.J. Chem., 10 (1957) 295.

83. Brown, J.K., J.Chem.Soc., 1955, 744.

84. Donnet, J.B., Hueber, F., Reitzer, C., Oddoux, J. and Reiss, G., Bull.Soc.Chim.France, 1727 (1962).

85. Herrick, J.W., Gruber, P.E., Jr., and Mansur, F.T., Surface Treatments for Fibrous Carbon Requirements, AFML-TR-66-178, Part 1, Air Force Materials Laboratory, July 1986.

86. Donnet, J.B., French Pat. 1,164,786 (1958).

87. Boehm, H.P., Adv.Catalysis, 16 (1966) 179.

88. Goan, J.C. and Prosen, S.P. in Interfaces in Composites, ASTM Special Tech.Publ., No.452, p.3.

89. Studebaker, M.L., Rubber Age, 77 (1955) 69.

90. Langmuir, J, J.Am.Chem.Soc., 40 (1918) 1361.

91. Walker, P.L., Jr., Austin, L.G. and Tientjen, J.J., Carbon, 2 (1965) 434.

92. Blench, E.A. and Garner, W.E., J.Chem.Soc., 1924, 1288.

93. Garner, W.E., Nature, 114 (1924) 932.

94. Garner, W.E. and McKie, D., J.Chem.Soc.,(1927) 2451.

95. Shilov, N.A., Shatunovska and Chmutov, K., Z.Physik. Chem. (Leipzig), A149 (1930) 421.

96. Lepin, L., Physik.Z.Sowjetunion, 4 (1957) 849.

97. Studebaker, M.L., Rubber Chem.Technol., 30 (1957) 1400.

98. Studebaker, M.L., Rubber Age (N.Y.), 80 (1957) 661.

99. Walker, P.L., Jr., Rusinko, F., Jr., and Austin, L.G., in D.D. Eley, et al., ed., Advances in Catalysis, Vol.II, Academic Press Inc., New York and London, 1959, p.133.

100. von Fredersdorff, C.G., and Elliott, M.A., in H.H. Lowry, ed., Chemistry of Coal Utilization, Supplementary Volume, John Wiley and Sons, Inc., New York - London, 1963, p.892.

101. Lavror, N.V., Korobov, V.V. and Filippova, V.I., in The Thermodynamics of Gasification and Gas Synthesis Reactions, G.H. Kinner, trans., The Macmillan Company, New York, 1963.

102. Ergun, S., U.S. Bur.Mines.Bull., 598 (1962).

103. Clark, T.J., Woodley, R.E. and de Halas, D.R., in R.E. Nightingale, ed., Nuclear Graphite, Academic Press Inc., New York, 1962, p.387.

104. Letort, M., Rev.Universelle Mines, 16 (1960) 255.

105. Boulangier, F., Duval, X., Letort, M., Proc.Conf.Carbon, 3rd Buffalo, 1957, 257 (1959).

106. Langmuir, I., J.Am.Chem.Soc., 37 (1915) 1139.

107. Strickland-Constable, R.F., Trans.Faraday Soc., 43 (1947) 769.

108. Vastola, F.J. and Walker, P.L.Jr., J.Am.Chem.Soc., Div.Gas and Fuel Chem., 1959, 1, 124.

109. Vastola, F.J. and Walker, P.L., Jr., J.Chim.Phys., 58 (1961) 20.

110. Lobenstein, W.V. and Deitz, V.R., J.Phys.Chem., 59 (1955) 481.

111. Savage, R.H., Ann.N.Y. Acad.Sci., 53 (1951) 862.

112. Gadsby, J., Long, F.J., Sleightholm, P., and Sykes, K.W., Proc.Roy.Soc., A193 (1948) 357.

113. Ingram, D.J.E., and Austen, D.E.G., in Industrial Carbon and Graphite, p.19, Society of Chemical Industry, London, 1957.

114. Winslow, F.H., Baker, W.O., and Yager, W.A., Proc. 1st and 2nd Conf. on Carbon, University of Buffalo, p.93 (1956).

115. Hennig, G.R. and Smaller, B., Proc. 1st and 2nd Conf. on Carbon, University of Buffalo, p.113 (1956).

116. Grisdale, R.O., J.Appl.Phys., 24 (1953) 1288.

117. Smith, W.R. and Polley, M.H., J.Phys.Chem., 60 (1956) 689.

118. Gadsby, J., Hinshelwood, C.N. and Sykes, K.W., Proc. Roy.Soc. (London), A187, 129 (1946).

119. Long, F.J. and Sykes, K.W., Proc.Roy.Soc. (London), A193 (1943) 377.

120. Reif, A.E., J.Phys.Chem., 56 (1952) 785.

121. Lewis, W.K., Gilliland, E.R. and McBride, G.T., Jr., Ind.Eng.Chem., 41 (1949) 1213.

122. Ergun, S., J.Phys.Chem., 60 (1956) 480.

123. Key, A., Gas Research Board Commun. (London) No. G.R.B. 40 (1948).

124. Strickland-Constable, R.F., J.Chim.Phys., 47 (1950) 356.

125. Bonner, F. and Turkevich, J., J.Am.Chem.Soc., 73 (1951) 561.

127. Bonner, F. and Turkevich, J., J.Am.Chem.Soc., 73 (1951) 561.

128. Brown, F., Trans.Faraday Soc., 48 (1952) 1005.

129. Orning, A.A. and Sterling, E., J.Phys.Chem., 58 (1954) 1044.

130. Petrenko, I.G., Khim.Tekhnol.Topliva Masel, 7 (1957) 15.

131. Petrenko, I.G., Tr.Inst.Goryuch.Iskop.Akad.Nauk SSSR, 11 (1959) 9.

132. Petrenko, I.G. and Krichko, I.B., Tr.Inst.Goryuch. Akad.Nauk.SSSR, 13 (1960) 10.

133. Stroeva, S.S., Kul'Kova, N.V. and Temkin, M.I., Dokl.Akad.Nauk.SSSR, 124 (1959) 628.

134. Meyer, L., Z.Physik.Chem., B17 (1932) 385.

135. Rhead, T.F.E. and Wheeler, R.V., J.Chem.Soc., 101 (1912) 831.

136. Eucken, A., Z.Angew.Chem., 43 (1930) 986.

137. Sihvonen, V., Z.Elektrochem., 40 (1934) 456.

138. Broom, W.E.J. and Travers, M.W., Proc.Roy.Soc. (London), A135 (1932) 512.

139. Tonge, B.T., Proc.Conf.Carbon, 4th Buffalo, 1959, 87 (1960).

140. Martin, H. and Meyer, L., Z.Elektrochem., 41 (1935) 136.

141. Semechkova, A.F. and Frank-Kamenetskii, D.A., Acta Physiochem., USSR, 12 (1940) 879.

142. Gadsby, J., Long, F.J., Sleightholm, P. and Sykes, K.W., Proc.Roy.Soc.(London), A193 (1948) 357.

143. Key, A., 53rd Rept.Joint Research Com., Gas Research Board and University of Leeds, Gas Research Board Commun., 40 (1948) 36.

144. Marsh, J.D.F., Int.Gas Engrs.Com. (London), No.393 (1951) 21

145. Reif, A.E., J.Phys.Chem., 56 (1952) 785.

146. Ergun, S. and Mentser, M., Chemistry and Physics of Carbon, Vol.1 (1965) 203.

147. Graham, H.S., D.Sc.Thesis, Mass.Inst.Technol., Cambridge, Mass., 1947.

148. Long, F.J. and Sykes, K.W., Proc.Roy.Soc., A193 (1948) 377.

149. Gadsby, J., Hinshelwood, C.N., and Sykes, K.W., Proc. Roy.Soc., A187 (1946) 129.

150. Johnstone, H.F., Chen, C.Y., and Scott, D.S., Ind. Eng.Chem., 44 (1952) 1564.

151. Jolley, L.J. and Poll, A., J.Inst.Fuel., 26 (1953) 33.

152. Ergun, S. and Mentser, M., Chemistry & Physics of Carbon, Vol.1 (1965) 203.

PART IV

(THE USE OF PGC IN LIQUID CHROMATOGRAPHY)

CHAPTER 8

CHROMATOGRAPHIC PERFORMANCE OF PGC

Note: Due to the large number of figures and tables
       presented in this chapter, they have been
       placed at the end of the chapter.

8.1   A Packing Method for PGC.

8.1.1   Introduction

Two methods are available for packing particles into HPLC columns; the dry packing method which is widely used in packing particles of 40 μm and above, and the slurry technique for microparticles in the range 3-20 μm. The slurry techniques have been reviewed by Bristow.[1] There appears to be five requirements for a satisfactory slurry - packing procedure namely:

(i)   The particles must not sediment too fast during the procedure.

(ii)   Each particle should have time to settle before it is bu ried by other particles landing on top.

(iii)   The particles must hit the accumulating bed at a high impact velocity.

(iv)   The particles must not agglomerate.

(v)   The liquid used to support the slurry must be easily washed out and must not react with the packing material.

There are two schools of thought regarding the selection of the slurry solvent. One school selects non-polar balanced density liquids. These proponents imply that since particles do not fall due to the high viscosity of the solvents there is no limit to time available to pack and that viscosity is unimportant. The solvents are generally brominated or iodinated alkanes. They are not to be recommended because of the toxicity and expense.

Others favour polar and low-viscosity liquids such as water, methanol or acetone. Particles, therefore, sink relatively rapidly but also pack rapidly.

The slurry technique has been mainly used in packing carbon columns. Colin and Guiochon[2,3] employed this technique even for particles greater than 20 μm. They used the balanced density method with a mixture of dibromo-ethane and acetonitrile (76:24 v/v) for packing both modified carbon black and carbon-coated silica particles. The packing pressures used were 300 bars for larger particles and 600 bars for the smaller particles. Unger et al[4] employed a high viscosity slurry of 17.5% w/w dioxan-paraffin oil (21:79 v/v) and the columns were packed downwards. Smolkova et al[5] used a slurry of 5% (w/w) of carbon adsorbents in tetrachloromethane. The slurry was treated in an ultrasonic bath for 5 minutes, and then packed in the column using heptane as the follower under a pressure of 20-30 MPa. Ciccioli et al[6], on the other hand, dry packed their graphitized carbon black particles greater than 20 μm. They found that the use of fritted metal ends were found to damage graphitized carbon black particles. The column ends were, therefore, separated from the packing by means of 180-200 μm metal particles. These were kept in place by a 10 μm metal screen supported on a PTFE o-ring placed in contact with the internal wall of the metal fritting. Polyamide ferrules were used to ensure a tight metal-glass connection.

8.1.2   Experimental , Materials & Equipment

PGC 72 was packed by the slurry technique using a number of solvents at different packing pressures. The solvents were of HPLC grade and bought from Rathburn Chemicals (Peebleshire, Scotland). The packing pump was purchased from Shandon Southern Products Ltd. (Runcorn, Cheshire, England). The columns used were also of the Shandon type (100 mm long and 5 mm internal diameter). The packing equipment that was used in packing columns is shown in figure 8.1-1. For a 100 x 5 mm column approximately 1.6 gms of packing material was dispersed in 33 cm^3 of slurry solvent by placing, for 10-15 minutes in an ultrasonic bath. The slurry was then poured in the packing chamber as quickly as possible. The columns were packed upwards until 100-150 cm^3 of the follower solvent was pumped through the column. The column and packing chamber was then inverted and another 50 cm^3 of the follower solvent was allowed to pump through the column before switching off the pump. Column F was packed using the Halasz and Maldener method[7]. In this method of packing, a packed restrictor column was placed at the outlet end of the column as shown in figure 8.1-2.

HPLC was performed using a home assembled equipment comprising of an Altex 110A or DuPont Instruments Chromatographic pump, a Rheodyne 7125 injection valve and a Cecil Instruments Ce212 or a Kratos ultraviolet photometric detector.

The columns were all tested using the standard phenol test mixture comprising of phenol, anisole, p-cresol, phenetole and 3,5-xylenol. The sharpness of the phenetole was an important criteria in deciding the quality of the packing.

8.1.3 Results and Discussion

Three main problems have been encountered in trying to pack earlier batches of PGC; firstly, the insufficient mechanical stability of the early batches of material; secondly, the agglomeration of particles, and thirdly the presence of 'needles' in PGC.

Table 8.1-1 lists the number of columns studied (A-U) using different solvents and solvent combinations. The columns have been graded according to the quality of the test chromatograms obtained; resolution of the five test solutes was essential and the phenetole peak should be sharp and symmetrical. The series of chromatograms are illustrated in figures 8.1-3 - 8.1-10.

In general, non-polar solvents appear to be very bad solvents for packing PGC (with reference to PGC 72). This would imply that the surface of PGC 72 studied is not totally hydrophobic and non-polar. Cyclohexane seems to give channeling effects. Acetone and methanol seem to be the best solvents for packing PGC. Furthermore, the columns packed with these solvents (Columns H, N and P) have all three been packed at 6000 psi, indicating that

PGC's have a mechanical stability comparable to chemically bonded phases. A low initial packing pressure is very important. There is the tendency of PGC crushing when in contact with the metal frits at the end of the column and, hence, an initial low pressure is important.

A stable packing pressure is also important. Column A was packed with methylene chloride but with the packing pressure increasing at the rate of 500 psi/minute. When the performance of this column is compared with column I, there is a marked decrease in performance and the resolution of the solutes is poor.

It has only recently been found that impurities in the solvents used for packing can deteriorate the performance of PGC's. After the column is flushed with a strong solvent for PGC, like Dioxan, the chromatographic performance is restored. Hence only very pure solvents should be used for packing carbon columns.

Furthermore, there is also a tendency for agglomeration of the particles. If the particles are placed in an ultrasonic bath for 10-15 minutes, a good dispersion of particles can be obtained.

Also, the presence of needles in PGC's and other forms of carbon can hinder packing. Since these needles are very fine their removal can pose a big problem. Therefore, it is highly desirable that the formation of these needles

should be avoided and appropriate precautions should be
taken. Figure 8.1-10 shows a test chromatogram of PGC
badly contaminated with needles. Badly tailed peaks
are seen for all the test solutes.

8.2   Analytical Separations of PGC

8.2.1   Introduction

Batches of porous carbons produced as in section 6.2, have been successfully used in liquid chromatography. The method of packing, as indicated in section 8.1, is straight forward and easy. Low back pressures are obtained allowing ease in operation. The porous carbon produced is compared with the existing reverse phase material, ODS. PGC has a selectivity quite different from ODS because of its flat graphitic surface. The retention of solutes on reversed-phase columns is mainly due to a balance between the non-specific interactions of the adsorbent with the solute and the eluent. Because of the absence of polar and hydrogen bonding surface group, carbon should be the ideal reverse-phase material and because of its chemical inertness, resist solvolysis.

The retention of a solute is defined in terms of its capacity factor (k') which is related to the thermo-dynamic adsorption constant (K) by the equation:

$$k' = K \frac{A_s}{V_o}$$

$$= K \cdot \frac{d_R}{\varepsilon_T} \cdot A_{sp}$$

where A_s is the total surface area of the adsorbent in a column of dead volume V_o. d_R is the packing density of the stationary phase which has a specific surface area of A_{sp}.

The total porosity of the column is ε_T. If d_R and ε_T can be assumed constant from one material to another, k' will be proportional to the specific surface area of the packing. While such an assumption will not generally hold due to variation in particle porosity (from the method of the preparation of the material) and packing density (from packing procedure). ε_T and d_R are often not quoted. The rough assumption is the best that can be made for comparison purposes. Also, we have evaluated k'_{100} as being the equivalent k' value if the carbon had an area of 100 m^2/g. k'_{100} is obtained for any measured k' value by the formula:

$$k'_{100} = k'_{obs} \times \frac{100}{A_{sp}} .$$

where k'_{100} is the observed capacity factor and A_{sp} is the specific surface area of the material.

A characteristic feature of the reverse-phase system is the linear dependance of log kR' on the number of carbon atoms. The selectivity, α, for a homologous series is given as:

$$\alpha = \frac{k'_{n+1}}{k'}$$

or $\log k' = \alpha n + \beta$

where n is the number of carbon atoms in the molecule. A true homologous series is obtained by adding successive CH_2 groups to a linear alkyl chain as, for example, in the n-alkylbenzenes. A quasi-homologous series is one where the CH_2 groups are not added into a straight alkyl

chain as seen in polymethybenzenes. Although smooth linear plots are obtained for true homologous series, isomeric effects give a considerable scatter of points for any series and α values are only approximate.

8.2.2 Experimental

Materials and Equipment

PGC's used were produced as described in section 6.1. Table 8.2-1 lists the various materials used in LC. Solvents of HPLC grade were obtained from Rathburn Chemicals, Walkerburn, Peebleshire, Scotland. The chemicals used were obtained from BDH and Fisons. HPLC was performed using a home assembled equipment comprising of an Altex 110A or DuPont high pressure pump, a rheodyne 7125 injection valve and a Cecil Instruments Ce212 or a Kratos ultra-violet photometric detector. Columns were either of the Shandon Southern Instruments pattern (100 mm long, 5 mm bore) or of the HETP pattern (100 mm long, 2 mm bore) when the quantity of material was limited. Columns were packed at 1000 psi either using dichloromethane as the slurry liquid and methanol as the follower or acetone as both the slurry liquid and follower. The upward-flow slurry method was adopted as indicated in Section 8.1.2.

8.2.3 Results and Discussion

All columns packed with PGC were tested with a test
mixture comprising of phenol, p-cresol, 3,5-xylenol,
anisole and phenetole. PGC shows a kinetic performance which
is comparable to ODS as illustrated in figures 8.2-1,
8.2-2 and 8.2-3 on three different batches of PGC. For
a good batch of PGC, the peaks are sharp and symmetrical.
Furthermore, the retention of solutes is also significantly
lower when compared with the retention on a bad batch of
PGC. Table 8.2-2 gives a comparative retention data, between
a good and bad batch of PGC and Figure 8.2-4(a) gives
comparative chromatograms. PGC that has been heated at
higher heating rates during high temperature treatment
shows asymmetrical peaks as shown in figure 8.2-4(b). It
has also been found that the order of elution in both the
materials, PGC and ODS, is different. On ODS, it is found
that ethers like anisole and phenetole are comparatively
more retained than the phenols. On the other hand, on PGC,
the phenols appear to be more retentive.

A functional group selectivity study on both PGC and
ODS further indicate that different potentials of the two
reversed phase materials as seen in figure 8.2-5. PGC
would appear to be the ideal reversed phase material for
the separations of benzenes, phenols and anilines. On
the other hand, nitrobenzene can be easily separated
from acetophenone using ODS as a reversed phase material. Such
a separation has not been possible on PGC in any kind of

solvent that has been studied so far. Furthermore, there is an interesting point to note - toluene is more retained on ODS than on carbon!

Homologous and quasi-homologous series

The plot obtained for n-alkylbenzenes is compared with plots obtained for quasi-homologous series in figure 8.2.6 using acetonitrile/H_2O as the eluent.

The α_{CH_2} for n-alkyl benzenes is found to be 0.19 and for pseudohomologous series is 0.44-0.47 using aceto-nitrile/H_2O as an eluent. A quasi-linear plot is obtained for alkylbenzenes which is similar to the plot obtained by Colin et al on modified carbon black.[8] They also obtained a different slope for n-alkyl and polymethyl-benzenes both on modified carbon black and carbon-coated silica particles similar to that obtained on PGC. The selectivity, α, for both PGC and ODS have been compared using the homologous and pseudo-homologous series (Table 8.2-3). On ODS, similar slopes of the plot corresponding to n-alkyl and polymethylbenzenes and polymethylphenols of about $\alpha = 0.14$ have been obtained using acetonitrile/H_2O as an eluent. Colin et al[8] obtained similar results on ODS. These results may suggest that adsorption on carbon packings is more specifically related to molecular configuration than adsorption on silica and that the projected area of a molecule is critical rather than the total surface area. Therefore, the selectivity for homologous series seems to be better on carbon adsorbents than for ODS. Also, it can

be observed in figures 8.2-7 and 8.2-8 that ODS seems to be more retentive for smaller aromatic molecules and PGC is more retentive for large aromatics, therefore, giving rise to crossing over effect in the selectivity plots. This further confirms the earlier observation on functional group selectivity where toluene is more retained on ODS than on carbon. For aromatic substitution, this crossing-over seems to occur with compounds having greater than 7 carbon atoms, and for aliphatic substitution crossing over occurs for compounds having more than 12 carbon atoms.

Furthermore, by using an eluent mixture of methanol-water (95:5 v/v) it is possible to obtain different slopes for methylbenzenes, phthalates and aliphatic ketones on PGC. This is illustrated in figure 8.2-9. Figures 8.2-10 - 8.2-19 gives separations of polymethylbenzenes, polymethylphenols and alkylbenzenes on different batches of PGC's and ODS.

The separation of polymethylbenzenes on two different good batches of PGCs is shown in figures 8.2-10 and 8.2-11. The separation can be compared with one obtained on a bad batch of PGC (shown in figure 8.2-12 for PGC 70-A) where the retention obtained is longer and the peaks are significantly broader. Separation of 1,2,3,4-tetramethylbenzene on PGC 26, an earlier batch of PGC, is shown in figure 8.2-14. A flow rate of 0.5 ml min^{-1} could only be used as the back pressure produced at this flow

rate was significantly high (2000 psi). The separation of polymethylphenols is also shown in two good batches of PGCs (figures 8.2-15 - 8.2-16). These chromatograms should be compared with that obtained on PGC 70-A shown in figure 8.2-17. The retention of polymethylphenols is longer and the peaks are badly tailed. The separation of polymethylphenols on PGC 26 is shown in figure 8.2-18. A good separation of alkylbenzenes on PGC 64 could also be obtained. This is shown in figure 8.2-19.

The study of selectivity or α values of polymethylphenols, polymethylbenzenes and alkylbenzenes indicate that different selectivity is obtained for aromatic and aliphatic substitution as shown in table 8.2-4. Very low selectivity is obtained with alkylbenzenes; acetonitrile giving the best selectivity and dioxan giving the least selectivity. For aromatic substituted solutes, greater selectivity is obtained for polymethylbenzenes than polymethylphenols; Acetonitrile and methanol giving the best selectivity and dioxan the least selectivity. For a particular solvent, the order of selectivity or α values would be alkyl benzenes < polymethylphenols < polymethylbenzenes.

Geometrical Isomers

As expected from the high values of α for quasi-homologous series PGC seems to give good selectivity for geometrical isomers. Positional isomers on an aromatic ring can be easily separated, for example, the separation

of 1,3,5- and 1,2,4-trimethylbenzene (figure 8.2-10).

On PGC, it is found that the meta-isomers are less retained

than the ortho- and para-isomers as seen in the separation

of xylenes, trimethylbenzenes (figure 8.2-10) and

xylenols (figure 8.2-20). The work of Colin et al[8] also

indicated that the m-derivative was the least retained

using acetonitrile as the eluent. The separation of three

isomers was achieved using PGC 26 as illustrated in

figure 8.2-21 where o-xylene appears to be the most

retained. These results are consistent with the observations

on alumina and silica. On the other hand, the case of

separations of polar positional isomers, the ortho-derivative

is less retained than the para-derivative. This is

illustrated in figures 8.2-22 and 8.2-23 for the

separations of o- and p-nitrotoluene and o- and p-nitro-

aniline using methanol and methanol:water (90:10, v/v) as

the eluents respectively. A similar result was obtained

by Colin et al on their carbon-coated silica particles

using acetonitrile as the eluent. The o-bromo nitrobenzene

was the least retained whilst the p-derivative had the

longest retention. It is, therefore, probable that this

could be due to the fact that the solvent-solute interactions

are different for polar positional isomers. On ODS, as

shown in figure 8.2-13, the retention of geometrical isomers is

quite different. The meta-isomers are, on the other hand,

more retained than the ortho- and para-isomers. Therefore,

m-xylene is more retained than o- and p-xylene, and

1,3,5-trimethylbenzene being more retained than 1,2,4-

trimethylbenzene.

A study of the isomeric selectivity of pairs of
isomers in different solvents have been tabulated in
table 8.2-5 and illustrated in figure 8.2-24. The results
do not seem to give any consistent results. Generally, one
can conclude that dioxan being the strongest solvent gives
poorest selectivity for small and large non-polar solutes
and small polar solutes. As the size of the non-polar
solute increases there is also a progressive tendency for
hexane, methanol and acetonitrile to give greater isomeric
selectivity! On the other hand, THF and DMF seem to be
suitable solvents for isomeric selectivity of small non-
polar and polar solutes.

Separation of Bases and Acids

The earlier batches of PGC (e.g. PGC 26) gave very
badly tailed peaks for bases and acids. With the improvement
of the method of production of PGC, the new material seems
to be an excellent material for the separations of small
molecular weight bases. Methanol/water systems or the
reversed phase system seems to be the best solvent system
for their separations as can be seen in figure 8.2-25.
A similar separation on ODS produces very badly tailed and
unsymmetrical peaks as shown in figures 8.2-26 and
8.2-27.

Acetonitrile is a bad eluent for bases on carbon.
The addition of water as a modifier brings about a drastic
change in peak symmetry as shown in figures 8.2-28 and
8.2-29 for pyridine and aniline respectively. This could

be explained by the presence of active sites on the surface which become deactivated by water, therefore, producing a more homogenous surface. A bad batch of PGC gives unsuitable base separations as illustrated in figure 8.2-30.

Good separations of acids have also been observed in the acetonitrile/water system. Under similar conditions, the acids are excluded on the ODS reversed phase system (figure 8.2-31).

Separation of Phthalates

Good separations of phthalates have also been obtained on PGC (figure 8.2-32) using acetonitrile. When compared with a similar separation on ODS an interesting observation can be made. Diethylphthalate is always less retained than dimethylphthalate on PGC in all solvents studied, but this is not true in the case of ODS (figure 8.2-33). A plot of log k' versus number of carbon atoms shows a minimum value as illustrated in figure 8.2-9.* This is again consistent with the earlier observation that PGC, unlike ODS, is less retentive for smaller molecules. A similar separation of phthalates using methanol/water as an eluent do not give good peak shapes as seen in figure 8.2-34. The importance of solute-solvent interactions, which shall be discussed in Chapter 9, therefore, cannot be over emphasized.

* A minimum value was only obtained with PGC 64 and not with PGC 26. Fig. 8.2-9 refers to PGC 26

Other Analytical Separations

Good separations of phenylketones have been
obtained. One such separation is shown on two different
batches of PGC (figures 8.2-35 and 8.2-36). The solutes
are eluted in increasing order of molecular size of the
solutes.

Acetonitrile is also a good eluent for the separation
of polyaromatic hydrocarbons (figure 8.2-37). A bad batch
of PGC (due to higher rates of heating) gives high
retention and badly shaped peaks for naphthalene as can
be seen in figure 8.2-38. A comparative retention data
between PGC 64 and PGC 26 for some solutes is given in
Table 8.2-6. The retention on PGC 64 is much less than
that on PGC 26.

Peak Shape Study of Solutes in Different Solvents on PGC

The peak shape of solutes in different solvents is an
important consideration when chromatographing solutes.
Table 8.2-7 gives a general idea of peak shapes of different
solutes in different solvents. This knowledge coupled with
a general understanding of the eluotropic series, which
will be discussed in Chapter 9, and of the isomeric selectivity
that can be achieved in different solvents can give a fairly
good idea of the type of solvent one can choose for
particular separations.

Variation of k' with Percentage Water Content

Figure 8.2-39 and Figure 8.2-40 show the variation of the retention of polymethylbenzenes, polymethylphenols and other polar solutes, alkylbenzenes, bases and polyaromatic hydrocarbons with the percentage water content. In each homolog ue studied (polymethylbenzenes, polymethylphenols and alkylbenzenes) as the size of the solute molecule is increased, increase in water content of the eluent brings about a greater change in retention of the solutes. There is, therefore, a progressive increase of slopes of the lines shown in figure 8.2-39 (a + b + c) as the size of the solute molecules are increased. Secondly, it can also be noticed that the effect of change of water content is lesser for polar solutes than for non-polar solutes. These two effects can be explained in terms of polarity of the eluent. Polarity cannot be neglected entirely as it influences the solubility of the solute in the mobile phase where moderately strong interactions can take place between the solute and the polar solvent. The solubility of phenols and polar solutes increases rapidly as solvent polarity increases due to formation of hydrogen bonds. On the other hand, solvent-adsorbent interactions decreases thereby causing the capacity factor k' of polar solutes to increase more slowly than non-polar or weakly polar solutes with increasing polarity of the solvent.

In the case of bases (Figure 8.2-40) the same
effect is seen; Aniline has a smaller slope than diethyl-
aniline. In the case of polyaromatic hydrocarbons
(Figure 8.2-41) biphenyl and acenaphthene show a peculiar
decrease in retention as the water content is increased
from 15% to 20%. O-terphenyl, on the other hand, show
a sharp increase in retention.

Deactivation and Reactivation of PGC

During the course of LC work, two batches of PGCs
underwent gradual reductions in retention behaviour. This
has been thought to be due to impurities in the eluent that
deactivate the material. It has been possible to reactivate
the column, fortunately, by washing the column with dioxan
which was chosen because of its stronger solvent strength
by the study of elu otropic series data in Chapter 9.
This deactivation and reactivation is illustrated in
figures 8.2-42 and 8.2-43 for the test mixture on two
different batches of PGC. Similar reductions in
retention of polymethybenzenes (shown in Figure 8.2-44)
and polymethylphenols were also observed. The phenomenon of
deactivation and reactivation for these compounds can
be seen in figures 8.2-45 - 8.2-47. After reactivation of
the material, the retention of non-polar and polar solutes
is greater than and less than the retention of the original
material, respectively. The capacity factors of these
solutes are compared in table 8.2-8. It is highly probable
that a high molecular weight contaminant had deactivated
the material.

The possibility of deactivating and reactiviting
PGC has opened a new field in the use of carbon in LC.
Highly retained solutes can be easily chromatographed
by the addition of suitable modifers in the eluent. Thus,
carbon, although more hydrophobic than ODS, can be used
for the separation of high molecular weight solutes.

The Use of Acetic Acid as a Modifier in the Eluent

Figures 8.2-48 - 8.2-52 illustrate the effect of
using acetic acid in the eluent. Significant changes
in the retention of solutes is observed on the addition of
less than 1% of acetic acid. Retention of non-polar solutes
and polyaromatic hydrocarbons is drastically decreased;
the decrease in retention is more significant in large size
molecules than in small size molecules (Figures 8.2-48 and
8.2-49). Minimum retention for non-polar solute values
are obtained using 4% acetic acid in the eluent. Poly-
methylphenols and nitrobenzene also undergoes significant
reductions in retentions as illustrated in figure 8.2-50.
For all acids, there is also a general trend in decrease
in retention with increase of percentage of acetic acid
(Figure 8.2-51). Peak shapes of acids are significantly
improved. 1% acetic acid gives good peak shapes and
good separations for acids. On the other hand, for bases
there is a general trend of increase in retention with
increase of percentage of acetic acid (Figure 8.2-52). The
peak shapes of bases worsened with the addition of acetic
acid. Peculiar shapes were obtained for some bases. At

about 3% acetic acid, the aniline peak is followed by
a negative displacement peak. Reactivation of the column
was done using sodium hydroxide. The retention of solutes
did not revert back to their original retention. Dioxan
was not used to wash the material and so the possibility of
activating the column is still not very definite.

The study of PGC of metallic impurities by X-ray
fluorescence before and after treatment of acetic acid
gave some interesting information. Figure 8.2-53 gives a
comparative X-ray fluorescence pattern of PGC before and
after treatment. There is a marked increase in chromium,
nickel, iron and zinc after treatment with acetic acid.
This could be due to the corrosive action of acetic acid on
the stainless steel column in an aqueous medium. The
metals released during the corrosion would have entirely
deactivated the column. Whether this deactivation is
permanent or reversible is still not conclusive.

Practical Applications

Some preliminary experiments show a promising future
for PGC. Aspirin or acetyl salicyclic acid can be easily
separated from its acid. Such a separation is extremely
difficult on ODS. This separation is illustrated in
figure 8.2-54. Other analgesics like paracetamol (figure
8.2-55) and phenacetin can also be separated using acetic
acid in the eluent to drastically improve peak shapes.
Caffeine can also be chromatographed as shown in
figures 8.2-56. Figure 8.2-57 shows a separation of all the
analgesics.

Chapter 8 - References

1. Bristow, P.A., J. Chromatogr., 131 (1977), 57.

2. Colin, H., and Guiochon, G., J. Chromatogr., 126 (1976), 43.

3. Colin, H., Eeon, C., Guiochon, G., J. Chromatogr., 119 (1976), 41.

4. Unger, K., Roumeliotis, P., Mueller, H. and Goetz, H., J. Chromatogr., 202 (1980), 3.

5. Smolkova, E., Zima, J., Dousek, F.P. and Jansta, J., J. Chromatogr., 191 (1980), 61.

6. Ciccioli, P., Tappa, R., DiCorcia, A., Liberti, A., J. Chromatogr., 206 (1981), 35.

7. Halasz, I. and Maldener, K., Anal. Chem., 55 (1983), 1842.

8. Colin, H., Ward, N., Guiochon, G., J. Chromatogr., 149 (1978), 169.

COLUMN

PACKING CHAMBER

PRESSURE GAUGE

ON/OFF

VALVE

RESERVOIR

AIR PUMP

N_2
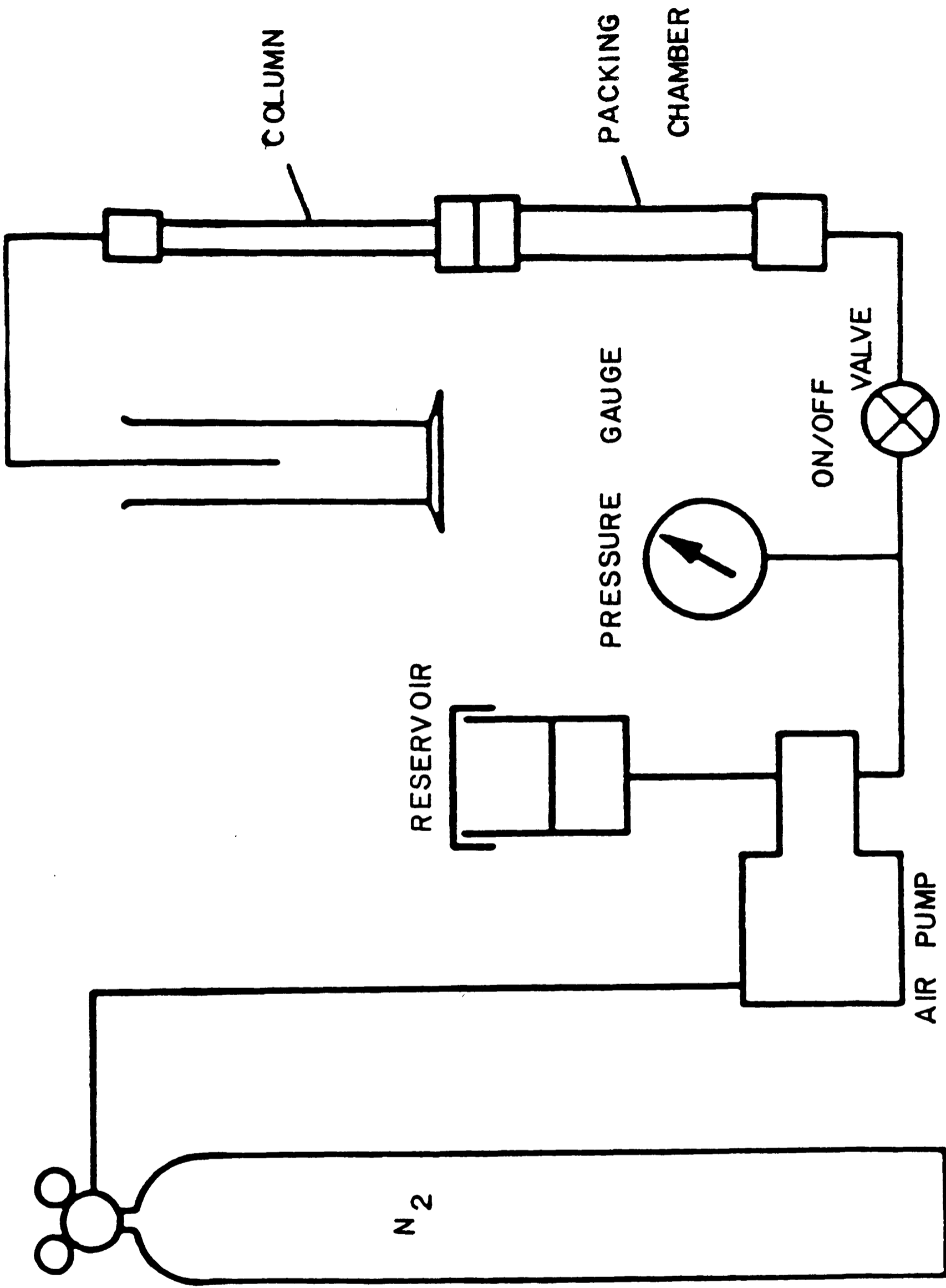
FIG. 8.1-1: SLURRY PACKING SYSTEM USING A PNEUMATIC INTENSIFIER PUMP

10 cm — Packed Restrictor Column

12cm — Column

Precolumn

Slurry Reservoir
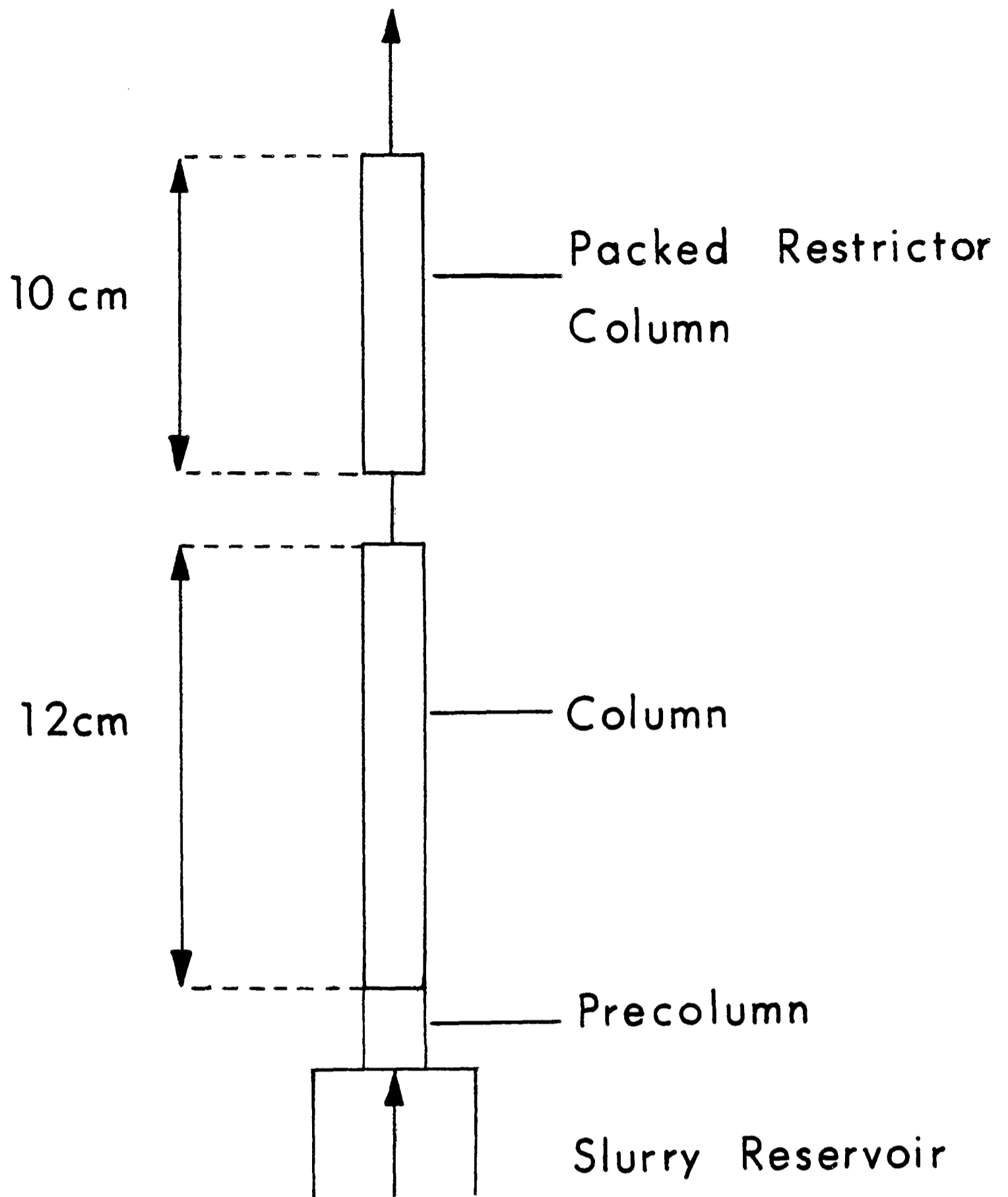
FIG. 8.1-2 : HALASZ AND MALDENER METHOD OF SLURRY PACKING (from Ref. 7)

Table 8.1-1   Grading of columns, from number 1 (the best) to number 19

(the worst), of PGC 72 packed with different solvents and

solvent combinations

Number of Column	Type of solvent slurry/follower	Packing Pressure psi	Outlet flow rate ml min^{-1} Bars	Back pressure at 1.0 ml min^{-1} Bars	Grading of column
A	CH_2Cl/CH_2Cl_2	500/min 1000→3000	6 - 8	61	19
B	CH_2Cl_2/CH_2Cl_2	1000	6 - 8	60	9
C	IPA/MeOH	1000	2	78	12
D	C_5H_{12}/C_5H_{12}	1-2 min 1000→2000	6	74	5
E	C_5H_{12}/C_5H_{12} *	2000	8	45	17
F	C_5H_{12}/C_5H_{12}	3000	2	14	18
G	IPA/MeOH	2 min 500→6000	2.5	125	14
H	MeOH	6000	5	117	3
I	$CH_2Cl_2KH_2Cl_2$	˙1000→6000	5.5	121	8
J	THF/THF	1000→6000	5	118	10
K	MeCN/MeCN	1000→6000	6.5	120	4
L	Toluene	1000→6000	4.0	269*	16
M	C_6H_{12}/ether	1000→6000	7.0	302*	13
N	Acetone	1000→6000	9.0	120	1
O	Cyclohexane/ IPA	1000→6000	5.0	116	15
P	50% MeOH+acetone /MeOH	1000→6000	8.0	65	2
Q	32% cyclohexane + 68% MeOH/MeOH	1000→6000	4.0	188	17
R	50% MeCN + 50% Acetone/acetone	1000→6000	7.5	119	10
S	12% cyclohexane 88% acetonitrile/ acetonitrile	1000→6000	6.2	164*	11

Table 8.1-1 (contd.)

Number of Column	Type of solvent slurry/follower	Packing Pressure psi	Outlet flow rate ml min^{-1} Bars	Back pressure at 1.0 ml min^{-1} Bars	Grading of column
T	76% Acetone + 24% CH$_3$COONa (0.2 g dm^{-3}) pH 1.7	1000→6000	6.5	106	7
U	76% acetone + 24% CH$_3$COONa (0.2 g dm^{-3}) pH 7.7	1000→6000	5.5	102	6

* Halasz and Maldener Method[7]
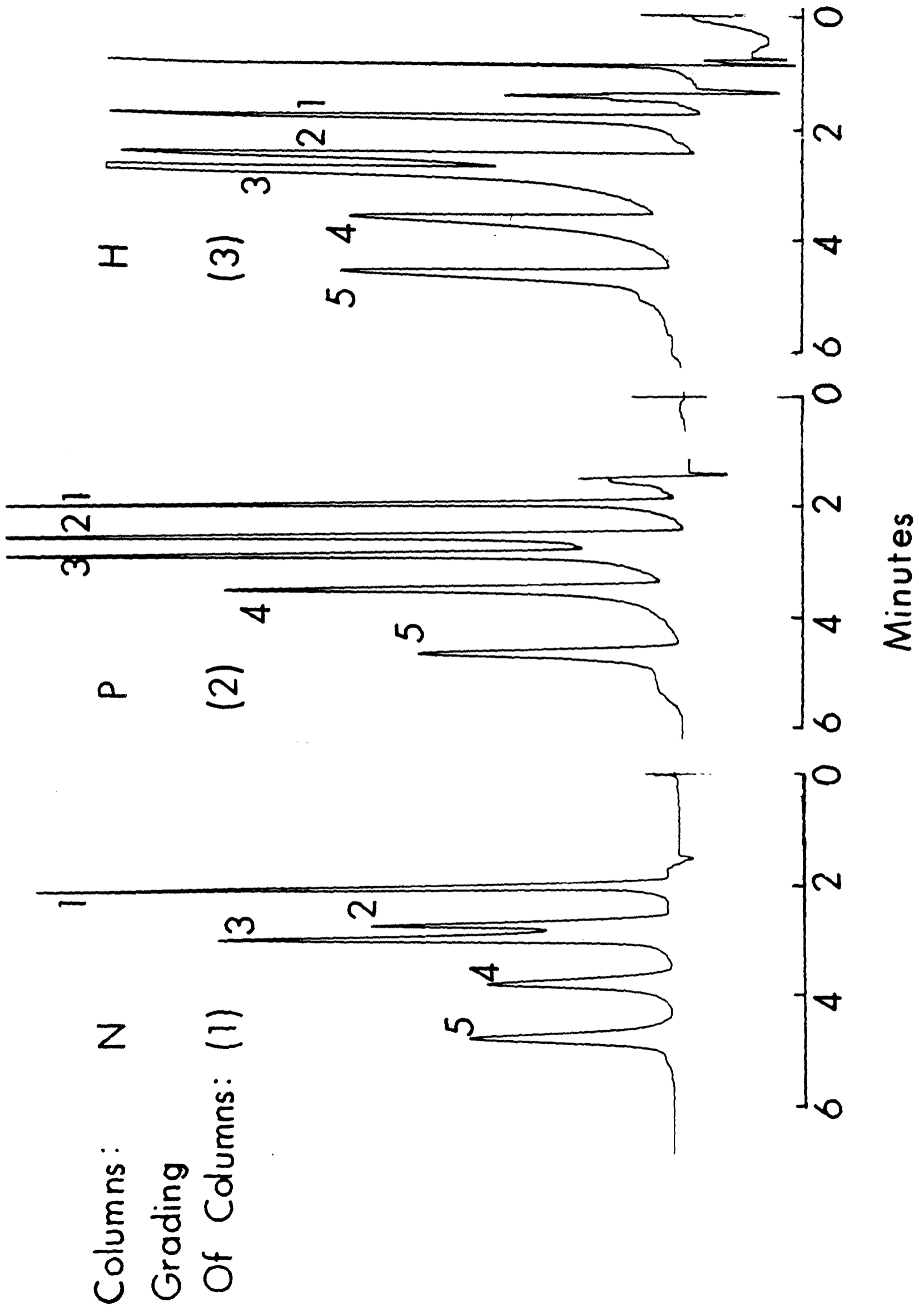
FIG. 8.1-3 : TEST CHROMATOGRAMS OF COLUMNS N, P & H.
Eluent: 95% MeOH/H₂O; Flow Rate: 1ml/min; Solutes: (1) Phenol
(2) Anisole, (3) p-Cresol, (4) Phenetole, (5) 3,5 Xylenol.

Columns: K D U

Grading
of Columns: (4) (5) (6)

Minutes
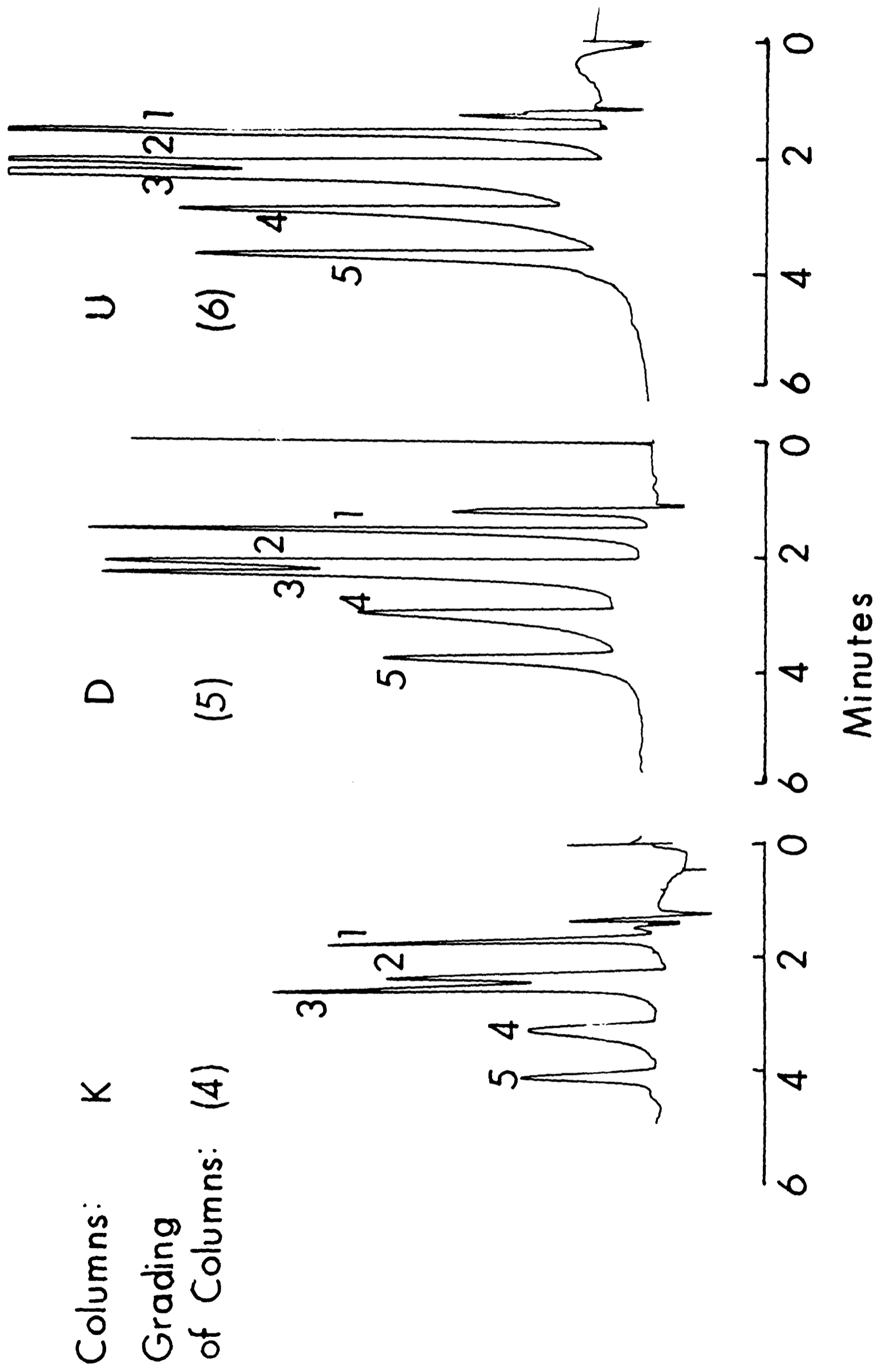
FIG. 8.1-4 : TEST CHROMATOGRAMS OF COLUMNS K, D & U

Conditions as in Fig. 8.1-3.
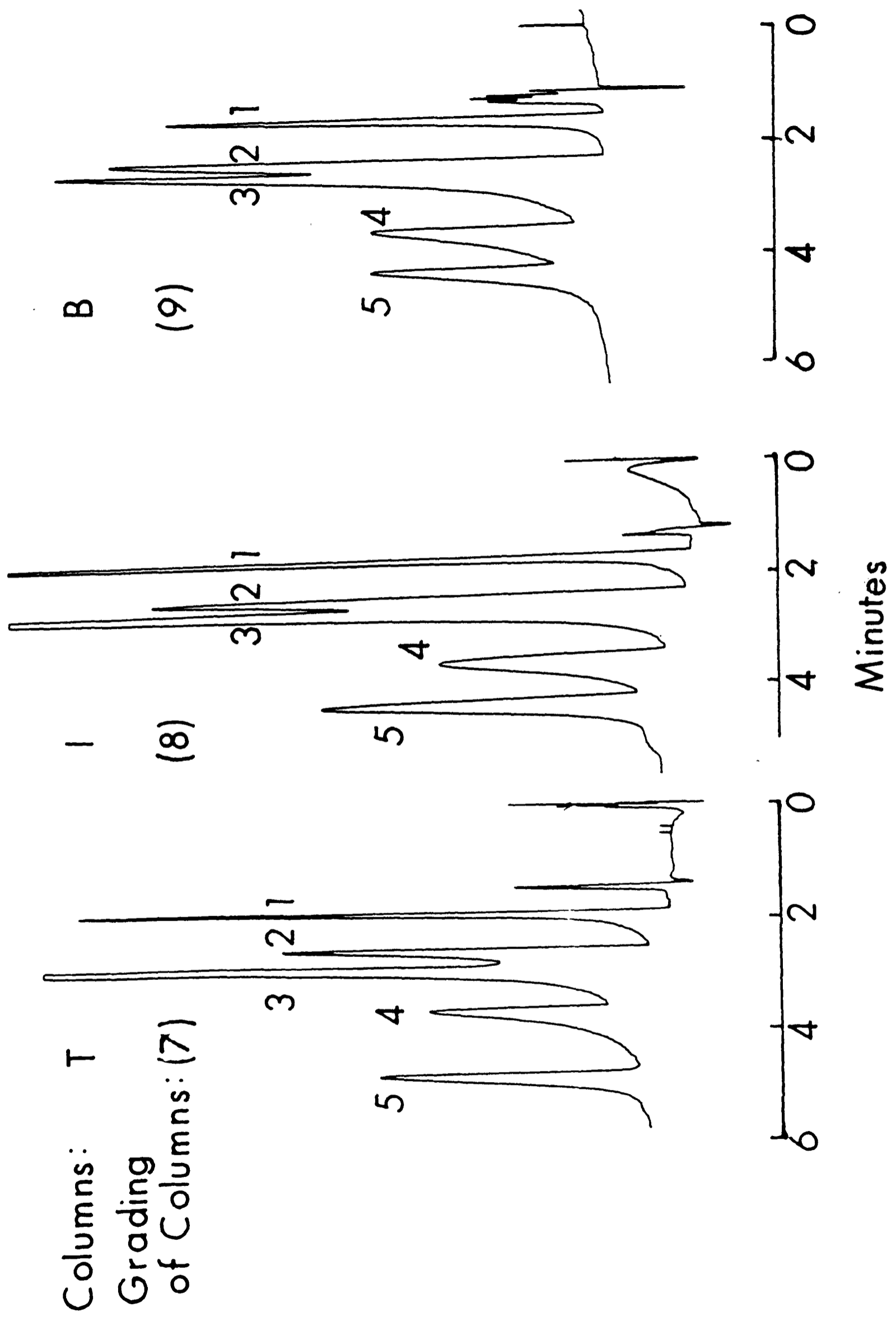
Columns: T

Grading
of Columns: (7)

Columns: I

(8)

Columns: B

(9)

Minutes

FIG. 8.1−5 : TEST CHROMATOGRAMS OF COLUMNS T, I & B

Conditions as in Fig. 8.1−3.

Columns: R

Grading
of Columns: (10)

J
(10)

S
(11)

Minutes
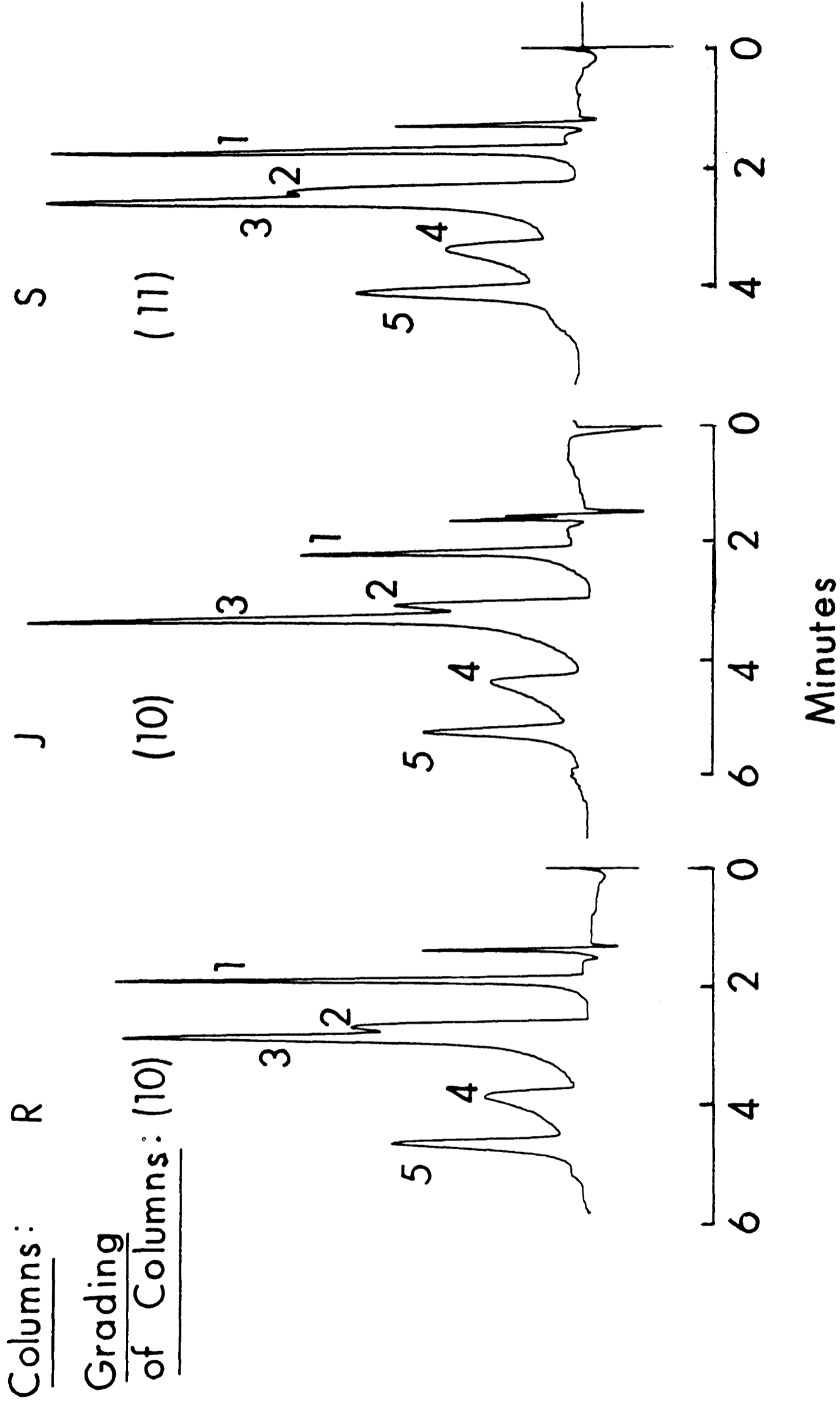
FIG. 8.1 - 6 : TEST CHROMATOGRAMS OF COLUMNS R, J & S

Conditions as in Fig. 8.1 - 3.

Columns:

Grading
of Column:

C (12)

M (13)

G (14)

Minutes
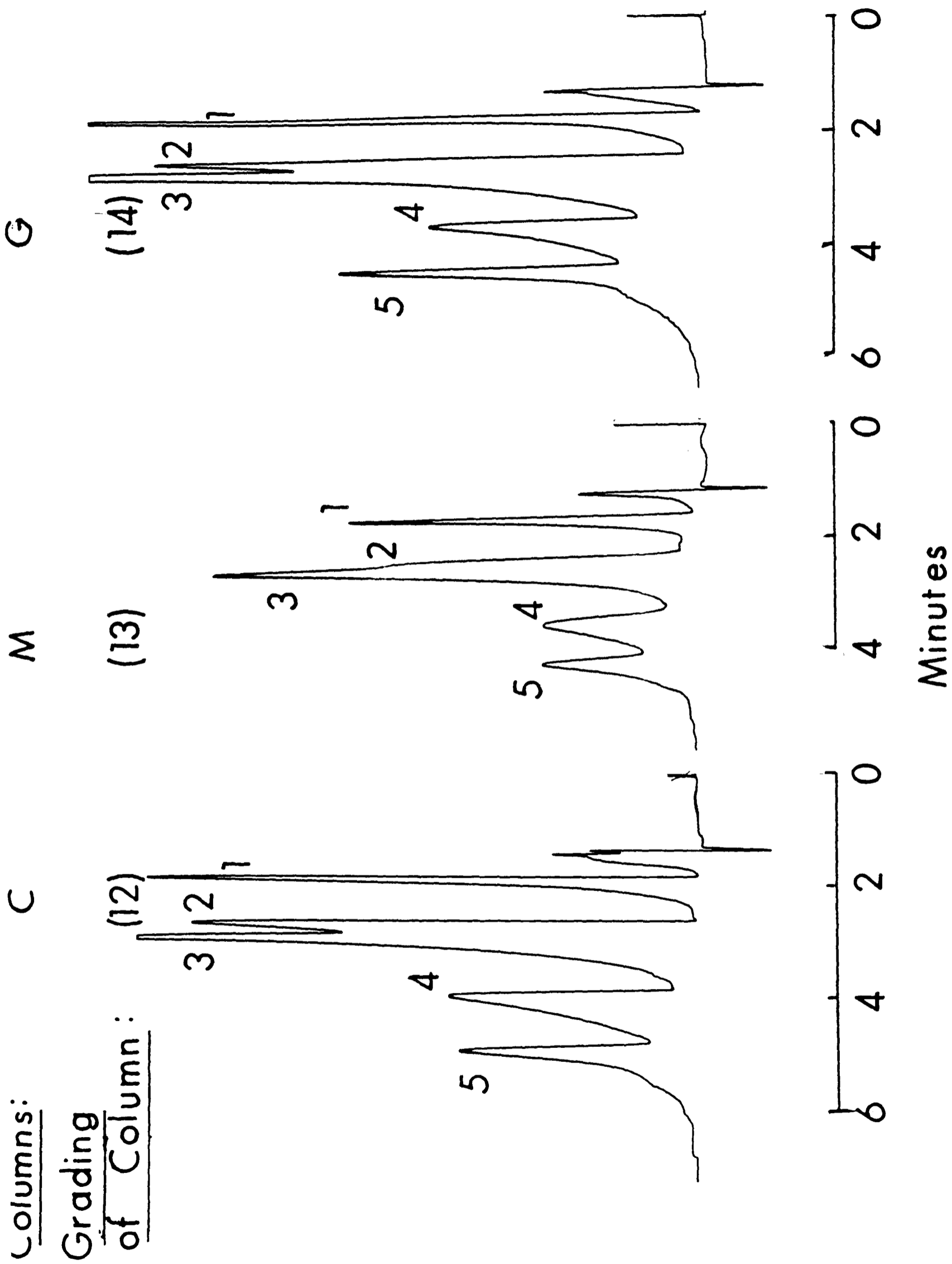
FIG. 8.1 – 7 : TEST CHROMATOGRAMS OF COLUMNS C, M & G

Conditions as in Fig. 8.1 – 3.

Columns: O   L   E

Grading
of Columns:

(15)   (16)   (17)

Minutes
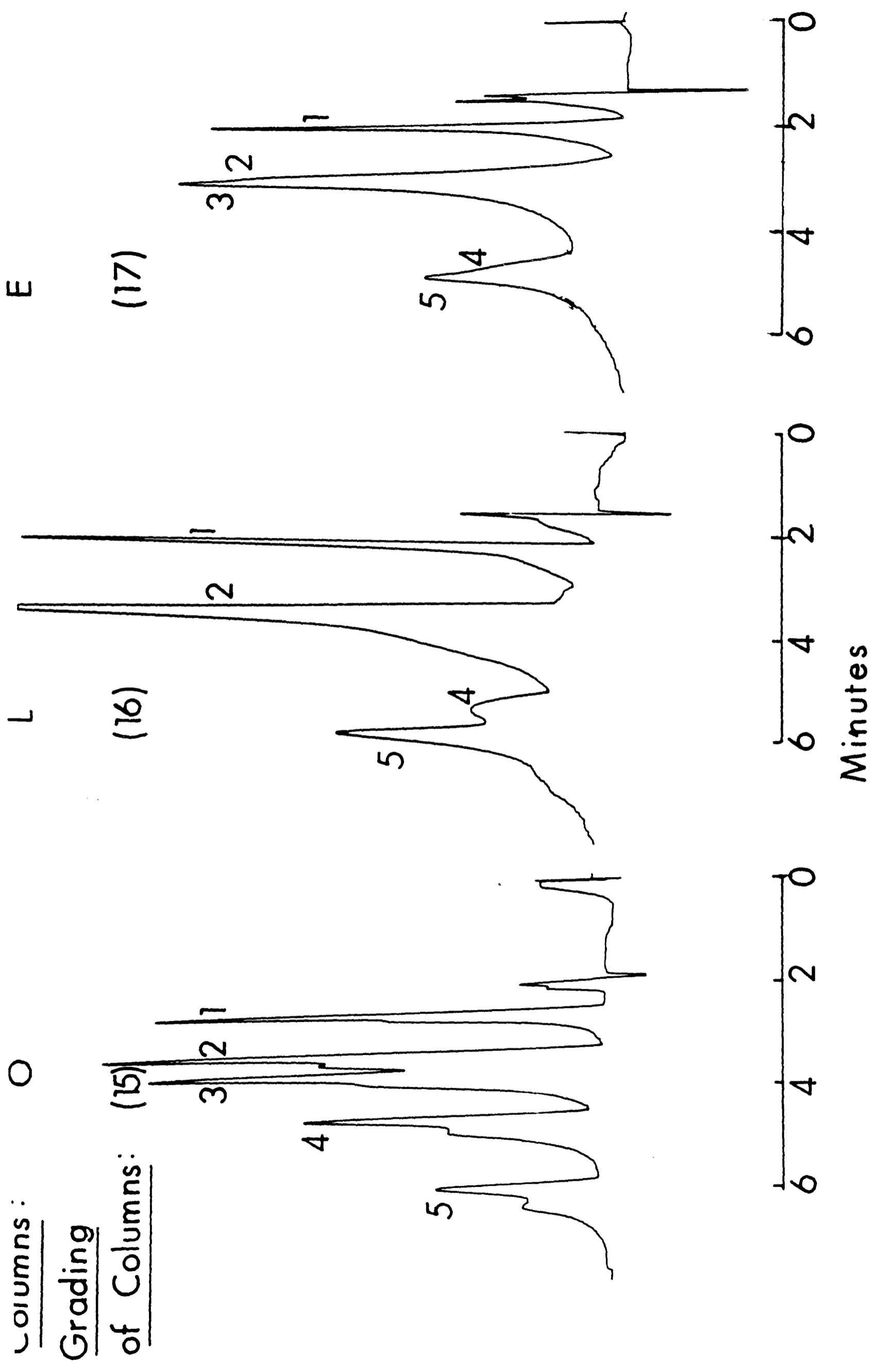
FIG.8.1 - 8 : TEST CHROMATOGRAMS OF COLUMNS O, L & E
Conditions as in Fig.8.1 - 3 .

Columns: Q   F   A

Grading
of Columns: (17)   (18)   (19)

Minutes
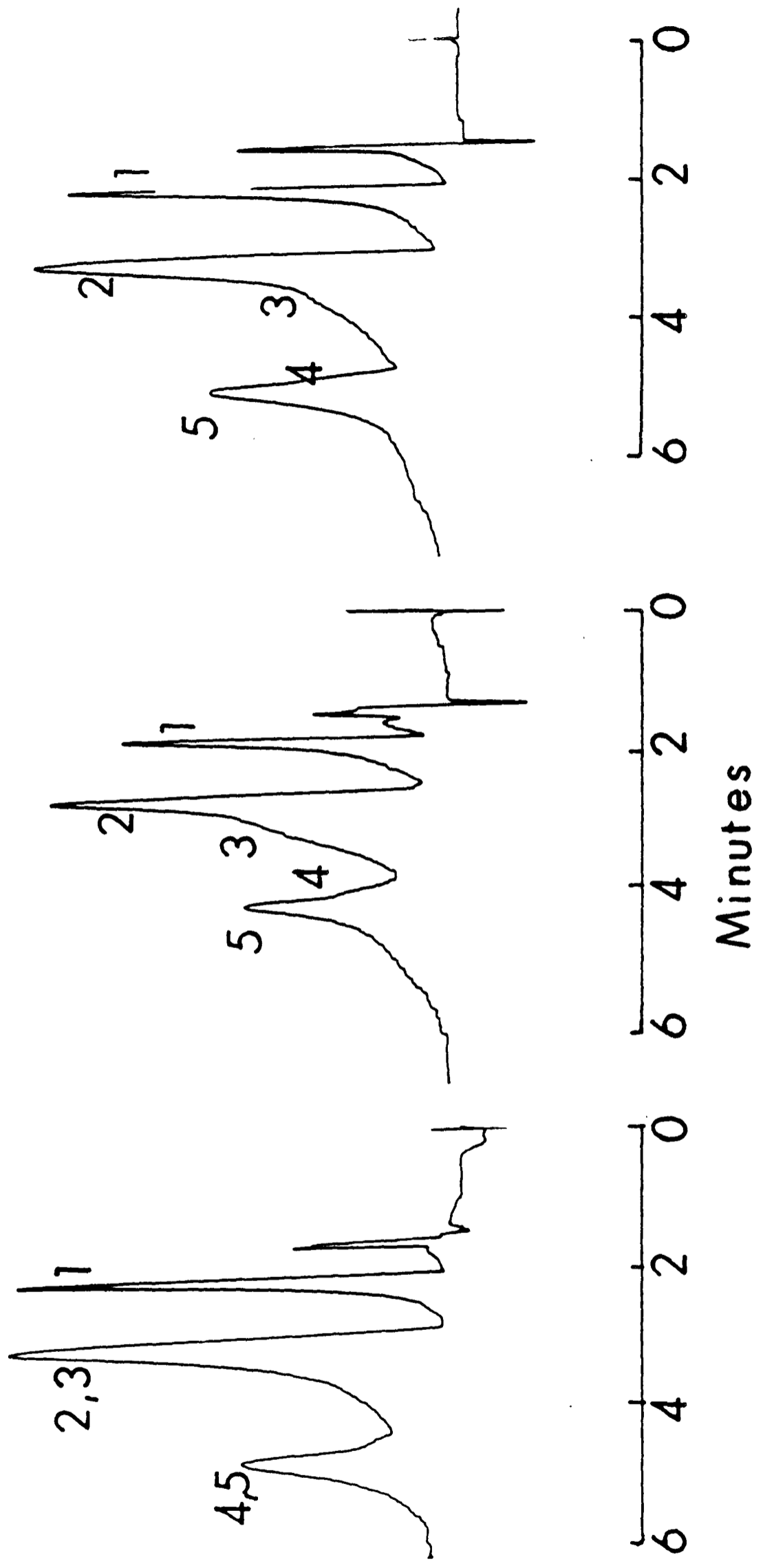
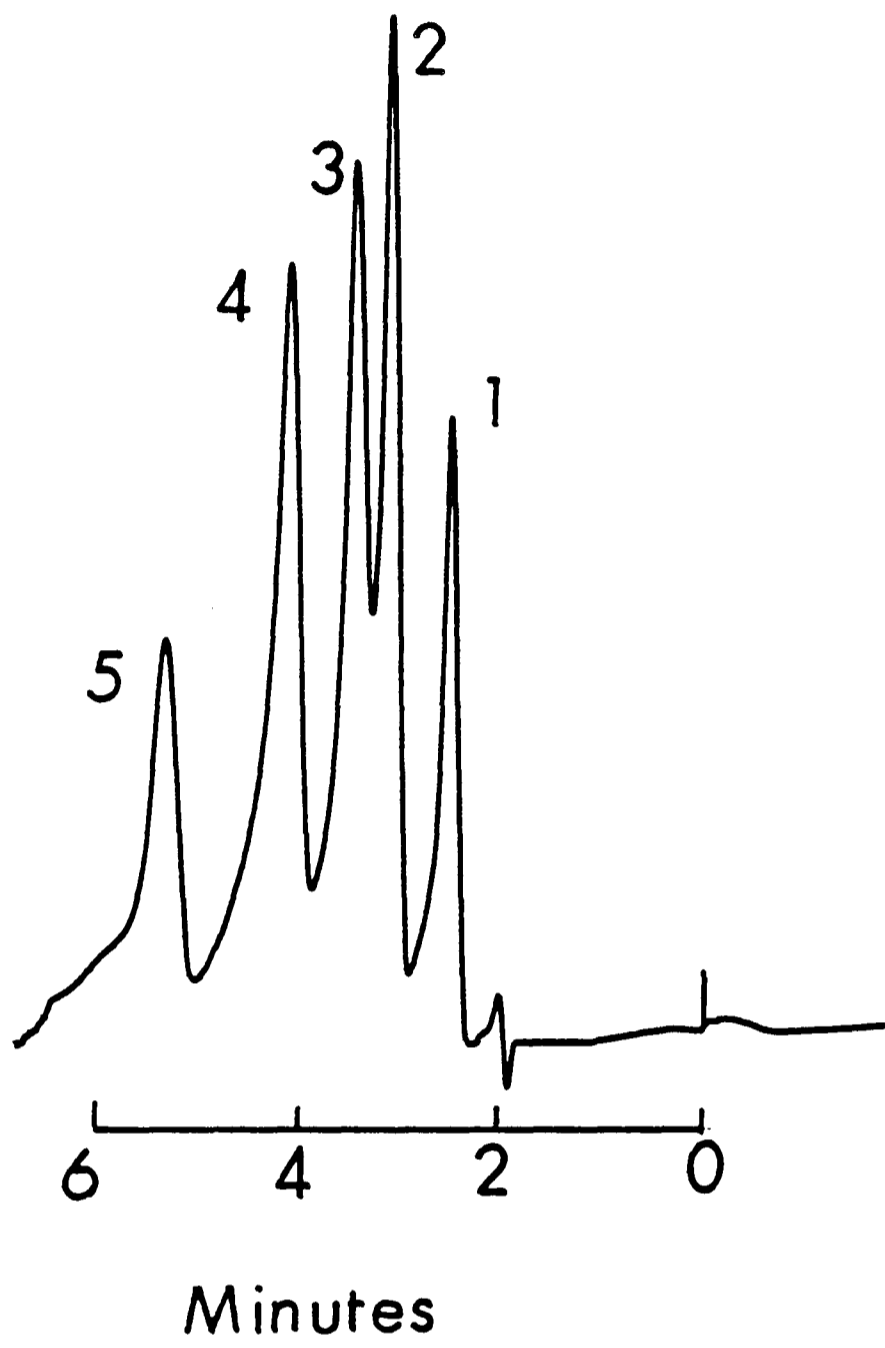FIG. 8.1 - 9 : TEST CHROMATOGRAMS OF COLUMNS Q, F & A

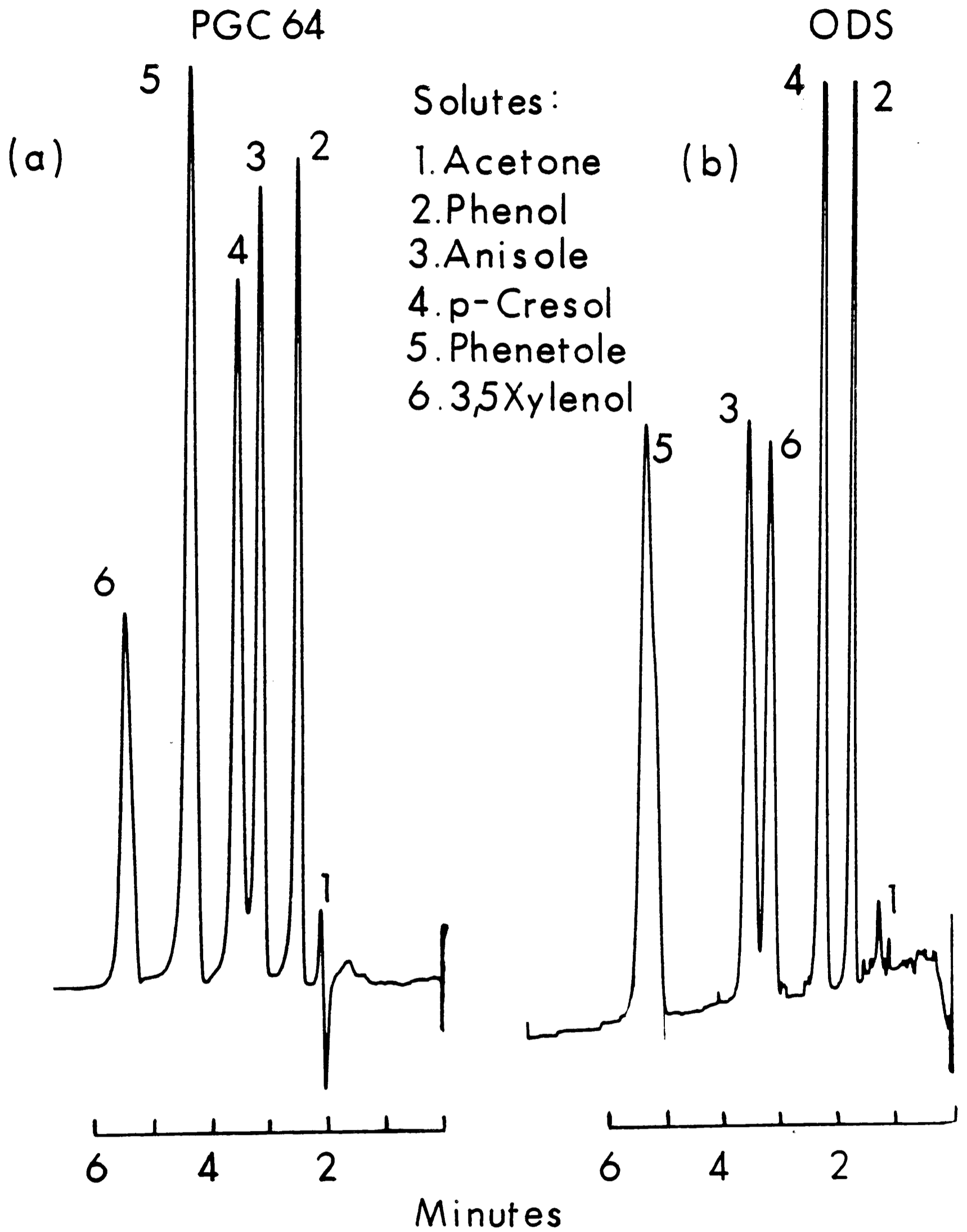Conditions as in Fig. 8.1 - 3.

FIG. 8.1 -10: TEST CHROMATOGRAM OF PGC CONTAMINATED WITH NEEDLES. Conditions as in Fig. 8.1 -3 .

Table 8.2-1   List of PGCs studied

Material	Particle size μm	Surface area $m^2 g^{-1}$
MTG-C-7d (spherical)	∿40	348
PGC 26 (spherical)	5	382
PGC 20	100	-
PGC 19 (chips)	37 - 74	21.18
PGC 57 (chips)	37 - 74	374
PGC 64	5	154
PGC 70B-B	5	149
PGC 70B-C	5	150
PGC 70B-A	5	160
72	5	144

PGC 64

(a)

Solutes:
1. Acetone
2. Phenol
3. Anisole
4. p-Cresol
5. Phenetole
6. 3,5 Xylenol

ODS

(b)

Minutes

Flow Rate : 1 ml / min
Eluent : (a) 95% MeOH / H_2O
(b) 60% MeOH / H_2O

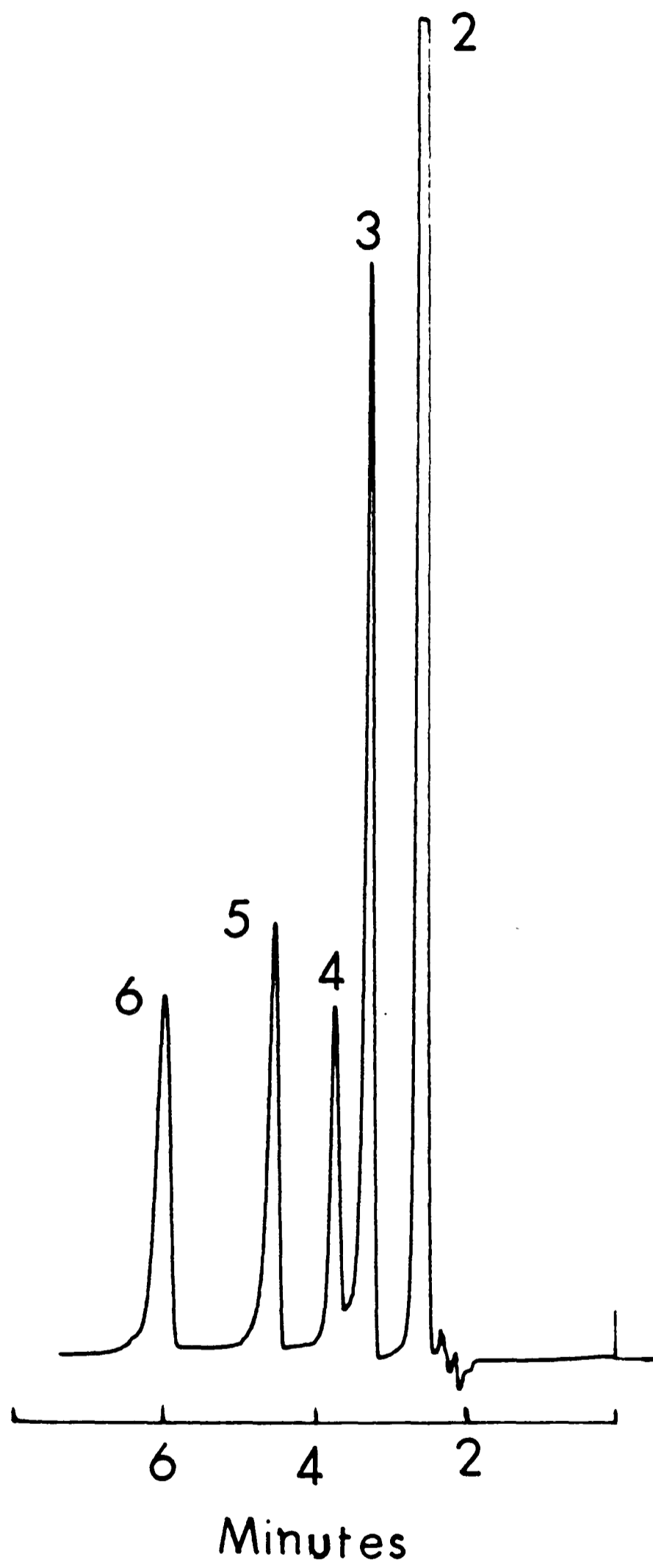FIG. 8.2 - 1 : SEPARATION OF TEST SOLUTES

PGC 70-C

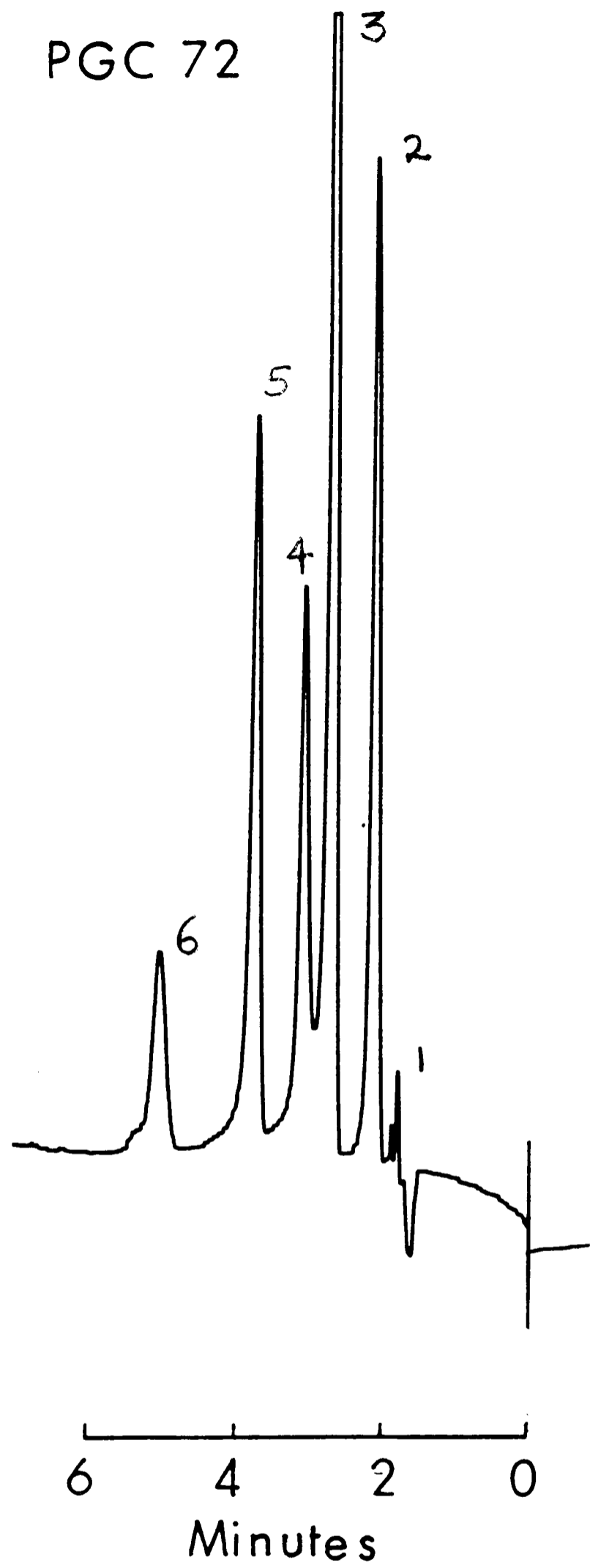FIG.8.2-2 : Conditions as in Fig.8.2-1(a)

PGC 72

FIG. 8.2 - 3 : Conditions as in Fig. 8.2 - 1(a)

Table 8.2-2   Retention data on a good batch of PGC

(PGC 64) and bad batch of PGC (PGC 70-A)

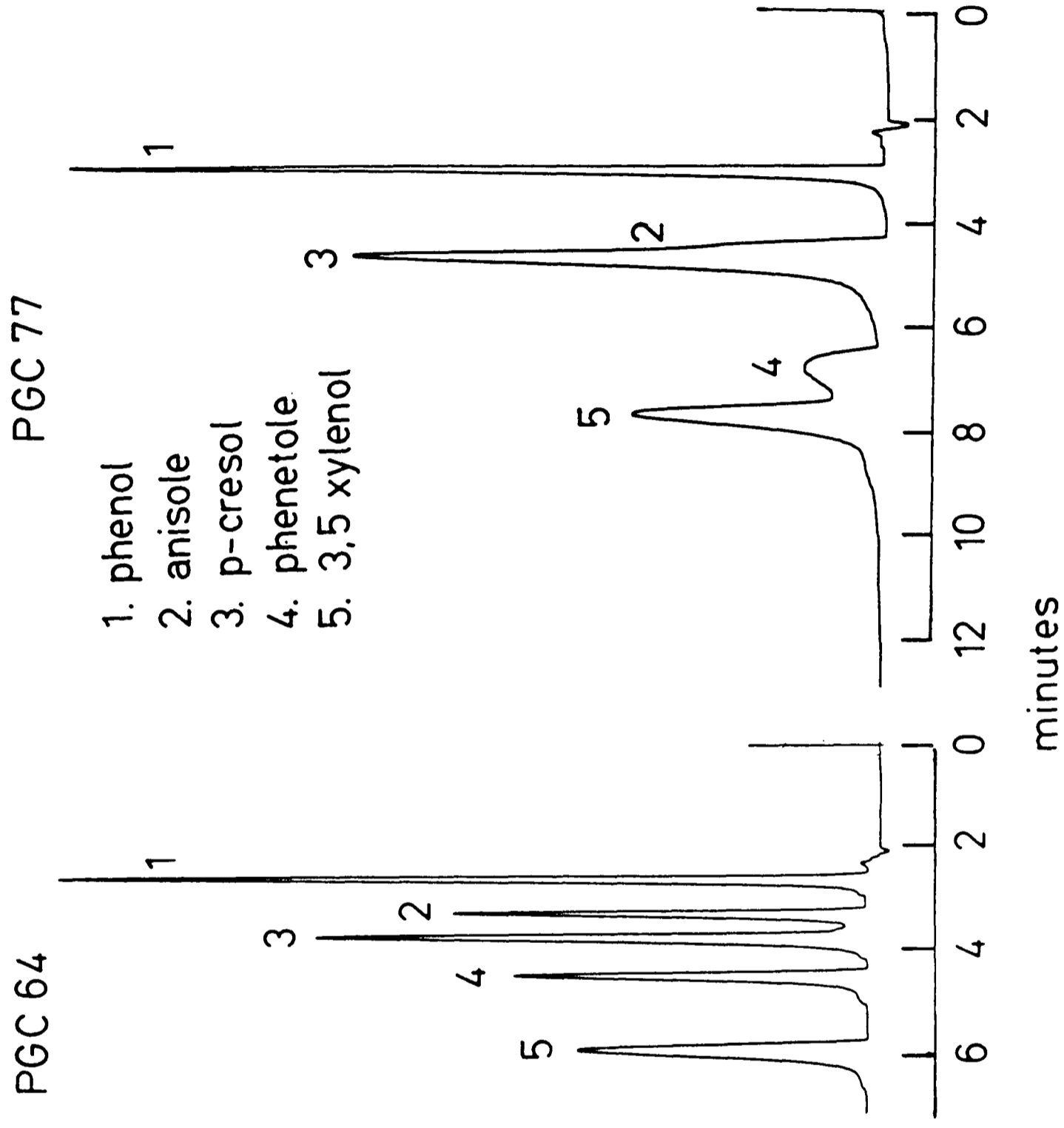| Solutes	PGC 64	PGC 70-A
Phenol	0.37	0.46
Anisole	0.63	1.10
p-Cresol	0.86	1.41
Phenetole	1.00	2.32
3,5-Xylenol	2.00	2.84

FIG. 8.2-4(a): COMPARATIVE CHROMATOGRAMS OF A GOOD BATCH OF PGC (PGC 64) AND A BAD BATCH (PGC 77)

PGC 70-A

Flow Rate : 0.5ml/min
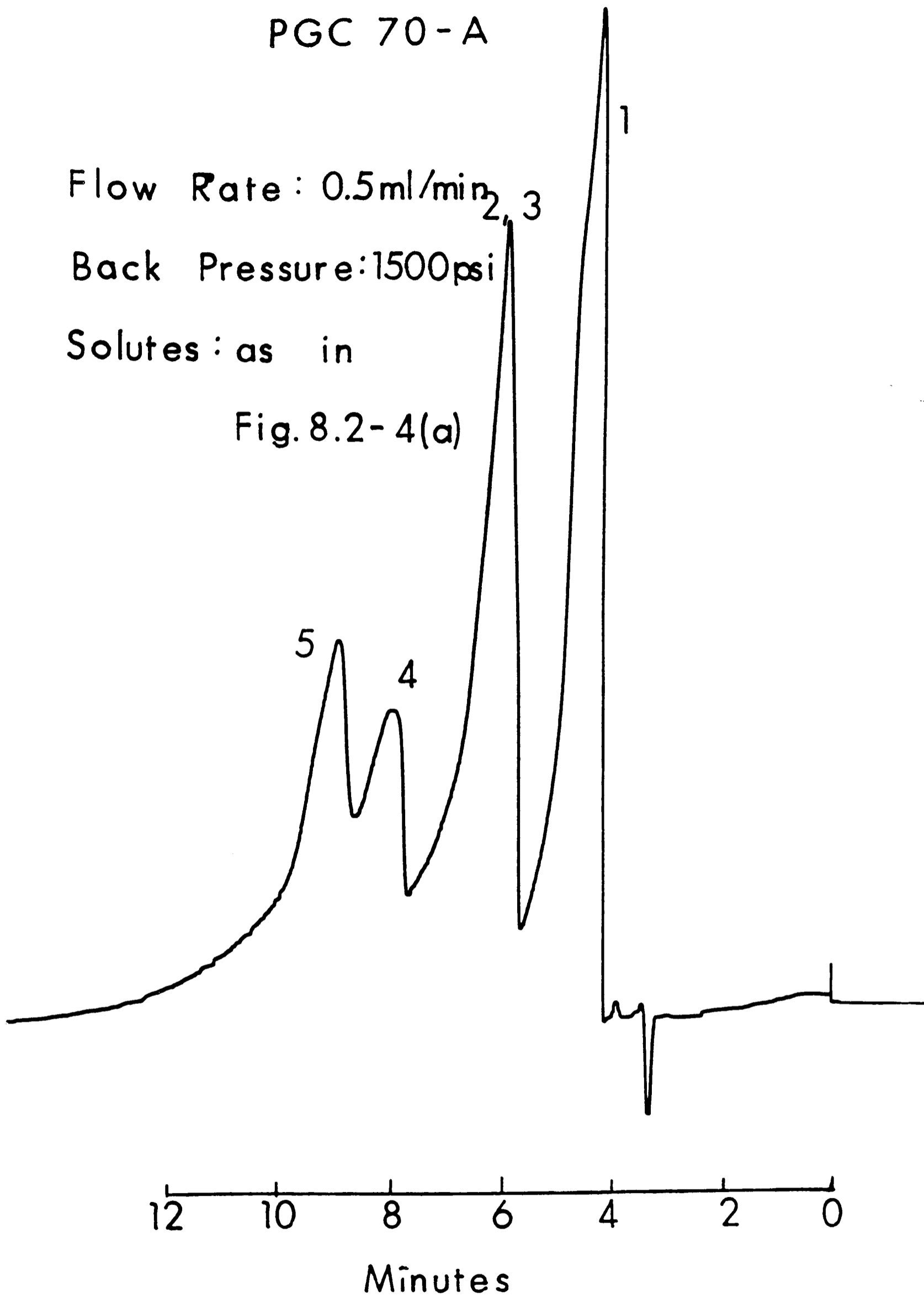
Back Pressure : 1500psi

Solutes : as in

Fig. 8.2-4(a)

FIG. 8.2 - 4 (b) : TEST CHROMATOGRAM OF
PGC HEATED AT A HIGH
RATE FROM 1000 TO 2500°C.

(a) PGC   (b) ODS

Eluent: (a) 90% MeOH/H$_2$O
        (b) 70% MeOH/H$_2$O

Flow Rate: 1 ml/min

Solutes:

1. Benzene
2. Aniline
3. Phenol
4. Benzyl alcohol
5. Toluene
6. Chlorobenzene
7. Anisole
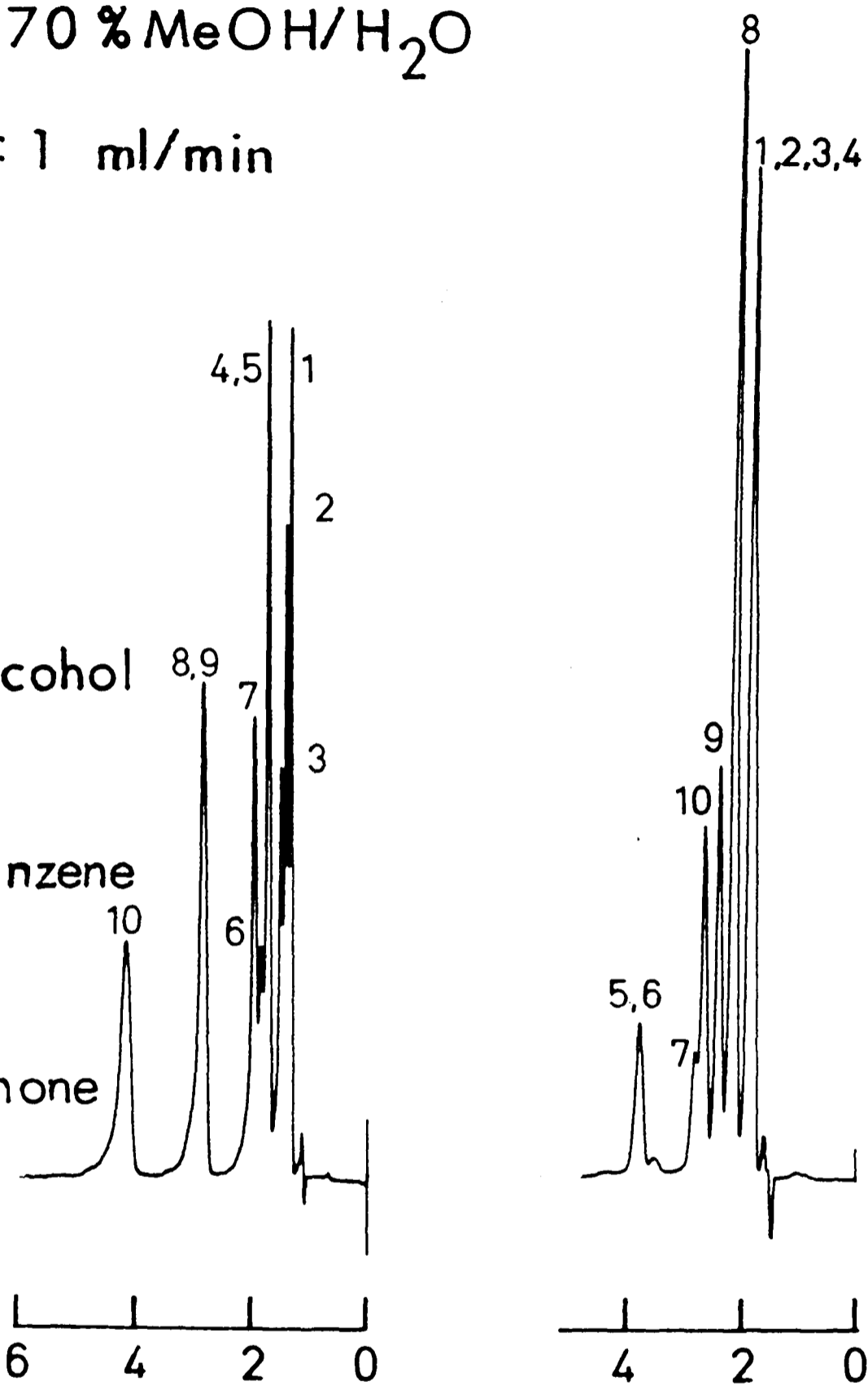8. Acetophenone
9. Nitro- benzene
10. Methyl- Benzoate
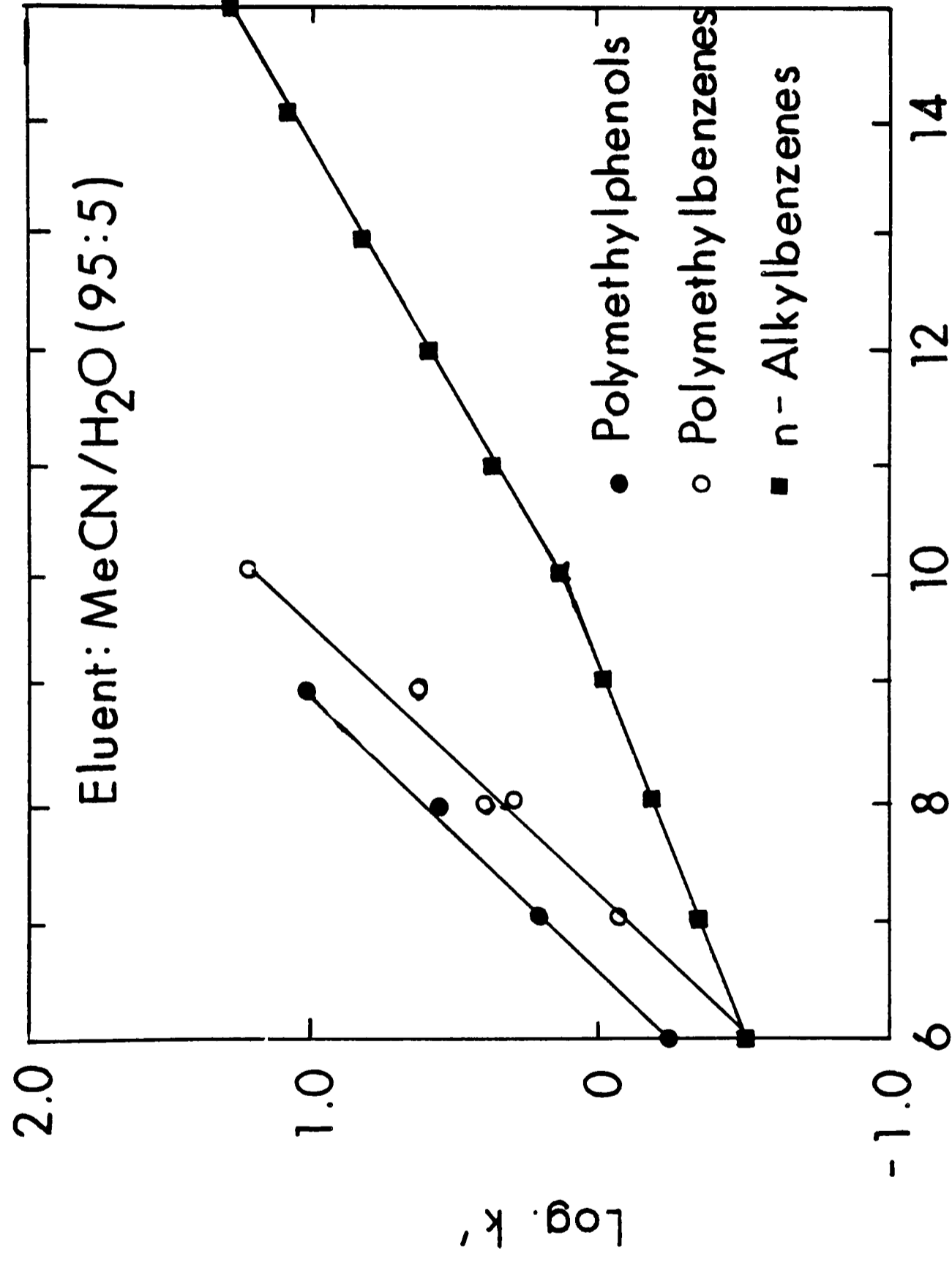
Minutes

FIG. 8.2 – 5: FUNCTIONAL GROUP SELECTIVITY

FIG. 8.2 - 6 : VARIATION OF LOG.k' WITH THE NUMBER OF CARBON ATOMS IN HOMOLOGOUS AND PSEUDO - HOMOLOGOUS SERIES

Table 8.2-3   Comparison of selectivity of ODS and PGC

using 90% acetonitrile + 10% H_2O as eluent

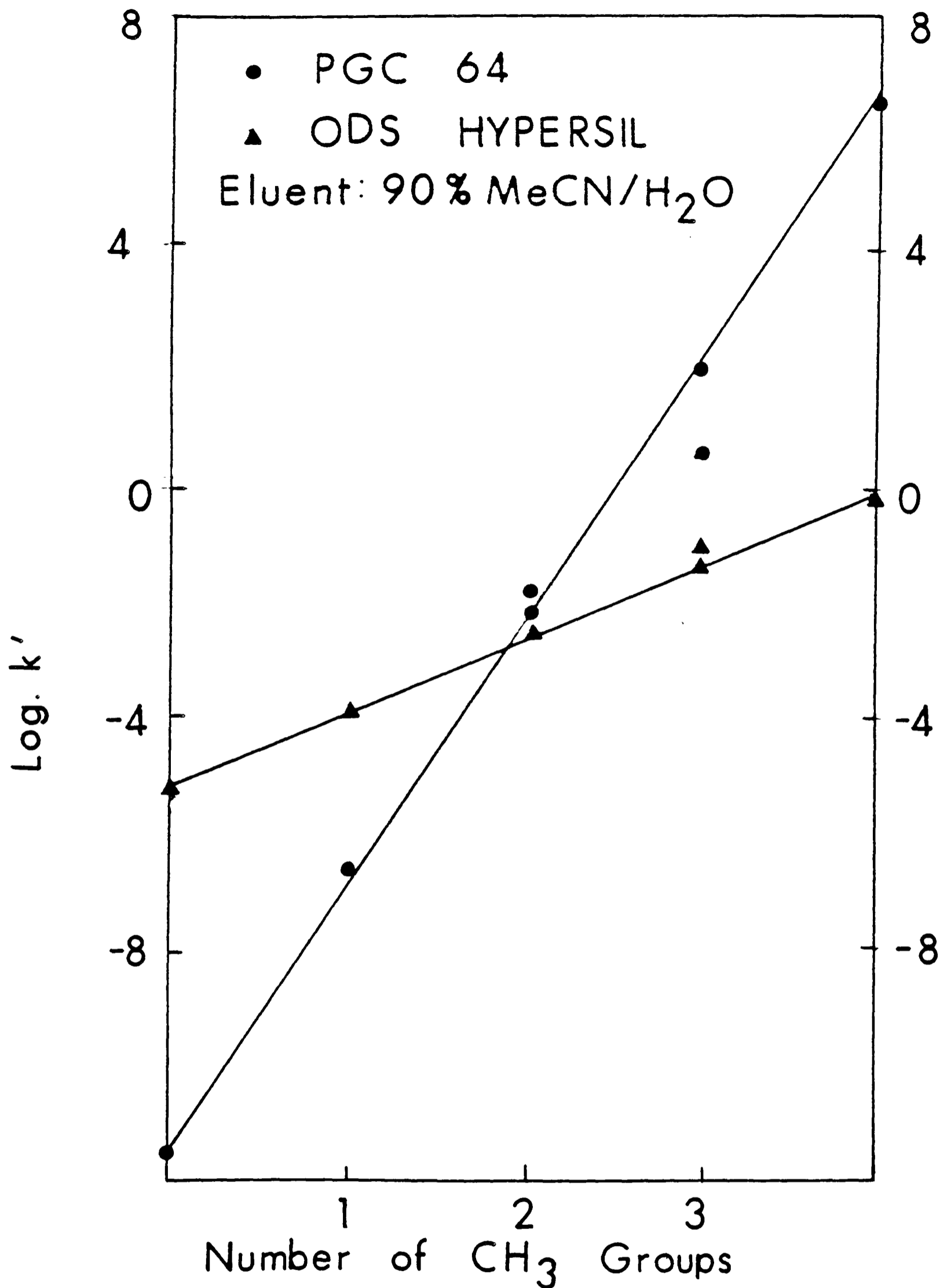|	α	
	ODS	PGC
Polymethybenzenes	0.13	0.44
Polymethylphenols	0.14	0.47
Alkylbenzenes	0.14	0.19

FIG. 8.2-7 : VARIATION OF LOG k' VS. NUMBER OF METHYL GROUPS IN POLY-METHYLBENZENES FOR PGC AND ODS
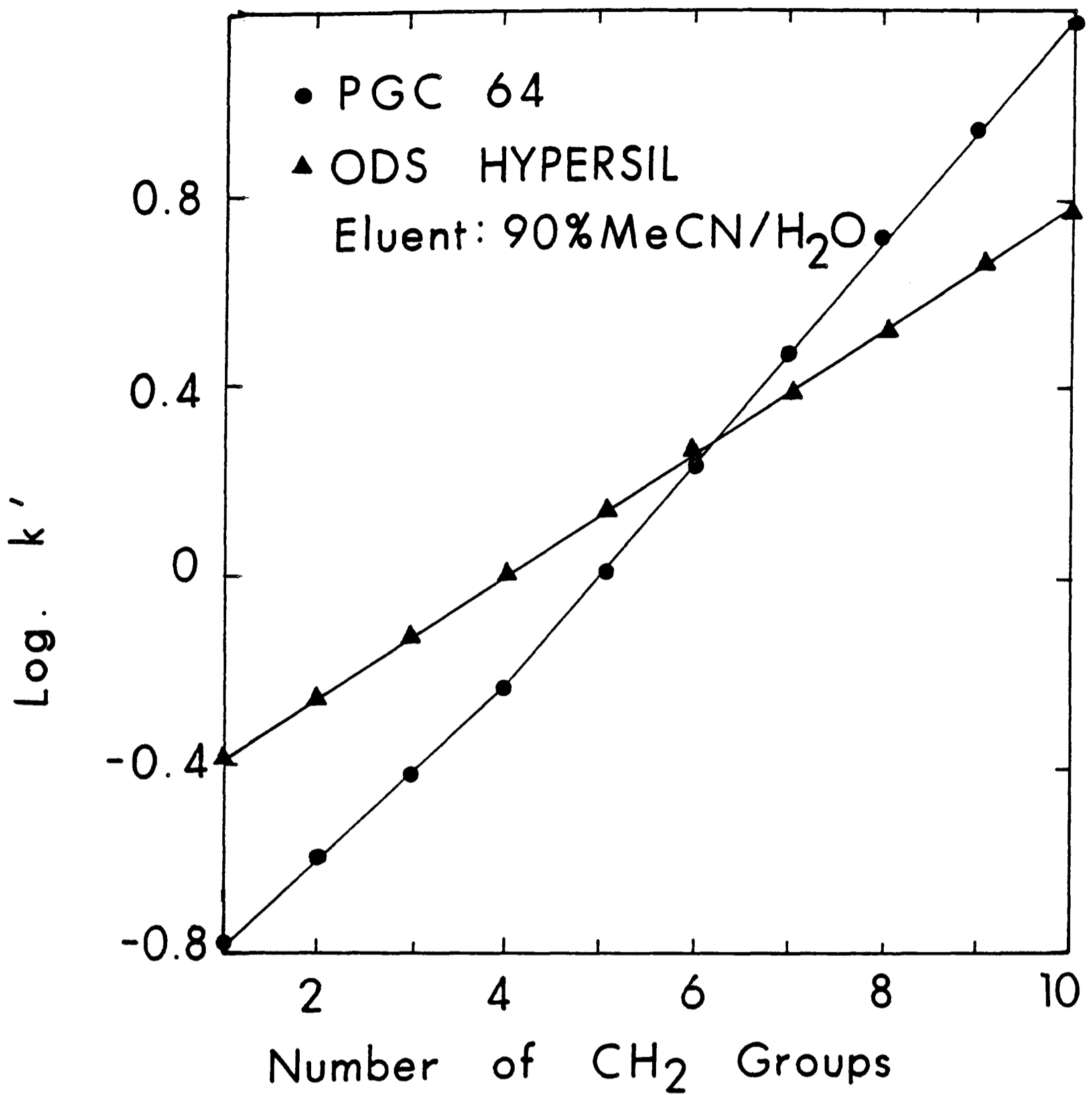
FIG.8.2-8: VARIATION OF LOG k' VS. NUMBER OF METHYL GROUPS IN ALKYLBENZENES FOR PGC AND ODS

Eluent: MeOH/H$_2$O (95:5)

Log. k'

Number of Carbon Atoms
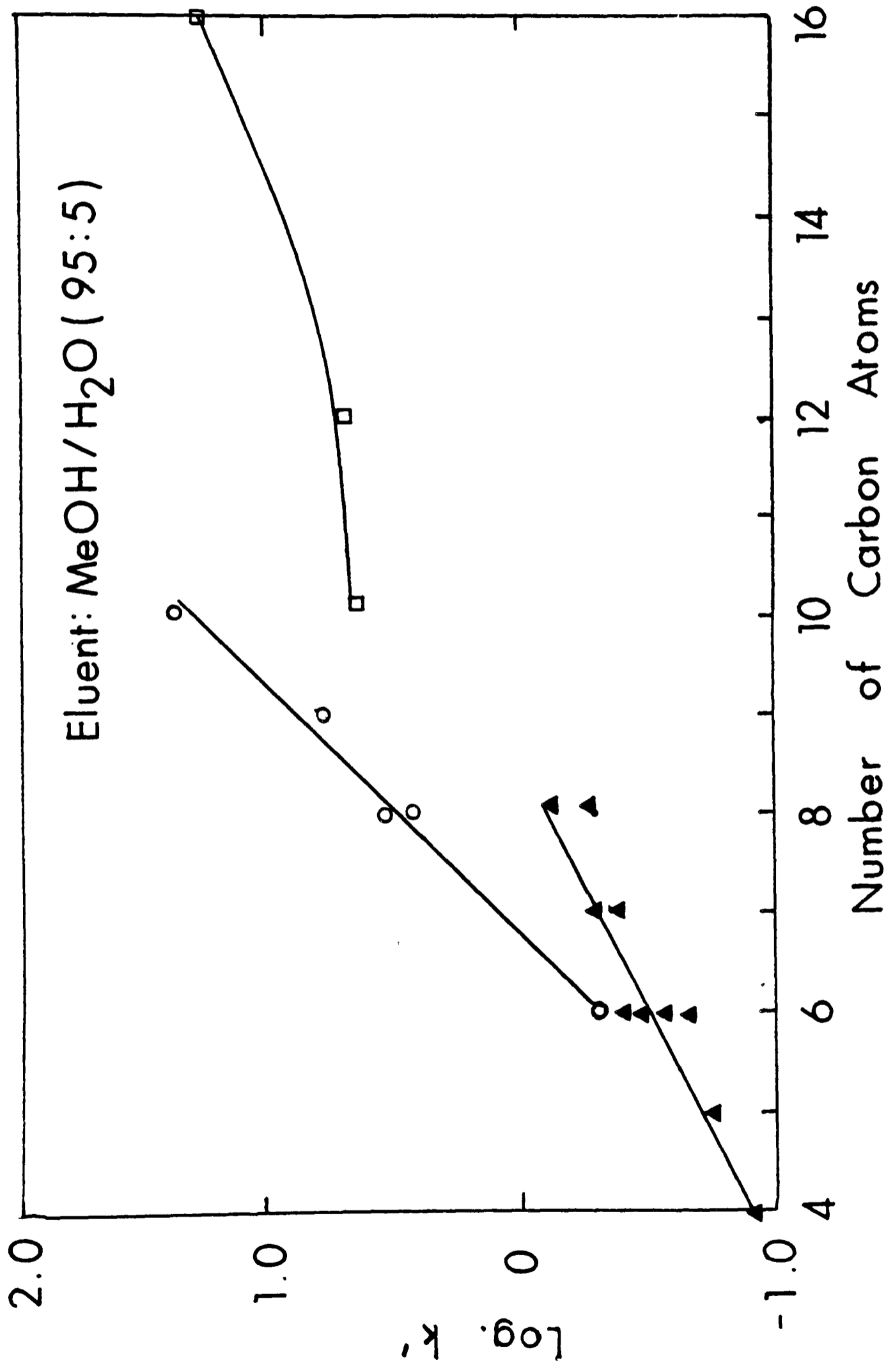
FIG. 8.2-9 : VARIATION OF LOG.k' WITH THE NUMBER OF CARBON ATOMS FOR POLYMETHYLBENZENES(○). PHTHALATES (□) AND ALIPHATIC KETONES(▲)

PGC 64

Eluent: 95% MeOH/H₂O
Flow Rate: 1 ml/min
Solutes:
1. Benzene
2. Toluene
3. m-Xylene
4. o-& p-Xylene
5. 1,3,5 Trimethylbenzene
6. 1,2,4 Trimethylbenzene
7. 1,2,4,5 Tetramethylbenzene

FIG. 8.2-10: SEPARATION OF POLYMETHYLBENZENES

PGC 70-C

FIG. 8.2-11: SEPARATION OF POLYMETHYLBENZENES
Conditions as in Fig. 8.2-10

PGC 70-A
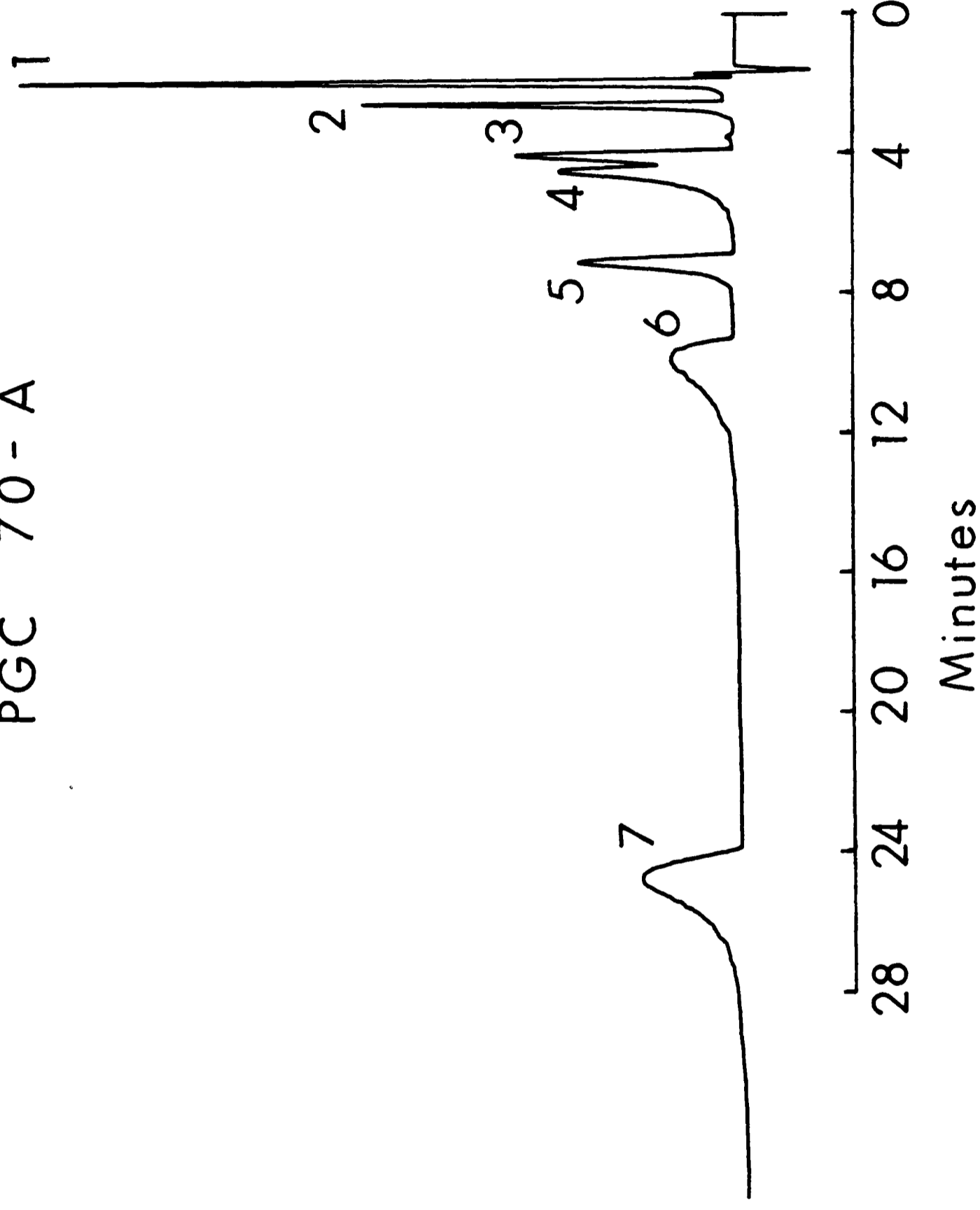
FIG.8.2-12 : SEPARATION OF POLYMETHYLBENZENES
Conditions as in Fig.8.2-10

ODS

Eluent : 70% MeOH/H_2O
Flow Rate : 1 ml/min
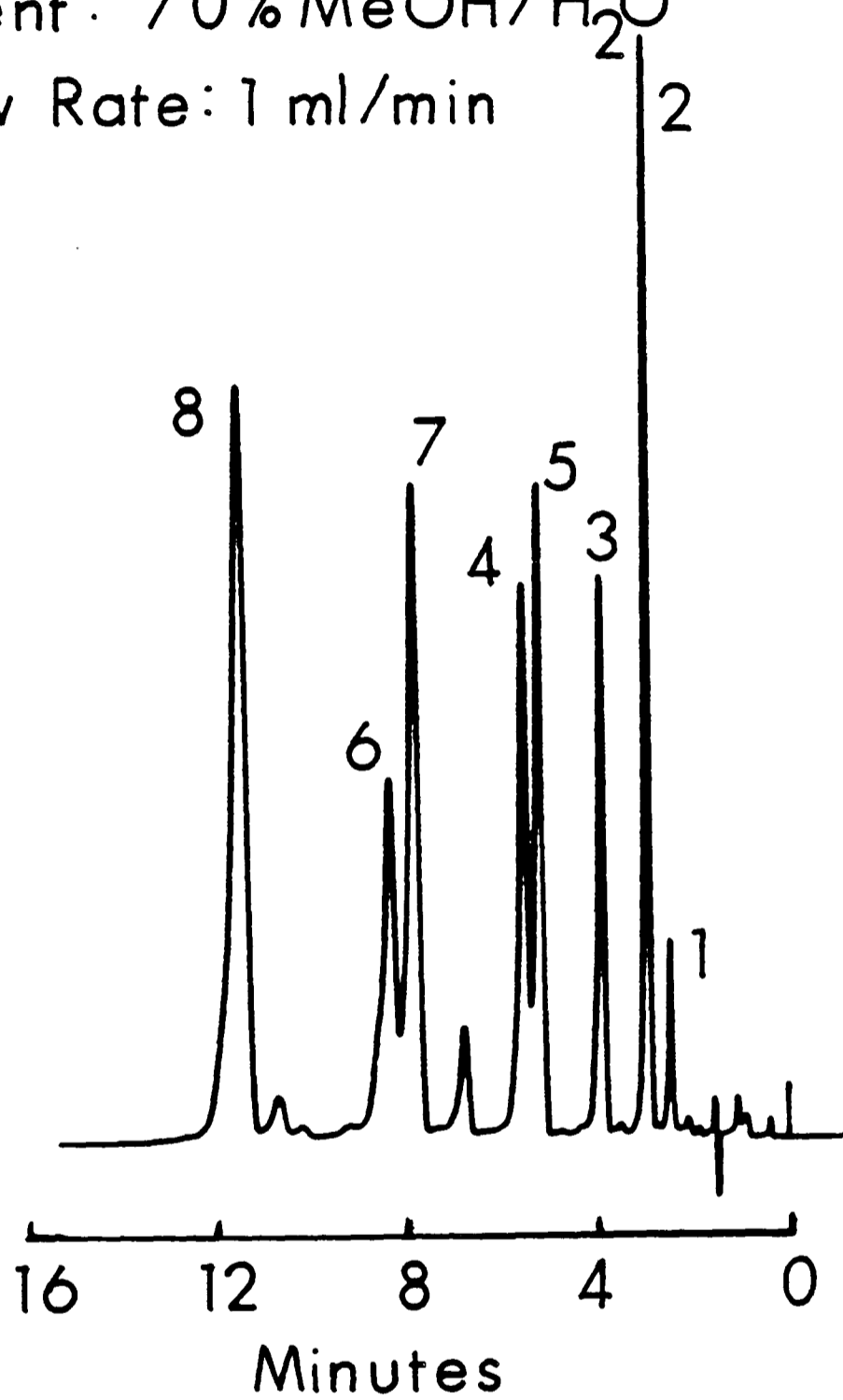
FIG. 8.2 -13 : SEPARATION OF POLY-

METHYLBENZENES

Solutes as in Fig. 8.2 -10

PGC 26

Eluent : MeOH
Flow Rate : 0.5 ml/min
Back Pressure : 2000 psi
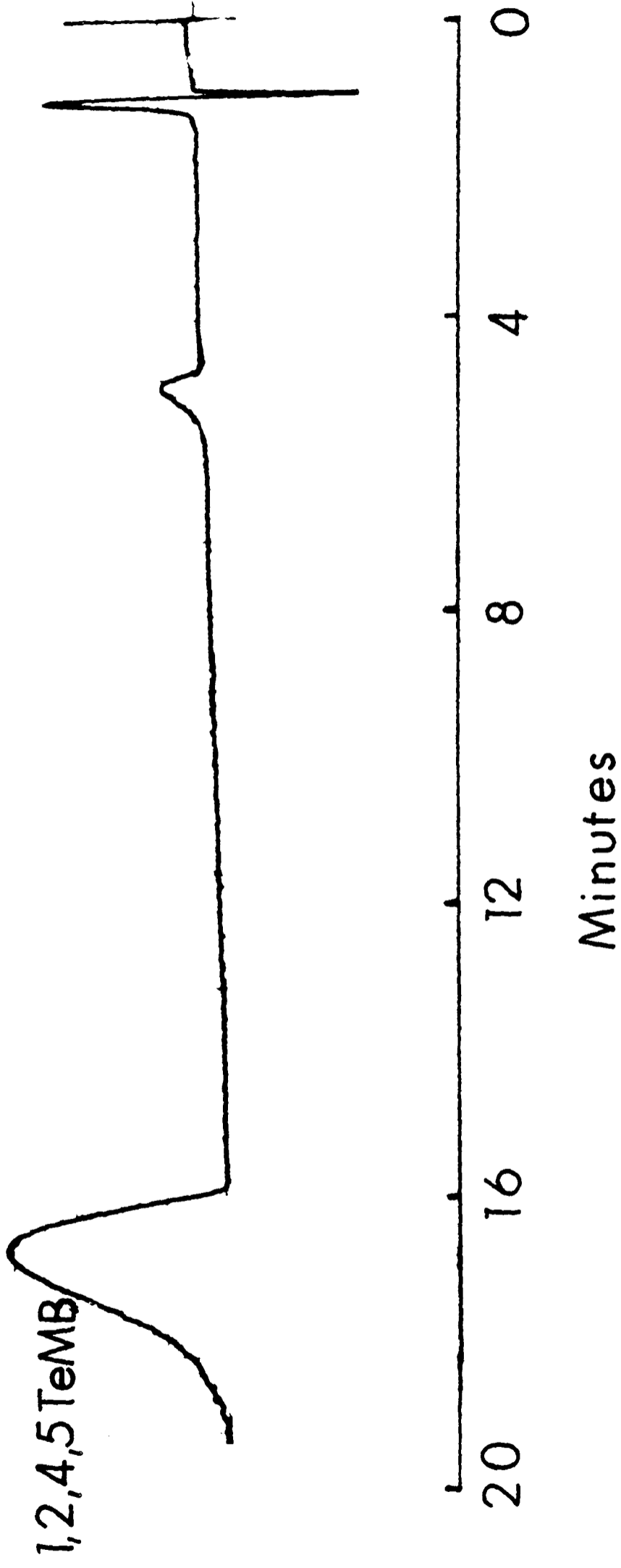
FIG. 8.2-14 : SEPARATION OF 1,2,4,5 TETRAMETHYLBENZENE

PGC   64

Eluent: 95% MeOH/H$_2$O
Flow Rate: 1 ml/min
Solutes:
1. Phenol
2. p-Cresol
3. 3,5 Xylenol
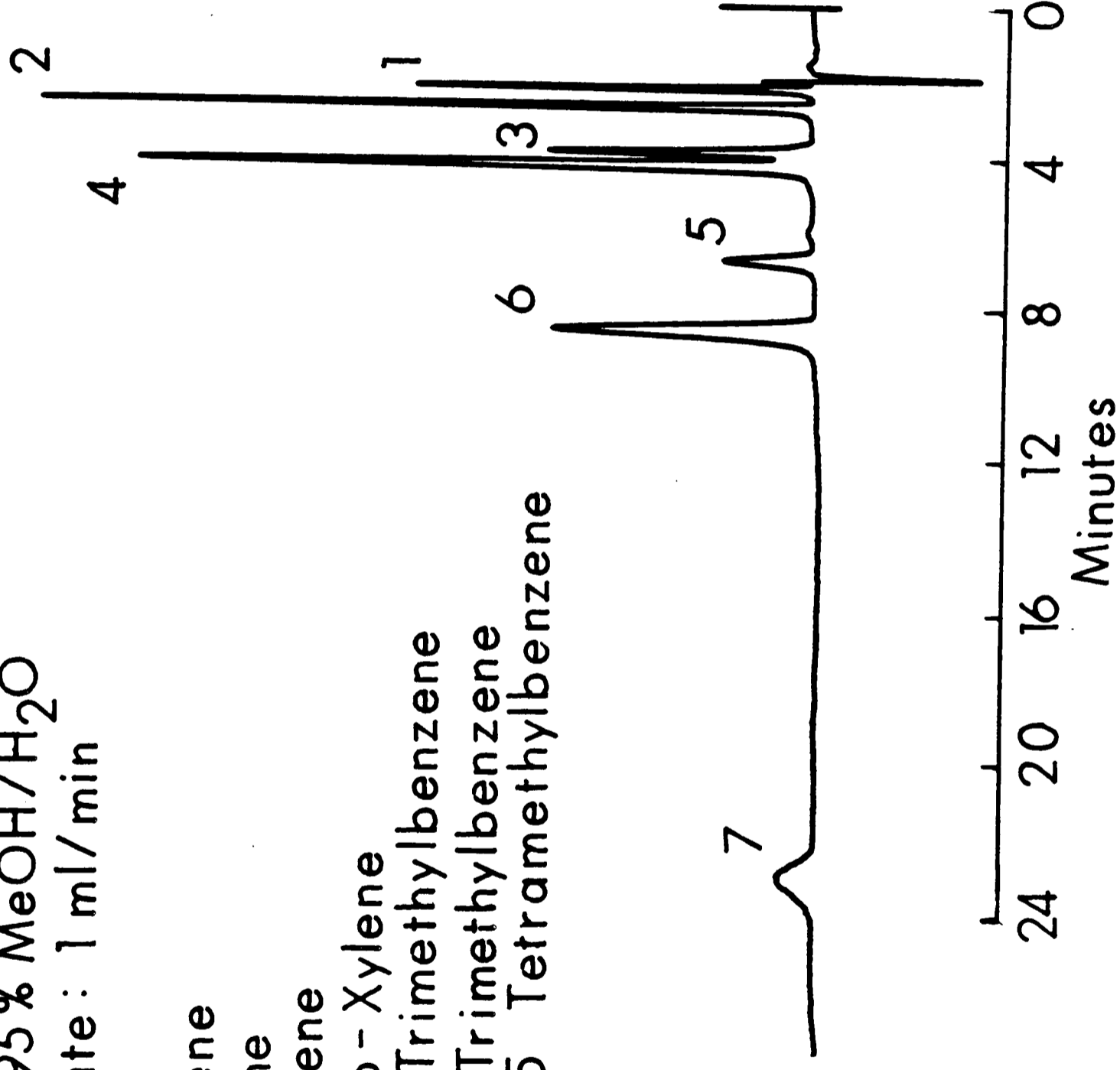4. 2,4,5 Trimethylphenol

Minutes
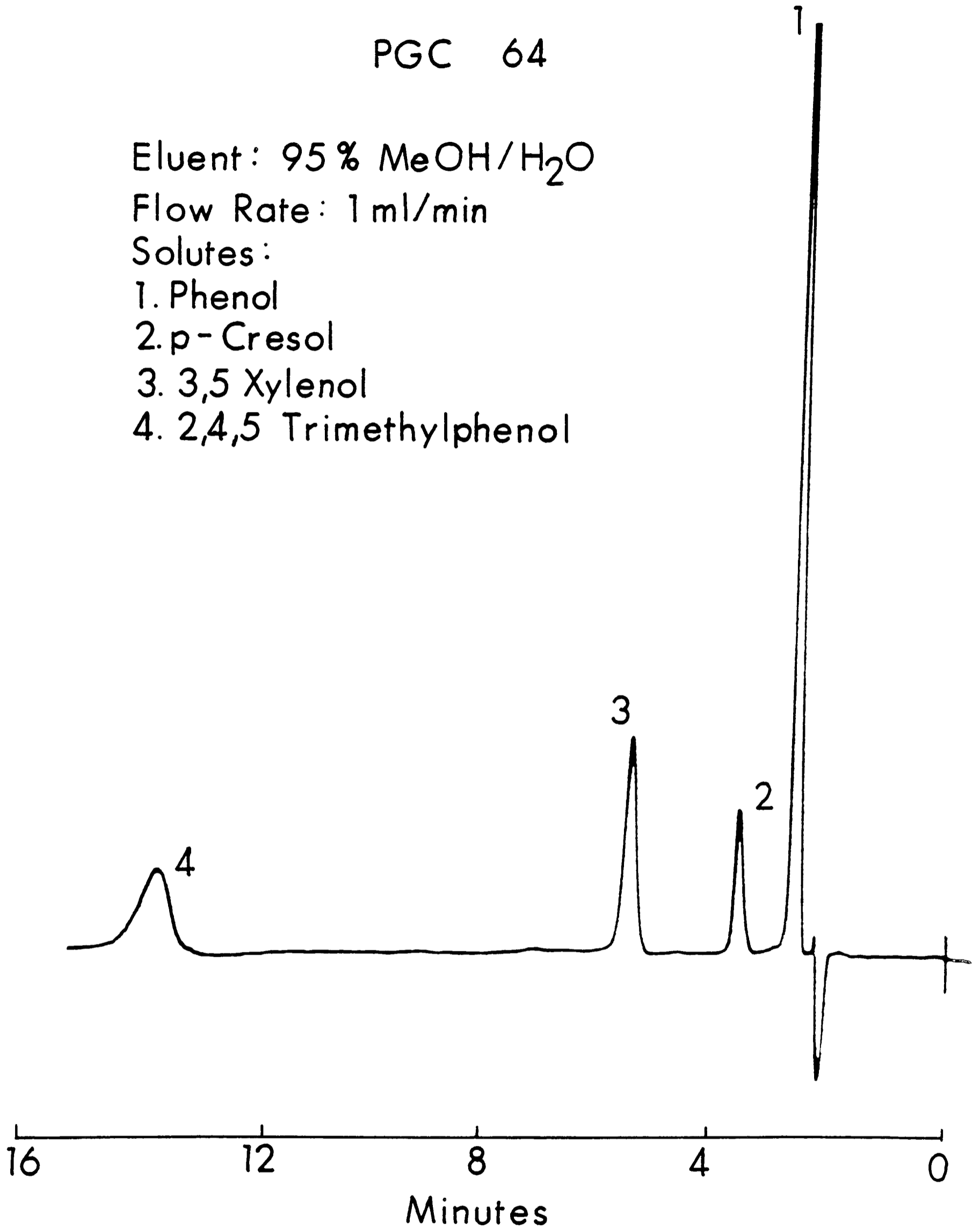
FIG. 8.2-15 : SEPARATION OF POLYMETHYL-
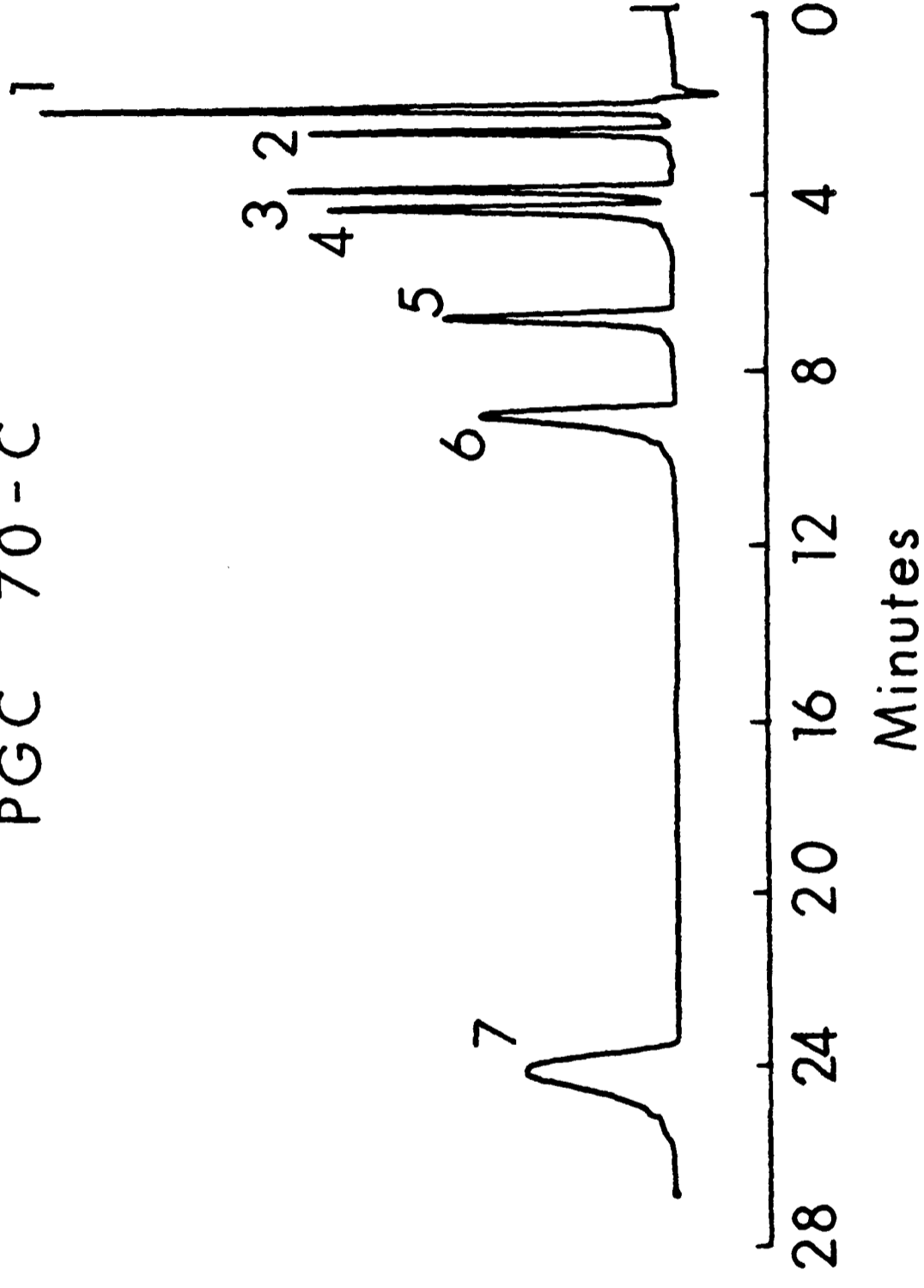PHENOLS

PGC 70-B
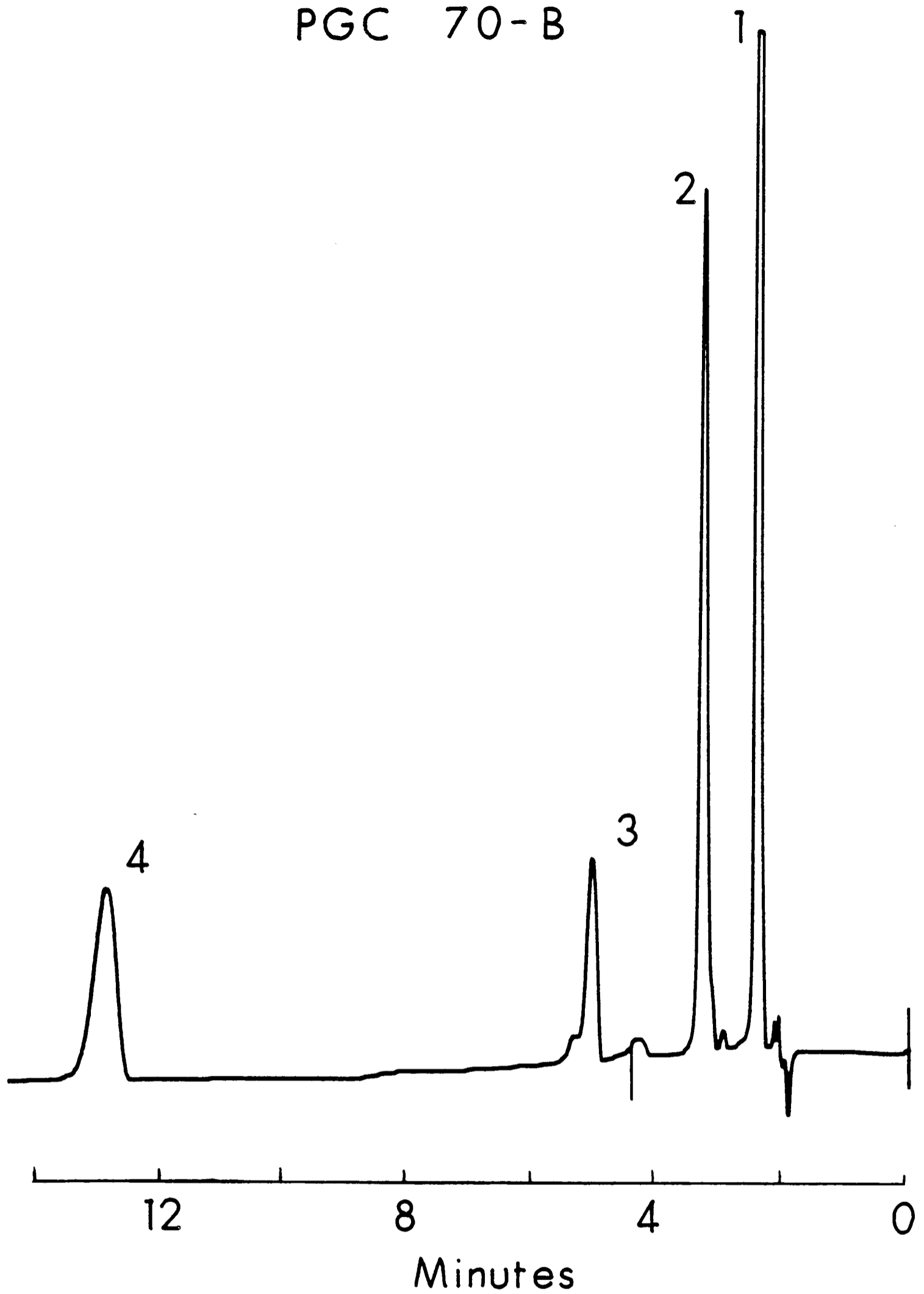
FIG. 8.2-16: SEPARATION OF POLYMETHYL-
PHENOLS. Conditions as in
Fig. 8.2-15

PGC 70-A
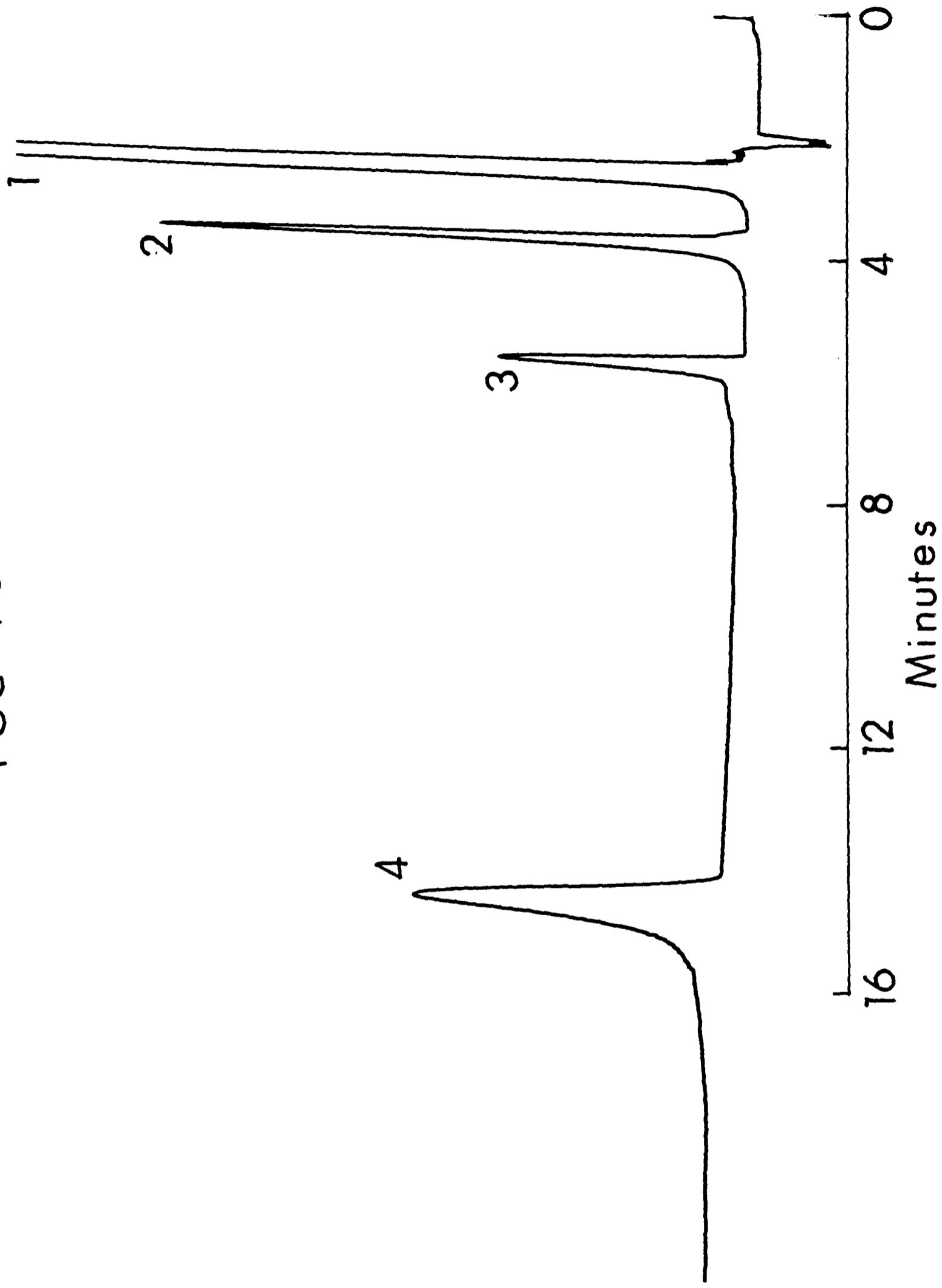
FIG. 8.2-17 : SEPARATION OF POLMETHYLPHENOLS.
Condition as in Fig. 8.2-15

PGC 26

Eluent : MeOH
Flow Rate : 0.5 ml/min
Back Pressure : 1800 psi
Solutes :
1. Phenol
2. p - Cresol
3. 2,4 Xylenol
4. 2,4,5 Trimethyl-
phenol
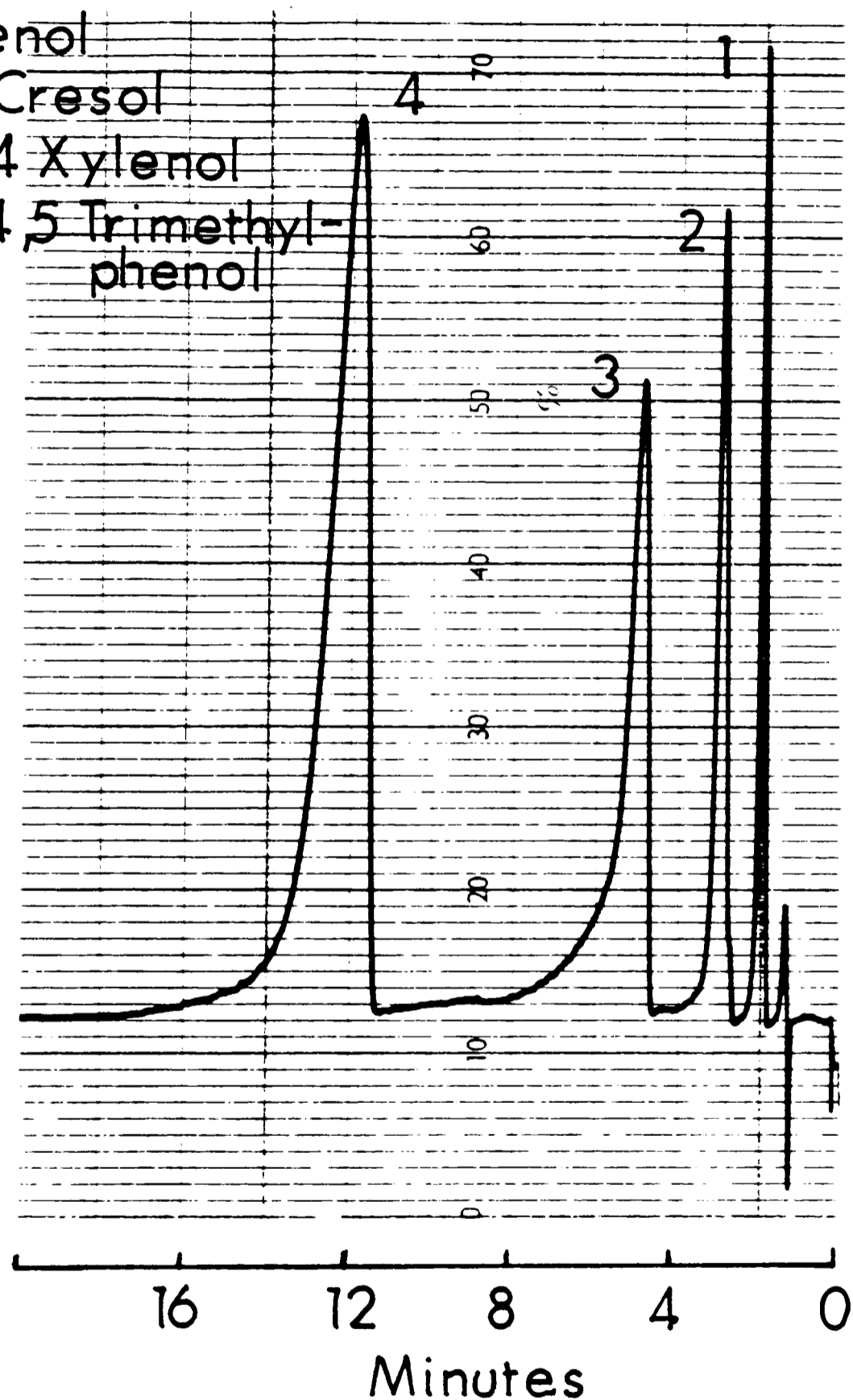
FIG. 8.2-18 : SEPARATION OF POLYMETHYL-
PHENOLS

PGC 64

Eluent: MeOH

Flow Rate: 1ml/min

Solutes:
1. Benzene
2. Ethyl Benzene
3. n-Propyl Benzene
4. n-Butyl Benzene
5. n-Amyl Benzene
6. n-Hexyl Benzene
7. n-Heptyl Benzene
8. n-Octyl Benzene
9. n-Nonyl Benzene
10. n-Decyl Benzene

Minutes
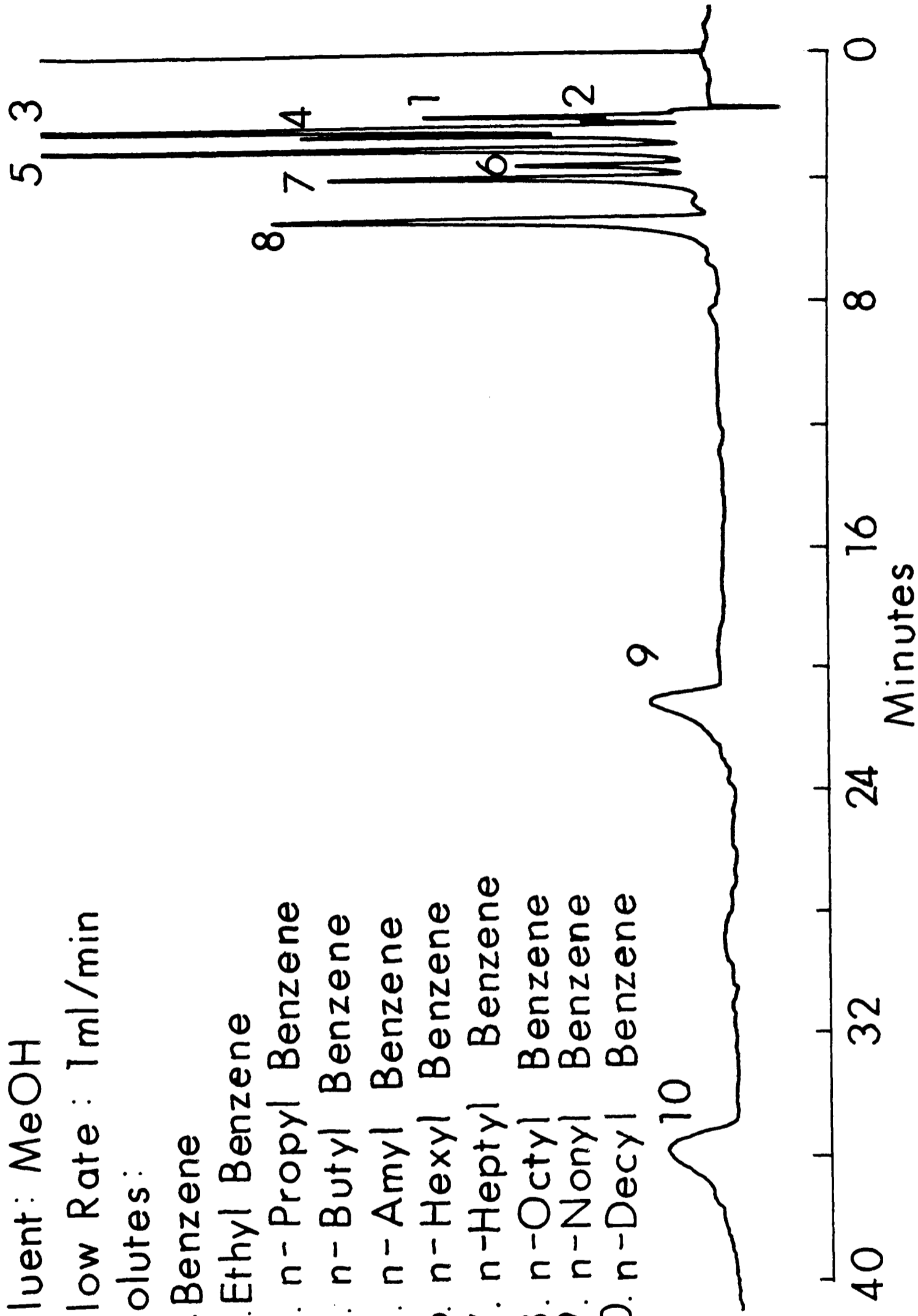
FIG. 8.2-19 : SEPARATION OF ALKYLBENZENES

<u>Table 8.2-4</u>   Homolog ue Selectivity

	α (selectivity)		
	Polymethylphenols	Polymethyl Øs	Alkyl Øs
Methanol	0.46	0.55	0.17
Acetonitrile	0.36	0.54	0.17
Ethylacetate	0.25	0.48	0.10
Methyl-terbutyl Ether	0.24	0.45	0.12
THF	0.24	0.46	0.06
DHF	0.24	0.50	0.12
n-Butylchloride	0.16	0.40	0.08
CH_2Cl_2	0.14	0.45	0.09
Chloroform	0.08	0.34	0.04
Dioxan	0.04	0.41	(0.03)
Hexane	-	0.44	0.09

(1) Different selectivity obtained for aromatic and aliphatic substitution.

(2) Very low selectivity is obtained for aliphatic alkyl Øs, acetonitrile giving the best selectivity and Dioxan giving the least selectivity.

(3) In aromatic substitution greater selectivity is obtained for polymethyl Øs than polymethyphenols.

PGC 64

Eluent: 95% MeOH/H₂O
Flow Rate: 1 ml/min
Solutes:
1. 3,5 Xylenol
2. 2,4 Xylenol
3. 2,5 Xylenol
4. 2,3 Xylenol

Minutes
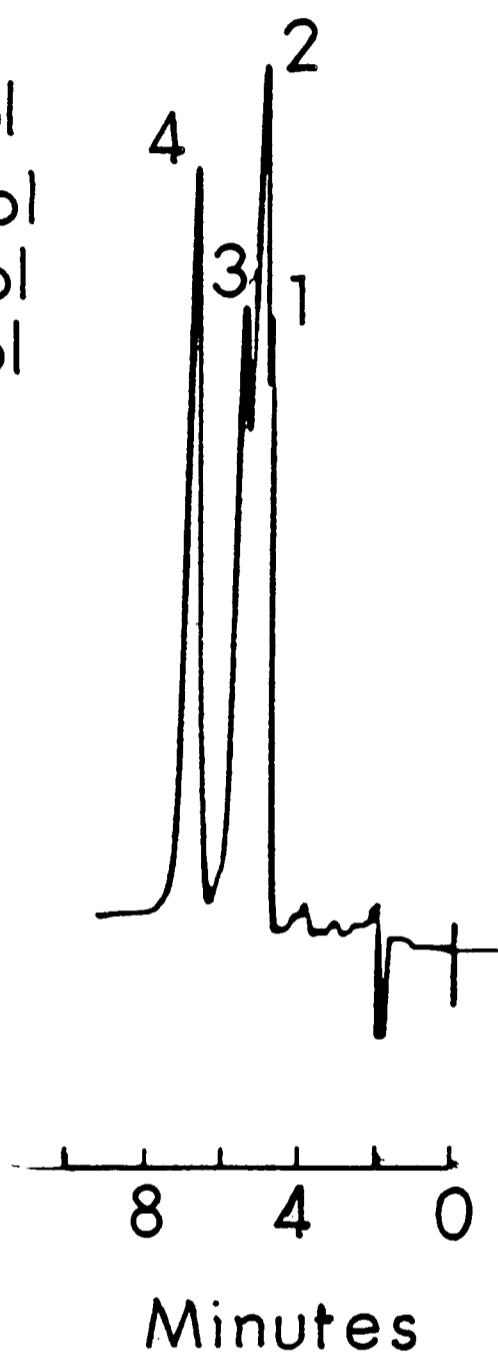
FIG.8.2 – 20: SEPARATION OF
XYLENOLS

PGC 26

Eluent: MeOH /
　　　　m-Terphenyl

Flow Rate: 0.5ml/min

Solutes:

1. p-Xylene
2. m-Xylene
3. o-Xylene

6　　4　　0
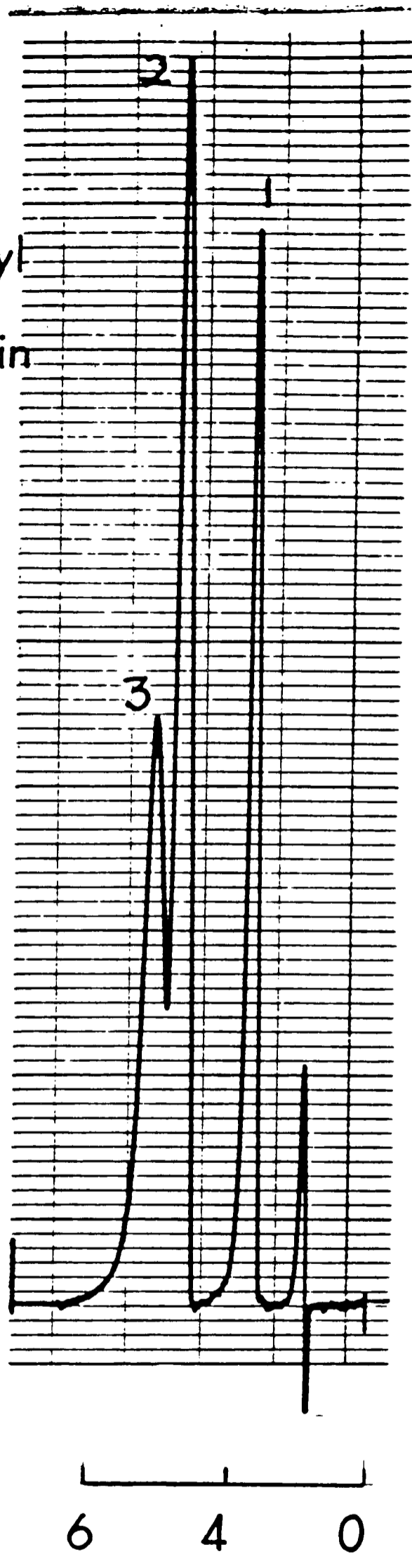
FIG. 8.3 - 21: SEPARATION　OF　XYLENES

MTG - 7d

Eluent : MeOH

Flow Rate : 1 ml /min

Solutes :

1. Toluene

2. o - Nitrotoluene

3. p - Nitrotoluene
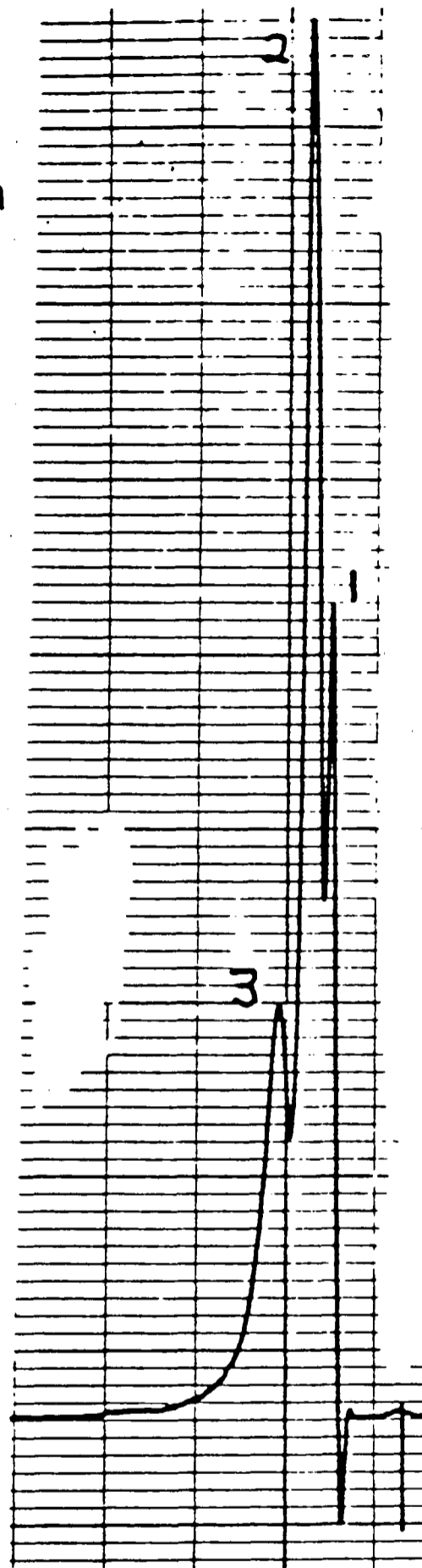
6 4 2 0

Minutes

FIG. 8.3 - 22 : SEPARATION OF o - AND p - NITROTOLUENE
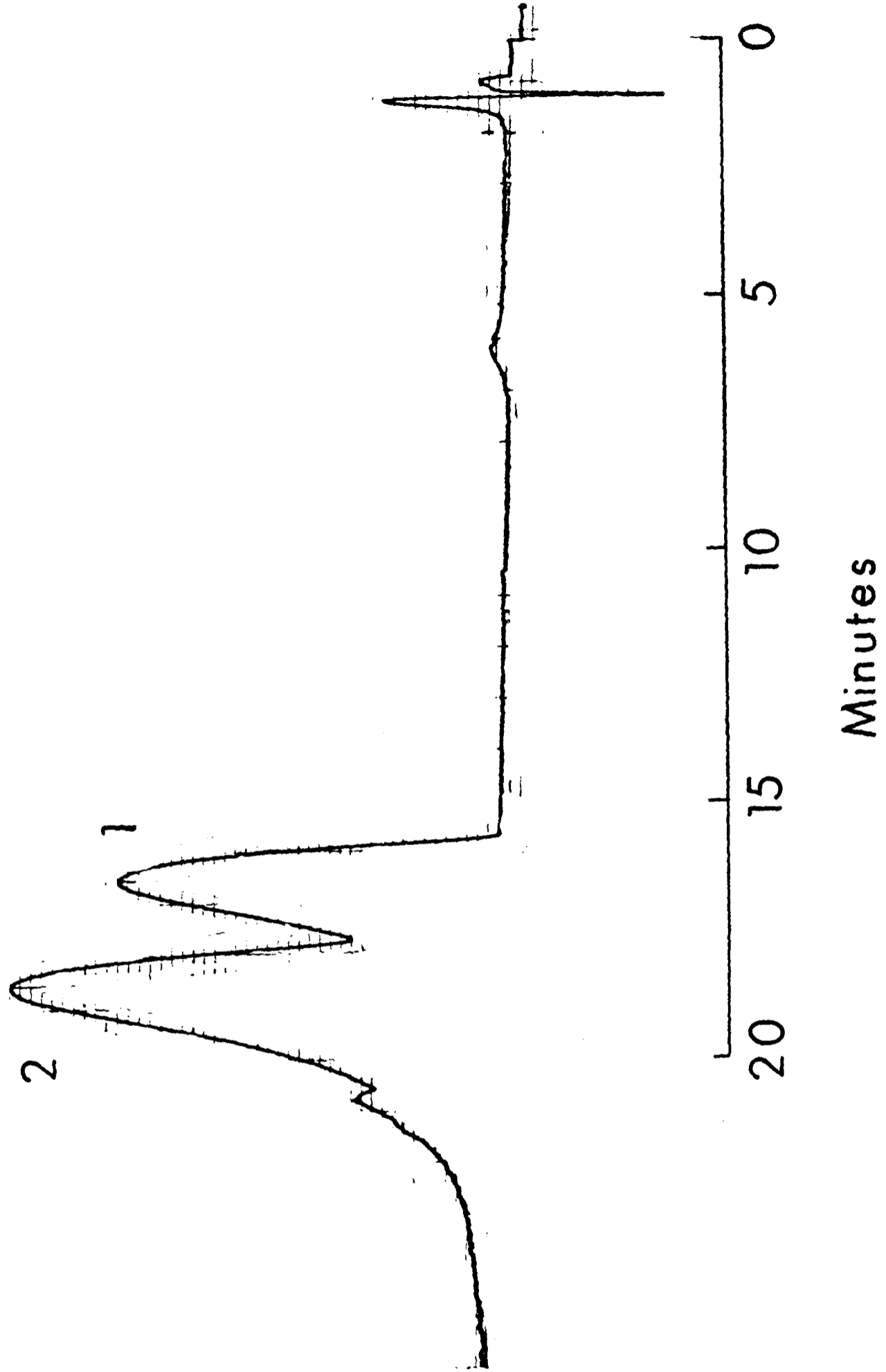
FIG.8.2 - 23 : SEPARATION OF o-NITROANILINE (1)
AND p-NITROANILINE (2)

Table 8.2-5 Variation of isomeric selectivity (Is) of polymethylbenzene isomers with different solvents

	Methanol	Aceto-nitrile	CH_2Cl_2	THF	Dimethyl formamide DMF	Ethyl acetate	Chloroform	Dioxan	Methyl ter-Butyl ether	n-Butyl chloride	Hexane
1. o+p-xylene m-xylene	1.19	1.05	1.33	1.56	1.25	1.18	1.05	1.06	1.21	1.19	1.10
2. 1,2,4-TMB[a] 1,3,5-TMB[a]	1.51	1.38	1.38	1.58	1.32	1.35	1.23	1.12	1.48	1.35	1.48
3. 1,2,3,4-TeMB[b] 1,2,4,5-TeMB[b]	1.74	1.45	1.45	1.35	1.20	1.38	1.29	1.10	0.66	1.45	2.8
4. 2,3-Xylenol 3,5-Xylenol	1.14	1.34	1.14	1.40	1.36	1.30	1.18	1.08	1.27	1.06	-

$$I_s = \frac{k' \text{ of isomer 1}}{k' \text{ of isomer 2}}$$

a = trimethylbenzene

b = tetramethylbenzene
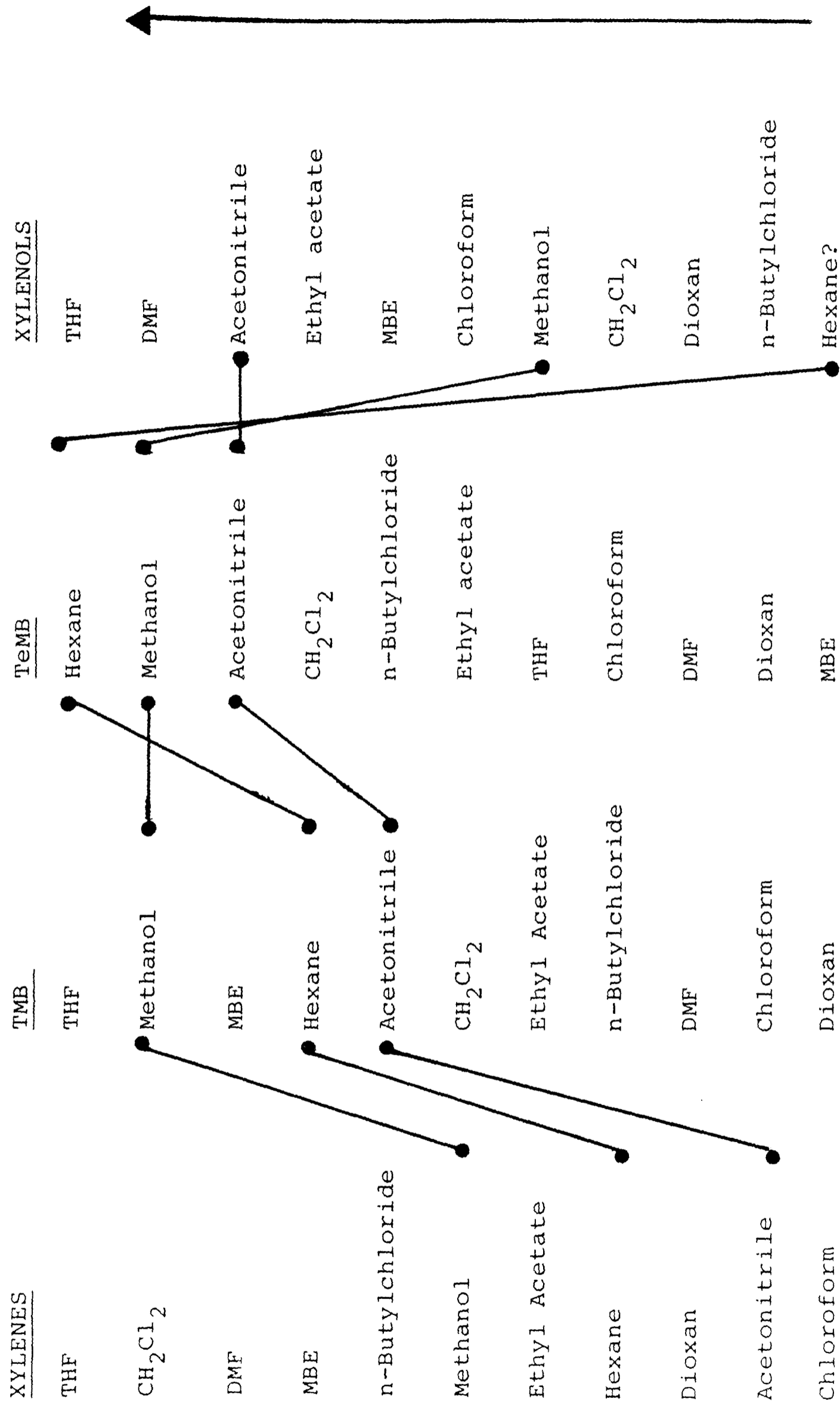
Figure 8.2-24   Isomeric Selectivity Scale for Different Solutes Placed in Decreasing Order of Strength

PGC 64

Eluent : 95 % MeOH/H$_2$O
Flow Rate : 1 ml /min
Solutes :
1. Aniline and Pyridine
2. 2-Methylpyridine
3. Methylaniline
4. Ethylaniline
5. Diethylaniline
6. Benzylaniline

Minutes
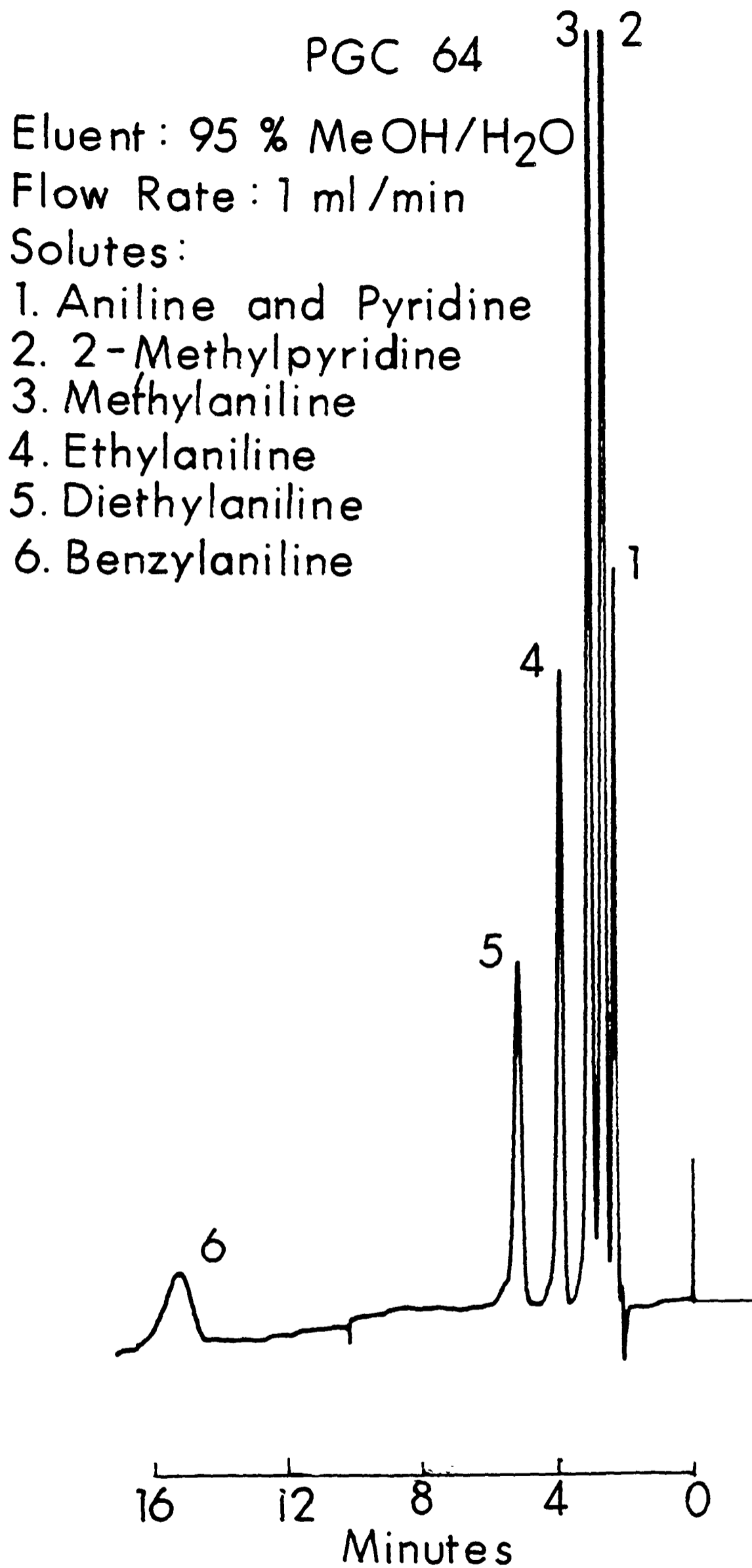
FIG.8.2 – 25 : SEPARATION   OF   AROMATIC
BASES

ODS

Eluent : 70 % MeOH/H_2O
Flow Rate : 1 ml/min
Solutes :
1. Aniline
2. Pyridine
3. Methylaniline and
   2-Methylpyridine
4. Ethylaniline
5. Dimethylaniline
6. Benzylamine
7. Diethylaniline

Minutes
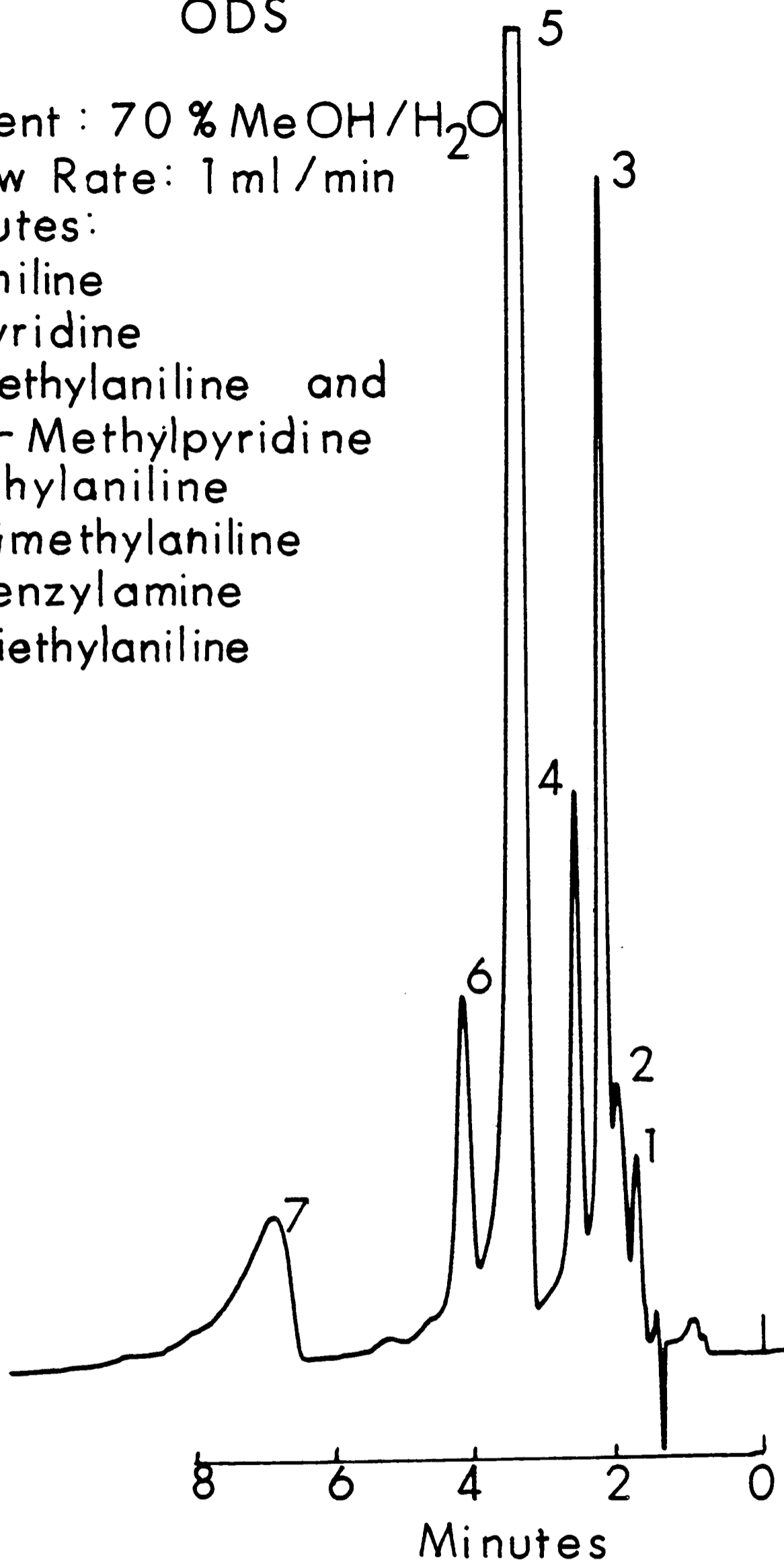
FIG. 8.2-26 : SEPARATION OF
AROMATIC BASES

Eluent : (a) 70 % MeOH / H$_2$O
(b) 90 % MeCN / H$_2$O
(c) 70 % MeOH / H$_2$O

PGC

ODS

(a)

(b)

(c)

4   2   0   6   4   2   0   4   2   0

Minutes
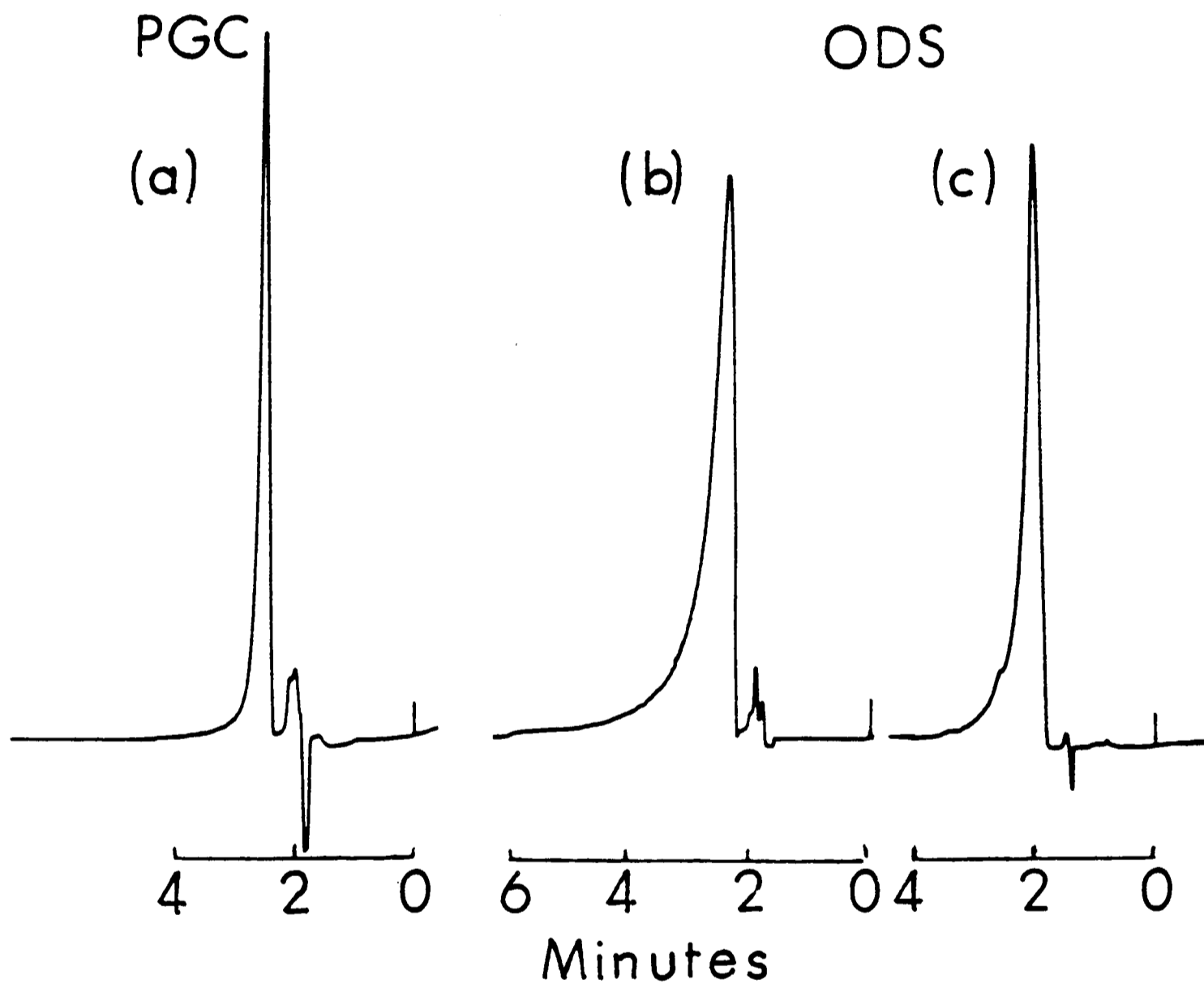
FIG. 8.2 - 27 : SEPARATION OF PYRIDINE
ON CARBON AND ODS

PGC 64

Eluent : (a) MeCN

(b) MeCN/H_2O (95:5)
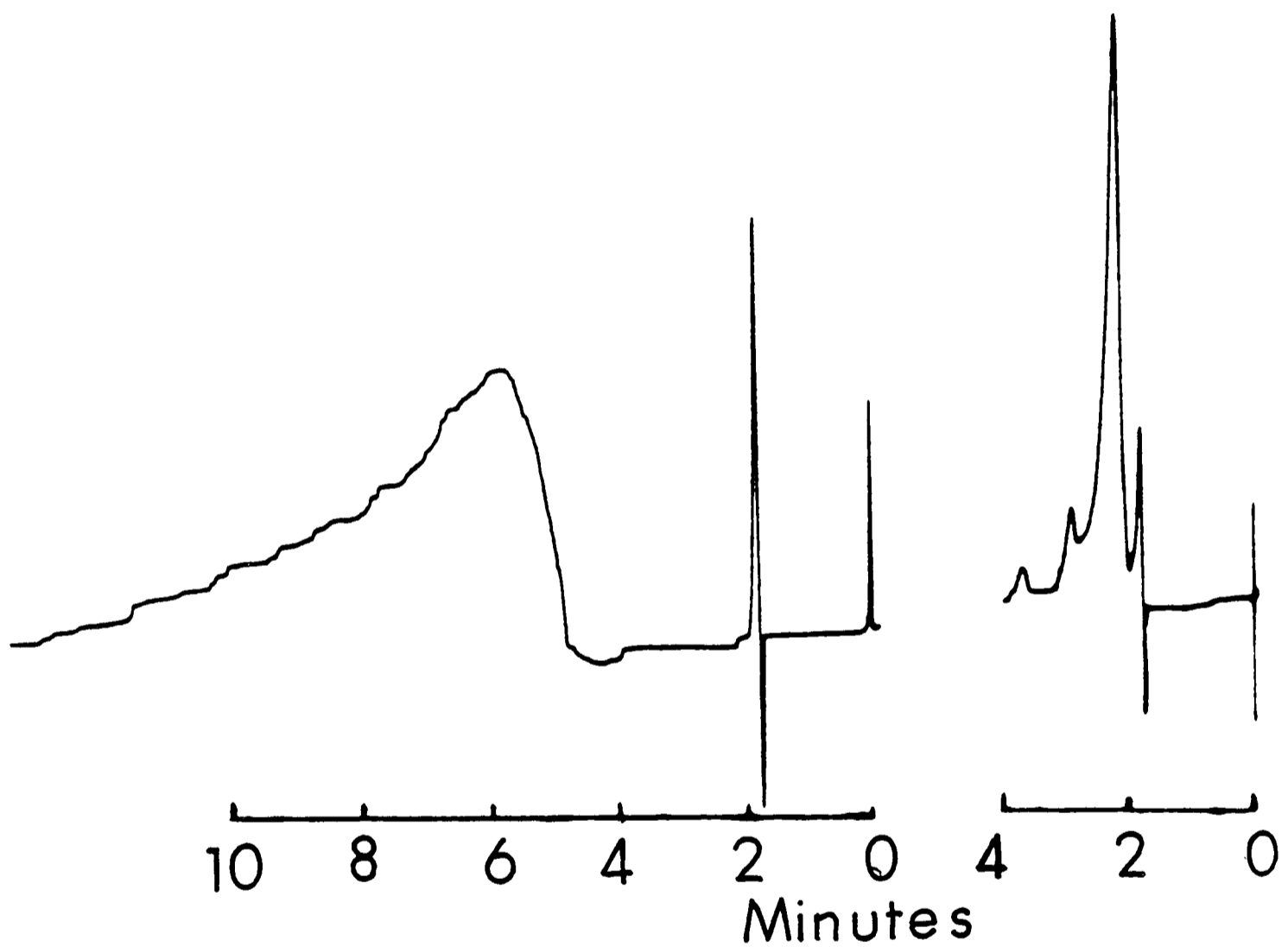
Flow Rate : 1ml/min

FIG.8.2-28: IMPROVEMENT OF PEAK
SHAPE OF PYRIDINE BY
ADDITION OF WATER
AS A MODIFIER

PGC   64

Eluent: (a) MeCN
        (b) MeCN/H$_2$O   (95:5)
Flow Rate : 1 ml / min
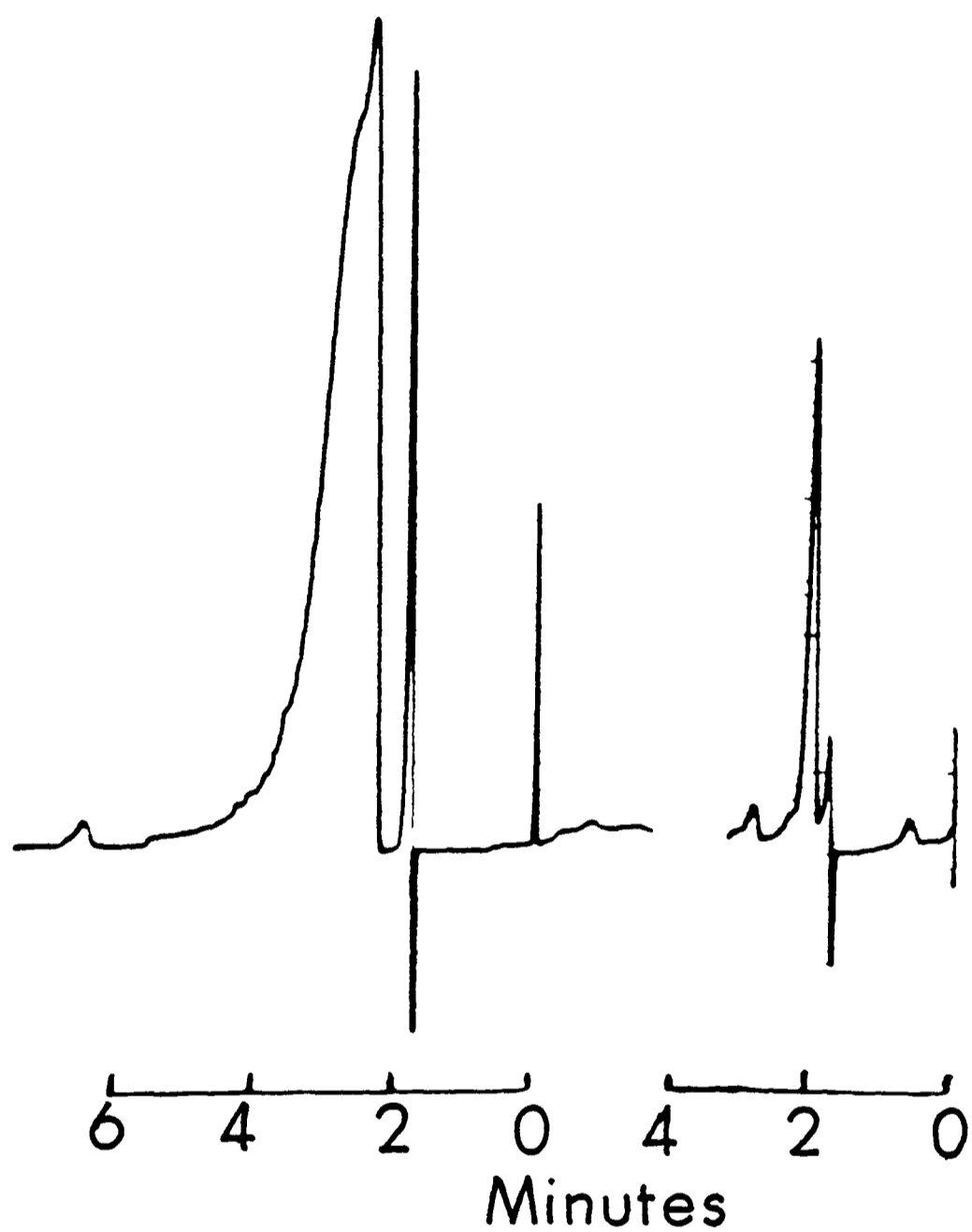
FIG. 8.2 - 29 : IMPROVEMENT OF PEAK
             SHAPE OF ANILINE BY
             ADDITION OF WATER
             AS A MODIFIER

PGC 70-A

Eluent: 95% MeOH/H₂O

Flow Rate: 1 ml/min

Solutes:

1. Pyridine
2. Aniline
3. 2-Methylpyridine
4. Methylaniline and
   Dimethylaniline
5. Ethylaniline
6. Dimethylaniline

Minutes
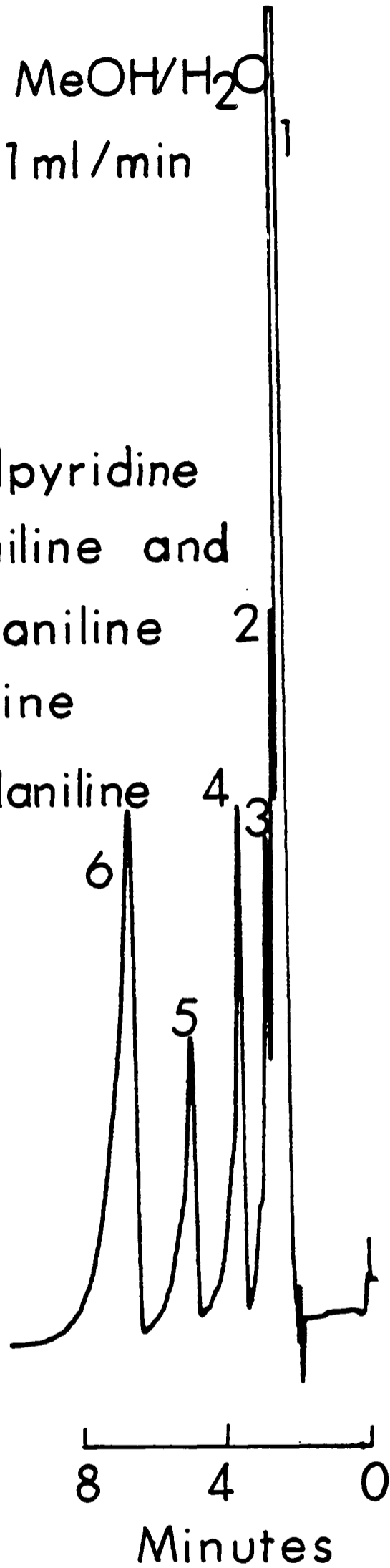
FIG. 8.2-30 : SEPARATION OF
AROMATIC BASES ON A
BAD BATCH OF PGC

Eluent: 90% MeCN/H₂O
Flow Rate: 1 ml/min
Solutes:

1. Benzoic Acid
2. o-Toluic Acid
3. Salicyclic Acid
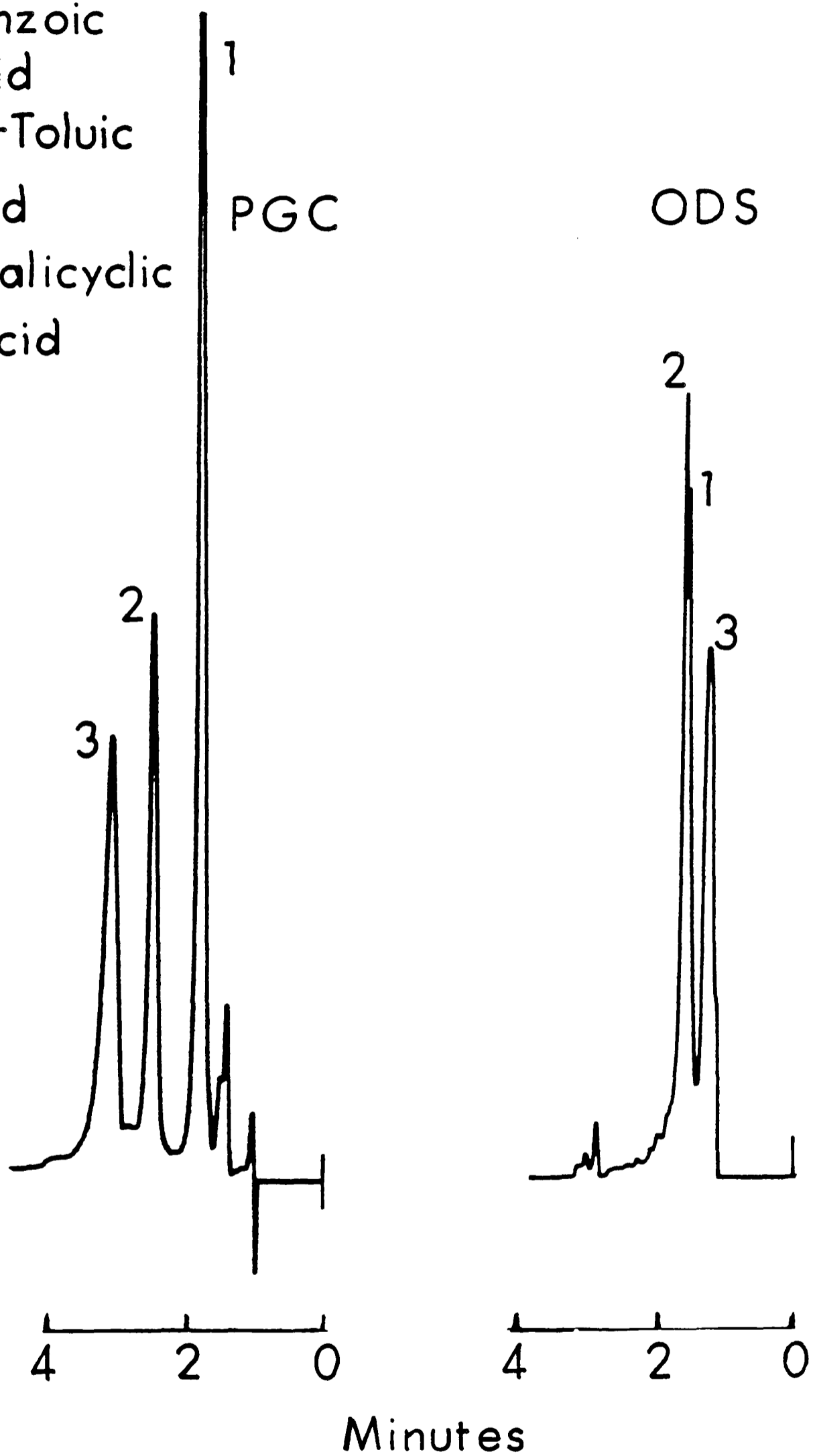
FIG.8.2-31: SEPARATION OF ACIDS

PGC 64

Eluent: MeCN
Flow Rate: 1 ml/min
Solutes:

1. Dimethylphthalate
2. Diethylphthalate
3. Di-n-Butyl-
   phthalate
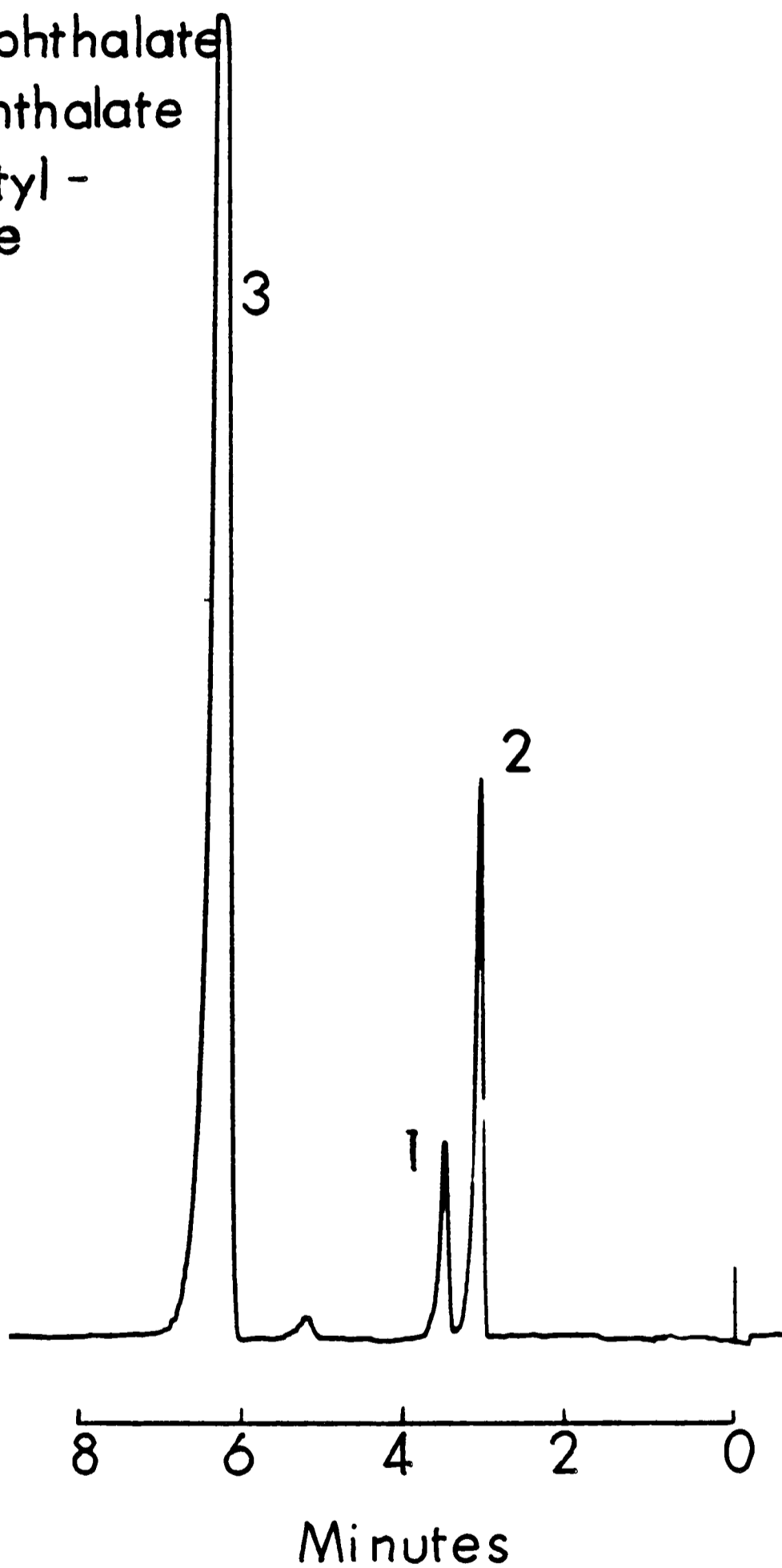
FIG. 8.2 - 32 : SEPARATION OF PHTHALATES

ODS

Eluent : 90 % MeCN/H$_2$O
Flow Rate : 1 ml/min
Solutes :
1. Dimethylphthalate
2. Diethylphthalate
3. Di-n-Butylphthalate
4. Di-n-Nonylphthalate
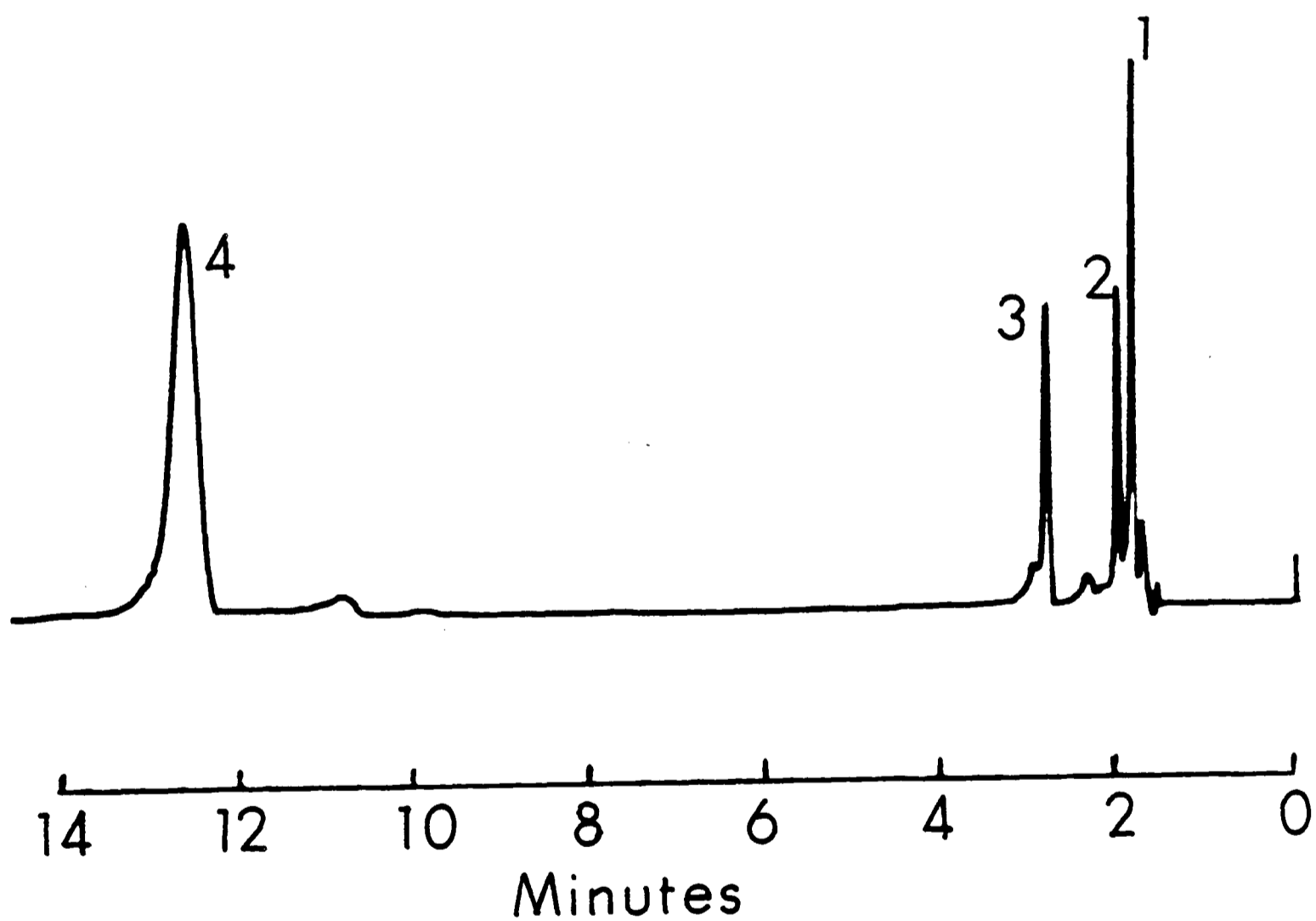
FIG. 8.2-33 : SEPARATION OF

PHTHALATES

ODS

Eluent: 70% MeOH/ H_2O
Flow Rate: 1ml/min
Solutes: as in Fig. 8.2 - 32
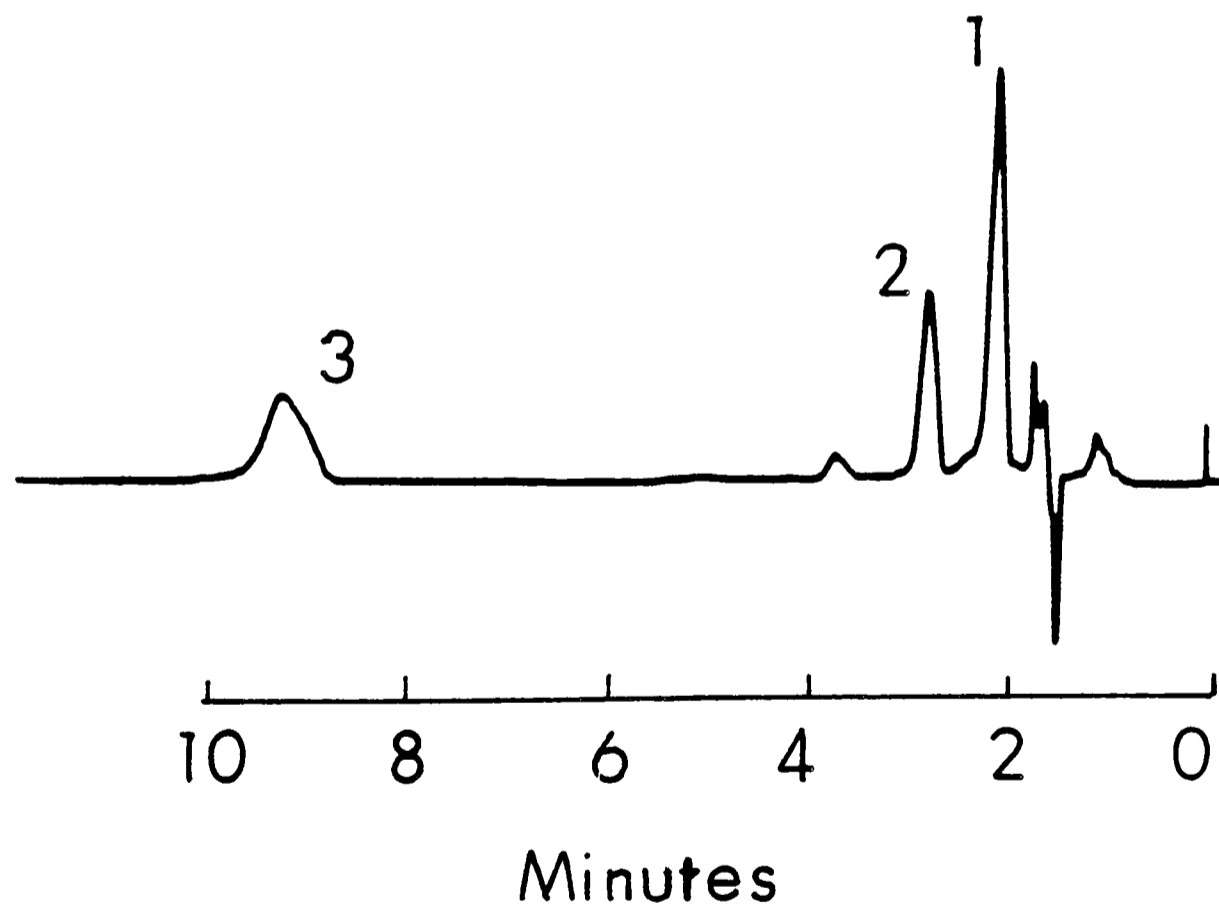
FIG. 8.2 - 34: SEPARATION OF

PHTHALATES

PGC 64

Eluent : MeOH

Flow Rate : 1 ml / min

Solutes :

1. Acetophenone
2. Propiophenone
3. Benzophenone
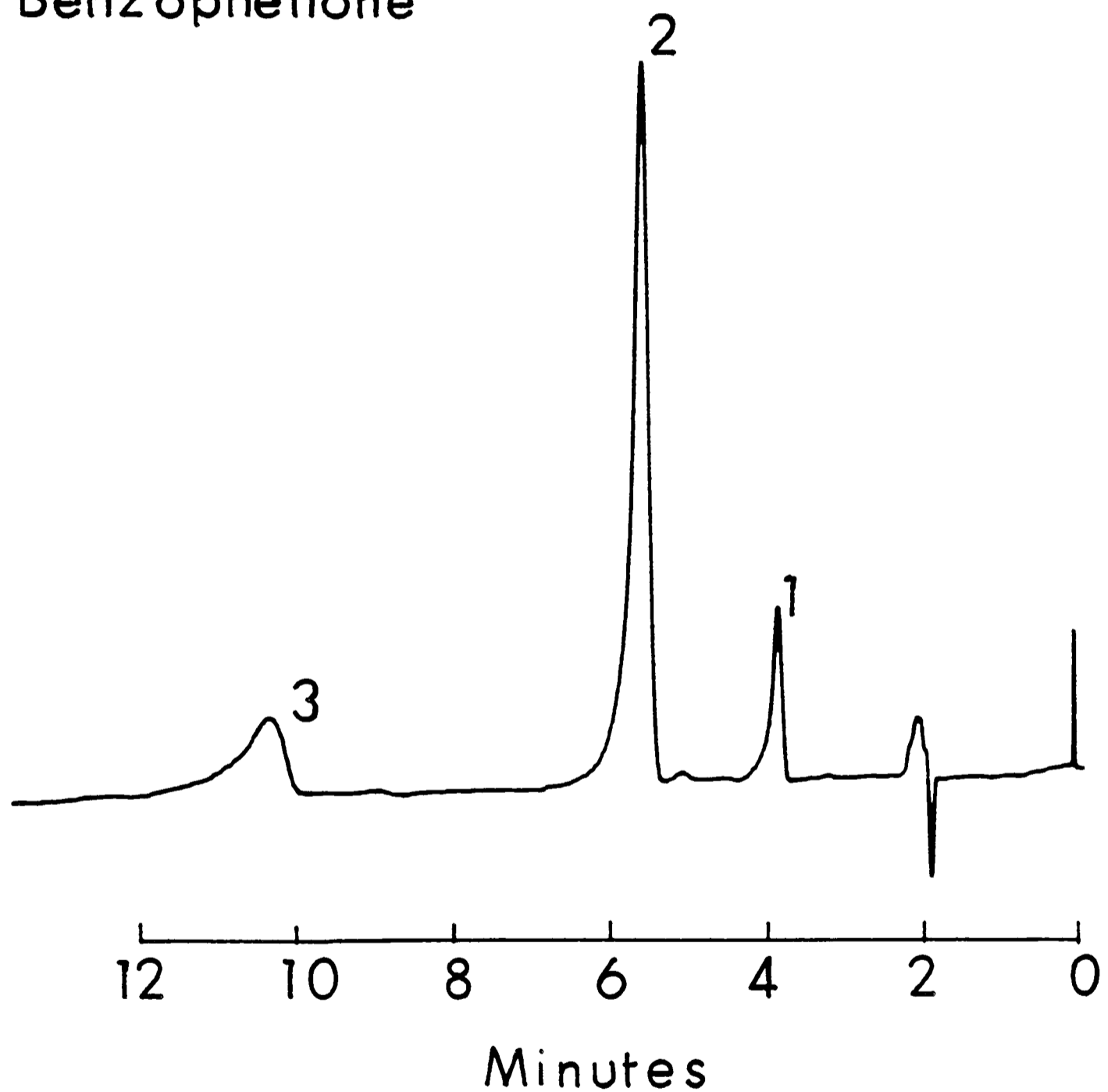
FIG. 8.2 - 35 : SEPARATION OF PHENYL KETONES

PGC 70-C

Eluent: 95% MeOH/H$_2$O
Flow Rate: 1 ml/min
Solutes: as in Fig.8.2-35

2

1

3

16   12   8   4   0

Minutes
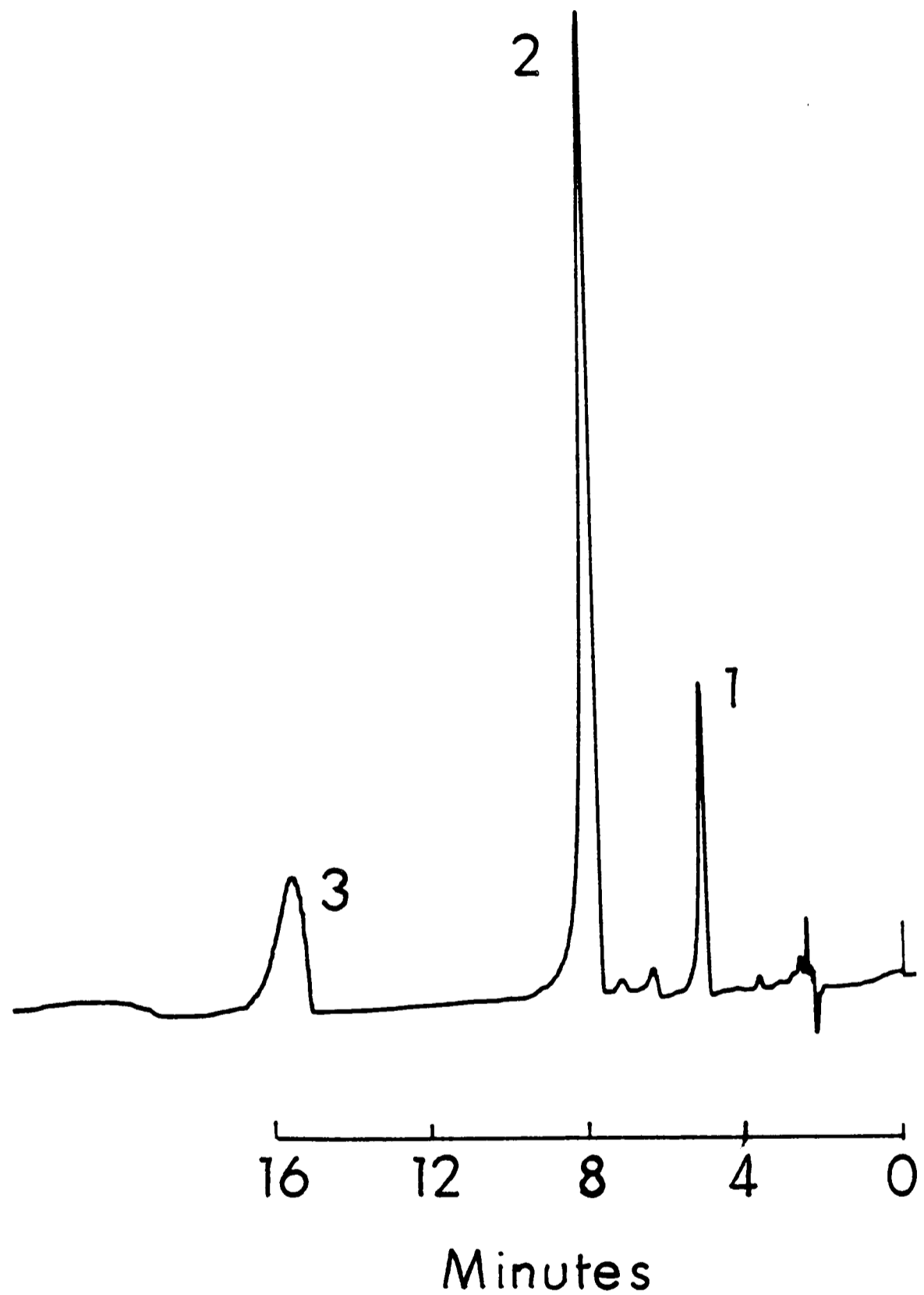
FIG.8.2-36: SEPARATION OF
PHENYL KETONES

PGC 64

Eluent: MeCN

Flow Rate : 3.5 ml/min

Solutes:

1. Tetrahydronaphthalene
2. Naphthalene
3. o-Terphenyl
4. Acenaphthene
5. Fluorene
6. Anthracene
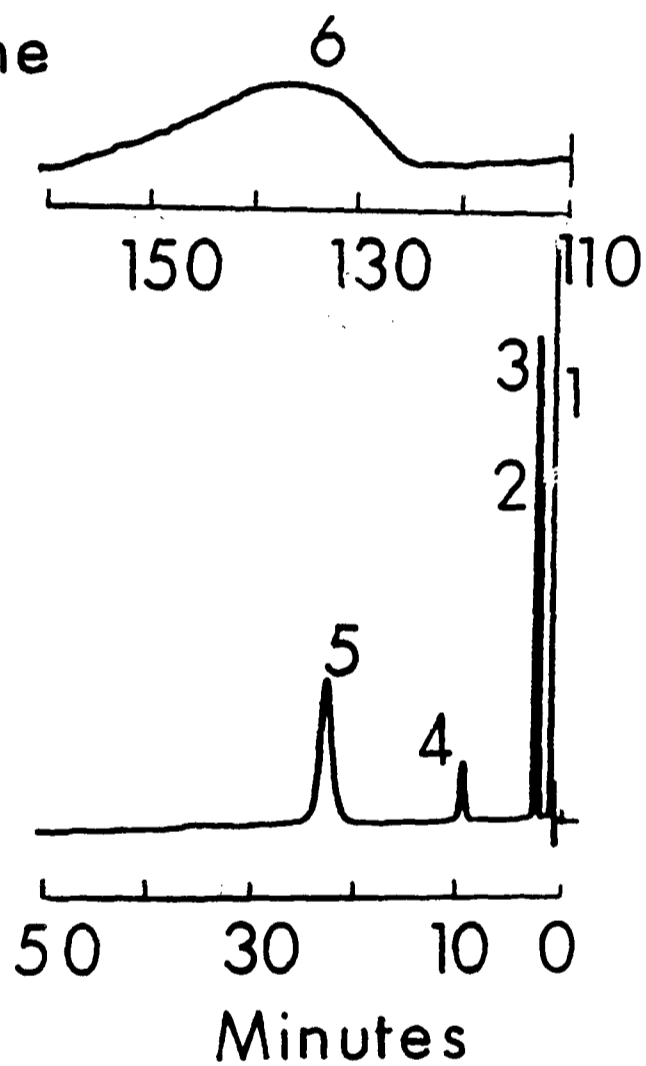
FIG. 8.2-37: SEPARATION OF POLYAROMATIC HYDRO-CARBONS

PGC   70-A

Eluent : MeCN
Flow Rate : 1ml/min
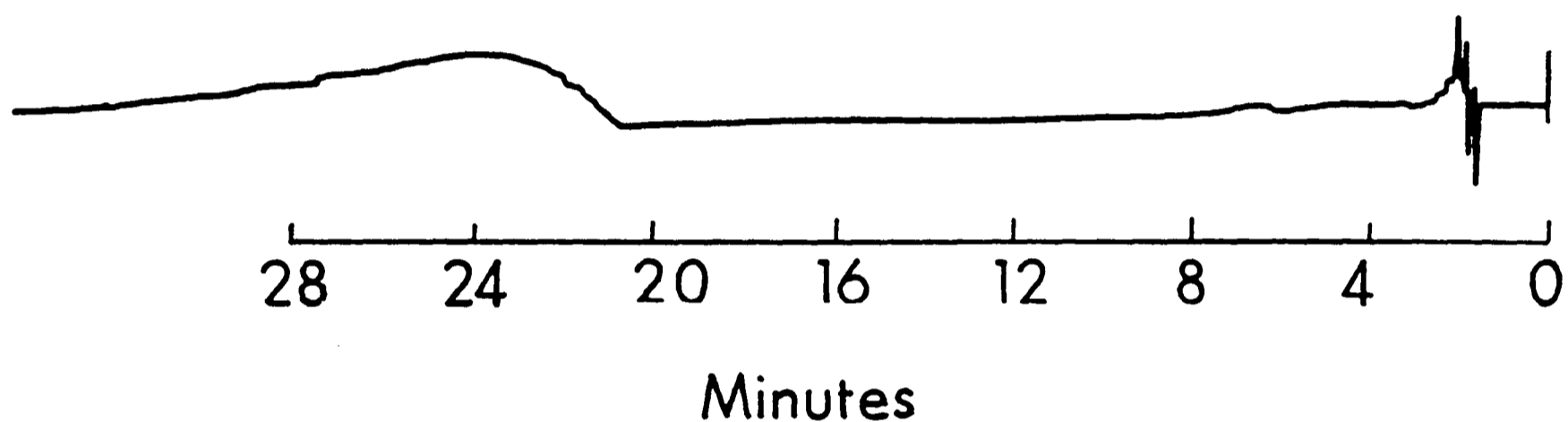
FIG. 8.2 - 38 : SEPARATION   OF   NAPHTHALENE
ON   A   BAD   BATCH   OF
PGC

Table 8.2-6   Comparative retention data of some solutes on PGC 64 and an earlier batch of PGC (PGC 26)

Solutes	CH_2Cl_2 R' PGC		MeOH PGC	
	26	64	26	64
Benzene	0.04	0.03	0.23	0.11
o-xylene	0.20	0.12	2.28	0.85
m-xylene	0.13	0.09	1.84	0.72
phenol	0.16	0.10	0.61	0.22
p-Gesol	0.25	0.36	1.62	0.67
2,3-xylenol	0.42	0.48	3.54	1.78
2,4,5-trimethylphenol	0.66	0.68	10.48	5.11
Aniline	0.14	0.12	-	0.17
Naphthalene	1.74	0.62	15.94	5.49
Acenaphthene	4.73	-	-	-
Nitrobenzene	0.37	0.15	2.48	3.55
Acetophenone	0.18	0.08	2.61	1.01
Benzophenone	0.75	0.24	-	4.58
Benzoic Acid	15.60	-	-	-
Methyl Benzoate	0.29	0.18	-	1.58
Dimethyl phth.	0.18	-	-	-
Diethyl phth.	0.05	-	-	-
Dibutyl phth.	0.03	-	-	-
1,2,4,5-TeMB	-	0.41	15.30	7.08
Anisole	0.10	0.07	1.23	0.44

SA   PGC 26:   382 m^2g^{-1}

64:   150 m^2g^{-1}

Table 8.2-7   Peak shape study of different solutes in different solvents

	MeOH	ACN	CH_2Cl_2	THF	DMF	Ethyl Acetate	n-Butyl chloride	Methyl t-butyl ether	Dioxan	Chloroform	Hexane
Homologous Series											
Substituted benzenes	1	1	1	1[m]	2	1	2	3	2	2	2
Substituted phenols	1	1	1	1	1	1	3	2	2	2	3
Bases	2	3[a]	2[k]	1[c]	1[i]	1[e]	1[f]	1[g]	3[h]	2	3[h]
Phthalates	2	1	2	1	1	1	2	2	1	2	3[j]
Aromatics	2	1	2	2	1	1	3	3	2	2	2
Alkyl øs	1	1	1	2	1	1	2	2	1	2	1
Aromatic ketones	1	1	1	1[ℓ]	1	2	2	3	2	1	3[j]
Single Cpds.											
-Cl	1	1	1	1	1	1	1	2	2	1	2
$-NO_2$	1	1	2	1	1	1	1	2	2	1	3
$-CH_2OH$	1	1	1	1	3	1	2	2	2	2	1
$-COOCH_3$	1	1	1	2	1	1	1	2	2	1	2
$-OCH_3$	1	1	1	1	1	1	2	2	2	1	1
Acid	2[n]	3[b]	2	1[d]	3	1	2[o]	3	2[p]	3	3

1 - good; 2 - moderate; 3 - bad

a,b = improvement of peak shapes of both acids + bases on the addition of 5% water

c = good for all bases except Benzylamine

d = good only for benzoic and o-toluic acid and not phthallic acid

e = except for pyridine and benzylamine

i = broad peak only for pyridine, benzylamine

g = except for aniline, pyridine + benzylamine

h = except methyl, ethylaniline   and dimethyl and diethylaniline

j = broad peaks with shoulders

k = bad for pyridine and 2-methyl pyridine

l = bad for benzophenone

m = moderate for hexamethyl Ø

n = Dimerization effect seen, as the traces go up slowly and come down rapidly

o = bad for salicyclic acid

p = bad for phthallic and salicyclic acid.
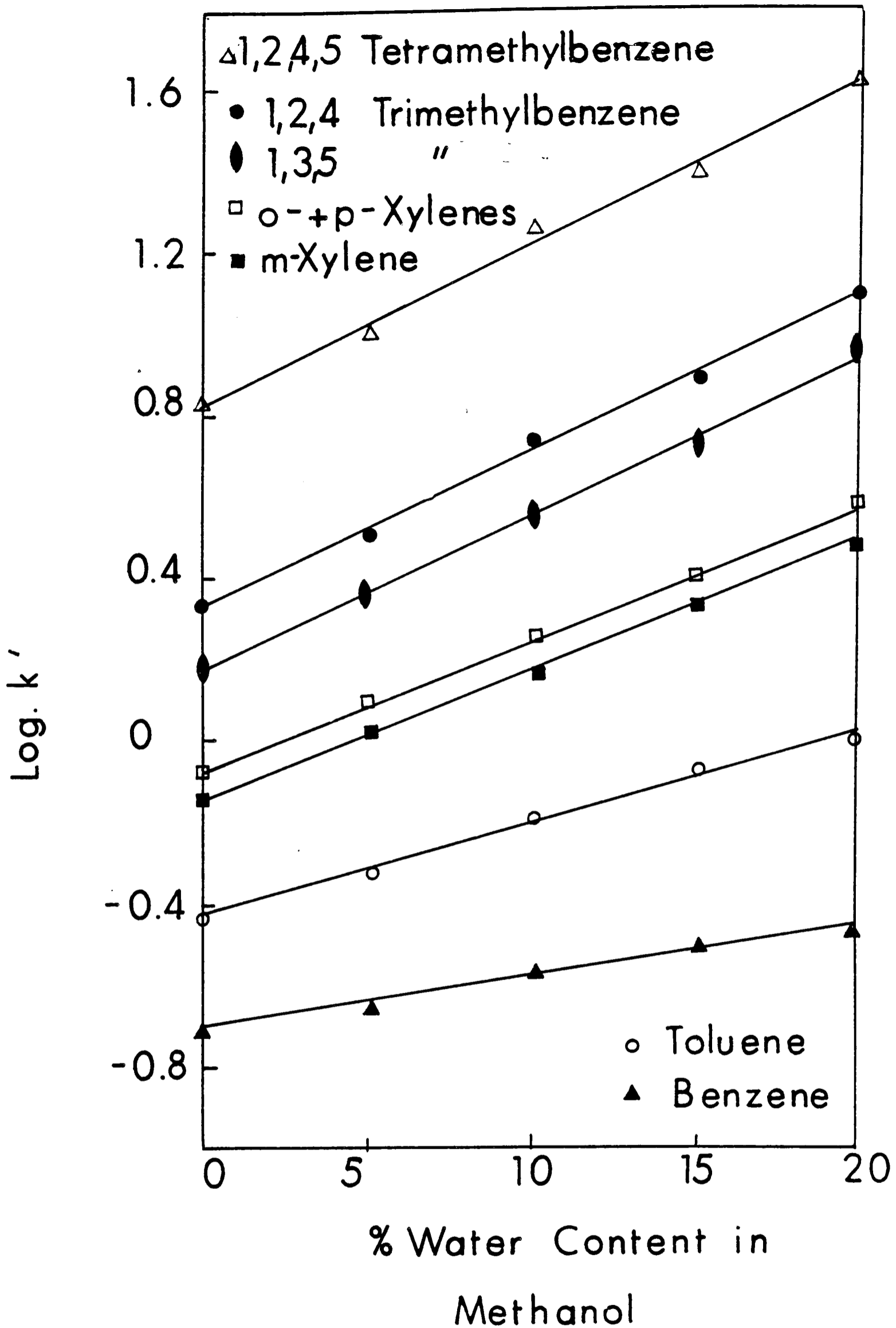
FIG. 8.2-39(a) : VARIATION OF LOG. k'
WITH PERCENTAGE WATER
CONTENT(POLYMETHYLBENZENES)
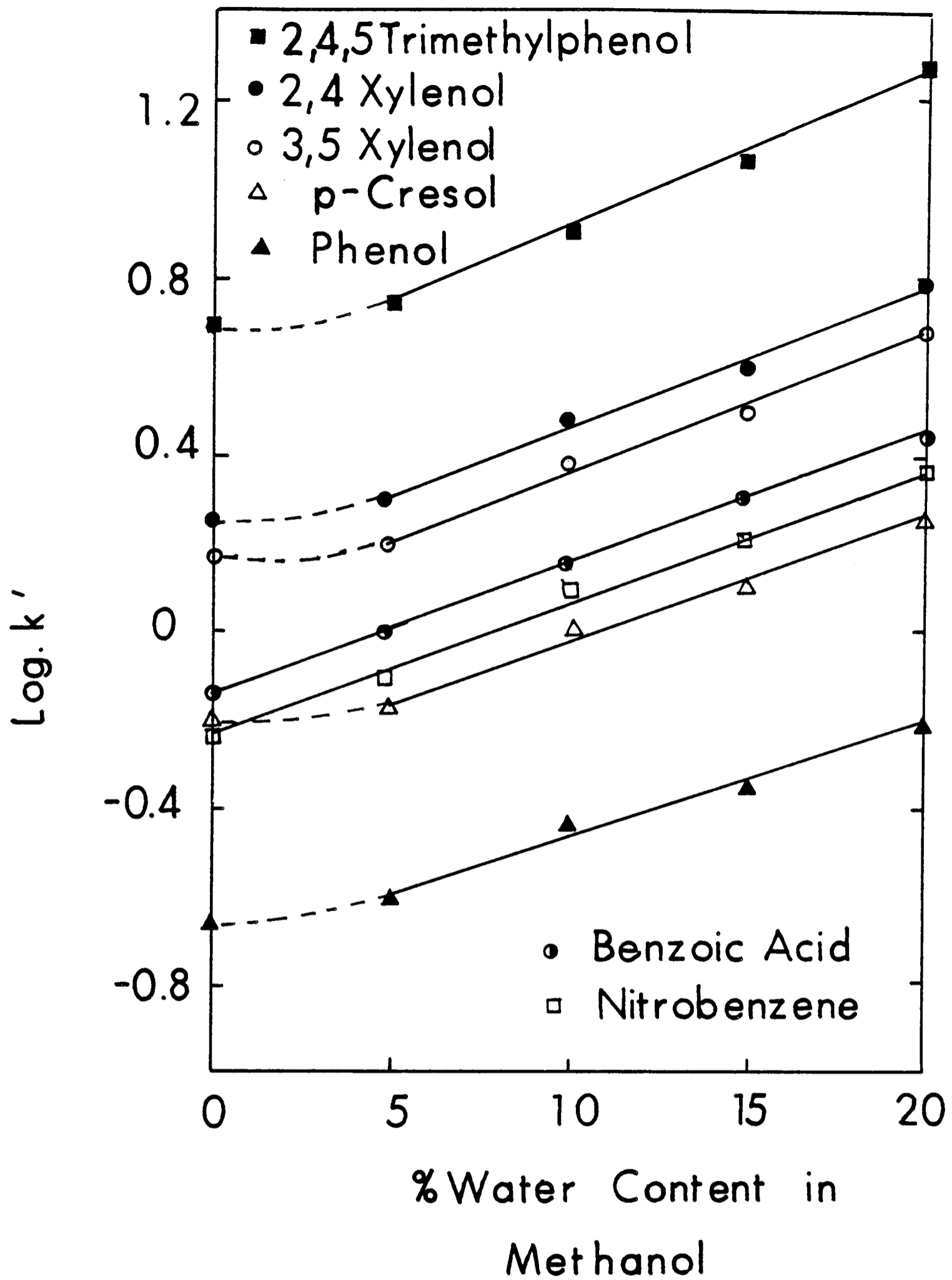
FIG. 8.2-39(b): VARIATION OF LOG. k' WITH PERCENTAGE WATER CONTENT (POLYMETHYLPHENOLS, POLAR SOLUTES)
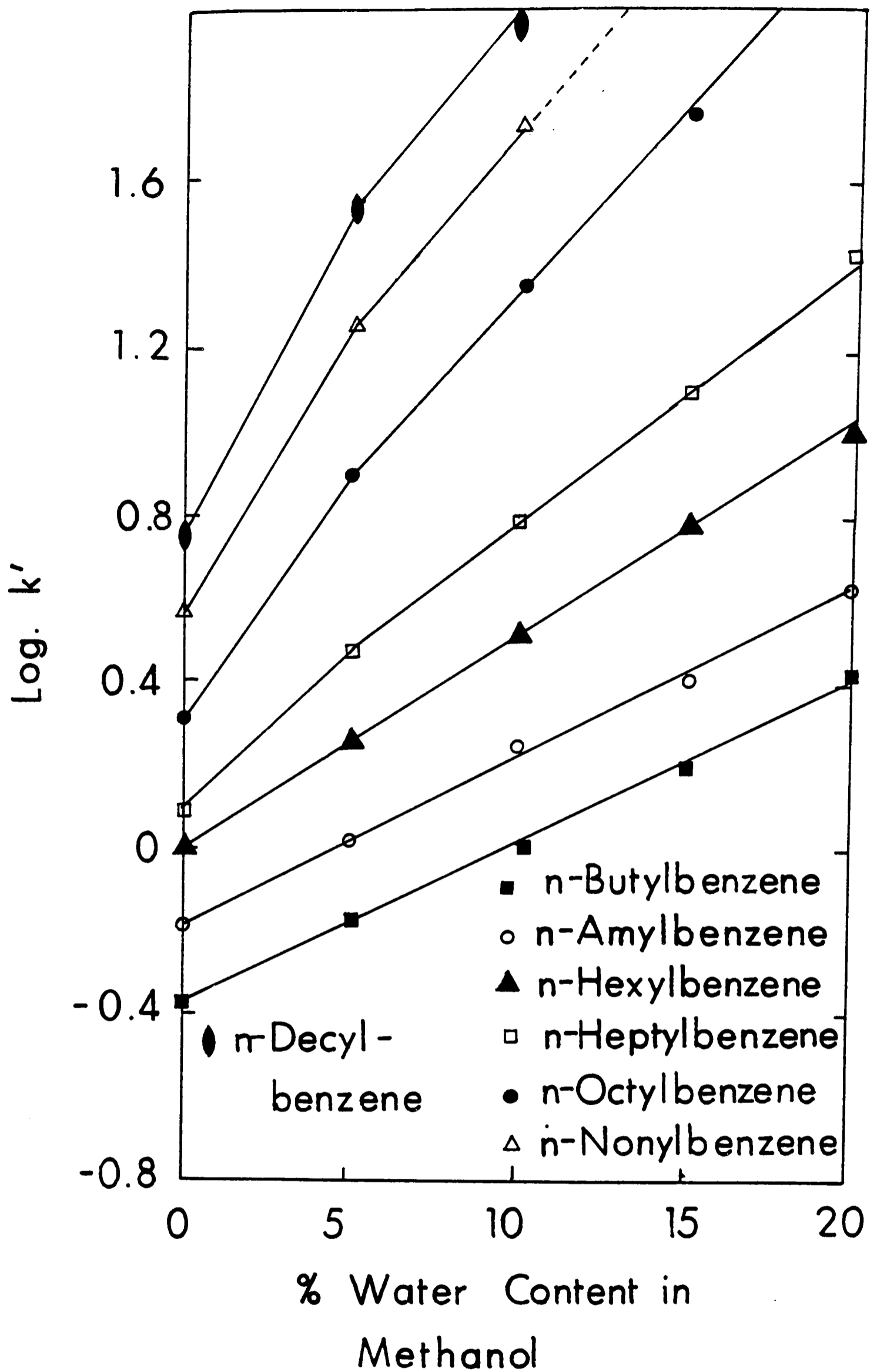
FIG. 8.2 - 39(c): VARIATION OF LOG. k' WITH PERCENTAGE WATER CONTENT (ALKYLBENZENE)
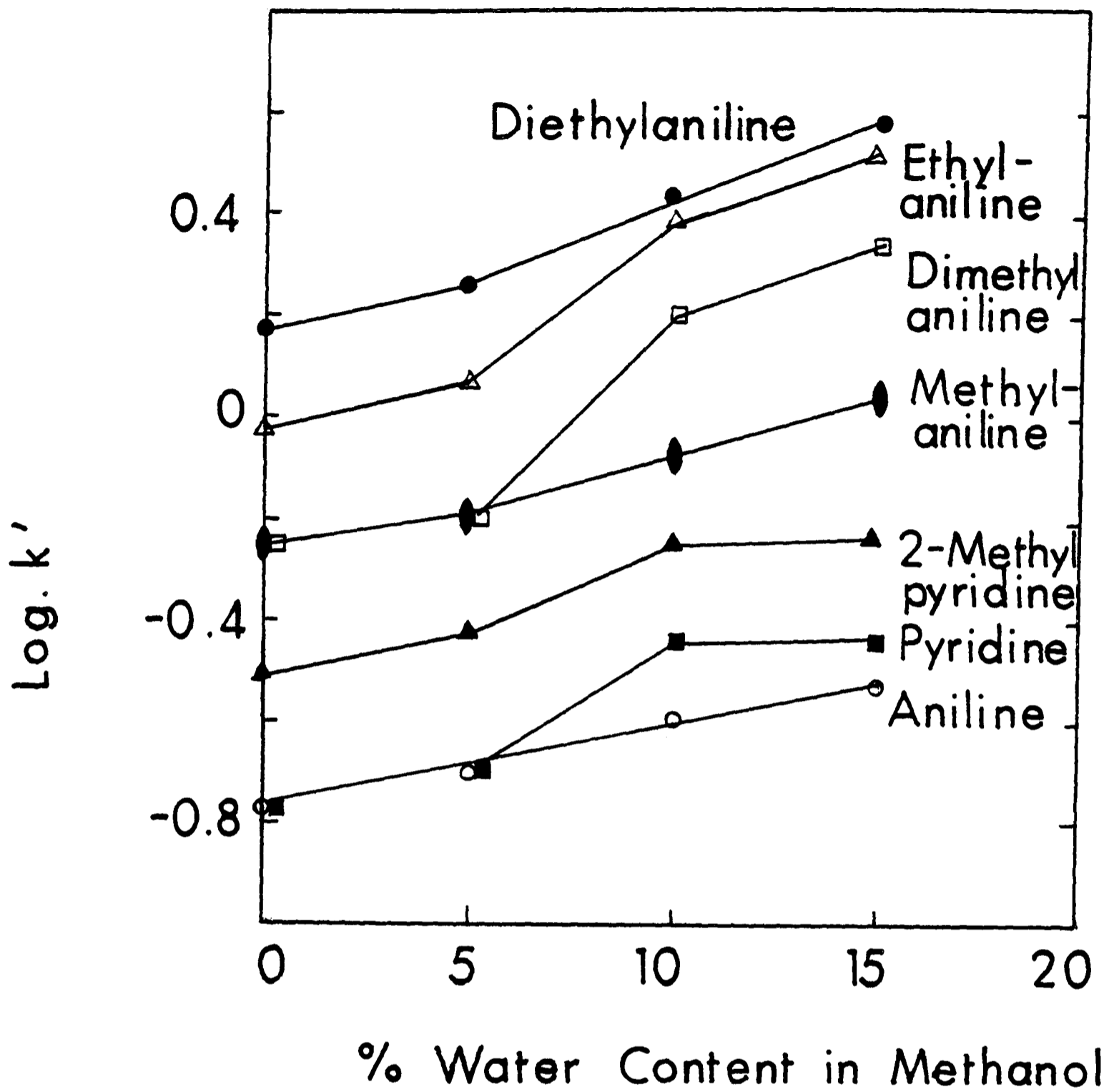
FIG. 8.2-40 : VARIATION OF LOG. k' WITH PERCENTAGE WATER CONTENT (BASES)
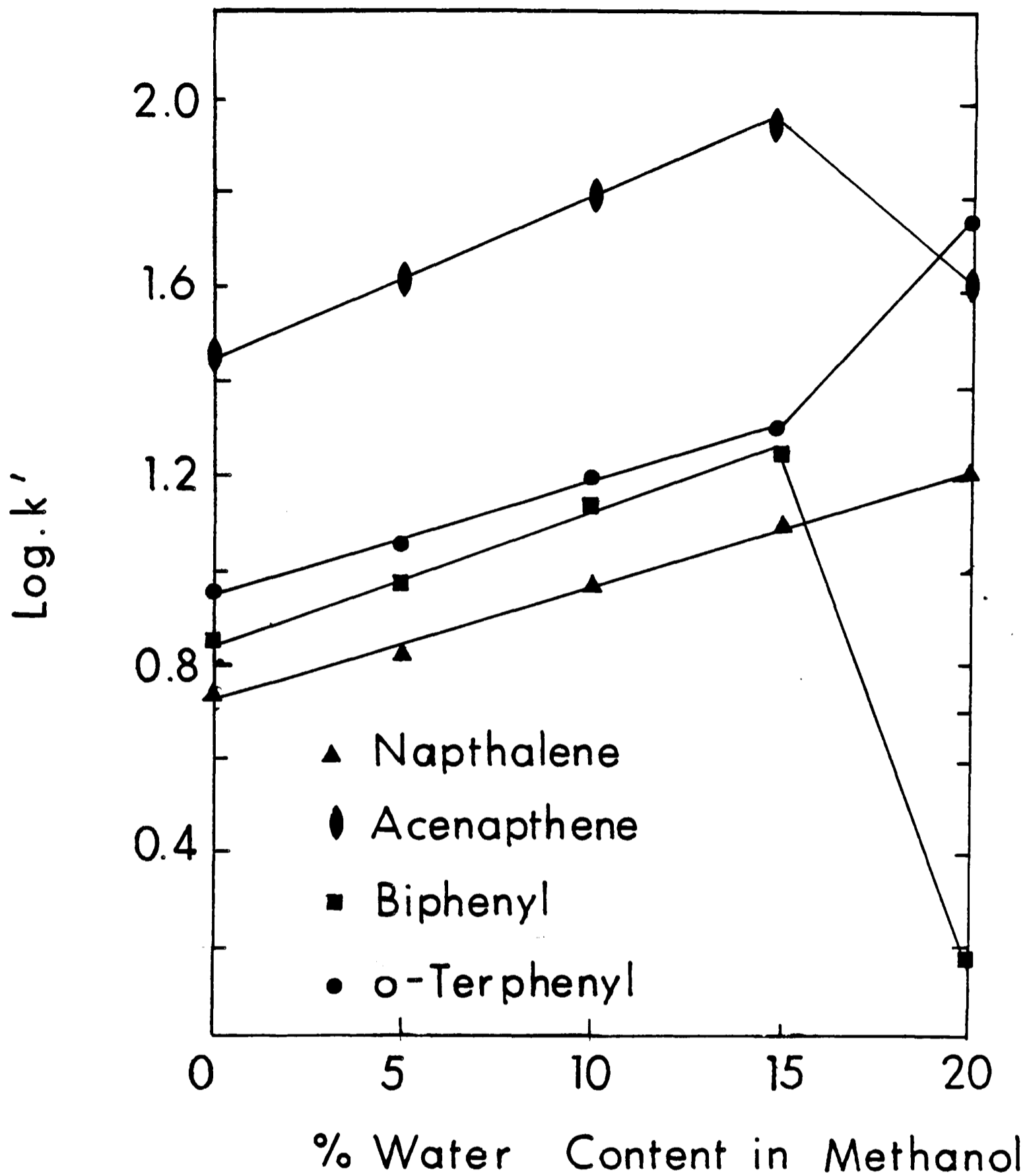
FIG.8.2 - 41:- VARIATION OF LOG.k' WITH
PERCENTAGE WATER CONTENT
(POLYAROMATIC HYDROCARBONS)

PGC 70-B
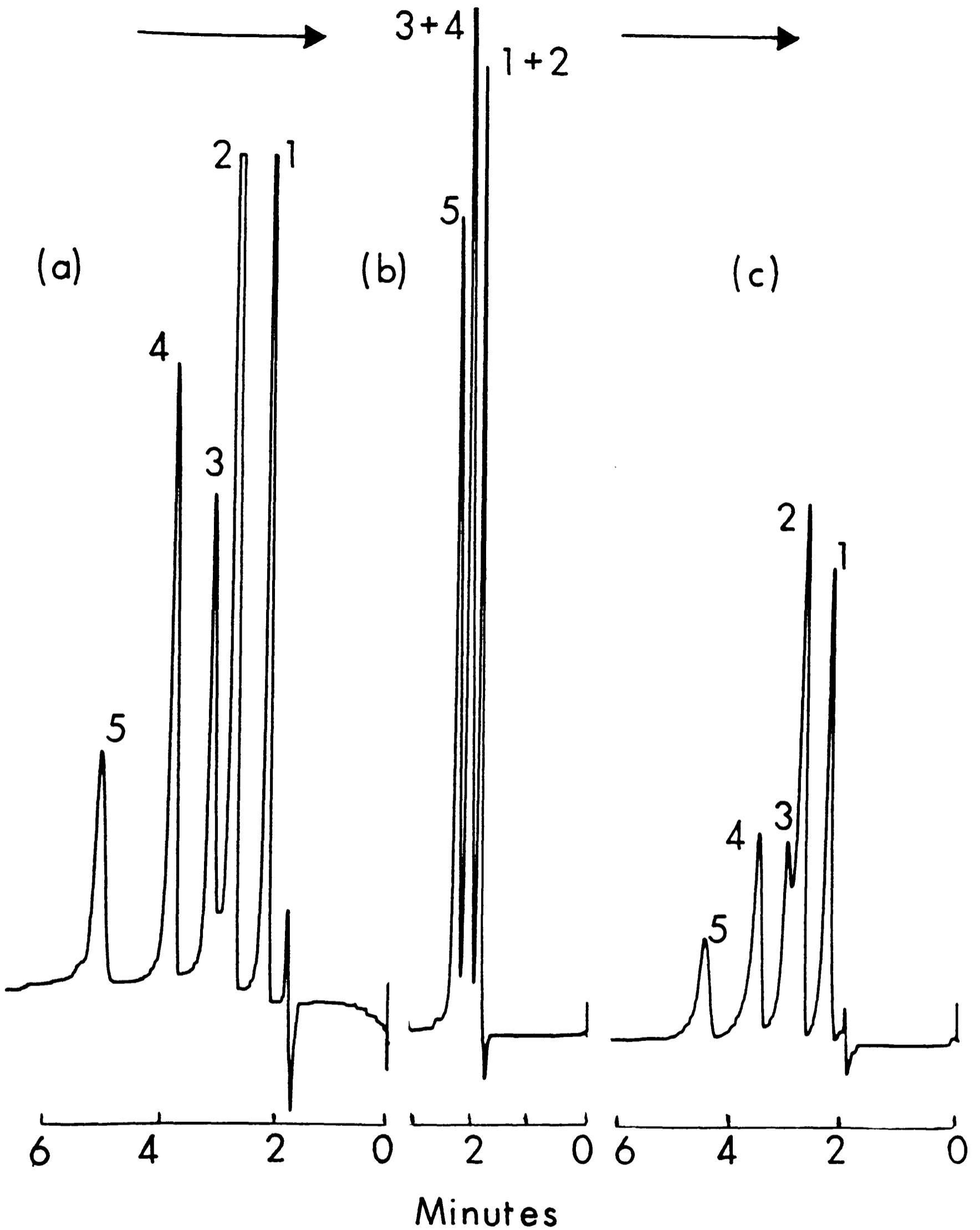
FIG. 8.2-42: DEACTIVATION (b) AND
REACTIVATION (c) OF PGC
Conditions as in Fig. 8.2-1(a)
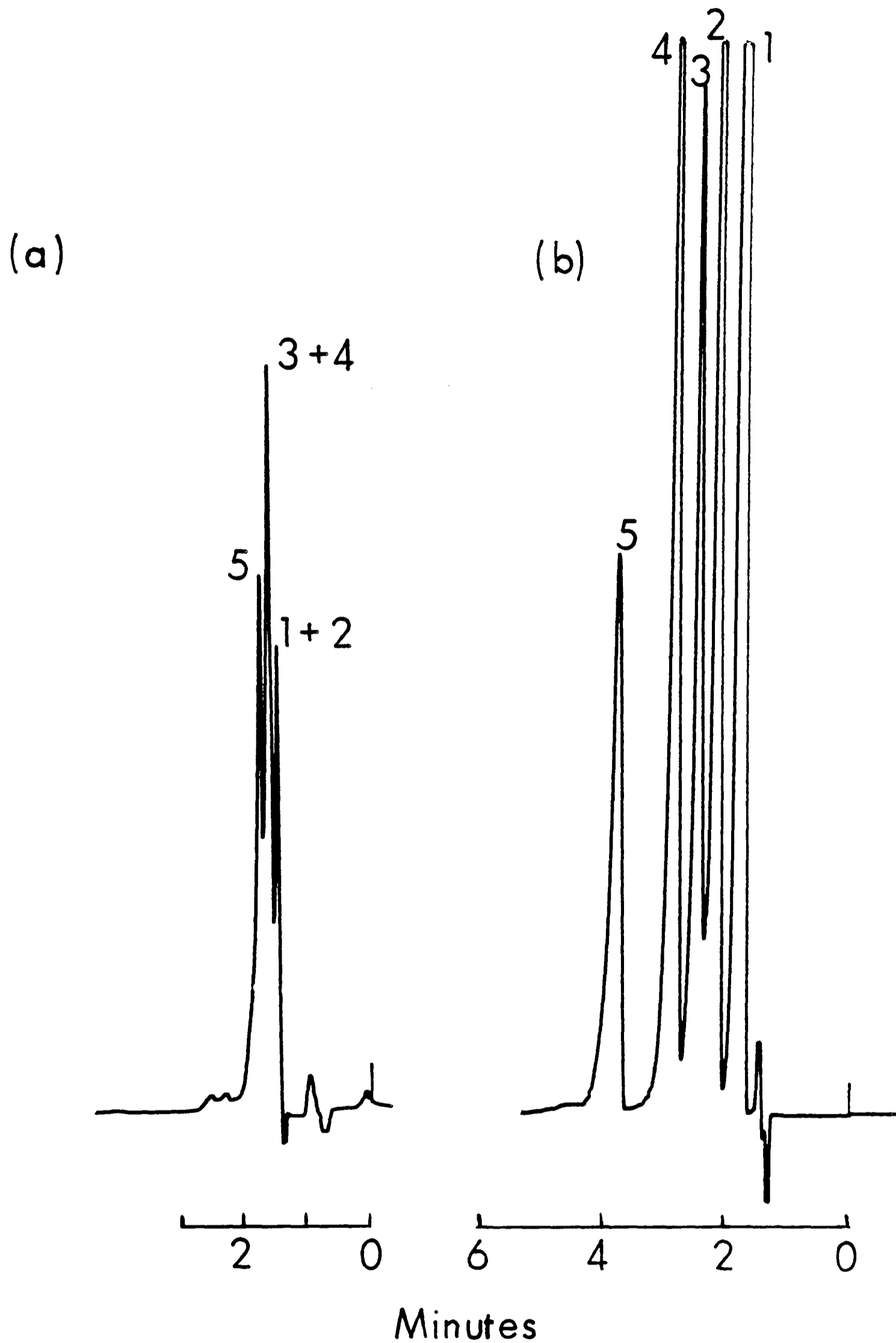
FIG.8.2-43 : DEACTIVATION (a) AND
REACTIVATION (b)
Conditions as in Fig. 8.2 -1(a)

POLYMETHYLBENZENES

PGC 70 - B

Minutes
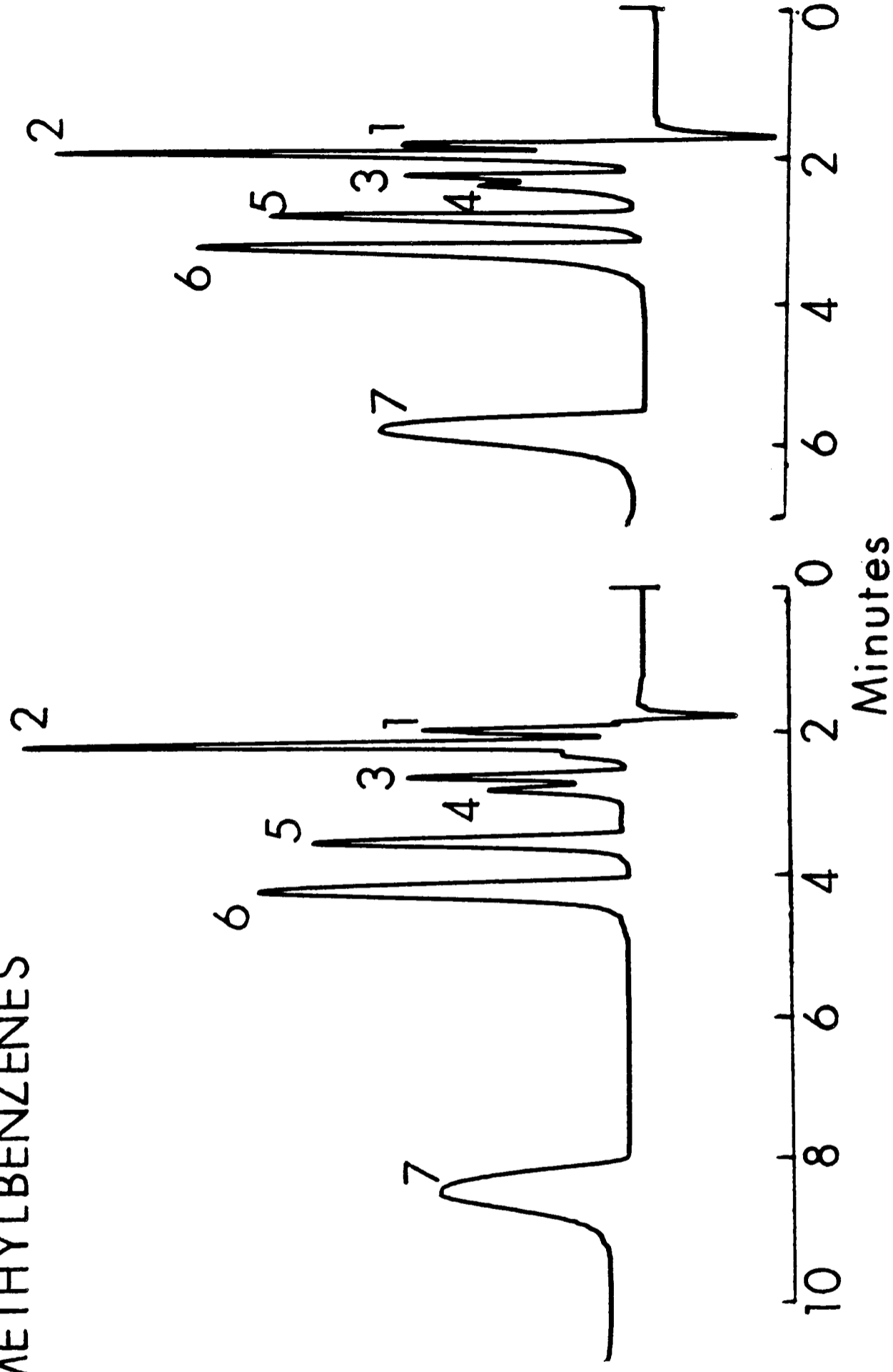
FIG. 8.2 - 44 : GRADUAL DEACTIVATION OF PGC.
Conditions as in Fig. 8.2 - 10

REACTIVATED PGC 70 - B
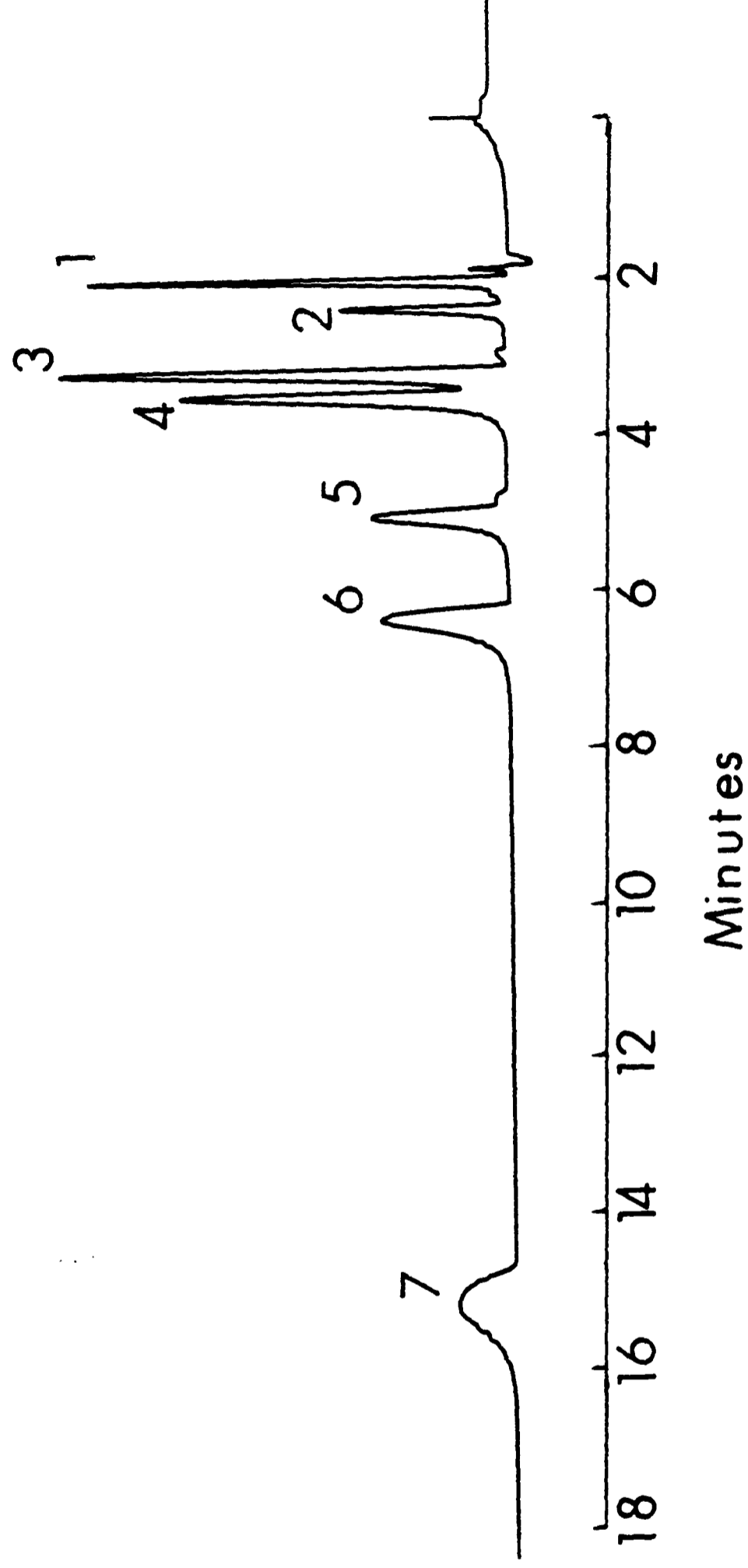
FIG.8.2 - 45 : SEPARATION OF POLYMETHYLBENZENES.

Conditions as in Fig.8.2 -10

REACTIVATED
PGC 64

PGC 64

Minutes
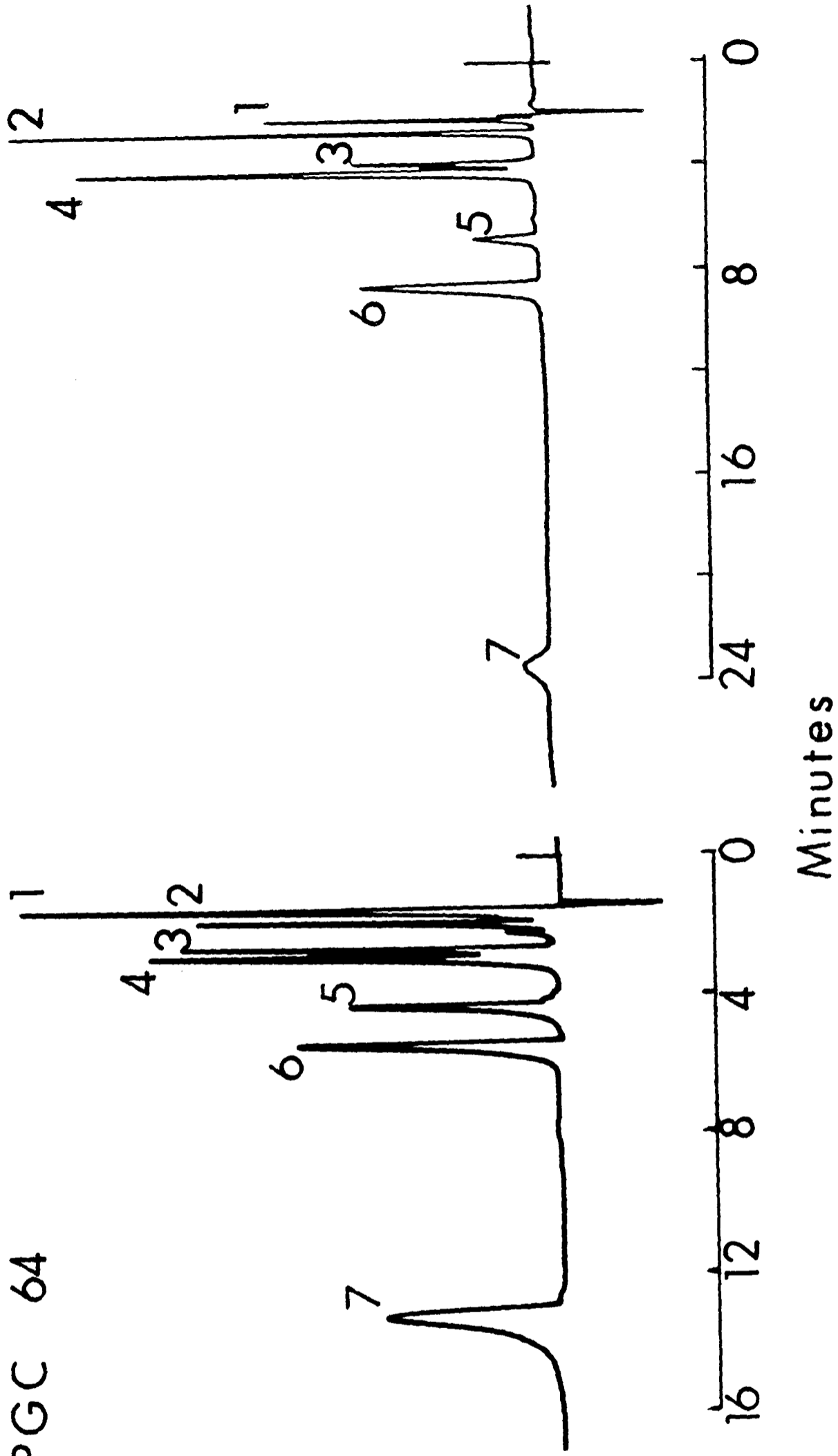
FIG. 8.2 - 46 : SEPARATION OF POLYMETHYLBENZENES.
Conditions as in Fig. 8.2 - 10

REACTIVATED PGC 64
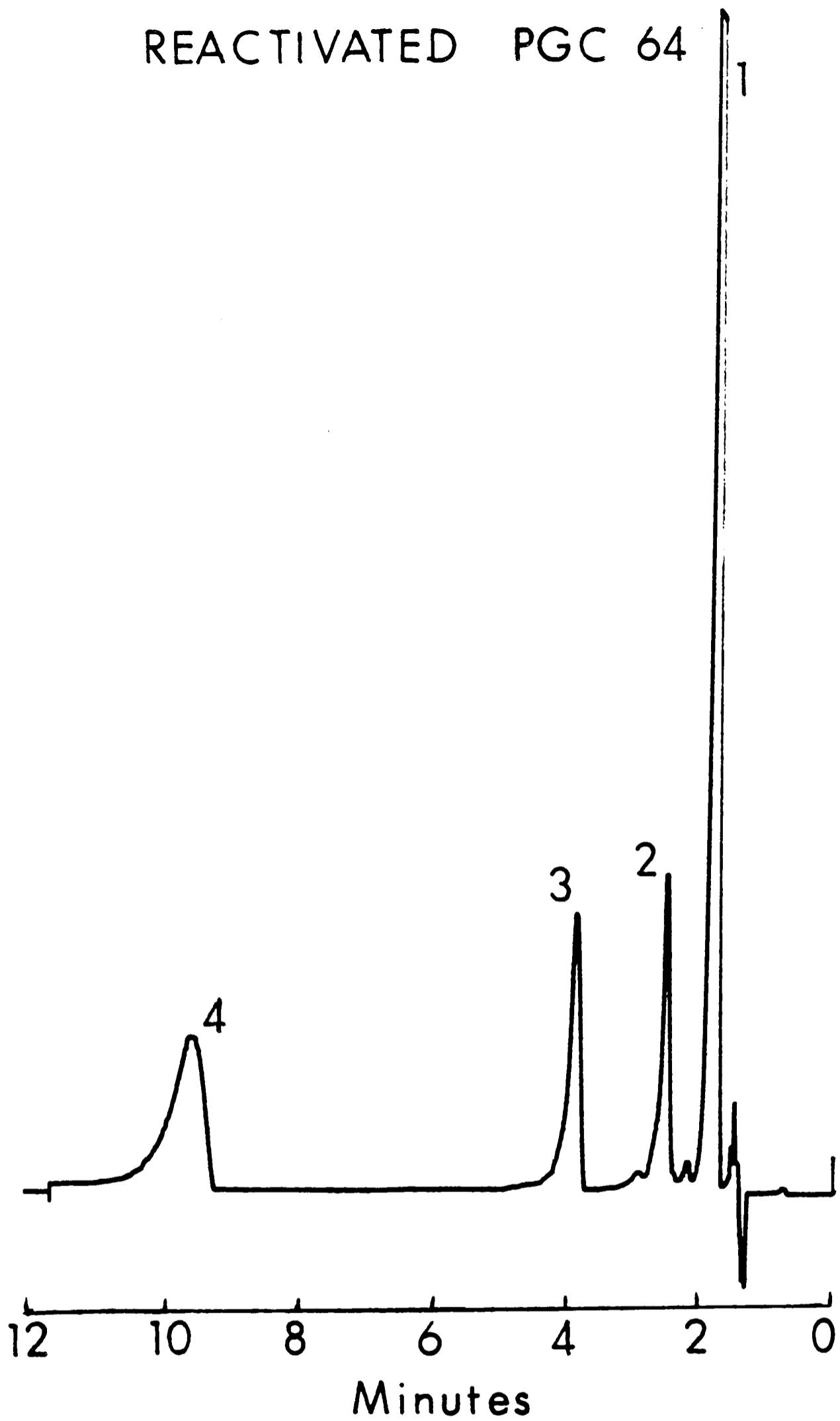
FIG. 8.2 - 47 : SEPARATION OF POLYMETHYL-
PHENOLS. Conditions as in Fig. 8.2 -15

Table 8.2-8   Variation of k' to show deactivation by an impurity

and reactivation by dioxan of PGC 70B

Solutes	k'		
	Before Adsorption of Impurity	After Adsorption of Impurity	Reactivation by Dioxan
Benzene	0.03	Unretained	0.08
Toluene	0.18	0.07	0.27
m-Xylene	0.54	0.22	0.69
o-,p-Xylene	0.68	0.28	0.85
1,3,5-TMB[1]	1.34	0.51	1.68
1,2,4-TMB[1]	1.91	0.73	2.35
1,2,4,5-TeMB[2]	-	2.02	6.98
Phenol	0.20	Unretained	0.17
p-Cresol	0.70	0.10	0.55
3,5-Xylenol	1.58	0.22	1.30
2,4,5-Trimethyl phenol	5.58	0.79	4.36
Anisole	0.51	0.10	0.41
Phenetole	1.06	0.22	0.81

1 = Trimethylbenzene

2 = Tetramethylbenzene
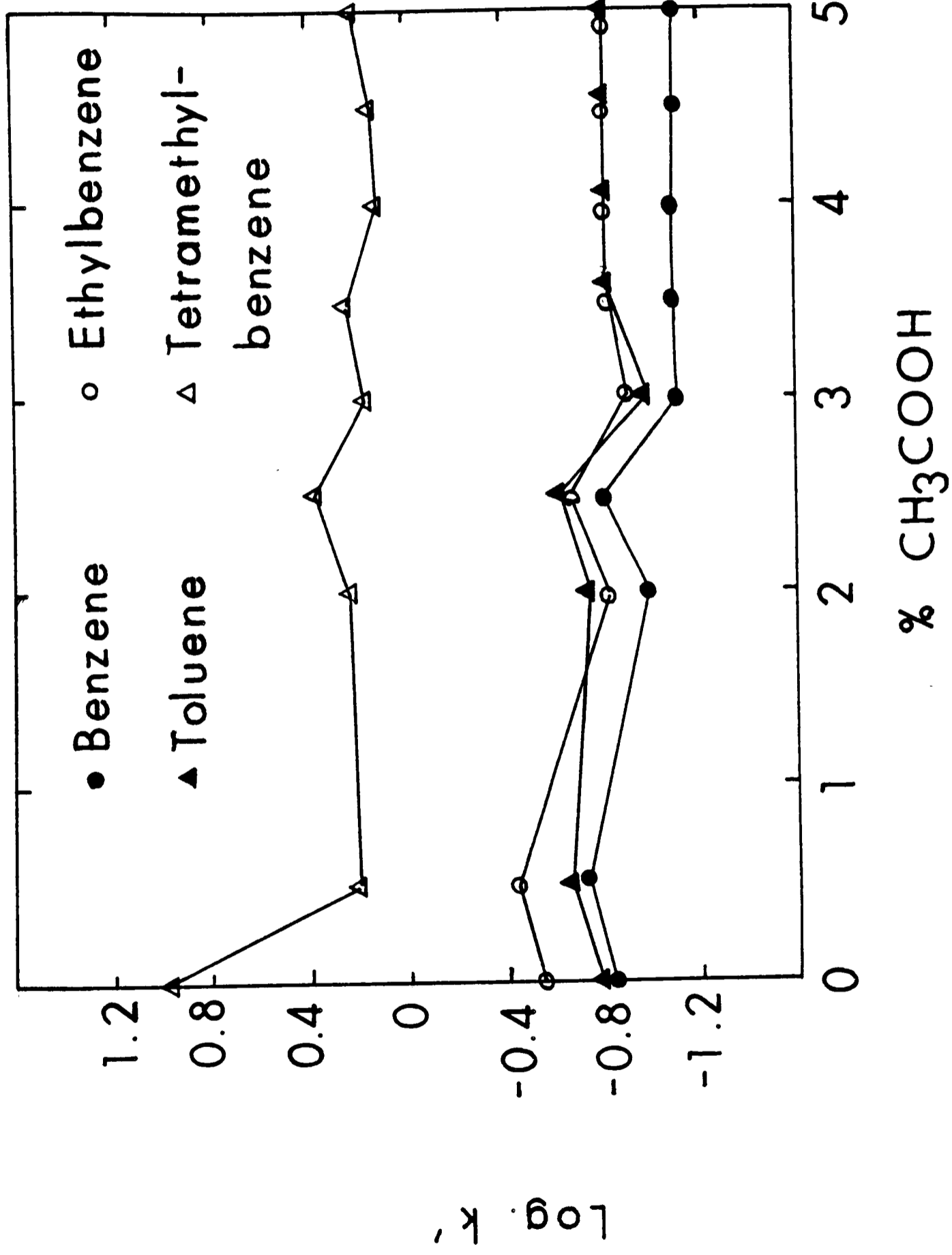
FIG. 8.2-48 : VARIATION OF LOG. k' OF NON - POLAR SOLUTES WITH PERCENTAGE OF ACETIC ACID
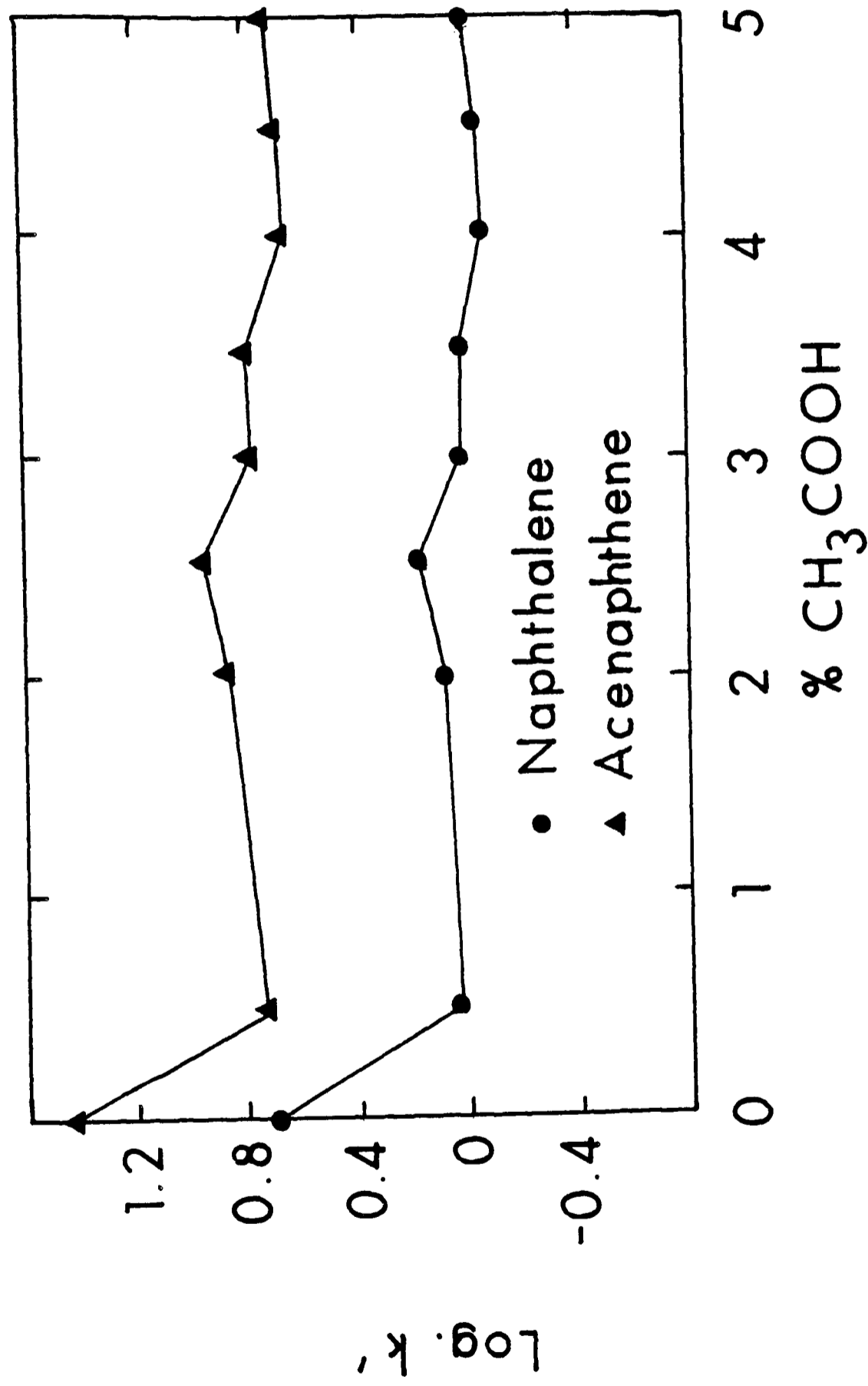
FIG. 8.2 -49 : VARIATION OF LOG. k' OF POLYAROMATIC
HYDROCARBONS WITH PERCENTAGE
OF ACETIC ACID.
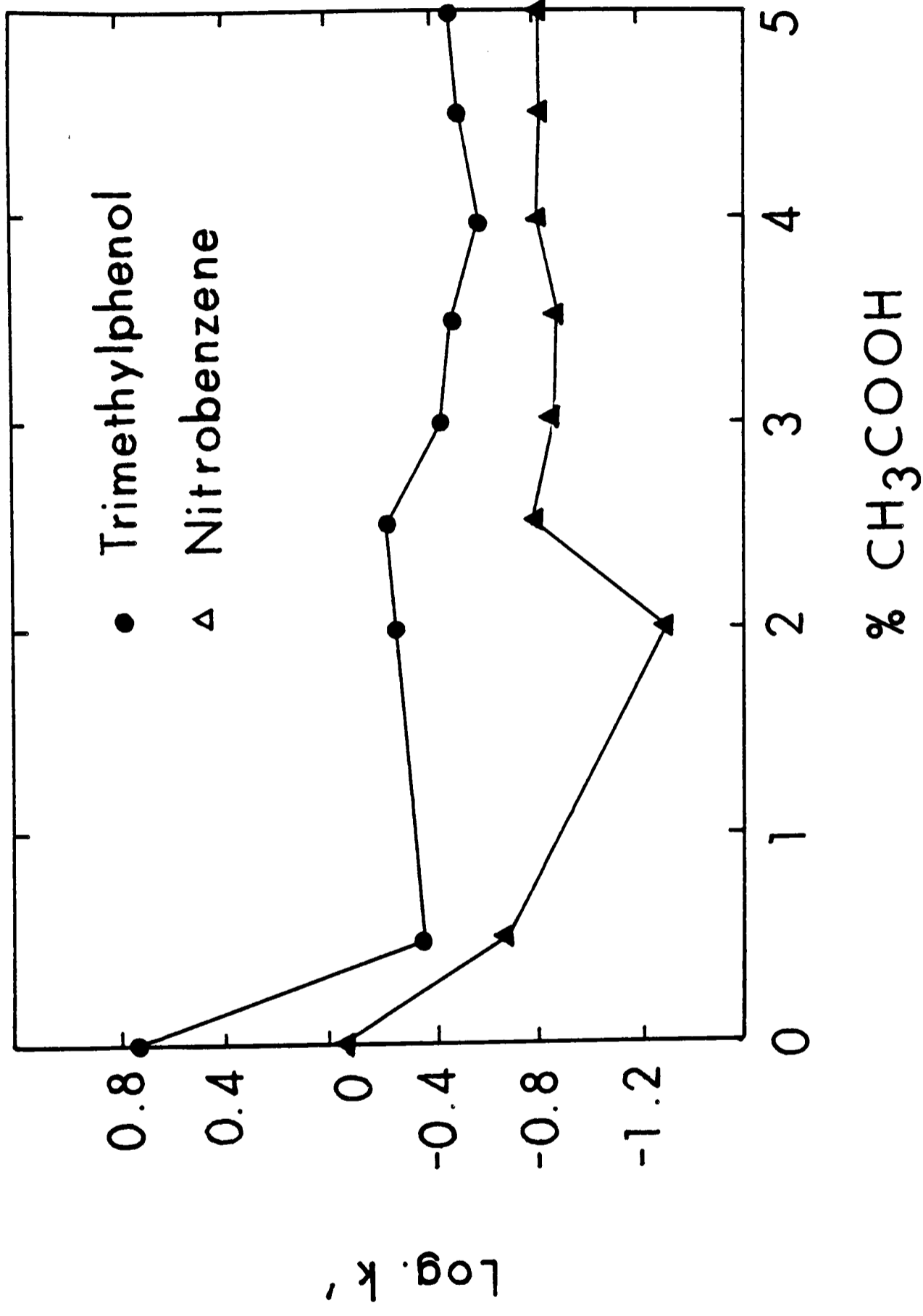
FIG. 8.2 - 50 : VARIATION OF LOG. k' OF POLAR SOLUTES WITH PERCENTAGE OF ACETIC ACID
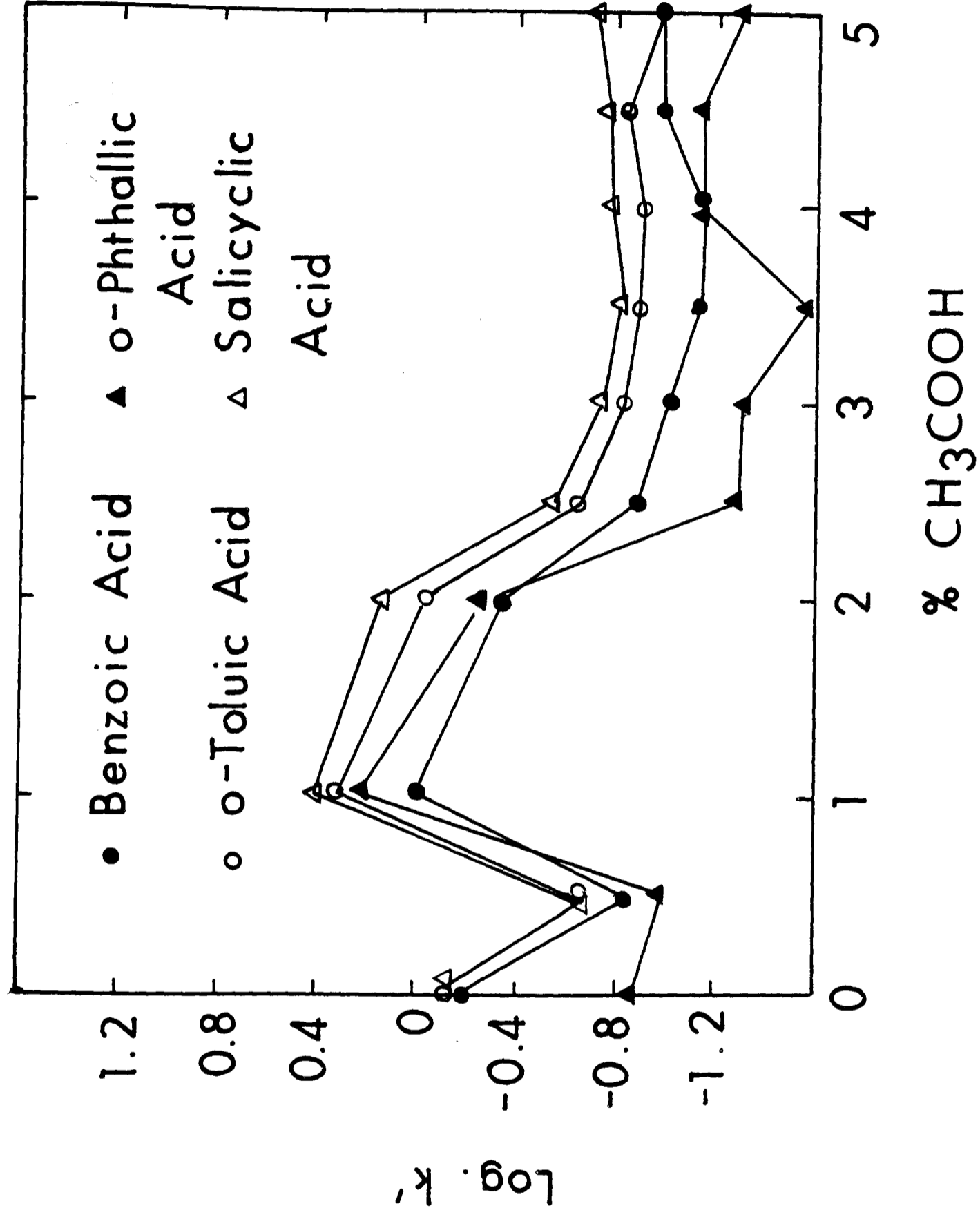
FIG. 8.2 - 51 : VARIATION OF LOG. k' OF ACIDS WITH
PERCENTAGE OF ACETIC ACID
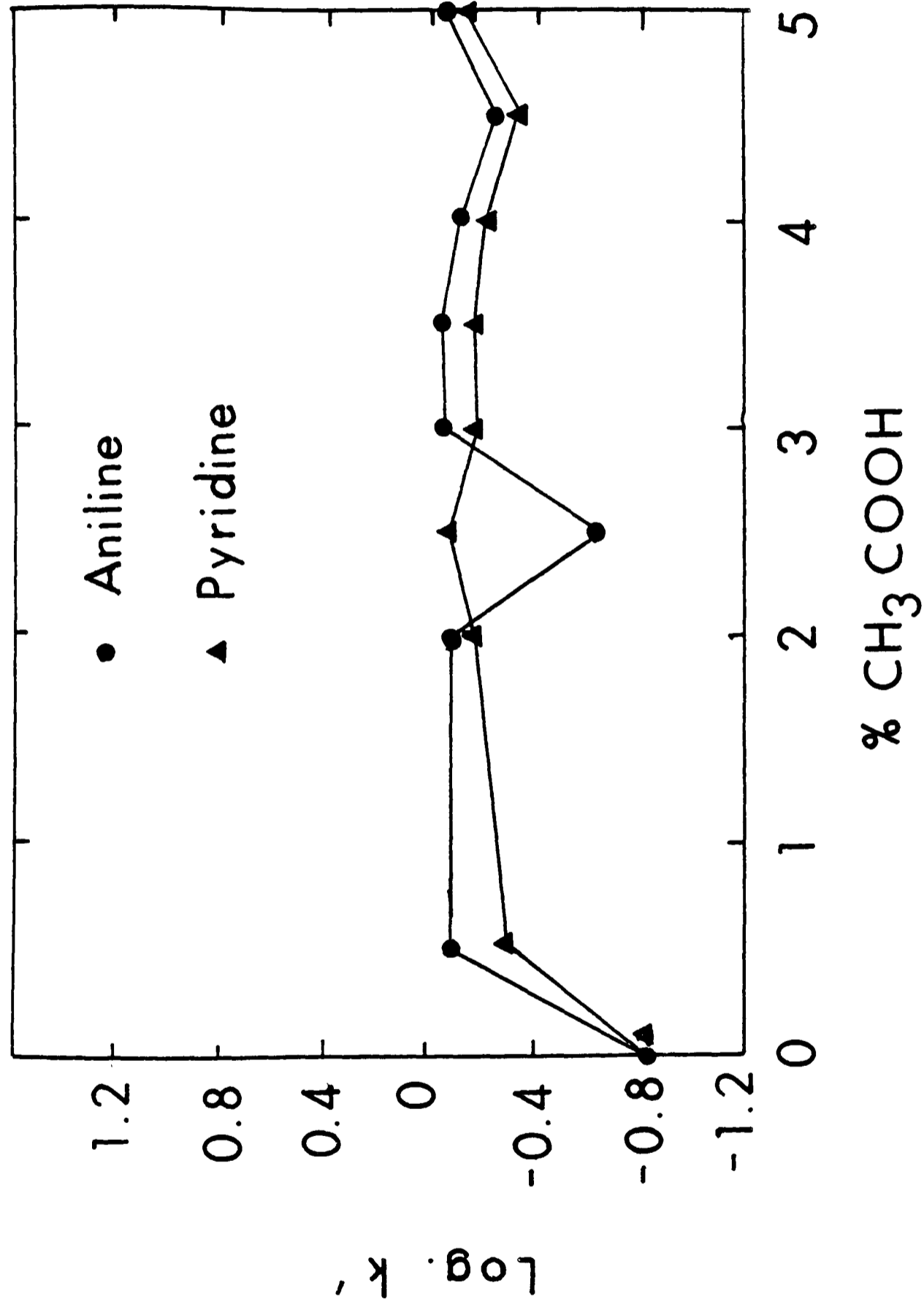
FIG. 8.2 - 52 : VARIATION OF LOG. k' OF BASES WITH PERCENTAGE OF ACETIC ACID

AFTER
TREATMENT
WITH CH₃COOH
IN 95% MeOH/H₂O

PGC 64
BEFORE
TREATMENT
WITH CH₃COOH

2θ/ Degree
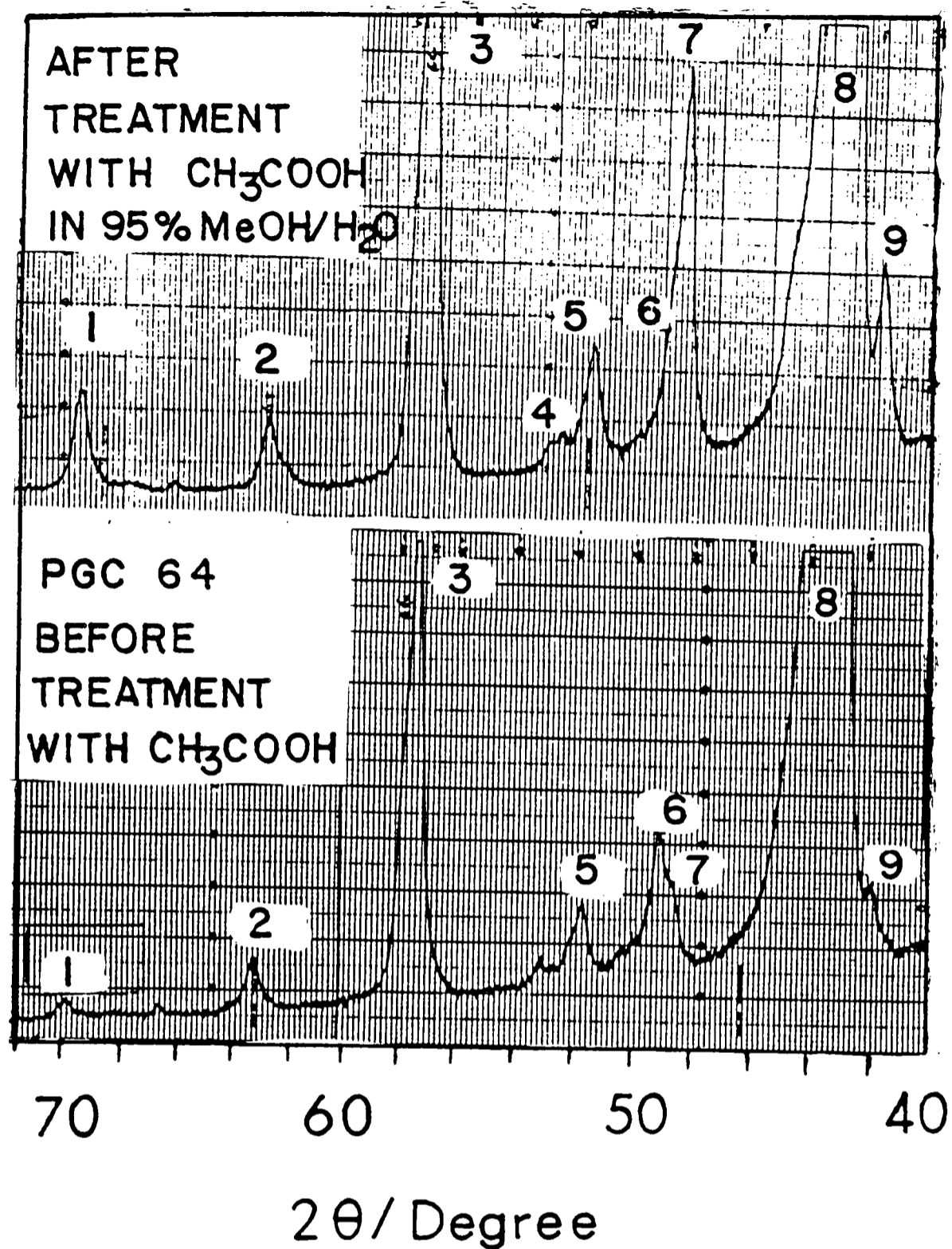
FIG. 8.2-53: X-RAY FLUORESCENCE OF PGC 64
BEFORE AND AFTER TREAMENT WITH
ACETIC ACID.

1. CrK_α 2. MnK_α 3. FeK_α 4. CoK_α 5. FeK_β
6. WL_α 7. NiK_α 8. WL_β 9. ZnK_α

Eluent: 95% MeOH/H$_2$O + 1% CH$_3$COOH

Flow Rate: 1ml/min

Minutes
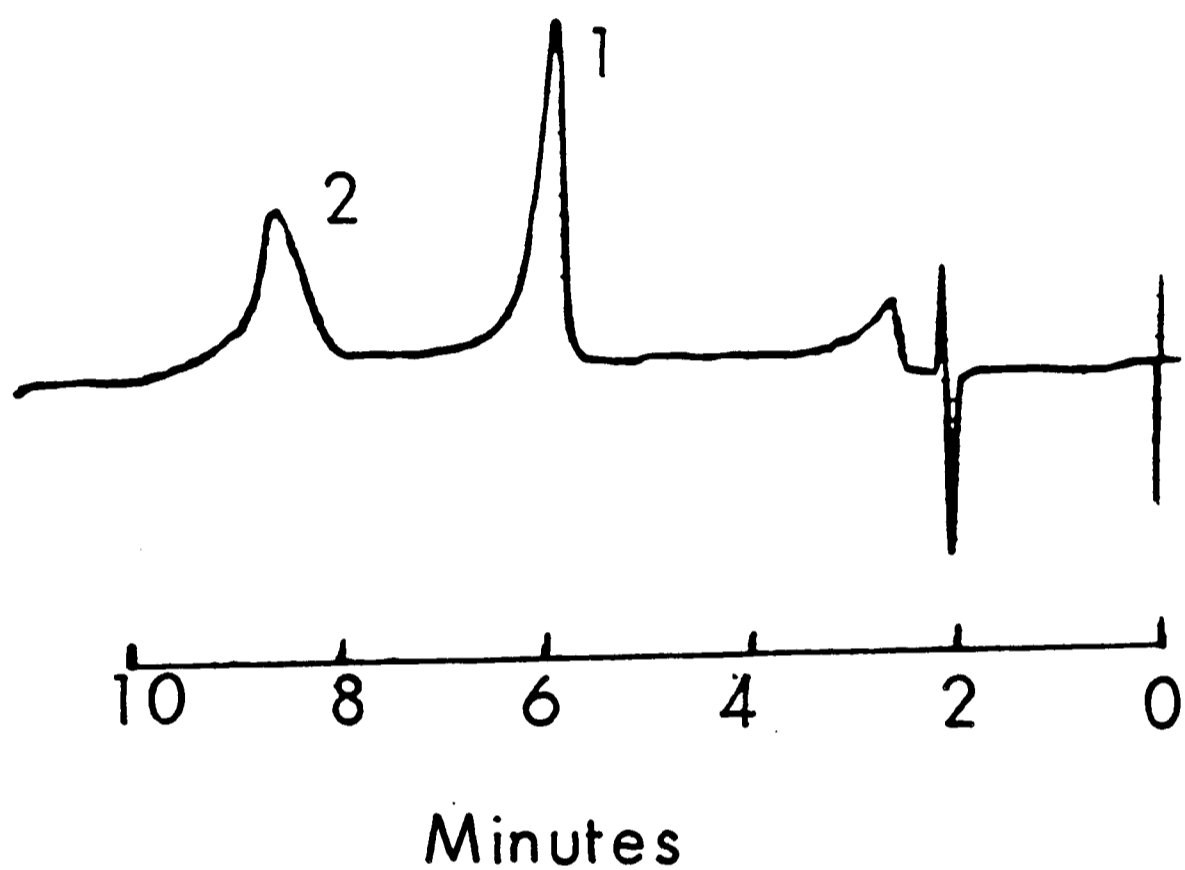
FIG. 8.2-54: SEPARATION OF ACETYL-SALICYCLIC ACID (ASPIRIN)(1) AND SALICYCLIC ACID(2)

Eluent: 95% MeOH/H_2O +
1% CH_3COOH

Flow Rate: 1ml/min

Minutes
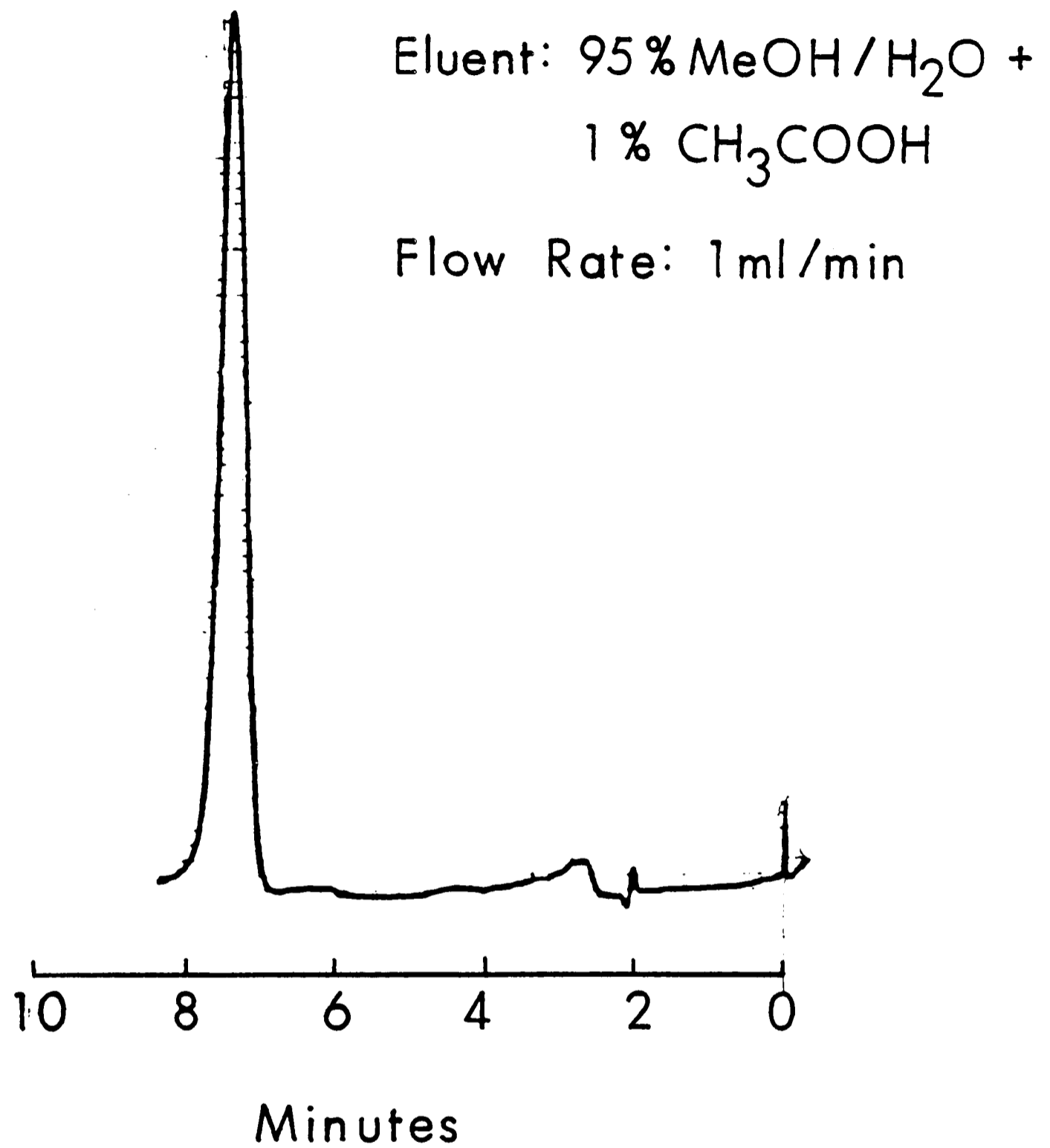
FIG. 8.2 -55: SEPARATION OF
PARACETAMOL

Eluent: 95% MeOH/H$_2$O + 1% CH$_3$COOH

Flow Rate: 1 ml/min

Solutes:

1. Phenacetin

2. Paracetamol
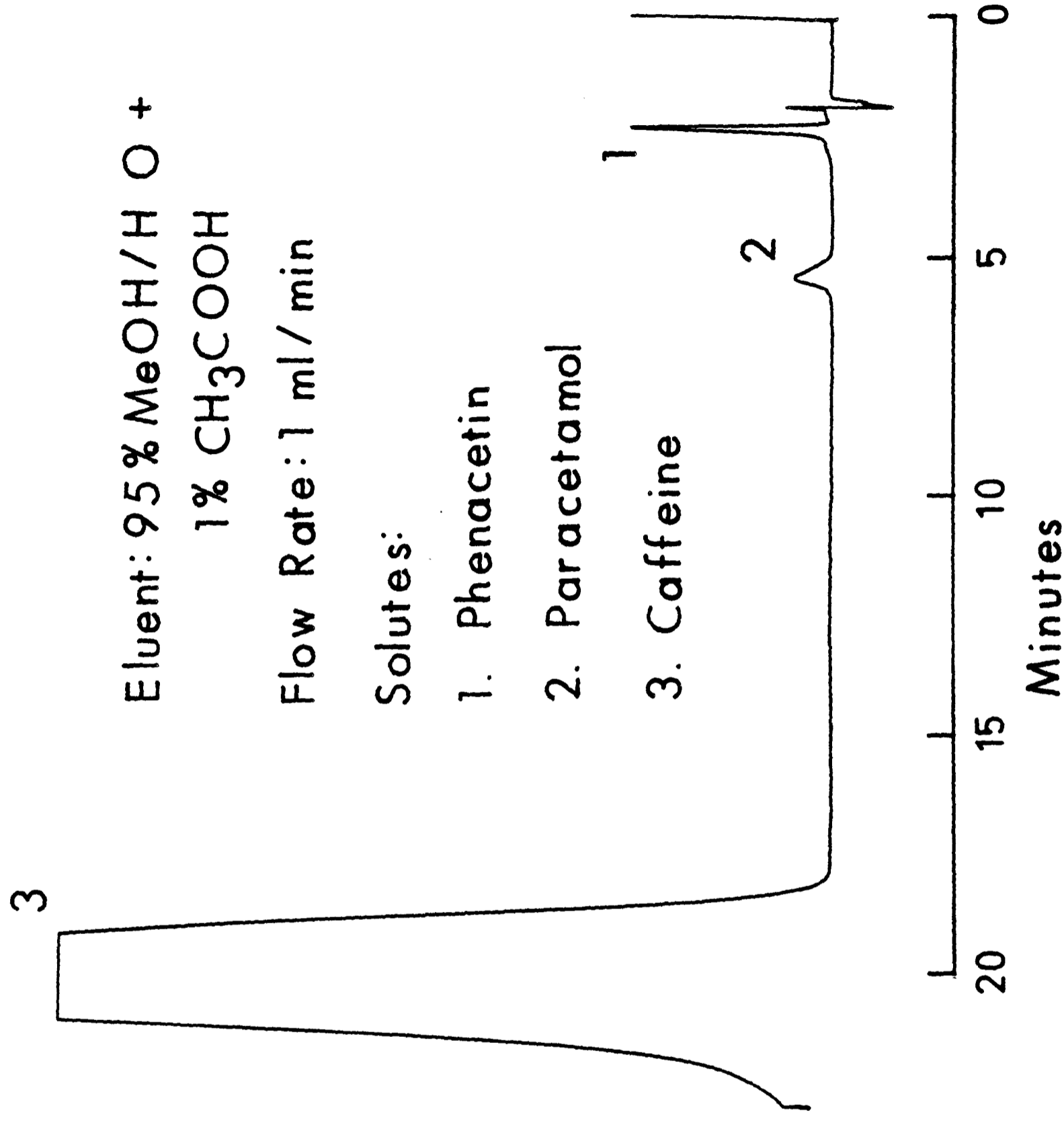
3. Caffeine

FIG. 8.2-56: SEPARATION OF PHENACETIN, PARACETAMOL AND CAFFEINE

Eluent: 95% MeOH/H_2O
+1% CH_3COOH

Flow Rate: 1ml/min

Solutes:

1. Phenatin
2. Aspirin
3. Paracetamol
4. Salicyclic Acid

Minutes
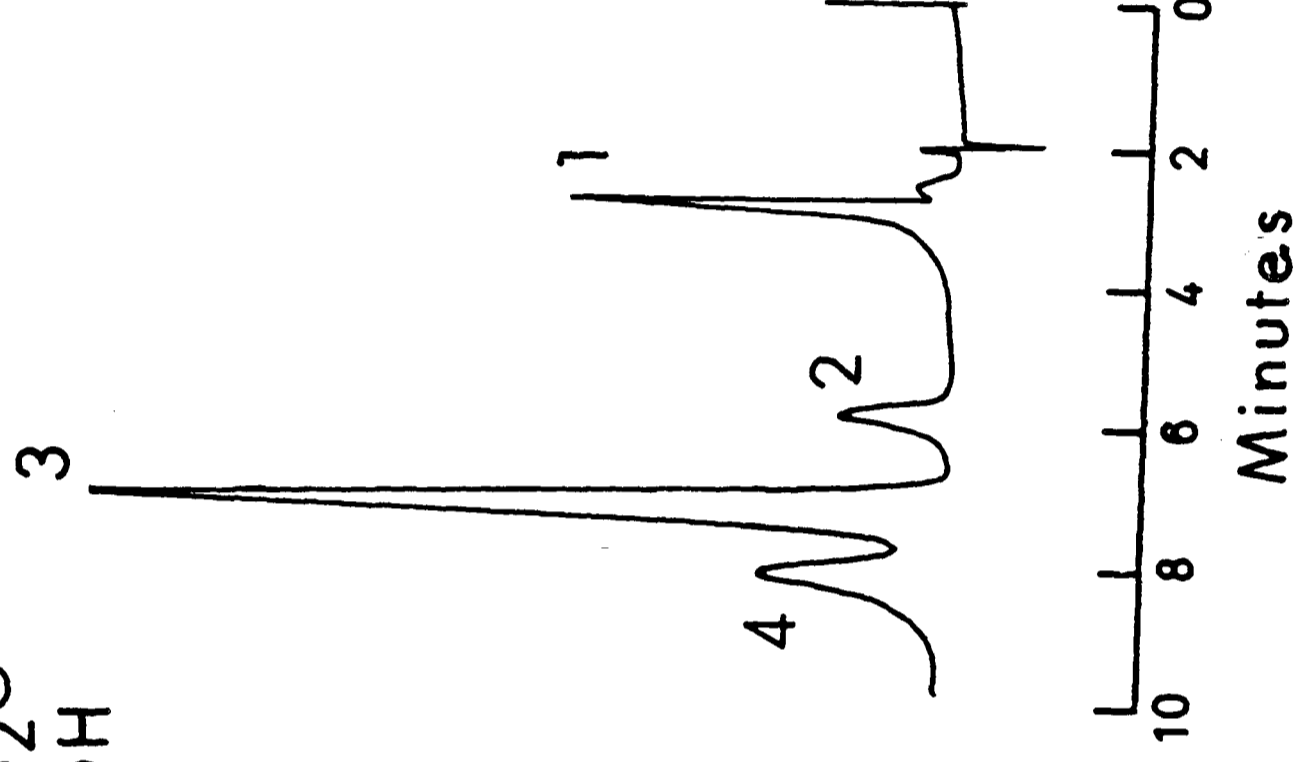
FIG. 8.2 –57: SEPARATION OF ANALGESICS AND
SALICYCLIC ACID

CHAPTER 9

ADSORPTION CHROMATOGRAPHY AND THE STUDY

OF SOLVENT STRENGTHS ON PGC

9.1   What is Adsorption?

When two phases are brought into contact with each other, it frequently happens that one phase or some constituent of it gets more concentrated at the interface than in the bulk. This phenomenon of higher concentration at the interface is called adsorption. Thermodynamically, adsorption is accompanied by a decrease in free energy as well as a decrease in entropy of the system. If accumulation at the interface arises from dispersion forces (van der Waals or London forces) the phenomenon is known as physical adsorption or "physisorption" and if it occurs as a consequence of exchange or sharing of electrons giving rise to ionic or covalent bonds, the phenomenon is known as "chemisorption". Chemisorption proceeds more rapidly with rise in temperature and, like most chemical reactions, involves activation energy. It is also termed activated adsorption. Hayward and Trapnell[1] who defined the difference between these two adsorption types "electron transfers take place between adsorbent and adsorbate in chemisorption but do not take place in physical adsorption". The major differences between the two types of adsorption have been tabulated in Table 9.1-1.

Most normal chromatographic adsorption is of the physical type. However, chemisorption may occur frequently involving perhaps only a fraction of the solute molecules in any one run but in doing so lead to anomalies well known in open as well as column chromatography, such as irreversible

Table 9.1-1   Differences between physical and

activated adsorption

Physical or van der Waals Adsorption	Activated Adsorption or Chemisorption
1. Energies involved are small, <15 kcal/mole	1. Energies generally are large (similar in magnitude to bond formation in chemical reaction) $\sim$20-100 kcal/mole
2. Adsorption and desorption normally rapid	2. Adsorption and desorption are slow (appreciable activated energy is involved for adsorption)
3. The intra-molecular forces responsible for physical adsorption are the van der Waals forces which hold non-ionic molecules together in the liquid or solid state.	3. An actual covalent or ionic bond is formed between adsorbing molecules and the adsorbent surface
4. Adsorbate gas may form mono-molecular or multi-molecular layers	5. A chemisorbed layer is only one molecule thick.

loss of sample, tailing, streaking and ghost spots.[2]
Dintenfass[3] and Matsen et al[4] have defined another kind
of adsorption termed polar adsorption, found in the
chromatographic separation of organic molecules where
the adsorption energies may be large, partial electron
transfer between adsorbate and absorbent is apparent. Actual
bonding of adsorbate and absorbent by chemical bonds is
absent.

9.2   Adsorption and Solution Interactions

According to Snyder, in a liquid-solid system, when a
solute molecule X is adsorbed on the surface of an adsorbent
it is subject to three main types of interactions, namely

(a) Interactions with the surface of the adsorbent.

(b) Interactions with adjacent molecules in the
adsorbed monolayer of solvent, S.

(c) Interactions with adjacent molecules of solvent S
in the (bulk) unadsorbed phase.

In classical liquid-solid chromatographic systems,
adsorbate-adsorbent interactions are important in determining
the relative adsorption of a sample molecule in either
gas-solid or liquid-solid chromatography. The various types
of adsorbate-adsorbent interactions have been classified
in figure 9.2-1 and table 9.2-1.

TYPES OF ADSORBATE-ADSORBENT INTERACTIONS

DISPERSIVE FORCES
or
LONDON FORCES

NON-DISPERSIVE FORCES
or
SPECIFIC INTERACTIONS

INDUCTION FORCES

ELECTRO-STATIC FORCES

HYDROGEN BONDING

CHARGE TRANSFER

COVALENT BONDING OR ION-EXCHANGE CHEMISORPTION
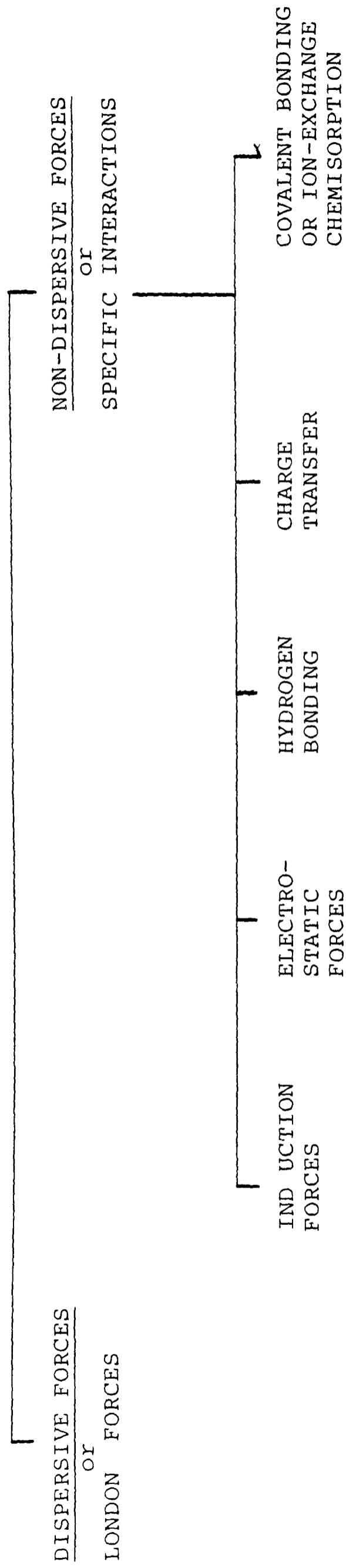
Figure 9.2-1   Types of Adsorbate-Adsorbent Interactions

Table 9.2-1 Types of Adsorbate-Adsorbent Interactions

ADSORBATE-ADSORBENT INTERACTIONS		ENERGY OF INTERACTIONS
DISPERSIVE FORCES (NON-SPECIFIC)	Exist between every non-bonded adjacent pair of similar or dissimilar atoms. Important in Graphite (15)	$E_{11} = \dfrac{-3\alpha_1^{\ 2} I_1}{4r_{11}^{\ 6}}$ and $E_{12} = \dfrac{-3\alpha_1 \alpha_2}{2r_{12}^{\ 6}} \left[\dfrac{I_1 I_2}{I_1 + I_2}\right]$ or $E_{12} = \sqrt{E_{11}} \ \sqrt{E_{22}}$
INDUCTIVE FORCES	Exist when one of two adjacent atoms or molecules has a permanent electrical field associated with it, e.g. a charged ion. It contributes to adsorption energy of alumina (17,18)	$E_i = -\tfrac{1}{2}\, \alpha_1 F^2$
ELECTROSTATIC FORCES	This type of forces contribute to the adsorption of polar molecules or polar adsorbents like alumina (23) since strong surface fields exist over base alumina surface	$E_e = -\mu F \cos\sigma$
HYDROGEN BONDING	Important in number of chromatographic systems like silica and alumina having hydroxyl groups which interact to basic or weakly basic adsorbates	
CHARGE TRANSFER	Bonding of many molecular complexes (24,25) through electron transfer to form charge transfer complexes. Unimportant in affecting the adsorption energy of a compound (Snyder)	

Table 9.2-1 (contd.)

ADSORBATE-ADSORBENT INTERACTIONS		ENERGY OF INTERACTIONS
COVALENT BONDING OR ION EXCHANGE (CHEMISORPTION)	Important in special purpose adsorbents which adsorb certain sample types (e.g. sulphur compounds, acetylenes, aldehydes)	

α_1 and α_2 = polarizabilies of atoms 1 and 2

I_1 and I_2 = Ionization potential of atoms 1 and 2

μ = dipole moment

F = field strength

σ = angle between the vectors of the dipole

9.2.1 Type of Adsorbate-Adsorbent Interactions

in Carbon

It is now generally accepted that dispersion forces account for all the adsorption energies of both polar and non-polar molecules on non-polar adsorbents such as graphite.[5,6] For a given adsorbent, the contribution of dispersion interactions to the adsorption energy of atom 1 is proportional to the polarizability of atom 1 and can be represented by the equation:

$$E_1 = C\alpha_1 \qquad (9.2-1)$$

where α_1 is the polarizability of atom 1. Kiselev[6] has shown that the adsorption energies of a wide variety of compounds (e.g. hydrocarbons, ether, acetone, pyridine) on graphite are proportional to the polarizabilities of the adsorbate.

In terms of surface tension of substances, the above equation can be expressed as:

$$E_1 = 2A_1 \sqrt{\gamma_i^d} \sqrt{\gamma_2^d} \qquad (9.2-2)$$

for the adsorption energy of a molecule 1 in a surface composed of atoms of 2 and where γ_i^d is the dispersion energy contribution to surface tension of substances 1. Fowkes[7] has shown that γ_i^d of most organic compounds are equal to their surface tension, γ.

Thus,

$$E_1 = 2A_1 \sqrt{\gamma_1} \sqrt{\gamma_2} \qquad\qquad (9.2-3)$$

Based on the retention volume data of Belyakova et al.[8] on graphitized carbon, Snyder found the logarithm of the retention volume (which is proportional to the free energy of adsorption) to be proportional to the quantity $A_1 (\gamma_1)^{\frac{1}{2}}$ as illustrated in figure 9.2-2 which further confirms that dispersion forces are responsible for the total adsorption energy.
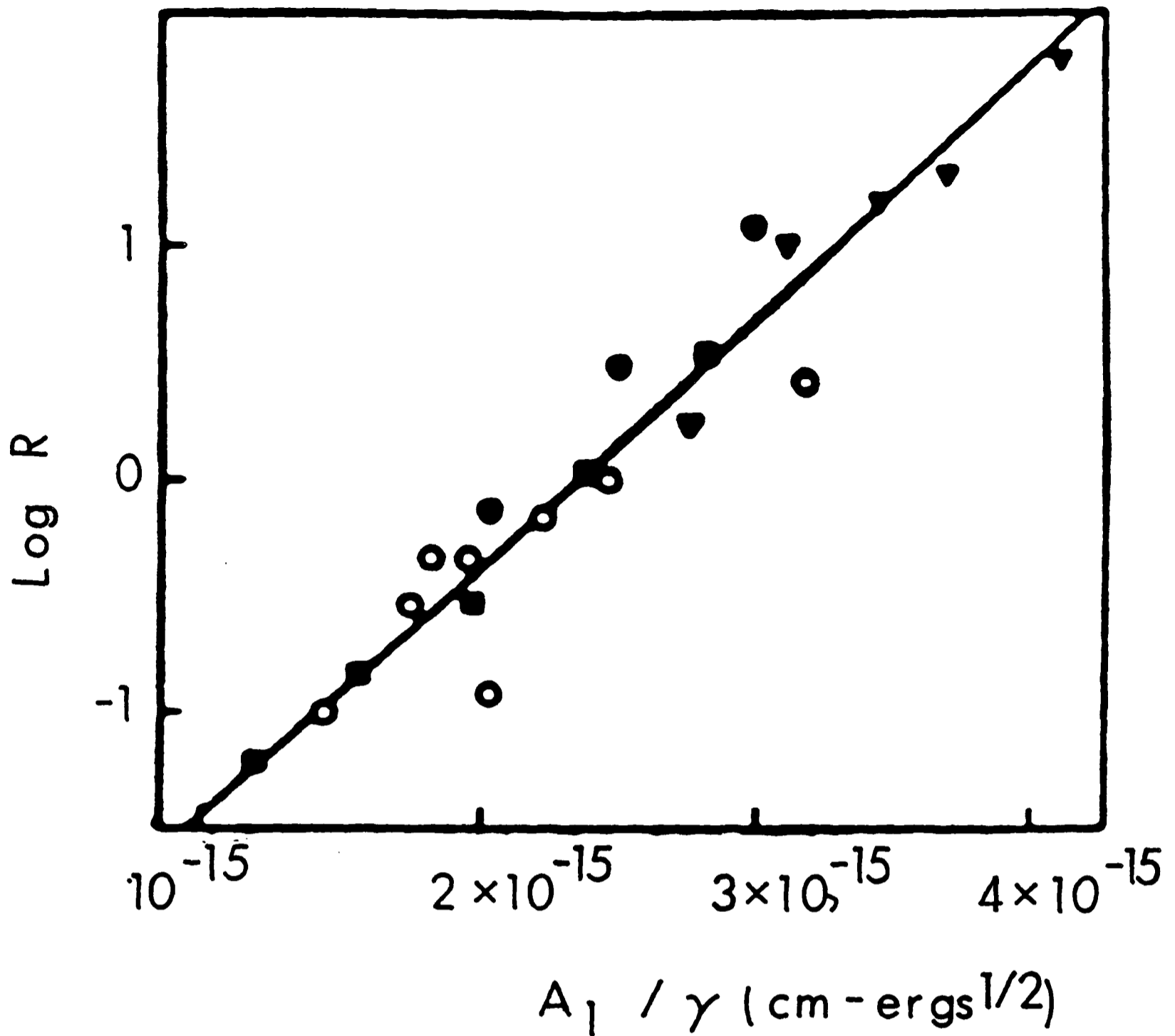
FIG. 9.2 - 2: DEPENDENCE OF SAMPLE
RETENTION VOLUME ON SAMPLE
MOLECULAR AREA A AND
SURFACE TENSION γ IN GAS-
SOLID CHROMATOGRAPHY
GRAPHITIZED CARBON.

■ ALCOHOLS, ○ ALKANES, OTHERS
▼ SUBSTITUTED BENZENES(Ref. 8)

9.3   Retention Mechanism in Liquid-Solid

        Chromatography

9.3.1   Introduction

        The theory of liquid-solid chromatography has now
been underway for several decades. In the 1960's, Snyder[5]
detailed a model for LSC. In 1969, Soczewinski[9] presented
a somewhat different model of retention but the two models
were essentially similar. This is referred to as the
Snyder-Soczewinski (S-S) or displacement model of LSC retention
from the assumption that an adsorbing molecule of solute
displaces adsorbed solvent molecules during the retention
process. In 1973, Scott and Kucera[10a] presented a third
model of retention in LSC which became known as the Scott-
Kucera model.

9.3.2   The Snyder-Soczewinski Model

        The S-S model assumes that in LSC systems the entire
adsorbent surface is covered by an adsorbate monolayer which
consists of mobile phase or solute molecules. This
adsorbed monolayer together with the adsorbent is termed
as the stationary phase. The volume of the adsorbed mono-
layer (ml/m^2 of adsorbent surface) will roughly be constant
and the concentration of the solute will be small; the
adsorbed monolayer will, therefore, consist mainly of mobile
phase molecules.

A competition exists between sample and solvent molecules in the liquid phase for a place on the adsorbent surface. Retention of a solute then occurs by displacing roughly equivalent volume of mobile phase molecules from the monolayer (see figure 9.3-1). The adsorption of a sample molecule X can be written as:

$$X_{(l)} + m\ S_{(a)} \rightleftharpoons X_{(a)} + m\ S_{(l)} \qquad (9.3\text{-}1)$$
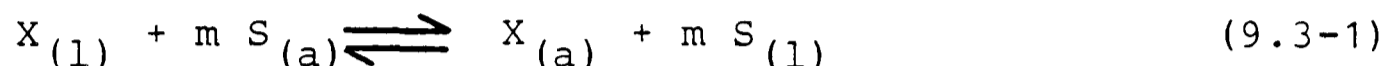
A sample molecule in the liquid phase displaces a certain number, m, of adsorbed solvent molecules, S, from a site complex. The net energy of adsorption is

$$\Delta E = E_{xa} + mE_{sl} - E_{xl} - mE_{sa} \qquad (9.3\text{-}2)$$

E_{xa}, E_{sl}, E_{xl} and E_{sa} refer to the dimensionless free energies (partial molal) of sample (x) and solvent (s) in adsorbed (a) or liquid (l) phases, respectively. To a first approximation,

$$\Delta E = E_{xa} - mE_{sa} \qquad (9.3\text{-}3)$$

on the assumption that various interactions between mobile phase and/or solute molecules in solution are normally cancelled by corresponding interactions in the adsorbed phase.

The S-S model also treats the relative solvent strength (ε^{O} values) of pure solvents as a function of their molecular structure. The S-S model states that the adsorption energy of the solvent molecule when the latter is injected as a sample divided by the molecular area (n_B) of the solvent molecule:
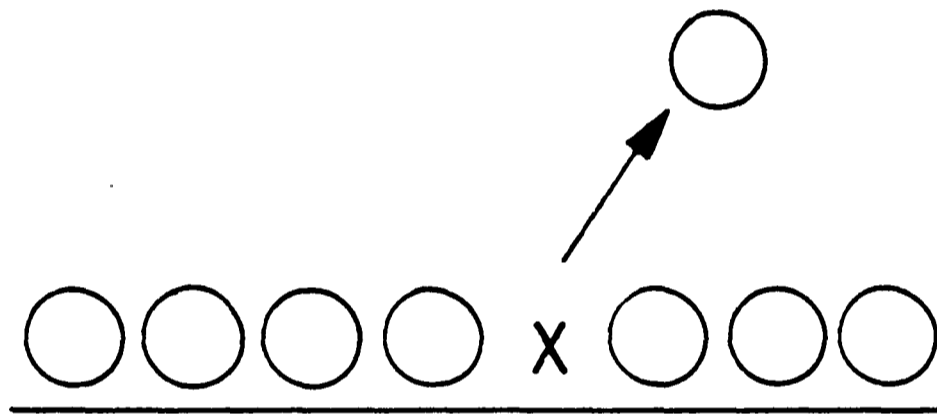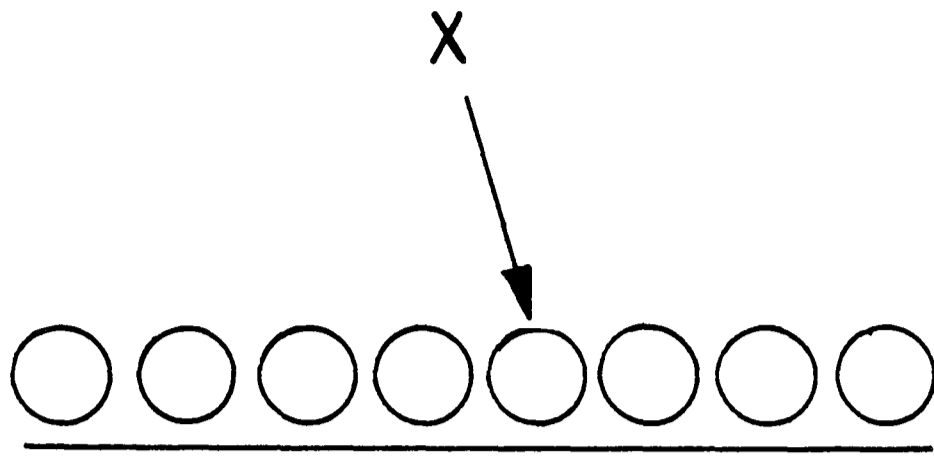
FIG. 9.3 - 1 : THE COMPETITION PROCESS.

◯ SOLVENT MOLECULE

X SOLUTE MOLECULE

$$\varepsilon^{O} = S^{O}_{M}/n_{B} \qquad\qquad (9.3-4)$$

According to Jermyn[10b], solvent strength on charcoal is seen to increase with the size of the solvent molecule and there is a good correlation between solvent strength and the calculated area (A_s) required by an adsorbed solvent molecule (Figure 9.3-2). This is due to higher polarizability per unit area of covered adsorbent surface for larger adsorbed molecules because of the van der Waal's separation between adsorbed solvent molecules.

9.3.3 Scott-Kucera Model[11-16]

The model of Scott and Kucera is based on binary solvent systems. Considering a binary system A-B, as the mobile phase concentration of B varies from 0 to 100%, a monolayer of B is formed within the first few percent addition of B to the binary mixture. Following completion of this monolayer, adsorbing solute molecules interact with the monolayer of B, rather than directly with the adsorbent surfaces by so called "sorption" process as illustrated in figure 9.3-3. As the concentration of B in the mobile phase increases the mobile phase becomes more polar, the strength of solvent-solute interactions increases and solute k' values decrease. Thus in the equation

$$\Delta E = E_{xa} + mE_{sl} - E_{xs} - mE_{sa}$$

E_{xs} determines the dependence of k' on solvent composition.
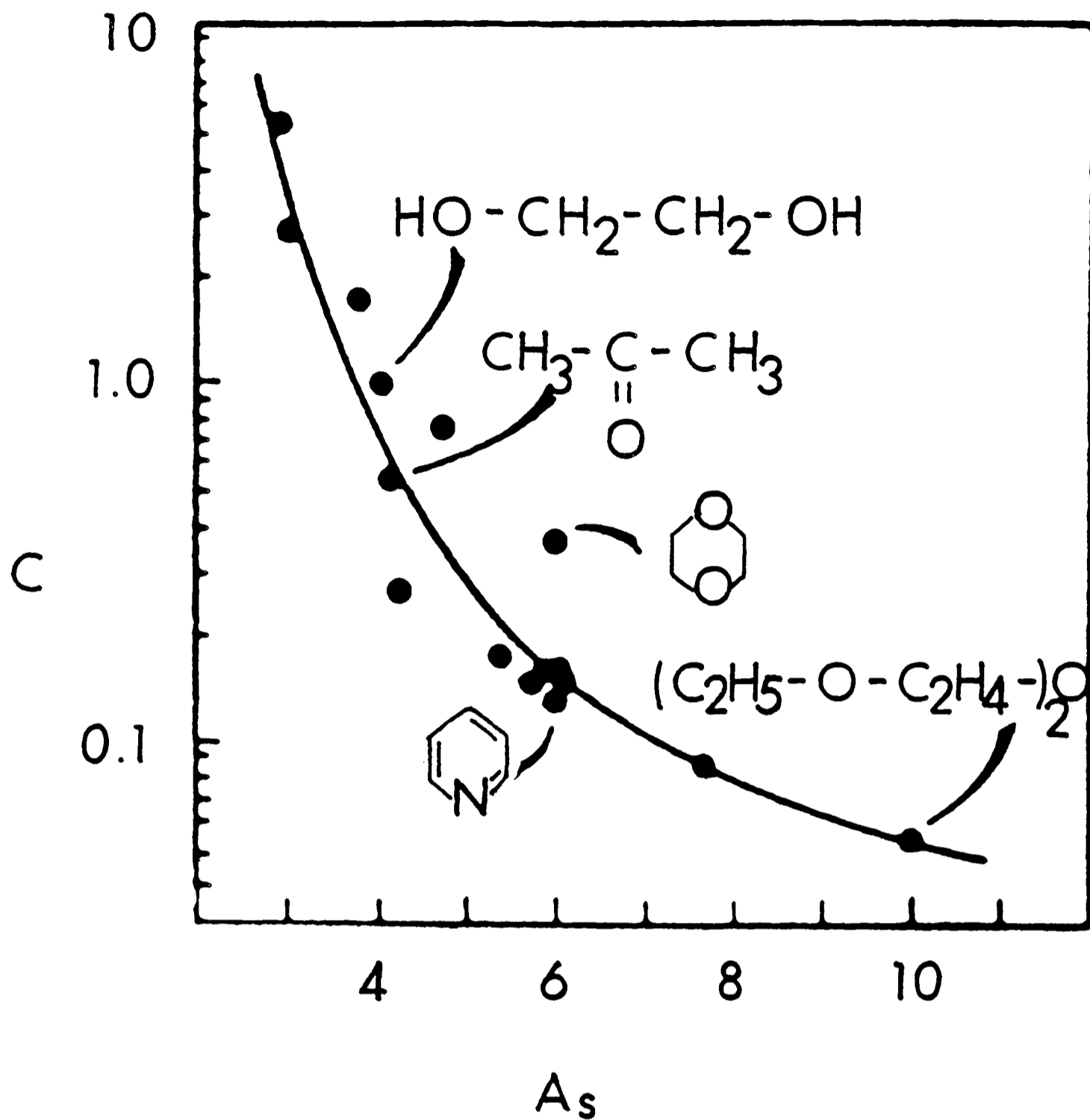
FIG. 9.3-2 : CORRELATION OF INVERSE SOLVENT STRENGTH (C) WITH SOLVENT MOLECULAR AREA(A_s) FOR ADSORPTION ON CHARCOAL (from Ref. 10 b)
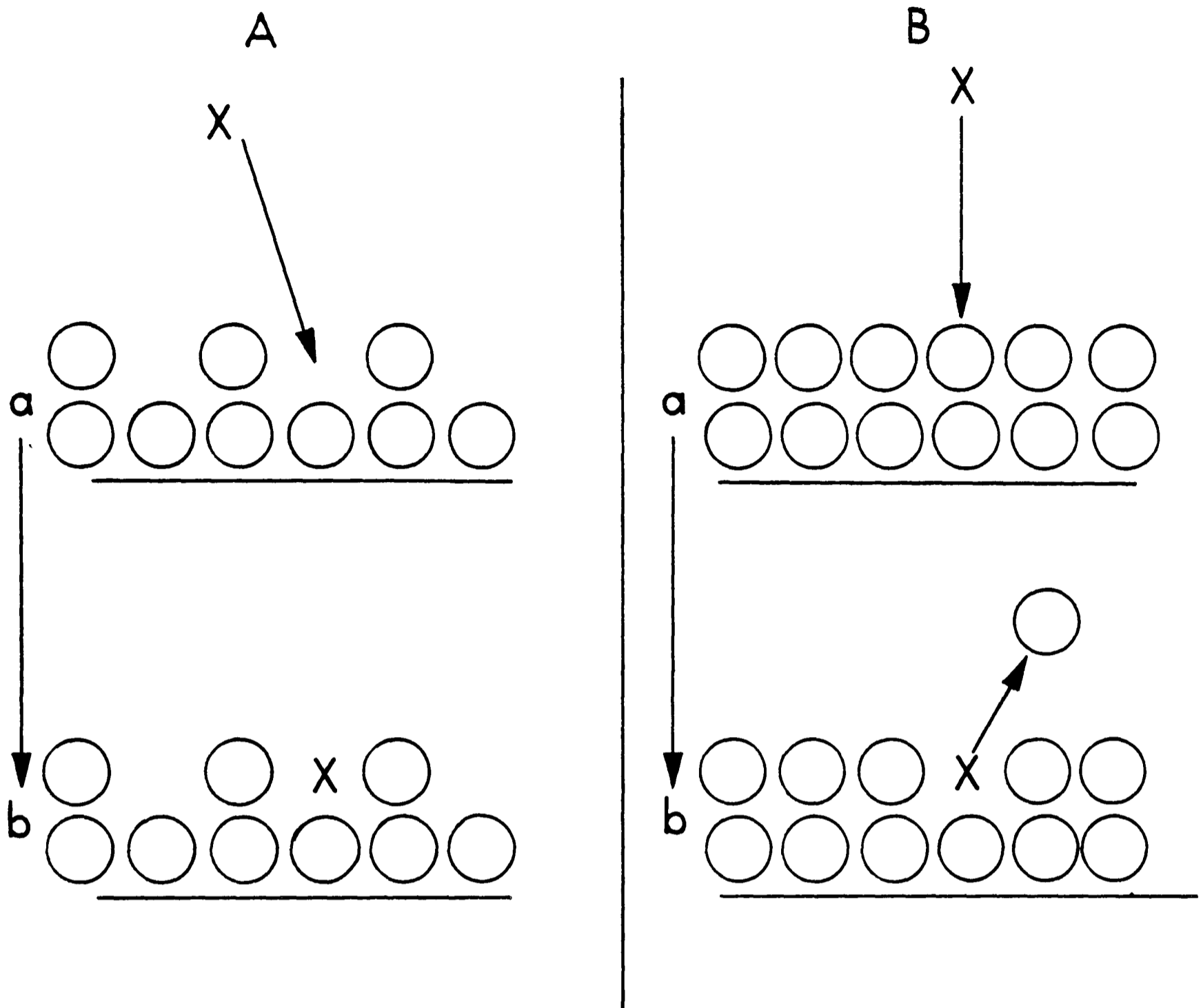
FIG. 9.3 - 3 : THE SORPTION PROCESS

⬤ SOLVENT MOLECULE

X SOLUTE MOLECULE

E_{xa} is assumed to be constant (as in the basic S-S model).
E_{sl} and E_{sa} do not influence ΔE because displacement is
assumed not to occur (m = 0).

They also gave an equation to predict the value of
solute k' in a binary system which is

$$1/k' = A' + B' cp \qquad\qquad (9.3-5)$$

Here A' and B' are constants for a particular solute and
polar solvent B and cp is the concentration of the strong
solvent B in the mobile phase binary. For cp greater than
a few percent, the composition of the stationary phase
remains constant and the assumption is, therefore, made
that both polar and non-polar interactions of the solute
in the stationary phase remain constant.

In references 15 and 16, Scott and Kucera state
that the sorption model is applicable only for non-amphoteric
polar mobile phases (e.g. methylethyl ketone, THF, ethyl
acetate and acetonitrile) which are capable of "hydrogen
bonding". The monolayer of the B-solvent, once formed,
then acts as a "hydrogen-bonded phase". Solutes are retained
by interaction with this phase (the Solution Interaction
Model, SIM) presumably by hydrogen bonding. With the
completion of monolayer formation by adsorbed B (at
concentrations of B equal to 1-3% v/v) a second adsorbed
layer begins to form (bilayer formation). Depending upon
the extent of formation of the second layer, solute
molecules may or may not displace a solvent molecule from

the second layer. However, once the first monolayer is formed, solute molecules do not displace solvent molecules from this layer unless the solute molecule is more polar than the solvent. The hypothesis that solute molecules can be retained in LSC without displacement of adsorbed solvent molecules was tested by both equilibrium and chromatographic means.[15] It was found that solutes with k' values less than about 20 do not displace full equivalent of the B-solvent thus apparantly confirming the concept of retention of solute under certain conditions in the second adsorbed layer.

9.4   Solute Retention in LSC

9.4.1   Introduction

The solute retention in LSC is governed by a number of factors which include the adsorbent type, the molecular configuration of the adsorbate molecule and the type of solvent used in affecting the separation. The different factors involved in solute retention are illustrated in figure 9.4-1 and will now be discussed in greater detail.

9.4.2   Adsorbent Type

The surface structure of any adsorbent is important in determining the selectivity of that adsorbent and its performance in chromatography. Table 9.4-1 shows the classification of LSC adsorbents according to Snyder.[5] Kiselev[17] has further subdivided polar adsorbents into those with predominantly positive or negative surface fields, thereby, interacting as electron donors and electron acceptors with the adsorbates respectively. According to Kiselev[17], the adsorbents are divided into three general types depending on the chemical structure of their surfaces; his classification is illustrated in figure 9.4-2. Polar adsorbents can also be classed as acidic adsorbents (e.g. florisil, silica) and basic adsorbents (e.g. alumina, magnesia) depending on the surface pH. Alumina contains both acidic and basic sites. Graphitized carbon blacks belong to adsorbents of the first class (non-specific adsorbents).

Figure 9.4-1   Factors involved in solute retention

Solute retention in LSC

TYPE OF SOLVENT

SOLUTE (SAMPLE) STRUCTURE

Planarity of Adsorbed Sample Molecules

Group Adsorption Energies and Surface Areas of Adsorbates

ADSORBENT TYPE

Adsorbent surface area

Pore Diameter

Plane of Adsorbent Surface

Surface Activity
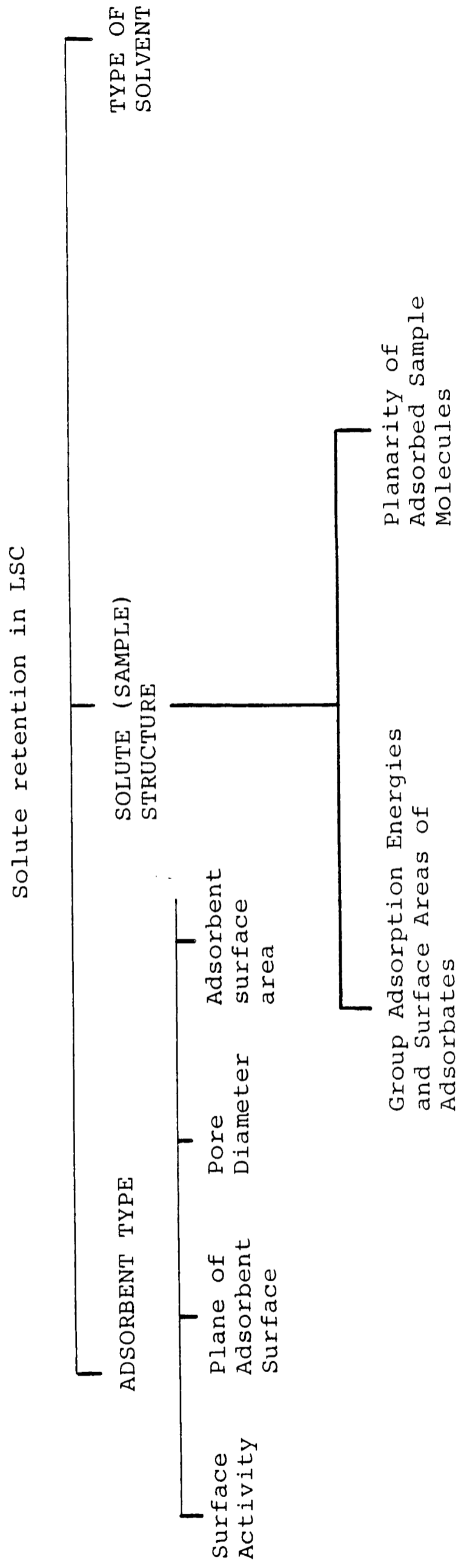
Table 9.4-1   Classification of LSC Adsorbents

(According to Snyder[5])

Adsorbents	General Class	Examples
I	Polar Inorganic	Silica
		Alumina
II	Non-Polar Inorganic	Graphite
		Charcoal
III	Polar Bonded Phase	Amino-propyl
		(C_3NH_2)
		Cyano-propyl
		(C_3CN)
		Diol phase
		$(-O-CH_2-CHOH-CH_2OH)$
IV	Non-Polar Bonded Phase	C_8, C_{18} bonded phase

ADSORBENTS

Non-Specific Adsorbents

(adsorbents that do not
carry on their surface
active functional groups,
ions or groups)

Specific Adsorbents

Adsorbents with
positive charges

Adsorbents with
negative charges
e.g. π bonds, or
Lone electron pairs
on O atoms in
ether
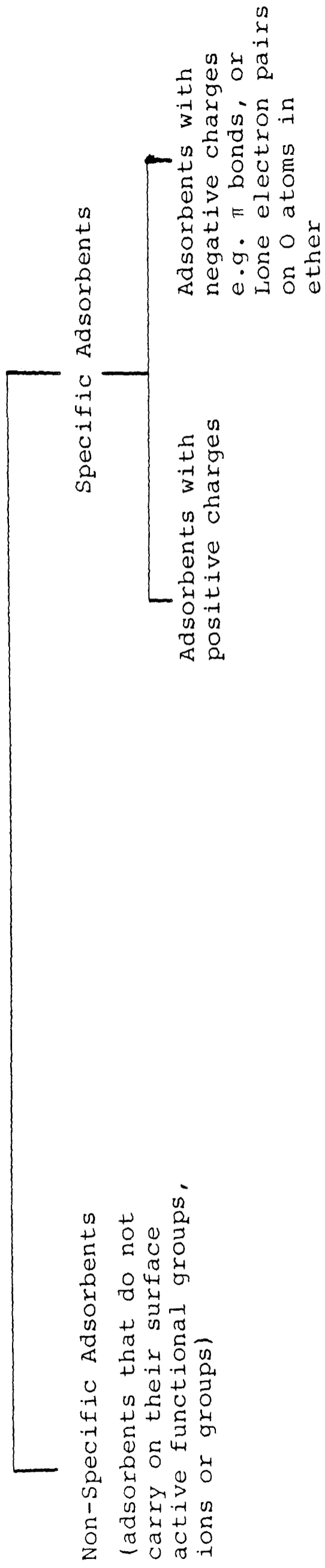
Figure 9.4-2   Classification of LSC Adsorbents

(According to Kiselev[17])

9.4.2.1 Surface Activity

As we have just noted, the surface of chromatographic adsorbents are generally heterogenous due to the presence of local concentrations of strongly interacting groups (active sites). The presence of relative active regions with high concentration of strong site and of less active regions will contribute to the surface activity of the adsorbent and, consequently, will affect the retention of solute molecules.

A monofunctional adsorbate molecule may be pictured as adsorbing on a single adsorbing site whereas a poly-functional molecule would require several distinct sites or a site group, the arrangement of which, in an optimum situation, should overlap the groups of the adsorbing molecule like a 'glove fitting a hand! This can be observed in the case of specific adsorbents which selectively adsorb certain compounds. In alumina, where there is a linear spacing of sites, linear solutes are preferentially adsorbed to angular or non-linear isomers. Preferential adsorption of aromatics on charcoal or graphite can be attributed to be due to the matching of adsorbate atoms and adsorbent sites. The graphite structure of the adsorbent precisely matches the aromatic rings of the adsorbate.

According to Snyder, adsorbents can be characterized by the values V_a (adsorbent surface volume or the volume of an adsorbed solvent monolayer per unit weight of adsorbent) and surface activity function α which are related by the equation:

$$\log K^O = \log V_a + \alpha f(X,S) \qquad (9.4\text{-}1)$$

This expresses one of the fundamental relationships of adsorption chromatography where

$$K^O = \frac{X \text{ adsorbed}}{X \text{ unadsorbed}} \qquad (9.4\text{-}2)$$

V_a and α are independent of the nature of solute molecule X and solvent molecule S.

V_a is related to the adsorbent surface area by means of

$$V_a = 0.00035 \times \text{(surface area, square metres per gram)}$$

9.4.2.2 Planarity of the Adsorbent Surface

The adsorbent surface is generally pictured as planar in most cases, and the HREM pictures shown in figure 6.2-4(a+b) confirm that this assumption holds well for PGC. The adsorption of planar or near-planar adsorbate molecules should be generally favoured relative to the adsorption of non-planar molecules of otherwise similar structure.

9.4.2.3 Pore Diameter

The internal pores of chromatographic adsorbents contribute to the adsorbent surface area, and adsorption onto such material occurs predominantly on the walls of such pores. The average pore diameter, d_{pore}, is related to the adsorbent specific surface area, SA, and pore volume V_p through the relationship

$$d_{pore} = 4V_p/SA \qquad (9.4\text{-}3)$$

if it is assumed that the pores are all cylindrical.

However, most adsorbents, including active carbons, contain pores with a wide variety of diameters from the largest ones to the smallest. In terms of size, these adsorbent pores can be divided into three basic varieties: mesopores (greater than 200 $\overset{o}{A}$), transitional pores (between 40 $\overset{o}{A}$ and 200 $\overset{o}{A}$) and the micropores (less than 40 $\overset{o}{A}$). According to Dubinin,[18] the smallest pores in active carbons play the principal role in adsorption but lead to a heterogenous spectrum of adsorption energies. Most chromatographic adsorbents, therefore, have $d_{pore} > 20$ $\overset{o}{A}$. Snyder[19] has shown that the adsorption of isomeric aromatic hydrocarbons (planar molecules) onto a 20 $\overset{o}{A}$ pore silica is unaffected by the width of the molecule.

9.4.2.4 Adsorbent Surface Area

Adsorbent surface area is important in deciding the suitability of the adsorbent in chromatography. According to Snyder[5], satisfactory adsorbents should possess a specific surface area of at least 50 m^2/g.

9.4.3 The Role of Sample Structure

Molecular structure of the sample is important in K^O determination. A practical knowledge of how K^O varies with sample structure can be useful in designing adequate separation procedures. The contribution of sample structure to K^O is expressed in the sample adsorption energy, S^O, which is mainly determined by the kinds of groups present in the sample molecule, by the total number of groups in the molecule (group composition) and by the arrangement of these various groups within the sample molecule (group arrangement).

9.4.3.1 Group Adsorption Energies and Surface Areas of Adsorbed Molecules

The total energy of interaction between a sample molecule and the adsorbent surface is the sum of the energies of interaction of each atom of group i in the molecule which contacts the surface, that is,

$$S^O = \overset{i}{\Sigma} Q_i^{\,O} \qquad\qquad (9.4-4)$$

where $Q_i^{\,O}$ is the dimensionless free energy ($\Delta G^{\ominus}/2.303\ RT$) of adsorption of a sample group i and S^O is the sample adsorption energy of the standard activity adsorbent.

From the fundamental equation (9.4 - 1) the following equation can be derived, as shall be discussed in section 9.5:

$$\log K^O = \log V_a + \alpha(S^O - A_x \varepsilon^O)$$

where ε^O is the solvent strength. Substituting equation (9.4-4) into the above equation gives:

$$\log K^O = \log V_a + \alpha(\overset{i}{\Sigma} Q_i^O - A_x \varepsilon^O) \qquad (9.4-5)$$

but,

$$A_X = \overset{i}{\Sigma} a_i \qquad (9.4-6)$$

that is, A_x is the sum of the areas of each sample group i. Then,

$$\log K^O = \log V_a + \overset{i}{\Sigma} \alpha(Q_i^O - a_i \varepsilon^O) \qquad (9.4-7)$$

For a given chromatographic system (fixed adsorbent and solvent) equation (9.4-7) predicts that the alteration of a particular molecule X by the addition of a group i to form the new compound X-i will result in a constant change in $\log K^O$ for the original compound, regardless of what this compound is, that is,

$$\log K_{X-i} - \log K_X \equiv \alpha(Q_i^O - a_i \varepsilon^O)$$

$$\equiv (\Delta R'_M)_i \qquad (9.4-8)$$

where K_{X-i} and K_X refer to the K^O values of the compounds X-i and X_1 respectively. For sample molecules, $X-i_n$, differing in the number n of some group i in the molecules (e.g. homologs) equation (9.4-7) assumes the form

$$\log K^O = \log K_X + n(\Delta R'_M)_i \qquad (9.4-9)$$

In most cases, however, it has been found that Q_i^O for a given group i will vary markedly when different groups j,k are attached to i in the sample molecule due to variability of group adsorption energies as the structure of the remainder of the sample molecule is changed. Considering the adsorption of a polyfunctional molecule composed of groups i, j, and k, the fixed arrangement of these groups within the molecule will preclude the possibility that each group can simultaneously overlap an adsorbent site. This leads to one of two possiblities, namely:

(a)   A compromise position might be adopted so that each group partially interacts with an adjacent site. This is referred to as semilocalized adsorption of all sample groups in the molecule.

(b)   On the other hand, some group k in the sample molecule, if it is strongly adsorbing, may localize on a particularly strong site leaving the rest of the sample groups delocalized. Localized adsorption is well accepted in classical adsorption theory.

The relative energy of adsorption of a group i in these various possibilities decreases in the order localized, semi-localized and delocalized. Equation (9.4-4) can now be corrected for the loss in sample adsorption energy of delocalized groups in the sample molecule

$$S^O = \overset{i}{\Sigma}\, Q_i^O - f(Q_k^O)\, \overset{i \neq k}{\Sigma}{}^O Q_i \qquad (9.4-10)$$

Since all groups i except k are assumed to be delocalized, the loss in adsorption energy due to delocalization must be summed over all groups except k. Equation (9.4-8) can now be written as

$$\log K^O = \log V_a + \alpha(Q_k^O - a_k \epsilon^O) + \overset{i \neq k}{\Sigma} \alpha\{(1-f[Q_k^O]Q_i^O - a_i \epsilon^O\}$$

$$(9.4-11)$$

For small aromatic molecules, $f(Q_k^O)$ is constant for a given localized group k and is independent of the relative positions of the localizing and delocalizing groups k and i. But as the size of the sample molecule is increased, as in alkyl benzenes, the delocalizing effect becomes less severe.

9.4.3.2 Planarity of adsorbed sample molecules

As noted in section 9.4.2.2, the surface of an adsorbent is generally regarded as planar. Consequently, planar sample molecules, or molecules which can most easily adopt a planar configuration will be adsorbed more strongly than corresponding non-planar isomers. Aromatic molecules are normally adsorbed in a "flat" or "parallel" configuration on the adsorbent surface. The flat adsorption of aromatic hydrocarbons on alumina from pentane is well known. Ortho- and para-isomers are more retained than meta-isomers in all of the known adsorbents; alumina, silica and carbon. This could be due partly to the planarity of the isomers and also due to the fact that

a para-methyl will increase the electron density (and adsorption energy) of the group i more than a methyl group in the meta position due to intramolecular electronic interactions.

9.4.3.3 Steric Hindrance in Adsorption

The optimum adsorption of a sample group i (corresponding to a maximum value of Q_i^o) requires the close approach to the adsorbent surface or to a particular site on the surface. A bulky adjacent group in the same molecule can interfere with this process by steric hindrance, resulting in a reduction in the adsorption energy of i. Steric hindrance to adsorption is an important and frequently encountered phenomenon. Steric effects are important in the adsorption of pyridine benzenes,[20-23] polysubstituted benzenes[24-26] and cyclohexane derivatives.[27,28]

9.4.4 The Role of Solvents in Adsorption Chromatography

9.4.4.1 General Background

The selection of a correct solvent for a chromatographic separation is very important. A change in solvent can alter the equilibrium constant, K^o, of a sample by several orders of magnitude. Jeulemans[29] has given a good review of the early theory of the principal factors which determine solvent strength in a given adsorption system. Solvent strength is determined by three basic contributions:

a.   Interactions between solvent molecules and a sample molecule in solution.   Solvent strength, therefore, will increase with increased tendency of the sample to dissolve in the solvent.

b.   Interactions between solvent molecules and a sample molecule in the adsorbed phase.

c.   Interactions between an adsorbed solvent molecule and the adsorbent.

In a ligand-solid adsorption system, Snyder-Soczewinski model (section 9.3) predicts a competition between the sample and solvent molecules for the adsorbent surface.   The adsorption of a sample molecule X can be written as equation (9.3-1)

$$X_{(1)} \; + \; mS_{(a)} \; \rightleftharpoons \; X_{(a)} \; + \; mS_{(1)}$$
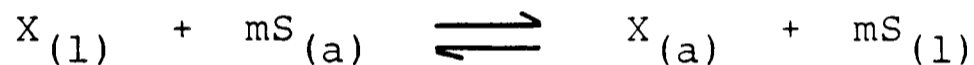
where a sample molecule displaces a certain number m of adsorbed solvent molecules S from a site complex, giving an adsorbed sample molecule and m solvent molecules in the liquid phase.   As discussed in section 9.3, to a first approximation

$$\Delta E \; = \; E_{xa} \; -mE_{sa} \qquad (9.3-3)$$

neglecting liquid phase energy terms, E_{sl} and E_{xl}, indicating that the net adsorption energy of the sample, ΔE, is equal to the adsorption energy of sample minus the total adsorption energy of the solvent which the sample displaces.   According to Snyder[5] the liquid phase or solution interactions can be neglected due to

a.   There is a net cancellation of dispersion energies in the .term $mE_{sl}-E_{xl}$ of equation (9.3-2) as the dispersion energies (per molecule) are proportional to molecular area A_x, and the area required by an adsorbed molecule is just equal to that required by m solvent molecules.   Selective interactions are, therefore, only considered in equation (9.3-3).

b.   There is an equivalent solvent-sample interactions in the adsorbed phase which cancels out the contribution of the individual terms E_{sl} and E_{xl} to ΔE.

The study of Janak[30] has shown that the liquid phase energy terms is 10% that for corresponding adsorbed phase energy terms.

The free energy of adsorption of X on the site i of an adsorbent is dependent upon some property of the adsorbate molecule and the particular adsorbent site and is given by

$$E_i = -F(X)f(A_i) \qquad (9.4-12)$$

Then we can write

$$E_{xa} = f(X)f(A_i) \qquad (9.4-13)$$

and

$$E_{sa} = f(S)f(A_i) \qquad (9.4-14)$$

Providing that the selective interactions between X or S and the adsorbent are of one type.   Substituting equations (9.4-13 and 9.4-14) into equation (9.3-3)

$$\Delta E = f(X)f(A_i) - f(S)f(A_i)$$

$$= fA_i[f(X) - f(S)]$$

$$= \alpha f(X,S) \qquad\qquad (9.4\text{-}15)$$

where α is the surface activity function and $f(X,S)$ is a sample-solvent function.

For adsorption of a sample molecule X, the thermodynamic equilibrium constant, K_{th}, is given by

$$K_{th} = N_{xa}/N_x \qquad\qquad (9.4\text{-}16)$$

where N_{xa} and N_x is the mole fraction of X in the adsorbed phase and unadsorbed phase respectively. In a linear isotherm system, where the sample concentration is low, the total number of moles of sample in the adsorbed (n_{xa}) and nonadsorbed (n_x) phase will be small compared to the total moles of solvent in the adsorbed (n_{sa}) and nonadsorbed (n_s) phases. The sample mole fractions are then equal to

$$N_x = n_x/n_s \qquad\qquad (9.4\text{-}17)$$

and

$$N_x = n_{xa}/n_{sa} \qquad\qquad (9.4\text{-}18)$$

Substituting equations (9.4-17) and (9.14-18) into equation (9.4-16)

$$K_{th} = n_{xa}n_s/n_x n_{sa} \qquad\qquad (9.4\text{-}19)$$

As described in section 2.1, $K°$, the equilibrium constant

is defined as

$$K^\circ = [X]_a / [X]_u$$

where $[X]_a$ and $[X]_u$ are the concentrations of X in the adsorbed (a) and non-adsorbed (u) phases in moles per gram and moles per millilitre repsectively. K° can be rewritten as

$$K^\circ = (n_{xa}/W)/(n_x/V_u) \qquad (9.4-20)$$

where V_u is the total volume of the unadsorbed phase in millilitres and W is the adsorbent weight in grams.

Elimination of n_{xa}/n_x between equations (9.4-19) and (9.4-20) gives

$$K^\circ = K_{th} n_{sa} V_u / n_s W \qquad (9.4-21)$$

If $V_a = n_{sa} V_u / n_s W$

where V_a is the volume of adsorbed solvent per gram of adsorbent in millilitres per gram , then substituting V_a into equation (9.4-22)

$$K^\circ = K_{th} V_a \qquad (9.4-23)$$

N_a is related to adsorbed surface area by

$V_a = 0.00035$ x (surface area, square metres per gram)

The quantity, V_a, is a fundamental property of the adsorbent and according to Snyder is independent of the nature of the solvent. Both the thermodyanmic and equilibrium constant

and adsorption energy, ΔE, are equal to

$$\log K_{th} = \Delta E = -\Delta G_a^\circ / 2.3RT \qquad (9.4\text{-}24)$$

where R and T refer to the gas constant and absolute temperature, respectively. Combining equations (9.4-23) and (9.4-24) gives

$$\log K^\circ = \log V_a + \Delta E \qquad (9.4\text{-}25)$$

Eliminating ΔE between equations (9.4-25) and (9.4-15) gives

$$\log K^\circ = \log V_a + \alpha f(X,S) \qquad (9.4\text{-}26)$$

Equation (9.4-26) expresses one of the fundamental relationships of adsorption chromatography.

For an adsorbed surface of standard activity ($\alpha=1$) using equation (9.4-15) gives

$$\Delta E = f(X,S)$$

and

$$E_{xa} = S^\circ$$

where S° is the sample adsorption energy of the standard activity adsorbent. Furthermore,

$$m = A_s / A_e$$

where A_s, A_e are the areas required by adsorbed sample and solvent molecules on the adsorbent surface.

The solvent parameter, ϵ°, can be defined as the

adsorption energy of the solvent per unit area of the standard activity surface, that is

$$\varepsilon^\circ = E_{sa}/A_e$$

For adsorption onto the standard activity adsorbent, equation (9.3-3) now takes the form

$$f(X,S) = S^\circ - A_x \varepsilon^\circ \qquad (9.4-27)$$

Eliminating $f(X,S)$ between equation (9.4-27) and equation (9.4-26)

Then

$$\log K^\circ = \log V_a + \alpha(S^\circ - A_x \varepsilon^\circ) \qquad (9.4-28)$$

For adsorbents of the same type equation (9.4-28) expresses K° as a function of certain fundamental properties of the adsorbent (V_a, α), sample (S°, A_x) and solvent (ε°). The solvent strength parameter, ε°, defines the effect of the solvent upon the adsorption of a given sample; the larger the solvent strength parameter the smaller is the value of K° for a given sample and adsorbent.

Equation (9.4-28) can also be rewritten in terms of capacity ratio, k', of a solute X by

$$\log k'_x = \log \frac{V_s}{V_m} + \beta(S^\circ_x - A_x \varepsilon^\circ_M) \qquad (9.4-29)$$

where

V_s = volume of adsorbed monolayer of eluent

V_m = volume of remaining eluent

$S^\circ_X = \Delta G^\circ_X / 2.303RT$ where ΔG°_X is the standard free energy of adsorption of solute X onto the surface from the reference solvent pentane

A_X = surface area of that part of X in contact with surface measured in units of 8.5 $\overset{\circ}{A}$. 8.5 $\overset{\circ}{A}^2$ is the notional area occupied by one aromatic cation.

$\varepsilon^\circ_m = \Delta G^\circ_m / 2.303\ RT$ where ΔG°_m is the standard free energy of adsorption of an amount of eluent sufficient to cover 8.5$\overset{\circ}{A}^2$. ε°_m is arbitrarily chosen as zero for the reference eluent R, that is $\varepsilon^\circ_R = 0$. The reference eluent in the polar adsorbents (Al_2O_3, SiO_2) is pentane and that, in case of non-polar materials like carbon, is methanol.

β = surface activity factor defined as unity for fully activated adsorbent and in practice falls in the range $0.7 < \beta < 1.0$.

In the calculation of the area covered by an adsorbed sample molecule the configuration of the adsorbed molecule must be known. For aromatic compounds one can assume flat adsorption. As discussed in section 9.4 the area A_X, would be the sum of contributions from each group i in the sample molecule as given in equation (9.4-6)

Thus,
$$A_X = \Sigma A_i \qquad\qquad (9.4-16)$$
where
$$A_i = (V_i/N)^{2/3} \qquad\qquad (9.4-30)$$

where V_i is the contribution to the molar volume of the solute from the group i, N is Avogadro's number and A_i is adjusted to be in units of 8.5 $\overset{\circ}{A}^2$.

Secondary Solvent Effects

According to Snyder[5] equation (9.4-29) is a reliable relationship only for adsorption systems with weak or moderately strong solvents. In the strongest solvent systems the equation is only a rough approximation due to secondary solvent effects. In its derivations two main assumptions have been made, namely

a. Interactions between solvent and sample molecules are assumed unimportant,

b. Interactions between the adsorbent and various adsorbate molecules are assumed to be fundamentally similar.

Equation (9.4-29) can now be corrected for secondary solvent effects by the addition of a correction term, Δeas. Thus

$$\log k'_x \ = \ \log \frac{Vs}{Vm} \ + \ (S^{\circ}_x - A_x \varepsilon^{\circ}_m) \ + \ \Delta eas \qquad (9.4-31)$$

The types of secondary solvent effects that can occur are

a. Hydrogen bonding in the liquid phase between sample and solvent which are highly specific and relatively strong.

b. The formation of strong-sample complexes which can affect k° of sample compounds.

9.4.4.2   The study of solvent strengths on PGC

9.4.4.2.1   Introduction

As noted in the earlier section the eluotropic strength, ε°, of the mobile phase is a very important

chromatographic parameter. In conventional liquid-solid chromatography on polar adsorbents such as silica gels and alumina the more polar the solvent the larger is its eluotropic strength. With carbon, a non-polar adsorbent, whose retention is based on the balance between the non-specific intermolecular interactions, the weakest solvents are supposed to be the most polar which is opposite to that of classical LC.

Using Snyder's assumption that specific molecular interactions between solute and eluent can be neglected, the eluotropic strength, ε°, can be determined from equation (9.4-29). For graphitic carbon, as shall be noted later solute-solvent interactions do actually play a major role. As a result of this, different scales of eluotropic strength are obtained depending upon the solute or method used to measure it.

In the calculation of the eluotropic strength parameter for carbon adsorbents, the surface activity factor, β, can be taken as unity. Water is undoubtedly the weakest solvent for carbon adsorbents and aromatic solvents such as benzene and xylene are generally the strongest. Methanol, which is a solvent of intermediate strength, is often, therefore, used as the standard solvent and arbitrarily given $\varepsilon_m^\circ = 0$. Further, since molecules are adsorbed flat on a graphitic surface equation (9.4-6) can be used to give the area A_x as a sum of contributions from the adsorbed groups. Table 9.4-2 lists values of A_x relevant to this work.

Table 9.4-2   Relevant Values of A_i in Snyder Units
of 8.5 $\overset{\circ}{A}{}^2$

Group	A_i/Su
Aromatic C	1.0
CH_3	1.0
CH_2	1.0
Cl	0.9
OCH_3	1.2
OH	0.4
CO	1.0
COOH	1.2
NH_2	0.6
$NHCH_3$	1.2
$N(CH_3)_2$	2.0
NO_2	0.6

(1 Su = 8.5 $\overset{\circ}{A}{}^2$)

It is widely believed that an eluotropic series should exist for carbon and that it should be the reverse of that for silica gel and alumina. If this were correct, the eleven solvents studied in this work should fall in the order given in Table 9.4-3 which lists Snyder's values for alumina and the values determined by Colin and Guiochon.[31]

Three different approaches can be used to calculate ε° from experimental values of retention of solutes. If the eluotropic concept is sound these should then give self-consistent results.

Method 1 Use of single solutes

The capacity factor, k', of a single solute X is measured in the reference solvent, R, and the solvent considered, M.

Thus

$$\log \frac{k'_{x,M}}{k'_{x,R}} = -A_x (\varepsilon^\circ_M - \varepsilon^\circ_R)$$

But $\varepsilon^\circ_R = 0$ (for methanol)

Then

$$\log \frac{k'_{x,M}}{k'_{x,R}} = -A_x \varepsilon^\circ_M$$

or

$$\varepsilon^\circ_M = \frac{1}{A_x} \log \frac{k'_{x,R}}{k'_{x,M}} \qquad (9.4\text{-}32)$$

Method 2 Use of homologous series

For a homologous series it is readily found that

$$\log k'_n = A + \alpha n \qquad (9.4\text{-}33)$$

Table 9.4-3 ε^O Values for Alumina[5] and Carbon

of Colin and Guiochon[31]

	ε^O	
	Al_2O_3	Carbon - Colin & Guiochon
Methanol	0.95	0
Acetonitrile	0.65	0.04
Dimethyl Formamide	-	-
Ethyl Acetate	0.58	0.13
Dioxan	0.56	-
Tetrahydrofuran	0.45	0.14
Dichloromethane	0.42	0.13
Chloroform	0.40	0.18
Methyl t-butyl Ether	0.30	-
Butyl Chloride	0.30	0.13
Hexane	0.01	0.10

When the logarithms of the capacity factors are plotted against the numbers of carbon atoms, n, the selectivity of the series, α, is given by the gradient of the linear plot.

Rewriting

$$\alpha_{CH_2} = \log \frac{k'_{n+1}}{k'_n} \qquad (9.4-34)$$

where k'_n, k'_{n+1} are the capacity ratios for homologues with n and $n+1$ carbon atoms. Then using the Snyder equation (9.4-29)

$$\alpha_{CH_2,M} = S^{\circ}_{CH_2} - A_{CH_2}\varepsilon^{\circ}_{M} \qquad (9.4-35)$$

where $S^{\circ}_{CH_2}$ and A_{CH_2} are the group contributions from the CH_2 group to S°_x and A_x. Thus

$$\alpha_{CH_2,M} - \alpha_{CH_2,R} = -A_{CH_2}(\varepsilon^{\circ}_{M} - \varepsilon^{\circ}_{R})$$

or

$$\varepsilon^{\circ}_{M} = \frac{1}{A(CH_2)}(\alpha_{CH_2,R} - \alpha_{CH_2,M}) \qquad (9.4-36)$$

Method 3   Use of functionality difference

ε°_{M} is calculated from the capacity factors, k', of pairs of solutes with a common difference in functionality. For example

Pair 1 $\emptyset - CO - CH_3$ and $\emptyset - CO - \emptyset$
                    A_1 B_1

Pair 2 $\emptyset - O - CH_3$ and $\emptyset - O - \emptyset$
                 A_2 B_2
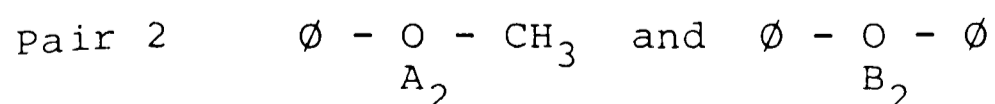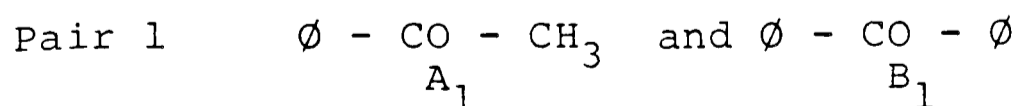
where $\emptyset = C_6H_5-$

Pairs 1 and 2 are similar in that B is made from A by replacing $-CH_3$ with $-\emptyset$. We can therefore write

$$\alpha_{A \to B} = \log \frac{k'_B}{k'_A}$$

and

$$\alpha_{A \to B,M} - \alpha_{A \to B,R} = -(A_B - A_A)(\varepsilon^\circ_M - \varepsilon^\circ_R)$$

or

$$\varepsilon^\circ_M = \frac{1}{(A_B - A_A)} (\alpha_{A \to B,R} - \alpha_{A \to B,M}) \qquad (9.4\text{-}37)$$

If the concept of an eluotropic series is to be useful, Methods 1-3 should give self-consistent results.

9.4.4.2.2 Experimental   Materials and Equipment

PGC was prepared as described in section 6.1. The specific surface of the adsorbent, PGC 64, is 154 m^2/g and its pore volume is 1.7 cm^3/g.

The pumping system used was Du Pont Instruments Chromatographic pump. The solutes were monitored with a Cecil UV detector. The solvents used were from Rathburn Chemicals and used without further purification. The solutes were obtained from various sources.

The column was of the Shandon type and was 120 mm long and 4 mm bore. PGC was packed at 1000 p.s.i. using methylene chloride as a slurry solvent and follower.

9.4.4.2.3 Results and Discussion

The capacity factors of a large number of solutes were measured in eleven different solvents. Different types of

solutes had been used namely alkyl and methyl benzenes, methylphenols, polyaromatic hydrocarbons acids and bases. The values of capacity factors of these solutes in the different solvents are given in Tables 9.4-4 - 9.4-10. These compounds are eluted over a large range of capacity ratios. ε° values of the eleven solvents were calculated using the three methods discussed earlier in the section. The results are reported in Tables 9.4-11, 9.4-12 and 9.4-13.

When many selected solutes are used in the determination of ε° by method 1, the ε°_M values do not fall in any self-consistent order as the solute is changed as indicated in Table 9.4-11. However, there is a general trend for dichloromethane and dimethylformamide to be the strongest solvents. Methanol and acetonitrile are both weak solvents for all solutes as in reversed phase except for phenols. This could be due to increased solute-solvent interactions of phenol in methanol; an important evidence that such solution interactions cannot be neglected as done by Snyder.[5] On the other hand, the surface also behaves as in classical adsorption chromatography. Dimethylformamide is generally a strong solvent for all solutes and hexane is a weak solvent for bases, phenols, ethers and aromatic hydrocarbons indicating the presence of specific sites for the adsorption of these solutes, most possibly acidic sites. As noted in section 9.4.3.1 localised adsorption is well accepted in classical adsorption theory and PGC is similar to silica and alumina in this respect. From Tables 9.4-3

Table 9.4-4
Variation in the value of k' of Alkylbenzenes
with different solvents

SOLUTE	MeOH	MeCN	CH_2Cl_2	THF	DMF	EtAc	B.Cl ^{a}	$CHCl_3$	Dioxan	MBE ^{b}	Hexane
Ethylbenzene	0.22	0.21	0.05	0.07	0.07	0.09	0.09	0.13	0.31	0.17	0.16
Propylbenzene	0.33	0.29	0.06	0.10	0.09	0.14	0.13	0.13	0.31	0.22	0.21
Butylbenzene	0.44	0.44	0.07	0.11	0.12	0.18	0.14	0.14	0.31	0.31	0.23
Amylbenzene	0.67	0.71	0.09	0.13	0.17	0.24	0.17	0.16	0.32	0.40	0.28
Hexylbenzene	1.00	1.09	0.12	0.16	0.19	0.29	0.19	0.17	0.34	0.50	0.34
Heptylbenzene	1.22	1.56	0.15	0.18	0.27	0.41	0.25	0.20	0.39	0.72	0.47
Octylbenzene	2.00	2.47	0.19	0.22	0.34	0.55	0.28	0.22	0.41	0.91	0.56
Nonylbenzene	3.72	4.83	0.24	0.26	0.44	0.69	0.36	0.24	0.47	1.25	0.69
n-Decylbenzene	5.62	8.76	0.30	0.29	0.60	0.93	0.44	0.27	0.50	1.73	0.88

a = Butyl Chloride

b = Methyl t-butyl Ether

Table 9.4-5

Variation in the value of k' of Polymethylbenzene
with different solvents

SOLUTE	MeOH	MeCN	CH$_2$Cl$_2$	THF	DMF	EtAc	B.Cl	CHCl$_3$	Dioxan	MBE	Hexane
Benzene	0.11	0.07	0.03	0.04	0.01	0.13	0.05	0.17	0.31	0.11	0.10
Toluene	0.31	0.16	0.06	0.09	0.04	0.15	0.12	0.19	0.32	0.25	0.13
m-Xylene	0.72	0.43	0.09	0.09	0.08	0.22	0.21	0.20	0.33	0.42	0.31
o-& p-Xylene	0.85	0.45	0.12	0.14	0.10	0.26	0.25	0.21	0.35	0.51	0.34
1,3,5 Trimethylbenzene	0.62	0.76	0.15	0.15	0.12	0.32	0.27	0.23	0.37	0.60	0.44
1,2,4 Trimethylbenzene	2.45	0.95	0.20	0.24	0.16	0.44	0.36	0.28	0.42	0.89	0.65
1,2,3,4 Tetramethylbenzene	4.27	3.89	0.59	0.63	0.40	1.29	0.93	0.51	0.69	2.69	1.91
1,2,4,5 Tetramethylbenzene	7.08	2.69	0.41	0.47	0.33	0.93	0.65	2.51	0.63	1.78	1.26
Pentamethylbenzene	17.40	10.23	1.15	1.26	0.96	2.75	1.70	0.79	1.17	5.62	3.72
Hexamethylbenzene	61.65	37.15	3.31	3.63	3.09	8.32	4.27	1.74	2.19	15.84	0.23

Table 9.4-6

Variation in the value of k' of Polymethylphenols
with different solvents

SOLUTE	MeOH	MeCN	CH_2Cl_2	THF	DMF	EtAc	B.Cl	$CHCl_3$	Dioxan	MBE	Hexane
Phenol	0.22	0.18	0.10	0.07	0.05	0.19	0.85	0.32	0.32	0.27	16.08
p-Cresol	0.67	0.70	0.36	0.12	0.09	0.33	1.26	0.38	0.36	0.46	High
3,5 Xylenol	1.56	1.27	0.42	0.15	0.11	0.47	1.72	0.39	0.38	0.62	-
2,3 Xylenol	1.78	1.70	0.48	0.21	0.15	0.61	1.63	0.46	0.41	0.79	-
2,4,5 Trimethylphenol	5.11	3.61	0.68	0.36	0.27	1.08	2.51	0.57	0.43	1.42	-

Table 9.4-7

Variation in the value of k' of Polyaromatic
Hydrocarbons with different solvents

SOLUTE	MeOH	MeCN	$CH_2 Cl_2$	THF	DMF	EtAc	BCl	$CHCl_3$	Dioxan	MBE	Hexane
Naphthalene	5.49	2.24	0.62	0.64	0.26	1.52	1.23	0.73	0.61	3.02	3.06
Acenaphthene	33.28	11.18	2.21	2.13	0.85	5.87	3.99	1.95	1.26	12.51	10.40
Tetralin	0.62	1.03	0.10	0.11	0.02	0.15	0.12	0.09	0.08	0.35	0.39
Biphenyl	7.19	2.24	0.50	0.67	0.25	1.32	1.11	0.54	0.65	3.18	3.05
o-Terphenyl	9.06	2.71	0.29	0.27	0.31	1.02	0.55	0.29	0.44	2.14	1.70

Table 9.4-8

Variation in the value of k' of Acids and
Phthalates with different solvents

SOLUTE	MeOH	MeCN	CH₂ Cl₂	THF	DMF	EtAc	BCl	CHCl₃	Dioxan	MBE	Hexane
Benzoic Acid	0.94	-	2.85	0.09	0.62	0.20	1.11	1.39	0.41	0.82	High
o-Toluic Acid	1.61	-	2.68	0.16	0.90	0.49	0.43	1.38	0.44	1.38	High
Phthallic Acid	-	0.40	-	0.39	Excluded	1.06	0.89	11.31	1.46	5.47	High
Salicyclic Acid	-	0.46	9.88	0.27	Excluded	2.95	3.82	2.50	1.05	0.16	High
Dimethyl Phthalate	1.92	1.09	0.15	0.15	0.10	0.45	0.43	0.24	0.34	1.15	0.65
Diethyl Phthalate	1.68	0.85	0.06	0.08	0.07	0.13	0.15	0.17	0.29	0.20	0.36
Di-n-Butyl Phthalate	1.92	2.74	0.09	0.08	0.13	0.48	0.30	0.17	0.31	1.32	2.27
Di-n-Nonyl Phthalate	2.61	17.12	0.16	0.11	0.32	1.23	0.45	0.17	0.32	3.58	3.85

Table 9.4-9

Variation in the value of k' of Bases
with different solvents

SOLUTE	MeOH	MeCN	CH₂ Cl₂	THF	DMF	EtAc	BCl	CHCl₃	Dioxan	MBE	Hexane
Aniline	0.17	Bad	0.12	0.08	0.04	0.22	0.23	0.18	0.31	0.37	1.24
Pyridine	0.17	-	0.62	0.17	0.06	0.62	0.41	0.33	0.63	0.69	1.29
2-Methyl Pyridine	0.31	-	1.06	0.10	0.09	0.24	0.29	0.21	0.38	0.37	1.18
Methyl Aniline	0.56	-	0.12	0.14	0.08	0.30	0.30	0.21	0.35	0.62	1.14
DiMethyl Aniline	0.56	0.80	0.15	0.24	0.12	0.48	0.44	0.27	0.40	1.10	1.10
Ethyl Aniline	0.94	-	0.15	0.18	0.13	0.38	0.35	0.24	0.38	0.76	0.62
Diethyl Aniline	1.44	0.59	0.15	0.14	0.15	0.32	0.27	0.22	0.36	0.69	0.63
Benzylamine	6.28	3.69	0.56	0.97	0.29	2.08	1.30	0.46	0.65	0.94	1.10

Table 9.4-10

Variation in the value of k' of Selected Solutes
with different solvents

SOLUTE	MeOH	MeCN	CH_2Cl_2	THF	DMF	EtAc	BCl	$CHCl_3$	Dioxan	MBE	Hexane
Acetophenone	1.01	0.67	0.08	0.18	0.10	0.32	0.31	0.27	0.37	0.74	1.05
Propiophenone	2.00	1.20	0.14	0.25	0.10	0.52	0.41	0.29	0.41	0.99	1.24
Benzophenone	4.58	2.26	0.24	0.44	0.13	0.76	0.69	0.28	0.52	2.45	4.05
Nitrobenzene	3.55	0.82	0.15	0.19	0.13	0.36	0.31	0.29	0.41	0.43	1.03
Anisole	0.44	0.31	0.07	0.13	0.06	0.20	0.19	0.22	0.29	0.39	0.38
Phenetole	0.81	0.50	0.12	0.16	0.10	0.27	0.24	0.30	0.36	0.54	0.46
Benzyl Alcohol	0.25	0.23	0.11	0.09	0.04	0.17	0.25	0.22	0.27	0.33	0.10
Chlorobenzene	0.44	0.40	0.11	0.11	0.73	0.19	0.17	0.23	0.33	0.31	0.27
Methyl Benzoate	1.58	1.06	1.18	0.25	0.13	0.46	0.39	0.30	0.41	0.89	0.97

Table 9.4-11 Eluotropic strength of solvents for

selected solutes
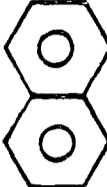
	Et	OH	NH$_2$	NO$_2$	naphthalene
Area/8.5 Å^2	8.0	6.4	6.6	6.6	10.0
Methanol	0.0	0.0	0.0	0.0	0.0
Acetonitrile	0.0	0.01	0.03	0.9	0.04
Dimethyl formamide	0.06	0.10	0.19	0.22	0.13
Ethyl Acetate	0.05	0.01	0.08	0.16	0.06
Dioxan	-0.02	-0.03	0.06	0.14	0.09
Tetrahydrofuran	0.06	-0.08	0.15	0.11	0.09
Dichloromethane	0.08	0.05	0.12	0.21	0.09
Chloroform	0.03	-0.03	0.21	0.17	0.09
Methyl t-butyl ether	0.01	-0.01	0.05	0.14	0.03
Butyl chloride	0.05	-0.10	0.08	0.17	0.06
Hexane	0.02	neg.	-0.03	0.08	0.03

Table 9.4-12 ε^O_M-values from homologous series

Eluent	Alkyl benzenes	Polymethyl benzenes	Polymethyl phenols	Mean
Methanol	0	0	0	0
Acetonitrile	-0.01	0.00	0.10	0.03
Dimethyl formamide	0.03	0.04	0.21	0.09
Ethyl Acetate	0.04	0.07	0.20	0.10
Dioxan	0.13	0.28	0.42	0.28
Tetrahydrofuran	0.08	0.10	0.22	0.13
Dichloromethane	0.06	0.09	0.32	0.16
Chloroform	0.11	0.21	0.36	0.23
Methyl t-butyl ether	0.04	0.07	0.21	0.11
Butyl chloride	0.08	0.14	0.31	0.18
Hexane	0.06	0.00	-	0.00

Table 9.4-13 ε^O_M-values from group replacement

	Pair 1 Acetophenone Benzophenone	Pair 2 Anisole Phenotole
Methanol	0.0	0.0
Acetonitrile	0.04	0.01
Dimethyl formamide	0.12	0.01
Ethyl acetate	0.07	0.03
Dioxan	0.12	0.04
Tetrahydrofuran	0.07	0.04
Dichloromethane	0.05	0.01
Chloroform	0.15	0.02
Methyl t-butyl ether	0.06	0.03
Butyl chloride	0.08	0.04
Hexane	0.03	0.04

and 9.4-11 it is immediately clear that

(i)   the range of ε° values on carbon is much smaller

        than on alumina (about 0.2 units compared to 1.0 units),

(ii)   there is, in fact, little correlation of ε° values

        on carbon with that on alumina,

(iii)   there is a slight indication that solvents with mid ε°

        values on alumina are the strongest solvents on

        carbon.

Method 2 was used in the determination of ε°_M for

three homologous series, alkylbenzene, polymethylbenzene

and polymethylphenols whose plots of log k' versus n are

shown in figures 9.4-3, 9.4-4 and 9.4-5 respectively.   The

gradients for each slope is α_M and represents the selectivity

of the solute.   Distinct differences in gradient are found.

Contrary to what a simple eluotropic theory would predict the

lines often cross indicating that ε°_M for the common

structural base differs from ε°_M for the homologous group (CH_2

or CH_3).   Table 9.4-12 lists ε°_M values obtained by this

method.   The ε°_M values is self-consistent for the three

homologous series and very similar to that noted by Colin

and Guiochon using pyrocarbon.[31]   Nevertheless the order

obtained is quite different from the order obtained by

Method 1.   The ε°_M values are also somewhat larger than

the values obtained from Method 1.   Polymethylphenols give

particularly large ε°_M values by this method.

In Method 3 the ε° values calculated from the first

pair are much greater than those from the second pair in
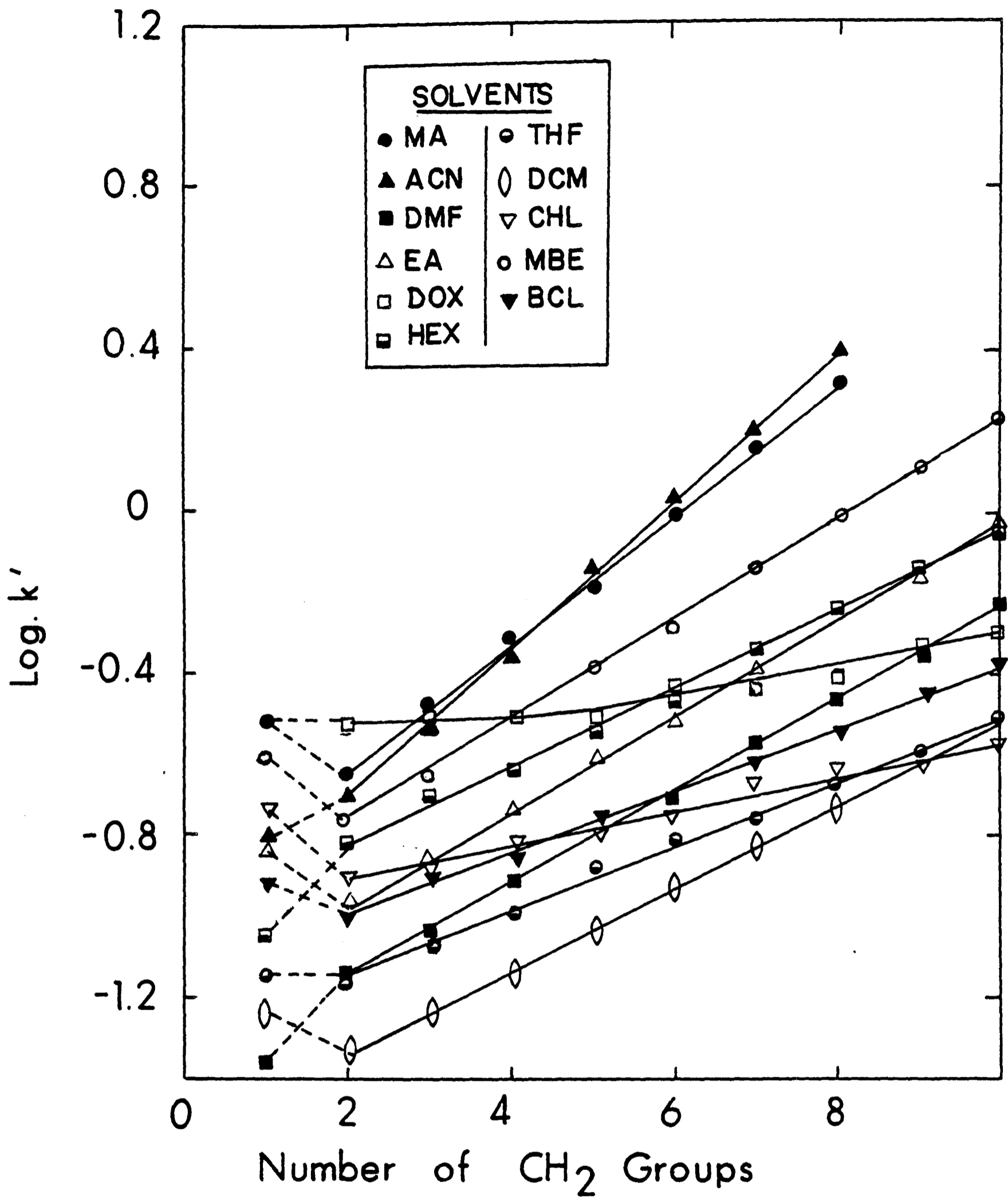
FIG. 9.4-3 : LOG. k′ VS. NUMBER OF CH$_2$ GROUPS
FOR ALKYLBENZENES IN DIFFERENT
SOLVENTS
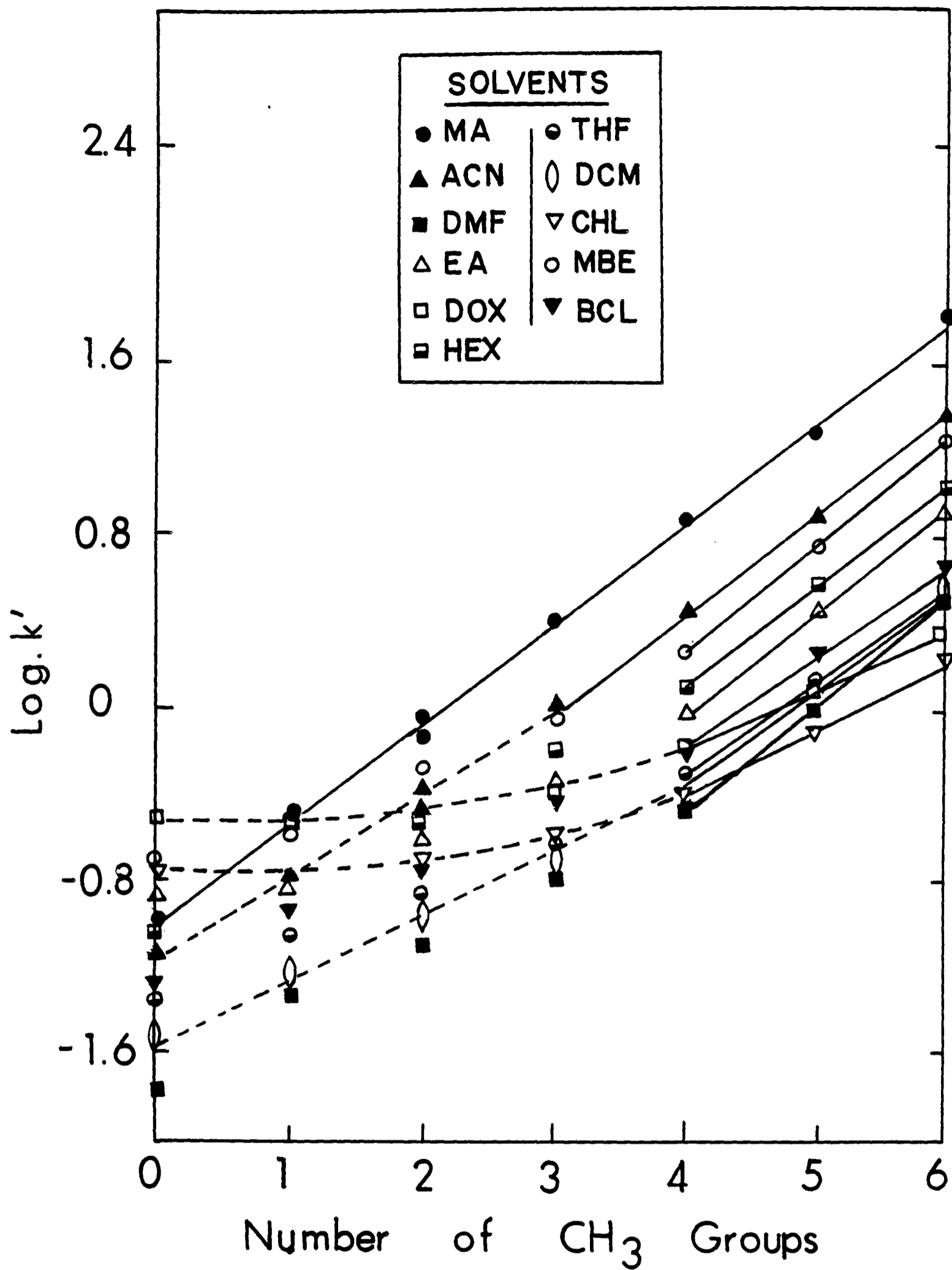
FIG. 9.4-4: LOG. k' VS. NUMBER OF CH₃
GROUPS FOR POLYMETHYLBENZENES
IN DIFFERENT SOLVENTS
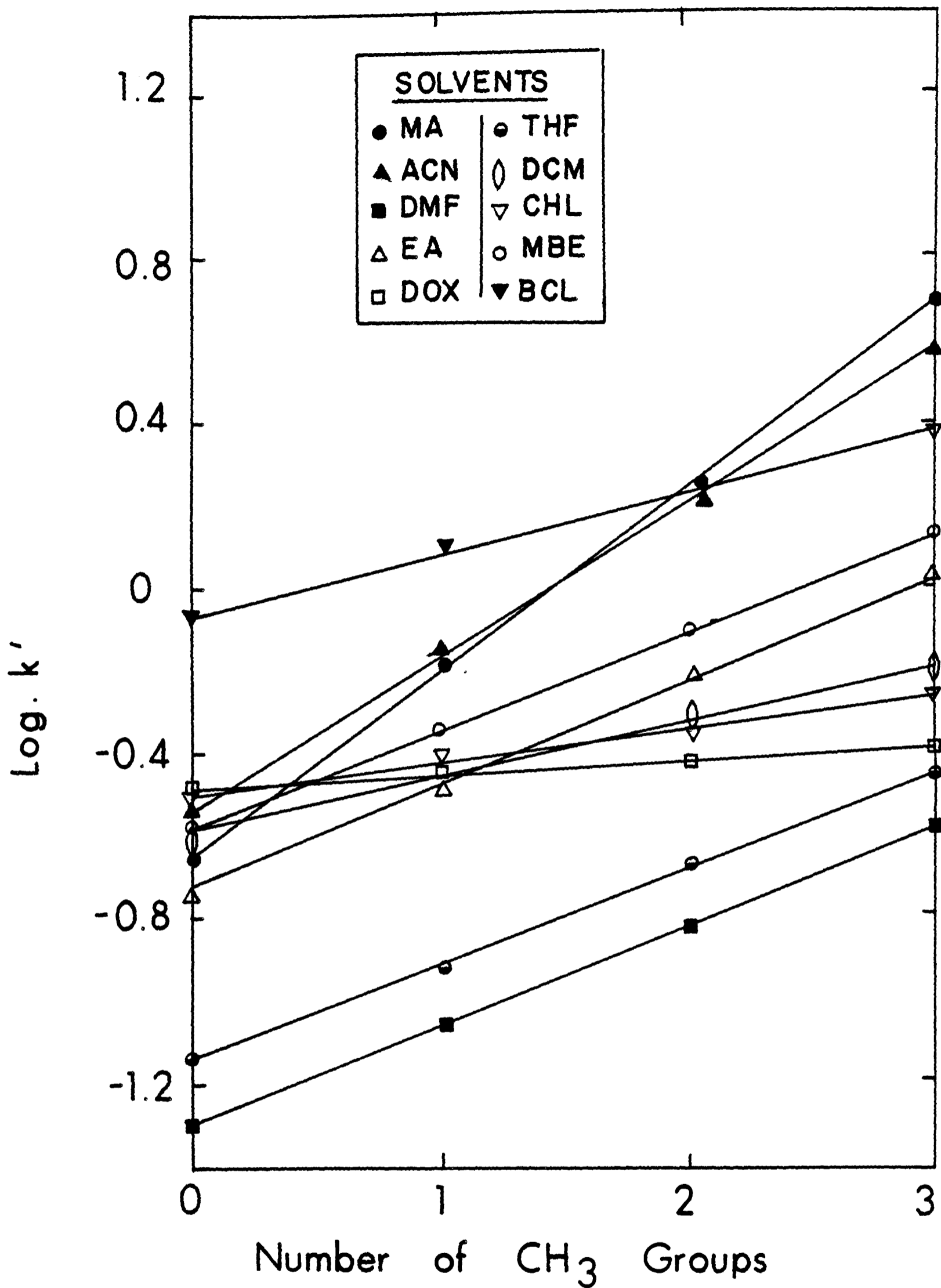
FIG.9.4-5 : LOG. k′ VS NUMBER OF CH₃ GROUPS FOR POLYMETHYLPHENOLS IN DIFFERENT SOLVENTS

spite of similarity of structure (Table 9.4-13).

Furthermore the orders of ε°_M values differ for the two

pairs. While methanol and acetonitrile are consistently

weak solvents, dioxan and chloroform are the strongest

as for the homologous series using Method 2.

9.4.4.2.4   Conclusions

(i)   The range of ε°_M values for porous 2D-graphitic

(PGC) is small in agreement with previous workers.

(ii)   Actual values of ε°_M for any eluent depend strongly

upon the solute or solute group used to determine

them.

(iii)   The three different methods of determining ε°_M

show little consistency either in regard to actual

values or in regard to ranking order.

(iv)   Notwithstanding conclusion (iii), there is evidence

for a weak eluotropic series, the order starting

with weakest eluents being

Methanol	Ethylacetate	Chloroform
Acetonitrile	Tetrahydrofuran	Dioxan
	Dichloromethane	Dimethyl Formamide
	Methylbutylether	
	Butyl chloride	
	Hexane	
Always weak	Variable dependent upon solute	strong for most solutes

Chapter 9 References

1. Hayward, D.O. and Trapnell, B.M.W., in Chemisorption, Butterworth, London, 1964.

2. Zweig, G., Anal. Chem., 31 (1959), 821.

3. Dintenfass, H.J., Chem. Ind. (London), 1957, 560.

4. Matsen, F.A., Makrides, A.C. and Hackerman, N., J. Phys. Chem., 22 (1954), 1800.

5. Snyder, L.R., in Principles of Adsorption Chromatography, 1968, Marcel Dekker, Inc., New York.

6. Kiselev, A.V., Discussions Faraday Soc., 40 (1965), 228.

7. Fowkes, F.M., Ind. Eng. Chem., 56 (1964), 40.

8. Belyakova, L.D., Kiselev, A.V. and Kovaleva, N.V., Zh. Fiz. Khim., 40 (1966), 1494.

9. Soczewinski, Anal. Chem., 46 (1974), 1384.

10. (a) Scott, R.P.W. and Kucera, P., Anal. Chem., 45 (1973), 749.

10. (b) Jermyn, M.A., Australian J. Chem., 10 (1957), 55.

11. Scott, R.P.W. and Kucera, P., J. Chromatogr. Sci., 13 (1975), 337.

12. Scott, R.P.W., Kucera P., J. Chr., 112 (1975), 425.

13. Scott, R.P.W., Kucera, P., J. Chr., 122 (1976), 35.

14. Scott, R.P.W., Analyst (London), 103 (1978), 37.

15. Scott, R.P.W. and Kucera, P., J. Chr., 149 (1978), 93.

16. Scott, R.P.W. and Kucera, P., J.Ch. 171 (1979), 37.

17. Kiselev, A.V., Zh. Fiz. Khim., 38 (1964), 2753.

18. Dubinin, M.M., Chemistry and Physics of Carbon, Vol. 2, 1966, p. 51.

19. Snyder, L.R., J. Phys. Chem., 67 (1963), 2622.

20. Snyder, L.R., J. Chromatogr., 6 (1961), 22.

21. Snyder, L.R., J. Phys. Chem., 67 (1963), 2344.

22. Snyder, L.R., J. Chromatogr., 8 (1962), 319.

23. Snyder, L.R., J. Chromatogr., 17 (1965), 73.

24. Charlton, J.K. and O'Neal, F.B., Talanta, 9 (1962), 39.

25. Bark, L.S. and Graham, R.J.T., J. Chromatogr., 23 (1966), 120.

26. Klemm, L.H., Chia, D.S.W., Kloppenstein, C.E. and Desai, K.B., J. Chr., 30 (1967), 476.

27. Jacques, J. and Kagan, H.B., in Chromatographie en Chimie Organique et Biologique, Vol. I (E. Lederer, ed.), Masson, Paris, 1959, pp. 559.

28. Feltkamp, H. and Koch, F., J. Chr., 15 (1964), 314.

29. Keulemans, A.I.M., in Gas Chromatography, Reinhold, New York, 1957.

30. Janak, J., in Chromatography (E. Heftmann, ed.), Reinhold, New York, 1967, Chap. 28.

31. Colin, H., Guiochon, G., J. Chromatogr., 122 (1976), 223.

Suppliers

1.	Alltech	28.	Laboratory Instrument Works, Prague, Czechoslovakia
2.	Altex	29.	Machery Nagel (Germany)
3.	Analabs	30.	MCB
4.	Anspec Co.	31.	Micromeritics
5.	Applied Science	32.	Perkin Elmer
6.	Beckman	33.	Phase Sep.
7.	Benson Co.	34.	Pierce
8.	Biolab Products	35.	Prolabo (France)
9.	BioRad Laboratories	36.	Rainen
10.	Brownlee	37.	Regis
11.	Calbiochem-Behring Corp.	38.	Rheodyne
12.	Chromanetics	39.	Rhone Poulene (France)
13.	Chromatix	40.	RSL
14.	Chrompak (Holland)	41.	Separations Group
15.	Dionex	42.	Shandon
16.	DuPont	43.	Shimadzu
17.	Es Industries	44.	Showa Denko
18.	Gow Mac	45.	Supelco
19.	Hamilton	46.	Synchrome
20.	Hetp	47.	Technicon
21.	Hewlett Packard	48.	Toyo Soda
22.	Hitachi	49.	Tracor
23.	HPLC Technology Ltd.	50.	Unimetrica Corp.
24.	ICN Inc.	51.	Varian
25.	Jasco	52.	Waters Associates
26.	Johns-Manville	53.	Whatman
27.	Jones Chromatography, Inc.		

Appendix 1

Packing materials for adsorption and conventional liquid-liquid partition chromatography

Type	Name	Shape[a]	Aver, d_p μm	Surface Area m^2g^{-1}	Suppliers
Pellicular	Corasil I[b]	S	37-50	7	52
Silica	Corasil II[b]	S	37-50	14	52
	Liqua-Chrom	S	44-53	<10	5
	Pellosil HC[c]	S	37-44	8	53
	Pellosil HS[c]	S	37-44	4	53
	SIL-X-II	S	30-44	12	41
	Zipax	S	25-37	∿1	16
Porous	Alltech Silica	I	10	–	1
Silica	Apex Silica	S	5	200	27
	BioSil HP	I	10	350	9
	Chromegasorb	I	5,10	500	6
	Chromosorb LC-6	I	5,10	400+	1,45
	Chrom Sep SI	I	5,10	400	49
	Finepak SIL-5	I	5	380	25
	Hitachi Gel 3030 Series	I	5-7	500	22
	HiChrom Si	S	5	220	37
	Hypersil	S	5-7	200	12,23,27,42
	ICN Silica	I	3-7 7-12	500-600	24
	LiChrosorb Si-60	I	5,10	550	2,5,10,12, 13,23,27, 18,45,50
	LiChrospher Si 100	S	5,10	250	1,5,21,23 27,45

Appendix 1 (cont.)

Type	Name	Shape[a]	Aver,dp μm	Surface Area $m^2 g^{-1}$	Suppliers
	Micropak Si	I	5,10	500	51
	Microsil	S	5,7	>400	31
	Nucleosil	S	5,7,10	300-500	1,14,23, 29,36,40, 45
	Partisil	I	5,10	400+	2,18,23,27 34,53
	μPorosil	I	10	300-350	1,52
	Polygosil 60	I	5,7,10, 15	500	14,23,29, 36,40
	R SIL	I	5,10	550	1,40
	Radial-Pak Si	S	10	200	52
	Sil-X-1	I	13,5	400	32
	Spherisorb SW	S	3,5,10	220	1,12,20,23, 27,33,37,45
	Separon Si VSK	S	5,7,10	450	28
	Supelcosil LC-Si	S	5	170	45
	Spheri-5 Silica	S	5	220	10,13,38
	Spherosil XOA600	S	5-7	600	3,39,45
	Techsil	I	5,10	385	35
	Ultrasphere-Si	S	5		2
	Vydac 101 TP	S	10	100	1,3,4,5,14, 41
Pellicular	Pellumina Hc[c]	S	37-44	8	53
Alumina	Pellumina HS[c]	S	37-44	4	53

Appendix 1 (cont.)

Type	Name	Shape[a]	Aver,dp μm	Surface area m^2g^{-1}	Suppliers
<u>Porous</u>	A5W, A10W, A20W	S	5,10,20	95	33
<u>Alumina</u>	Alox 60-D	I	5,10	60	14,29,36, 40
	Bio-Rad AG	I	<75	>200	9
	LiChrosorb AloxT	I	5,10	70	10,13,27,38
	Spherisorb AY	S	5,10	95	23,33,37,45

[a] S=spherical; I=irregular

[b] Corasil II has a thicker silica coating than Corasil I.

[c] HC (high capacity) material has a thicker coating than the HS (high speed) material.

Appendix 2

Packings for Ion-exchange Chromatography

Type	Name	Aver,dp μm	Functional Group	Suppliers
Anion-silica based	Partisil 10 SAX	10	$-NR_3^+$	2,18,23,27, 34,53
	LiChrosorb-AN	10	$-NR_3^+$	5,8,10,13, 27,18
	R SIL AN	5,10	$-NR_3^+$	1,40
	Vydac 301 TP	10	$-NR_3^+$	1,3,4,5,14, 41,45
	Nucleosil 5B	5,10	$-NR_3^++Cl^-$	1,2,10,14, 23,36,40
	Synchropak AX-300	10	Polymeric amine	4,5,37,46, 51
	Chromegabond SAX	10	$-NR_3^+$	6
	Microsil SAX	10	$-NR_3^+$	11
	Zorbax	7	$-NR_3^+$	16,23
	Micropak Ax	5,10	Difunction-alamino	51
	Micropak SAx	10	$-NR_3^+$	51
Anion-resin based (Porous Polymer)	Hitachi Gel 3011-N	10-15	$-NR_3^+$	22
	Benson BA-X	7-10	$-NR_3^+, Cl^-$	1,7,11
	Benson BWA	7-10	$-NR_2H\ Cl^-$	7
	Shodex Axpak	-	$-NR_3^+$	44
	Chromex	11	$-NMe_3^+$	15
	Aminex A Series	A-27,13 A-28, 9 A-29, 7	$-NR_3^+$	9,51

Appendix 2 (cont.)

Name	Name	Aver,dp μm	Functional Group	Suppliers
<u>Cation</u>	Partisil-10SCX	10	Benzyne-SO_3^-	1,2,18,23, 27,34,53
Silica	Lichrosorb-KAT	10	$-SO_3^-$	1,5,8,10, 13,23,38
based	RSIL-CAT	5,10	$-SO_3^-$	1,40
	Nucleosil SA	5,10	$-SO_3Na$	1,2,14,23, 29,36,40
	Vydac 401 TP	10	$-SO_3^-$	1,3,4,14, 15,41,45
	Chromega Bond SCX	10	$-SO_3H$	6
	Microsil SCX	10	$-SO_3^-$	31
	Zorbax SCX	6-8	$-SO_3^-$	16,23
Resin based	Aminex A Series	A-5, 13 A-7, 7-11 A-8, 5-8 A-9, 11	$-SO_3^-$	9,51
	Chromex Cation	11	$-SO_3^-$	15
	Hitachi Gel 3011-C	10-15	$-COOH$	22
	Hitachi Gel 3011-S	10-15	$-SO_3^-$	22
	Benson BC-X	7-10 10-15	$-SO_3^-Na^+$	1,7,11
	Beckman AA	W-1, 12 W-2, 9 W-3, 8	$-SO_3^-$	6
	Aminex HPX-87	AA 8 9	$-SO_3^-$	9
	Hamilton HC	10-15	$-SO_3^-Na^+$	19
	Shodex Cxpak	-	$-SO_3^-$	44
	Dionex Dc	9-14	$-SO_3^-$	15,34

Appendix 3

Chemically bonded stationary phases for HPLC

Bonded Phase	Designation	Base Material	Aver,dp μm	Supplier(s)
Octadecyl	ODS-Hypersil	Hypersil	5	42
hydrocarbon	Finepak SILC$_{18}$	Finepak SIL	10	
(C$_{18}$H$_{37}$Si$^-$)	Partisil ODS-1	Partisil	5,10	1,18,23,27, 34,53
	Partisil-10 ODS-2	Partisil	10	1,12,18,23, 34,53
	Partisil-10 ODS-3	Partisil	10	18,34,53
	LiChrosorb RP-18	LiChrosorb Si	5,10	1,5,10,12, 13,21,23,27, 38,45,50
	Spherisorb ODS	Spherisorb	5,10	1,12,20,23, 27,33,37,45
	Chromosorb LC-7	Chromosorb LC-6	3,5, 10	1,45
	Hitachi Gel 3050 Series	Hitachi Gel	5-7, 10-15	22
	μBondapak C$_{18}$	μPorasil	10	1,23
	Zorbax ODS	Zorbax SIL	6	1,12,16,23 45
	Vydac 201 C$_{18}$	Vydac TP	5,10	1,3,4,5,14,41,45
	Nucleosil C$_{18}$	Nucleosil 100	5,7, 10	1,14,23,29, 36,40
	Bio-Sil ODS-10	BioSil HP-10	5,7	31
	Ultrasphere-ODS	Ultrasphere -Si	3,5	2
	Rodiak Pak C$_{18}$	Radial-Pak Si	10	52
	Micropak CH	LiChrosorb Si60	5,10	51
	Spherosil-C$_{18}$	Spherosil	5-7	3,32,39,45

Appendix 3 (cont.)

Bonded Phase	Designation	Base Material	Aver,dp μm	Supplier(s)
Short Chain Hydro-carbon	Finepak SIL C$_8$	Finepak SIL	10	25
	LiChrosorb Rp-8	LiChrosorb	–	1,5,10,12,13, 21,23,27,38, 45,50
	Alltech C$_8$	Alltech Si	10	1
	Nucleosil C$_8$	Nucleosil	5,7,10	1,14,23,29,36, 40,45
	SAS-Hypersil	Hypersil	5	
	Ultrasphere-Octyl	Ultrasphere-Si	5	2
	Radial Pak C$_8$	Radial Pak Si	10	52
	Techsphere C$_8$	Techsphere	5,10	23
Phenyl-silane	μBondapak Phenyl	μPorosil Corasil	10	1,23
	Nucleosil Phenyl	Nucleosil 100	5-7	1,14,29,36 40
	Spherisorb P	Spherisorb	5	1,12,23,33
Allylphenyl	Allylphenyl-SIL-X-I		8-18	32
Fluroether	Fe-SIL-X-1		8-18	32
Ether	Permaphase ETH		25-37	16
Nitro	Nucleosil NO$_2$		5,10	29

Appendix 3 (cont.)

Bonded Phase	Designation	Base Material	Aver, d_p μm	Supplier(s)
Cyano	Co.Pell PAC		41	53
	Vydac Polar Phase		30-44	41
	μBondapak CN		10	52
	Nucleosil CN		5,10	29
	Micropak CN		10	51
	Partisil-10-PAC		10	53
	Spherisorb S5CN		5	33
Hydroxyl	Durapak Carbowax 400/Corasil		37-50	52
	Durapak Carbowax 400/Corasil		37-75	52
	LiChrosorb Diol		10	
Amino	APS-Hypersil		5	42
	Amino-SIL-X-I		8-18	32
	μBondapak NH_2		10	52
	LiChrosorb NH_2		10	
	Micropak NH_2		10	51
	Nucleosil NH_2		5,10	29
	Nucleosil $N(CH_3)_2$		5,10	29
Anion	Bondapak Ax/Corasil		37-50	52
Exchanger	Perisorb AN		30-40	
	Permaphase AAX		25-37	16
	Partisil-10 SAX		10	53
	Vydac TP Anion Exchanger		10	41
Cation	Bondapak CX/Corasil		37-50	52
Exchanger	Perisorb KAT		30-40	
	Partisil-10 SCX		10	53
	Vydac TP Cation Exchanger		10	41

Porous Glassy Carbon, A New Columns Packing Material for Gas Chromatography and High-Performance Liquid Chromatography

M. T. Gilbert / J. H. Knox / B. Kaur

Wolfson Liquid Chromatography Unit, Department of Chemistry, University of Edinburgh, West Mains Road, Edinburgh EH9 3JJ

Key Words

Gas and liquid chromatography
Porous glassy carbon stationary phase
Preparation and evaluation

Summary

A new carbon for liquid and gas chromatography, called "porous glassy carbon" (PGC) is described. The material is made using a porous template filled with carbonizable resin. After firing in an inert atmosphere the template is removed. PGC has been made with surface area ranging from 20 m²/g to 400 m²/g. It is of adequate strength for gas and high-performance liquid chromatography. In gas chromatography it is similar to the commerical graphitized thermal carbon black (GTCB) "Carbopack B", but has somewhat less retention per unit surface area and is much more robust. It gives symmetrical peaks for hydrocarbons with k'-values up to at least 100. In liquid chromatography it is similar to the GTCB's coated with pyrolytic carbon described by Guiochon. It behaves as a strong reversed phase adsorbent. Fairly good peak symmetry is maintained for k'-values up to at least 10 but trace additives to the eluent may be necessary to control peak asymmetry. PGC has considerable potential as a new packing material in both gas and liquid chromatography.

Introduction

Active carbons have long been used as adsorbents in classical liquid chromatography [1]. With the advent of gas chromatography attention turned to graphitized thermal carbon black (GTCB) [2]. These were found to be suitable nonpolar adsorbents either for gas-solid chromatography [3, 4] or, when coated with a small percentage of liquid phase as a "tailing reducer", for gas liquid/solid chromatography [5–7]. The carbon surface could also be modified by adsorp-

tion of small quantities of suitable involatile compounds to effect specific separations [8, 9]. These applications have been extensively reviewed [10]. Recently high efficiencies have been reported for short columns (21 mm long) packed with 20–25 μm GTCG particles coated with ≈ 1% stationary phase [11], and a novel active carbon, prepared by the reduction of polytetrafluorethylene by lithium amalgam [12], has been examined as an adsorbent for gas chromatography.

The poorly defined surface properties of active carbons used in classical liquid chromatography have been responsible for their almost complete neglect as adsorbents for high-performance liquid chromatography (HPLC). However, the desire for non-polar adsorbents with improved pH stability over the alkyl-bonded silica materials has led to renewed interest in the production of suitable carbons for this purpose. Unfortunately the otherwise attractive GTCB's are unsuitable because of their extremely poor mechanical stability: several attempts have been made to overcome this limitation either by treating GTCB, or by developing entirely new materials. Initial experiments by Guiochon and co-workers [13–15] involved the consolidation of GTCB aggregates by deposition of pyrolytic carbon from the vapour phase pyrolysis of benzene followed by graphitization of the product. Later, pyrolysis was performed on silica [16, 17]: this resulted in a more robust material but one that could not be graphitized due to the volatility of silica. In addition it was difficult to obtain adequate coverage of the internal surface of the silica without completely plugging the pores of the material. The active carbon prepared by the electrochemical reduction of PTFE [18, 19] also turned out to be a relatively strong material but contained a high content of oxygen and was of exceedingly high surface area, which could, however, be reduced by various treatments. The surface was also modified by an octyl Grignard reagent to give a material with properties intermediate between those of the original carbon and of octyl silica [20]. Porous carbons have also been produced by calcination of purified active carbons and cokes [21]. Unfortunately none of the above materials has given adequate chromatographic efficiency for solutes with capacity ratios exceeding about 2. Undoubtedly the best liquid chromatographic results have

been obtained using a weakly consolidated GTCB, Carbopack C, which was ground and fractionated to provide small particles [22]. The material was, however, very fragile and can hardly be regarded as a useful HPLC column packing material. Nevertheless this important piece of work showed clearly that the ideal surface, as in gas chromatography, is that of graphite.

The lack of success with the existing carbon materials is almost certainly due to the difficulty of obtaining hard materials which are free from micropores [23]. Active carbons, for instance, tend to lose all their porosity when heated to a sufficient temperature to eliminate the micropores, whereas graphitized materials, as already noted, are too fragile. The optimum compromise has not yet been achieved but may lie with a composite material having a strong particle framework coated with a thin graphitic layer.

With these problems in mind we were led to examine the possibility of avoiding micropores by preparing a macro- or meso-porous, but otherwise dense carbon, by using a template of appropriate porosity within those interstices a non-porous carbon could be deposited: the template could then be subsequently removed [24]. This paper describes initial experiments aimed at preparing porous glassy carbons suitable for both gas chromatography and high-performance liquid chromatography.

In brief, porous glassy carbon (PGC) is produced by impregnating a suitable silica gel or porous glass with a phenol-formaldehyde resin mixture. After polymerisation within the pores of the template material the polymer is converted to glassy carbon by heating in an inert atmosphere to about 1000 °C. The silica template is then removed by alkali to give PGC. Finally the material is fired in an inert atmosphere at a high temperature in the range 2000–2800 °C to anneal the surface, remove micropores and, depending upon the temperature, produce some degree of graphitization. The particle size, shape, porosity and pore size are determined by the choice of the template material; the surface chemistry is determined by the final heat treatment and any subsequent chemical treatment. It is thus possible in principle to produce PGC's with a range of pore and surface properties tailored to specific requirements.

Experimental

Materials

Batches of PGC were prepared according to the published procedure using analytical grade reagents [24]. Samples were fired in argon at temperatures from 1400 °C to 2600 °C. The products were characterised by C.H.N. analysis (Departmental Analytical Service) and by thermogravimetric analysis and by using a Stanton Redcroft TG770 thermobalance; specific surface area was determined by the B.E.T. method [25] using equipment constructed in the department, and pore volume was determined by a home-made medium pressure mercury porosimeter which enabled the total particle volume to be determined; the pore volume was then obtained assuming a density of 2.20 g/cm³ for the carbon structure. Some products were examined by a Cambridge Instruments "Stereoscan 604" scanning electron microscope.

Products for use in gas chromatography were sized by sieving, and those for HPLC either by sieving (down to 37 μm) or by sedimentation. A sample of uncoated Carbopack B was kindly provided by Supelco Inc.

Chromatographic Equipment

Gas chromatography was carried out using a Varian Series 1400 gas chromatograph fitted with a flame ionisation detector. The carrier gas was nitrogen. Columns were of 1/8″ outer diameter 2 mm bore stainless steel (0.9 m in length) or silanized glass of the same diameter and bore (1.5 m in length). The injector temperature was maintained at least 20 degrees above the column temperature.

HPLC was performed on home assembled equipment comprising an Altex 110A high pressure pump, a Rheodyne 7125 injection valve, and a Cecil Instruments CE212 ultraviolet photometric detector. Columns were either of the Shandon Southern Instruments pattern (100 mm long, 5 mm bore) or of the HETP pattern (100 mm long, 2 mm bore) when the quantity of material was limited. Columns were packed at 1000 psi (70 bar) by the upward-flow slurry method with dichloromethane as the slurry liquid and methanol as follower. Solvents of HPLC grade were obtained from Rathburn Chemicals, Walkerburn.

Table I. Physical properties of porous glassy carbons

Batch No.	Template			Carbon before firing		Firing conditions		Carbon after firing	
	Material	A/m² g⁻¹	Vp/cm³ g⁻¹	A/m² g⁻¹	% carbon	Temp °C	Time/min	A/m² g⁻¹	Vp/cm³ g⁻¹
PGC 6	Porasil A60X	~400	0.85	644	92.1 (a)	1400 (c) 1600 (c)	150 150	563 593	— —
PGC 7	Porasil B60X	~400	0.85	621	88.9 (a)	1800 (a) 2000 (d) 2200 (d)	45 30 15	403 370 347	— — —
PGC 19	Corning Porous Glass	12.5	0.99	—	81.0 (a)	2340 (d)	15	21.2	1.54
PGC 20	Corning Porous Glass	94	0.85	—	73.3 (a)	2340 (d)	15	—	—
PGC 26	6 μm spherical Silica Gel	~200	0.6	—	83.6 (a)	2400 (d)	15	382	1.40
PGC 57	Silica Gel irregular	~200	1.50	374 (f)	97 (b)	2600 (e)	30	80	0.35
Carbopack B — as supplied —								80	1.03

(a) by CHN analysis   (c) firing by Carbolite   (e) firing by Anglo Great Lakes
(b) by TGA analysis   (d) firing by AERE Harwell   (f) pore volume before firing 1.06 cm³/g

Results and Discussion

Materials

The physical properties of the batches of PGC and of their respective template materials are listed in Table I. Materials of a wide range of surface area, A, and pore volume, Vp, were prepared by appropriate choice of the template material and firing conditions. Unlike the active carbons which initially possess very high surface areas but lose them on heating, PGC's retain a substantial proportion of their original surface areas even when heated to very high temperatures. Thus up to about 1600 °C the surface area is unchanged (entries for PGC6) even with a duration of firing of 150 min. With firing temperatures of 1800 °C to 2200 °C there is a significant reduction in the original area (PGC 7) with moderate duration of heating (45 to 15 min). Heating for 30 min at 2600 °C (PGC 57) has a fairly dramatic effect on the surface area and pore volume (the pore volume of the unfired material was $1.06 \, cm^3/g$). Indeed the volume of $0.35 \, cm^3/g$ may be partly or even largely present as closed pores since the medium pressure mercury porisimetric method makes no distinction between open and closed pores.
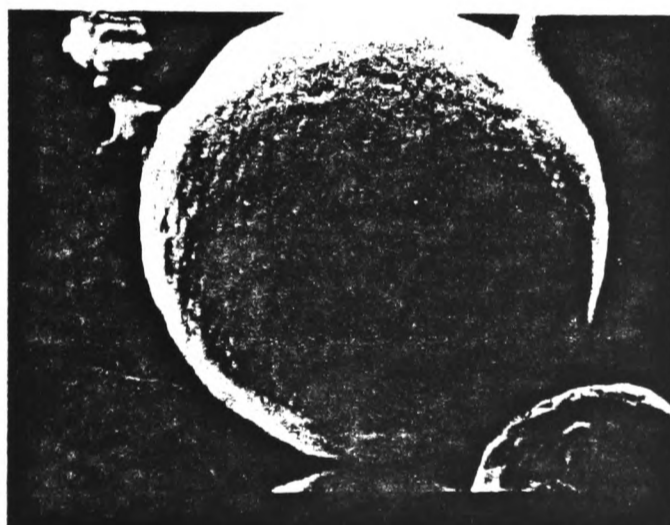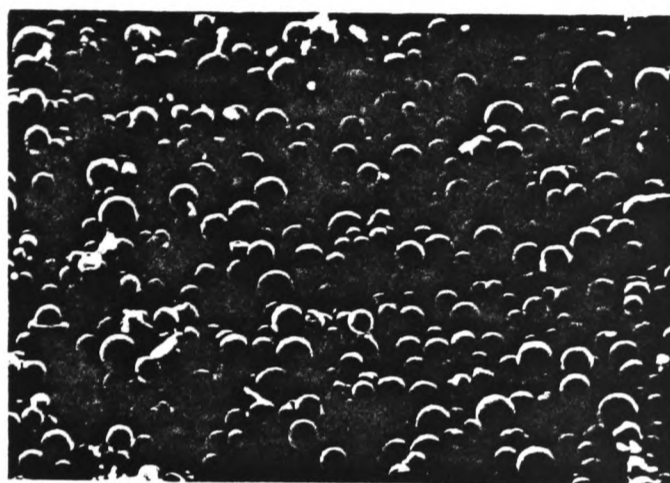

Fig. 1
Scanning electron micrographs of PGC 26, mean particle diameter of template 6 μm. Pore size ~ 10 nm.

The materials tested for chromatography were PGC's 19, 20, 26 and 57. These materials were all sufficiently hard to be useful under both GC and HPLC conditions although those materials with high pore volumes were rather too fragile for routine HPLC use. However, PGC 57 made from a highly porous template was of sufficient strength for normal HPLC use both before and after high temperature firing. Unfortunately (see below) the pore structure of fired PGC 57 appears to be unsatisfactory in that its chromatographic performance is substantially poorer than that of the more open PGC 19.

It is a noteworthy feature of the process for preparing PGC that the shape of the original template material is retained in the final product. This is clearly shown by the scanning electron micrograph of PGC 26 shown in Fig. 1: the particles are not only spherical but of the correct mean diameter of around 6 μm.

It becomes clear from the above that the firing temperature, the duration of firing and the initial template porosity require to be carefully chosen to obtain the optimum combination of particle hardness, porosity, surface area, and surface structure for any chromatographic purpose.

Gas Chromatography

To establish the GC characteristics of PGC the retention of a number of representative solutes was determined on PGC 19 (low surface area and high porosity) and PGC 57 (moderate surface area and low porosity). The results were compared with those obtained on uncoated Carbopack B.

A selection of the solutes used by McReynolds [26] to characterise liquid stationary phases gave the k'-values and retention indices, I, listed in Table II. The ΔI-values are those for the carbons less those obtained by McReynolds for squalane. The ΔI-values are all significantly negative and indicate the extremely non-polar nature of the two types of carbon. The similarity in the retention indices of the two carbons indicates the similarity in their surface chemistry. However, retention on Carbopack B is much stronger than

Table II. Retention data for McReynolds' solutes on PGC 19 at 120 °C and Carbopack B at 200 °C

Solute	0.9 m PGC 19/120 °C			1.5 m Carbopack B/ 200 °C		
	k'	I	ΔI	k'	I	ΔI
benzene	4.7	570	− 83	8.4	565	− 88
pyridine	6.4	600 (a)	− 99	9.6	675 (a)	− 124
1,4-dioxane	2.5	520	− 134	3.6	496	− 159
butanol	2.4	520	− 70	3.9	500	− 90
pentan-2-one	4.7	570	− 57	8.7	565	− 62
nitropropane	2.5	520	− 132	5.1	625	− 127
n pentane	1.9	500 (b)	−	4.2	500 (b)	−
n hexane	6.4	600	−	12.0	600	−
n heptane	23	700	−	−	700	−

(a) Peaks for Pyridine were severely tailed thus values are subject to considerable uncertainty and likely to be larger at limit of zero sample size.
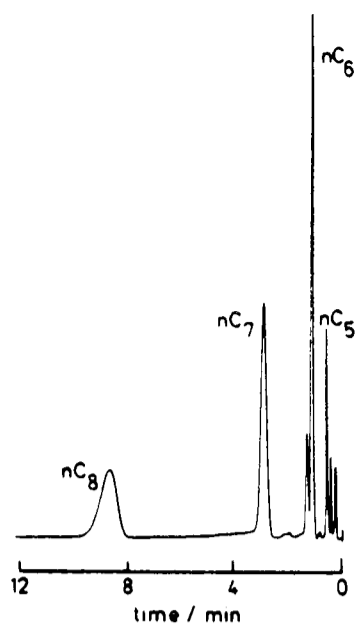
(b) Values by definition for n-alkanes.

Fig. 2

Gas chromatogram of n-al-kanes on PGC 19 at 140 °C.

benzenes. In general the plate number for the later peaks in these chromatograms is about 900 giving a plate height of about 1 mm for k' values in the range 40–90, and a reduced plate height h = H/d$_p$ ≅ 6. The peak symmetry throughout is seen to be excellent. Fig. 4 shows that the expected linear relationship holds between Log$_{10}$ k' and the carbon number in a homologous series for alkanes and alkyl benzenes for both Carbopack B and PGC 19. The logarithmic separation factors defined in eq. (1)

Separation factor, $\alpha' = \mathrm{Log}_{10}\,(k'_{n+1}/k'_n)$ (1)

(where k'_{n+1} and k'_n are the k'-values corresponding to molecules with n + 1 and n carbon atoms respectively) are 0.45 for alkanes and 0.42 for alkyl benzenes with PGC 19 and 0.43 for alkanes and 0.38 for alkyl benzenes with Carbopack B. A similar value of 0.41 for alkanes on GTCB may be obtained from ref. [2]. The k' values obtained by us are also similar to those obtained by Kiselev and Yashin [2] after allowance is made for the different specific surface areas of the materials. PGC 19 is a highly selective adsorbent as can be seen from the separation of the four butyl benzenes shown in Fig. 5. The excellent peak symmetry

on PGC in spite of the higher temperature of elution from the former. Table II lists data for alkanes and alkyl benzenes. The similarity between the two materials is again evident. k'-values on Carbopack B at 270 °C are on average 5.2 times those on PGC 19 and 200 °C. At first sight this factor might be attributed to the differences in surface area per cm^3 of material (54 m^2/cm^3 for Carbopack B and 10.5 m^2/cm^3 for PGC 19, a ratio of exactly 5.2). However, this does not take into account the difference of 70 °C in elution temperature. Assuming a mean heat of adsorption for the solutes of about 50 kJ/mol, it is readily calculated using the Van't Hoff equation that the k' values on Carbopack B are about five times those expected on PGC 19 at the same temperature allowing for the area difference. Thus Carbopack B is intrinsically more retentive than PGC 19. The reason for this may be a higher degree of graphitization of Carbopack B is required, but further work is required.

Fig. 2 shows a typical chromatogram of C$_5$ and C$_8$ alkanes on PGC 19 and Fig. 3 shows a chromatogram of some alkyl
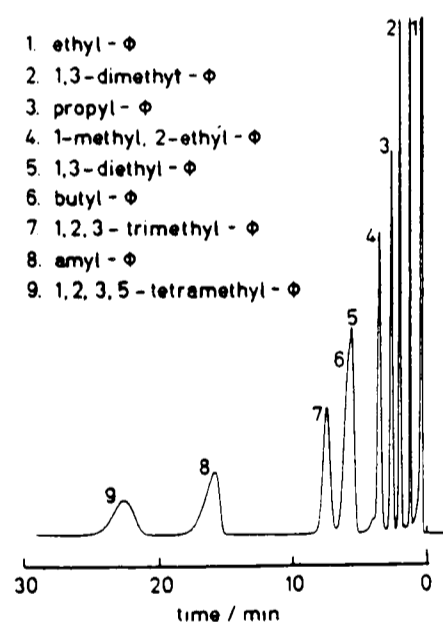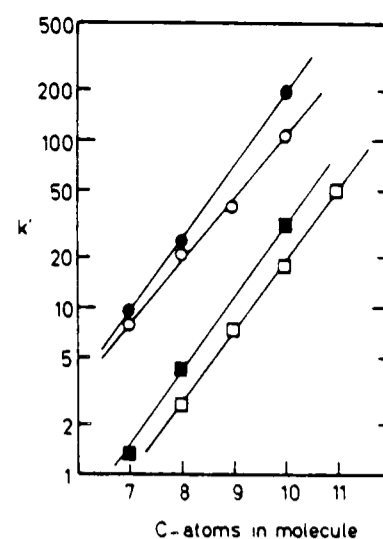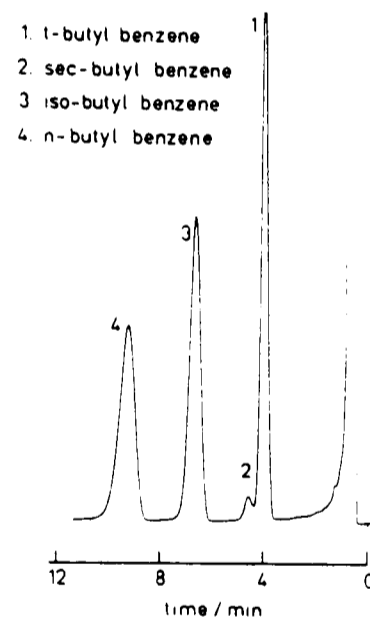

1. ethyl - Φ
2. 1,3-dimethyl - Φ
3. propyl - Φ
4. 1-methyl, 2-ethyl - Φ
5. 1,3-diethyl - Φ
6. butyl - Φ
7. 1,2,3 - trimethyl - Φ
8. amyl - Φ
9. 1,2,3,5 - tetramethyl - Φ

Fig. 3

Gas chromatogram of alkyl benzenes on PGC 19 at 200 °C. Φ indicates benzene ring.

1. t-butyl benzene
2. sec-butyl benzene
3. iso-butyl benzene
4. n-butyl benzene

Fig. 5

Gas chromatogram of butyl benzenes on PGC 19 at 200 °C.

Table III. Retention data for n-hydrocarbons and aromatic hydrocarbons on PGC 19 at 200 °C and Carbopack B at 270 °C

Solute	0.9 m PGC 19/ 200 °C		1.5 m Carbopack B/270 °C	
	k'	I	k'	I
Heptane	1.33	700 (a)	9.4	700 (a)
Octane	4.4	800	24.5	800
Decane	32	1000	19.5	1000
Toluene	1.33	700	7.8	690
Ethylbenzene	2.6	760	20.6	775
n-propylbenzene	7.3	850	39.8	840
n-butylbenzene	17.6	940	107	945
n-amylbenzene	50	1050	–	–
Isopropylbenzene	4.6	795	25.8	800
t-butylbenzene	7.8	845	42.6	850
Isobutylbenzene	14	905	73.4	905
sec-butylbenzene	9.3	865	51.4	865
o-xylene	6.6	830		
m-xylene	5.6	815		
p-xylene	6.6	830		
p-ethyltoluene	11.6	885		
m-ethyltoluene	12.2	890		
o-ethyltoluene	12.2	890		
o-diethylbenzene	21.6	935		
m-diethylbenzene	22.0	935		
p-diethylbenzene	23.3	945		
1,2,3-trimethylbenzene	29.5	975		
1,2,4-trimethylbenzene	25.5	960		
1,3,5-trimethylbenzene	22.0	940		
1,2,3,5-tetramethylbenzene	91.0	1085		
1,2,3,4-tetramethylbenzene	109.4	1105		
1,2,4,5-tetramethylbenzene	103.4	1100		

(a) Values by definition for n-alkanes

Table IV. Retention data for polar aromatic compounds on a 0.9 m column of PGC 19 at 180 °C

Solute	k'	As (a)	I
Aniline	9.0	1.33	745
Phenol	6.0	2.0	710
Anisole	15.0	1.0	790
Phenetole	43.5	1.5	900
Nitrobenzene	29.0	1.6	855

(a) Asymmetry factor measured at 10% peak maximum height

found with the hydrocarbons is also observed with polar compounds as noted from Table IV. The asymmetry factors are calculated at 10% of maximum peak height.

Graphitized carbon blacks have been particularly widely used for separations of lower hydrocarbons. PGC 19 with its low surface area is suitable for the separation of the lower alkanes as shown in Fig. 6a. The separation of the four isomeric butenes is particularly noted: Fig. 6b shows the separation on Carbopack B at 100 °C and Fig. 6c shows the separation on PGC 19 at 50 °C. There is a slight difference in selectivity but both materials separate all four isomers. PGC 19 does not have sufficient retentive power to separate the C_2 hydrocarbons but PGC 57 with a surface area of about 80 m²/g gives a good separation of methane, acetylene, ethylene and ethane (Fig. 6d). This order is an excellent indication of the nonpolar nature of the PGC. The poor plate efficiency of around 300 was not a function of the sample size and therefore cannot be due to a non-linear adsorption isotherm and surface heterogeneity: it is most likely to be due to poor mass transfer characteristics which in their turn probably arise from severely constricted pores in this material which has an unusually low pore volume.

Heats of adsorption of the C_2-C_5 alkanes were determined on PGC 57 and PGC 19 from measurements of k' over suitable temperature ranges from 20–130 °C. The results are compared with those of Kiselev and Yashin [2] and with heats of vapourisation in Fig. 7. The values of ΔH_{ads} are generally self consistent and greater than ΔH_{vap} in agreement with observations of strong retention of the solutes at
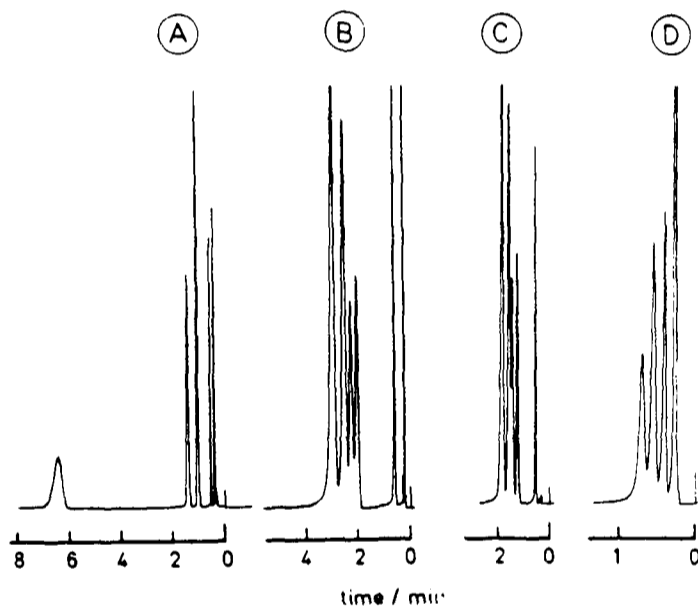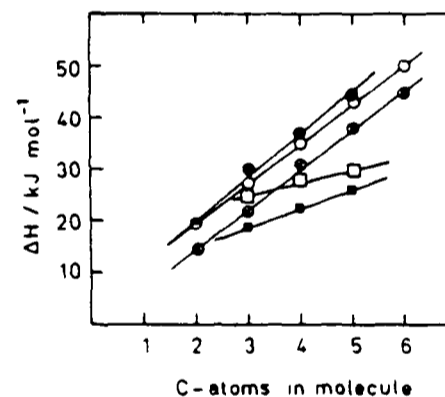

Fig. 6

Gas chromatograms of lower hydrocarbons: major peaks are identified in order of elution.

A C_1 + C_2; C_3; i-C_4; n-C_4; nC_5 alkanes on PGC 19 at 30 °C.

B C_1 + C_2; C_3=; 1-C_4=; i-C_4=; cis2-C_4=; tr2-C_4= alkenes on Carbopack B at 100 °C.

C As B omitting C_1 + C_2 on PGC 19 at 50 °C.

D CH_4, C_2H_2, C_2H_4, C_2H_6 on PGC 57 at 20 °C.

Fig. 7

Dependence of ΔH_{ads} and ΔH_{vap} of alkanes on carbon numbers for GC of n-alkanes.

● PGC 57, ○ Kiselev and Yashin [2] GTCB (theoretical)

⊗ Kiselev and Yashin [2] GTCB (experimental)
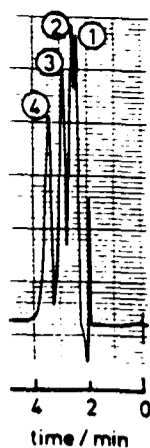
□ PGC 19, ■ Heat of vapourization.

Fig. 8

Liquid chromatogram of phenols on PGC 26; eluent, CH_2Cl_2: solutes (1) phenol, (2) 4 methyl phenol, (3) 2,3 dimethyl phenol, (4) 2,4,5 trimethyl phenol.

Fig. 10

Liquid chromatogram of polynuclear aromatic hydrocarbons: Eluent CH_2Cl_2 + 0.1% 1,3-terphenyl; solutes (1) naphthalene, (2) acenaphthene, (3) fluorene, (4) replenishment of displaced 1,3-terphenyl.

temperatures well above their boiling points. Our values for PGC 57 are about 5kJ mol^{-1} greater than the experimental values Kiselev and Yashin obtained on GTCB but agree well with their theoretically calculated values. The results broadly confirm that PGC 57 is a highly graphitized material. This view was also supported by x-ray analysis which indicated an amorphous structure for unfired PGC but showed a strong reflection corresponding to the crystal spacing of graphite in the sample fired at 2600 °C. Calculations using the standard formula [21] gave a degree of graphitization of about 70%. More limited measurements of ΔH_{ads} on PGC 19 gave lower values than on PGC 57 and they showed less dependence on carbon chain length. Values for benzene, toluene and ethyl benzene were 36, 46 and 51 kJ mol^{-1} respectively compared to 42, 49 and 54 obtained by Kiselev and Yashin [2] on GTCB. By comparison with PGC 57 the values for PGC 19 are again somewhat lower than might be expected on graphite.

The heat of adsorption on the less graphitized materials is apparently less than on highly graphitized material but, unfortunately, in obtaining a high degree of graphitization on PGC 57, the porosity and pore-accessibility were reduced to such an extent that the kinetic properties of the material were seriously compromised.

Further experiments should probably concentrate in intermediate firing conditions which will produce reasonable
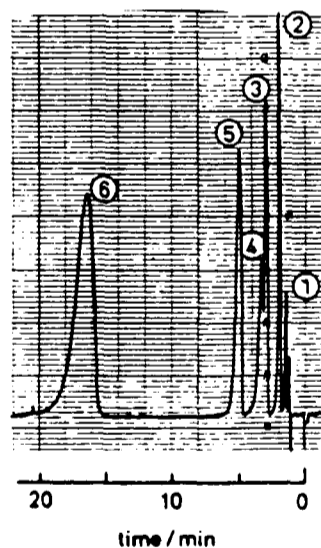
degrees of graphitization while retaining adequate pore volume and accessibility.

Liquid Chromatography

Previous efforts to prepare carbons for HPLC [13–15, 18, 22] met with only partial success. Where the materials have been sufficiently rigid to stand high pressures [13–15, 18–21] the chromatograms have generally been poor, showing severe peak tailing when k'-values exceed about 2; where good chromatograms have been obtained [22] the material has been too fragile for routine use.

As has been shown by experiments on GC, porous glassy carbons (PGC) appear to offer an alternative to graphitized thermal carbon black (GTCB) in that PGC's can give equally good separations while at the same time they are much less fragile. When used for liquid chromatography PGC's show substantial advantages over previous hard carbons in terms of peak shape at high values of k' and their performance approaches that of GTCB. Figure 8–10 show respectively separations of phenols, methyl substituted benzene and of some polynuclear aromatics.

Using fired but otherwise untreated PGC26, phenols, phthalates and other simple aromatics gave reasonably symmetric peaks but polynuclear aromatic hydrocarbons and more highly retained solutes generally gave poorly shaped peaks. However, the peak symmetry of such solutes was much improved by the addition of 0.1% of m-terphenyl to the eluent. This concentration was sufficiently low that the UV photometer used could still be zeroed. Terphenyl was strongly retained and acted as a "tailing reducer". Fig. 10 shows an interesting effect in that following the final peak of fluorene, a negative peak occurs due to the replenishment of terphenyl displaced by the previous solute or solutes. In order to elute nitrocompounds and acids as symmetrical peaks it was necessary in addition to add an acid to the eluent. In this context a concentration of 1% of pure acetic acid added to the eluent was effective.

As in GC, a stationary phase/eluent combination in LC can be characterised by the α'-value defined by equation 1 for a homologous series. Fig. 11 demonstrates that linear relationships hold between log k' and the carbon number for

Fig. 9

Liquid chromatography of methyl benzenes on PGC 26; eluent, CH_3OH; solutes (1) benzene, (2) toluene + 1,4-dimethylbenzene, (3) 1,3-dimethyl benzene, (4) 1,2-dimethyl benzene, (5) 1,2,4-trimethyl benzene, (6) 1,2,4,5-tetramethyl benzene.
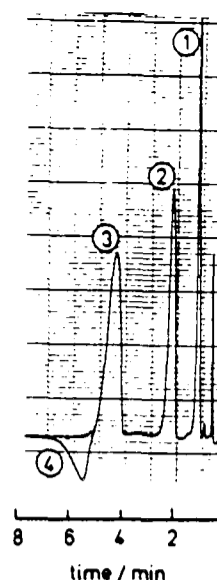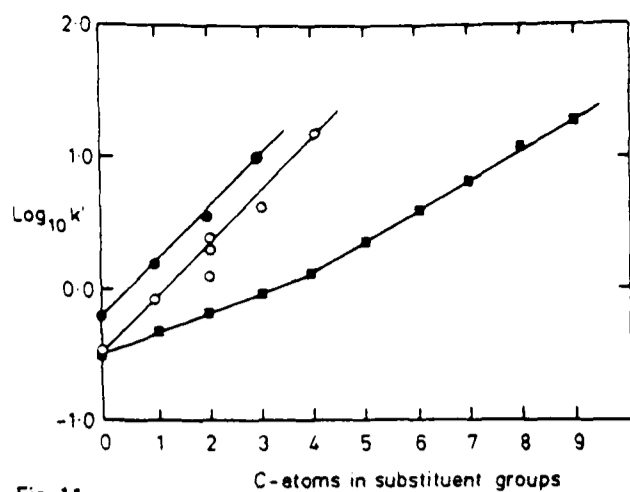
Fig. 11

Dependence of $\log_{10} k'$ on number of carbon atoms in substitueny groups on PGC 26; eluent CH_3OH; solutes ●, methyl phenols, ○, methyl benzenes, ■, n-alkyl benzenes.

n-alkyl benzenes and for the pseudo-homologous series of methyl substituted benzenes and phenols. For the former $\alpha' = 0.23$ and for the latter $\alpha' \cong 0.4$. These values are similar to those obtained by other workers as shown by the data collected in Table V. In particular our values are, within

experimental error, the same as those obtained by Guiochon and co-workers [13, 14], using pyrocarbon on GTCB. Rather lower values of α' are obtained from the data of Unger et al. [21]. The carbon examined by Smolkova et al. [19] illustrates the different eluotropic strengths of the solvents ranging from heptane to methanol. The data of Ciccioli et al. [22] are unfortunately insufficient to provide reliable α'-values but they appear to be a little lower than those obtained by Guiochon and co-workers and by ourselves.

Absolute values of k' on different carbons are difficult to compare owing to the different surface areas of the materials and, as already shown for GC, they are not necessarily comparable even when due allowance is made for the differences in surface area. However, it is perhaps worthwhile to make rough comparisons by normalizing k'-values to a standard surface area of $100 \text{ m}^2/\text{g}$. To do this eq. (2) has been used:

$$k'_{100} = \frac{100}{A} \cdot k'_{obs} \qquad (2)$$

where k'_{100} is the normalized value of k', k'_{obs} is the observed value and A is the surface area of the material in m^2/g. It may be pointed out that, strictly, normalization

Table V. Values of methylene selectivities on carbons using homologous series $\alpha'_{CH_2} = \log_{10} (k'_{(n + 1)}/k'_n)$

Material	Surface area m^2g^{-1}	Eluent composition v/v	Solutes	Range of n	α'_{CH_2}	Ref.
PGC 26	380	CH_3OH	alkyl benzenes	0 — 4	0.15	this work
				4 — 9	0.23	
		CH_3OH	methyl benzenes (a)	0 — 4	~ 0.4	
		CH_3OH	methyl phenols (a)	0 — 2	~ 0.4	
15% Pyrocarbon on Sterling GTCB.	6.4	$CH_2CN:H_2O$ 46:54	alkyl benzenes	0 — 4	0.26	13
		CH_3CN	n alcohols	5 —12	0.25	
		CH_3CN	methyl benzenes	1 — 3	~ 0.36	
55% Pyrocarbon on black pearls GTCB	37	CH_3OH	n alkyl benzenes	1 —12		14
		CH_3OH	n alkyl bromides	4 —10	0.24	
		CH_3OH	n alkyl chlorides	5 — 8		
		CH_3OH	n alcohols	6 —16		
		CH_2Cl_2	methyl naphthalenes	1 — 3	~ 0.3	14
		CH_3CN	methyl benzenes	2 — 5	~ 0.43	
		CH_3CN	methyl phenols	1 — 3	~ 0.45	
14% Pyrocarbon on Sterling FTFF GTCB	12 (b)	CH_3CN	methyl naphthalenes	1 — 3	~ 0.41	4
Purified coke calcined 2800 °C	2.5 (b)	$CH_3OH:H_2O$ 55:45	dialkyl phthalates (c)	1 — 4	~ 0.17	21
		$CH_3OH:H_2O$ 55:45	methyl benzenes	1 — 4	~ 0.16	
Carbon III (grahitized carbon from PTFE)	20	$C_2H_5OC_2H_5$	n-alkanes	12—14	0.13	19
		n C_5H_{12}	n-alkanes	8 —16	0.14	
		n C_7H_{16}	1-chloroalkanes	6 —16	0.11	
		CH_3OH	n-alcohols	3 — 6	0.32	
Carbosorb B	80	CH_3OH	dialkyl phthalates (c)	1 — 8	~ 0.15	22
		CH_5H_{12}	methyl naphthalenes	0 — 2	~ 0.3	

(a) For the pseudo-homologous series a geometric mean value has been taken of the k'-values for isomeric homologues.

(b) Estimated from the author's data.

(c) n refers to the number of carbon atoms in each alkyl chain: α refers to single CH_2 groups.

should be carried out on the basis of surface area of support per unit volume of eluent. However, the volume of eluent per gram of support is rarely deducible from the published data whereas surface area per gram of support is normally quoted. Eq. (2) is thus the only approximation that can be used in practice.

Tables VI and VII compare k'_{100}-values for polynuclear aromatics (PNA's) and methyl substituted benzenes (MB's). While there are wide variations in the values from one carbon to another when the same eluent is used these are a number of correlations which can be made. The elution order of PNA's on all carbons is the same and there is clear evidence from our work on PGC26 that solvent strength decreases in the order CH_2Cl_2, C_6H_{14}, $CH_3COOC_2H_5$, CH_3CN, CH_3OH and that the addition of the tailing reducer, terphenyl, reduces retention by about 30%. The retention on the pyrocarbons is similar to that on the PGC's, with benzene apparently a stronger solvent than CH_2Cl_2.

For MB's analogous similarities are evident. Addition of water to methanol increases retention as expected.

Table VI. Values of k'_{100} for representative solutes on Carbons

Material	Surface m^2g^{-1}	Eluent	k'_{100}					
			Naphthalene	Acenaphthene	Fluorene	Phenanthrene	Anthracene	Ref.
PGC 7	350	CH_2Cl_2	0.2	0.3	0.7	2.4	4.7	this work
		C_6H_{14}	0.2	0.4	1.6			
		$CH_3COOC_2H_5$	0.2	0.6				
		CH_3CN	1.4	1.8	5	.		
		CH_3OH	1.4	7	18			
PGC 26	380	CH_2Cl_2	0.5	1.4	3.3			this work
		$CH_2CL_2 + 0.1\%$ m-Terphenyl	0.3	0.9	2.1			
		CH_3OH	4.2					
PGC 19	21	C_6H_{14}		3.3				this work
		$C_6H_{14} + 2\%$ $CH_3COOC_2H_5$		2.9	11	50		
15% Pyrocarbon on Sterling GTCB	6.4 (a)	CH_3CN	6		80			13
55% Pyrocarbon on black pearls GTCB	37	CH_2Cl_2	0.8		0.9	2.2	2.7	
		C_6H_6	0.2	0.7				
Purified coke graphitized 2800°C	2.5 (a)	CH_3OH	2.8		14	21		
Carbon III	20	$C_2H_5OC_2H_5$					37	
Carbopack B	80	C_5H_{12}	1.8					

(a) Estimated from authors' data.

Table VII. k'_{100} values on carbons for methyl substituted benzenes

Material	Surface area m^2g^{-1}	Eluent	k'_{100} (a)						
			Benzene	Toluene	Xylenes	Trimethyl benzenes	Tetramethyl benzenes	Penta methyl benzene	Ref.
PGC 26	380	$CH_2Cl_2 + 0.1\%$ m-Terphenyl	0.02	0.04	0.04	0.08	0.15		this work
		CH_3OH	0.06	0.22	0.4	1.0	4.0		
		$CH_3OH:H_2O:HAc$							
		94:5:1	0.13	0.3	0.6	1.5	6		
		89:10:1	0.15	0.4	0.7	1.7	7		
		84:15:1	0.2	0.5	—	2.5	11		
44% Pyrocarbon on black pearls GTCB	38 (b)	CH_3CN	0.4		1.0	2.3	6.6	18	14
33% Pyrocarbon on black pearls GTCB	45 (b)	CH_3CN	—		0.7	1.6	5.4	16	14
Purified coke graphitized 2800°C	2.5 (b)	$CH_3OH:H_2O$ 55:45	—	16	19	48	64		21
Carbopack B	80	C_5H_{12}				0.2			22

(a) k'_{100}-values are the geometric means of k'_{100}-values for individual isomers of any homologue
(b) Estimated from authors' data

It may be concluded that PGC's are similar in their retentive characteristics to GTCB's which have been coated with pyrocarbon. Peak symmetry is, however, somewhat better and the materials are much easier to make. They therefore provide a form of carbon for HPLC which has real potential for further development.

PGC behaves as a reversed phase packing material. Its retentive power is much greater than that of reversed-phase bonded silica gels as shown by the requirement for fairly strong eluents such as methanol, acetonitrile and dichloromethane where aqueous mixtures would be used for alkyl bonded silica gels.

Conclusions

Porous Glassy Carbon (PGC) can be produced with a wide range of surface area from 20 to 400 m²/g. It can be used for both gas and high performance liquid chromatography.

In gas chromatography it has retentive characteristics and heats of adsorption similar to Carbopack B, a weakly consolidated graphitized thermal black (GTCB) but is substantially more robust.

In liquid chromatography it has retentive characteristics similar to those of the GTCB's hardened by deposition of pyrolytic carbon but peak symmetry is somewhat better and the material is easier to produce. Broadly PGC provides a new reversed phase material with strong adsorptive strength compared with reversed phase bonded silica gels.

Acknowledgements

References

[1] A. V. Kiselev, in Advances in Chromatography, 4, 113, Marcel Dekker, New York (1967).
[2] A. V. Kiselev, J. P. Yashin, Gas Adsorption Chromatography, Plenum Publishing, New York (1969).
[3] L. D. Belyakova, A. V. Kiselev, Anal. Chem. 36, 1517 (1964).
[4] A. V. Kiselev, E. A. Paskonova, R. S. Petrova, D. K. Shcherbakova, Russ. J. Phys. Chem. 38, 84 (1964).
[5] A. V. Kiselev, N. V. Kovaleva, Yu. S. Nikitin, J. Chromatogr. 58, 19 (1971).
[6] F. Bruner, P. Ciccioli, G. Crescentini, M. T. Pistolesi, Anal. Chem. 45, 1851 (1973).
[7] F. Bruner, G. Bertoni, P. Ciccioli, J. Chromatogr. 120, 307 (1976).
[8] A. Di Corcia, R. Samperi, J. Chromatogr. 107, 99 (1975).
[9] A. Di Corcia, A. Liberti, R. Samperi, J. Chromatogr. 122, 459 (1976).
[10] A. Di Corcia, A. Liberti, Advances in Chromatography 14, 305, Marcel Dekker, New York (1976).
[11] A. Di Corcia, A. Liberti, R. Samperi, J. Chromatogr. 167, 243 (1978).
[12] V. Patzelova, J. Jansta, F. P. Dousek, J. Chromatogr. 148, 53 (1978).
[13] H. Colin, C. Eon, G. Guiochon, J. Chromatogr. 119, 41 (1976).
[14] H. Colin, C. Eon, G. Guiochon, J. Chromatogr. 122, 223 (1976).
[15] H. Colin, G. Guiochon, J. Chromatogr. 137, 19 (1977).
[16] H. Colin, G. Guiochon, J. Chromatogr. 126, 43 (1976).
[17] H. Colin, N. Ward, G. Guiochon, J. Chromatogr. 149, 169 (1978).
[18] Z. Plzak, F. P. Dousek, J. Jansta, J. Chromatogr. 147, 137 (1978).
[19] E. Smolkova, J. Zima, F. P. Dousek, J. Jansta, J. Chromatogr. 191, 61 (1980).
[20] T. A. Zwier, M. F. Burke, Anal. Chem. 53, 812 (1981).
[21] K. Unger, P. Roumeliotis, H. Mueller, H. Goetz, J. Chromatogr. 202, 3 (1980).
[22] P. Ciccioli, R. Tappa, A. Di Corcia, A. Liberti, J. Chromatogr. 206, 35 (1981).
[23] K. K. Unger, J. H. Knox, J. Liquid Chromatogr., in preparation (June 1982).
[24] J. H. Knox, M. T. Gilbert, U.K. Patent 2035282 B/ US Patent No. 4,263,268, Fed. Rep. Germany P2946688-4.
[25] S. J. Gregg, K. S. W. Sing, Adsorption, Surface Area and Porosity, Academic Press, New York, 1967.
[26] W. O. McReynolds, J. Chromatogr. Sci. 8, 685 (1970).

CHROMSYMP. 740

STRUCTURE AND PERFORMANCE OF POROUS GRAPHITIC CARBON IN LIQUID CHROMATOGRAPHY

JOHN H. KNOX* and BULVINDER KAUR

Wolfson Liquid Chromatography Unit, Department of Chemistry, University of Edinburgh, West Mains Road, Edinburgh EH9 3JJ (U.K.)

and

G. R. MILLWARD

Department of Physical Chemistry, University of Cambridge, Lensfield Road, Cambridge (U.K.)

SUMMARY

The structure of the porous carbon (designated PGC) has been studied in detail by X-ray diffraction, scanning electron microscopy, electron diffraction, and high-resolution electron microscopy. These techniques provide a self-consistent picture: PGC which has not been heated above 1000°C is an amorphous glassy carbon containing micropores and mesopores. PGC which has been heated to above 2000°C has the atomic-molecular structure of a 2-dimensional graphite which is essentially indistinguishable from that of graphitised carbon black (GCB), both being made up from crystallites of around 100 Å in size. By contrast, at the colloidal level, PGC and GCB are very different: where GCB consists of loosely aggregated colloidal units having only weak Van der Waals bonding between them, PGC has a strong sponge-like structure, capable of withstanding considerable shearing forces, such as those met with in high-performance liquid chromatography (HPLC).

During the heating of PGC from 1000°C to above 2000°C, needle- and plate-like structures are also formed. These consist of dense 3-dimensional crystalline graphite. They have negligible surface area and are not useful in chromatography.

The porous 2-dimensional graphite (PGC) consists of 3–10 μm spherical particles which are about 80% porous and have a specific surface area of about 150 m²/g. This material has been used for HPLC and gives peak shapes comparable to those from bonded silica gels of the same particle size. PGC acts as a very strong hydrophobic adsorbent with unique selectivity. Its elution patterns are compared to those from a commercial ODS-bonded silica for methyl benzenes, phenols, ethers, monosubstituted benzenes, amines, and acids. Examples are shown of HPLC separations of simple analgesics. Deactivation by adsorption of high-molecular-weight impurities and reactivation of PGC is also briefly noted.

INTRODUCTION

In 1982 Gilbert *et al.*[1] described the production and performance in gas and

liquid chromatography (GC and HPLC) of a new carbon material which they called "porous glassy carbon" (PGC). The material was produced[2] by impregnating a silica gel template with a phenol–hexamine mixture, polymerising this mixture within the pores of the silica gel, pyrolysing the resin in nitrogen, dissolving out the silica template, and finally heating the remaining porous carbon to a temperature in excess of 2000°C. Large-particle material (100–200 μm) was examined as a GC adsorbent and small-particle material (<40 μm) as an HPLC material. In GC, the material showed selectivity and retention which was very similar to that of Carbopack B, a commercial graphitised carbon black (GCB) marketed by Supelco. In HPLC, the material behaved as a strong hydrophobic adsorbent but at that stage in development gave rather poor peak shapes with strongly retained solutes[1].

Shortly before the publication of this paper[1], Ciccioli et al.[3] had shown that carefully fractionated 20-μm Carbopack B gave excellent results in LC with a high degree of peak symmetry, even for strongly retained solutes. Unfortunately, the fragility of this material made it impracticable as a routine HPLC packing material. Nevertheless, these two papers[1,3] showed that a porous graphitised carbon would probably be the ideal carbon material for HPLC, if it could be made strong enough. Accordingly, a more appropriate name for the carbon developed by Gilbert et al. might be "porous graphitised carbon". Fortunately, the initials PGC cover both descriptions equally well.

The present work presents evidence from X-ray analysis and electron microscopy to support this contention and it establishes the close similarity between the bulk and surface atomic arrangements in PGC and GCB. However, unlike GCB, which is composed of loosely aggregated colloidal particles and very fragile, PGC has a continuous sponge-like structure with a mechanical strength comparable to that of silica gels having similar porosity and is therefore of adequate strength for both GC and HPLC.

The sample of PGC tested by Gilbert et al.[1] in HPLC showed significant peak tailing when compared to the GCB tested by Ciccioli et al.[3]. This difference can probably be attributed to imperfections in the graphitic surface of PGC. In this paper, we show that improved methods of preparation of PGC have led to samples which exhibit chromatographic properties in HPLC very similar to those of ODS-bonded silicas in terms of peak symmetry and sharpness.

STRUCTURE OF CARBONS

Many varieties of carbon are produced industrially on a large scale[4]. The most important of these are: electrographite (for industrial electrodes), nuclear graphite (as a moderator in nuclear reactors) active carbons or charcoals (for adsorption of vapours, extraction of organics from water, decolourising), carbon blacks (fillers in rubber), glassy carbons, and carbon fibres.

Electrographites and nuclear graphites, as the names suggest, are "graphitised". This term, as used commercially, implies little more than that the materials have been heated to high temperatures (e.g. 3000°C). The actual degree of graphitisation achieved may vary widely over the range of materials which are loosely termed "graphitised" and is discussed in more detail below. The other forms of carbon are not normally heated much above about 1000°C in the course of manufacture and are

therefore amorphous. Active carbons are made from cokes and charcoals by controlled oxidation, and possess highly oxygenated surfaces, bearing functional groups such as -OH, =O, C–O–C, COOH, etc. They behave as polar adsorbents and are hydrophilic, whereas graphite is hydrophobic. Carbon blacks are made by combustion of oils in a deficiency of oxygen, and are converted to graphitised carbon blacks (GCB) by heating in an inert atmosphere to 3000°C. Carbon blacks are generally hydrophobic. Glassy carbons and carbon fibres are produced by controlled pyrolysis of materials such as phenol–formaldehyde resins and poly(acrylonitrile) fibres in an inert atmosphere. They are amorphous but will develop some degree of graphitisation, as discussed later, when heated to temperatures above 2500°C.

For good chromatographic performance an adsorbent such as carbon must have adequate surface area and a uniform free energy of adsorption of solutes at low surface coverage. Too low a surface area leads to inadequate load capacity, whereas an energetically heterogeneous surface leads to tailed peaks. In general, active carbons have strongly heterogeneous surfaces and are unsuitable for chromatography, unless the most active sites can be eliminated. These sites occur mainly in micropores and can be removed by heating to high temperatures. However, as shown by Unger et al.[5], who explored this route to effective chromatographic carbons, the removal of micropores reduces the surface area to such a degree that the material is of very limited usefulness in HPLC.

The requirements for a good chromatographic carbon would thus appear to be a high surface area, a graphitic surface, and good structural strength. Unfortunately, industrial graphites are all designed to be dense and non-porous, while the carbon blacks, which have the necessary area, are much too fragile. Glassy carbons, like industrial graphites, are also dense and non-porous. It is thus evident that no industrial carbon can readily be converted into a carbon suitable for chromatography, and the few attempts to modify them for this purpose[5,6] or to develop special carbons by electrochemical reduction[7] have failed. This previous work has been re-
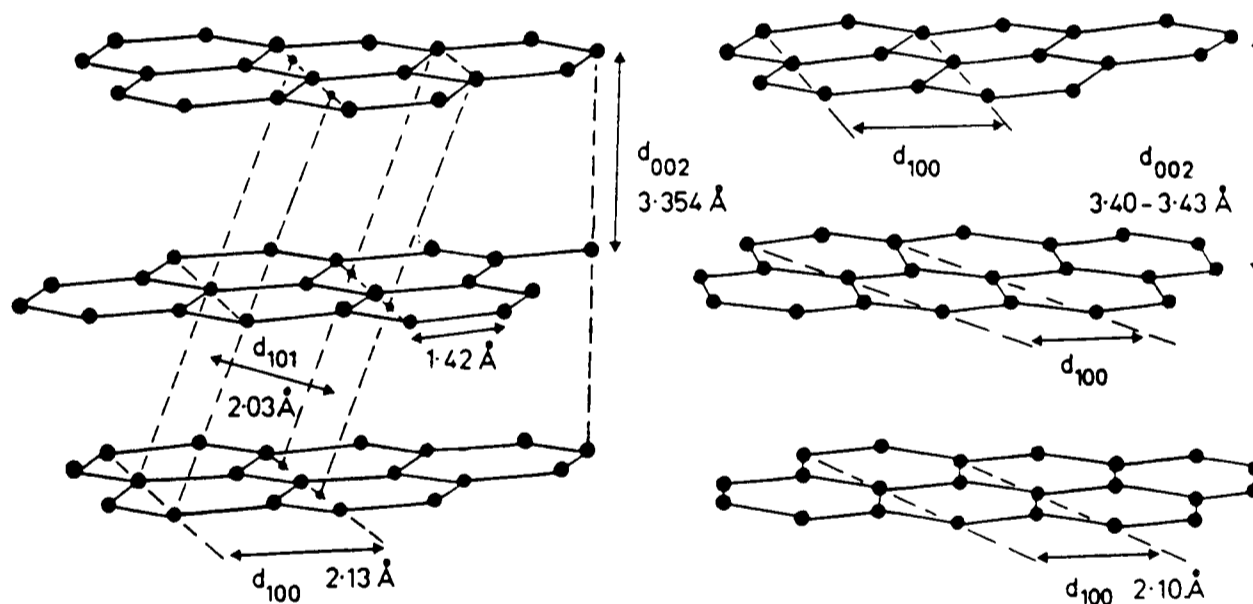

Fig. 1. Atomic structures of graphites. Left: Bernal structure of perfect 3-dimensional graphite with ABAB·· layer registration. Right: Warren structure of two-dimensional turbostratic graphite with no layer registration.

viewed comprehensively by Knox and Unger[8]. We therefore believe that the process described by Knox and Gilbert[2] may offer a unique method of producing chromatographic carbons.

The term "graphitised carbon" is widely misused and misunderstood. As noted above, "graphitised" generally means that a particular carbon has been heated to a temperature in the region of 3000°C in a graphitising furnace. In crystallographic terms, the degree of graphitisation of such a carbon may fall within wide limits, supposedly "graphitised" carbons ranging from almost amorphous materials to perfect three-dimensional crystalline graphites. There are, in fact, three distinct forms of carbon to which the term "graphitised" can reasonably be applied and which have well-defined crystal structures. Two of these forms are shown in Fig. 1. The Bernal structure of perfect three-dimensional graphite[9] as shown in Fig. 1 consists of layers of carbon atoms, organized in a hexagonal array and ordered ABABAB···. This form of graphite is termed hexagonal graphite. A second, rarer form of three-dimensional graphite, the Lipson and Stokes form, also exists, but here the layers are ordered ABCABC···. This is termed rhombohedral graphite[10]. In both crystalline forms the layer spacing is 3.354 Å and the atomic spacing within the layers is 1.42 Å. Perfect graphite is rarely formed synthetically from amorphous solid carbon, since the bonding between the carbon atoms within the graphitic planes is extremely strong, while the interlayer bonding is weak. Thus, graphitisation tends to develop by the formation of graphitic sheets which are initially randomly oriented. The reorganization of these sheets into ordered three-dimensional graphite requires such a high activation energy that formation of three-dimensional crystalline graphite is generally impossible below 3000°C. Thus, most synthetic carbons, when heated to about 3000°C, assume the second structure shown in Fig. 1. This is a two-dimensional graphite in which graphitic sheets are randomly oriented relative to one another. In
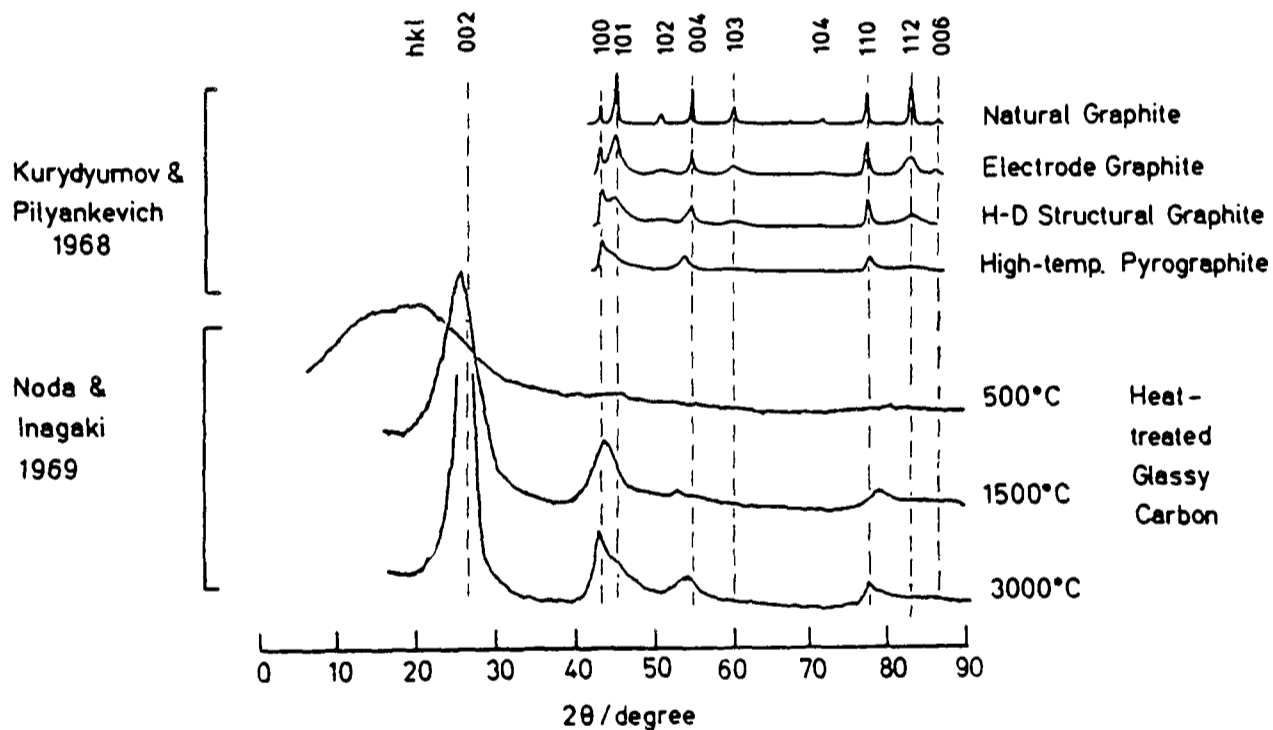

Fig. 2. Published X-ray diffractograms of various carbons, showing different degrees of crystallinity (see refs. 15 and 16).

two-dimensional graphites the layer spacing is slightly greater than in three-dimensional graphites at 3.40–3.43 Å, and the atomic spacing within the layers is slightly less. Two-dimensional graphites are often said to have a turbostratic structure, a term first coined by Warren[11] in referring to graphitised carbon blacks. Glassy carbons, when heated to high temperatures, appear to assume a similar structure, except that, unlike carbon blacks, which are composed of loosely aggregated colloidal units, high-temperature glassy carbons are thought to be made up of intertwined graphitic ribbons[12]. At an early date, Franklin[13] discussed the problem of two-phase graphites and the process of graphitisation and concluded that many carbons consisted of mixtures of amorphous and graphitic crystallites. She also distinguished between "hard" and "soft" carbons, depending upon whether they could be readily graphitised or were difficult to graphitise. However, it appears that at that time the distinction between three-dimensional and two-dimensional graphites was not well understood. In general, turbostratic, two-dimensional graphites are not converted into three-dimensional graphites below 3000°C.

While three-dimensional graphites rarely arise from heating amorphous solid carbons, they can nevertheless arise by high-temperature pyrolytic deposition from organic vapours in the gas phase[14]. Presumably, properly oriented layers are laid down in the first place, and no reorganization is required.

Fig. 2 shows X-ray diffraction patterns of various carbons, taken from the literature[15,16]. The X-ray diffractogram of true graphite (topmost tracing) shows a range of sharp (hkl) reflections and, in particular, a prominent 101 reflection of greater intensity than the 100 reflection. The small angular spread of the reflections indicates relatively large crystallites (see below). As the degree of graphitisation decreases, the (hkl) reflections first become diffuse and then disappear altogether, leaving only the (hk0) and (001) reflections, which are characteristic of two-dimensional graphites. A good example is the tracing for "high-temperature pyrographite" which gives only a 002 peak (not shown), a 004 peak, and a typical asymmetric 100 peak. In such materials, the 002 and 004 reflections occur at slightly lower angles than in true 3-dimensional graphites, indicating that the graphitic planes are slightly further apart (3.40–3.43 Å, compared to 3.354 Å). The tracings in the lower part of Fig. 2 show that glassy carbon, as produced at 500°C, possesses no structure and gives only very diffuse reflections at about 20° and possibly at 40–50°. As the material is heated, these diffuse reflections become sharper, and by 3000°C they have become the 002, 004, and 100 reflections of two-dimensional graphite. The X-ray diffractogram of glassy carbon heated to 3000°C is almost identical to that of "high-temperature pyrocarbon" but with wider peaks indicating smaller crystallites.

Fig. 3 shows X-ray diffractograms of a number of so-called graphitised carbons, along with the ungraphitised carbon black Vulcan®. These diffractograms were obtained with the equipment employed for the main part of the X-ray study reported below. Ungraphitised Vulcan black (Cabot Corporation) shows a relatively wide reflection at 25° and a second, more diffuse reflection at 45°. With heating, these peaks become narrow and move to higher angles into the positions of the 002 and 100 peaks for graphitised carbon black, as shown at the top of Fig. 3. This diffractogram of GCB shows the symmetrical 002 and 004 reflections and the unsymmetrical 100 reflection, which is characteristic of two-dimensional graphites. Carbon fibre shows less extensive two-dimensional graphitisation, as indicated by the wider and
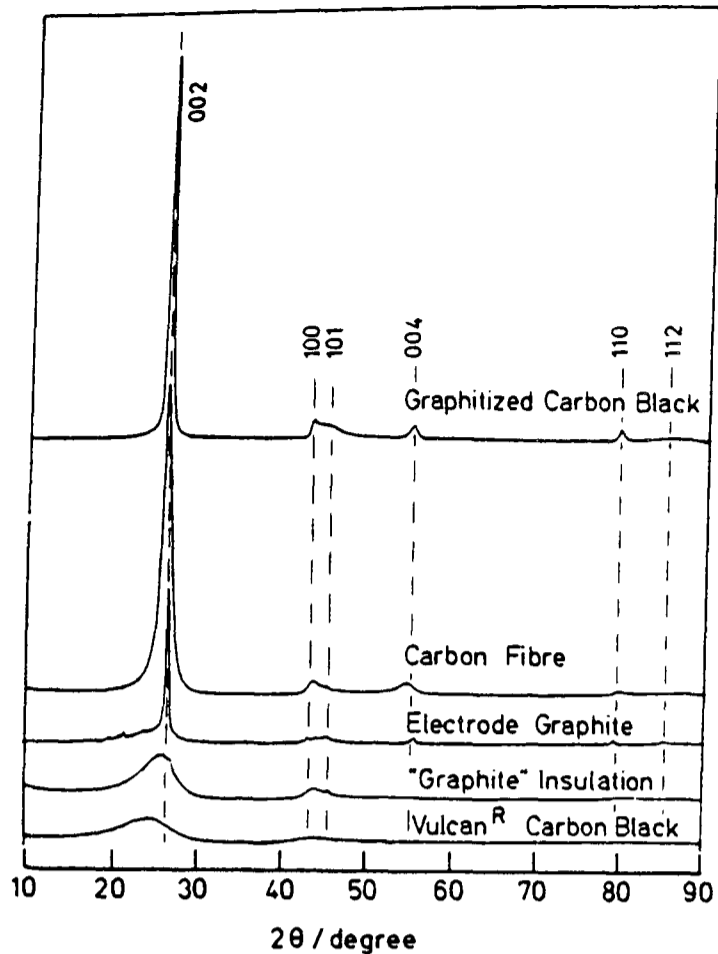
Fig. 3. X-ray diffractograms of commercial carbons, obtained in this study.

less symmetrical 002 and 004 reflections. In this tracing there is slight evidence of some three-dimensional graphitisation, as shown by the blip at the position expected for the 101 reflection. Electrode graphite gives a much sharper 002 reflection, superimposed on a broad, amorphous background reflection, and shows definite evidence of a 101 peak, superimposed on a wide unsymmetrical 100 peak. This material appears to have a significant proportion of three-dimensional crystallites within an otherwise amorphous or two-dimensional graphitic matrix. Finally, "graphite furnace insulation", supplied in the form of a felt, shows only slightly more graphitisation than does Vulcan carbon black.

The angular widths of X-ray reflections, discounting instrumental broadening, gives useful information about crystallite size. In the case of graphites the width of the 002 and 004 reflections (usually measured at half the maximum peak height) give an indication of the mean stack height of the graphitic planes, while the width of the (100) reflection indicates the mean diameter of the graphitic sheets. The relationship was originally derived by Scherrer[17]:

$$L = k\lambda/B \cos \theta \tag{1}$$

where L is the crystallite dimension, λ is the wavelength of the X-rays, B is the peak width in radians, θ is the Bragg angle of reflection, and k a constant around unity. There has been considerable discussion as to the best value for k[18-20]. For the

002 reflection, 0.84 is thought to be an optimum value, while for the unsymmetrical 100 peak, Biscoe and Warren[20] advocate a value of 1.84. Using these values, a typical stack height in a graphitised carbon black (uppermost tracing in Fig. 3) would be about 50 Å, and a typical plate diameter about 100 Å. These values correspond to crystallites having about 15 graphitic layers with about 3000 C-atoms in each layer.

EXPERIMENTAL

Equipment, materials, and methods

Thermogravimetric analysis was carried out with a Stanton Redcroft TG770 thermogravimetric analyser (Stanton Redcroft, London, U.K.). Scanning electron microscopy was carried out on a Cambridge Instruments type 604 stereoscan instrument (Cambridge Instruments, Cambridge, U.K.) fitted with a Praktica LC camera. Samples of PGC were deposited on aluminium stubs and coated with gold to prevent accumulation of charge. The coating was carried out with an E5100 coating unit (Polaron Equipment). Transmission electron microscopy and electron diffraction were carried out using a JEOL 200-CX instrument (JEOL UK, Colindale, London, U.K.) at Cambridge University. The instrument, operated at 200 keV, was fitted with a top-entry goniometer stage, modified to enable the specimens to be moved parallel to the incident beam (z-lift), as described by Thomas et al.[21]. Under the operating conditions used, it had a resolution of 2.4 Å. Specimens for examination were deposited from a suspension in acetone onto carbon "holey" films. Only particles positioned over the holes were imaged under high resolution.

X-ray diffraction was carried out on a Philips powder diffractometer (Pye Unicam, Cambridge, U.K.). Samples on slide holders were loaded by an automatic sample changer (type PW 1170/02). The goniometer (type PW 1050/80) was mounted on a highly stabilized X-ray generator (PW 1130/10) that provided Cu $K_{\alpha 1,2}$ radiation of a mean wavelength of 1.5418 Å. Angular scanning was by a motor control unit, type PW 1394. Detection was by a channel control unit, type PW 1390, and fed to a pen recorder, Type PM 8203. Normally, a scan rate of 0.5°/min was used (in 2θ units) with a time constant setting of 4.

High-temperature treatment of PGC up to 2500°C was carried out by the Atomic Weapon Research Establishment (Aldermaston, U.K.), by Carbon Lorraine (Gennevilliers, France), and by Dr. C. Jenkins (Department of Metallurgy, University of Swansea, U.K.). Samples were generally heated slowly in argon from ambient temperature to 2500°C over a period of several hours.

The rocking autoclave used in the preparation of the silica gel template was designed and constructed by C. W. Cook & Sons (Birmingham, U.K.) and was rated to 300 bar at 400°C; it had a 2-1 capacity.

The furnace used to pyrolyse the silica–polymer particles in the preparation of PGC could heat up to 2 l of material to 1100°C in a rotating monel tube. The tube could be purged with nitrogen through a rotary seal. The furnace was designed and constructed by Carbolite Furnaces (Bamford Mill, Sheffield, U.K.).

Liquid chromatography was carried out using laboratory-assembled components from a variety of sources. Pumps used were an Altex Model 110 (Beckman RIIC, High Wycombe, U.K.), a Kontron Model 410 (Kontron Intertechnique, St. Albans, U.K.) and a Du Pont chromatographic pump, Type 861001 (Du Pont, Hitch-
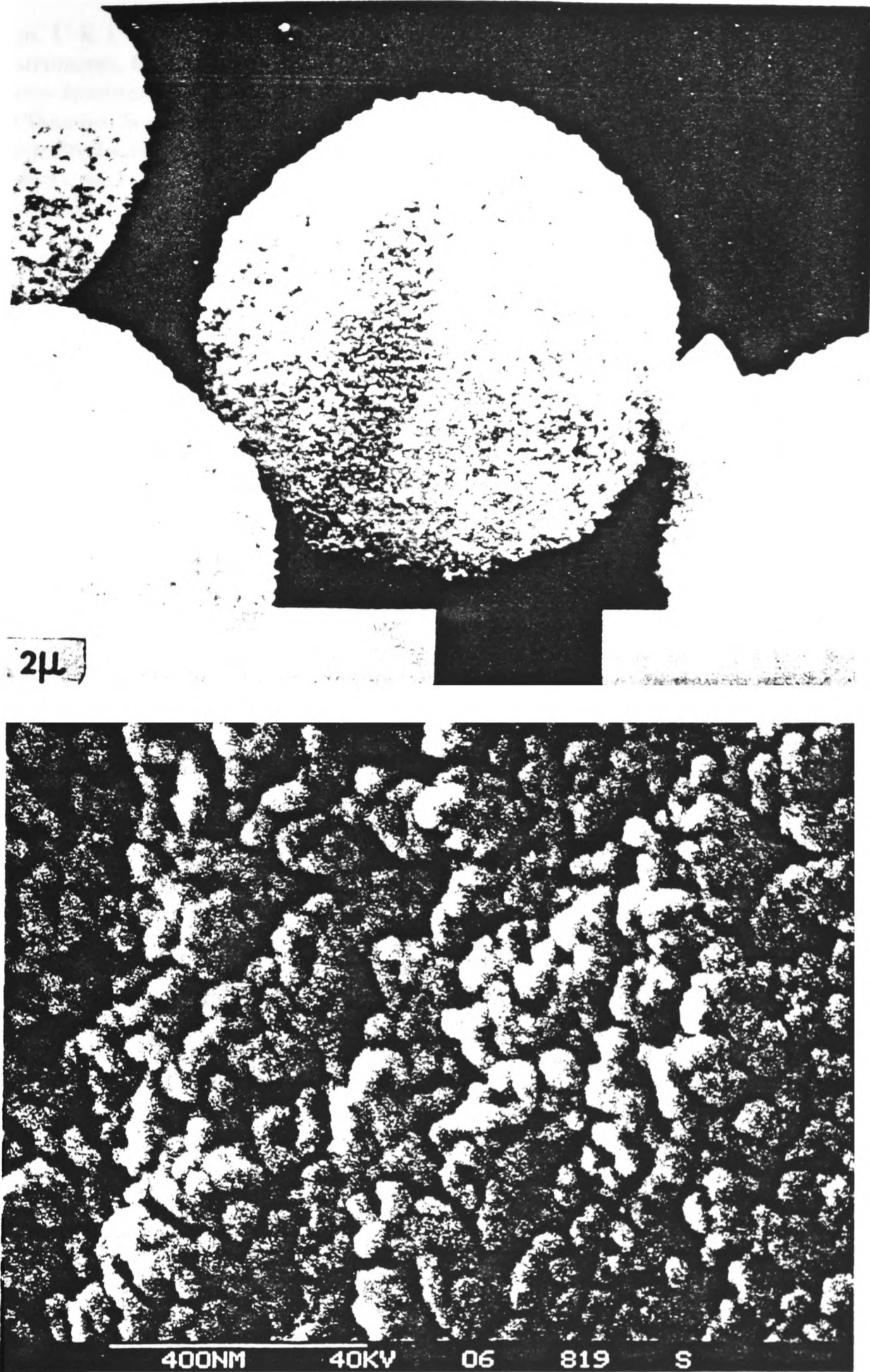
Fig. 4. Scanning electron micrographs of PGC. Upper: spherical particle of PGC; black band represents 2 μm. Lower: high magnification of surface; white horizontal line represents 400 nm.

in. U.K.). Detectors used were a Cecil Model 212 UV spectrophotometer (Cecil Instruments, Cambridge, U.K.) and a Kratos Model 773 UV spectrophotometer (Spectros International, Urmiston, Manchester, U.K.). Injection was by a Rheodyne valve (Shandon Southern Products, Runcorn, U.K.). Columns were from Shandon Southern Products and were 100 mm long, 5 mm bore. PGC was packed using a Shandon slurry packer at 100 bar. Both the slurry support liquid and the follower liquid were acetone. It was important to use ANALAR-grade or HPLC-grade solvents for column packing because of the strong adsorption by PGC of any high-molecular-weight impurities. Columns were normally operated at 1 ml/min with pressure drops of 50–75 bar.

Chemicals used in the preparation of PGC were BDH ANALAR Reagents (BDH, Poole, U.K.). HPLC eluents were obtained from Rathburn Chemicals (Walkerburn, U.K.). ODS Hypersil was obtained from Shandon Southern Products.

BET surface areas were measured using a laboratory-constructed instrument.

Pore volumes were determined by a laboratory-constructed low-pressure (up to 30 bar) mercury porosimeter or by liquid titration.

Preparation of PGC

The template required for the production of PGC should be a well-bonded silica gel of high porosity. The spherical silica gel was specially prepared and had a
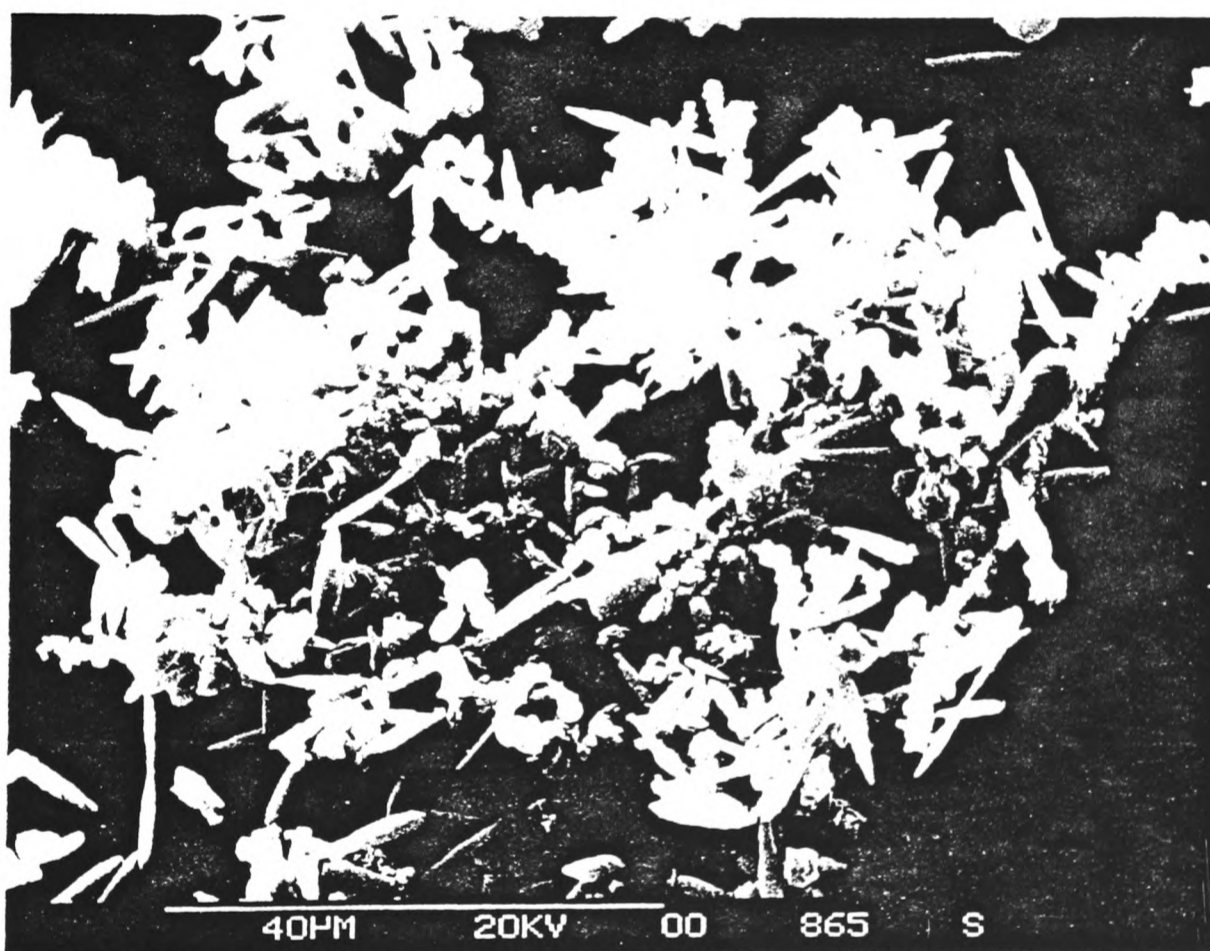
Fig. 5. Scanning electron micrograph of sample of "needles", separated from spheres of PGC; horizontal white line represents 40 μm.
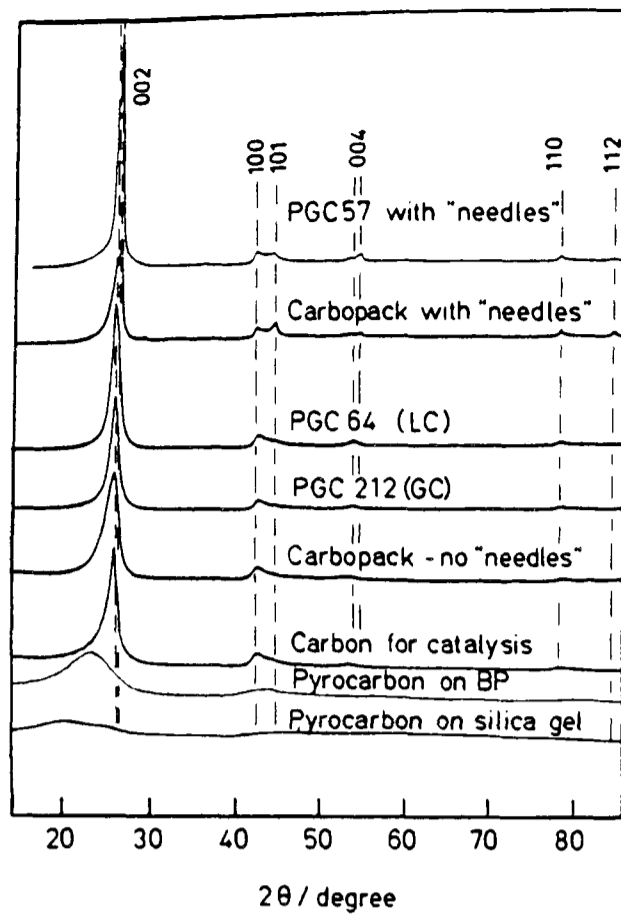
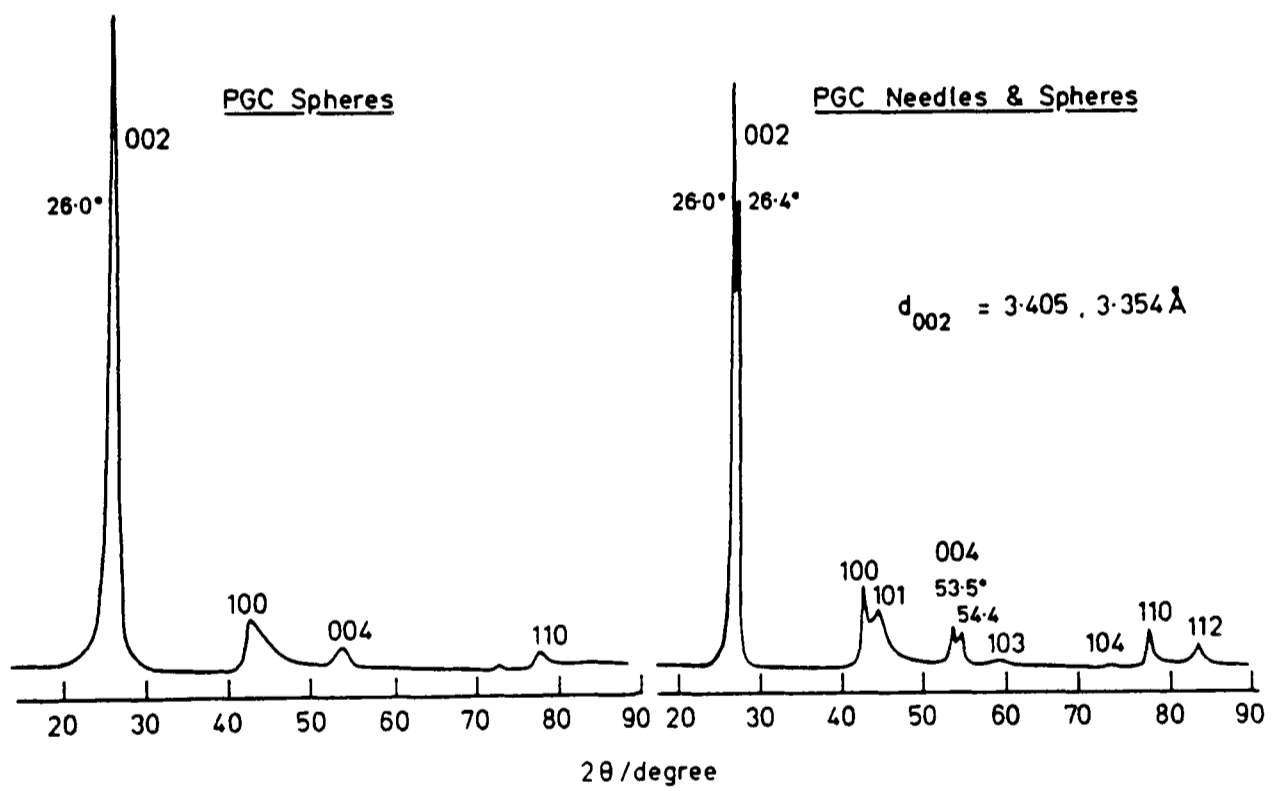Fig. 6. X-ray diffractograms of potential chromatographic carbons.

Fig. 7. X-ray diffractograms of PGC 201 (2600°C) with and without needles present.

pore volume of 1.4 cm^3/g with a specific surface area of 50 m^2/g. The mean particle diameter was 7 μm. This template was impregnated with a melt of phenol and hexamine in a 6:1 weight ratio. The impregnated material was heated gradually to 150°C to form phenol–formaldehyde resin within the pores of the silica gel. This silica-polymer was then heated slowly to 900°C in a stream of oxygen-free nitrogen in a specially designed rotary furnace. Approximately 50% of the weight of the polymer was thereby lost, and the density of what remained was increased to about 2 g/cm^3. The silica–carbon particles were then treated with hot aqueous potassium hydroxide to dissolve the silica template. Dissolution of silica was determined with a Stanton Redcroft TG770 thermogravimetric analyser to be at least 99% complete. The remaining porous glassy carbon had a BET surface area of 450–600 m^2/g and a pore volume of 2.0 cm^3/g, corresponding to a particle porosity of about 80%. This carbon was then heated to 2500°C in oxygen-free argon. The final carbon had a surface area of about 150 m^2/g and a pore volume similar to that of the carbon before high-temperature treatment. The carbon retained the spherical form and the particle size of the original silica template. The scanning electron micrographs in Fig. 4 clearly show the spherical shape of the particles and their sponge-like structure.

After high temperature firing, most samples of PGC contained needle-like or spine-like structures with lengths of a few micrometres and diameters of around 1 μm. An example of some needles separated from spherical particles is shown in Fig. 5. Both the porous spheres and the needles were examined by X-ray diffraction and by electron microscopy.

RESULTS AND DISCUSSION

X-ray diffraction

Fig. 6 shows diffractograms of a number of carbons which have been proposed for use in chromatography. "Pyrocarbon on silica" was prepared by Colin and Guiochon[22] by deposition from benzene vapour at 900°C into the pores of silica gel.

TABLE I

BRAGG SPACING AND CRYSTALLITE SIZE IN VARIOUS CARBONS

Material*	θ_{002} (deg)	d_{002} (Å)	θ_{100} (deg)	d_{100} (Å)	θ_{101} (deg)	d_{101} (Å)	L_c** (Å)	L_a*** (Å)
Graphite	13.3	3.35	21.2	2.13	22.3	2.03	–	–
Needles	13.3	3.35	21.2	2.13	22.3	2.03	–	–
Carbopack B	13.0	3.43	21.2	2.13	–	–	50	100
PGC64 (2350)	13.0	3.43	21.2	2.13	–	–	70	100
PGC205 (2500)	13.0	3.43	21.2	2.13	–	–	70	140
PC on BP	12.2	3.65	21.0	2.15	–	–	15	20

* The bracketted figure in designation of PGC gives the highest temperature in °C to which the PGC was heated. PC on BP = pyrocarbon on Black Pearls, kindly supplied by Dr. H. Colin, Ecole Polytechnique, Palaiseau, France.
** Constant k = 0.86 in eqn. 1.
*** Constant k = 1.84 in eqn. 1.

EM of PGC 64 (2340° C)

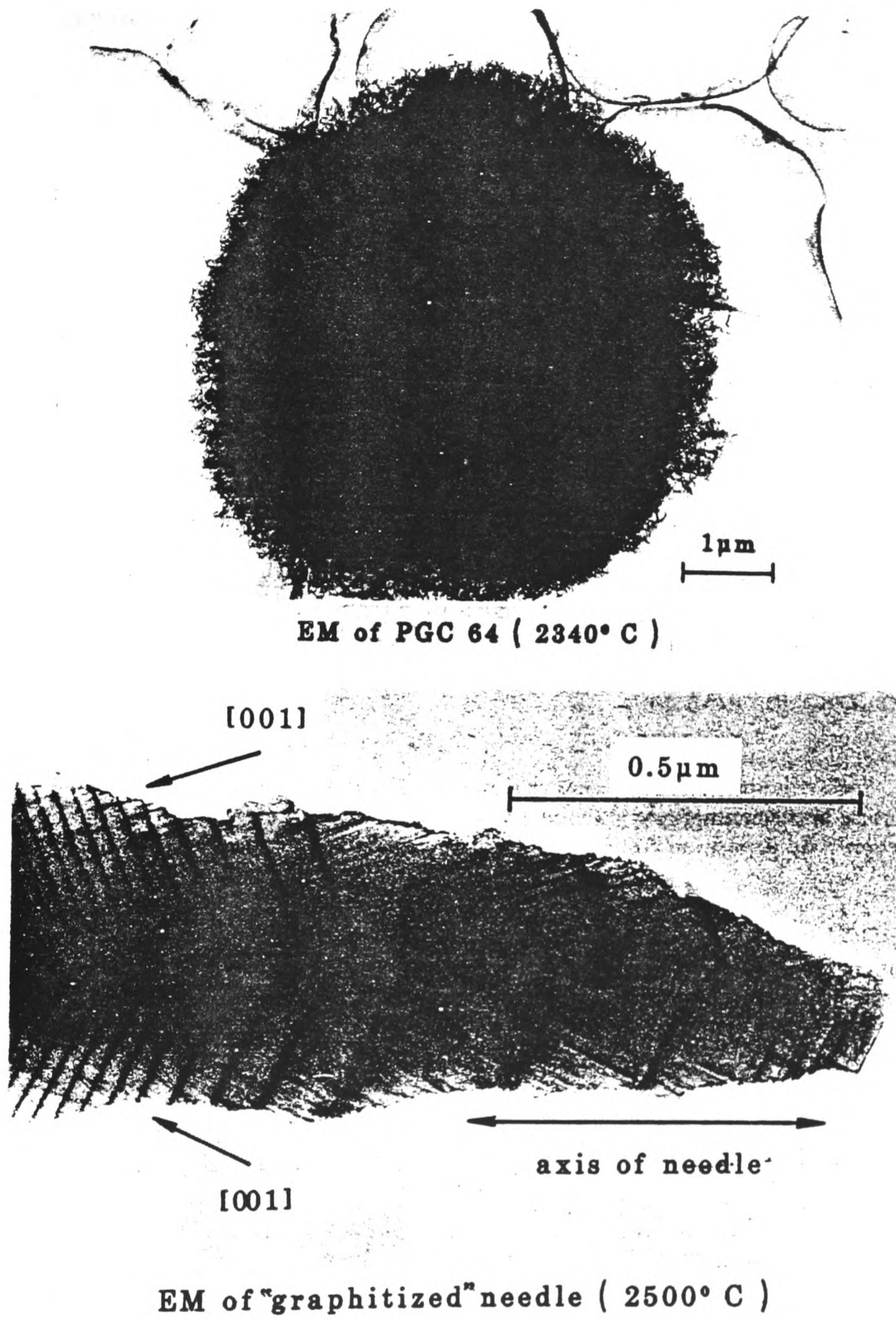
EM of "graphitized" needle (2500° C)

Fig. 8. Transmission electron micrographs. Upper: Spherical particle of PGC. Lower: "Needle", showing twinning.

"Pyrocarbon on Black Pearls" was similarly prepared using Black Pearls (a carbon black) as the supporting structure. Neither material shows significant graphitisation and, indeed, the tracing for the "Pyrocarbon on BP" shows the expected diffuse reflections of a carbon black (Fig. 3). The still wider reflections for "Pyrocarbon on silica gel" are analogous to those of low-temperature glassy carbon (Fig. 2). Neither of these materials gave satisfactory chromatograms in liquid chromatography.

"Carbon for Catalysis" was an active carbon which had been treated at a high
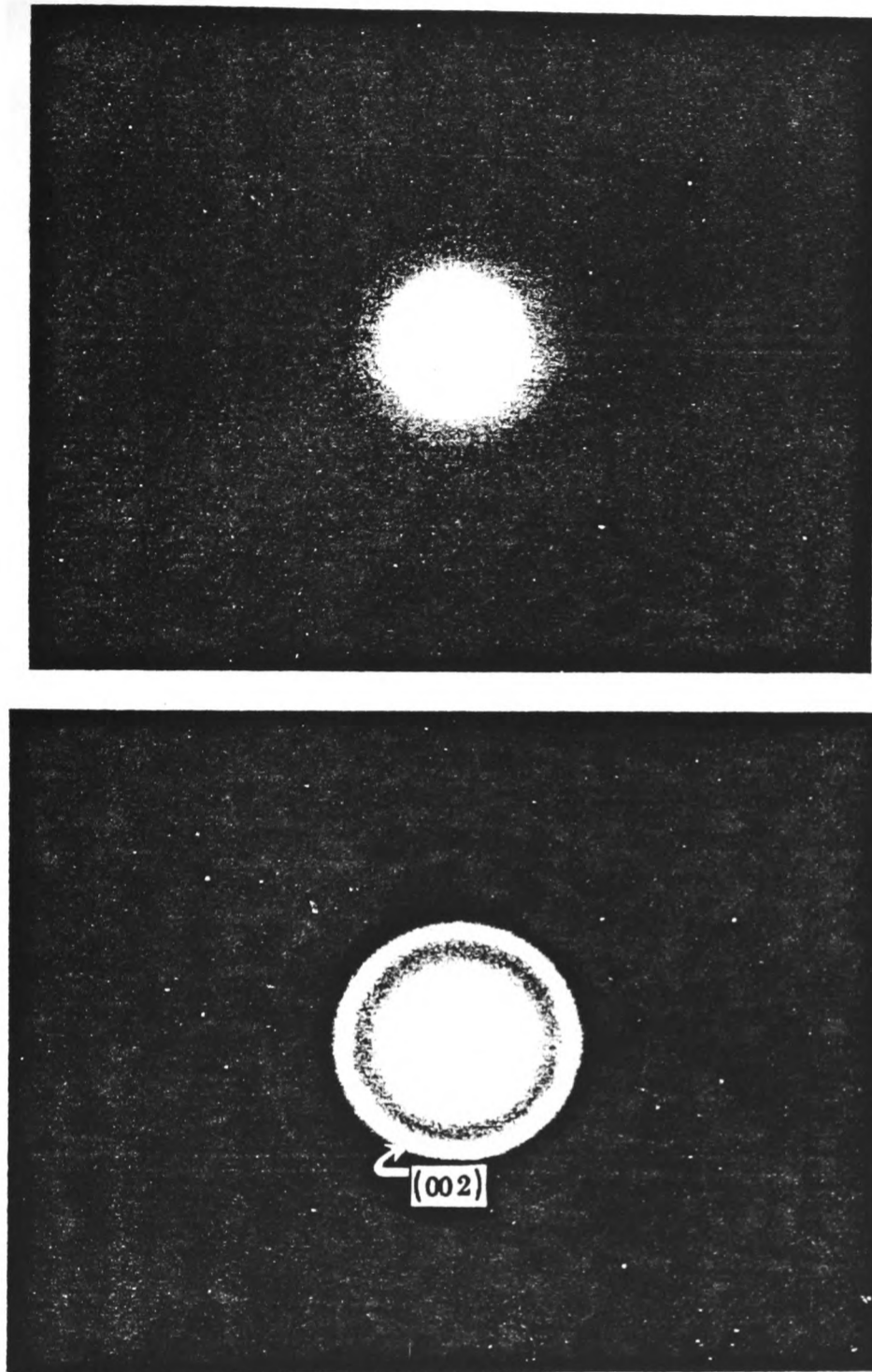
Fig. 9. Electron diffractograms of PGC. Upper: sample, as prepared at 1000°C. Lower: after heating to 2500°C, showing 002 and other diffractions.
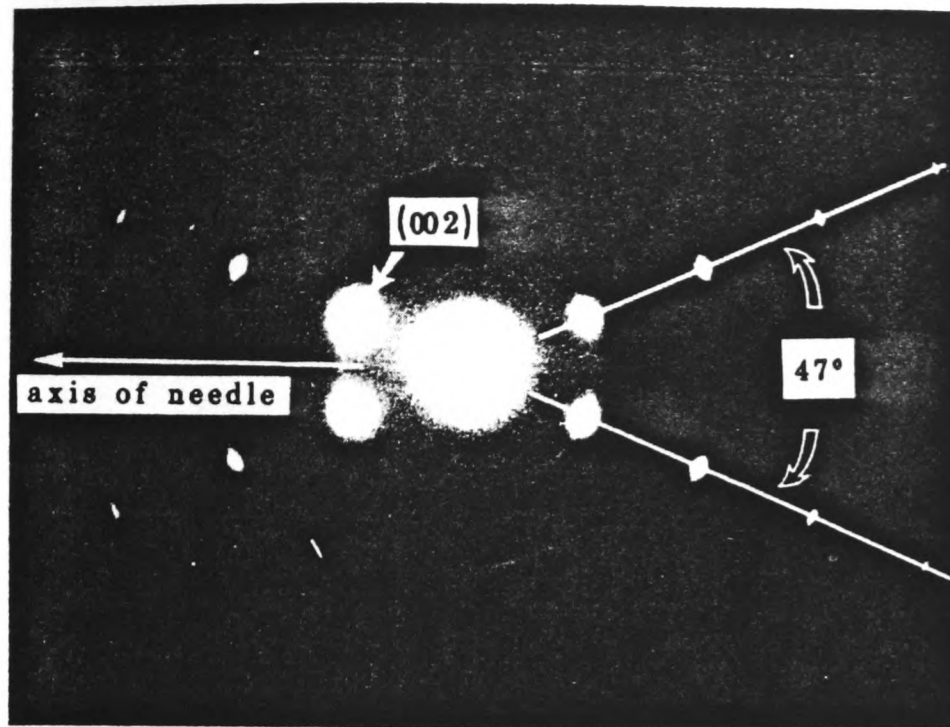
Fig. 10. Electron diffractogram of "needle", showing twinning.

temperature by a proprietary process. It shows two-dimensional graphitisation, but the rather wide asymmetric 002 peak characteristic of a material with a relatively high proportion of amorphous material. "Carbopack" from which needles have been removed shows a more symmetrical 002 reflection, indicating good graphitisation —but its width suggests that the crystallites are small. Both PGC64 and PGC212 show narrower 002 reflections, indicating good graphitisation with larger crystallites. When needles are present in "Carbopack" and PGC, additional 002 and 004 reflections are present, as well as 101 reflections. This is illustrated more clearly in Fig. 7.
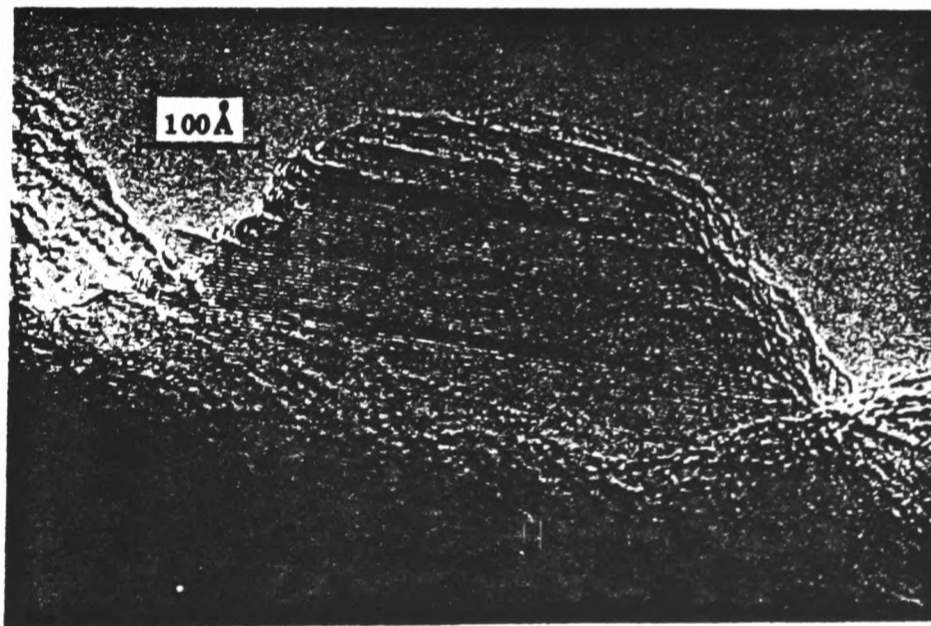
Fig. 11. High-resolution electron micrograph of plate or needle, heated to 2500°C.

The additional peaks indicate that the material containing needles consists of two distinct phases. The needles appear to be three-dimensional pyrolytic graphite, while the spherical, porous particles are two-dimensional graphite with the wider l-spacing of about 3.40 Å. Often, a shoulder is seen on the 002 reflection of PGC samples heated above 2000°C. We believe that this shoulder arises from a small proportion of needles in these samples.

Typical crystallite sizes from some PGC samples are given in Table I. The
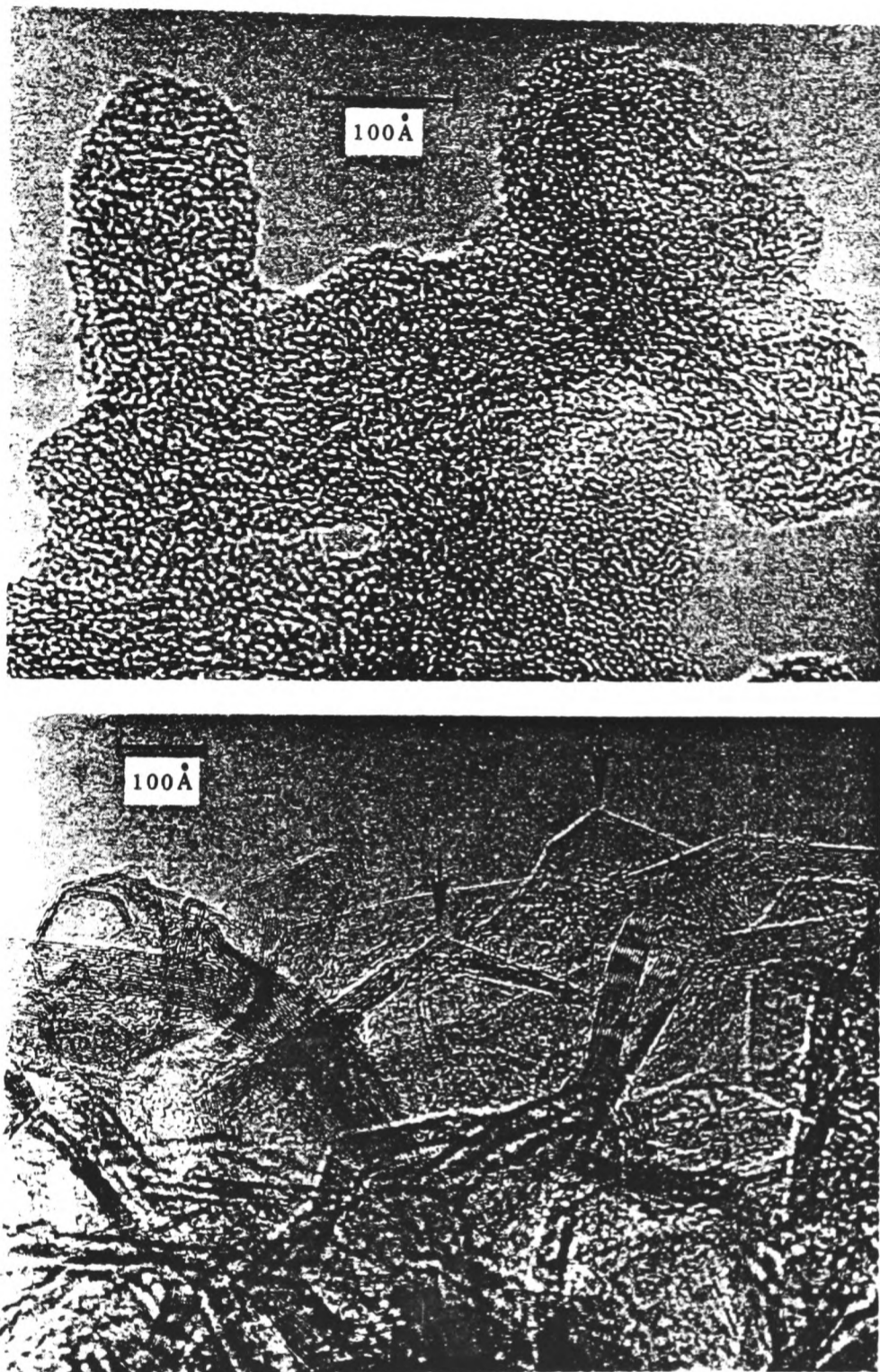
Fig. 12. High-resolution electron micrographs of PGC. Upper: PGC, as prepared at 1000°C. Lower: after heating to 2340°C.

crystallite sizes are typical for two-dimensional graphites and are comparable to the thickness of the connecting bridges in the sponge-like PGC structure. These may be estimated to be about 100 Å on the basis of a surface area of 150 m² g.

Electron diffraction and transmission electron microscopy

Fig. 8 shows transmission electron micrographs of a spherical particle of PGC and of a "needle". The porous nature of PGC contrasts with the much denser structure of the needle. The needle shows clear evidence of twinning with an angle between the layers of about 45°. Fig. 9 shows two electron diffractograms of the spherical particulate material, the upper of PGC heated to 1000°C, the lower of material heated to 2500°C. The presence of the 002 band and the increased sharpness of the diffraction patterns in the latter are consistent with the evidence from X-ray analysis which indicate layer ordering during high-temperature treatment. The lower diffractogram clearly shows the crystal spacing of two-dimensional graphite. Fig. 10 shows the electron diffractogram from a needle. The two sets of reflections correspond to two sets of crystal planes at an angle of 47°, in complete agreement with the transmission electron micrograph of Fig. 8.

Fig. 11 shows high-resolution electron micrography (HREM) of a fragment of a pyrolytic carbon needle. The graphitic layers are clearly visible. Fig. 12 shows HREM of PGC. The upper part shows the totally amorphous structure of the material, heated only to 1000°C, while the lower part shows the high degree of two-dimensional graphitisation of PGC after heating to 2500°C. Particularly notable are the straight, parallel lines, indicating ordered graphitic sheets, and the sharp angles at which the "booklets" of sheets meet. Also seen are a number of rounded corners and several groups of curved or bent sheets. There is also some evidence of surface
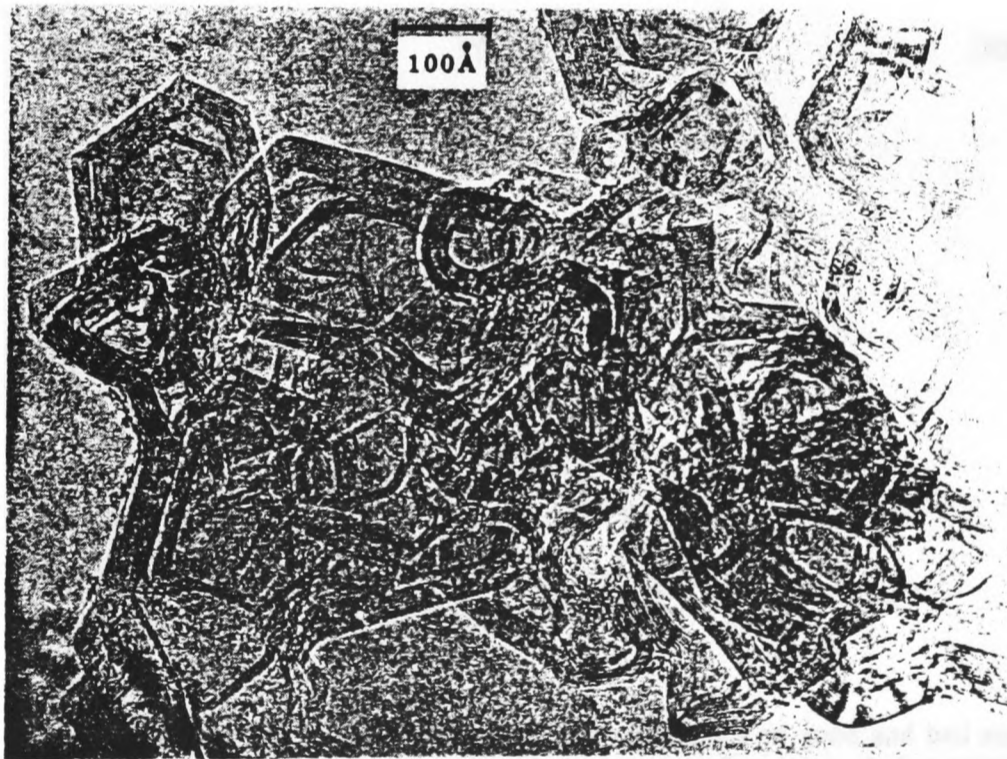

Fig. 13. High-resolution electron micrograph of Carbopack B, a typical graphitized carbon black.

defects. Fig. 12 should be compared with Fig. 13, which shows HREM of graphitised carbon black. Again, one notes flat sheets, meeting at well-defined angles, rounded corners, and bent or distorted sheets. The degree of two-dimensional graphitisation shown in Fig. 12 and 13 are very similar. However, there is a striking difference between the two: Fig. 13 shows that graphitised carbon black is made up of colloidal particles which are not interconnected, whereas Fig. 12 shows that PGC is in the form of a continuous structure in accord with our original intention in developing a template method for producing PGC.

HREM of PGC shows that the crystallites comprise tens of layers of graphitic sheets, thus giving stack heights of 30–60 Å, in agreement with the X-ray evidence cited in Table 1. The widths of the sheets appear somewhat greater than their thicknesses.

Conclusions from X-ray analysis and electron microscopy

From the foregoing, a number of firm conclusions can be drawn regarding the nature and structure of PGC:

(1) PGC heated to 2500°C is a two-dimensional graphitised carbon.

(2) PGC heated to 2500°C has an atomic structure almost identical to that of a graphitised carbon black, but its structure at a colloidal level (*i.e.* > 1000 Å) is quite different. PGC has a sponge-like form, whereas GCB is made up of loosely aggregated colloidal particles.

(3) PGC, when heated only to 1000°C, is totally amorphous, but HREM clearly shows its sponge-like structure.

(4) On heating PGC from 1000 to 2500°C, pyrolytic deposition of carbon needles takes place, presumably from organic vapours liberated just above 1000°C, rather than from evaporation of carbon itself. The atomic arrangement in these
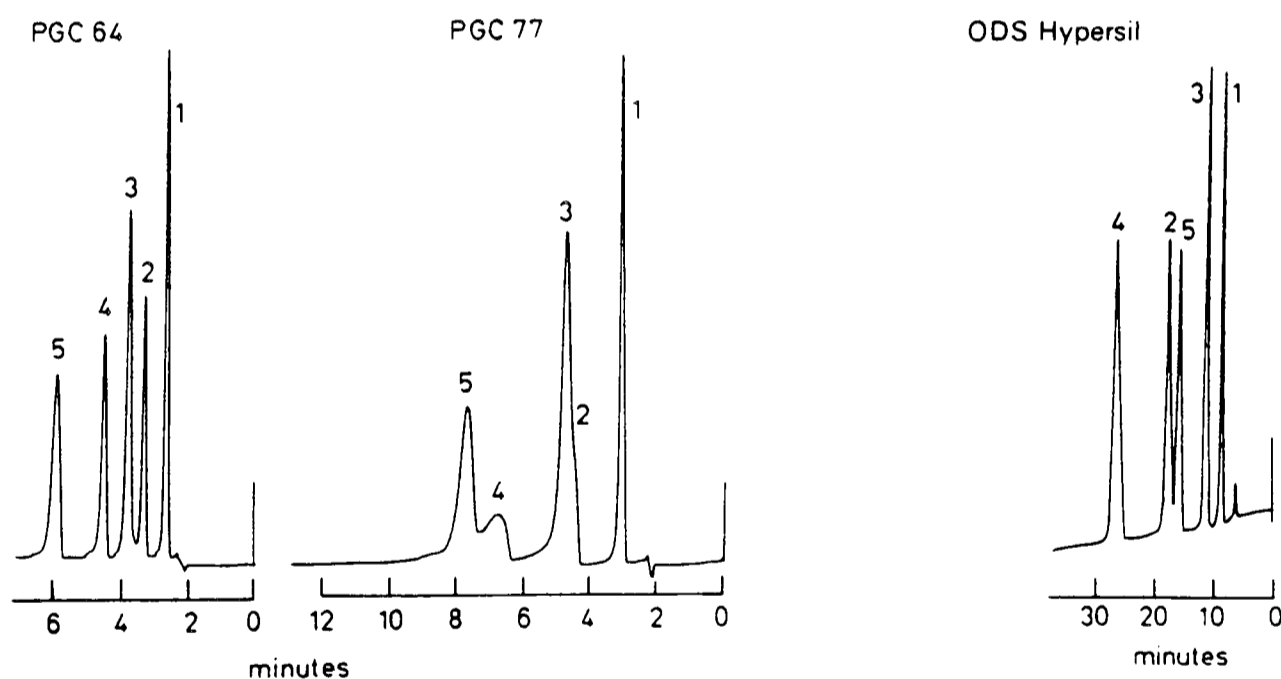

Fig. 14. Comparative chromatograms, showing separations on good and bad samples of PGC (Eluent: methanol–water, 95:5). Peaks: 1 = phenol; 2 = anisole; 3 = *p*-cresol; 4 = phenetole; 5 = 3,5-xylenol.

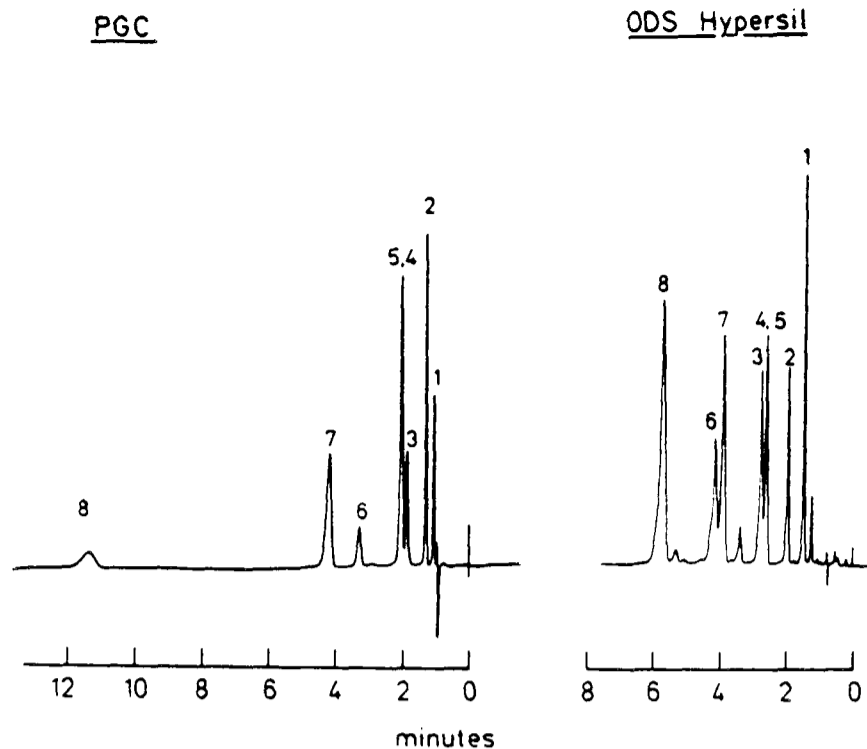Fig. 15. Separation of mixture of Fig. 14 on ODS Hypersil (methanol–water, 60:40). Peaks as in Fig. 14.

PGC   ODS Hypersil

Fig. 16. Separations of methylbenzenes on PGC64 (methanol–water, 95:5) and on ODS Hypersil (methanol–water, 70:30). Peaks: 1 = benzene; 2 = toluene; 3 = *m*-xylene; 4 = *p*-xylene; 5 = *o*-xylene; 6 = 1,3,5-trimethylbenzene; 7 = 1,2,4-trimethylbenzene; 8 = 1,2,4,5-tetramethylbenzene.
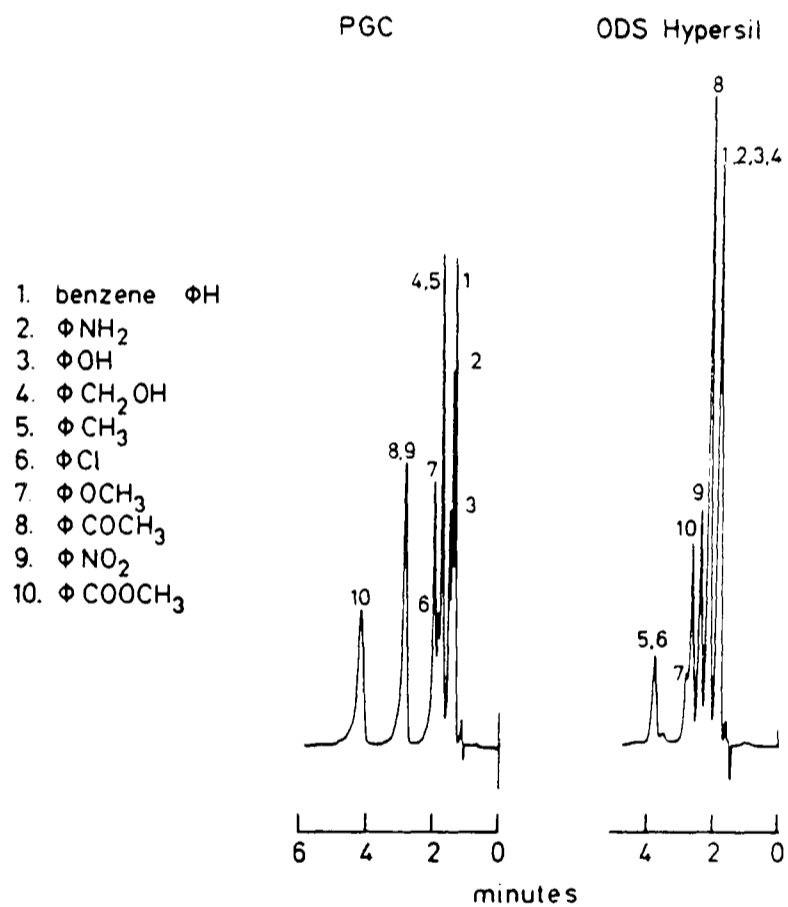
PGC   ODS Hypersil

1. benzene ΦH
2. ΦNH₂
3. ΦOH
4. ΦCH₂OH
5. ΦCH₃
6. ΦCl
7. ΦOCH₃
8. ΦCOCH₃
9. ΦNO₂
10. ΦCOOCH₃

Fig. 17. Separations of monofunctional derivatives of benzene on PGC64 (methanol–water, 90:10) and on ODS Hypersil (methanol–water, 70:30).

needles is that of a three-dimensional crystalline graphite. Whereas the spheres of PGC are highly porous, the needles have no porosity.

(5) For chromatographic purposes, the needles, having no significant surface area, are of no value and should, if possible, be removed or, preferably, their formation should be avoided. The chromatographically useful particles are those of the porous two-dimensional graphite.

(6) The original intention of producing a porous graphite of adequate surface area and appropriate structure for chromatography has been achieved.

Liquid chromatography: typical separations

Figs. 14–22 show illustrative chromatograms on PGC. Figs. 15–19 show comparisons of separations on PGC and ODS Hypersil.

One of the problems encountered in the production of PGC for liquid chromatography is illustrated in Fig. 14. Satisfactory batches of PGC, such as PGC64, show well-shaped peaks with good plate efficiency, whereas unacceptable batches, such as PGC77, show tailed peaks and higher capacity factors. Comparing the two chromatograms, it is particularly noted that the peaks for the ethers, anisole and phenetole, are more strongly retained relative to the phenols on PGC77, and that the
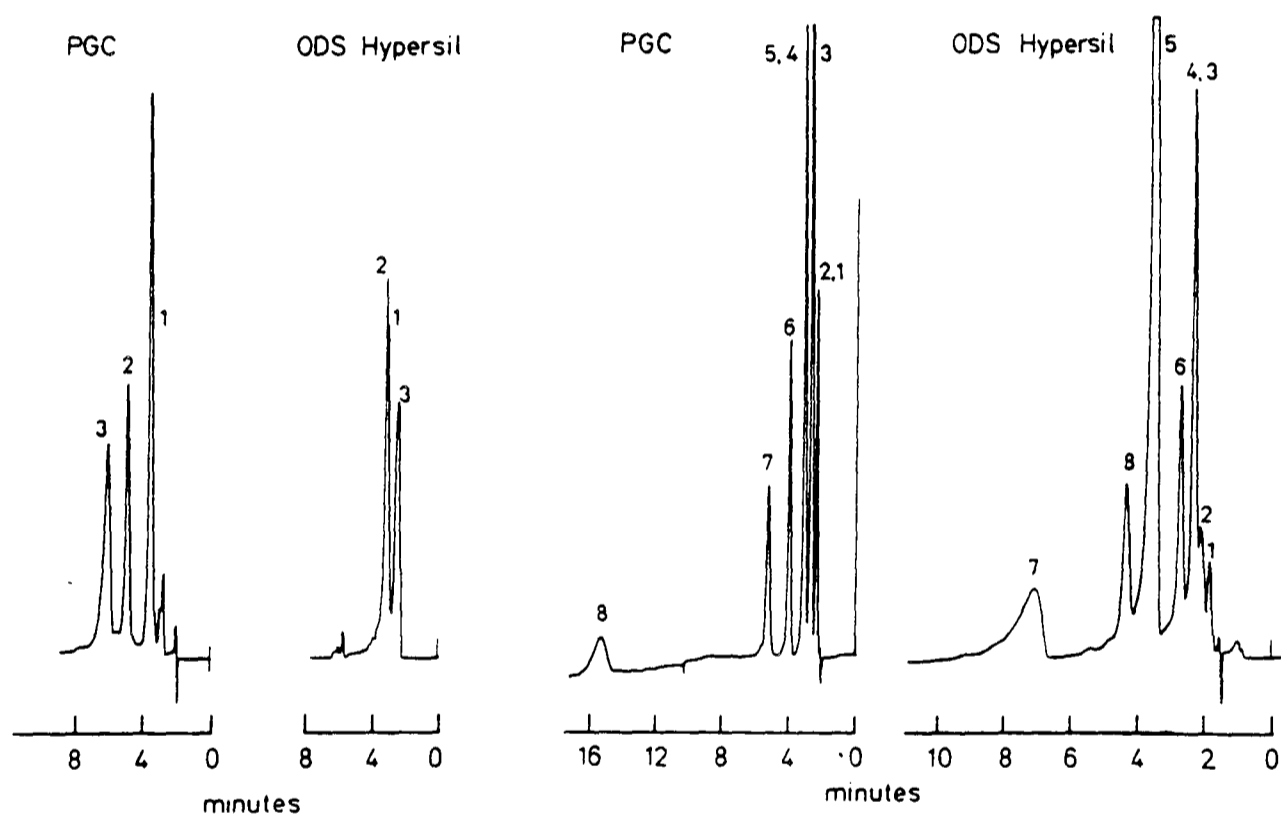

Fig. 18. Separations of acids on PGC64 and ODS Hypersil (acetonitrile–water, 90:10). Peaks: 1 = benzoic acid; 2 = o-toluic acid; 3 = salicylic acid.

Fig. 19. Separations of amines on PGC64 (methanol–water, 95:5) and on ODS Hypersil (methanol–water, 70:30). Peaks: 1 = aniline; 2 = pyridine; 3 = 2-methylpyridine; 4 = methylaniline; 5 = dimethylaniline; 6 = ethylaniline; 7 = diethylaniline; 8 = benzylamine.

peak for phenetole is badly tailed. It appears that the unacceptable material arises when traces of oxidation can occur, either during the pyrolysis to 1000°C or during the subsequent heating above 1000°C.

Fig. 15 shows the separation of the same mixture on ODS Hypersil. It is noted that the selectivity with regard to phenols vs. ethers is different, although the order within each group is the same. On ODS Hypersil, the ethers are more retained relatively to phenols than on PGC.

Fig. 16 shows comparative separations of methylbenzenes. Attention is drawn to the reversal of the order of elution of m-xylene and o- plus p-xylenes. The elution order for carbon has been explained by Kiselev and Yashin[23] on the basis that when o-xylene and p-xylene are adsorbed onto the flat graphitic surface, four carbon atoms contact the surface (two from the methyl groups and two from the ring) whereas with m-xylene only three atoms contact the surface (two from the methyl groups and one from the ring). A similar order reversal is noted with 135 and 124 trimethylbenzenes. In addition, PGC shows a greater spread of retention than does ODS Hypersil.

Fig. 17 compares separations of a range of singly substituted benzenes. Again, similar peak symmetry and plate efficiencies are observed, but significant differences in elution order. In particular, solutes 4 and 7–10 appear much later on PGC, whereas 5 and 6 appear later on ODS. The more strongly retained solutes on PGC are those with the greater number of C, N and O atoms in the functional groups. Fig. 18 shows comparative separations of some acids, again showing different selectivities. From PGC, the acids are eluted in the order of molecular weight.

Fig. 19 illustrates the superior performance of PGC when used for the separation of amines. Whereas ODS Hypersil gives tailed peaks for several of the solutes, no tailing is observed with PGC. Tailing on ODS silica is presumably due to the effect of residual silanol groups. This is confirmed by the late elution of the most tailed peaks (dimethylaniline, 5, and diethylaniline, 7) from ODS Hypersil.
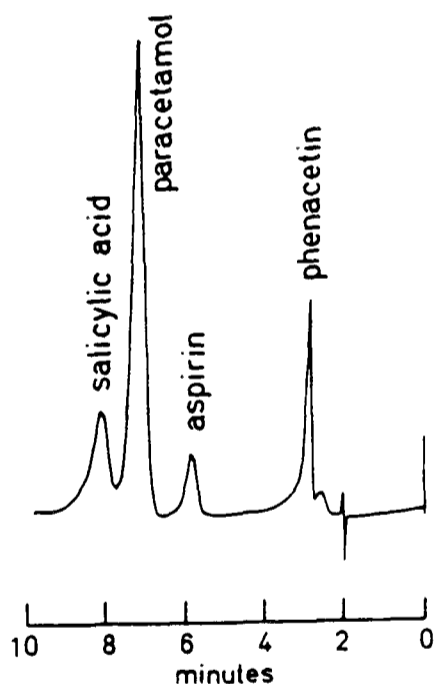

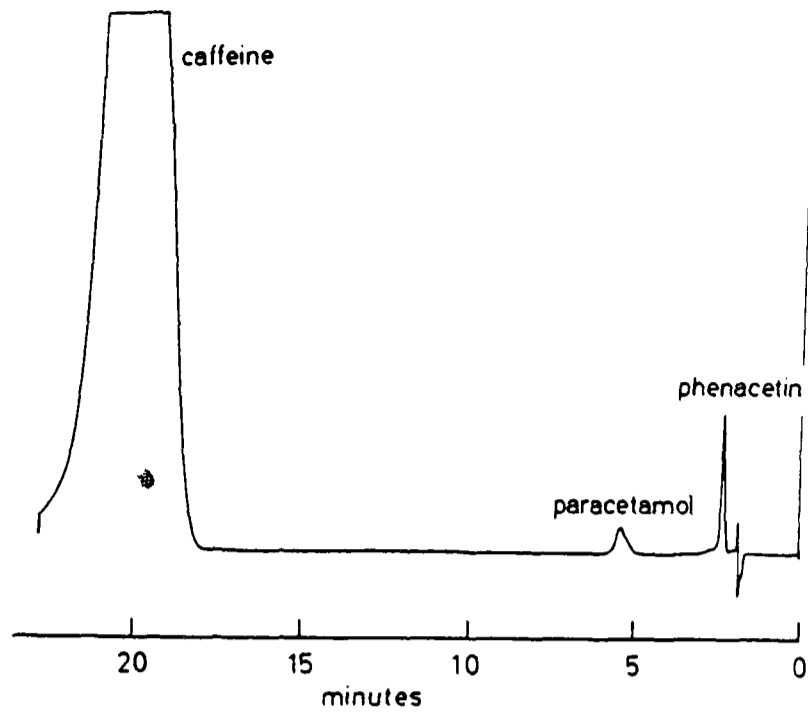Fig. 20. Separation of simple analgesics on PGC64 (methanol–water–acetic acid, 94:5:1).

Fig. 21. Separation of analgesics on PGC64 (methanol–water, 95:5).

Figs. 20 and 21 show separations of typical analgesic mixtures on PGC.

Fig. 22 illustrates an aspect of LC on PGC which is likely to be of great importance in the future. A column of PGC after long use became deactivated so that the retention of solutes was much reduced. The column was stored for several
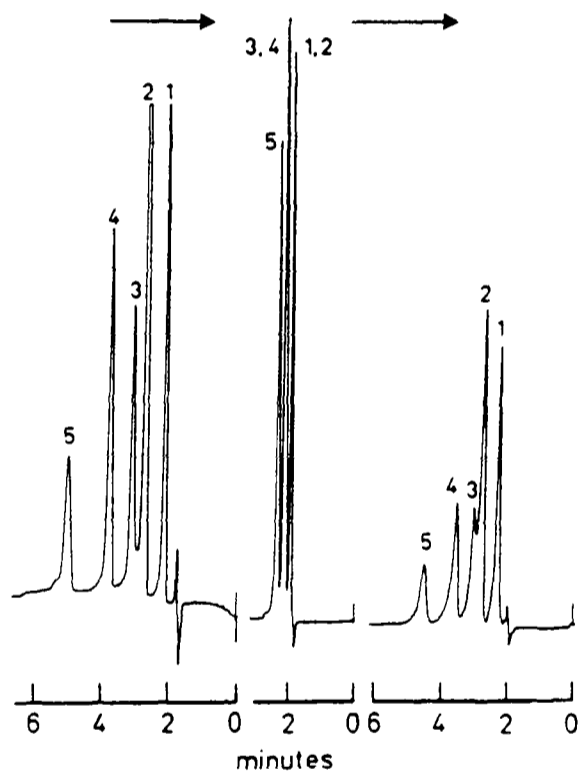

Fig. 22. Deactivation and reactivation of PGC64. From left to right: column, as originally tested with methanol–water (95:5); column, after becoming deactivated; column, after reactivation by washing with dioxane. Solutes as for Fig. 14.

months and was subsequently eluted with pure dioxane, whereupon the original activity returned. This observation leads to some important conclusions.

Firstly, if PGC becomes deactivated, it can generally be reactivated by washing with a suitable solvent. This makes it clear that the deactivation observed must have been due to the adsorption of some high-molecular-weight impurity in the eluent. Accordingly, it is important when using PGC that the eluents contain no traces of plasticisers, etc., and it is probably desirable to include a precolumn before the analytical column to avoid contamination. Secondly, we note that, even when deactivated, PGC provides excellent peak shape. Controlled deactivation of PGC by the preadsorption of high-molecular-weight additives may thus provide an important method of modifying its adsorption characteristics. It may be noted that it is probably impossible to derivatise the graphitic surface of PGC, which is made up of a totally aromatic sheet of carbon atoms. Pre-adsorption of long-chain additives provides the nearest equivalent to the chemical bonding method so widely used with silica gel.

In general, it is noted from the examples just given that, for roughly equal degrees of retention, eluents for PGC contain high proportions of the organic component (90-100%), whereas eluents for ODS silica contain considerable proportions of water (around 50%). Evidently, the very strong retention by PGC may be a disadvantage when eluting molecules of high molecular weight. However, as with silica gel, the addition of a strongly adsorbed modifier can be used to reduce and modify this activity. Accordingly, we anticipate that by adsorbing long-chain molecules, bearing different functional groups, it will be possible not only to control the degree of retention by PGC but also to modify the selectivity of PGC in novel ways. Extensive work in this area has been carried out on modifications of GCB for use in GC by adsorption of small quantities of high-molecular-weight modifiers[24,25].

Conclusions —Chromatographic

(1) PGC acts as a strong hydrophobic adsorbent in LC.

(2) PGC can be operated under typical HPLC conditions of pressure and flow-rate.

(3) Spherical PGC (7 μm) gives peak sharpness (number of plates) very similar to a typical bonded silica gel.

(4) PGC requires eluents containing a higher proportion of organic components than does ODS-bonded silica gel; typically 95% methanol compared to 50% methanol.

(5) PGC gives good peak shapes for elution of a wide range of monofunctional benzenes (phenols, ethers, acids, and amines) and for some simple analgesics.

(6) PGC can be deactivated by prior adsorption of high-molecular-weight additives.

CONCLUSION

PGC is a two-dimensional graphite with a unique sponge-like structure which gives it good mechanical strength, adequate for HPLC, while maintaining an adequate surface area (around 150 m^2/g) and porosity (around 80%). PGC has unique chromatographic properties, being the only truly hydrophobic adsorbent. It shows strong retention of simple organics and novel stereoselectivity. It gives chromatograms of high efficiency.

REFERENCES

1 M. T. Gilbert, J. H. Knox and B. Kaur, Chromatographia, 16 (1982) 138.
2 J. H. Knox and M. T. Gilbert, U.K. Pat., 7939449 (1982); U.S. Pat., 4,263,268 (1982); W. German Pat., P 2946688-4 (1982).
3 P. Ciccioli, R. Tappa, A. Di Corcia and A. Liberti, J. Chromatogr., 206 (1981) 35.
4 A. Standen (Editor), Kirk Ottmer Encyclopaedia of Chemical Technology, Wiley Interscience, New York and London, 2nd ed., 1964, Vol. 4, pp. 149–335.
5 K. K. Unger, P. Roumeliotis, H. Mueller and H. Gotz, J. Chromatogr., 202 (1980) 3.
6 H. Colin, C. Eon and G. Guiochon, J. Chromatogr., 119 (1976) 41; 122 (1976) 223.
7 Z. Plzák, F. P. Dousek and J. Jansta, J. Chromatogr., 147 (1978) 137.
8 J. H. Knox and K. K. Unger, J. Liq. Chromatogr., 6 (1983) 1.
9 J. D. Bernal, Proc. Roy. Soc. London Ser. A, 100 (1924) 749.
10 H. Lipson and A. R. Stokes, Proc. Roy. Soc. London Ser. A, 181 (1942) 93.
11 B. E. Warren, Phys. Rev., 59 (1941) 693.
12 J. M. Jenkins and K. Kawamura, Polymeric Carbons, Cambridge University Press, Cambridge, 1976.
13 R. E. Franklin, Proc. Roy. Soc. London Ser. A, 209 (1951) 196.
14 T. V. Barmakova, A. V. Kiselev and N. V. Kovaleva, Kolloid Zh., 36 (1974) 133.
15 T. Noda, M. Inagaki, S. Yamada, J. Non-crystalline Solids, 1 (1969) 285.
16 A. V. Kurydyumov and A. N. Pilyankevich, Crystallography, 13 (2) (1968) 245.
17 P. Scherrer, Nachr. Ges. Wiss. Göttingen, 2 (1918) 98.
18 J. T. Randall, H. P. Rooksby and B. S. Cooper, Z. Krist., 15 (1930) 196.
19 R. Diamond, Acta Cryst., 10 (1957) 359.
20 J. Biscoe and B. E. Warren, J. Appl. Phys., 13 (1942) 364.
21 J. M. Thomas, D. A. Jefferson and G. R. Millward, Jeol News, 23 (1985) 7.
22 H. Colin and G. Guiochon, J. Chromatogr., 126 (1976) 43.
23 A. V. Kiselev and Y. I. Yashin, Gas Adsorption Chromatography, Plenum Press, New York, 1969.
24 A. Di Corcia and A. Liberti, Adv. Chromatogr., 14 (1976) 305.
25 F. Bruner, P. Ciccioli, G. Crescentini and M. T. Pistolesi, Anal. Chem., 45 (1973) 1851.

ELUOTROPIC RELATIONSHIPS FOR POROUS GRAPHITIC CARBON

by John H. Knox and Bulvinder Kaur
Wolfson Liquid Chromatography Unit, Department of Chemistry, University of Edinburgh, West Mains Road, Edinburgh, UK.

The concept of an eluotropic series has proved to be of great value in understanding the eluting power of solvents when used with oxide-based adsorbents such as silica gel and alumina. It is widely held that there exists a corresponding eluotropic series for carbon which is the reverse of that for the oxide adsorbents.

We have examined eleven common eluents with a wide range of solutes of different functionality and with three homologous series in order to determine the relevance of the eluotropic concept to porous graphitised carbon (PGC).

The following results have been obtained:

(1) The total range of eluotropic strength using the Snyder scale is only about 0.2 units for PGC compared to about 1.0 units for the oxide adsorbents.

(2) The order of elution strengths of the eleven solvents depends markedly upon the solute or functional group used to determine the elution strength.

(3) The strongest solvents are those whose eluotropic strength for oxide adsorbents lie in the middle of the range, while solvents with extreme eluotropic strengths, such as methanol, acetonitrile and hexane are weak solvents on PGC.

(4) For a given solute type (e.g. an acid, an alcohol or a base etc.), peak symmetry depends markedly upon the eluent used. Thus the optimum eluent for any separation has to be chosen on the basis both of the eluotropic strength of the solvent and the peak symmetry which it provides.

Our results lead to the following general conclusions:

(1) The main assumption made by Snyder in applying the surface displacement theory to oxide adsorbents does not hold when applied to PGC.

(2) There is no unique eluotropic series for carbon, and broadly speaking the strong solvents on carbon are not the weak solvents on the oxide adsorbents.

(3) The concept of an eluotropic series for carbon is not of much use in guiding the selection of eluent.

Some guidelines for the selection of optimum eluents are discussed and have been applied to particular separation problems including the separations of paracetamol metabolites in urine, of hop acids, and of aromatic amino acids.